NEW ENGLAND INTERCOLLEGIATE GEOLOGICAL CONFERENCE

*110TH ANNUAL MEETING*

NEW YORK STATE GEOLOGICAL ASSOCIATION

*90TH ANNUAL MEETING*

# Guidebook for Fieldtrips in New York and Vermont

A meeting in honor of Bruce Selleck and William Kidd

Edited by
Tim Grover
and
Helen Mango

Hosted by Castleton University and Colgate University

# NEW ENGLAND INTERCOLLEGIATE GEOLOGICAL CONFERENCE

*110TH ANNUAL MEETING*

# NEW YORK STATE GEOLOGICAL ASSOCIATION

*90TH ANNUAL MEETING*

## Guidebook for Fieldtrips in New York and Vermont

October 12-14, 2018

*Edited by*
Timothy W. Grover and
Helen Mango

*Hosted by*
Castleton University and Colgate University

NEIGC
New England Intercollegiate Geological Conference

Copies of this guidebook may be purchased for $35 from the
following address:
Geology Program Coordinator
Natural Sciences Department
Castleton University
Castleton, VT 05735

## Front Cover Credit

The front cover photo credits are clockwise from top right: William Peck, John Rayburn, Tim Grover, Jean Crespi, Tim Grover

The NEIGC logo is courtesy of Lindley Hanson.



All field tripguides are available for free download by following this link: www.castleton.edu/neigc-nysga

## DISCLAIMER

Before visiting any of the sites described in New England Intercollegiate Geological Conference guidebooks, you must obtain permission from the current landowners.

Landowners only granted permission to visit these sites to the organizers of the original trips for the designated dates of the conference. It is your responsibility to obtain permission for your visit. Be aware that this permission may not be granted.

Especially when using older NEIGC guidebooks, note that the conditions and accessibility at field trip locations may have changed drastically. Likewise, geological interpretations may differ from current understandings.

Please respect any trip stops designated as "no hammers," "no collecting" or the like.

Consider possible hazards and use appropriate caution and safety equipment.

NEIGC and the hosts of these online guidebooks are not responsible for the use or misuse of the guidebooks.

**TABLE OF CONTENTS**

## Welcome

Welcome to the 110th Annual Meeting of the New England Geological Conference, the 90th meeting of the New York State Geological Association, and the beautiful Lake George Region. Trips during this meeting will range from the High Peaks region of the Adirondacks to the summits in the Green Mountains, the Taconics, and the Berkshires in Massachusetts. Trips will also visit the Champlain Valley and the upper reaches of the Hudson Valley. Participants will have the opportunity to examine geologic features ranging from Mesoproterozoic, granulite facies, metamorphic rocks that formed in the middle to lower crust to mud and sand presently on the surface of the Earth. Topics of discussion will range from major and trace element bulk rock geochemistry to REE behavior in monazite to cosmogenic isotopes to chemical contamination from burn piles; from climate in the Early Paleozoic to relatively recent periods of glacial advance and retreat; and from ductile to brittle deformation mechanism. There is something for everyone!

This meeting is dedicated to Bruce Selleck and William Kidd. Bruce Selleck, who unexpectedly passed away just over a year ago, began his work in the region studying the Paleozoic platform sedimentary rocks and later, along with Jim McLelland, published many papers on the Proterozoic rocks of the Adirondacks. Bill Kidd has published many papers on the rocks in the Taconics and the deformed foreland basin rocks. Many of us have learned a great deal from these two distinguished geologists and geologic educators at meetings such as this one or other field excursions. More on Bruce and Bill follows in the dedication in this guidebook.

The hosts of this combined NEIGC and NYSGA also wish to recognize the support of the Malcolm ’54 and Sylvia Boyce endowment for Geology at Colgate University. Our current students represent the future of the NEIGC and the NYSGA. The organizers tried to encourage student attendance at this conference by keeping the costs of registration and the banquet low. These reduced costs were made possible by the generous support of the Malcolm ’54 and Sylvia Boyce endowment for Geology at Colgate University. Thank you!

## Foreword

The NEIGC and NYSGA are amazing organizations that we all believe in and feel are incredibly valuable. Both of these organizations are completely run by many folks generously volunteering their time. We thank the many people that made this NEIGC and NYSGA happen. First thanks to all the field trip leaders who gave generously of their time to put their field guides together and run the trips. Thanks also to Dyk Eusden who set a high bar running the previous NEIGC meeting. We did our best to try to achieve that standard. Dyk was very patient answering our many questions. Thanks also to Brigette Olsen at Castleton University Camps and Conferences office for designing and implementing the online registration process and thanks to Castleton University’s Office of Advancement for hosting the conference webpage. Thanks to Tom Wysocki and the staff at the Fort William Henry Hotel for their assistance with the lodging, welcoming reception, and banquet. Thanks to Lindley Hanson of Salem State for updating and maintaining the official NEIGC website and to Joe Kopera for serving as Secretary of the NEIGC. Thanks also to Dave Valentino for his years of dedicated service to the NYSGA and for helping us with many aspects of this meeting. We would also like to thank Brain Carl for his work on the NYSGA website. Finally, thanks to everyone that is attending the meeting. We hope you find that it is both educational and enjoyable.

Helen Mango  Tim Grover  William Peck  Martin Wong

**Memorial to Bruce Warren Selleck**
**1949-2017**

William H. Peck[1], Department of Geology, Colgate University, Hamilton, New York 13346
Martin S. Wong[2], Department of Geology, Colgate University, Hamilton, New York 13346
Email addresses: [1]wpeck@colgate.edu, [2]mswong@colgate.edu

Bruce Selleck, Thomas A. Bartlett Chair and Professor of Geology at Colgate University, died unexpectedly but peacefully in his sleep July 31, 2017. Bruce was born September 30, 1949 in Potsdam, NY. He was the son of Fred W. and Helen Spanik Selleck, and was raised on the family dairy farm in the town of Pierrepont. On the Albert Marsh USGS 7.5-minute sheet the family farm is designated "Sellecks Corners", and Bruce began his formal education there in a one-room schoolhouse. Bruce graduated from Colton-Pierrepont Central School in 1967 and received a scholarship to attend Colgate University. Bruce was already interested in geology at that point, and had even attended SUNY Potsdam's field geology course as a high school student. Bruce would often credit his early interest in geology to a excellent ninth grade science teacher, and the particularly good mineral collecting around the farm where he grew up. At Colgate he played varsity soccer and was influenced by Jim McLelland and Bob Linsley, the magnetic poles of the department at that time. Bruce graduated from Colgate with an AB, High Honors in Geology in 1971. That year Bruce also married Nancy Barlow, who he had met when they were both 4-H camp counselors in the Adirondacks. Bruce earned his MA (1972) and PhD (1975) degrees at the University of Rochester, where he was a student of Zeddie Bowen and Bob Sutton and worked on Cambro-Ordovician sedimentology in northern New York for his dissertation.

In 1974 Bruce returned to Colgate as a one-year visiting instructor, but subsequently was asked to interview for a permanent position, and joined the staff as an assistant professor. Bruce would jokingly refer to his three years at Rochester as "the inter-Selleckian period", the only hiatus in his 50 year affiliation with Colgate. Colgate came to rely on Bruce, calling him to serve in many leadership roles, including chair of the geology department (1983–1986 and 2003–2006), associate dean of the faculty (1988–1990), dean of the faculty and provost (1990–1994), and interim dean of the faculty and provost (2011–2012), as well as chair and director of university committees and institutes, and as advisor to a range of sports teams, clubs, and Greek organizations. Bruce also believed strongly in contributing to the community beyond Colgate, and he served on the Town of Lebanon planning board as well as in leadership roles with the Friends of Rogers Environmental Center and the Adirondack Research Consortium. Bruce was a generous and inspirational mentor to many young faculty in and outside of the Geology department, and was well-known to be a gifted and loved teacher. Many of Bruce's students over the years cherish their memories of wonderful field trips with Bruce, and also his words of encouragement at critical moments, and thoughtful advice. Bruce received the Colgate Alumni Corporation Distinguished Teaching Award (1998), the AAUP Teacher of the Year Award (2006), and the Sidney J. and Florence Felten French Prize (2010) in recognition of his outstanding teaching.

Bruce was a very broad geologist with wide-ranging interests. His initial research focused on the Paleozoic sedimentology of New York, but as his career progressed he worked on a variety of projects with students and collaborators around the world. Bruce also diversified his approach to geological problems by learning stable isotope geochemistry and fluid inclusion analysis, turning some of his attention to diagenesis and alteration studies. In the 1990s, with longtime colleague and friend Jim McLelland, Bruce later expanded the scope of his research to include tectonic and geochronologic studies of the Adirondack Mountains. Bruce, who would always describe himself as a sedimentologist, was to co-author over twenty articles on the petrology and structural evolution of the Adirondacks with Jim, Jeff Chiarenzelli, Colgate colleagues, students, and others. Bruce's work on the Carthage-Colton shear zone eventually brought him back to some of the places where he collected rocks and minerals around Sellecks Corners, and he and Eric Johnson took us to some of them during the Friends of the Grenville field conference in 2005. Many geologists will know Bruce from field trips, and he was a active participant in Friends of the Grenville and The New York State Geological Association (NYSGA), leading or co-leading 12 NYSGA trips over the years and organizing the 2008 NYSGA in Lake George. A session on Adirondack and Grenville geology

was held in Bruce's honor at the 2018 Northeastern Geological Society of America meeting in Burlington, VT, and the Adirondack Research Consortium has inaugurated an annual forum on Adirondack Contemporary Issues in his name.

Bruce is survived by his wife of 46 years, Nancy Barlow Selleck, their two daughters, Caity Selleck (Jim Murphy) and Beth Selleck Fiore (Chris Fiore), grandchildren Cooper Murphy and Ellie Fiore; Bruce's two sisters, Linda Selleck Kershlis and Laura Selleck (John Jenkins); Nancy's sister, Cindy Lawrence (Kevin Lawrence); and his nephews, Zachary and Adam.

**Dedication to William S. F. Kidd**

Adam Schoonmaker, Department of Geosciences, Utica College, Utica, New York 13502
James H. MacDonald[1], Department of Marine and Ecological Sciences, Florida Gulf Coast University, Fort Meyers, Florida 33965

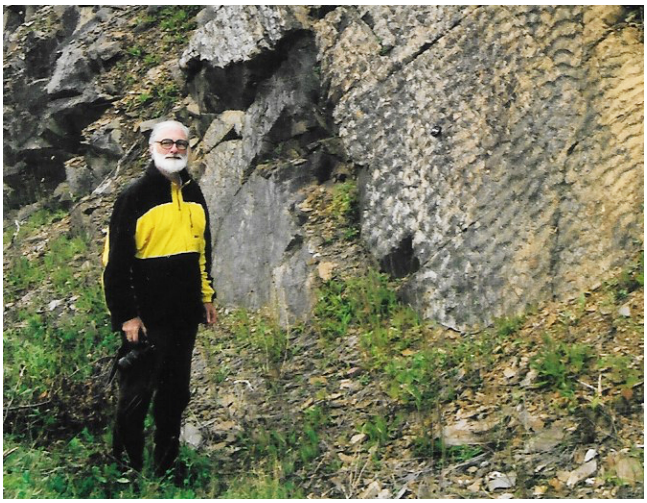

William S. F. Kidd is an Emeritus Professor of Geology from the University at Albany, SUNY. Bill arrived at Albany in 1974 after completing his Ph.D. in Geology from Cambridge University (via Wales), and a visiting position at the University of Toronto. Bill developed a number of courses at Albany, including teaching Field Mapping for 32 consecutive years! Bill supervised or co-supervised 43 graduate students while at Albany, including numerous students that went on to academic positions at significant colleges and universities. Bill's tenure at Albany coincided with the plate tectonic revolution; the Albany Geology Department at this time was highly influential in that revolution with seminal papers from Bill, John Dewey, Kevin Burke, Akiho Miyashiro, John Bird, Win Means, and the department's graduate students. Bill's work in the Taconic foreland is an important contribution to our understanding of the processes of plate interactions on subducting margins.

Bill's research focused on the tectonics of continental collisions, specifically the Tibetan Plateau, the Himalayas, and the Appalachians of Newfoundland and New England. Bill's has created many meticulous, highly detailed and amazingly accurate maps, many drawn in the pre-GPS era. Bill's diverse research interests also took him to the depths of the Tamayo and Oceanographer transform faults via ALVIN dives along the East Pacific Rise and Mid-Atlantic Ridge. Bill has been awarded over 1.3 million dollars in grant funding to conduct his research. He has published 91 peer reviewed papers, and over 150 referred abstracts presented at conferences.

Bill has shown great dedication to his students over the years. For many, he emphasized the importance of field observations of rocks and structures. In particular, he stressed the significance of stratigraphy as an indicator of tectonic processes. He has also devoted an incredible amount of energy preserving the work of his students by digitizing their reports and maps to keep their work accessible and relevant to the academic community. Bill's great observational humor translated in the classroom as well as outside. Pepsi University or the Pakistan Institute of Nuclear Science and Technology are just two of many examples of this wonderful observational humor. Notably, he will always call out bullshit.

## DATES, LOCATIONS, AND ORGANIZERS OF PREVIOUS NEIGC MEETINGS

| | | |
|---|---|---|
| 110 - 2018 | Lake George, NY | Tim Grover and Helen Mango |
| 109 - 2017 | Bethel, ME | Beverly Johnson and Dykstra Eusden |
| 108 - 2016 | Bath, ME | Henry Berry and David West |
| 107 - 2015 | Middletown, CT | Martha Gilmore |
| 106 - 2014 | Wellesley, MA | Margaret Thompson and David Hawkins |
| 105 - 2013 | Millinocket Lake, ME | Lindley Hanson |
| 104 - 2012 | Sunapee, NH | Peter Thompson and Timothy Allen |
| 103 - 2011 | Middlebury, VT | David West |
| 102 - 2010 | Orono, ME | Martin Yates, Chris Gerbi, Alice Kelley, Dan Lux |
| 101 - 2009 | Lyndon, VT | David Westerman and Alison Lathrop |
| 100 - 2008 | Westfield, MA | Mark Van Baalen and Mike Young |
| 99 - 2007 | Quebec City, PQ | Louise Corriveau, Tom Clark and Michel Malo |
| 98 - 2006 | Rangeley, ME | David Gibson, Julia Daly and Douglas Reusch |
| 97 - 2005 | New Haven, CT | Brian Skinner and Tony Philpotts |
| 96 - 2004 | Salem, MA | Lindley Hanson |
| 95 - 2003 | Amherst and Northampton, MA | John Brady and Jack Cheney |
| 94 - 2002 | Lake George, NY | James McLelland and Paul Karabinos |
| 93 - 2001 | Fredericton, NB | Dave Lentz and Ron Pickerill |
| 92 - 2000 | Orono, ME | Martin Yates, Daniel Lux and Joseph Kelley |
| 91 - 1999 | Burlington, VT | Barry Doolan |
| 90 - 1998 | Kingston, RI | Dan Murray |
| 89 - 1997 | Killington-Pico, VT | Timothy Grover and Helen Mango |
| 88 - 1996 | Mount Washington, NH | Mark Van Baalen |
| 87 - 1995 | Brunswick, ME | Arthur Hussey and Robert Johnston |
| 86 - 1994 | Millinocket, ME | Lindley Hanson and Dabney Caldwell |
| 85 - 1993 | Boston, MA | National GSA: Jack Cheney and Chris Hepburn |
| 84 - 1992 | Amherst, MA | Peter Robinson and John Brady |
| 83 - 1991 | Princeton, ME | Allan Ludman |
| 82 - 1990 | La Gaspésie, PQ | Walter Trzcienski |
| 81 - 1989 | Farmington, ME | Archie Berry |
| 80 - 1988 | Keene, NH | Wallace Bothner |
| 79 - 1987 | Montpelier, VT | David Westerman |
| 78 - 1986 | Lewiston, ME | Donald Newberg |
| 77 - 1985 | New Haven, CT | Robert Tracy |
| 76 - 1984 | Danvers, MA | Lindley Hanson |
| 75 - 1983 | Greenville-Millinocket, ME | Dabney Caldwell and Lindley Hanson |
| 74 - 1982 | Storrs, CT | Ray Joesten and Sidney Quarrier |
| 73 - 1981 | Kingston, RI | Jon Boothroyd and Don Hermes |
| 72 - 1980 | Presque Isle, ME | David Roy and Richard Naylor |
| 71 - 1979 | Troy, NY | Gerald Friedman |
| 70 - 1978 | Calais, ME | Allan Ludman |
| 69 - 1977 | Quebec City, PQ | René Béland and Pierre LaSalle |
| 68 - 1976 | Boston, MA | Barry Cameron |
| 67 - 1975 | Great Barrington, MA | Nicholas Ratcliffe |
| 66 - 1974 | Orono, ME | Philip Osberg |
| 65 - 1973 | Fredericton, NB | Hugo Grenier and Nick Rast |
| 64 - 1972 | Burlington, VT | Barry Doolan and Rolfe Stanley |
| 63 - 1971 | Concord, NH | John Lyons and Glenn Stewart |
| 62 - 1970 | Rangeley Lakes-Dead River, ME | Gary Boone |
| 61 - 1969 | Albany, NY | John Bird |
| 60 - 1968 | New Haven, CT | Phil Orville |
| 59 - 1967 | Amherst, MA | Peter Robinson, David Drake and Richard Foose |
| 58 - 1966 | Katahdin, ME | Dabney Caldwell |
| 57 - 1965 | Brunswick, ME | Arthur Hussey |
| 56 - 1964 | Chestnut Hill, MA | James Skehan |
| | | ***Note: individual trip leaders are listed for earlier meetings*** |

| | | |
|---|---|---|
| 55 - 1963 | Providence, RI | Quinn, Mutch, Shafer, Agron, Chapple, Feiniger & Hall |
| 54 - 1962 | Montreal, PQ | Gill, Clark, Kranck, Stevenson, Stearn, Elson, Eakins, & Gold |
| 53 - 1961 | Montpelier, VT | Doll, Cady, White, Chidester, Matthews, Nichols, Baldwin, Stewart, Dennis, Smith, and Ferris |
| 52 - 1960 | Rumford, ME | Griscom, Milton, Wolfe, Caldwell, and Peacor |
| 51 - 1959 | Rutland, VT | Zen, Kay, Welby, Bain, Theokritoff, Osberg, Shumaker, Berry, and Thompson |
| 50 - 1958 | Middletown, CT | Rosenfeld, Eaton, Sanders, Porter |
| 49 - 1957 | Amherst, MA | George Bain |
| 48 - 1956 | Portsmouth, NH | Novotny, Billings, Chapman, Bradley, Freedman and Stewart |
| 47 - 1955 | Ticonderoga, NY | Rodgers, Walton, MacClintock, Bartolome |
| 46 - 1954 | Hanover, NH | Elston, Washburn, Lyons, McKinstry, Stoiber, McNair, and Thompson |
| 45 - 1953 | Hartford, CT | Flint, Gates, Peoples, Cushman, Aitken, Rodgers and Troxell |
| 44 - 1952 | Williamstown, MA | Perry, Foote, McFaden, and Ramsdell |
| 43 - 1951 | Worcester, MA | Lougee and Little |
| 42 - 1950 | Bangor, ME | Trefethen and Raisz |
| 41 - 1949 | Boston, MA | Nichols, Billings, Shrock, Currier, and Stearns |
| 40 - 1948 | Burlington, VT | Charlie Doll |
| 39 - 1947 | Providence, RI | Alonzo Quinn |
| 38 - 1946 | Mt. Washington, NH | Marland P. Billings, Kathrine F. Billings and R.W. Chapman |
| 37 - 1941 | Northampton, MA | Balk, Jahns, Lochman, Shaub, and Willard |
| 36 - 1940 | Hanover, NH | J. W. Goldthwait, Denny, Shaub, Hadley, Bannerman, and Stoiber |
| 35 - 1939 | Hartford, CT | Troxell, Flint, Longwell, Peoples and Wheeler |
| 34 - 1938 | Rutland, VT | George W. Bain |
| 33 - 1937 | NYC-Dutchess Co., NY | O'Connell, Kay, Fluhr, Hubert and Balk |
| 32 - 1936 | Littleton, NH | Marland P. Billings, Hadley, Cleaves and Williams |
| 31 - 1935 | Boston, MA | Morris, Pearsall, and Whitehead |
| 30 - 1934 | Lewiston, ME | Lloyd Fisher and Edward Perkins |
| 29 - 1933 | Williamstown, MA | Herdman Cleland, Perry, and Knopf |
| 28 - 1932 | Providence-Newport, RI | C. W. Brown |
| 27 - 1931 | Montreal, PQ | O'Neill, Graham, T. M. Clark, Gill, Osborne, and McGerrigle |
| 26 - 1930 | Amherst, MA | F. B. Loomis and Gordon |
| 25 - 1929 | Littleton, NH | Irving B. Crosby |
| 24 - 1928 | Cambridge, MA | Marland P. Billings, Kirk Bryan, and Kirtley Mather |
| 23 - 1927 | Worcester, MA | Perry, Little, and Gordon |
| 22 - 1926 | New Haven, CT | C. R. Longwell |
| 21 - 1925 | Waterville, ME | Edward H. Perkins |
| 20 - 1924 | Providence, RI | C. W. Brown |
| 19 - 1923 | Beverly, MA | A. C. Lane |
| 18 - 1922 | Amherst, MA | Ernst Antevs |
| 17 - 1921 | Attleboro, MA | J. B. Woodworth |
| 16 - 1920 | Hanging Hills, Meriden, CT | W. N. Rice and Wilbur Foye |
| 15 - 1917 | Gay Head, Martha's Vineyard, MA | J. B. Woodworth and E. Wigglesworth |
| 14 - 1916 | Blue Hills, MA | W. O. Crosby and C. H. Warren |
| 13 - 1915 | Waterbury-Winsted, CT | Jos. Barrell |
| 12 - 1912 | Higby-Lamentation Blocks, CT | W. N. Rice |
| 11 - 1911 | Nahant-Medford, MA | A. C. Lane and D. W. Johnson |
| 10 - 1910 | Hanover, NH | James W. Goldthwait |
| 9 - 1909 | Northern Berkshires, MA | H. F. Cleland |
| 8 - 1908 | Long Island, NY | Jos. Barrel |
| 7 - 1907 | Providence, RI | C. W. Brown |
| 6 - 1906 | Meriden-East Berlin, CT | H. E. Gregory |
| 5 - 1905 | Boston-Nantasket, MA | D. W. Johnson and W. O. Crosby |
| 4 - 1904 | Worcester, MA | Benjamin Emerson |
| 3 - 1903 | West Peak, Meriden, CT | W. N. Rice |
| 2 - 1902 | Mount Tom, MA | Benjamin Emerson |
| 1 - 1901 | Westfield River Terraces, MA | William Morris Davis |

# MIGMATITES OF THE EASTERN ADIRONDACK MOUNTAINS: NEW CONSTRAINTS ON THE TIMING, PETROLOGY, AND TECTONIC SETTING OF PARTIAL MELTING

MICHAEL L. WILLIAMS
*Department of Geosciences, University of Massachusetts, Amherst, MA 01003*

TIMOTHY W. GROVER
*Department of Earth and Atmospheric Sciences, University of Northern Colorado, Greeley, CO 80639*

CLAIRE R. PLESS
*Department of Geosciences, University of Massachusetts, Amherst, MA 01003*

KAITLYN A. SUAREZ
*Department of Geosciences, University of Massachusetts, Amherst, MA 01003*

SEAN P. REGAN
*Department of Geosciences, University of Alaska Fairbanks, Fairbanks, AK 99775*

GRAHAM B. BAIRD
*Department of Earth and Atmospheric Sciences, University of Northern Colorado, Greeley, CO 80639*

## INTRODUCTION

The Adirondack Mountains of New York are a classic example of a high-grade, polydeformational terrane that has been used as an analog for mid/deep crustal continental collisional and extensional tectonism (Mezger, 1992; Selleck et al., 2005; Rivers, 2008). Numerous studies have characterized the nature and grade of metamorphism and deformation (Bohlen et al., 1985; Spear and Markussen, 1997; Storm and Spear, 2005). Many rocks show evidence for significant degrees of partial melting, and it seems likely that, at least in some rocks, significant amounts of melt have been lost from the local system. Previous workers have interpreted the melting to have occurred during one (or several) orogenic or thermal/magmatic events, but in many regions, questions remain about the timing, melt producing reactions, tectonic setting, and even the number of partial melting events. In order to interpret the tectonic history of the region and use the region as an analog for modern deep crust, it is critical to constrain the timing, setting, and rheologic implications of melting.

Migmatitic rocks in the eastern Adirondack Mountains can be very similar to one another in appearance. They tend to be gray-colored gneisses with layers of garnet-rich Qtz-Fsp-Sil-Bt gneiss interlayered with pink or white Qtz-Fsp leucosome with or without garnet. Leucosomes range from centimeters to a meter or more in width. The proportion of K-feldspar and plagioclase in both leucosome and gray gneiss varies widely. Many of the leucosomes are interpreted to be the product of in-situ melting although some have been interpreted to have been injected from outside of the local system (Bickford et al., 2008). Distinctive garnet- and sillimanite-rich gneisses with little biotite, “khondalite”, are relatively common, and are interpreted to be restitic rocks, where a significant amount of melt has been lost from the local rock.

The timing of melting is one of the critical outstanding questions in the Adirondack Mountains. Different rocks in different regions have been interpreted to have melted during one (or several) of four possible events: the 1190-1160 Shawinigan orogeny, the 1160-1140 AMCG intrusive event, the 1090-1050 Ottawan orogeny, or 1050-1030 extensional tectonism. In some regions, cross-cutting or contact relationships constrain the timing of melting although the interpretation is rarely unambiguous. In general, the gray gneisses and leucosomes form sub-parallel layers, and timing constraints tend to come from geochronology, particularly of zircon and monazite. Even though the migmatitic paragneisses can contain abundant zircon and monazite, interpretations of melting relationships are commonly constrained by relatively subtle textures and compositions of chronometer phases.

Multiscale compositional mapping combined with high-spatial-resolution (micron-scale), in-situ geochronology and geochemistry of monazite can provide significant insight into the nature of melting reaction(s), the timing of melting, the relationship to deformational events, and the ultimate significance of companion zircon geochronology (Williams et al., 2017). This field trip will visit localities in the eastern Adirondack Mountains where

we have applied this technique to samples of migmatite. The results suggest that melting did indeed occur at different times, producing rocks of very similar appearance. Although the relative intensity of the different events may have varied regionally, the degree of melting and melt segregation also played a role in controlling how fertile a rock was for melting in a subsequent event. The results presented here have a number of implications for the tectonic history of the region and for the rheology of the deep crust in general. They also provide a template for future studies in this region and in other regions in order to compare and interpret the tectonic setting of migmatitic rocks.

## OVERVIEW OF ADIRONDACK GEOLOGY

The Grenville Province is a Proterozoic orogenic belt that represents the culminating continental collision(s) during assembly of the supercontinent of Rodinia (Rivers, 2008). The Grenville Province extends from northeastern Canada through the eastern and southern portion of the U.S. into Texas with proposed correlations in Australia, Antarctica, Baltica and others (Karlstrom et al., 1999). In eastern Canada, the Grenville Province forms a northeast trending belt approximately 2000 km long and 400-500 km wide. The Adirondack Mountains, located in northeastern New York, are a domical uplift of Mesoproterozoic rocks that are part of the Grenville Province (Fig. 1). The Green Mountain and Berkshire massifs represent outliers of the Grenville Province and lie to the east and southeast of the Adirondacks respectively.

The Adirondack Mountains have been divided into the Adirondack Lowlands and Highlands (Fig. 1), separated by the Carthage-Colton shear zone (Selleck et al., 2005). Most workers now recognize several major stages in the overall tectonic history (Fig. 2). The ca. (1300-1200 Ma) Elsevirian orogeny is interpreted to represent a period of arc and back-arc accretion on or near the margin of Laurentia (McLelland et al., 2013). The (ca.1180-1140 Ma) Shawinigan orogeny is interpreted to represent a period of accretionary orogenesis with closure of the Trans Adirondack Basin with subduction-related magmas forming above a westward-dipping subduction zone. The culminating collisional phase of the Shawinigan Orogeny is the result of the collision of the Adirondack Highlands-Green Mountain terrane with the Adirondack Lowlands terrane, which was part of the eastern margin of Laurentia. (Chiarenzelli et al., 2010). The effects of this orogenic event have been increasingly recognized in the Adirondack Lowland in recent years (Chiarenzelli et al., 2011) largely due to an expanding geochronologic database.

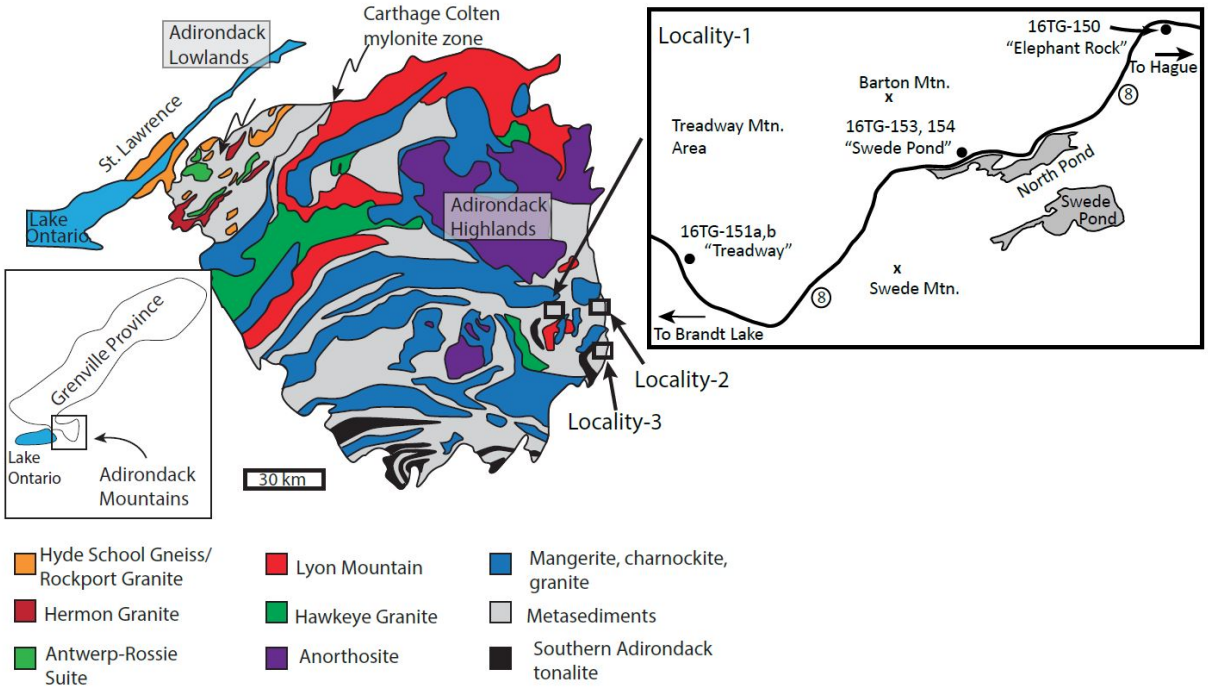


Figure 1. Generalized geologic map of the Adirondack Mountains (after McLelland, 2010) showing the location of the three main localities discussed in this paper. Inset shows the location of the three main outcrops discussed from Locality-1.

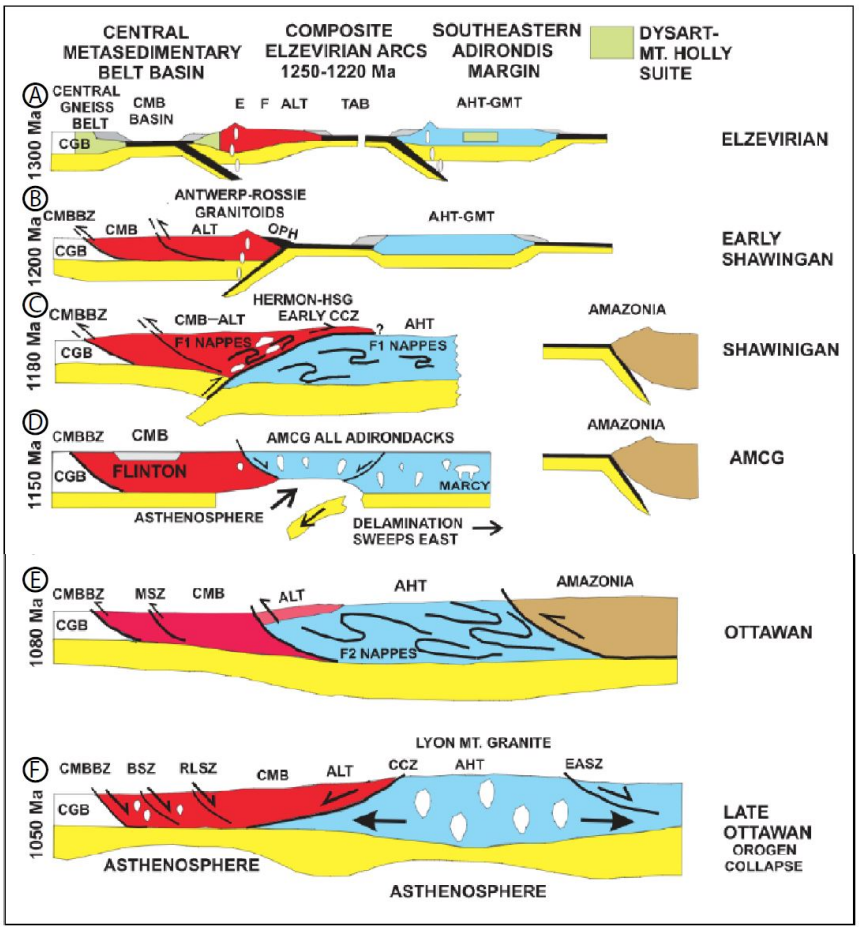


Figure 2. Schematic summary of the tectonic history of the Adirondack Mountains (Modified from McLelland, et al, 2013)

A voluminous suite of igneous rocks was emplaced near the end of the Shawinigan Orogeny (ca. 1155Ma). The magmatic event involved gabbro, anorthosite, mangerite, charnockite, and granite; the suite of intrusives is commonly referred to as the "AMCG suite". They are interpreted to be the result of lithospheric delamination (McLelland et al., 2004; Regan et al., 2011). The 3000 km$^2$ Marcy anorthosite massif (1154 +/- 6 Ma; McLelland et al. 2004; Hamilton et al. 2004), a member of this suite, is the dominant plutonic body in the Adirondack Highlands (Buddington, 1939).

The (ca. 1090-1030 Ma) Ottawan orogeny has been interpreted as a major continent-continent collision, involving large-scale thrusting and folding of rocks in the Adirondack Highlands (McLelland et al., 1996, 2001). Recently, however, at least the later part of the orogeny (<1050 Ma) has been interpreted as an extensional event with localized normal shearing on the Highlands-bounding, Carthage Colton and East Adirondack shear zones (Selleck et al., 2005; Wong et al., 2012; Regan et al., in review). The latest events in the cycle involved pegmatite emplacement, metasomatism, and local (ca, 980 Ma) disturbance. Tectonism during this final phase has been termed the Rigolet stage or orogeny (Rivers, 2008), which is currently interpreted to have had a minimal impact on the structural and metamorphic architecture in the Adirondack region.

In addition to plutonic rocks, the Adirondack Highlands contains abundant garnet-rich migmatitic gneisses, interpreted to have been derived from Al-rich sedimentary protoliths (Storm and Spear, 2005). Although leucosome layers, veins, and pods are common, many rocks are dominated by garnet (10s of percent), sillimanite, quartz, and feldspar, with variable amounts of prograde and retrograde biotite. Many of the biotite-poor, sillimanite-rich rocks have been termed "khondalite" (McLelland et al., 2002), and have been interpreted to be residues (restites), having lost some component of partial melt.

Bickford et al. (2008) and Heumann et al. (2006) carried out U-Pb zircon (IDTIMS) analyses, and Heumann combined in-situ monazite dating, in order to constrain the timing and setting of melting in the

Adirondack Highlands. Heumann et al. (2006) concluded that melting occurred primarily during the Shawinigan orogeny, which was cited as 1210-1160 Ma and also during AMCG magmatism, cited as 1165-1150 Ma. Bickford et al. (2008) investigated additional localities and concurred that melting occurred in many regions during the Shawinigan and AMGC events, but they also found evidence for melting at ca. 1050 Ma (Ottawan), particularly in the eastern Adirondack Highlands. They suggested that Ottawan metamorphic temperatures were probably high, but melting occurred only locally due to fluid influx or local decompression melting.

Samples discussed here and on the associated field excursion came from several commonly-visited localities in the eastern Adirondack Mountains. These include: Locality-1: outcrops along Route 8, west of Hague, NY, including the Elephant Rock, Swede Pond, and Treadway Mountain areas; Locality-2: the Dresden Station area along Rt. 22 south of Ticonderoga, NY; and Locality-3: outcrops along Route 22 south of Whitehall, NY. The Treadway Mountain area was also studied by Bickford et al., (2008), their Locality-9. Each of these localities contain migmatitic gray gneisses with abundant monazite and zircon. They represent a particularly appropriate target for in-situ monazite dating (i.e. "reaction dating", Williams et al., 2017), in order to evaluate the degree to which monazite analysis can provide insight into the melting history of these rocks.

## METHODS

The outcrops described here have been visited on many field trips and described in numerous publications and field guides. For this study, oriented hand samples of gray garnet-rich gneisses with a variety of textures and grain sizes were collected from each outcrop. Polished thin sections were prepared for petrographic analysis, microstructural analysis, electron microprobe analysis, and in-situ microprobe dating. The general approach to *in-situ* monazite dating is summarized in Williams et al. (2006) and updated in Williams et al. (2017). Full-section compositional maps are collected early in the analytical process using the Cameca SX50 electron microprobe. For this study, maps were collected for Mg, K, Ca, Ce, and Zr. The Mg, K, and Ca maps show the distribution of the major silicate phases. Ce and Zr maps show the location of all monazite and zircon grains respectively (See Williams et al., 2006).

Next, high resolution maps are collected for a number of monazite grains (typically 20 or more) in the section. Maps for Y, Th, U, Ca, and one other element (Si, Nd, Gd, As, etc.) are collected. The maps are processed simultaneously such that intensities are comparable from grain map to grain map (Williams et al., 2006; 2017). It is particularly informative for high-resolution maps to be placed around the full-section image with links to the actual grain locations. This allows the zonation within a particular grain to be interpreted in the context of its textural and microstructural setting within the thin section. Important domain types are selected from the combined assemblage of grain maps; commonly between 3 and 6 domain types are present in a typical thin section. A dating strategy is developed whereby each domain type is sampled (dated) several times with preference given to grains where two or more domains can be sampled from the same grain.

Monazite dating was carried out on the Cameca Ultrachron electron microprobe at the University of Massachusetts. The instrument was specifically designed for trace-element analysis and geochronology (Jercinovic et al., 2008a, 2008b). The analytical protocol is described in Williams et al. (2017) and is briefly summarized here. For each compositionally-defined domain, a single background analysis is acquired first, followed by 6-8 peak measurements near the background location. Background intensities are determined using the "multipoint" method (Allaz et al., 2018); measurements are made in four to eight locations on either side of the peak position. The bremsstrahlung curve (background) is determined by regression of acceptable measurements and then the background is calculated at the peak position. One "date" is calculated for each domain. Uncertainty is calculated by propagating measurement and background errors through the age equation (Williams et al., 2006). Dates are typically shown as a single Gaussian probability distribution function for the dated domain.

Zircon U-Pb analyses were carried out at the Arizona Laserchron Laboratory. Analyses were made on bulk zircon separates and in-situ in thin section. Bulk analyses were carried out according to methods outlined in Gehrels et al., (2008); and (https://drive.google.com/file/d/0B9ezu34P5h8eTU9PaUczTGc5elk/view). Polished thin sections for in-situ analysis were first mapped for Zr (as described above) in order to locate all zircon crystals. Individual zircon grains were imaged by high-resolution backscattered electron imaging and then by cathodoluminesence imaging in order to select domains for dating. Polished sections were analyzed with either 10 or 15 µm laser beam size with standards mounted adjacent to the thin section. Data were reduced using procedures outlined in Gehrels et al., (2008).

## METAMORPHIC CONDITIONS AND MELTING REACTIONS

Metamorphic assemblages from aluminous metasedimentary rocks are similar in all three localities. Most samples contain K-feldspar, garnet, quartz, biotite, sillimanite, +/- rutile, monazite, zircon, and apatite. Biotite is interpreted to be mainly a retrograde phase, but in some samples, some biotite was certainly present at peak conditions. Phase diagrams have been calculated by a number of workers for pelitic bulk compositions, and relationships for moderate-pressure granulites are very similar (Storm and Spear, 2005; White et al., 2007; Yakumchuk and Brown, 2014; Yakumchuk, 2017), see Figure 3.

The lack of peak biotite and plagioclase and the abundance of garnet and K-feldspar suggests that the following were important melting reactions.

$$Bt + Pl + Als + Qtz = Grt + Kfs + melt \quad (1)$$

$$Bt + Als + Qtz = Grt + Kfs + melt \quad (2)$$

Some initial melting may have occurred earlier associated with muscovite dehydration, but modeling suggests that the amount of melting (i.e. melt production) was probably limited (Storm and Spear, 2005; Yakumchuk and Brown, 2014). We suggest that the P-T conditions of metamorphism for these samples generally fall within the region shown on Figure 3.

Estimates of peak metamorphic temperatures and pressures are rather uniform, on the scale of kilometers, across the Adirondack Highlands (Bohlen et al., 1985; Spear and Markussen, 1997; Storm and Spear, 2005). All previous workers agree that peak conditions were on the order of 750 °C (or higher), 0.7-0.8 GPa in the central Adirondack Highlands. Bohlen et al. (1985) showed a concentric pattern of P's and T's and suggested that the pattern may reflect doming of preexisting isograds. However, a persistent question concerns the age of the metamorphism. Calculated conditions could represent late (ca. 1150 Ma) Shawinigan, Ottawan (ca. 1090), or late Ottawan (ca. 1050-1030) metamorphism, and it is likely that a combination of these events resulted in the preserved assemblages and compositions.

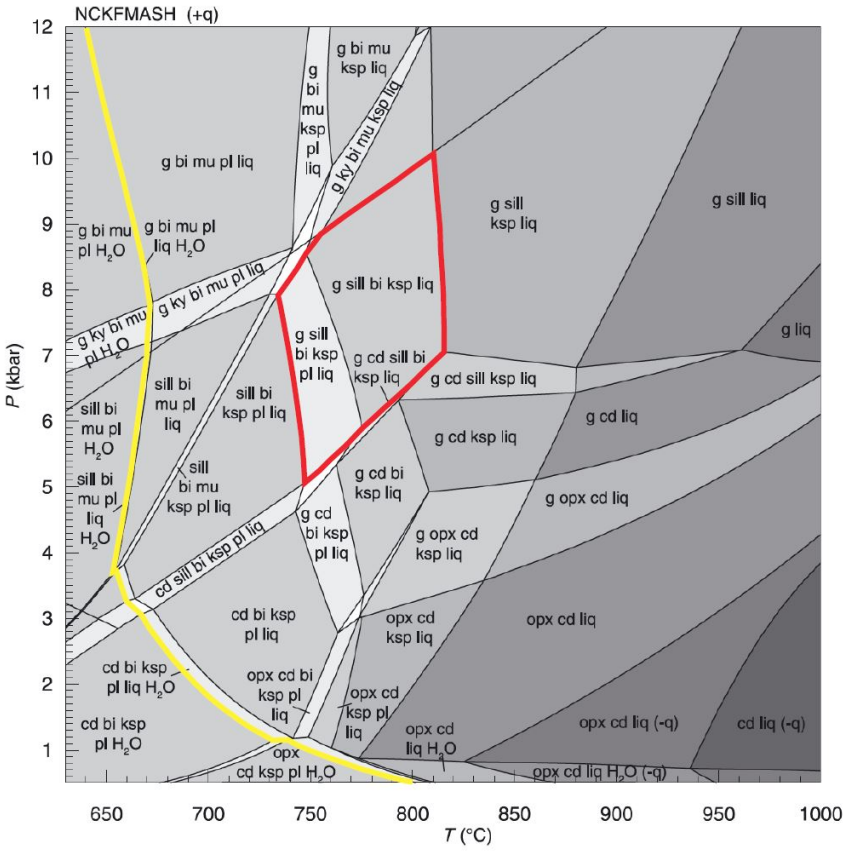


Figure 3. Model phase diagram for a theoretical pelitic (Al-rich shale). From White et al., (2007). Rocks from this study are interpreted to have been metamorphosed within the area outlined in red.

## RESULTS

### Locality-1: Rt. 8 Migmatites, Hague, NY

Samples have been investigated from three separate outcrops along Rt. 8, west of Hague New York (Williams et al., in review). From west to east, these are Treadway Mtn, Swede Pond, and Elephant rock (Fig. 1). Figure 4 shows full-thin-section compositional maps from the samples. All three samples contain the common assemblage: biotite, garnet, quartz, sillimanite, apatite, rutile, zircon, and monazite. However, major differences occur in the mode, composition and distribution of feldspar and also in the mode and distribution of biotite.

Sample 16TG-154 (Swede Pond) contains no plagioclase, only K-feldspar (Fig. 4a,b). The K-feldspar is extremely abundant making up much of the matrix of the sample (Fig. 4b). The complete lack of plagioclase and prograde biotite in this sample suggests that Reaction-1 was exceeded. That is, the sample underwent extensive bt-dehydration melting. Also, the lack of plagioclase suggests that the melting reaction was not reversed, i.e. the melt did not crystalize within this sample. Instead, we suggest that a significant portion of the melt component was removed or segregated from the local (residual) rock.

Samples 16TG-151 (Treadway Mtn.) and 16TG-150 (Elephant Rock) contain both plagioclase and K-feldspar, but have distinctly different textures. 16TG-150 contains coarse grained K-feldspar and plagioclase, particularly in the shadows of large garnet porphyroblasts (Fig. 4 d,e). Leucosome layers with annealed or undeformed feldspars wrap around the garnet porphyroblasts. Samples from locality151 (Treadway Mtn.) contain dispersed, fine to medium grained, plagioclase and K-feldspar (Fig. 4 g,h). Both of these samples are interpreted to have undergone melting by a similar bt-dehydration reaction, but at least some leucosome crystalized locally, that is, the melting reaction was at least partially reversed in these samples. The differences between the three samples may reflect subtle differences in the original bulk composition, but they may also involve different amounts of strain partitioning that, in turn, helped to facilitate melt segregation/removal (see below).

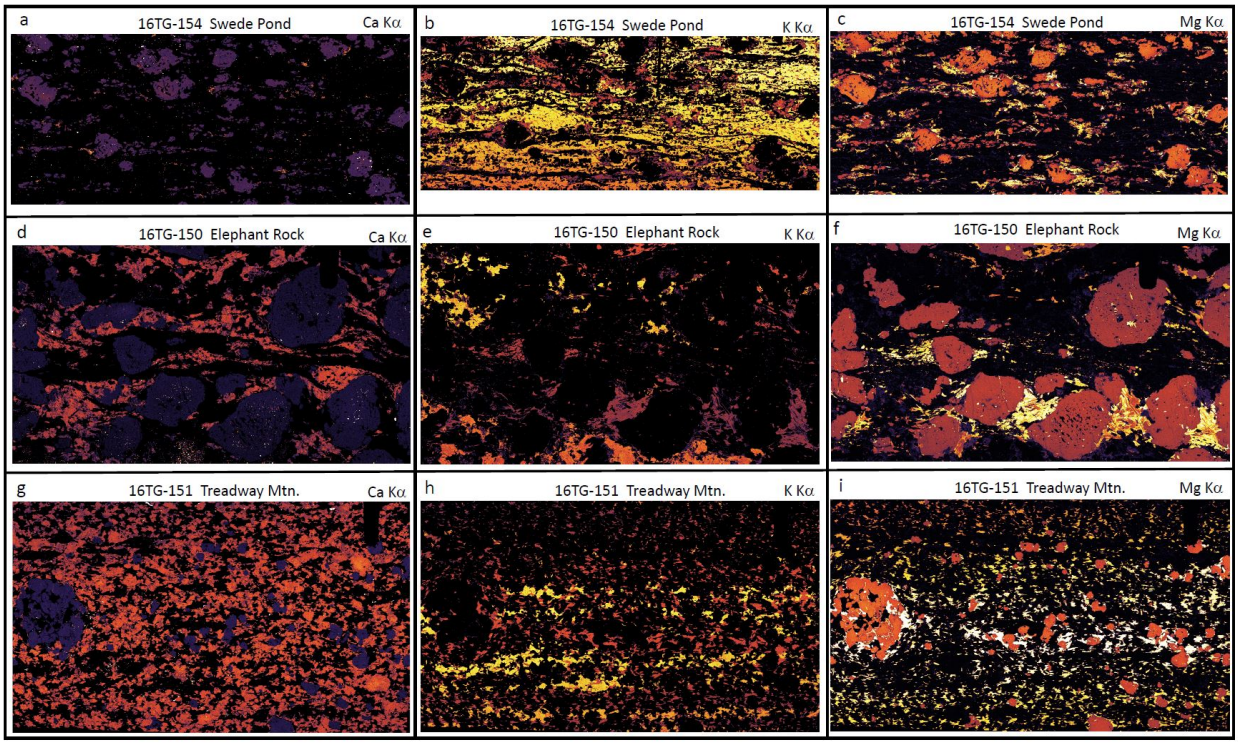


Figure 4. Compositional maps for samples from Locality-1, Rt. 8, Hague, NY. Each map covers a full-thin section for the specified elements. Brighter colors represent greater abundance of the element. See text for discussion.

**Monazite Data** Figure 5 is a summary of monazite data from the three Rt.8 outcrops discussed above. As noted, each probability distribution represents one monazite date, obtained from one compositional domain in a single monazite grain as delineated by grain mapping. Color codes show the main domain types (i.e. core, outer

core, main, rim). Details about the analyses, monazite compositions, and interpretation are presented in Williams et al., in review). Typical uncertainties (2σ) range from ca. 4 m.y. to very rarely greater than 20 m.y.

*Note: We use the term "date" to refer to the results of the age equation using measured U-Th-Pb values. The term "age" refers to the interpretation of a date such as the age of a particular rock or process.*

Figure 5 d,e,f show Y-content in monazite vs. calculated date for the three samples. Horizontal scales are equal so that each point in the composition plot corresponds to one probability distribution. Arrows connect cores and rims when analyses come from the same grain. Y is strongly partitioned into garnet and has been used in many studies to link monazite growth with garnet growth and breakdown (see references in Williams et al., 2007). The characteristic 'U-shaped' profile (Fig. 5d) is interpreted to result from significant garnet growth (decreasing Y) and garnet breakdown (increasing Y).

Figures 5 g,h,i show U content in monazite vs. calculated date. Partitioning data from Stepanov et al. (2012) indicate that the actinides (U, Th) have positive monazite/melt fractionation, but U has a significantly lower ratio than Th and most REEs. During partial melting U and other trace and REEs will be partitioned from the whole rock into melt. Monazite in equilibrium with the melt will be depleted in uranium relative the other actinides or REEs, and monazite in restite will be expected to equilibrate with the lower bulk-rock uranium abundance. Thus, a decrease in U in monazite is interpreted to result from partial melting of the sample. A reduction in U synchronous with a Y and HREE reduction is consistent with melting by reactions 1 and 2 where garnet is produced as a peritectic phase during melting. If the U content of monazite remains low during cooling or subsequent thermo-tectonic events, we suggest that a significant component of the melt was removed from the local system.

**Interpretation – Locality-1.** The three samples/localities summarized here are similar in outward appearance. They are all garnet-rich migmatitic gray gneisses. But compositional maps and the monazite record suggest that they have very different petrologic, microstructural, and petrotectonic histories, especially with regard to melting and melt loss. Sample 16TG-154 (Swede Pond) experienced significant melting at ca. 1160-1150 Ma and judging by the dominance of garnet and K-feldspar and lack of plagioclase, the sample shows little evidence for back reaction and melt crystallization. Much of the partial melt in this sample is interpreted to have left the system. The monazite record suggests that little garnet growth or melting occurred during the Ottawan orogeny (ca. 1090-1050 Ma).

Sample 16TG-150 (Elephant Rock) contains a significant amount of plagioclase in addition to K-feldspar, garnet, biotite and quartz. One characteristic feature of this sample is the coarse segregation of minerals, especially feldspar and biotite into distinct layers. Like sample 16TG-154, the monazite record suggests that significant melting occurred at ca. 1150 Ma and that little if any melting or garnet growth occurred at ca. 1050 Ma. However, unlike 16TG-154 (Swede Pond), U does not show a significant decrease after 1150 Ma. Although the leucosome was segregated into distinct layers, any U partitioned into the melt was apparently released back into the rock on crystallization and was thus, available for incorporation into later monazite. We suggest that, even though the components were present for melting, the segregation of minerals, especially feldspars and biotite at the end of the early melting event, may have left the sample relatively infertile for subsequent melting (Williams et al., in review).

Sample 16TG-151 (Treadway Mtn.) shows evidence for garnet growth and melting at 1150 Ma and also at 1050 Ma. Y and HREEs decrease in two sharp steps, one at ca. 1150 Ma and one at ca. 1050 Ma. This sample also has by far the greatest volume of ca. 1050 monazite domains, interpreted to have grown during melt crystallization. Because the U-content remains relatively high and constant from the ca. 1150 Ma to ca. 1050 Ma (Fig. 5), the 1150 melt component is interpreted to have remained dispersed within the rock, releasing U back to monazite on crystallization. Consequently, this sample was more fertile for melting during the Ottawan Orogeny.

All three samples investigated in this study have a strong, shallowly-dipping foliation and weak (if any) lineation. It would be tempting to correlate this fabric from locality to locality in the three closely-spaced localities. However, based on the fabric and monazite record, samples 16TG-150 and 154 largely preserve their 1150 Ma migmatitic fabric while the fabric in 16TG-151 was reactivated at 1050 Ma. The Shawinigan Orogeny apparently involved crustal thickening culminating in partial melting at ca. 1160-1150 Ma (Rivers, 2008; McLelland et al., 2013). The associated melt weakening is interpreted to have led to the subhorizontal migmatitic fabric preserved in samples 150 and 154. Both samples do have subtle evidence for west-directed shearing. We suggest that at ca. 1050 Ma localized melting in certain fertile localities led to a second phase of melt weakening and fabric development roughly parallel to the preexisting fabric.

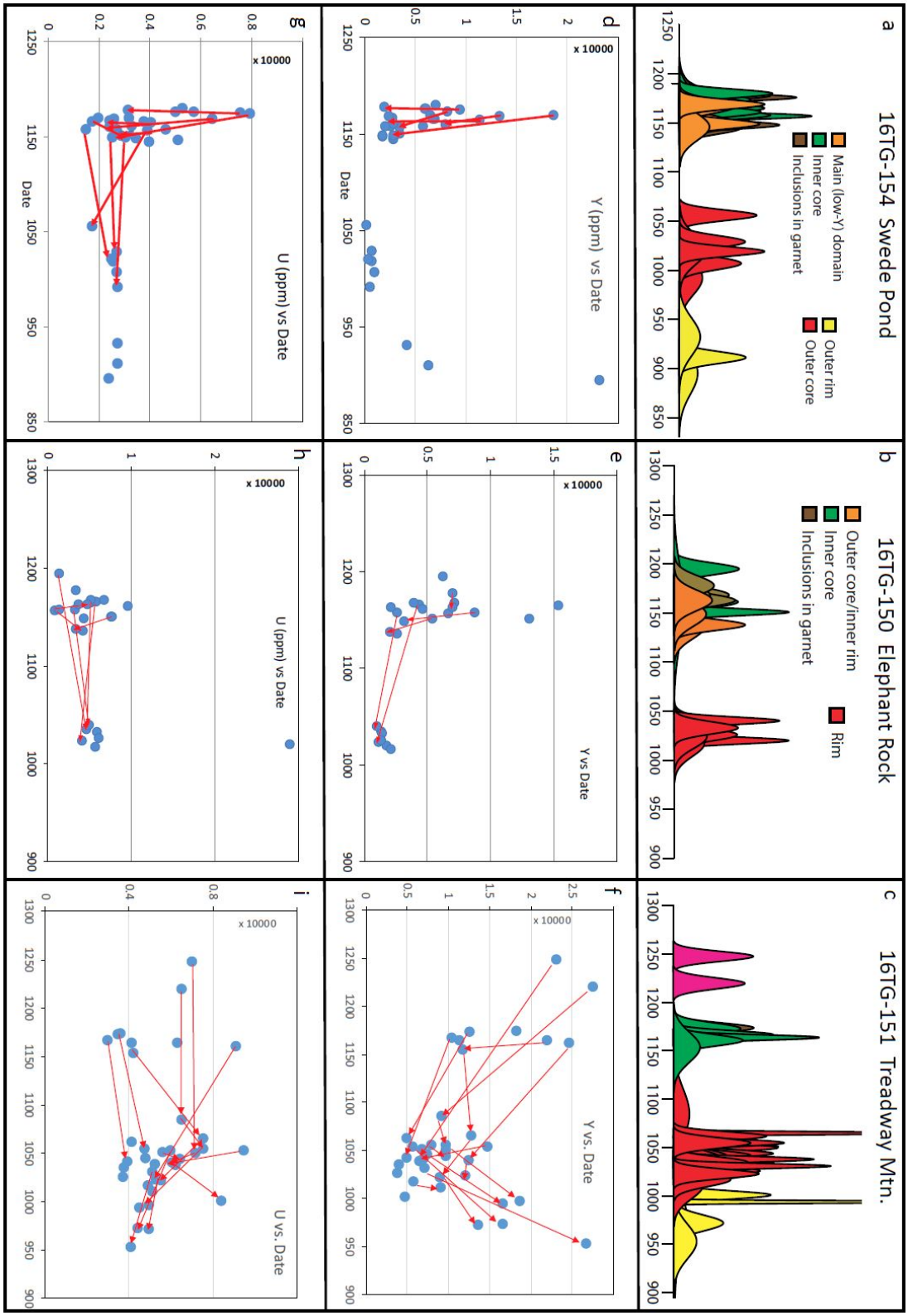


Figure 5. Monazite-date-composition relationships for samples from three outcrops along Rt. 8, Hague, NY. See text for discussion.

**Locality-2 Dresden Station**

The Dresden Station outcrops have been the focus of a number of publications and field excursions. McLelland et al. (1988a) cite evidence from this outcrop to show that there were multiple phases of metamorphism recorded by the rocks in the Adirondack Mountains. A sharp contact between garnet-sillimanite gneiss and a coronitic metagabbro is well-exposed. The gneiss is a garnet-sillimanite-plagioclase-K-feldspar-quartz gneiss with a small amount of biotite, commonly referred to as khondalite. The garnet-sillimanite gneiss is penetratively deformed with a well-developed foliation and a lineation that plunges gently to the east. Much of the metagabbro is undeformed and a coarsely crystalline texture is preserved throughout portions of the unit. The gabbro is finely crystalline right at the contact with the gneiss and appears to get more coarsely crystalline towards the interior of the body suggesting a chilled margin formed at the contact between the gabbro and the gneiss. The foliation in the khondalite gneiss is sharply cut by the contact between the gneiss and the metagabbro. This contact relationship suggests that the gneiss was deformed and metamorphosed prior to the intrusion of the gabbro (McLelland et al., 1988a). McLelland et al. (1988b) report a U-Pb zircon, multigrain age of 1144 ± 7 Ma for the metagabbro. This is interpreted as an igneous crystallization age and is consistent with the gabbro belonging to the AMCG suite.

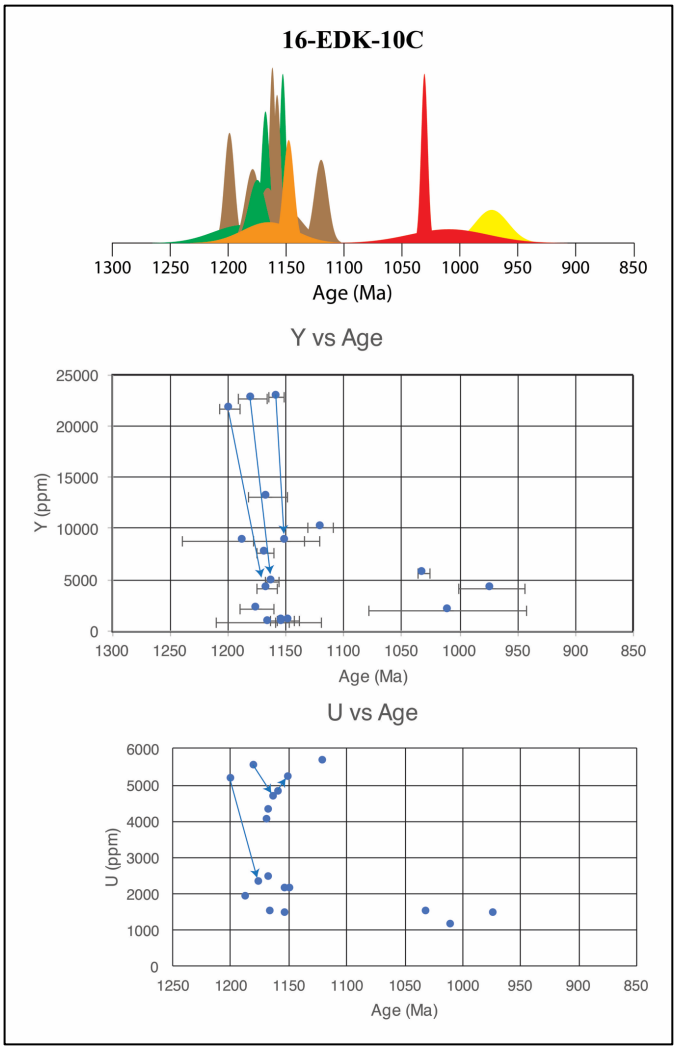


Figure 6. Monazite date-composition relationships from sample EDK-09-10C, Dresden Station khondalite. See text for discussion.

We analyzed monazite from several thin sections of the garnet-sillimanite gneisses (Fig. 6). The data broadly suggest three distinct periods of monazite growth. The oldest population has a weighted mean of 1179 ± 9 Ma. We suggest that this is the age of prograde metamorphism and fabric development in the garnet sillimanite gneisses. The next population yielded dates that cluster around 1151 Ma. We hypothesize that this represents a period of monazite growth driven by a thermal perturbation resulting from the intrusion of the AMCG gabbroic rocks. The date correlates well with the reported age of the gabbro at this outcrop. The third population yields dates of 1030 Ma or younger. These are too young to correlate with the proposed timing of the peak of the Ottawan Orogeny (~1090-1050 Ma). Instead we interpret this generation to represent the period of post-Ottawan decompression and uplift.

The following model is consistent with the field observations and data from this outcrop. The mineral assemblage and the fabric in the garnet-sillimanite gneisses formed during the Shawinigan Orogeny. The gabbro was emplaced at approximately 1150 Ma, after the prominent fabric developed in the gneisses. This time frame is consistent with both the monazite ages from the gneisses and the multigrain age from the gabbro. Following the emplacement of the gabbro there was another period of deformation and metamorphism. This is when the nearby AMCG rocks were deformed and metamorphosed. This is also when the coronitic texture developed in the metagabbro. This requires in influx of an $H_2O$–bearing fluid. Unlike the nearby rocks, the coronitic metagabbro was not pervasively deformed at this time nor did any new monazite grow in the garnet-sillimanite gneiss. Perhaps strain was partitioned around this outcrop and the lack of strain resulted in little recrystallization in the largely anhydrous garnet-sillimanite gneisses. The 1020 Ma and younger monazite ages in the garnet-sillimanite gneisses record monazite growth during post Ottawan extensional collapse.

**Locality-3: Migmatites of the East Adirondack Shear Zone**

Outcrops of garnet, sillimanite, biotite, quartz, feldspar gray gneisses with abundant leucosome layers are common along Rt. 22 south of Whitehall, NY. Locality-3 was also the focus of a study by Wong et al. (2012) and of one M.S. thesis (Suarez et al., 2017; Suarez, 2018). The outcrop contains interlayered garnet-biotite-sillimanite gneisses with greenish calcsilicate lithologies. The well exposed foliation surfaces of the gneisses commonly have well-lineated, coarsely crystalline sillimanite. The lineation is gently plunging to the southeast on an east-dipping foliation. Variations in the amount of biotite, garnet, and the proportions of feldspars are interpreted to reflect variation in the amount of melting by Reaction 1 and 2 and also in the amount of melt segregation and melt loss.

Wong et al. (2012) investigated deformational fabrics in this outcrop and in granite-bearing outcrops immediately to the south. They report a U-Pb zircon date of the granite of ca. 1140 Ma. This date suggests that the granite is part of the AMCG suite and was emplaced towards the end or after the Shawinigan Orogeny. Following this reasoning, they suggest that most of the strain in the rock is therefore related to Ottawan compression or post Ottawan extension. They examined the asymmetric K-feldspar porphyroclasts as kinematic indicators to document shear sense. Although they found some porphyroclasts that suggested top to the west, thrust sense motion and others that suggest top to the east, normal-sense motion, those that indicate top to the east movement were more abundant by a ratio 3:1. From this they concluded that this rock experienced both shortening and extension, but the extensional event was younger and overprinted the shortening event.

**Geochronology.** In-situ monazite analyses have been carried out as part of this work (Suarez et al., 2017) and also as part of the Wong et al (2012) study. Six distinct compositional populations (generations) have been recognized in the migmatitic metasedimentary samples: 1178 Ma, 1139 Ma, 1064 Ma, 1049 Ma, 1030 Ma, and ca. 1000 Ma (Fig. 7); see also Suarez et al. (2017). Uncertainties are on the order of 10-20m.y. (2σ). There is a distinct drop in Y and HREE between the ca. 1140 and ca. 1060 populations. An additional decrease occurs between 1064 and 1049 Ma. Uranium also shows decreases in the 1060-1050 Ma range. Although work is still underway, there is little evidence in these rocks for significant melting at ca. 1150 Ma. The data are consistent with the dominant melting event to have occurred at ca. 1060 Ma. The lowest Y and REE and U contents are associated with the ca. 1050 Ma population, suggesting that garnet growth and additional melting continued to this time (Fig. 7). It is possible that there was one prolonged melting event or alternatively melting may have occurred during the culmination of Ottawan shortening (1090-1060 Ma) and a second event associated with post Ottawan extension and intrusion of the Lyon Mountain granite (ca. 1050 Ma).

The 1030 Ma population is interpreted to represent shearing associated with the East Adirondack shear zone (Wong et al., 2012). Y and HREE contents increase dramatically after 1050 Ma, probably reflecting garnet break-down during exhumation (Fig. 7). The relatively high-Y overgrowths on monazite grains are commonly located along the foliation and in extensional quadrants of the grains further supporting the connection between this monazite generation, extensional shearing, and exhumation (see Wong et al., 2012). Based on the extremely low Th-content, the youngest population (ca. 1000 Ma) is interpreted to represent monazite associated with fluid infiltration and hydrothermal alteration events.

Monazite is present in thin leucosome layers within the gray migmatitic gneiss and also in thicker leucosome layers in the outcrop (Fig. 8). Monazite from a thin (~ 1 cm) leucosome layer yielded dates 1050 Ma and younger. Because monazite is expected to dissolve into partial melt, i.e. most partial melts are undersaturated in monazite components (Kelsey et al. 2008; Yakymchuk and Brown 2014; Harley and Nandakumar, 2014), we interpret the ca.1050 date to be the time of crystallization of this leucosome layer. Monazite from larger, more discrete leucosomes also yielded ca. 1050 Ma dates. However, these monazite grains have much greater U-content than the gray gneiss or the thin leucosome. We suspect that these leucosomes represent injections of external partial melts that have fractionated and evolved to higher U contents.

We have carried out in-situ and bulk zircon (U-Pb) analysis of some rocks from this outcrop. Analyses were done by Laser-ICP-MS at the Arizona Laserchron Laboratory. Bulk separates from gray gneiss yielded only ca. 1050 dates but in-situ samples of the gray gneiss yielded both ca. 1150 and ca. 1050 dates (Fig. 7, 8). We suspect that this reflects a sampling bias where only the larger zircon grains were recovered during mineral separation and these are dominated by the younger populations. An analysis of a zircon separate from the thin leucosome layer from which monazite was also analyzed, yielded both ~1150 and ~1050 dates (Fig. 8). We suspect that the older dates represent inherited zircon incorporated into the partial melt from the gray gneiss (see Suarez et al., 2017).

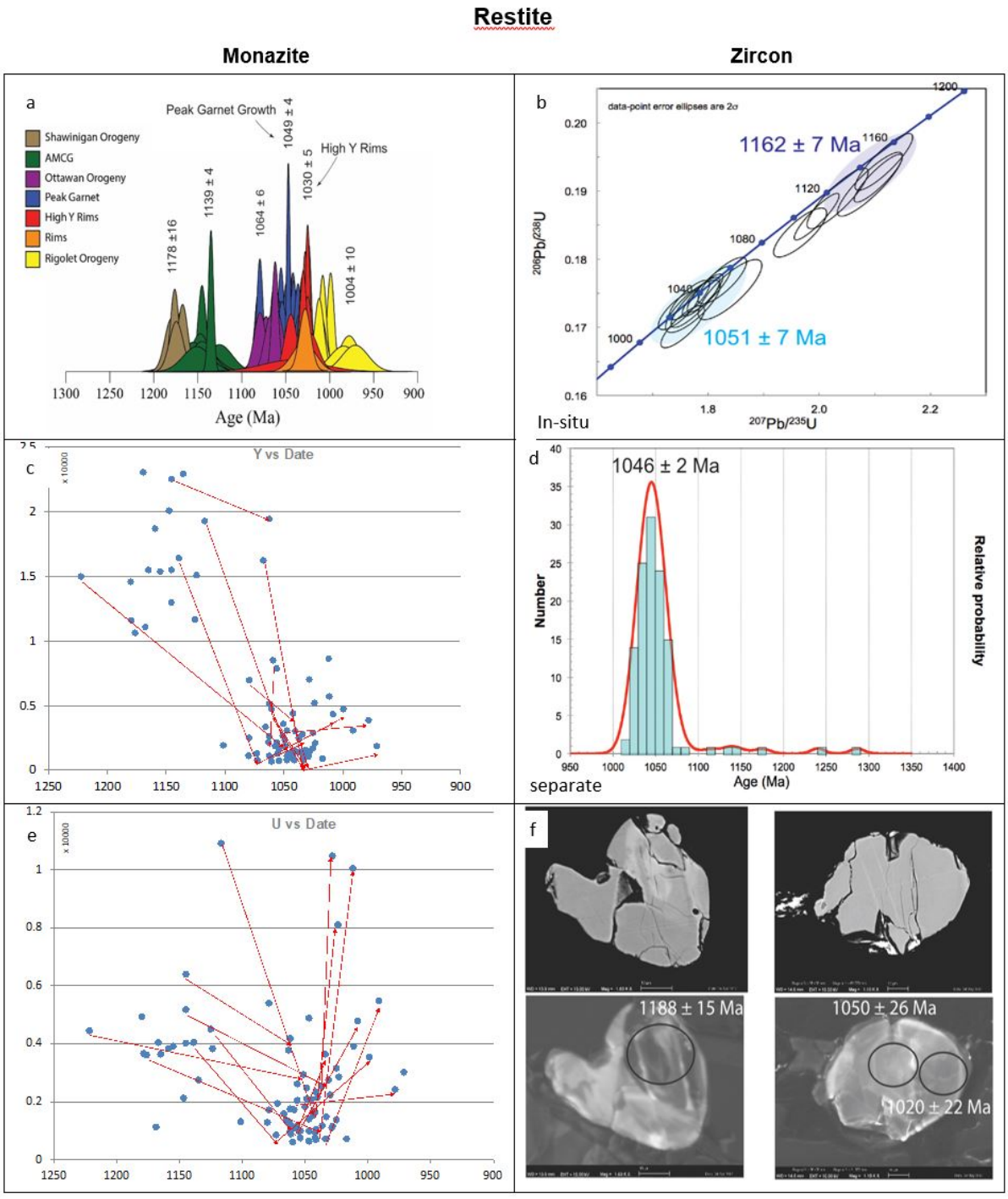


Figure 7. Monazite and zircon date-composition relationships from the restite layer, Rt. 22, south of Whitehall, NY. See text for details. A) Monazite dates for the restite. The results show six distinct populations at 1178, 1139, 1064, 1049, 1030, and 1004 Ma. B) Concordia diagram from in-situ restite zircon with two major populations at 1162 and 1051 Ma. C) Monazite yttrium composition vs date. The sharp decrease in Y in the 1050 Ma population suggests significant garnet growth. D) Zircon probability density plot for the restite mineral separate, showing one population at 1046 ± 2 Ma. E) Monazite uranium composition vs date. The U decreases at 1050 Ma and increases at 1030 Ma, suggesting melt loss and hydrothermal alteration, respectively. F) BSE and CL images of in-situ zircon with associated dates.

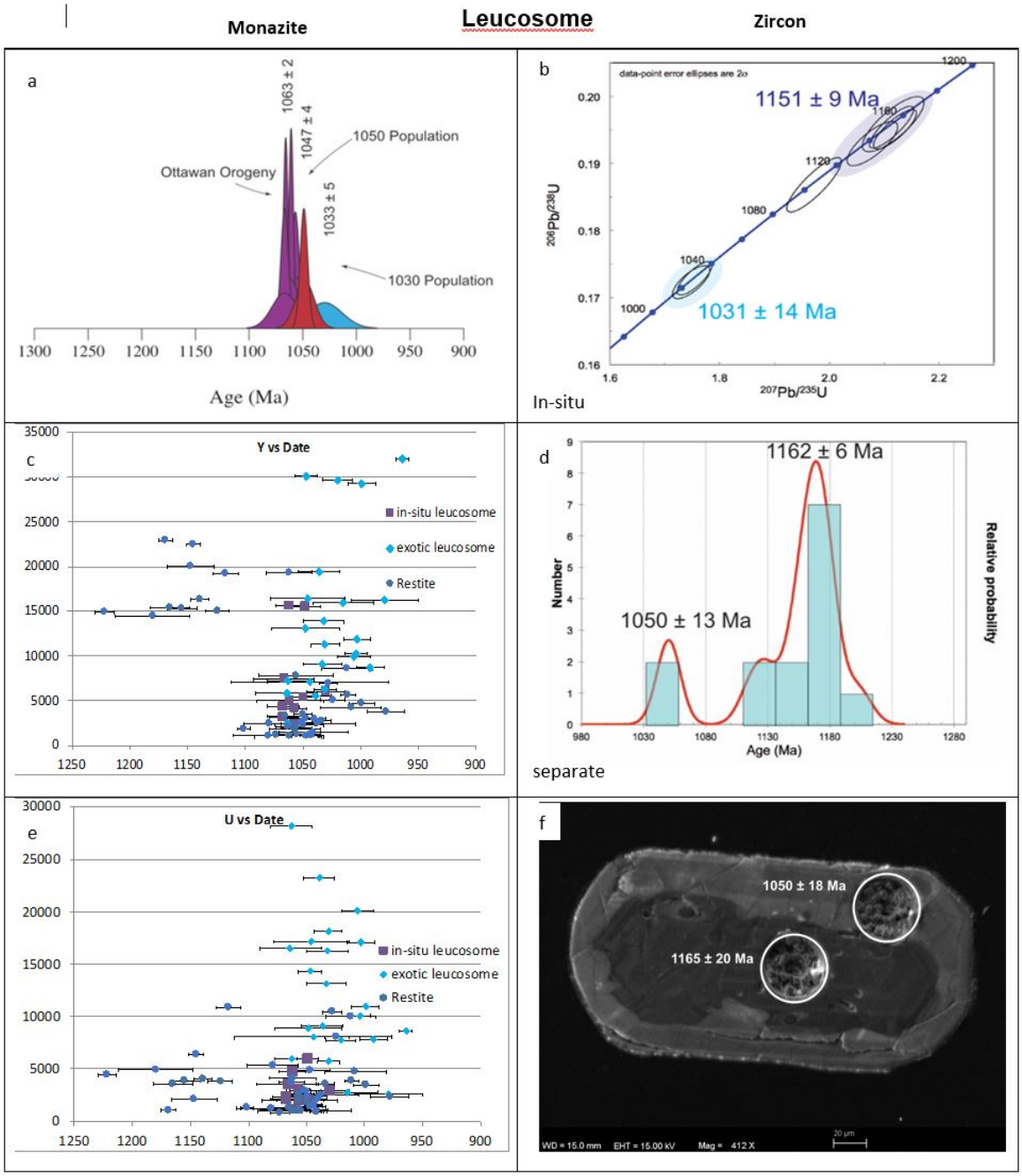


Figure 8. Monazite and zircon date-composition relationships from a leucosome layer from the same sample as Figure-7. See text for details. A) Monazite dates for the leucosome layer showing three distinct populations: 1063, 1047, and 1030 Ma. B) Concordia diagram from the in-situ leucosome zircon with populations at 1151 and 1031 Ma. C) Monazite yttrium composition vs date for in-situ leucosome, exotic leucosome and restite. The exotic leucosome has the highest Y values. D) Zircon probability density plot for the leucosome mineral separate, showing two populations: 1162 ± 6 Ma and 1050 ± 13 Ma. E) Monazite uranium vs. date for in-situ leucosome, exotic leucosome and restite. The exotic leucosome has significantly higher uranium. F) Cathodoluminescence photograph of the zircon with a 1165 ± 20 Ma core and a 1050 ± 18 Ma rim. The 1050 Ma rim date is interpreted to be the age of the leucosome.

## DISCUSSION

At least three regional tectonothermal events have been recognized in the Adirondack Highlands: the (1190-1140 Ma) Shawinigan orogeny, the (1090-1020 Ma) Ottawan orogeny, including post-Ottawan extension, and the poorly understood (1010-980 Ma) Rigolet stage/orogeny (Rivers, 2008; McLelland et al., 2013; Chiarenzelli et al., 2017). One of the major challenges for interpreting the tectonic history of the region involves placing fabrics, textures, and metamorphic assemblages into the context of these events. This is particularly true of the Shawinigan and Ottawan orogenies, which have both been interpreted to involve granulite facies metamorphism, partial melting, and penetrative deformation (Heumann et al., 2006; Bickford et al., 2008). Monazite and zircon domains from this study have yielded dates in each of the main age ranges including abundant data that span the (ca. 1160-1140 Ma) time of AMGC plutonism. Compositional mapping and composition-date relationships provide a number of insights into the significance of these generations and into the tectonic history of the region in general.

In the following discussion, dates and interpreted ages will be presented mainly without uncertainties for brevity and clarity. Errors on most monazite dates are on the order of 10-20 m.y. and the two major granulite facies events are separated by approximately 100 m.y. (Shawinigan: 1190-1140 Ma vs. Ottawan: 1090-1020 Ma). For the following discussion, the Shawinigan/AMCG event will be considered to be ca. 1150 Ma and the Ottawan event will be considered to be ca. 1050 Ma.

### Timing of Partial Melting

**Shawinigan/AMCG Melting.** Samples from all three localities investigated here have Shawinigan/AMCG monazite domains. These tend to occur as cores in zoned monazite grains or as monazite inclusions in garnet. Localities 1 and 2 show a dramatic decrease in Y, HREEs and U at approximately 1160-1150 Ma. In agreement with Heumann et al. (2006) and Bickford et al. (2008), these data are taken to indicate a significant period of partial melting and garnet growth. Importantly, this overlaps with the age of AMGC plutonism, near the end of the Shawinigan orogeny. We suggest that heating from AMGC intrusions and associated gabbroic intrusions may have contributed to the high temperature of metamorphism and may help to explain the abundance of migmatite in paragneiss across the Adirondack Highlands. There is little evidence for Shawinigan melting in samples from Locality-3. We suspect that temperatures were not high enough for extensive biotite-dehydration melting in this locality. This may be due to variations in the depth of exposure and thus temperature (i.e. Bohlen et al., 1985), but it may also reflect the greater distance to high-T, AMCG gabbro and anorthosite.

Samples from Swede Pond (Locality-1) contain the silicate assemblage Bt (retrograde)-Sil-Grt-Ksp-Qtz and are interpreted to reflect the almost complete progression of Reactions 1 and 2. That is, biotite and plagioclase were exhausted, and the assemblage is dominated by the solid products of melting (garnet and K-feldspar). The lack of plagioclase-bearing (leucosome) domains and the stability of the product assemblage suggests that partial melt was lost from the local assemblage. Other samples do contain biotite and plagioclase, either dispersed or localized in discrete layers. Importantly, many of these samples do not show the distinct decrease in U that is seen in the K-feldspar dominated samples. We suspect that, at least in some locations, a portion of the Shawinigan-AMCG partial melt did crystallize locally, producing plagioclase and biotite and maintaining high U-levels in monazite. However, the abundance of garnet suggests that some melt was also lost. If not, one would expect that much of the garnet produced during melting would be consumed during melt crystallization (White et al., 2002).

**Ottawan Melting.** The Ottawan orogeny is interpreted to have occurred in the range 1090-1020 Ma, based on regional constraints (Rivers, 2008). However, locally, some workers would break the event into an early prograde or peak phase (1090- ca.1070 Ma) and a later extensional phase (1070-1020 Ma) (Wong et al., 2012; Chiarenzelli et al., 2017). Peak conditions are estimated to have been in the granulite facies, perhaps similar to those in the Shawinigan orogeny (Spear and Markussen, 1997; Peck et al., 2018). Samples from Swede pond, at Locality-1, and all samples form Locality-2 (Dresden Station) have yielded essentially no monazite grains/domains with dates in the 1090-1060 range, and there is little evidence for new melting in these samples. Y and HREEs were depleted at 1150 Ma. U shows no additional change after approximately 1150 Ma.

Samples from Locality-3 and some samples from Locality-1 (i.e. Treadway Mountain) are very different. Numerous monazite domains and whole grains yielded dates in the 1090-1050 Ma range, especially between 1060 and 1050, the presumed prograde/peak phase of the Ottawan event. Importantly, numerous grains show a core-to-rim drop in Y, HREEs, and U at this time. We interpret this to indicate new garnet growth and a new phase of partial melting by reactions 1 and/or 2. So far, garnet compositional mapping and quantitative traverses have not definitively shown two distinct garnet compositions or textures. This may not be surprising because the Ottawan

event is interpreted to have involved high temperatures (>800 C) (Spear and Markussen, 1997) and thus, rapid diffusion. Also, the operation of similar reactions at similar grades may have produced similar garnet compositions.

**Retrograde Metamorphism**

Monazite examined in this study, as well as monazite from around the eastern Adirondack Mountains, shows evidence of retrograde metamorphism starting at approximately 1030 Ma. Y and HREEs in monazite increase significantly in monazite domains younger than ca. 1050 Ma. The increases are interpreted to reflect breakdown of garnet and release of HREES and Y. The Y- and HREE enriched domains typically occur as narrow rims, and are never present on grains completely enclosed in garnet.

Several samples are characterized by decreasing Th in monazite domains younger than approximately 1000 Ma. This seems somewhat contradictory to the interpretation that Th is strongly partitioned into monazite relative to melt of other major minerals (Stepanov et al,2012; and see above). However, there is some evidence that Th may be removed from monazite during fluid alteration by a dissolution reprecipitation mechanism (Putnis and Austrheim, 2010; Harlov and Hetherington, 2010; Williams et al., 2011). Several of the low-Th domains show textural evidence of alteration rather than overgrowth, for example, irregular low-Th domain boundaries cutting earlier domain boundaries (see Williams et al., 2011). Dissolution reprecipitation may be particularly effective in the presence of Na-bearing fluids (Harlov and Hetherington, 2010; Harlov et al., 2011). This would be consistent with the characteristic Na-metasomatism associated with late iron mineralization in the eastern Adirondacks (Valley et al., 2010; 2011). We tentatively suggest that this late depleted Th signature may be a signal of the late hydrothermal phase of evolution of the Adirondack Highlands.

It is interesting that, although there is widespread preservation of early, ca. 1150 Ma and older, monazite cores, there are no high-Y/REE rim domains of this late-Shawinigan age. Exhumation/collapse has been interpreted to have occurred soon after the Shawinigan orogeny (Rivers, 2008; McLelland, 2013) and would be required if the 1155 Ma Marcy anorthosite was emplaced into shallow crust (Valley and O'Neill, 1982). However, the fact that monazite in these samples is very sensitive to decompression and garnet break-down after 1050 Ma, but there is little evidence for garnet break-down after 1150 Ma suggests that there may have been less post-Shawinigan decompression in the Adirondack Highlands than previously thought.

**Timing of Deformation**

Textural evidence suggests that one major gneiss-forming deformational event occurred synchronous with partial melting at ca. 1160-1150 Ma (Williams et al., in review). K-feldspar-rich leucosomes from Locality-1 show evidence for pooling of leucosome in garnet shadows. Also, imbricated garnet that is wrapped by annealed K-feldspar suggests flow of garnet crystals during leucosome formation (Williams et al., in review). The ca. 1150 Ma monazite domains are distinctly aligned in the main migmatite layering. These domains probably reflect local melt crystallization, and they support interpretation of syn-melting deformation. Older monazite inclusions in garnet are not aligned in the migmatitic fabric.

Mineral lineations and kinematic indicators are poorly developed in many of the migmatite samples interpreted to have formed in the ca. 1150 event. This is in distinct contrast to a meta-quartzite at Locality-1, which has a strong mineral lineation (see Williams et al., in review). We suspect that the melt-weakened rocks at ca. 1150 Ma were not particularly amenable to lineation formation, but it is possible that some annealing occurred during later (Ottawan) orogenesis. Pooling of leucosome, possible imbrication of garnet, and subtle shear bands provide a low-confidence top-west sense of shear. This is opposite of the sense interpreted for the (ca. 1050-1030 Ma) East Adirondack shear system along the eastern edge of the uplift (Wong et al., 2012) and may characterize Shawinigan deformation in this area.

Late-stage monazite domains (>1050 Ma) have little preferred orientation in Localities 1 and 2. However, ca. 1050-1030 monazite overgrowths from Locality-3 are distinctly oriented along the SE-plunging mineral lineation. In fact, some overgrowths form sigma-tails consistent with top-east normal shearing (Wong et al., 2012). Locality-3 occurs within the region that Wong et al (2012) interpreted to be part of the East Adirondack shear zone, related to orogenic collapse following the Ottawan orogeny. Interestingly, these rocks also have some of the strongest mineral lineations of any of the migmatitic gray gneisses sampled. We suggest that the high temperatures and presence of partial melt may have contributed to weakening and localization in the East Adirondack shear zone, but shearing may have outlasted melting leading to the development of a stronger lineation due to solid state deformation. Late-stage, decompression-related monazite overgrowths are present in all sampled localities, but the

lack of alignment of the overgrowths suggests that the other two localities were not specifically located within a collapse-related structure.

## CONCLUSIONS

Partial melting can play a key role in the tectonic history of orogenic belts. Melting events can lead to weakening and thus, deformation of the crust and strengthening again when the melts crystallize. In addition, melting events record thermal perturbations that can have large-scale geodynamic significance. It is critical to illuminate the timing of melting and the relationship to deformation events and other tectonic events both before and after anataxis. Monazite can be a powerful tool for constraining the timing of metamorphism, melting, melt crystallization, and deformation.

Rocks from the three sample localities summarized here are similar in outward appearance, they are all garnet-rich migmatitic gray gneisses. However, compositional maps and the monazite record suggest that they have different petrologic, microstructural, and petrotectonic histories, especially with regard to melting and melt loss. All samples show evidence of monazite growth ca. 1150 Ma, but only localities 1 and 2 experienced significant melting. Judging by the abundance of garnet and K-feldspar some partial melt was lost from most rocks. Rocks in Locality-3 did not melt significantly during this early event perhaps because temperatures were lower near the margin of the present Adirondack dome and farther away from AMGC rocks.

The degree of partial melting and garnet growth during the Ottawan orogeny (ca. 1090-1050 Ma) was highly variable from locality to locality and, to some degree, from sample to sample. Although there is no evidence for melting or new garnet growth at Swede Mountain (Locality-1) or at Dresden Station (Locality-2), there is strong evidence for two periods of melting, Shawinigan and Ottawan, at Treadway Mtn. (Locality-1). Rocks at Locality-3 apparently underwent their first melting event during the Ottawan orogeny. These rocks have by far the greatest volume of ca. 1050 monazite domains, interpreted to have grown during melt crystallization.

A full explanation of the differing behavior must await additional analysis and more samples. Original bulk compositional differences probably played a role in controlling the degree of melting, especially at ca. 1160-1150 Ma. However, the dynamics of melt segregation and removal may have also played a role (see Williams et al, in review). We suggest that a significant proportion of melt at Localities 1 and 2 was removed and either lost from the system or segregated into distinct compositional layers. This apparently left these rocks relatively infertile for melting during the younger thermotectonic event. Rocks from Treadway Mountain may have undergone less melting during the earlier event, but importantly, it seems likely that any melt component remained dispersed in the rock producing a finer-grained, more homogeneous texture. After crystallization, the melt and restite components were more finely and evenly distributed, leaving these rocks more fertile for the second melting event. The rocks at Locality-3 were apparently fertile for melting at 1150 Ma, but did not melt, probably because metamorphic conditions were not high enough for significant biotite dehydration melting. These rocks were fully fertile for melting under Ottawan high-T granulite facies conditions.

All three localities investigated in this study have a strong, shallowly-dipping foliation. It would be tempting to correlate this fabric from locality to locality. However, based on the fabric and monazite record, deformational fabrics in gneisses from Locality-2 and parts of Locality-1 formed during the Shawinigan orogeny, while the fabrics at Treadway Mountain and Locality-3 formed or were reactivated at 1050 Ma. One would hope to be able to map, in the field, the effects of Shawinigan vs. Ottawan metamorphism and the effects of Shawinigan vs. Ottawan deformation. As noted earlier, the three localities investigated here are extremely similar in terms of outcrop appearance, fabrics and kinematics. However, some samples experienced Shawinigan melting and deformation, some record mainly Ottawan melting and deformation, and some record both events. At least for these gray gneisses, compositional mapping, detailed monazite analysis, and the integration of results from multiple samples is necessary to extract the full history.

## ROAD LOG and FIELD GUIDE

**Goals:** The main goals of this trip are to look at and discuss migmatitic paragneisses (partially melted meta-sedimentary rocks) in the Adirondack Highlands. We will focus on three main localities, although several other outcrops may be visited in passing. Rocks from each of the three main localities are similar in appearance. They are gray, garnet-rich gneisses. However, recent monazite studies suggest that they may have very different histories. They may have been melted at different times, in different tectonic settings, at with different amounts of deformation.

**Logistics:** The trip will have two starting points. Some vans and cars will leave from the Fort. William Hotel at 8:00 AM. Additional vans and cars can meet at the first stop (North Pond/Swede Pond). The official trip begins at North Pond at 9:00 AM.

Most of the stops are road-side stops. It will be grassy, possibly wet, and as usual, there is potential for ticks, chiggers, mosquitos, etc.

**Meeting Point** (for those not meeting at the Fort William Hotel)

Meet at the parking area at the east end of North Pond on Rt.8, ~5mi west of Hague, NY. Note, there are two pull-offs, one at the east end and one near the western end of North Pond. The trip will meet at the east end pull-off. Park along the edges of the pull-off road.

The meeting point is also the first stop. We will have an introductory talk and then visit outcrops across Route 8. **UTM: NAD 83, 18T 0614217; 4844335**

### Stop 1: North Pond/Swede Pond (Rt. 8, Hague, NY) -

#### Stop 1a. Dixon schist-marble-quartzite-khondalite

(Description partly taken from McLelland et al., 2002).

Rocks along Rt. 8 are dominated by metamorphosed sedimentary rocks; partially melted metapelitic rocks are particularly common. Bedding and a strong early foliation are shallowly dipping (east or west). Recumbent isoclinal folds have been described in a number of outcrops, including those at Stop-1. McLelland et al. (2002) described a large recumbent isoclinal fold at the southwestern end of the stop-1 outcrop. The fold axis plunges gently to the east or west and has been folded about upright E-W axial planes.

Rocks directly across from the pull-off are dominated by Dixon schist and marble. Dixon schist is a rusty slabby sulfidic rock that varies from garnet-bearing impure quartzite to garnet-rich schist. The more schistose varieties are similar to sillimanite-garnet-quartz-feldspar (khondalite) gneiss that we will see throughout the trip. Of particular note here is the strong mineral lineation on shallow, east-dipping foliation surfaces. The lineation plunges 20° => 090° on a foliation oriented 012°,21°.

Both Dixon schist and the khondalite were mined for flake graphite during the early part of the 20$^{th}$ century. The region around Swede Pond is known as the Dixon National Forest and the former mining hamlet of Graphite is located just to the East.

#### Stop-1b – Khondalite

Walk westward (carefully – traffic moves very fast!) along the road to the outcrops near the sign: “Parking Area 800 Ft.”). Most of the rocks along the way consist of shallowly-dipping Adirondack marble. This is a highly recrystallized, primarily calcite marble. Although the rocks are almost completely recrystallized, there are a number of very heterogeneous folds varying from isoclinal to open.

Just west of the “Parking Area 800 Ft.” is an excellent exposure of khondalite gneiss. The name “khondalite” originated in India, and refers to sillimanite-garnet-quartz-feldspar gneiss with notably little biotite. Sample 16TG-154 (Williams et al., this guidebook; Williams et al., in review) came from this outcrop. Here, the rock contains biotite, garnet, quartz, sillimanite, apatite, rutile, zircon, and monazite. Much of the biotite is interpreted to be a retrograde phase. K-feldspar is extremely abundant making up much of the matrix of the sample.

It occurs in continuous layers wrapping around garnet, forming strain shadows near garnet, and locally occurs as sigma-style porphyroclasts. Importantly, plagioclase is absent in the sample (Fig. 4).

The lack of peak biotite and plagioclase and the abundance of garnet and K-feldspar suggests that the following were important melting reactions.

$$Bt + Pl + Als + Qtz = Grt + Kfs + melt \quad (1)$$

$$Bt + Als + Qtz = Grt + Kfs + melt \quad (2)$$

Some initial melting may have been associated with muscovite dehydration, but modeling suggests that the amount of melting was probably limited (Storm and Spear, 2005; Yakumchuk and Brown, 2014). The complete lack of plagioclase suggests that Reaction-1 was exceeded. Peak conditions are interpreted to be in the range of 0.6-0.8 GPa, 700-800 °C based on phase relationships Storm and Spear, 2005; White et al., 2007; Yakumchuk and Brown, 2014) and also on calculated P-T conditions (Bohlen et al., 1985; Essene, Storm and Spear, 2005). We suggest that P-T conditions were within the region shown on Fig. 3.

The lack of plagioclase in sample 16TG-154 indicates that Reaction-1 was not significantly reversed during melt crystallization and retrograde metamorphism. The abundance of K-feldspar and garnet, similarly, suggests that Reaction-2 was not significantly reversed. Sample 16TG-154 does contain biotite, but at least some of this biotite may reflect late biotite growth associated with fluid influx long after melting. Because of the lack of reversal of the melting reactions and the lack of plagioclase-bearing leucosome, it seems likely that a significant portion of the melt component was removed from the local rock.

**Monazite results.** Figure 9 shows calculated monazite dates for sample 16TG-154 (see also Fig. 5). Figure 9 b,c shows Y-content in monazite vs. calculated date for the same sample. Arrows (Fig. 9c) connect core and rim analyses from single monazite grains. Figure 9d shows the sum of heavy rare earth elements (HREEs) in monazite vs. calculated date. HREEs and Y are strongly partitioned into garnet. The characteristic 'U-shaped' profiles in Figure 9 b,c,d are interpreted to result from significant garnet growth at ca. 1150 Ma and garnet breakdown after ca. 1000 Ma.

Figure 9e shows U content in monazite vs. calculated date. Like Y and HREEs, U decreases dramatically prior to 1150 Ma. However, unlike Y and HREEs, there is no late-stage increase in U. Partitioning data from Stepanov et al. (2012) indicate that the actinides (U, Th) have positive monazite/melt fractionation, but U has a significantly lower ratio than Th and most REEs. During partial melting U and other trace and REEs will be partitioned from the whole rock into melt. The decrease in U in monazite in sample 16TG-154 is thus, interpreted to result from partial melting of the sample. The fact that this reduction occurred at the same time as the Y and HREE reduction is consistent with melting by reactions 1 and 2. The fact that the U content of monazite remains low during cooling and during subsequent events is taken as evidence that a large component of the melt was removed from the local system.

Importantly, sample 16TG-154 shows little evidence for garnet growth or melting at ca. 1050 Ma, suggesting that little or no melting occurred in this sample during the Ottawan orogeny.

*Return to vehicles. We will head west on Rt. 8.*

***Mileage***

0 Head west on Rt. 8

1.7 Pull-off on left (south). Drive to the second entrance to the parking area and turn in facing East.

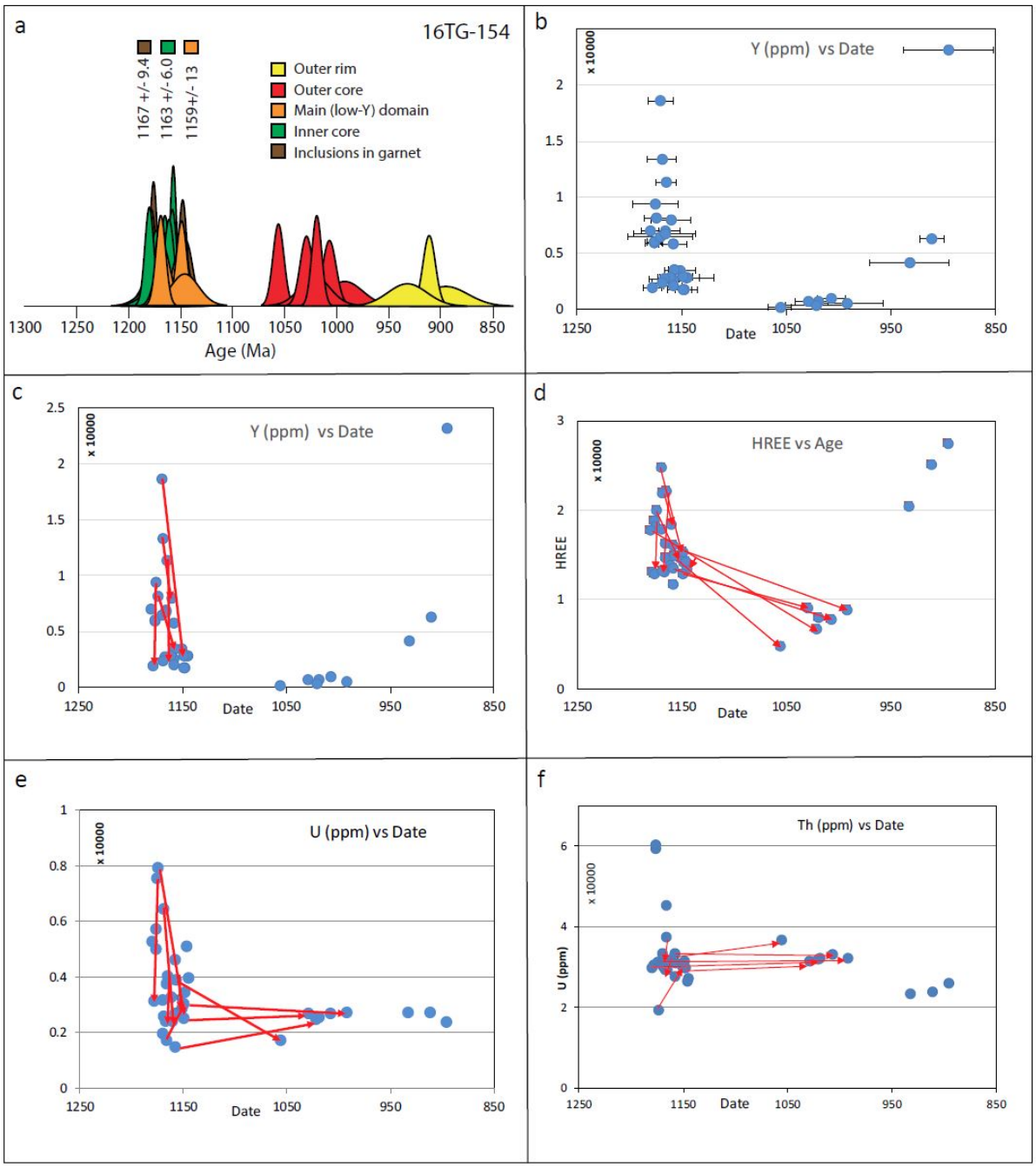


Figure 9. Monazite data from sample 16TG-154 North Pond - Swede Pond. See Figure 5 and text for discussion.

**Stop 2. Treadway Mountain, UTM: 0612067; 4843537**

A large outcrop of biotite-quartz-feldspar +/- sillimanite metapelite occurs along the north side of Rt. 8. Leucosome layers are abundant, ranging from centimeters to one meter in thickness. Similar to the North Pond outcrops, the foliation is shallowly dipping. Mineral lineations are poorly developed (preserved), but where present, trend to the east.

Several samples have been collected from this outcrop, including 16Tg151-a, b. In addition, this is Locality-9 from Bickford et al., 2008 (see below). The samples contain the common assemblage K-feldspar, garnet, quartz, sillimanite, with apatite, rutile, zircon, and monazite. Biotite is relatively abundant compared to samples from the previous stop. Most of the biotite is interpreted to be a retrograde phase, but some biotite may have been present at peak conditions. Samples contain both plagioclase and K-feldspar. The feldspars are fine to medium grained and are dispersed through the rock. Most samples have plagioclase richer and poorer layers, but distinct leucosome segregations with sharp boundaries are not present in the analyzed samples.

**Monazite Results:** Monazite date-composition relationships in sample 16TG-151 (Fig. 10) show some distinct differences from the North-Pond samples. Both Y and HREEs decrease significantly at ca. 1150 Ma, consistent with a significant period of garnet growth at this time (Fig.10 b, c, d). Yttrium and HREEs increase after 1000 Ma, consistent with garnet breakdown. However, there is considerably more variability in monazite composition at ca. 1050 Ma than in samples from Swede Pond. Importantly, several monazite grains show a distinct decrease in Y and HREEs at ca, 1050 Ma. This is interpreted to indicate a second period of garnet growth.

Uranium in sample 16TG-151 shows fairly little change from 1150 through 1050 Ma (Fig. 10e). There is some evidence for an averaging effect (that is, grain-to-grain variability decreases in younger monazite) and possibly a slight decrease in U is apparent after 1000 Ma. This is distinctly different from the trend in 16TG-154 where U was dramatically depleted at ca. 1150 Ma.

Two grains (M-3 and M-19) illustrate the behavior in this sample particularly well (Fig. 11, 12)). Monazite grain #3 has eight distinct domains (Fig. 11). HREEs drop at ca. 1150 from the innermost core to the next domain. HREES are relatively constant to the outermost core domain (1060 Ma) Then, there is a second decrease in Y and HREEs at approximately 1060-1050 Ma. This decrease is taken to be a second period of garnet growth at ca. 1050 Ma. The relatively constant Y and HREEs in grain 3 from 1150 to 1060 suggests that there was relatively little garnet growth (or breakdown?) during this 100 m.y. period. Grain 19 has no domains in the 1150 Ma range, but has at least nine domains that are ca. 1060 and younger (Fig. 12). This grain documents the progressive decrease in Y and HREEs at ca. 1050. The fact that U also decreases at this time is taken to indicate further melting, probably by a reaction such as reaction 1 and/or 2.

*Return to Vehicles* **Reset odometer to zero!**

Head east toward Hague, NY

1.7 North Pond pull-off (Stop-1)

2.5 Elephant Rock

We will discuss results from Elephant Rock, but will not make a stop. Parking is limited and the traffic can be heavy. See results in Williams et al., this guidebook; Williams et al., in review).

6.5 Town of Hague, NY

6.8 Turn left (north) on Rt. 9N

15.6 Intersection Rt. 9N and Montcalm St. Turn left toward 9N

16.3 Intersection Rt. 9N, Rt. 74 (west), and Rt. 22 (east). - Turn Left on Rt. 74

17.4 Pull off on right shoulder.

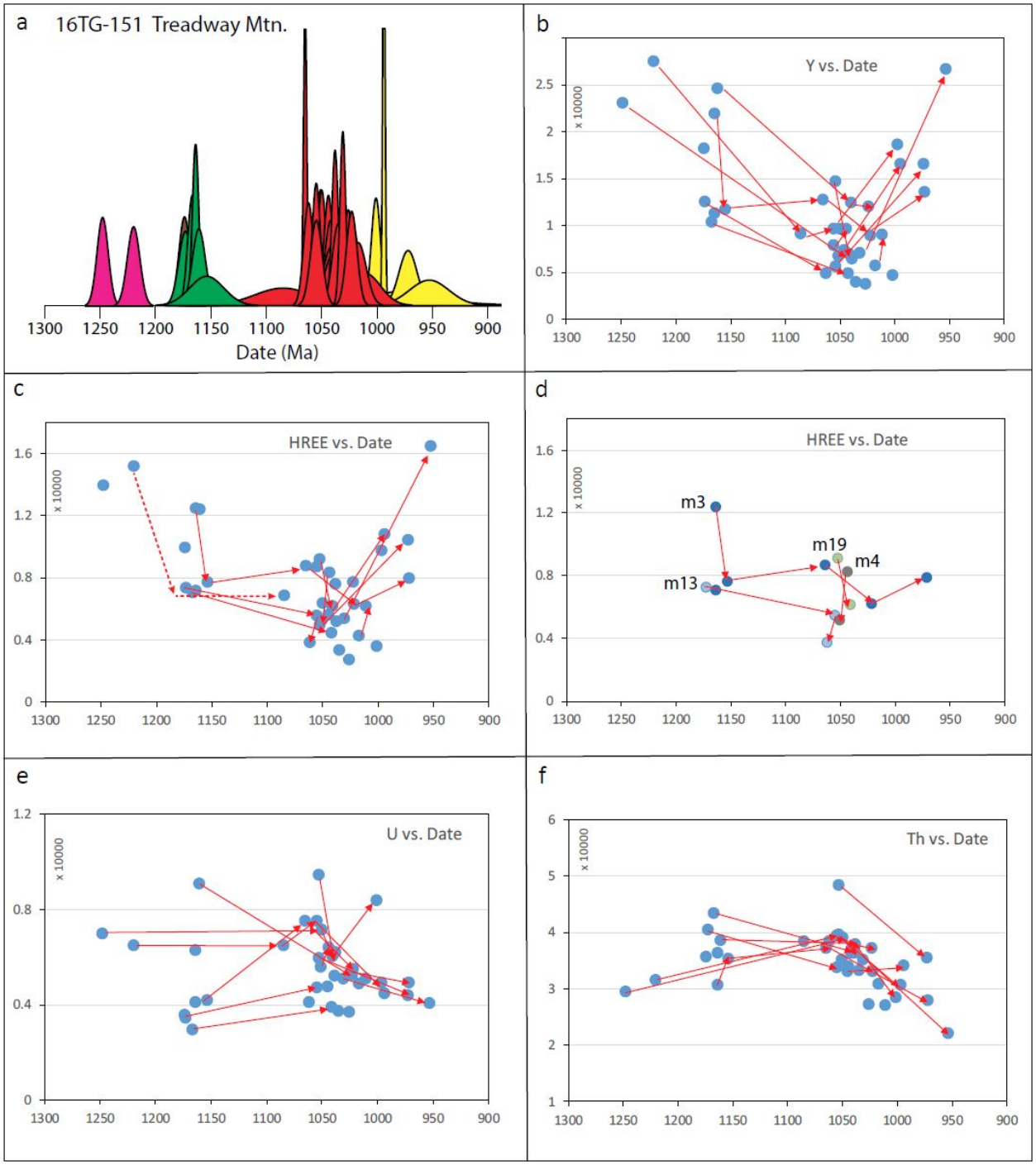


Figure 10. Monazite data from sample 16TG-151, Treadway Mountain outcrop, Rt. 8, Hague, NY. See text for discussion.

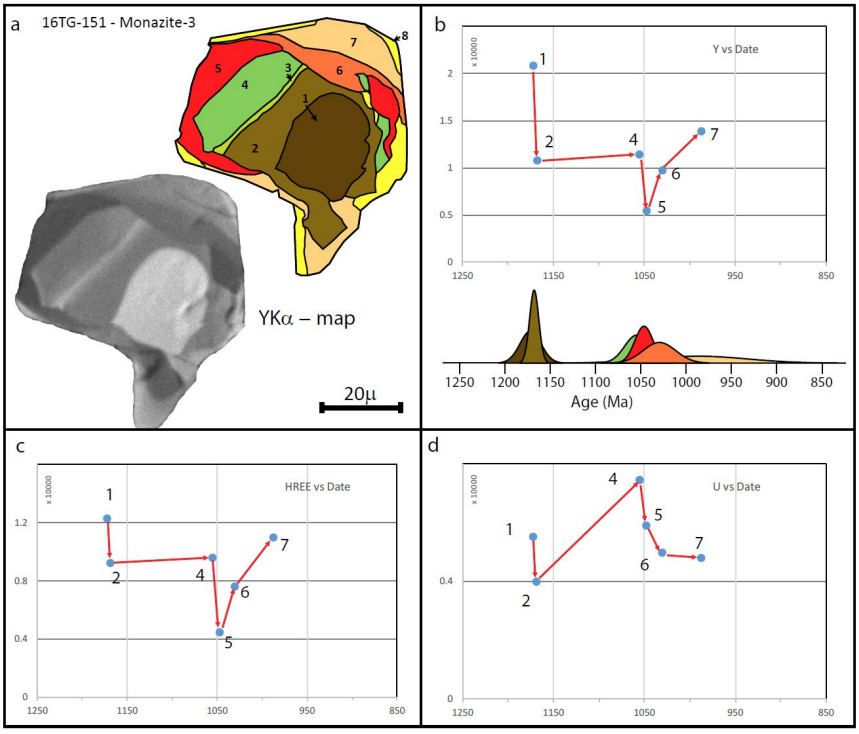


Figure 11. Monazite composition-date relationships from Monazite-3 from sample 16TG-151. See text for discussion.

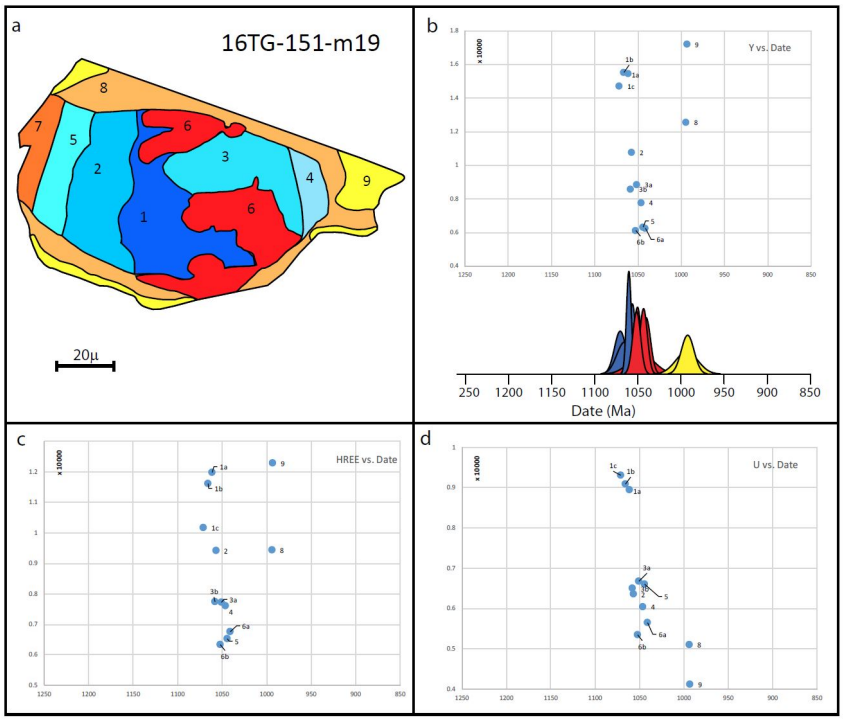


Figure12. Monazite composition-date relationships from Monazite-19 from sample 16TG-151. See text for discussion.

**Stop 3. Roadcut on NY-74, west of Ticonderoga, NY**

The easternmost rock at this outcrop is a poikiloblastic garnet amphibolite that contains garnet, clinopyroxene, plagioclase, and hornblende. Fe-Ti oxides are present as well, although they can only be seen in thin section. The garnet crystals can reach upwards of 3 cm in diameter. The best examples are concentrated in the westernmost part of the garnet amphibolite. Schistosity, mostly defined by aligned hornblende, appears to both traverse and wrap around the garnet poikiloblasts, suggesting garnet growth was syn-kinematic. Geochemistry of the amphibolite (Fig. 13) is consistent with other metamorphosed mafic members of the AMCG suite, constraining intrusion of the protolith to ca. 1160-1140 Ma.

Further west along the outcrop is a transition zone, marked by a vegetated slope, containing some layers of marble and a rusty weathering paragneiss. West of the transitions zone the vast majority of the outcrop is composed of a garnet-biotite-plagioclase-perthitic microcline-quartz ± sillimanite migmatitic paragneiss. Leucosome proportion is estimated to be 30-50%. Leucosomes preferentially contains garnet, while biotite is concentrated in the melanosome. Both leucosome and melanosome layers are deformed and define a foliation parallel to a schistosity defined by aligned biotite. Quartz and feldspar are granoblastic in both the leucosome and melanosome.

Within the migmatitic paragneiss are a number of garnet rich boudins. These are possibly deformed and metamorphosed dikes. The boudins indicate stretching in all directions parallel to gneissic layering suggesting a flattening finite strain. Also present within the migmatitic paragneiss are bodies of amphibolite similar to what is present at the east end of the outcrop. Three, 5 to 30 meters wide, unstrained, amoeboid-shaped, pegmatitic granitic plutons also occur in the migmatitic paragneiss.

The pegmatites contain feldspar, quartz, and biotite and are likely an alkali-feldspar granite, but some feldspars are striated. Locally associated with the pegmatites, the host migmatite contains cm-size books of graphite.

The fabric is essentially parallel among the garnet amphibolite, the migmatitic paragneiss, and the transitional contact zone (Fig. 14). The in the eastern half of the outcrop the foliation is ~062, 43 SE but changes to ~103, 45 SW by the westernmost end of the outcrop. A mineral lineation, defined by aligned hornblende, biotite, or sillimanite, depending on location, predominately plunges gently to the ESE (~20 → 100). This fabric is identified as the second regional fabric, forming after AMCG intrusion. Asymmetric tails on garnet poikiloblasts in the garnet amphibolite suggest top to the west transport.

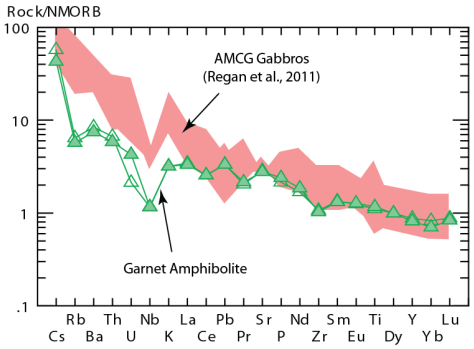


Figure 13. Multielement diagram (Sun and McDonough, 1989) for the garnet-amphibolite compared to other mafic members of the AMCG suite. Both are tholeiitic and have identical REE profiles.

Samples of the migmatitic paragneiss and of pegmatite were processed for U-Pb zircon geochronology (see also Regan et al., 2015). Presented here are preliminary results from a new sample that is solely of a structurally late migmatite leucosome that connects to adjacent leucosome boudinaged by $S_2$.

Two distinct generation of zircon can be identified in this sample by both CL and geochronology. Oscillatory zoned zircon with a bright CL response are found as cores within grains or forms entire grains. The most concordant, best cluster of ages for this zircon type provide a weighted $^{207}Pb/^{206}Pb$ age of ca. 1177 +/- 10 Ma (Fig. 15), interpreted to reflect zircon growth during Shawinigan migmatization, consistent with previous results from this outcrop. Oscillatory zircon with a dark CL response is found as rims surrounding the bright zircon or as entire grains. The oldest, concordant, tightly grouped analyses of this zircon produce a Concordia age of ca. 1067 +/- 6 Ma (Fig. 15), which is taken to be the age of a second, Ottawan-aged migmatization event and formation of the penetrative $S_2$ fabric.

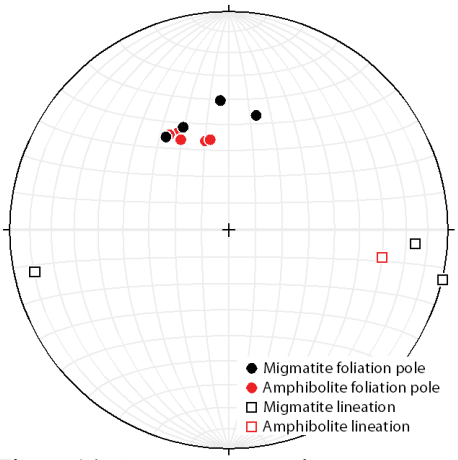


Figure 14. Outcrop structural pattern.

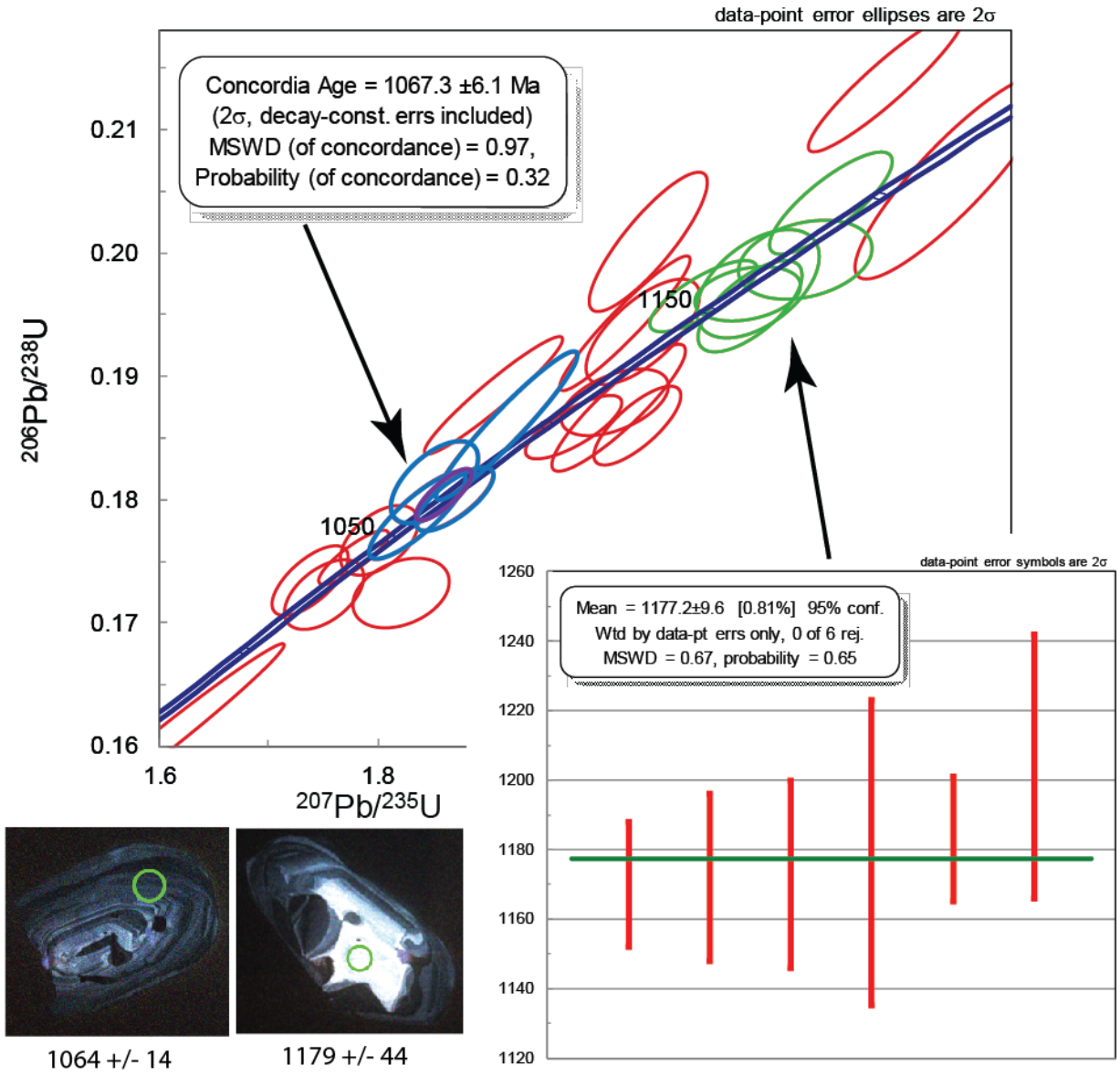


Figure 15. Concordia diagram for zircons isolated from the late-leucosome analyzed by LA-ICP-MS. Green analyses best date Shawinigan migmatization (weighted average given), blue analyses best date Ottawan migatization (Concordia age). Representative CL images and spot ages shown.

One pegmatite body produced uniform oscillatory or sector zoned zircon with a dark CL response. Nine analyses of this zircon are concordant or near concordant and produce a Concordia age of 1015 ± 10 Ma (Fig. 16), thought to best represent the age of pegmatite formation.

We have completed analyses of monazite from several samples from the migmatite. The overwhelming majority of monazite are ca. 1050 Ma and younger (Fig. 17), with only one small core domain yielding ca. 1150 date. Decreasing Y for some monazite grains (Fig. 18), the presence of ca. 1050 Ma monazite inclusions in garnet, and given the zircon data, demonstrate most monazite crystallization occurred late during or following Ottawan leucosome crystallization. Increasing Y in 1030 Ma and younger monazite supports garnet breakdown and retrograde metamorphism beginning at this time, as seen throughout the region. With the zircon data suggesting an earlier period of melting during the Shawinigan orogeny, it is likely that virtually all earlier monazite was consumed during this early or subsequent melting events. No age pattern is convincingly evident in the monazite U concentration, suggesting melt largely did not escape during either melting event (Fig. 18).

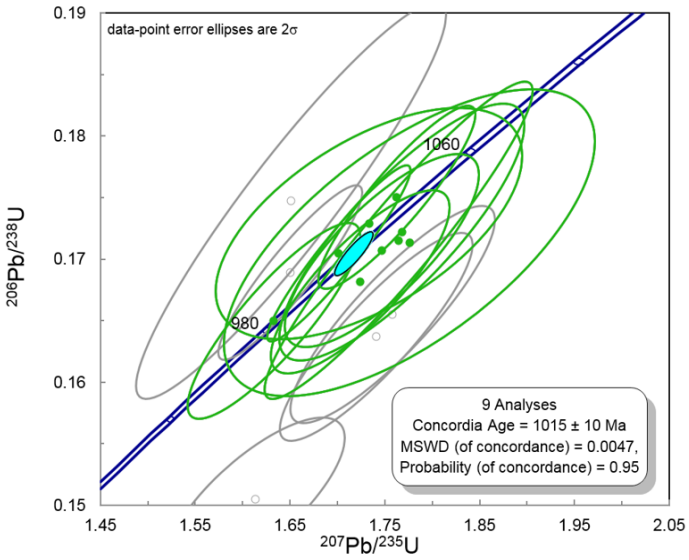


Figure 16. Concordia diagram for pegmatite zircon analyzed by SHRIMP-RG. Green analyses best date crystallization (Concordia age).

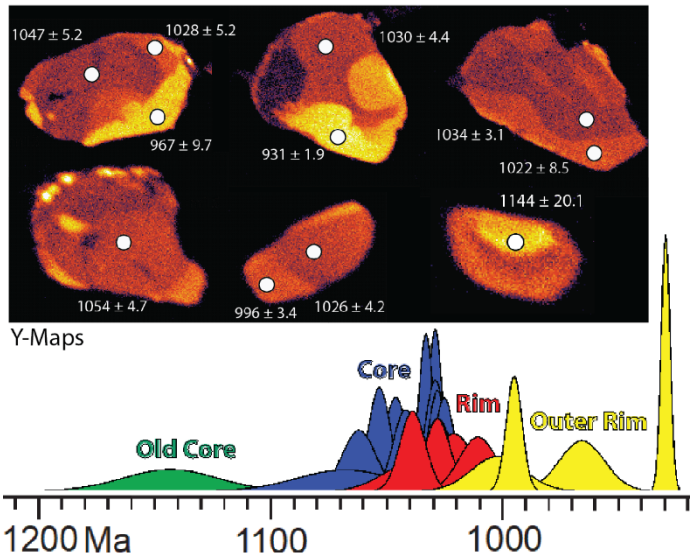


Figure 17. Summary of migmatite monazite ages with representative spot analyses.

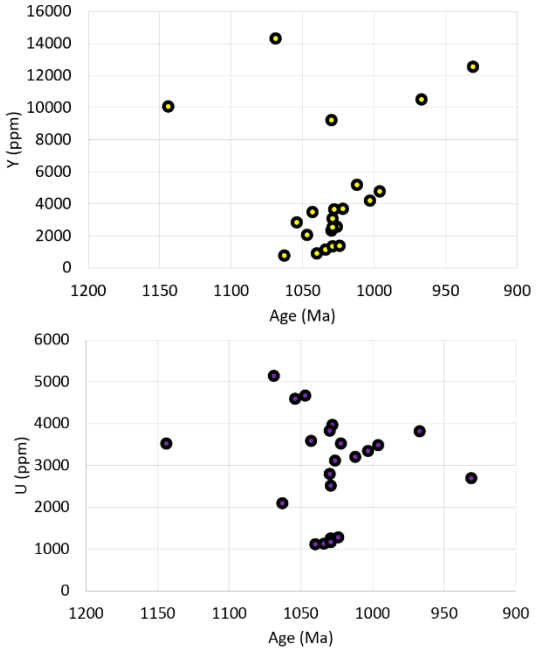


Figure 18. Monazite Y and U concentration.

*Return to vehicles. Turn around (carefully) and return to intersection of Rt. 74, 9N, and 22.*

**Note Reset Trip Mileage to ZERO.**

**0 – Miles from Rt. 72-22 Intersection**

At this point some cars may want to take a bathroom break at McDonalds or the Maplefield's gas station (northeast corner). The trip will collect at the rest-stop/lunch stop.

**1.6** Blinking traffic light, intersection with east end of Montcalm St.

**5.0** Turn into rest area on right.

This is a brief lunch stop, for those who bring lunch. People who stop for long in Ticonderoga may have to eat in vehicles on the way to the next stop!!

**9.9** Putnam Station – note Cambrian Potsdam sandstone on right above the Great Unconformity

**15.2** Turn right into Belden Road

**15.4** Turn around at Manning Rd. and return on Belden Rd.

**15.6** Park on right side of Belden Rd.

**Stop 4. Dresden Station: Garnet-sillimanite gneisses and coronitic metagabbro (UTM 18 NAD83 - 628107 E, 4837420 N)**

Many field trips have stopped at this location over the years. This description comes partly from Grover et al. (2015). McLelland et al. (1988a) used this outcrop to show that there were multiple phases of metamorphism recorded by the rocks in the Adirondacks. A sharp contact between garnet-sillimanite gneiss and a coronitic metagabbro is well-exposed in this outcrop (Fig. 19). The gneiss is a garnet-sillimanite-plagioclase-K-feldspar-quartz (khondalite) gneiss with a small amount of biotite. The khondalite is associated with quartzite and calc-silicate rocks as in many other parts of the Adirondacks.

The garnet-sillimanite gneiss is penetratively deformed with a well-developed foliation and a lineation that plunges gently to the east (21° => 091°). Much of the metagabbro is undeformed and a coarsely crystalline texture is preserved throughout much of the unit. There are places within the gabbro however that are deformed and foliated. Adjacent to the khondalite contact, the gabbro is fine grained (Fig 19c). It appears to coarsen toward the interior of the body, suggesting that a chilled margin formed at the contact. The contact between the gneiss and the gabbro is, in places, at a high angle to the foliation in the gneiss. These field relationships suggest that the gneiss was deformed and metamorphosed prior to the intrusion of the gabbro (McLelland et al., 1988).


Figure 19. Contact between garnet-sillimanite gneiss and coronitic metagabbro. Figure 19a shows that locally the foliation in the gneiss is parallel to the contact and locally it is at a high angle to the contact. Figure 19b illustrates the sharp nature of the contact. Figure 19c shows that the metagabbro is finely crystalline in the immediate vicinity of the contact.

Coronitic metagabbro bodies are found throughout the Adirondacks (Whitney and McLelland, 1973; Whitney and McLelland, 1983; Regan et al., 2011). Figure 20 illustrates the typical corona texture with an olivine core, surrounded by a rim of orthopyroxene, which in turn is rimmed by symplectic intergrowths of garnet and clinopyroxene. Ilmenite is typically rimmed by Ti-rich hornblende. Clouding in the plagioclase is due to microscopic spinel inclusions. This mineral assemblage and texture developed via subsolidus recrystallization from a rock that was originally an olivine-clinopyroxene-plagioclase gabbro. Preliminary P-T estimates suggest this mineral assemblage developed at approximately 9 kb and 750 °C. The growth of amphibole also requires an influx of an $H_2O$-bearing fluid.

To the south and west of this outcrop of gabbroic rocks, ferrogabbroic rocks and anorthosites, all thought to be associated with the metagabbro, have a very strong penetrative fabric and in many locations are mylonites. These rocks contain garnet, clinopyroxene, plagioclase, and local orthopyroxene, similar to the mineral assemblage found in the coronitic metagabbro. Kinematic indicators in these rocks suggest a west-directed thrust sense of motion. This period of deformation and metamorphism must postdate the emplacement of the AMCG rocks, but it is not clear if it reflects the late Shawinigan orogeny or the Ottawan orogeny. McLelland et al. (1988b) reported a U-Pb zircon, multigrain age of 1144 ± 7 Ma for the metagabbro. This is interpreted as an igneous crystallization age, consistent with the gabbro belonging to the AMCG suite. However, Aleinikoff and Walsh (2015) report a SHRIMP age of ca. 1134 +/- 3 Ma which suggests emplacement was during the waning stages of, or slight after the Shawinigan Orogeny.

We dated monazite from several samples of the garnet-sillimanite gneiss. The data fall into three broad populations (Fig. 6). The oldest population has a weighted mean of 1179 ± 9 Ma. We suggest that this represents the timing of prograde Shawinigan metamorphism. The next population yields ages that cluster around 1151 Ma. This is interpreted to represent the peak of metamorphism and melting driven by a thermal perturbation resulting from the intrusion of the gabbroic rocks. Most of the remaining monazite dates are 1020 Ma or less. These are too young to correlate with the proposed timing of the peak of the Ottawan Orogeny (~1090-1050 Ma). Instead, this generation probably represents post-Ottawan decompression and uplift.

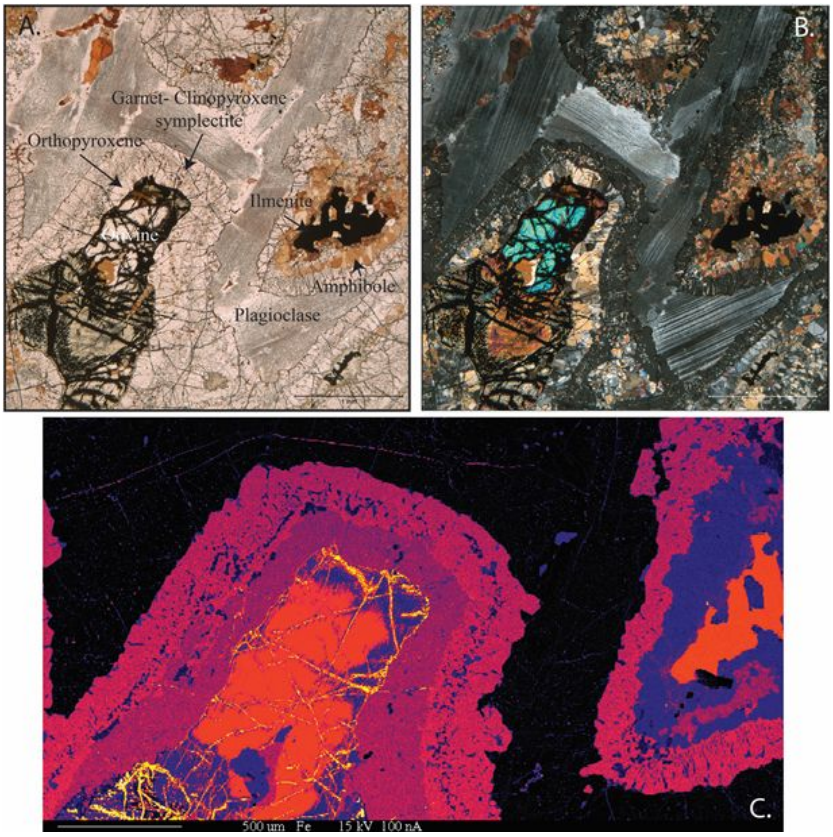


Figure 20. Photomicrographs and Fe-x-ray map of coronitic metagabro. Figure 20 a,b are photomicrographs under plane and cross polarized light respectively. Orthopyroxene surrounds olivine, and is in turn surrounded by garnet-clinopyroxene symplectite. Figure 20c is a Fe-Kα map of a portion of the thin section shown in 20 a,b.

The following model is consistent with the field observations and data from this outcrop. The mineral assemblage and the fabric in the garnet-sillimanite gneisses formed during the Shawinigan Orogeny. The gabbro was emplaced at approximately 1150 Ma, after the prominent fabric developed in the gneisses. This time frame is consistent with both the monazite dates from the gneisses and the multigrain age from the gabbro. Following the emplacement of the gabbro there was another period of deformation and metamorphism. This is when the nearby AMCG rocks were deformed and metamorphosed. This is also when the coronitic texture developed in the metagabbro. This requires in influx of an $H_2O$–bearing fluid. Unlike the nearby rocks, the coronitic metagabbro was not pervasively deformed at this time nor did any new monazite grow in the garnet-sillimanite gneiss. Perhaps strain was partitioned around this outcrop and the lack of strain resulted in little recrystallization in the largely anhydrous garnet-sillimanite gneisses. The 1020 Ma and younger monazite ages in the garnet-sillimanite gneisses record monazite growth during post Ottawan extensional collapse.

*Return to vehicles and proceed south on Rt. 22.*

**25.0** Large outcrop of khondalite gneiss on right, referred to as "Whitehall khondalite"

**26.9** Town of Whitehall; intersection of Rt. 22 and Rt.4. Continue south on Rt. 22.

**33.0 Parking area on left**

Be careful turning across traffic. Rt. 22 is busy and fast here!

**Stop 5. Lineated Sillimanite Gneiss and the East Adirondack Shear Zone**
Coordinates: UTM Z18 NAD83 (626163 E, 4813714 N)

*Walk south (left) along Rt.22 to the first set of low outcrops.*

**Stop 5a. Sillimanite Gneiss.** This outcrop contains interlayered garnet-biotite-sillimanite gneiss with greenish calc-silicate layers. The well exposed foliation surfaces of the sillimanite-bearing gneiss commonly have well-lineated, coarsely crystalline sillimanite. The lineation plunges gently to the southeast (18° => 130°). This lineation is distinctly different than that at the previous stops. It may represent a completely different stage of the tectonic history. These rocks are interpreted to have been affected by the East Adirondack shear zone (Wong et al., 2012), although kinematic indicators are better developed in outcrops just to the south (Stop 5b).

In-situ monazite analyses have been carried out as part of this work (Suarez et al., 2017) and also as part of the Wong et al (2012) study. Six distinct compositional populations (generations) have been recognized in the migmatitic metasedimentary samples: 1178 Ma, 1139 Ma, 1064 Ma, 1049 Ma, 1030 Ma, and ca. 1000 Ma (Fig. 8); see also Suarez et al. (2017). Uncertainties are on the order of 10-20m.y. (2σ). There is a distinct drop in Y and HREE between the ca. 1140 and ca. 1060 populations. An additional decrease occurs between the 1064 and 1049 Ma populations. Uranium also shows decreases in the 1060-1050 Ma range. Although work is still underway, there is little evidence in these rock for significant melting at ca. 1150 Ma. The data are consistent with the dominant melting event to have occurred at ca. 1060 Ma. The lowest Y and REE and U contents are associated with the ca. 1050 Ma population, suggesting that garnet growth and additional melting occurred at this time. It is possible that there was one prolonged melting event or alternatively melting may have occurred during the culmination of Ottawan shortening (1090-1060 Ma) and a second event associated with post Ottawan extension and intrusion of the Lyon Mountain granite (ca. 1050 Ma).

The 1030 Ma monazite population is interpreted to represent shearing associated with the East Adirondack shear zone (Wong et al., 2012). Y and HREE contents increase dramatically after 1050 Ma, probably reflecting garnet break-down during exhumation. The high(er)-Y overgrowths on monazite grains are commonly located along the foliation and in extensional quadrants of the grains, further supporting the connection between this monazite generation, extensional shearing, and exhumation (see Wong et al., 2012). This period of extension is synchronous with the extension along the Carthage-Colton shear zone (McLelland et al., 2001; Streepey et al., 2001; Johnson et al., 2004). Based on the extremely low Th-content, the youngest population (ca. 1000 Ma) is interpreted to represent monazite associated with fluid infiltration and hydrothermal alteration events.

Monazite is present in thin leucosome layers within the gray migmatitic gneiss and also in thicker leucosome layers in the outcrop. Monazite from a thin (~ 1 cm) leucosome layer yielded dates 1050 Ma and younger. Because monazite is expected to dissolve into partial melt, i.e. most partial melts are undersaturated in

monazite components (Kelsey et al. 2008; Yakymchuk and Brown 2014; Harley and Nandakumar, 2014), we interpret the ca.1050 date to be the time of crystallization of this leucosome layer. Monazite from larger, more discrete leucosomes also yielded ca. 1050 Ma dates. However, these monazite grains have much greater U-content than the gray gneiss or the thin leucosome. We suspect that these leucosomes represent injections of external partial melts that have fractionated and evolved to higher U contents.

We have carried out in-situ and bulk zircon (U-Pb) analysis of some rocks from this outcrop. Bulk separates from gray gneiss yielded only ca 1050 dates but in-situ samples of the gray gneiss yielded both ca. 1150 and ca. 1050 dates. We suspect that this reflects a sampling bias where only the larger monazite grains were recovered during mineral separation and these are dominated by the younger populations. An analysis of a zircon separate from the thin leucosome layer from which monazite was also analyzed, yielded both ~1150 and ~1050 dates. The older dates are interpreted to represent inherited zircon incorporated into the partial melt from the gray gneiss (see Suarez et al., 2017).

It is interesting to compare these data with that from stop 3. The monazite data from the stop 3 rocks had a strong Shawinigan, AMCG, and post Ottawan signature but virtually no peak Ottawan monazite growth. The monazite data from this outcrop have Shawinigan and Ottawan monazite populations, but the data suggest that melting occurred mainly during the Ottawan event(s).

*Follow the outcrop to the south remaining on the east side of Highway 22 for the time being.*

**Stop 5b. East Adirondack Shear Zone.**

Note the interlayer folds in the upper part of the road cut on the east (Fig. 21). This exposure illustrates an older foliation that was transposed into a new foliation. Perhaps this is an example of a Shawinigan S1 transposed into a younger Ottawan or post-Ottawan S2. Across the highway is an asymmetric mafic boudin with a long tail that continues to the south in the upper part of the road cut (Fig. 22). Although it is clear that the boudin was involved in a period of ductile deformation, the road cut is oriented almost at right angles to the lineation direction so it is difficult to use the boudin for kinematic analysis.

Figure 21. Interlayer folds in paragneiss along Hwy22 at Stop 5b. Red line traces some folds. Note hammer for scale.

The granitic rocks to the left of the mafic boudin in the picture below are mylonitic, LS-tectonites with megacrystic K-feldspar porphyroclasts Fig. 23). The prominent lineation plunges gently to the southeast. Data from this outcrop was cited by Wong et al. (2012) as evidence for the East Adirondack Shear Zone. They report a U-Pb zircon age obtained using the SHRIMP-RG at Stanford, of the granite in Figure 23 of ca. 1140 Ma. This date suggests that it is part of the AMCG suite and was emplaced towards the end or after the Shawinigan Orogeny.

Figure 22. Photomosaic of a mafic boudin enveloped by mylonitic, granitic gneiss at stop 5b. The mylonitic rocks pictured in Fig. 23 are located approximately in the center of this photo.

Following this reasoning they suggested that most of the strain in the rock is therefore related to Ottawan shortening or post Ottawan extension. They examined the asymmetric K-feldspar porphyroclasts as kinematic indicators to document shear sense motion. Although they found some porphyroclasts that suggested top to the west, thrust sense motion more suggest top to the east, normal-sense motion. They concluded that this rock experienced both early shortening (west-directed thrusting) and later extension.

*Optional: cross the road and return to the vehicles along the west-side outcrops. This side gives an excellent view of the east-side outcrops, and to the north, there are excellent examples of coarse biotite-sillimanite-feldspar gneiss.*

*Be careful crossing the road. It is busy and fast.*

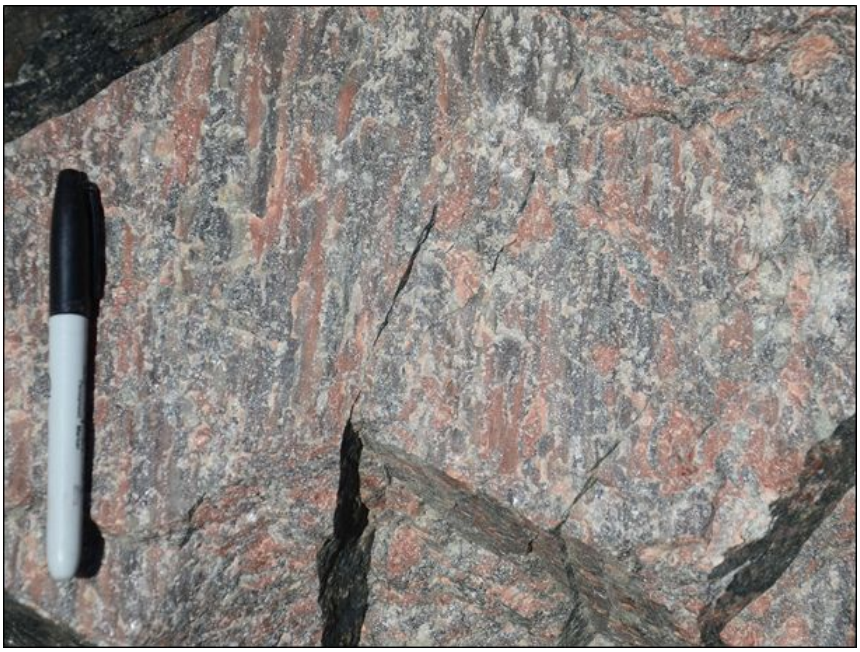

Figure 23. Strongly lineated granitic rock in the East Adirondack Shear zone.

*Return to vehicles and continue south on Rt.4.*

**34.1** Turn right on Kelsey Pond Road.
Park on the side of the road. Carefully cross the highway to outcrop on the east side.

**STOP 6. Mylonitic, Migmatitic "Straight" Gneiss**

Coordinates UTM 18 NAD83: (625497 E, 4812086 N)

This is a beautiful exposure of a garnet-biotite-plagioclase-K-feldspar-quartz sillimanite gneiss. Most of the white layers are interpreted as leucosomes that formed during partial melting via a reaction such as Reaction-1. The strongly attenuated nature of the leucosomes, along with also remnants of pegmatite dikes that are now sheared into the foliation plane attest to the significant strain recorded by these rocks. The rocks have the same strong southeast-trending, gently plunging lineation that was seen at the last stop. We suggest that some of the strain in these rocks may be the result of post-Ottawan extensional collapse in the East Adirondack shear zone.

This outcrop was part of a study by Bickford et al. (2008). They concluded that these rocks underwent partial melting at approximately 1050 Ma at the tail end of the Ottawan Orogeny. They suggest anatexis was facilitated by an influx of $H_2O$-bearing fluids and decompression as a result of extensional collapse.

Figure 24 shows our preliminary U-Th-Pb electron microprobe monazite data from this outcrop. The data indicate monazite growth from approximately 1150 Ma through 1000 Ma with most monazite growth after 1100 Ma.

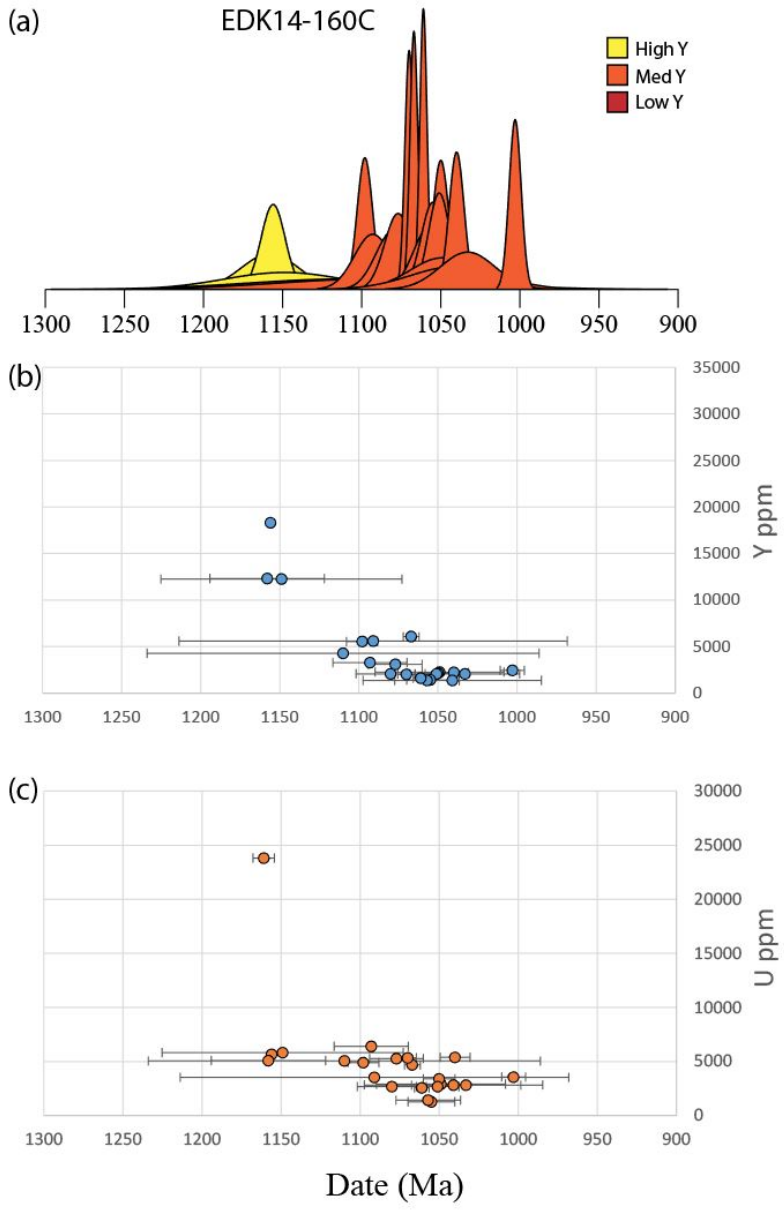


Figure 24. Monazite-composition data from the Rt. 22 "Straight Gneiss". (a) Dates from individual monazite domains; (b) Yttrium composition of monazite domains; (c) Uranium composition of monazite domains. See text for discussion.

Post-1100 Ma monazite have distinctly lower yttrium content than ca. 1150 monazite. The data are consistent with garnet growth and melting associated with the Ottawan orogeny and post Ottawan extension in agreement Bickford et al. (2008). However, there is also evidence for Shawinigan/AMCG monazite growth, and some suggestion that some melting may have occurred at this time. Combining these results with those of the precious stop, we see evidence for significant partial melting during Ottawan/post-Ottawan time. The extent of melting during Shawinigan/AMCG time is less certain, but the evidence from monazite or from zircon is certainly much less compelling. The may partly due to the intensity of the ca. 1050 Ottawan metamorphism, melting, and deformation, but we suspect that the earlier melting was much less extensive. Because the rocks were clearly fertile for melting during the later event, we suggest that Shawinigan temperatures were not sufficient for extensive biotite dehydration melting. This may reflect decreasing temperatures toward the outer parts of the Adirondack dome (as originally suggested by Bohlen et al., 1985). However, the observation that Shawinigan melting was synchronous with the AMCG plutonism suggests that the larger distance to AMGC gabbro and anorthosite may have contributed to higher temperatures during late Shawinigan time. We are in the process of collecting more data in order to further explore the effects of the Shawinigan and Ottawan Orogenies and post Ottawan orogenic collapse on these rocks.

**End of Trip.**

## REFERENCES CITED

Allaz, J. M., Williams, M. L., J., J. M., Goemann, K., and Donovan, J., 2018- In Review, Multipoint Background Analysis: Gaining precision and accuracy in microprobe trace element analysis: Microscopy and Microanalysis.

Bickford, M.E., McLelland, J.M., Selleck, B.W., Hill, B.M., and Heumann, M.J., 2008, Timing of anatexis in the eastern Adirondack Highlands: Implications for tectonic evolution during ca. 1050 Ma Ottawan orogenesis: Geological Society of America Bulletin, v. 120, no. 7-8, p. 950–961.

Bohlen, S. R., Valley, J. W., and Essene, E. J., 1985, Metamorphism in the Adirondacks. I. Petrology, Pressure and Temperature: Journal of Petrology, v. 26, no. 4, p. 971-992.

Buddington, A. F., 1939, Adirondack igneous rocks and their metamorphism.: Geological Society of America Memoir - 7, 354p.

Chiarenzelli, J., Regan, S., Peck, W.H., Selleck, B.W., Cousens, B., Baird, G.B., and Shrady, C.H., 2010, Shawinigan arc magmatism in the Adirondack Lowlands as a consequence of closure of the Trans-Adirondack backarc basin: Geosphere, v. 6, no. 6, p. 900–916, doi: 10.1130/GES00576.1.

Chiarenzelli, J., Lupulescu, M., Thern, E., and Cousens, B., 2011, Tectonic implications of the discovery of a Shawinigan ophiolite (Pyrites Complex) in the Adirondack Lowlands: Geosphere, v. 7, no. 2, p. 333–356, doi: 10.1130/GES00608.1.

Chiarenzelli, J., Selleck, B., Lupulescu, M., Regan, S., Bickford, M. E., Valley, P., and McLelland, J. M., 2017, Lyon Mountain ferroan leucogranite suite: Magmatic response to extensional thinning of overthickened crust in the core of the Grenville orogen: GSA Bulletin, v. 129, no. 11-12, p. 1472-1488.

Gehrels, G. E., Valencia, V. A., and Ruiz, J., 2008, Enhanced precision, accuracy, efficiency, and spatial resolution of U-Pb ages by laser ablation–multicollector–inductively coupled plasma–mass spectrometry: Geochemistry, Geophysics, Geosystems, v. 9, no. 3.

Harley, S. L., and Nandakumar, V., 2014, Accessory Mineral Behaviour in Granulite Migmatites: a Case Study from the Kerala Khondalite Belt, India: Journal of Petrology, v. 55, no. 10, p. 1965-2002.

Harlov, D. E., and Hetherington, C. J., 2010, Partial high-grade alteration of monazite using alkali-bearing fluids: Experiment and nature: American Mineralogist, v. 95, no. 7, p. 1105-1108.

Harlov, D. E., Wirth, R., and Hetherington, C. J., 2011, Fluid-mediated partial alteration in monazite: the role of coupled dissolution–reprecipitation in element redistribution and mass transfer: Contributions to Mineralogy and Petrology, v. 162, no. 2, p. 329-348.

Heumann, M., Bickford, M., Hill, B., McLelland, J., Selleck, B., and Jercinovic, M., 2006, Timing of anatexis in metapelites from the Adirondack lowlands and southern highlands: A manifestation of the Shawinigan orogeny and subsequent anorthosite-mangerite-charnockite-granite magmatism: Bulletin of the Geological Society of America, v. 118, no. 11-12, p. 1283.

Jercinovic, M. J., Williams, M. L., and Lane, E., D., 2008, In-situ trace element analysis of monazite and other fine-grained accessory minerals by EPMA: Chemical Geology, v. 254, p. 197-215.

Jercinovic, M. J., Williams, M. L., and Snoeyenbos, D. R., 2008, Improved analytical resolution and sensitivity in EPMA – Some initial results from the Ultrachron development project: Microscopy and Microanalysis 14, supplement 2, p. 1272-1273.

Karlstrom, K. E., Harlan, S. S., Williams, M. L., McLelland, J., Geissman, J. W., and Ahall, K. I., 1999, Refining Rodinia; geologic evidence for the Australia-Western U.S. connection in the Proterozoic: GSA Today, v. 9, no. 10, p. 1-7.

Kelsey, D. E., Clark, C., and Hand, M., 2008, Thermobarometric modelling of zircon and monazite growth in melt-bearing systems; examples using model metapelitic and metapsammitic granulites: Journal of Metamorphic Geology, v. 26, no. 2, p. 199-212.

McLelland, J., Chiarenzelli, J., Whitney, P., and Isachsen, Y., 1988a, U-Pb zircon geochronology of the Adirondack Mountains and implications for their geologic evolution: Geology, v. 16, no. 10, p. 920–924, doi: 10.1130/0091-7613(1988)016<0920:UPZGOT>2.3.CO;2.

McLelland, J., Lochhead, A., and Vyhnal, C., 1988b, Evidence for multiple metamorphic events in the Adirondack Mountains, NY: The Journal of Geology, doi: 10.2307/30068728.

McLelland, J., Daly, J. S., and McLelland, J. M., 1996, The Grenville orogenic cycle (ca. 1350-1000 Ma); an Adirondack perspective: Tectonophysics, v. 265, no. 1-2, p. 1-28.

McLelland, J., Hamilton, M., Selleck, B., Walker, D., and Orrell, S., 2001, Zircon U-Pb geochronology of the Ottawan orogeny, Adirondack highlands, New York: regional and tectonic implications: Precambrian Research, v. 109, no. 1, p. 39–72.

McLelland, J. M., Bickford, M. E., Spear, F. S., and Storm, L. C., 2002, Geology and Geochronology of the Eastern Adirondacks: New York State Geological Association Field Trip Guide, Trip B1.

McLelland, J. M., Bickford, M. E., Hill, B. M., Clechenko, C. C., Valley, J. W., and Hamilton, M. A., 2004, Direct dating of Adirondack massif anorthosite by U-Pb SHRIMP analysis of igneous zircon: Implications for AMCG complexes: GSA Bulletin, v. 116, no. 11-12, p. 1299-1317.

McLelland, J., Selleck, B., Hamilton, M., and Bickford, M., 2010, Late-To Post-Tectonic Setting of Some Major Proterozoic Anorthosite–Mangerite–Charnockite–Granite (AMCG) Suites: Canadian Mineralogist, v. 48.

McLelland, J.M., Selleck, B.W., and Bickford, M.E., 2013, Tectonic Evolution of the Adirondack Mountains and Grenville Orogen Inliers within the USA: Geoscience Canada, v. 40, no. 4, p. 318, doi: 10.12789/geocanj.2013.40.022.

Mezger, K., 1992, Temporal evolution of regional granulite terranes: Implications for the formation of lowermost continental crust, *in* Fountain, D. M., Arculus, R., and Kay, R. W., eds., Continental Lower Crust: Amsterdam, Elsevier, p. 447-478.

Peck, W. H., Selleck, B., Regan, S., Howard, G. E., and Kozel, O. O., 2018, in Revision, In-situ dating of metamorphism in Adirondack anorthosite: American Mineralogist - Preprint.

Putnis, A., and Austrheim, H., 2010, Fluid-induced processes: metasomatism and metamorphism: Geofluids, v. 10, no. 1-2, p. 254-269.

Regan, S.P., Chiarenzelli, J.R., and McLelland, J.M., 2011, Evidence for an enriched asthenospheric source for coronitic metagabbros in the Adirondack Highlands: …,, doi: 10.1130/GES00629.1.

Regan, S., Walsh, G. J., Williams, M. L., Chiarenzelli, J. R., Toft, M., and McAleer, R. J., 2018, in Review, Syn-collisional exhumation of hot middle crust in the Adirondack Mountains: implications for extensional orogenesis in the southern Grenville Province: Geosphere.

Rivers, T., 2008, Assembly and preservation of lower, mid, and upper orogenic crust in the Grenville Province--Implications for the evolution of large hot long-duration orogens: Precambrian Research, v. 167, no. 3-4, p. 237–259.

Selleck, B., McLelland, J. M., and Bickford, M. E., 2005, Granite emplacement during tectonic exhumation: The Adirondack example: Geology, v. 33, no. 10, p. 781-784.

Spear, F. S., and Markussen, J. C., 1997, Mineral Zoning, P–T–X–M Phase Relations, and Metamorphic Evolution of some Adirondack Granulites, New York*: Journal of Petrology, v. 38, no. 6, p. 757-783.

Stepanov, A. S., Hermann, J., Rubatto, D., and Rapp, R. P., 2012, Experimental study of monazite/melt partitioning with implications for the REE, Th and U geochemistry of crustal rocks: Chemical Geology, v. 300–301, p. 200-220.

Storm, L. C., and Spear, F. S., 2005, Pressure, temperature and cooling rates of granulite facies migmatitic pelites from the southern Adirondack Highlands, New York: Journal of Metamorphic Geology, v. 23, no. 2, p. 107-130.

Suarez, K., Williams, M. L., Grover, T. W., and Pless, C. R., 2017, Constraining the Timing of Melting in the Eastern Adirondack Mountains, NY Using a Combination of In-Situ Monazite and Zircon U/Pb Dating Techniques: Geological Society of America Abstracts with Programs, v. 49, no. 6.

Suarez, K., 2018, Constraining the Timing of Melting in the Eastern Adirondack Mountains [MS: University of Massachusetts – In Progress.

Valley, J. W., and O'Neil, J. R., 1982, Oxygen isotope evidence for shallow emplacement of Adirondack anorthosite: Nature, v. 300, p. 497.

Valley, P. M., Fisher, C. M., Hanchar, J. M., Lam, R., and Tubrett, M., 2010, Hafnium isotopes in zircon: A tracer of fluid-rock interaction during magnetite–apatite ("Kiruna-type") mineralization: Chemical Geology, v. 275, no. 3, p. 208-220.

Valley, P.M., Hanchar, J.M., and Whitehouse, M.J., 2011, New insights on the evolution of the Lyon Mountain Granite and associated Kiruna-type magnetite-apatite deposits, Adirondack Mountains, New York State: Geosphere, v. 7, no. 2, p. 357–389, doi: 10.1130/GES00624.1.

Walsh, G.J. and Aleinikoff, J.N, 2016, New U-Pb zircon ages and field studies support Shawinigan deformation in the Eastern Adirondacks: Geological Society of America Abstracts with Programs, v. 48, no. 2.

White, R. W., and Powell, R., 2002, Melt loss and the preservation of granulite facies mineral assemblages: Journal of Metamorphic Geology, v. 20, no. 7, p. 621-632.

White, R. W., Powell, R., and Holland, T. J. B., 2007, Progress relating to calculation of partial melting equilibria for metapelites: Journal of Metamorphic Geology, v. 25, no. 5, p. 511-527.

Williams, M.L., Jercinovic, M.J., Goncalves, P., and Mahan, K., 2006, Format and philosophy for collecting, compiling, and reporting microprobe monazite ages: Chemical Geology, v. 225, no. 1-2, p. 1–15, doi: 10.1016/j.chemgeo.2005.07.024.

Williams, M.L., Jercinovic, M.J., and Hetherington, C.J., 2007, Microprobe Monazite Geochronology: Understanding Geologic Processes by Integrating Composition and Chronology: Annual Review of Earth and Planetary Sciences, v. 35, no. 1, p. 137–175, doi: 10.1146/annurev.earth.35.031306.140228.

Williams, M. L., Jercinovic, M. J., Harlov, D. E., Budzyn, B., and Hetherington, C. J., 2011, Resetting monazite ages during fluid-related alteration: Chemical Geology, v. 283, no. 3-4, p. 218-225.

Williams, M. L., Jercinovic, M. J., Mahan, K. E., and Dumond, G., 2017, Electron microprobe petrochronology, *in* Kohn, M. J., Engi, M., and Lanari, P., eds., Petrochronology: Methods and Applications, Volume 83, Reviews in Mineralogy and Geochemistry v. 83 p. 153-182.

Williams, M. L., Grover, T. W., M.J., J., Regan, S., Pless, C. R., and Suarez, K., 2018-In Preparation, Constraining the timing and character of extreme crustal melting in the Adirondack Mountains using multiscale compositional mapping and in-situ geochronology.

Wong, M.S., Williams, M.L., McLelland, J.M., Jercinovik, M.J., and Kowalkoski, J., 2012, Late Ottawan extension in the eastern Adirondack Highlands: Evidence from structural studies and zircon and monazite geochronology: Geological Society of America Bulletin, v. 124, no. 5-6, p. 857–869, doi: 10.1130/B30481.1.

Yakymchuk, C., and Brown, M., 2014, Behaviour of zircon and monazite during crustal melting: Journal of the Geological Society, v. 171, no. 4, p. 465-479.

Yakymchuk, C., 2017, Behaviour of apatite during partial melting of metapelites and consequences for prograde suprasolidus monazite growth: Lithos, v. 274–275, p. 412-426.

# GEOLOGY OF THE CARTHAGE-COLTON SHEAR ZONE AND LYON MOUNTAIN GRANITE AN ADIRONDACK FIELD TRIP IN HONOR OF BRUCE SELLECK

William H. Peck[1], Department of Geology, Colgate University, Hamilton, New York 13346
Eric L. Johnson[2], Department of Geology, Hartwick College, Oneonta, New York 13820
Martin S. Wong[3], Department of Geology, Colgate University, Hamilton, New York 13346
Email addresses: [1]wpeck@colgate.edu, [2]johnsone@hartwick.edu, [3]mswong@colgate.edu

## INTRODUCTION

This field trip is in honor of Bruce Selleck, Thomas A. Bartlett Chair and Professor of Geology at Colgate University, who passed away unexpectedly on Monday, July 31 2017. Bruce had deep ties to the upstate New York region, growing up on a farm on the western edge of the Adirondack Park. Bruce received his AB in Geology in 1971 from Colgate University, and returned to his alma mater as a faculty member in 1974, after taking MA and PhD degrees at the University of Rochester. His scholarship initially focused on the Paleozoic sedimentology of New York, but as his career progressed Bruce later expanded the scope of his research to include study of the tectonic development of the Adirondack Mountains, with longtime colleague and friend Jim McLelland.

This field trip revisits some of the key localities first described by Bruce and his collaborators in the Carthage-Colton shear zone, a major structure in the southern Grenville Province that separates the Adirondack Highlands from the Adirondack Lowlands and underlies the crossroads of Selleck's Corners, and the farm where Bruce grew up. This guide draws heavily on the Friends of the Grenville field trip to look at these rocks led by Eric Johnson and Bruce in 2005, Bruce's papers on the Carthage-Colton shear zone and the syntectonic Lyon Mountain granite, and subsequent research by Bruce, the field trip leaders, and our colleagues.

## GEOLOGIC SETTING

The area of the Carthage-Colton shear zone has long been recognized as a major geologic discontinuity in the Mesoproterozoic crust of the Adirondack mountains, dividing the Adirondack Highlands from the Adirondack Lowlands (Fig. 1). The Lowlands are for the most part dominated by upper amphibolite facies metasedimentary rocks, while the Adirondack Highlands are made up of granulite facies metaplutonic rocks with only a minor metasedimentary component. When U-Pb age determinations became available for the Adirondacks in the late 1980s and early 1990s it became clear that magmatic suites of the Lowlands and Highlands have different age groupings (McLelland and Chiarenzelli 1988), and that the Highlands and Lowlands have different metamorphic ages. In the Adirondack Lowlands U-Pb ages of metamorphic minerals and partial melting reflect the 1190-1140 Ma accretionary Shawinigan orogeny, while in the Highlands both the Shawinigan and the 1090-1020 Ma Himalayan-style Ottawan orogeny are represented (Mezger et al. 1991; Heumann et al. 2006).

Mezger et al. (1992) framed the newly-available geochronology and overall tectonic setting of the Carthage-Colton shear zone in the terms of orogenic collapse, where the Lowlands was down-dropped during the waning Ottawan orogeny and juxtaposed the terranes at ca. 1030 Ma. In one of their tectonic scenarios the Lowlands was at a higher, and cooler (<400°C) crustal level above the Highlands during the Ottawan Orogeny. This basic tectonic interpretation has been extended to elsewhere in the southern Grenville Province to explain discontinuities in metamorphic grade, age of metamorphism, and tectonic style across several terrane-bounding shear zones. In this model regions such as the Adirondack Lowlands lacking Ottawan resetting of metamorphic chronometers are part of the orogenic lid during the Ottawan orogeny, making up the suprastructure of the orogen. The Adirondack Highlands make up part of the Ottawan orogenic infrastructure, which underwent mid-crustal channel flow and eventually collapse (see Rivers, 2011).

The west-dipping Carthage-Colton shear zone is structurally complex and records several kinematic regimes. Ottawan granulite-facies transpression is recorded in some fabrics, and is followed by rapid cooling during extensional collapse (Streepey et al. 2001; Johnson et al., 2004; Bonamici et al. 2015). Much of the Carthage-Colton shear zone deforms the 1164±11 Ma Diana complex (Hamilton et al., 2004), the westernmost major pluton of the Highlands Anorthosite- Mangerite- Charnockite- Granite (AMCG) suite. The Diana complex is for the most part made up of pyroxene syenite and related rocks, but also includes hornblende granite and associated small bodies of anorthosite (Hargraves, 1969). Rocks of the Diana complex are often penetratively deformed, mylonitized, and metasomatized in the Carthage-Colton shear zone (Johnson and Selleck, 2005; Bonamici et al. 2015).

For this field trip we will revisit several locations where intrusions related to the Lyon Mountain granite suite intrude the footwall of the Carthage-Colton shear zone (ie. the Adirondacks Highlands). Selleck et al. (2005) recognized that these synkinematic intrusions were emplaced at ca. 1050 Ma, similar in age to other ferroan & potassic granites elsewhere in the Adirondack Highlands (Chiarenzelli et al. 2018). The Lyon Mountain granite is regionally associated with hydrothermal alteration and iron oxide mineralization, and is interpreted to be the product of crustal melting caused by gravitational collapse of the Ottawan orogen (Selleck et al. 2005; Chiarenzelli et al. 2018).

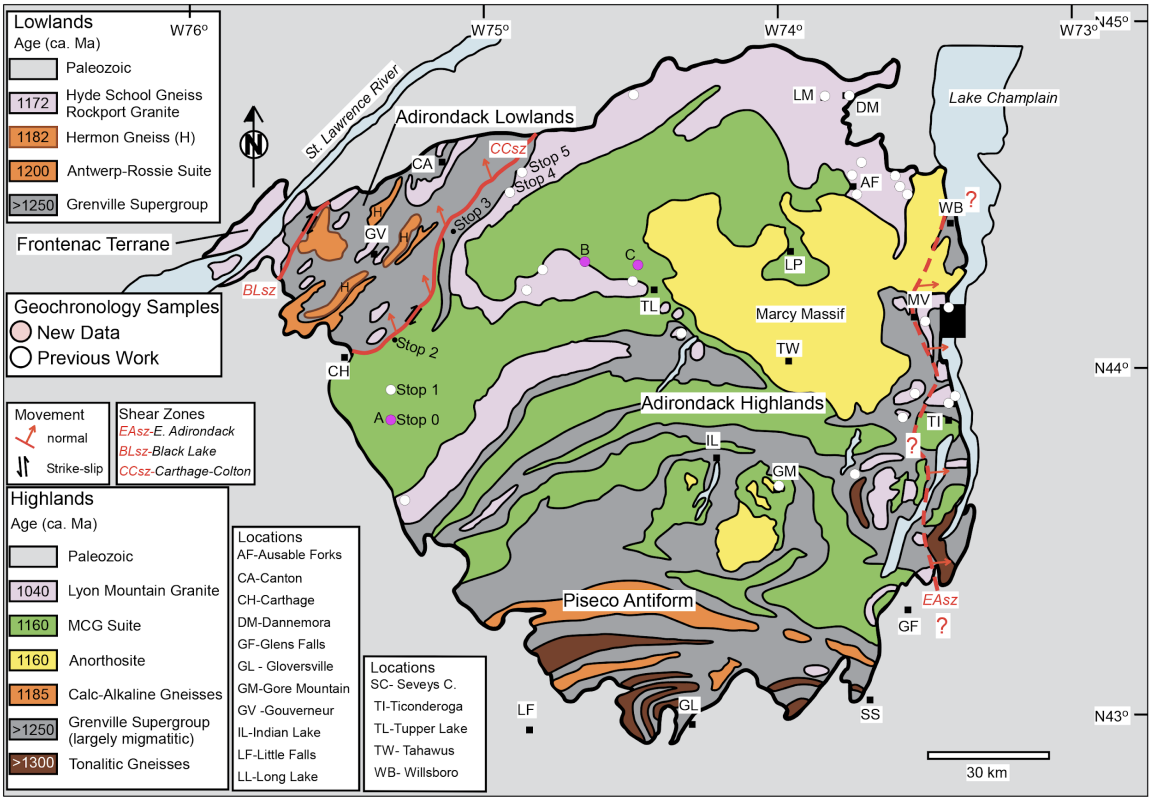


Figure 1. Geological map of the Adirondack region (from Chiarenzelli et al. 2018). Colored units are igneous rocks dated by U-Pb zircon geochronology, with ages indicated in the legend. Separate legends are given for the Adirondack Highlands and Adirondack Lowlands terranes. Small white circles note sampling locations for U-Pb zircon analyses of the Lyon Mountain granite tabulated by Chiarenzelli et al. (2018). Pink circles are new U-Pb zircon age localities: (A) Croghan, (2) Seveys Corners West, (C) Long Lake. Field trip stops are numbered.

## PRE-TRIP STOP

### STOP 0: DEFORMED AMCG GRANITOIDS SOUTH OF CROGHAN

Extensive outcrops on both sides of NY-812 (LAT-LONG 43.87477 -75.38969)

This stop, 1.2 miles south of the Citgo gas station, is included for field trip participants traveling from the south to the meeting place in Croghan as a 'guide your own' stop. Extensive outcrops of penetratively deformed and folded rocks are exposed on both sides of NY-812, showing a variety of granites, syenites, and amphibolites (Fig. 2). Lithologically these exposures are similar to the Diana syenite and other AMCG-suite granitoids elsewhere in the Adirondacks. These rocks are mapped as hornblende and biotite granites on the state geologic map.

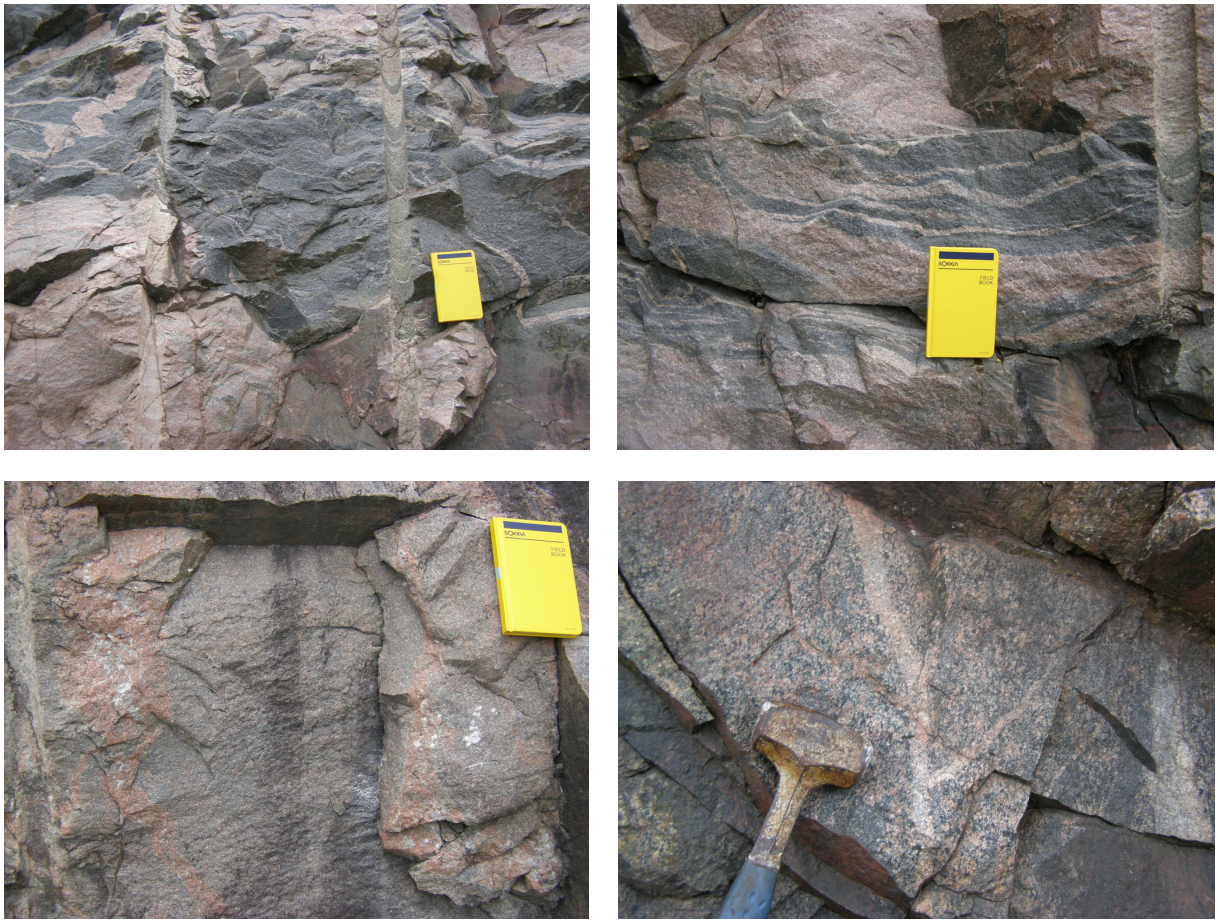

Figure 2. Deformed anorthosite-suite syenite and amphibolite (above) intruded by granite pegmatite (lower left) and granitic dikes (lower right), south of Croghan, NY.

In 2017 Bruce Selleck dated several rocks thought to be part of the Lyon Mountain granite suite to test the relationship with mineralogically similar, but deformed AMCG suite granitoids, including two rocks from this site (Fig. 3). The sample CRO-16-H is a deformed granitoid from this outcrop, and 29/31 analyzed euhedral zircon with oscillatory zoning yields a $^{207}Pb/^{206}Pb$ weighted mean age of 1176±10 Ma (MSWD=2.1), similar to other members of the AMCG suite. The sample CRO-16-PEG is coarse pegmatite dike that cuts fabric in the host syenite. Fourteen analyses of zircon with broad zoning in BSE from this sample have a $^{207}Pb/^{206}Pb$ weighted mean age of 1047±10 Ma (MSWD=1.7), which is identical to typical igneous ages determined in the Lyon Mountain granite elsewhere. Three older analyses overlap those of the host gneiss, and are likely inherited. Bruce Selleck (personal communication 2017) thought that this sample (lower left, Figure 2) might represent in-situ melting of AMCG suite granitoids to produce Lyon Mountain granite pegmatite.

Croghan host gneiss
1176±10 Ma (n=29)
MSWD=2.1

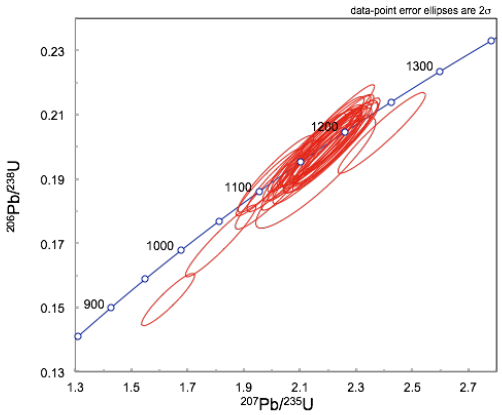


Croghan pegmatite
1047±10 Ma (n=14)
MSWD=1.7

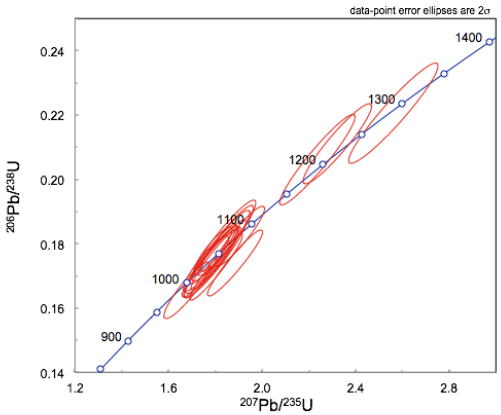


Long Lake pegmatite
1050±7 Ma (n=27)
MSWD=1.5

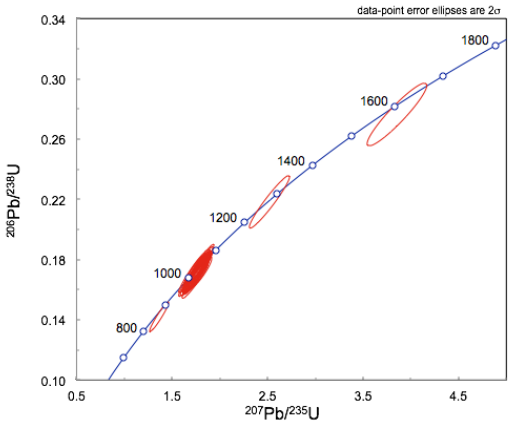


Seeleys Corners West
Amphibolite
1056±7 Ma (n=33)
MSWD=1.4

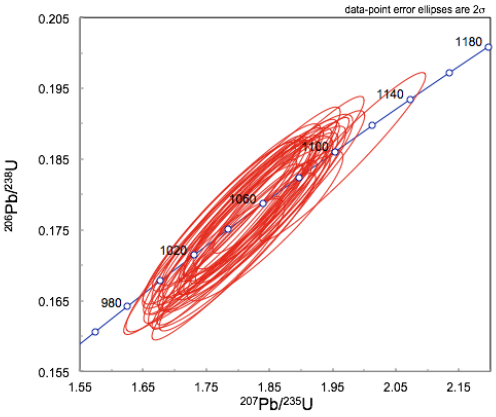


Figure 3. New laser ablation ICP-MS age determinations of Lyon Mountain granite and host rocks. $^{207}Pb/^{206}Pb$ weighted mean ages are given for zircon analyses interpreted to date igneous growth.

## ROAD LOG

This field trip begins at the Citgo Gas Station in Croghan, NY, street address 9741 NY Route 812. The geology caravan will depart at 9 AM on Friday Morning, October 12, 2018. LAT-LONG 43.89162, -75.39191

**Mileage**

0.0 Citgo Gas Station in Croghan, NY
4.4 Proceed north on NY-812 (Indian River Road ). Park next to prominent outcrops east side of road.

**STOP 1: INTRUSIVE RELATIONSHIPS ON INDIAN RIVER ROAD**
Indian River Road near Croghan, NY (LAT-LONG 43.95181 -75.38115)

This roadcut exposes dikes of leucogranite intruding mafic syenite. The location is south of the mapped extent of the Carthage-Colton shear zone and thus within the Adirondack Highlands. This outcrop and nearby exposures represent a zone of extension within the lower plate (Adirondack Highlands) of the CCSZ that accommodated granite emplacement. The undeformed quartz mesoperthite leucogranite dikes crosscut foliation in the syenite and contain xenoliths of the mafic country rock. The outcrop is also crosscut by later hematite-stained quartz-feldspar-calcite veins that resemble the late mineralized veins associated with the Lyon Mountain granite elsewhere in the Adirondack Highlands (Johnson and Selleck, 2005).

Figure 4. Ca. 1039 Ma leucogranite intruding foliated mafic syenite at Stop 1. Note xenolith of foliated mafic rock in leucogranite

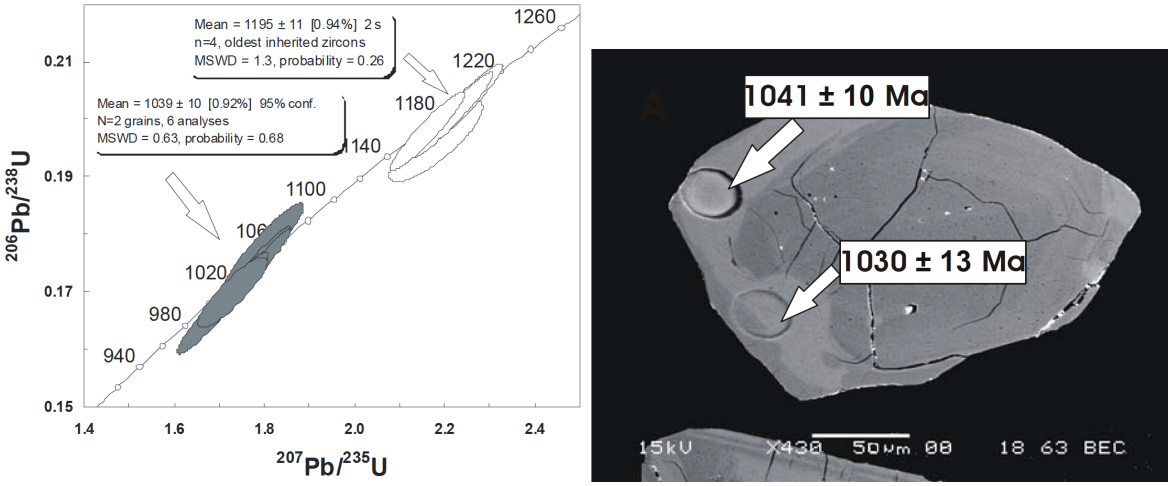


Figure 5a. Concordia plot of U-Pb SHRIMP data from leucogranite at Stop 1.
Figure 5b. BSE image of zircon from leucogranite. The finely zoned overgrowth is interpreted as igneous. Darker (lower U content) cores from this suite are older and represent xenocrysts.

Zircon from the leucogranite are subequant to elongate with faintly zoned cores and finely-zoned rims (Selleck, et al, 2005). Four reliable core analyses yield an upper intercept age of 1195 ± 11 Ma (Fig. 5, MSDW = 1.3). Six analyses of zoned rims on yielded 1039 ± 10 Ma with MSDW of 0.63. The core ages are older than zircons dating intrusion of the Diana Complex (1164 ± 11 Ma) but overlap the ages of some older cores (1180–1190 Ma) in the Diana reported by Hamilton et al. (2004). The rims represent igneous overgrowths on xenocrysts, as observed in other studies of the Lyon Mountain Granite suite in the Adirondack Highlands (Chiarenzelli et al. 2018), and fixes the minimum age of penetrative deformation in this part of the Adirondack Highlands.

16.7 Continue north on NY-812 N, turn left onto NY-3 West
17.0 Turn right onto Hermitage Road, park on right shoulder of Hermitage Road

**STOP 2: THE VALENTINE WOLLASTONITE DEPOSIT**
Hermitage Road near the intersection with NY-3 (LAT-LONG 44.12217 -75.3775)

The Gouverneur Talc Company No. 4 Quarry is at the northern contact between the 1164 Ma Diana Syenite and marble country rocks, which exposes the spectacular blue calcite marble and coarse wollastonite of the Valentine deposit. This relatively quick visit to the deposit will examine representative lithologies dumped by the mine operators next to the entry gate, which is a working site.

Mining of wollastonite in the Valentine deposit began in 1977, and the deposit is well-known as a mineral collecting locality (Chamberlain et al. 1999). Calcite marbles (containing blue or white calcite) contain high-grade mineral assemblages including diopside, spectacular euhedral graphite, and other accessory minerals such as phlogopite, titanite, and chondrodite (Gerdes and Valley 1994). Secondary minerals include talc, prehnite, quartz, secondary vein wollastonite, and a host of other alteration minerals (Chamberlain et al. 1999). Visible in the dump next to the entry gate are also cemented crushed ore from the mine. This phenomenon was first noticed by Bruce Selleck in 2017 at the Lewis deposit, and now that we know what to look for, cementation of wollastonite mine wastes seems to be a common process. Crushed wollastonite rock is cemented by calcite and silica, probably by the carbon sequestration reaction wollastonite + $CO_2$ = calcite + quartz occuring passively in wollastonite mine waste rock and old stockpiles. Current research on wollastonite weathering and carbon sequestration is ongoing.

Wollastonite is relatively common in marbles and calc-silicates of the Adirondacks, and often forms during closed-system metamorphism of protolith sediments via the reaction calcite + quartz = wollastonite + $CO_2$. Large wollastonite ore deposits are found associated with 1155 Ma AMCG-suite rocks: around the Westport anorthosite dome in the eastern Adirondack Highlands (Fig. 1) and adjacent to the Diana Syenite at the boundary of the Adirondack Highlands and Adirondack Lowlands. Large wollastonite deposits require the infiltration of large

volumes of water-rich fluids into the contact aureole, producing wollastonite via reaction with calcite country rocks, where fluids bring in dissolved silica and remove evolved $CO_2$ (Gerdes and Valley, 1994).

The Willsboro-Lewis wollastonite district around the Westport dome has low oxygen isotope ratios (as low as -1.3‰ SMOW), which is indicative of interaction with large volumes of heated meteoric water, and places important constraints on the depth of emplacement of the Marcy anorthosite in the Adirondack High Peaks. (Valley and O'Neil 1982; Clechenko and Valley 2003). Large volumes of surface water during contact metamorphism is strong evidence of shallow (<10 km) anorthosite emplacement (Valley and O'Neil 1982). Interestingly, the main wollastonite ore of the Valentine deposit does not share the low oxygen isotope ratios of the Willsboro-Lewis wollastonite district (Gerdes and Valley 1994), nor does wollastonite at the contact of the the contemporaneous Morin or Lac St. Jean anorthosites of Quebec (Peck 1996; Higgins et al. 2001; Peck et al. 2005). This may indicate deeper emplacement in the crust or differences in hydrothermal flow for these other AMCG plutons.

The Valentine deposit shows steep gradients in oxygen isotopes ratios across skarn/hostrock boundaries, revealing that fluid infiltration was channelized and not pervasive (Gerdes and Valley 1994). Carbon isotope fractionations between co-existing calcite and graphite are consistent with equilibration at 675°C during overprinting Ottawan metamorphism (Gerdes and Valley 1994), although for the most part the rocks are not very deformed by this event.

17.1 Turn around on Hermitage Road, heading back to NY-3 E. Turn left onto NY-3 East
27.6 Drive on NY-3 East to the junction with Co Rd 23A, turn left on Co Rd 23A
33.5 Take Co Rd 23A to NY-58 N. Turn left on NY-58 N
37.6 Follow NY-58 N to Co Rd 24. Turn right on Co Rd 24
43.1 Proceed on Co Rd 24 5.5 miles to park on broad shoulder, right side of road.

**STOP 3: DANA HILL METAGABBRO**

Co. Rt. 24 near Edwards, NY (LAT-LONG 44.3838, -75.1781). This stop involves a short hike uphill.

Park the vans and climb the hill on the north side of the road. On the trail up the hill we will pass several sub-meter width EVENT 4 shear zones.

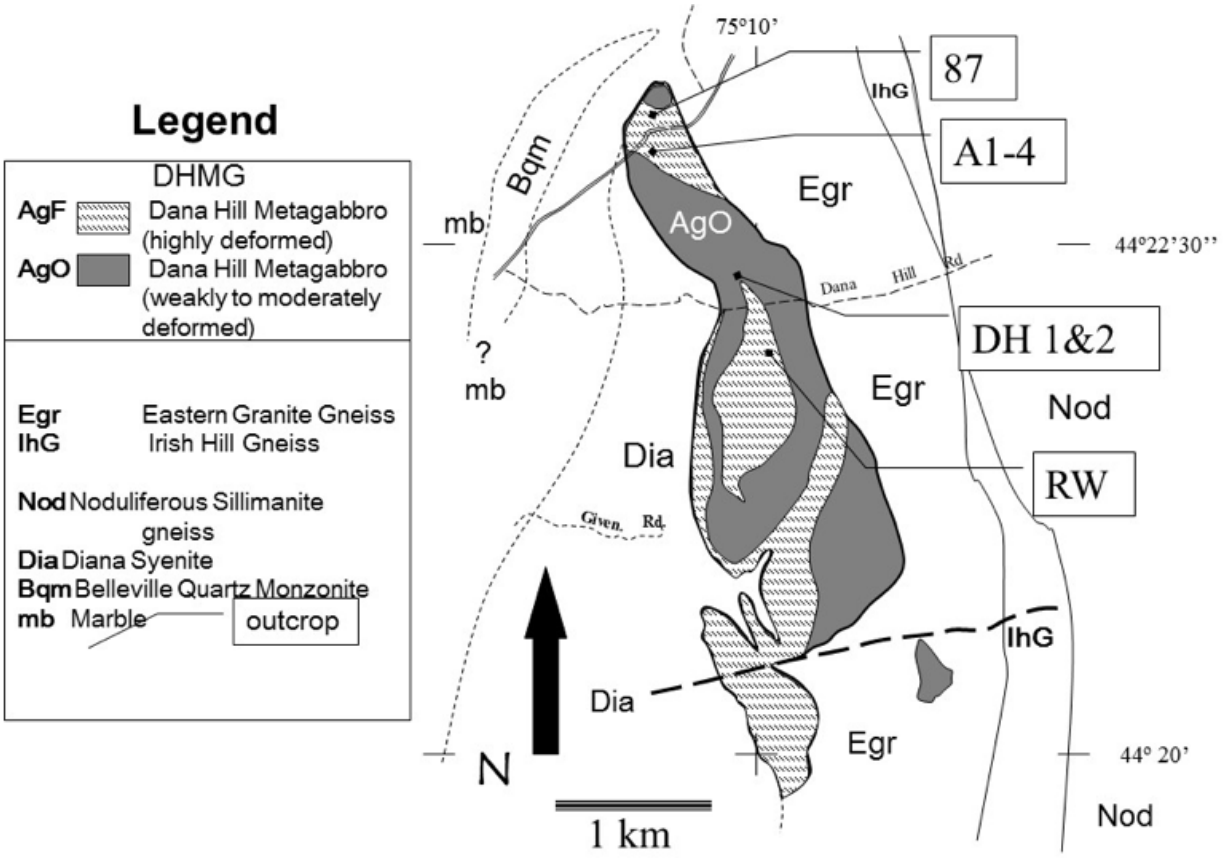


Figure 6. Map of the Dana Hill Metagabbro Body.

The Dana Hill Metagabbro preserves multiple deformation and veining events ranging from granulite facies ductile to sub-greenschist facies brittle events (see appendix). In many cases, cross-cutting relationships allow for the determination of a sequence of events. To date, six major deformational/veining events have been identified (Johnson et al. 2004; Streepey et al. 2001). At this stop we will examine the complex deformational events recorded in the body. This outcrop along with the outcrops at the top of the hill across the road, exhibit all 6 deformational events. We will start at the far southern end of the outcrop and examine the deformational sequence of events recorded. From the oldest to the youngest, this outcrop preserves EVENT 1 mega-shearing, EVENT 3 hornblende veining, EVENT 4 sub-meter shearing, and EVENT 6 folding and brecciation. EVENTS 2 and 4 can be observed at the top of the hill across the road. Events 3 through 5 take place in the presence of a fluid or fluids that drive scapolite replacement of original plagioclase feldspar in the host metagabbro. In the Diana Syenite, cm to dm-wide shear zones (dated to 1052-1034 Ma) also exhibit scapolite replacement of plagioclase feldspar. This scapolitization event is widespread in and around the CCSZ from just north of Harrisville to Colton and is present in both the Highlands and Lowlands terranes, therefore, marks a common event for both terranes. Continuing north to the far end of the outcrop lone finds a weakly to un-deformed pod of cumulate gabbro.

The goal of this stop is to demonstrate that the Dana Hill Metagabbro body acted as a rigid block during deformation. In some instances, cumulate igneous textures have been completely preserved while in other exposures the gabbro is ultramylonitic in texture. The resistance to deformation in the Dana Hill Metagabbro resulted in an

episodic response to the applied stress leading to discrete pulses of deformation. This body preserves individual and distinct events that record the much of deformational history of the region. The earliest shear zones are massive (30m wide) and mylonitic to ultramylonitic. These shear zones record recrystallization temperatures in excess of 700°C. Subsequent shearing events are dramatically different forming sub-meter wide anastomosing shear zones at recrystallization temperatures at or below 700°C. The last deformation events to affect the Dana Hill Metagabbro transition to brittle failure at low to sub greenschist facies conditions. The deformational history is one of an exhuming footwall with deformation beginning in the granulite facies and eventually passing through the brittle-ductile transition at greenschist to sub greenschist facies conditions. We will examine these events and the available geochronologic data for this complex outcrop.

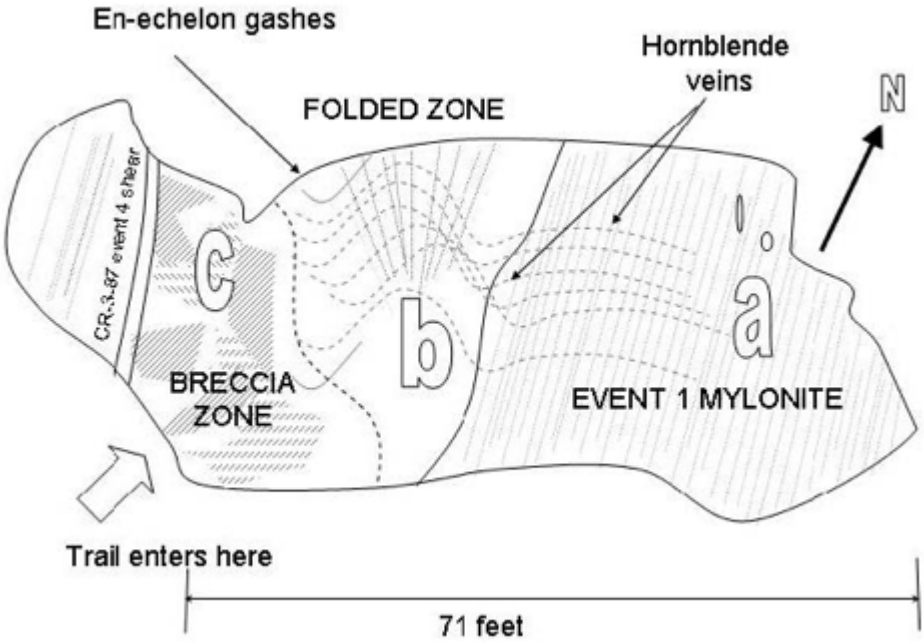


Figure 7. Map view of the outcrop at stop 3. We will begin at the western edge of exposure in zone a. The small oval shapes in zone a represent feldspar (albite)+quartz veins and tension gash fills that are undeformed internally.

EVENT 1 shearing accounts for the mylonitic character of the outcrop as a whole. The foliation here dips steeply yet transport lineation orientations plunge shallowly to the north-northwest. Kinematic indicators yield dextral shear sense. These mylonites contain recrystallized clinopyroxene + amphibole + sphene+ plagioclase (An45-51) along with accessory minerals (apatite, zircon, +/-quartz). Amphibole compositions for these samples range from Ferroan Pargasite to Magnesian Hastingsite. Chlorine contents are high for all amphiboles studied ranging from 2 to 18% hydroxyl site occupation. Amphibole and plagioclase chemistries are presented in Johnson et al. (2004). All samples exhibit a well-annealed polygonal fabric with perfect 120° triple junctions between grains. Grain sizes show a narrow range of variation for these samples averaging in the range of 100-300 μm for polygonal plagioclase. Re-crystallization temperatures for event 1 samples using the quartz-free geothermometer Holland and Blundy (1994) range from 744 to 770°C (for 6 kbar). Scapolite replacement of plagioclase is not present in EVENT 1 shears at this location.

Hornblende veins cut the foliation at high angles in zone a. Hornblende veining belongs to EVENT 3 (we do not see EVENT 2 shear zones in this outcrop.). The hornblende veins are surrounded by reaction halos were scapolite replaces plagioclase feldspar in the host metagabbro. These halos can extend several mm into the surrounding metagabbro. In zone b (see Fig. 7), the metagabbro is folded and the open to nearly chevron folds are marked by EVENT 3 hornblende veins. What looks like a rotated cleavage fanning across the folds are in fact the old EVENT 1 mylonitic foliation surfaces. This zone transitions into the chaotic breccia zone (EVENT 6; zone c). Brecciation (EVENT 6) was accompanied by the growth of actinolite, biotite and chlorite after hornblende, and the breakdown of scapolite to a mixture of albite, epidote, and calcite Breccia sample H-6A preserves rafts and clots of scapolite-

rich mylonitic metagabbro with an invasive matrix of fibrous mats of chlorite, epidote, and actinolite. Hornblende (ferroan pargasite) that has not suffered alteration to actinolite is fluorine-rich (average F = .75 wt %; average Cl = .57 wt %).

At the eastern margin of the breccia zone, an EVENT 4 sub-meter scale shear zone is exposed. This shear (sample CR-3-87 Johnson et al. 2004; Streepey et al. 2001) preserves deformation textures (little annealing) and contains the assemblage hornblende + recrystallized clinopyroxene + plagioclase An 32 + Fe-Ti oxides + scapolite (minor). Plagioclase-amphibole equilibrium pairs where present yield re-crystallization temperatures for event 4 shearing in the range of 730°C to 680°C ±50°C for a pressure of 6 kbar.

GEOCHRONOLOGY OF STOP 3

Figure 8 shows the U/Pb isochron data for shear-zone grown sphene (titantite) for this outcrop. U/Pb data presented represent EVENTS 1, and 4 and yield a tightly constrained age of 1020.7 +/- 3.1 Ma. Since recrystallization temperatures for events 1 through 4 occur at temperatures above the closure temperature for U/Pb in titanite, these dates represent cooling ages for the body. The consistency of U/Pb titanite ages for samples throughout the body indicate that all (Events 1-5) shearing and veining occurred prior to 1020 Ma.

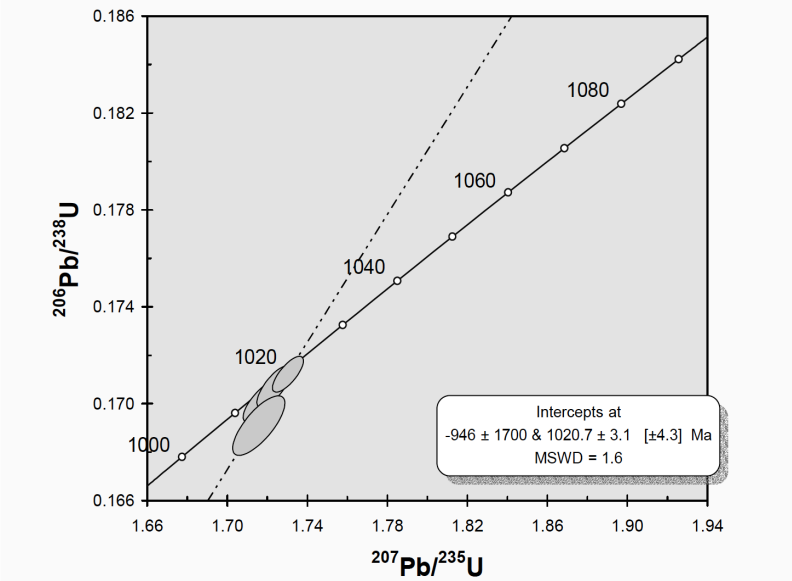


Figure 8. U/Pb isochron plots for samples from the Dana Hill Metagabbro

The $^{39}Ar/^{40}Ar$ results for hornblende in these samples is presented in figure 9. These data mark the date at which these samples cooled through the 500-550°C closure temperature for hornblende. The data from this and outcrop A-4 (opposite side of the road) are quite interesting. The results yield two cooling ages: one at ~985-1000 Ma and a second (recorded in two shear zones) of ~935-940 Ma. The latter and younger ages were determined from two samples at this outcrop. The 945 Ma age was used by Streepey et al. (2001) to constrain the timing of the last stage of movement along the CCSZ. Only one of these samples (CR-2A2) yields a statistically clear plateau. Both shear zones are overprinted by the later brecciation event and, therefore, may have suffered some Ar loss during this event. Conversely, hornblende overgrowths on undeformed cumulate textured Dana Hill Metagabbro sample from the outcrop across the road also yield a 945 Ma age indicating hornblende growth at this time. Whether or not the 945 Ma age represents renewed deformation remains a point of controversy. The bulk of the shear zones and veins studied in the Dana Hill Metagabbro (and surrounding Diana Syenite body) record $^{39}Ar/^{40}Ar$ hornblende cooling ages of 985-1010 Ma. The generally flat spectra for $^{39}Ar/^{40}Ar$ data indicate rapid cooling with little to no post-closure disturbance.

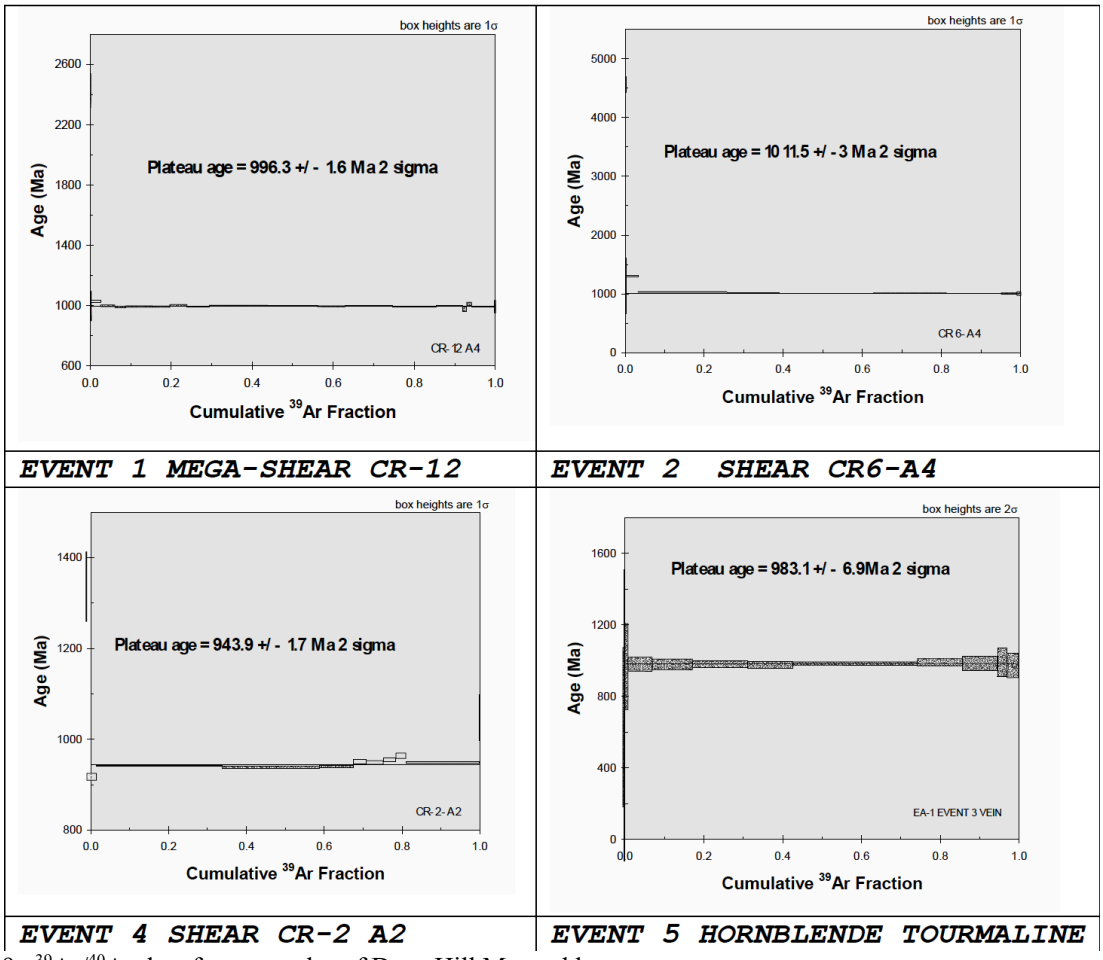


Figure 9. $^{39}Ar/^{40}Ar$ data from samples of Dana Hill Metagabbro.

The Dana Hill Metagabbro outcrops visited today provide an overview of the deformational and thermal history associated with movement along the CCSZ. Since this body is located at the CCSZ detachment, it records the entire deformational history. During exhumation of the footwall (Highlands), the width of the deformation zone narrows with falling temperature and confining pressure and eventually, deformation is confined to regions directly adjacent to the detachment surface. Due to its the resistance to strain, preexisting deformational fabrics in the Dana Hill body were not completely overprinted, leading to the complexly deformed body that we see today. Deformation in the Dana Hill can be broken down into three distinct regimes with falling temperature and pressure: 1. mega-shearing, 2. sub-meter width shearing, 3. brittle failure. Early veining episodes may have been driven by fluid infiltration into the body (driving scapolite and high Cl hornblende-forming reactions). The origin(s) of these fluids (CO2 and HCl/NaCl rich) is unknown, but a likely source is from exhalation/mobilization of evaporite deposits in the adjacent lowlands hanging wall block. This origin for the metasomatic fluids fits well with the observed and widespread scapolite veining and scapolite replacement of original plagioclase feldspar in the lowlands near Pierrepont (Tyler, 1980; Selleck , pers. comm.).

44.9 Continue east on Co Rd 24 for 1.8 mi. Turn right on on Co Rd 24

*Note, this is different from the 2005 FOG guidebook; the bridge in Russell was closed earlier in the summer*

49.9 Continue on Co Rd 17, turns into Clare Rd/Fine-Canton-Lisbon Rd heading north from Degrasse.

52.7 Continue north on Fine-Canton-Lisbon Rd (Co Rd 27) to the intersection with Donnerville Road, across from large roadcuts. Pull over.

**STOP 4: LYON MOUNTAIN LEUCOGRANITE, MYLONITE, AND ULTRAMYLONITE AT BROUSES CORNERS**

Brouces Corners (LAT-LONG 44.44050 -75.06017)

Dark mylonitic gneiss and coarse calcsilicate granulite are intruded by coarse, pink leucogranite pegmatite at this locality (Figure 10). Strong foliation in the mylonitic gneiss and local bands of ultramylonite dip gently northwest with a prominent NW-trending lineation. The pegmatite contains xenoliths of mylonitized wall rock and pegmatite veins invade and crosscut mylonitic foliation. However, the pegmatite shows mylonitic deformation along portions of its intrusive margins. One m-scale mass of pegmatite forms a large strain sigmoid indicating deformation consistent with a top-NW sense of shear. These field relationships suggest that the pegmatite was intruded during the waning phases of mylonitization and provides a key age constraint on deformation. Pseudotachylite veins crosscut mylonitic foliation but do not apparently crosscut granite pegmatite. Note the quartz veins within the tabular pegmatite masses; the veins appear to have formed as extension fractures within the pegmatite. Some quartz veins are strongly mylonitic.

Zircons from sample BC-PEG, a coarse, undeformed pink granite pegmatite, are equant, and faintly zoned in CL and BSE images (Figure 11). These analyses (based on 9 spot ages) yield a mean age of 1044 ± 7 Ma (Selleck, et al. 2005), which overlaps within error the ages of leucogranite at Indian River Road and Selleck's Corners. This age fixes the timing of mylonitic strain, as the pegmatite intrudes mylonitic rock but is itself mylonitized along its margins. The pegmatite does not contain pseudotachylite veins, suggesting that these veins developed prior to pegmatite intrusion, although no unequivocal crosscutting relationships have been observed.

Petrographic and electron backscatter diffraction (EBSD) analyses provide further insight into the kinematics of this late Ottawan deformation. Kinematic indicators in the mylonites and ultramylonites include sigma-type porphyroclasts and a strong oblique grain shape fabric that is well developed in quartz-rich mylonites (Figures 12 and 13). These kinematic indicators consistently indicate a top-NW sense of shear. Petrographic observations suggest that quartz largely was dynamically recrystallized by sub-grain rotation (SBR) recrystallization, which typically occurs between 400-500°C (Stipp et al., 2002). EBSD analyses of these mylonites yield strong lattice preferred orientations (LPO), with c-axes showing patterns that are a combination of single girdle and y-strain axis maxima (Fig. 13). This pattern suggests quartz deformation via a combination of rhomb and prism <a> slip, which is also consistent with deformation temperatures of 400-500°C (e.g. Law, 2014), matching the petrographic data. A-axes patterns also illustrate a sense of rotation consistent with a top-NW sense of shear consistent with other kinematic indicators. Taken together, these data are consistent with the interpretation of extensional motion on the CCSZ during late Ottawan time and that deformation continued through cooling to upper greenschist-facies temperatures following peak metamorphism.

Figure 10. Interlayered pegmatitic leucogranite and mylonite/ultramylonite at Brouses Corners. Note contact relationships between pegmatite and mylonite and possible mylonitic xenoliths in pegmatite. Scale in cm.

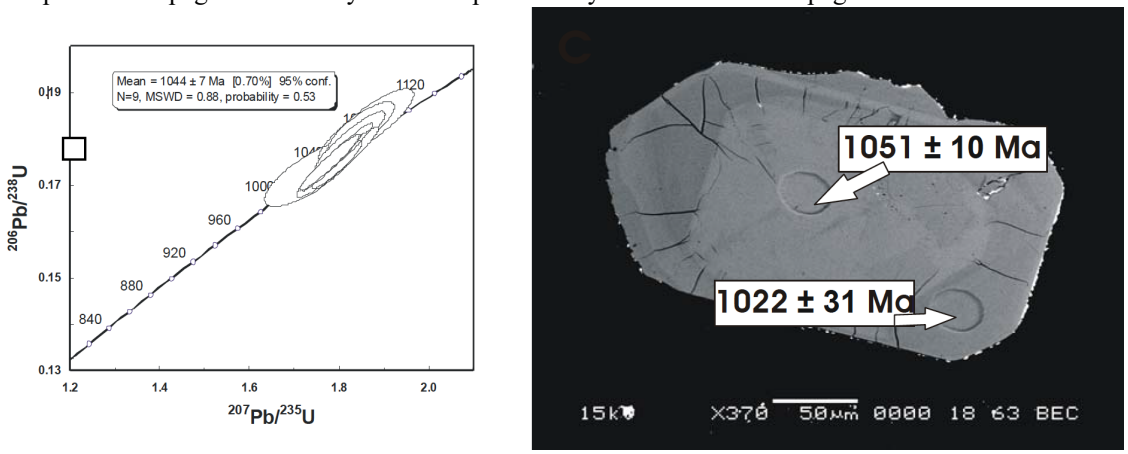


Figure 11. Left - Concordia diagram of SHRIMP results from Brouses Corners pegmatite yielding a mean age of 1044 ± 7 Ma. Right - Typical pegmatite zircon from Brouses Corners pegmatite showing SHRIMP analysis spots. BSE image.

Figure 12. Left - σ−type grain-tail complex around pyrite spheroid in ultramylonite, Brouses Corners; shear sense indicates top down to the northwest transport. Dark bands are magnetite-rich. Width of field is ~12 mm. Right - Pseudotachylite in mylonitic gneiss, Brouses Corners. Note crosscutting relationship with mylonitic foliation. Dark, microlitic-textured areas are ksp+qtz+mag. Width of field is ~ 10 mm.

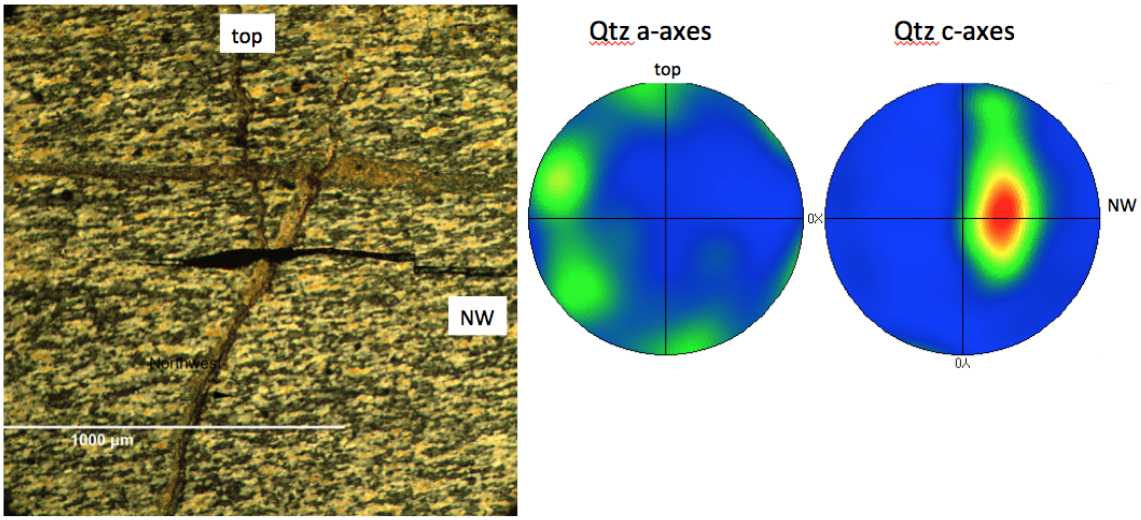


Figure 13. Left - Photomicrograph of mylonitic quartz vein at Brouses Corners showing clear top-NW sense of shear indicators such as the sigma-porphyroclast of hematite and a strong oblique grain shape foliation in quartz. Quartz dynamic recrystallization is dominated by sub-grain rotation (SBR) recrystallization. Field of view is ~1.4 mm. Right - Orientations of a and c-axes in quartz from this sample showing the development of a strong lattice preferred orientation (LPO). C-axes show a combination of single girdle and Y-axis maximum patterns indicating a combination of rhomb and prism <a> slip during deformation.

55.7 Continue north on Co Rd 27 (becomes Stone School- Waterman Hill Rd). Turn right onto Clare Town Line-Pierrepont Center Rd (Co Rd 24).
56.9 Turn right on Selleck Road.
57.9 On the right is the turnoff to the world-class Selleck Road mineral collecting locality, where spectacular tremolite, diopside, tourmaline, and other minerals can be collected from high grade marble on state land (Chamberlain et al., 2016).
60.7 On the left is the farm where Bruce Selleck grew up, and the one-room school-house where he attended Elementary School.
60.8 Turn right onto *Buck Pond Rd.*
62.0 Park on the right next to small outcrops.

**STOP 5: SYNTECTONIC LYON MOUNTAIN GRANITE WITH QUARTZ-SILLIMANITE SEGREGATIONS**

Buck Hill Road near Sellecks Corners (LAT-LONG 44.47166 -74.98360)

Numerous natural outcrops and small road cuts along Buck Pond Road expose quartz-microcline and quartz-mesoperthite leucogranite with common centimeter- to meter-scale quartz-sillimanite segregations, veins, and nodules. The leucogranite is locally gneissic with northwest-dipping banding. Quartz-sillimanite segregations (Figure 14) are commonly drawn out into elongate, cm-scale rods surrounded by equigranular quartz- mesoperthite granite. Sillimanite crystals form a mineral lineation in deformed segregations, but these oriented segregations are also crosscut by slightly later granitic veins that contain sillimanite. Sillimanite is often partially replaced by muscovite. Networks of quartz-sillimanite veins, quartz-sillimanite ribbons, and smaller quartz-sillimanite segregations and nodules are interpreted as representing progressively dismembered magmatic-hydrothermal features, forming via leaching of granite and granitic magma by Cl-rich, acidic fluids during granite pluton emplacement (McLelland et al. 2002). Equigranular, coarse, pegmatitic quartz-microperthite granite surrounds some quartz-sillimanite in strain sigmoids that indicate a top-down to the northwest transport. Outcrops of leucogranite south of Buck Pond Road are more massive and contain diffuse pegmatitic zones and quartz veins typical of the Lyon Mountain granite of the Adirondack Highlands. This quartz-sillimanite nodular granite is mappable for ~ 12 km along strike to the southwest as a 1-2 km wide belt immediately southeast of the mapped extent of the CCSZ.

This outcrop was sampled for U-Pb SHRIMP zircon geochronology (Selleck et al. 2005). Zircons were separated from coarse-textured quartz-microperthite granite that forms a 10-cm-thick band irregularly intrusive into quartz-sillimanite nodule–bearing quartz-microcline gneiss. Nine age determinations on well-developed, oscillatory-zoned rims (Figure 15) give a weighted mean age of 1046 ± 7 Ma. We interpret this result as documenting intrusion of 1046 Ma granite during active extension on the Carthage Colton shear zone at this site.

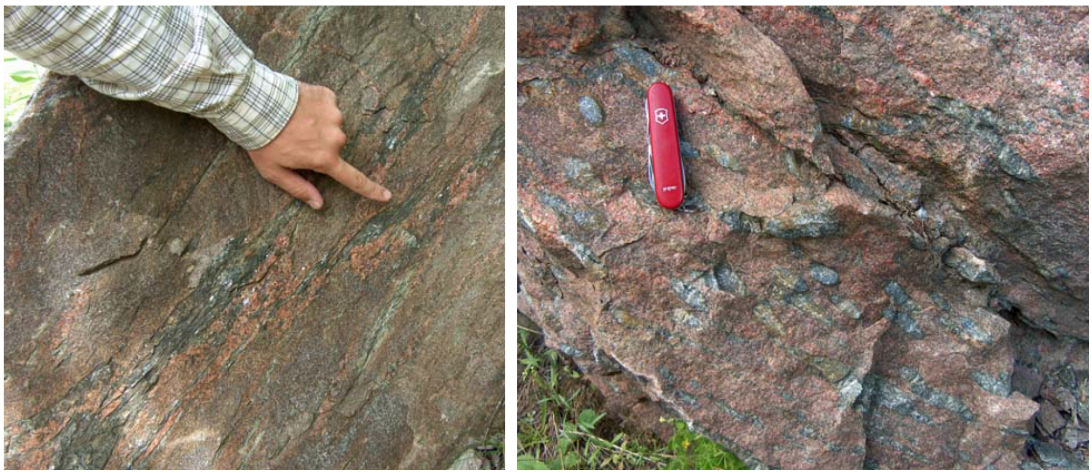

Figure 14. Left - σ−type strain marker formed by quartz-sillimanite segregation surrounded by equigranular leucogranite. View looking northeast; tectonic transport is top down to the northwest. Right - Quartz-sillimanite segregations in leucogranite. Q-S segregations are elongate nodules; long axes plunge NW. Note equigranular texture of granite between q-s segregations. Knife is ~12 cm long.

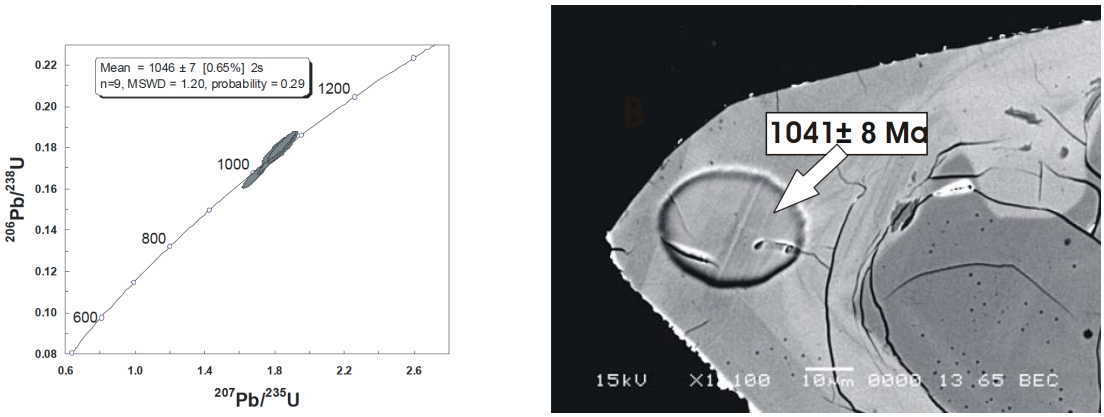


Figure 15. Left - Concordia plot of SHRIMP data from oscillatory-zoned igneous rims on zircons from leucogranite at Buck Pond Road. Right - BSE image of zircon showing SHRIMP analysis pit. Note the fine-scale zoning that is accentuated by ion beam milling.

Figure 16. Polished slab of quartz-sillimanite granite from Buck Pond Road locality showing relationships between quartz-sillimanite segregations, equigranular leucogranite, gneissic 'country rock' and quartz veins. Note magnetite within quartz-sillimanite nodule at right-center. Slab is approximately 25 cm wide.

*Thank you for joining us on this field trip in honor of the memory of Bruce Selleck.*
*Mileage to Lake George via Tupper Lake is 132 miles, two and a half to three hours drive.*
*The Welcoming Reception in Lake George is from 5:30 to 8:00 PM.*

## REFERENCES

Bonamici, C.E., Fanning, C.M., Kozdon, R., Fournelle, J.H., and Valley, J.W., 2015, Combined oxygen-isotope and U-Pb zoning studies of titanite: New criteria for age preservation: Chemical Geology, v. 398, p. 70-84.

Chamberlain, S.C., King, V.T., Cooke, D., Robinson, G.W., and Holt, W., 1999, Minerals of the Gouverneur Talc Company Quarry (Valentine Deposit), Town of Diana, Lewis County, New York: Rocks & Minerals, v. 74, no. 4, p. 236-249.

Chamberlain, S.C., Robinson, G.W., Walter, M.R., and Bailey, D.G., 2016, The Selleck Road Tremolite and Tourmaline Locality, West Pierrepont, St. Lawrence County, New York: Rocks & Minerals, v. 91, no. 2, p. 116-131.

Chiarenzelli, J., Selleck, B., Lupulescu, M., Regan, S., Bickford, M., Valley, P., and McLelland, J., 2017, Lyon Mountain ferroan leucogranite suite: Magmatic response to extensional thinning of overthickened crust in the core of the Grenville orogen: GSA Bulletin, v. 129, no. 11-12, p. 1472-1488.

Gerdes, M., and Valley, J., 1994, Fluid flow and mass transport at the Valentine wollastonite deposit, Adirondack Mountains, New York State: Journal of Metamorphic Geology, v. 12, no. 5, p. 589-608.

Hamilton, M.A., McLelland, J., Selleck, B., Tollo, R., Corriveau, L., and Bartholomew, M., 2004, SHRIMP U-Pb zircon geochronology of the anorthosite-mangerite-charnockite-granite suite, Adirondack Mountains, New York: Ages of emplacement and metamorphism. *in* Tollo, R., Corriveau, L., McLelland, J. and Bartholomew, M., eds., Proterozoic Tectonic Evolution of the Grenville Orogen in North America, Geological Society of America Memoir 197, p. 337-356.

Hargraves, R., 1969, A contribution to the geology of the Diana syenite gneiss complex: Origin of Anorthosite and Related Rocks: New York Museum Science Service Memoir 18, p. 343-356.

Heumann, M.J., Bickford, M., Hill, B.M., McLelland, J.M., Selleck, B.W., and Jercinovic, M.J., 2006, Timing of anatexis in metapelites from the Adirondack lowlands and southern highlands: A manifestation of the Shawinigan orogeny and subsequent anorthosite-mangerite-charnockite-granite magmatism: Geological Society of America Bulletin, v. 118, no. 11-12, p. 1283-1298.

Higgins, M.D., Beisswenger, A., and Hoy, L.D., 2001, Geochemistry and oxygen isotopic composition of the Canton Saint-Onge wollastonite deposit, central Grenville Province, Canada: Canadian Journal of Earth Sciences, v. 38, no. 8, p. 1129-1140.

Holland, T., and Blundy, J., 1994, Non-ideal interactions in calcic amphiboles and their bearing on amphibole - plagioclase thermometry: Contributions to Mineralogy and Petrology, v. 116, no. 4, p. 433-447.

Johnson, E.L., and Selleck, B.W., 2005, The nature and significance of the Carthage-Colton Shear Zone and related late- to post-tectonic granites and ore deposits; Adirondack Mountains, New York , Friends of the Grenville Annual Field Trip Guidebook, 46 p.

Johnson, E.L., Goergen, E.T., and Fruchey, B.L., 2004, Right lateral oblique slip movements followed by post-Ottawan (1050-1020 Ma) orogenic collapse along the Carthage-Colton shear zone: Data from the Dana Hill metagabbro body, Adirondack Mountains, New York. *in* Tollo, R., Corriveau, L., McLelland, J. and Bartholomew, M., eds., Proterozoic Tectonic Evolution of the Grenville Orogen in North America, Geological Society of America Memoir 197, p.357-378.

Law, R. D., 2014, Deformation thermometry based on quartz c-axis fabrics and recrystallization microstructures: A review: Journal of Structural Geology, v. 66, p. 129-161.

McLelland, J., Morrison, J., Selleck, B., Cunningham, B., Olson, C., and Schmidt, K., 2002, Hydrothermal alteration of late-to post-tectonic Lyon Mountain Granitic Gneiss, Adirondack Mountains, New York: Origin of quartz–sillimanite segregations, quartz–albite lithologies, and associated Kiruna-type low-Ti Fe-oxide deposits: Journal of Metamorphic Geology, v. 20, no. 1, p. 175-190.

McLelland, J.M., Bickford, M., Hill, B.M., Clechenko, C.C., Valley, J.W., and Hamilton, M.A., 2004, Direct dating of Adirondack massif anorthosite by U-Pb SHRIMP analysis of igneous zircon: Implications for AMCG complexes: Geological Society of America Bulletin, v. 116, no. 11-12, p. 1299-1317.

McLelland, J., Chiarenzelli, J., Whitney, P., and Isachsen, Y., 1988, U-Pb zircon geochronology of the Adirondack Mountains and implications for their geologic evolution: Geology, v. 16, no. 10, p. 920-924.

McLelland, J.M., and Chiarenzelli, J.R., 1990, Geochronological studies in the Adirondack Mountains and the implications of a middle Proterozoic tonalitic suite: Special Paper - Geological Association of Canada, v. 38, p. 175-194.

Mezger, K., Rawnsley, C., Bohlen, S., and Hanson, G., 1991, U-Pb garnet, sphene, monazite, and rutile ages: implications for the duration of high-grade metamorphism and cooling histories, Adirondack Mts., New York: The Journal of geology, v. 99, no. 3, p. 415-428.

Mezger, K., Van Der Pluijm, B., Essene, E., and Halliday, A., 1992, The Carthage-Colton mylonite zone (Adirondack Mountains, New York): The site of a cryptic suture in the Grenville orogen?: The Journal of geology, v. 100, no. 5, p. 630-638.

Peck, W.H., 1996, Stable isotope geochemistry of Precambrian anorthosite [M.S. thesis], University of Wisconsin--Madison, 96p.

Peck, W.H., DeAngelis, M.T., Meredith, M.T., and Morin, E., 2005, Polymetamorphism of marbles in the Morin terrane, Grenville Province, Quebec: Canadian Journal of Earth Sciences, v. 42, no. 10, p. 1949-1965.

Rivers, T., 2011, Upper-crustal orogenic lid and mid-crustal core complexes: signature of a collapsed orogenic plateau in the hinterland of the Grenville Province: Canadian Journal of Earth Sciences, v. 49, no. 1, p. 1-42.

Selleck, B.W., McLelland, J.M., and Bickford, M., 2005, Granite emplacement during tectonic exhumation: The Adirondack example: Geology, v. 33, no. 10, p. 781-784.

Streepey, M., Johnson, E., Mezger, K., and Van Der Pluijm, B., 2001, Early history of the Carthage-Colton shear zone, Grenville Province, Northwest Adirondacks, New York (USA): The Journal of geology, v. 109, no. 4, p. 479-492.

Stipp, M., StuÈnitz, H., Heilbronner, R., & Schmid, S. M. (2002). The eastern Tonale fault zone: a 'natural laboratory' for crystal plastic deformation of quartz over a temperature range from 250 to 700 C: Journal of Structural Geology, v. 24(12), p. 1861-1884.

Tyler, R., 1980, Chloride metasomatism in the southern part of the Pierrepont Quadrangle: Adirondack Mountains, New York [Ph.D.thesis], State University of New York at Binghamton, Binghamton, New York, 527p.

Valley, J., and O'Neil, J.R., 1982, Oxygen isotope evidence for shallow emplacement of Adirondack anorthosite: Nature, v. 300, no. 5892, p. 497-500.

# STRUCTURAL AND STRATIGRAPHIC FEATURES OF THE TACONIC FORELAND, NW VERMONT

By

Adam Schoonmaker[1], Department of Geosciences, Utica College, Utica, NY 13502
William S.F. Kidd[2], formerly of Geological Sciences, University at Albany, Albany, NY 12222
Email addresses: [1]adschoon@utica.edu, [2]wkidd@albany.edu

## INTRODUCTION

This trip will focus on some of the spectacular structural and stratigraphic features exposed in NW Vermont at the Highgate Gorge, and at Lessor's Quarry, and the outcrop known as "The Beam", on South Hero Island. The last two are Rolfe Stanley Memorial outcrops. The trip will cover the nearly continuously exposed upper Cambrian to Ordovician section in the Highgate Gorge. This section exposes the shelf to basin transition including bedded limestone and massive dolomite, a spectacular shelf slope limestone breccia, as well as basinal slates containing likely turbidite-transported carbonate shelf beds. The out-of-sequence cataclastic Highgate Falls Thrust is well-exposed, as well as a number of other Taconic-aged structures including folds, axial plane cleavage, and rotated en echelon fractures. The "Beam" is a superb meso-scale illustration of duplex faulting in thin-skinned foreland belts, while Lessors Quarry exposes fault-bend fold structures as well as a number of fault zone features, and an excellent example of an out-of-sequence thrust. This trip is highly recommended for students to see a number of well-exposed and instructive stratigraphic and structural features. Part of this material has appeared in a previous NEIGC field trip (Schoonmaker and Kidd, 2009).

***Walking in the gorge can be treacherous and difficult both on the boulder field in the channel and the outcrop; both may be very slippery if wet. Care should be observed, and adequate footwear is advised.***

### Regional Geology

The Highgate area exposes rocks that were previously correlated to the Stanbridge Nappe of Southern Quebec and include shelf and shelf edge rocks on the west, passing upward and eastward in the exposed section to basinal shales including carbonate shelf-derived beds. Similar changes from shelf to basin have been mapped in a generally north-south direction (Shaw, 1958; Mehrtens and Dorsey, 1987) leading to the proposal of a small depositional basin ("Franklin Basin" and "St. Albans Reentrant, respectively) in northwestern Vermont. In Quebec, the overlying shales (now slates) of the Stanbridge Group are interpreted to be part of an allochthon (Stanbridge Nappe) that is in fault contact with the underlying carbonate shelf units along a tectonically significant thrust fault (Charbonneau, 1980; Globensky, 1981). In Vermont, the slates are in depositional contact with the underlying shelf and slope section. The Highgate Gorge exposes an excellent section of shelf slope deposits overlain by deeper water shales.

Stanbridge Nappe of Southern Quebec. Adjacent to the International Border, in southern Quebec (Figure 1), the east-dipping Ordovician-aged Stanbridge Nappe has previously been interpreted to be an allochthonous group of carbonates and argillaceous slates derived from the Laurentian continental rise, which was detached and thrust over the upper Cambrian Milton Dolomite, part of the imbricated, parauthochthonous Laurentian shelf, along a major, structural boundary (St. Julien and Hubert, 1975; Charbonneau, 1980; Globensky, 1981). Although it is not exposed, the western boundary of the Stanbridge Complex comprises the southernmost section of Logan's Line in Quebec.

The Stanbridge Nappe is the southernmost of the Quebec Allochthons, part of the larger belt of allochthons that extend discontinuously from Newfoundland, across to the Gaspé and southwards to just across the International Border in northwestern Vermont; the allochthons reappear in west-central Vermont and continue southwards as the Taconic Allochthons. They are generally composed of far-traveled low-grade metamorphosed deep-marine mud-rocks and clastics originally deposited on the Laurentian continental lower slope and rise, and thrust westward, up and over the Laurentian shelf. The two belts are separated by parauthochthonous carbonate and siliciclastic rocks deposited on the Laurentian shelf and upper slope, that were subsequently imbricated during the Taconic Orogeny (e.g. the Champlain Thrust). While these parauthochthonous rocks have undergone transport along thrust faults, they are still in structural contact with related rocks deposited in a similar setting (e.g. the continental shelf), This contrasts with the allochthons that have seen significant transport from an original lower slope and rise setting and are now structurally emplaced against shelf rocks. All of the Quebec allochthons are structurally emplaced on top of younger rocks, and many are floored by flysch that in places contains olistostromal units.

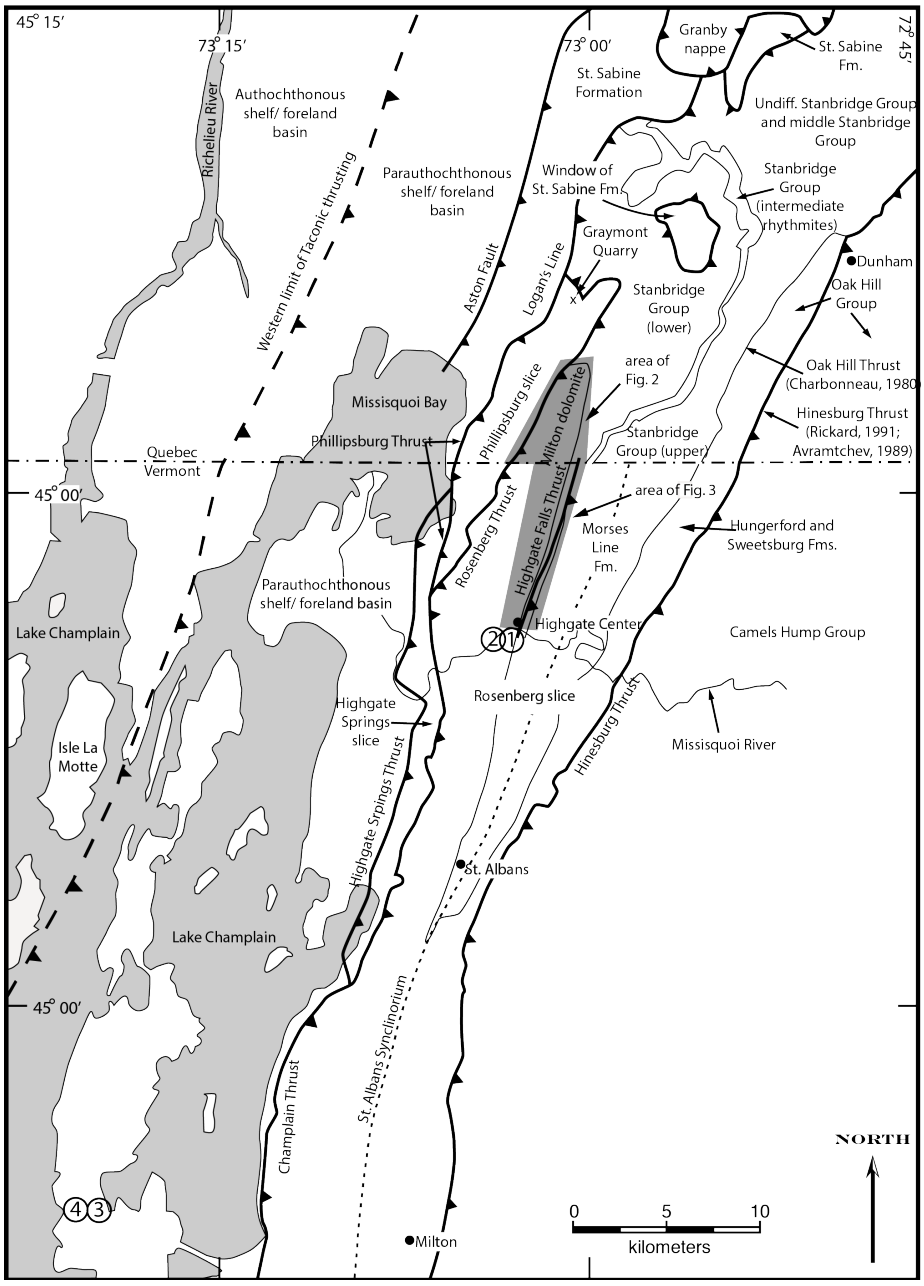


Figure 1. Regional map of significant structures and lithologic units in northwestern Vermont and southern Quebec. Based in part on Doll et al. (1961), Fisher (1968), Charbonneau (1980), Globensky (1981), and Avramtchev (1989).

The Stanbridge Nappe is composed of the dominantly argillaceous Stanbridge Complex of Charbonneau (1980; Figures 1and 2). The complex is divided into three sequences: 1) the lower sequence, composed of bedded slaty limestone and limestone conglomerates, overlain by thick sequences of bedded calcareous slate with sparse individual limestone beds and ribbon limestone bed sequences (usually not more than a few meters thick); 2) an intermediate rhythmite unit, composed of thinly laminated siltstone-argillite-mudstone beds; and 3) an upper sequence of calcareous slate, slaty limestones and calcareous conglomerates. The entire complex is an internally

coherent package that structurally overlies massive dolomites, chert-bearing and sandy dolomites, and dolomitic conglomerates of the Milton Dolomite along an unnamed (and unobserved) thrust fault. The Milton Dolomite (a term abandoned south of the International Border) is the northern extension of the Dunham Dolomite, and Saxe Brook and Gorge formations of northwestern Vermont, and is part of the imbricated carbonate-siliciclastic shelf sequence. The inferred structural relationship between the slaty Stanbridge Complex and underlying non-slate-bearing shelf carbonates is first reported in St. Julien and Hubert (1975) who include the bedded limestones of the lower sequence of the Stanbridge Complex as part of the transported Stanbridge Nappe. Significantly, the Stanbridge Complex does not contain flysch or olistostromes, and structurally overlies older, or approximately coeval rocks of the Rosenberg and Phillipsburg slices (Figure 1).

**Correlative rocks in Northwestern Vermont.** In Vermont, the lower slaty limestones and overlying calcareous slates of the lower unit of the Stanbridge Nappe are correlated with the Highgate and Morses Line Formations, respectively (Figure 4; Charbonneau, 1980; Globensky, 1981; Schoonmaker, 2007). The intermediate rhythmite and upper sequence correlate with higher sections of the Morses Line Formation above the Corliss Conglomerate, an internal member of the Morses Line Formation. Underlying the Highgate Formation are a series of massive dolomites, sandy dolomites, and dolomite breccias, including the Dunham, Saxe Brook, and Gorge Formations (in ascending order), all part of the Rosenberg Slice of Clark (1934) and equivalent to the Milton Dolomite in Quebec (Figure 3). These dolomitic units beneath the Highgate Formation have long been assigned to the imbricated shelf sequence of the Champlain Thrust slice (e.g. Stanley and Ratcliffe, 1985).

Previous workers in Vermont are divided on the presence of a major structural boundary in this section. Mehrtens and Dorsey (1987), and Schoonmaker and Kidd (2007) have interpreted the contacts between the Gorge and Highgate, and Highgate and Morses Line Formation to be conformable, and it is similarly shown on the Centennial Map of Doll et al. (1961) and the more recent bedrock Geological Map (Ratcliffe et al, 2011). Shaw (1958) and Pingree (1982) placed a thrust fault at the contact between the Highgate Formation and Morses Line Slates, while Haschke (1994) placed a normal fault at that same position. However, all these workers concluded that that bedded limestones and limestone breccias of the Highgate Formation were deposited on top of the dolomites and dolomitic breccias of the Gorge Formation. This contrasts with the interpretation in Quebec where the base of the bedded limestones and limestone breccias (Highgate Formation) is interpreted to be in thrust fault contact with the underlying dolomites and dolomitic breccias of the Milton Dolomite (Gorge Formation).

We will observe the contact relationships between the dolomitic units of the Gorge Formation and overlying bedded limestones and limestone breccias of the Highgate Formation (Stop 2), as well as the overlying partly calcareous slates, previously referred to as the Highgate Slate (e.g. Keith, 1923), but which we reclassify as the lower part of the Morses Line Formation. These are beautifully exposed in the Highgate Falls Gorge (Stop 1; Figures 3 and 5). The relationships we will observe show that the Highgate and Morse Line formations are internally conformable (with the exception of minor thrusts, and the younger, out-of-sequence Highgate Falls Thrust) and depositionally overlie the shelf-derived dolomitic Gorge Formation.

**Thin-skinned imbrication of the continental shelf.** At stops 3 and 4 we will observe excellent examples of imbricate duplexes formed in the thin-skinned Taconic foreland fold-thrust belt. The structures that can be observed include roof and floor faults, flat and ramp sections, horses, variably rotated en echelon fractures, slickenlines and slickensides, and fault-bend folds.

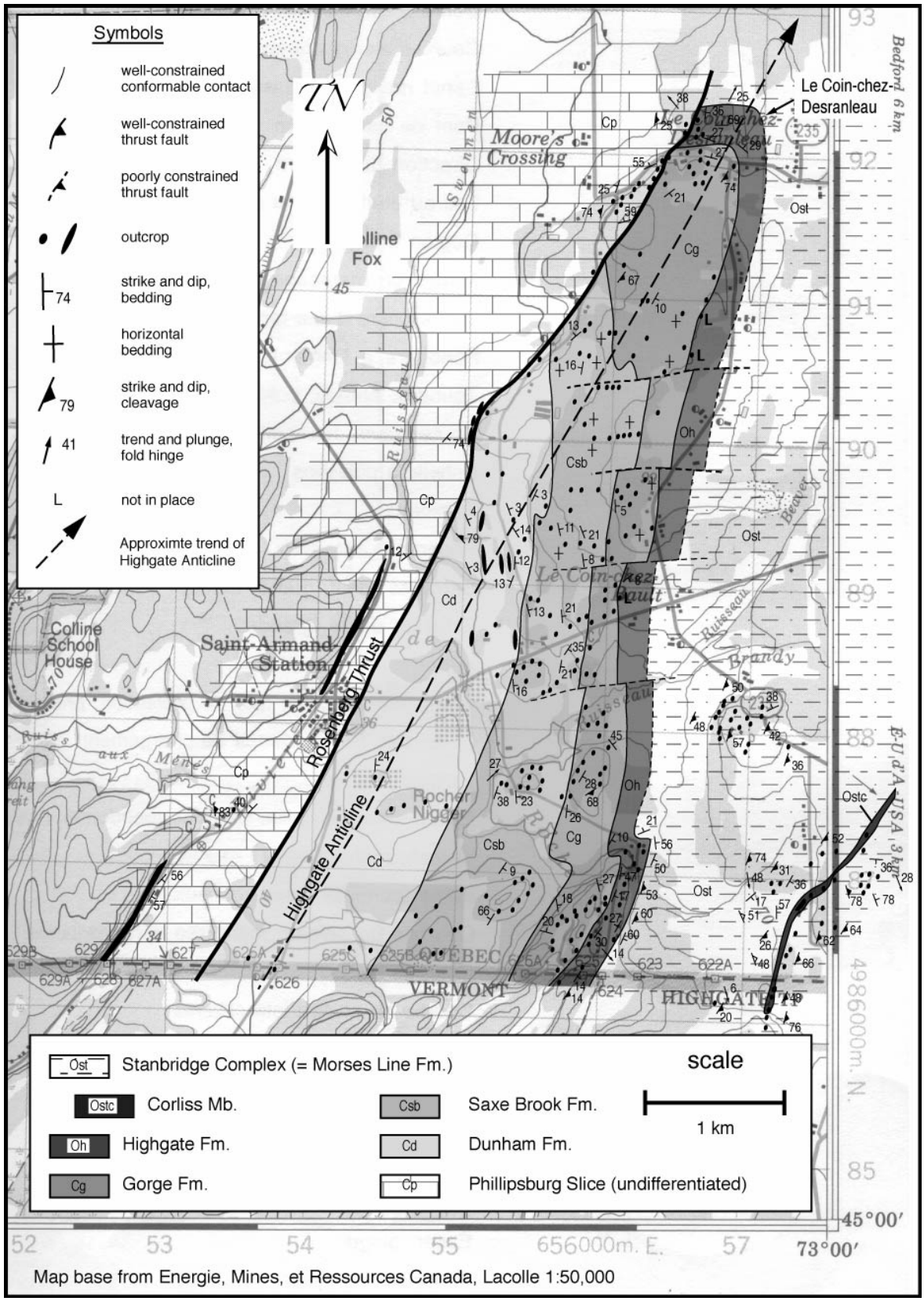


**1**

Figure 2. Geologic map, St. Armand Station area, southern Quebec. (Schoonmaker and Kidd, 2007)

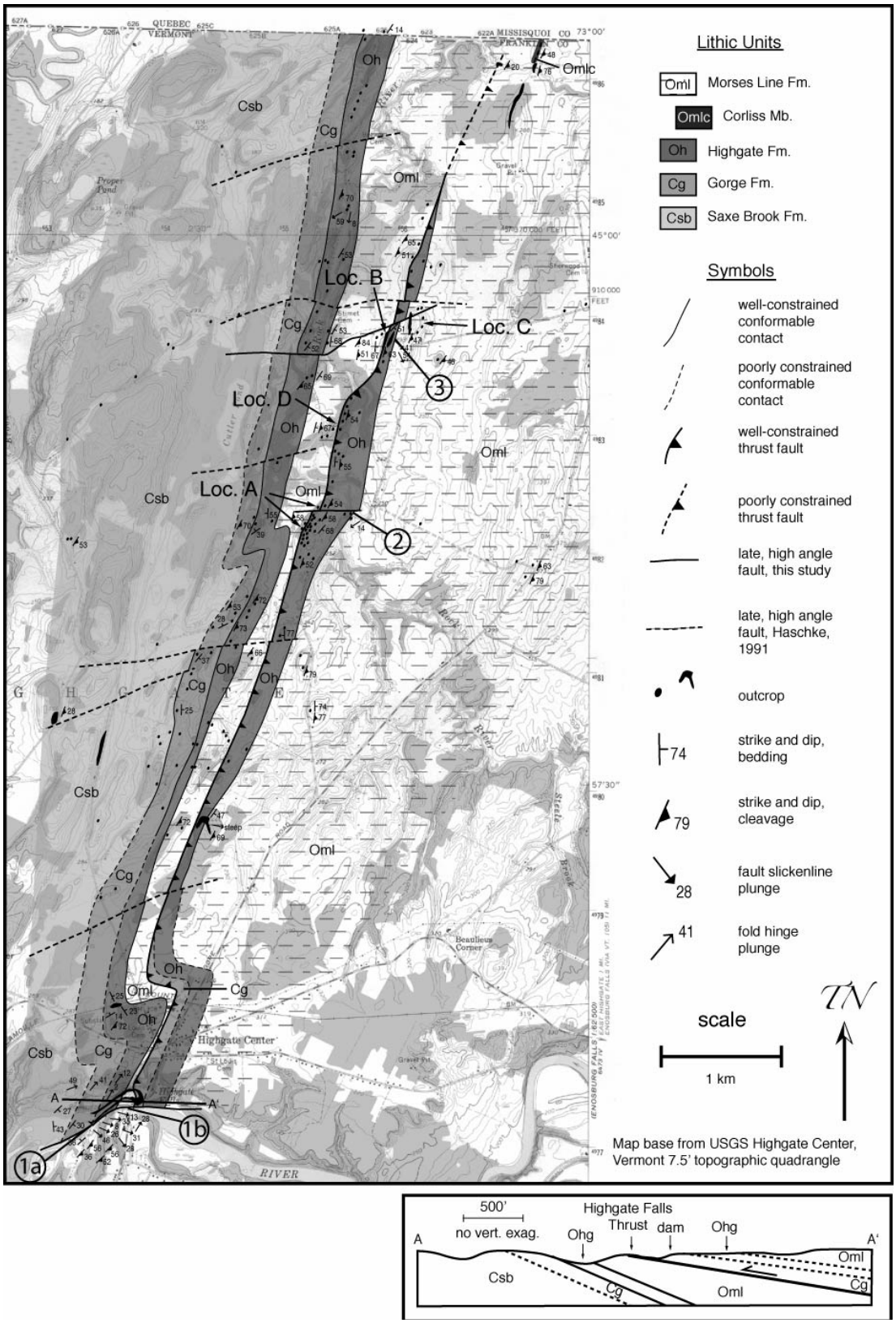


Figure 3. Geologic map, Highgate Center area, Vermont. (Schoonmaker and Kidd, 2007)

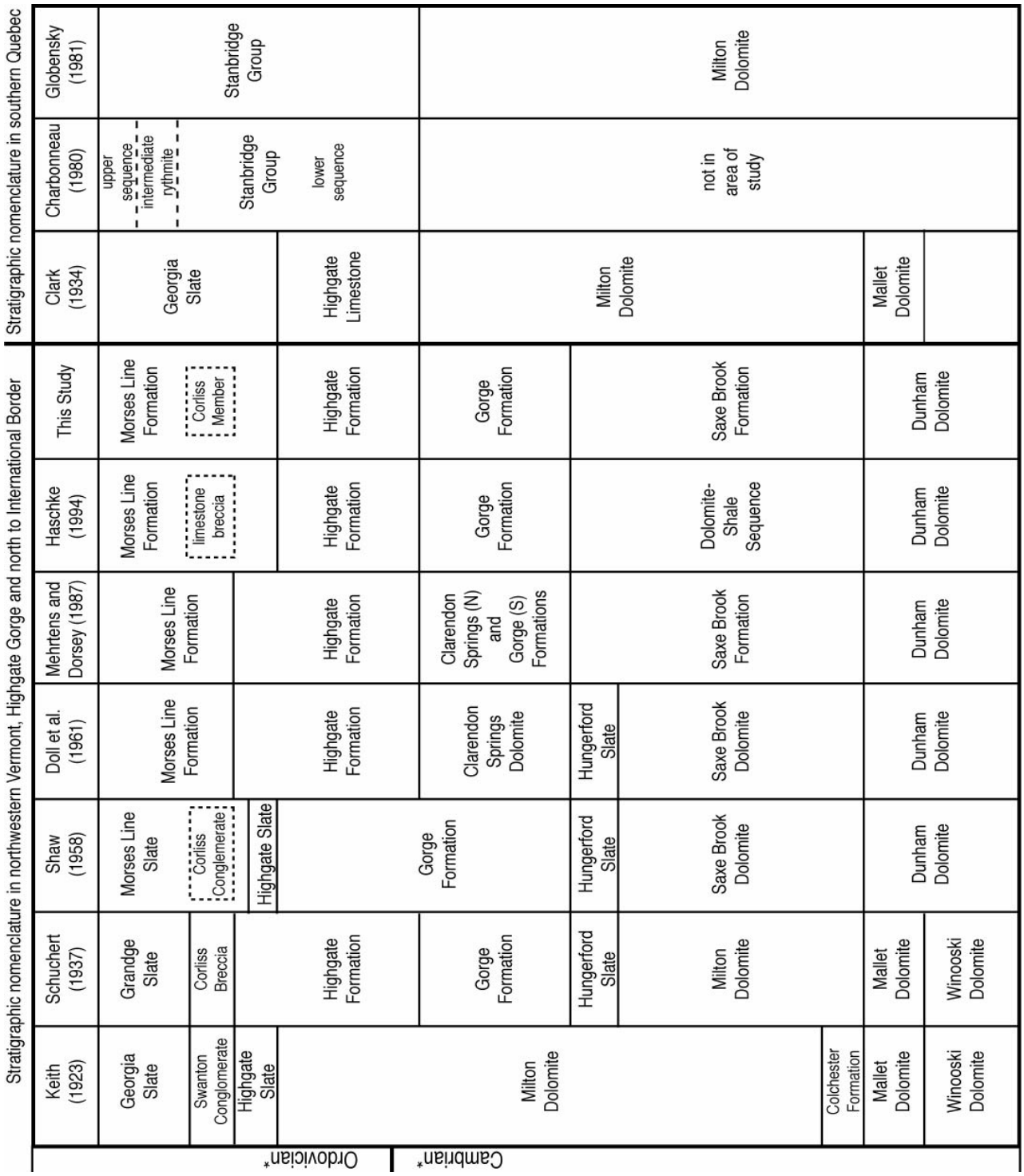


Figure 4. Lithostratigraphic correlation chart of the Cambrian through Middle Ordovician formations of the Rosenberg slice (Schoonmaker and Kidd, 2007). * Cambrian-Ordovician boundary located after Landing (1983) as it applies to our study and does not necessarily represent placement of this boundary by other workers.

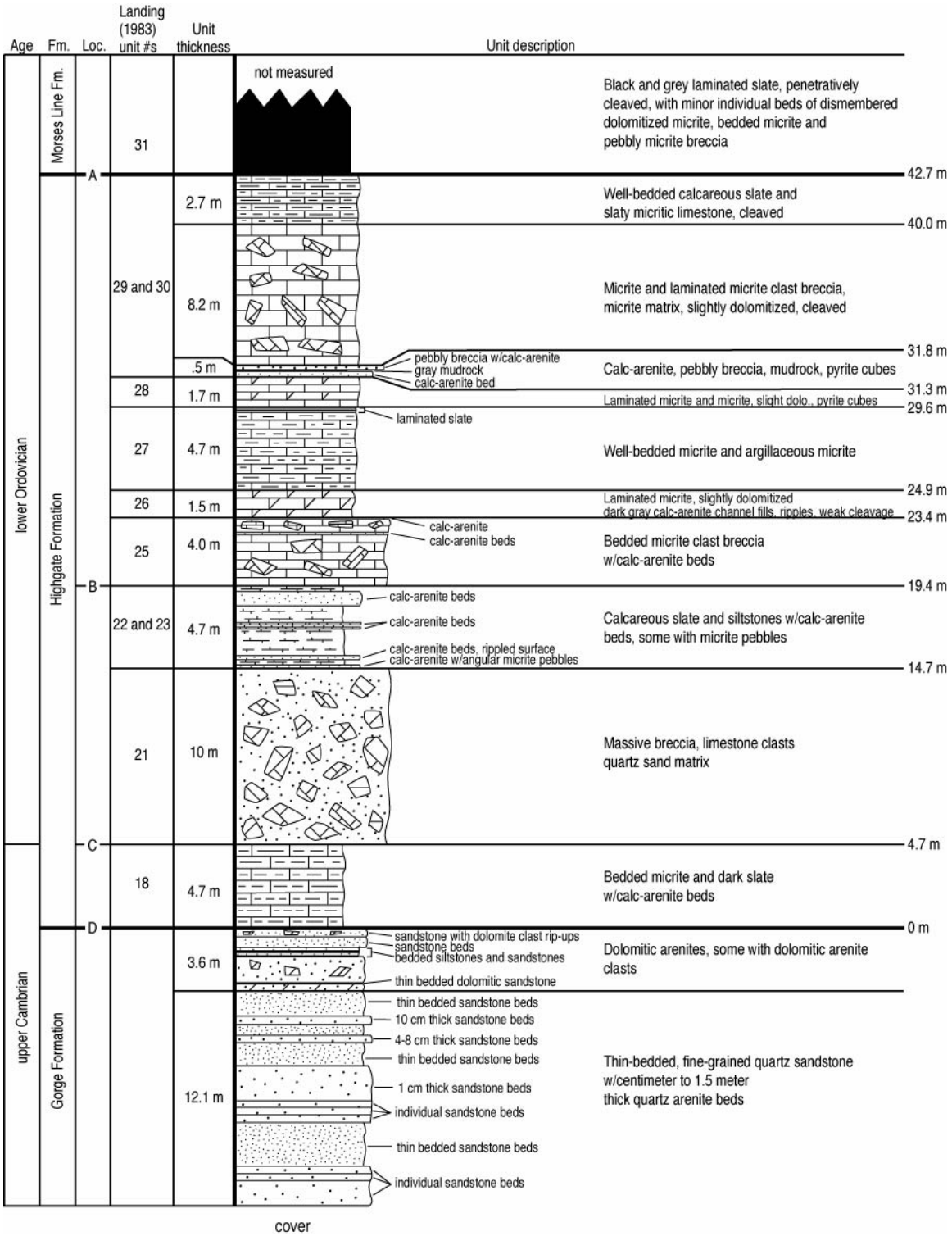


Figure 5. Measured detailed lithostratigraphy of part of the continuously exposed section on the north shore of the Mississquoi River gorge at Highgate Center (Schoonmaker and Kidd, 2007). Cambrian-Ordovician boundary from Landing (1983).

## ROAD LOG

**Assembly Point** – Price Chopper Parking Lot, Prosser Road (off of Rt. 9), Warrensburg. We will consolidate vehicles and proceed to the village green at Highgate Center VT, approximately 2.5 hours travel time via Interstate 87 North.

For some, it may be more convenient to meet in Highgate Center. Those folks can meet us at the village green in Highgate Center at about 10:30 am.

**Time:** 8:00 am, Friday, October 12th, 2018.

**MILEAGE**

| Miles | Incr. | Directions |
|---|---|---|
| 0.0 | 0.0 | Exit parking lot and take right onto Prosser Road. |
| 0.1 | 0.1 | Turn left onto Bakers Crossing. |
| 0.2 | 0.1 | Turn left onto US 9. |
| 0.3 | 0.1 | Turn right onto Diamond Point Road (crosses over I-87). |
| 0.5 | 0.2 | Turn left onto entrance ramp for Interstate 87 North. |
| 115.5 | 115 | Take Exit 42 (Rouses Point and US Rt. 11). |
| 115.6 | 0.1 | Turn right onto US Rt. 11. |
| 120.3 | 4.7 | Turn left staying on US Rt. 11 and State Rt. 9B. |
| 121.5 | 1.2 | Turn right onto Bridge Road (US Rt. 2). Cross bridge into Vermont. |
| 128.5 | 7.0 | Turn left onto VT Rt. 78. |
| 143.1 | 14.6 | Turn right onto Lamkin St. Pull over next to village green for a bathroom/coffee break. |
| 143.4 | 0.3 | Continue straight and immediately bear right onto Mill Hill Road. Park at bottom of hill at terminus of pedestrian bridge and hydroelectric dam. A nice view of the gorge can be seen from the pedestrian bridge including the Highgate Falls Thrust. Proceed by foot along canoe portage westward through the woods along the north side of the gorge for about 50 feet. Find trail on the left that leads down to the gorge floor below the dam. |

**CAUTION!**

**ACCESS TO GORGE FLOOR WILL REQUIRE SCRAMBLING DOWN STEEP ROCKS AND ONCE ON THE GORGE FLOOR, WALKING ON THE BOULDER FIELD CAN BE TREACHEROUS, ESPECIALLY WHEN WET.**

**PLEASE ALSO NOTE THAT IF HORN SOUNDS, EXIT GORGE AS QUICKLY AS POSSIBLE IN THE EVENT OF AN UNLIKELY, BUT POSSIBLE DAM RELEASE.**

**STOP 1: UPPER HIGHGATE FALLS GORGE.**
(N 44.93540°, W 73.04866°; NAD 83)

The Mississquoi River laps against the walls in part of the gorge, so it is cut into upper (Stop 1) and lower (Stop 2) sections with different access points.

The entire (both upper and lower) east-west oriented Highgate Falls Gorge on the Mississquoi River continuously exposes a cross-section (Figure 3) of upper Cambrian to lower Ordovician rocks that include the upper section of the Gorge Formation (dolomitic arenites and quartz sandstones), the entire Highgate Formation (a variable unit containing bedded micrite, limestone clast breccias, calcareous slate, and argillaceous micrite), and the lower part of the Morses Line Formation (argillaceous slates with dolomitized, boudinaged micrite beds, bedded micrite, and limestone breccias;). The Highgate Falls Thrust repeats part of this section (Gorge Fm.) in the part of the gorge nearest the dam. In the upper gorge we can see the upper part of the Highgate Formation, lower section of the Morses Line Formation, and part of the Gorge Formation above the Highgate Falls Thrust.

Once in the gorge, the Highgate Falls Thrust is clearly visible in the north wall, approximately 200' downstream from the point where the path descends (Figure 6E). A dolomite clast breccia with dolomitic matrix of the Gorge Formation is thrust over dark slates and a bedded argillaceous micrite and carbonate breccia interval within the Morse Line slates along a shallowly east-dipping surface characterized by phyllonitic fault zone cleavage (cataclastic breccia- to gouge-sized material); beds and cleavage in the lower block are bent in the direction of transport of the upper block. In the lower block, directly beneath the thrust, regional cleavage in the slates and bedded micrite can be seen to be bent as it approaches the fault zone indicating a westward sense of motion of the upper block. Because the regional cleavage is deformed by the motion of the upper block, the Highgate Falls Thrust is inferred to be an out-of-sequence thrust fault.

To the west and slightly downstream from the highway bridge that can be seen high above the gorge and upstream from the powerhouse and tailrace visible on the south bank, the contact between calcareous slates of the uppermost Highgate Formation are overlain by black slates of the Morses Line Formation (Loc. A, Figure 5). The contact on the north bank is mesoscopically folded and marked by a minor thrust fault containing a slickenlined and stepped calcite vein on the north limb (Figure 6C). On the south bank, the south limb is an observable depositional contact. Landing (1983) interpreted the micrite clast breccia (unit 29, Figure 5) that occurs beneath the calcareous slate as a tectonic breccia and the base of the black slates as an unnamed thrust. In contrast, Haschke (1994) suggested the slickensided surface on the north limb was a detachment that cut out a major thrust between the Highgate and Morses Line Formations, similar to relationships described by Hayman and Kidd (2002) for the northern part of the Taconic Allochthon. The observable conformable contact relationships on the south bank in the Highgate Falls Gorge do not support either of these hypotheses. Further, minor thrust faults are observed in the Morse Line slates (Figure 6D) and cleavage can also be seen in the Highgate Formation limestones, suggesting that a significant structural boundary is not present within this section, which contrasts to the Quebec and Taconic allochthons where deformation and cleavage deformation occurred prior to final emplacement (Rowley and Kidd, 1981; St. Julien, 1977; Lebel and Kirkwood, 1998).

Within the Morses Line Formation, dismembered dolomitized micrite beds can be observed, wrapped by the regional cleavage. Some of these beds are cut by small pre-cleavage faults with a normal sense of displacement. These normal faults are interpreted to be from passive continental margin downslope slumping. Similar dolomite beds in slate are observed further north in Vermont and in Quebec, well east of the strike of these beds, where they form part of the upper block of the Highgate Falls thrust and are mapped as Stanbridge Slates (Figure 3).

Structurally just below the Highgate Falls Thrust, there is a small fold of bedding in slate and thin limestone beds whose axial plane is parallel to the regional cleavage in the slates; this can be seen in the outcrop close to the river channel.

> Return to canoe portage on north bank of river and proceed westward (away from vehicles).
> Proceed approximately 250 yards and cross VT Rt. 207.
> Continue west along canoe portage.
> Follow canoe portage signs, descend to the riverbank. CAUTION! ABUNDANT POISON IVY ALONG SHORELINE.
> Walk upstream to the outcrop starting at a point slightly downstream from the turbine building of the Highgate Center Hydroelectric Plant on the far bank.

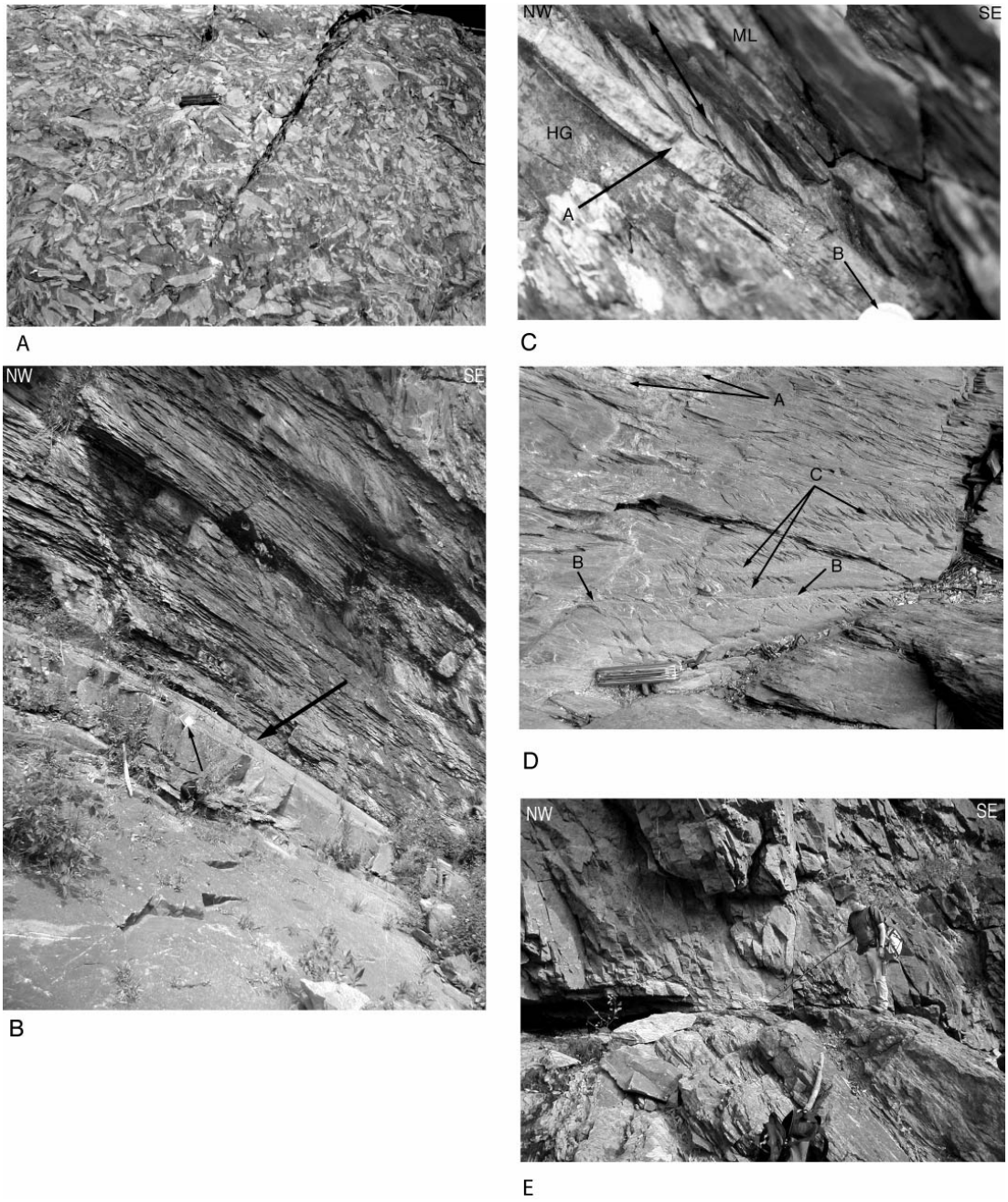


Figure 6. Field photos are all from the north bank of the Mississquoi River in the gorge at Highgate Center. A) The sedimentary breccia identified as "fault breccia" by Schuchert (1937). Pocketknife is 9 cm long. B) Large arrow indicates contact between the lowest beds of the Highgate Formation, above, and the uppermost sandstone bed of the Gorge Formation, below (Loc. D, Figure 5). Small arrow points to 15 cm tall notebook. C) Minor, locally impersistent thrust fault at contact between Highgate and Morses Line Formations. Arrow (A) = calcite slickenfiber vein, approximately 1 cm thick. Arrow (B) = dime for scale, only partially visible. Large bi-directional arrow indicates cleavage orientation. D) Minor thrust faults and en echelon fractures in Morses Line Formation. Arrow (A) points to deformed fault, slip surface parallels ground surface in photo. Arrows (B) indicate relatively undeformed planar thrust that cuts oblique to ground surface. Both faults are surrounded by extension fractures (arrows C). Pocketknife is 9 cm long. E) Highgate Falls Thrust exposed in the Mississquoi River Gorge. Geologist (A.S.) points to slip surface. Upper block moved to the west (left in photo). Photo courtesy of Marjorie Gale.

**STOP 2: LOWER HIGHGATE FALLS GORGE.**
(N 44.93372°, W 73.05165°; NAD 83)

The lower gorge displays the contact between the Gorge and Highgate Formations, slightly below the Cambrian-Ordovician boundary (Figures 3 and 4). Here, the depositional contact the Gorge Formation and the overlying Highgate Formation can be observed (Figure 3, Loc. D). In contrast, Landing (1983) placed the contact at Loc. B (Figure 3). Very similar argillaceous limestones and limestone breccias are present both below and above this level. We prefer to define the contact at the lower horizon (Figure 3, Loc. D; Figure 6B), which separates dolomitic sandstones below (Gorge Formation) from the argillaceous limestones and limestone breccias above (Highgate Formation), as a much more readily identifiable contact in the field and likely representing a significant change in depositional environment from sand-dominated carbonate deposition to shale-dominated carbonate deposition. Regardless of the placement of the Gorge-Highgate contact (Figure 3. Loc. D vs. Loc. B) within the Highgate Falls Gorge, no major structural boundary is observed in this section, up to the position of the out-of sequence Highgate Falls Thrust.

The contact is readily identifiable in the gorge by the abrupt change from thick-bedded dolomitic arenites of the Gorge Formation below, to thinner bedded argillaceous micrites and limestone breccias of the Highgate Formation above (Figure 6b). In Quebec, this contact is inferred to be a major fault boundary between the autochthonous shelf platform rocks (Milton Dolomite) and allochthonous, deep marine rocks (Stanbridge Complex).

Return along canoe portage to vehicles. Proceed back up hill along Mill Hill Road.

| | | |
|---|---|---|
| 143.7 | 0.3 | Turn left onto VT Rt. 78. |
| 143.9 | 0.2 | Turn left onto VT Rt. 207. |
| 150.9 | 7.0 | Turn left onto Interstate 89 South entrance ramp. |
| 170.5 | 19.6 | Take exit ramp 17 for US Rt. 2. |
| 170.6 | 0.1 | Turn right onto US Rt. 2. |
| 179.8 | 9.2 | Park on right side of Rt. 2 at McBride Lane (private drive). |

**STOP 3: "THE BEAM", A ROLFE STANLEY MEMORIAL OUTCROP.**
(N 44.65130°, W 73.31649°; NAD 83)

NO HAMMERS, PLEASE. "The Beam" is one of two Rolfe Stanley Memorial Outcrops visited on this trip. Over the years, many thousands of introductory geology students, as well as undergraduate and graduate students in Rolfe's structural geology courses have visited these sites. Both beautifully expose important features of foreland deformation, including thrust faulting, fault duplexes, fault bend folds, ramps and ramp faults, en echelon fractures and rotation, and pressure solution cleavage. Detailed descriptions and interpretation for both of these outcrops can be found in Stanley (1988).

"The Beam" occurs in the Cumberland Head Formation, and is a ~1 foot thick micrite bed sandwiched between calcareous shale, and is bounded by bedding parallel thrust faults that display slickensided and stepped calcite veins, and fault zone cleavage (Figure 7). The micrite bed is relatively uncleaved while the surrounding shale displays a strong, steeply east-dipping spaced pressure solution cleavage, similar to that seen throughout the region, containing clay selvedges. Along the thin fault zones, a fault zone cleavage dips more shallowly to the east. Near the fault zone, the spaced cleavage in the shale is rotated towards parallelism with the fault zone cleavage indicating westward transport along the thrust faults. This is consistent with fiber orientation and slickenside fracture steps developed within veins in the fault zones.

Several ramps have been cut through the micrite bed, merging with the bounding bedding-parallel floor and roof faults, creating several horsts. Ramp faults show progressive development from initial slight buckle folding, en echelon fracture formation along the west-dipping limb, and subsequent rotation and failure through the trace of the fractures. Some fractures show diachronous development where older fractures are rotated and cut by younger, unrotated ones. Fracture arrays dominantly dip to the east (west-climbing), parallel and are cut by ramps, but a few dip to the west (east-climbing) and are not cut by through-going faults.

Deformation in “the Beam” contrasts with that in the surrounding calcareous shale. “The Beam” has shortened through rigid body displacement along thrust faults with little cleavage development within the bed, and minor folding over the ramps (~13%), while shortening in the shale is accommodated by pressure solution development (~11-16%), with some minor bedding parallel faults present in the shale. Stanley (1988) interpreted the development of ramp faults to be time transgressive, from east to west across the outcrop. This diachronous shortening in “the Beam” was accompanied by a concurrent progressive pressure solution cleavage development from east to west in the surrounding shale (Figure 8).

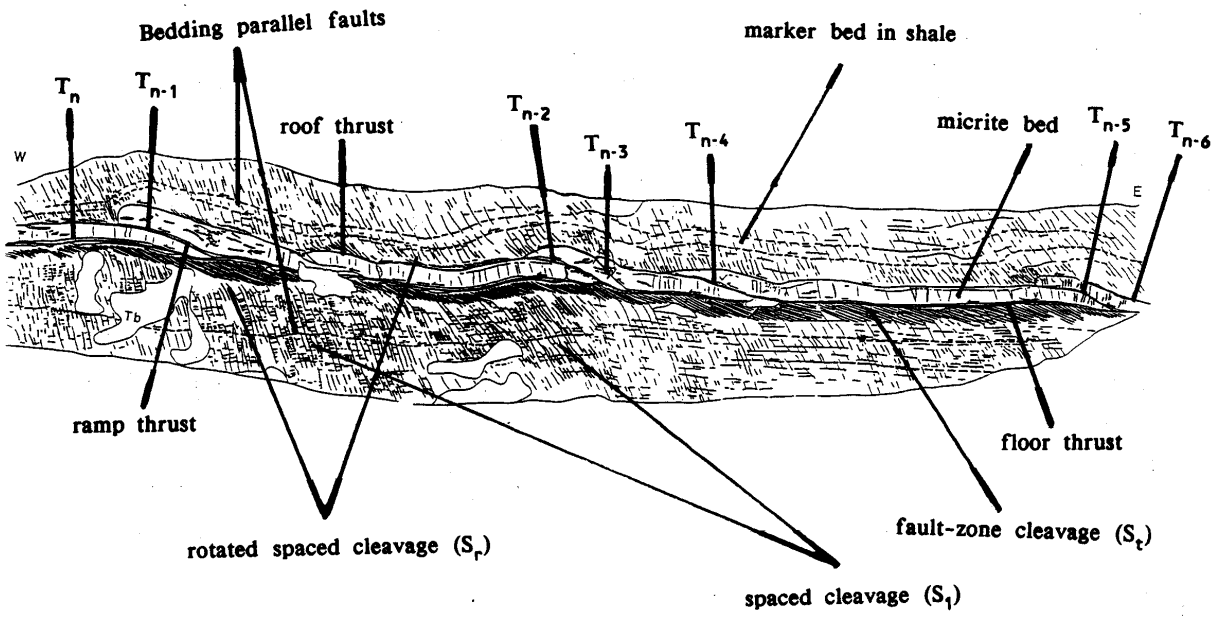


Figure 7. “The Beam” (view looking north). Duplex-faulted micrite bed surrounded by calcareous, cleaved shale. Modified from Stanley (1988). Ramp thrusts evolved from east to west, based on crosscutting fabrics in ramp, roof, and floor thrusts.

When traffic permits, turn out and continue north on US Rt. 2. Be prepared to make an immediate left.

| | | |
|---|---|---|
| 179.9 | 0.1 | Turn left onto Sunset View Road. |
| 180.5 | 0.6 | Turn left onto dirt track; this turn is just before high voltage power lines cross the road. |
| 180.6 | 0.1 | Park in small dirt area adjacent to old gravel quarry. |

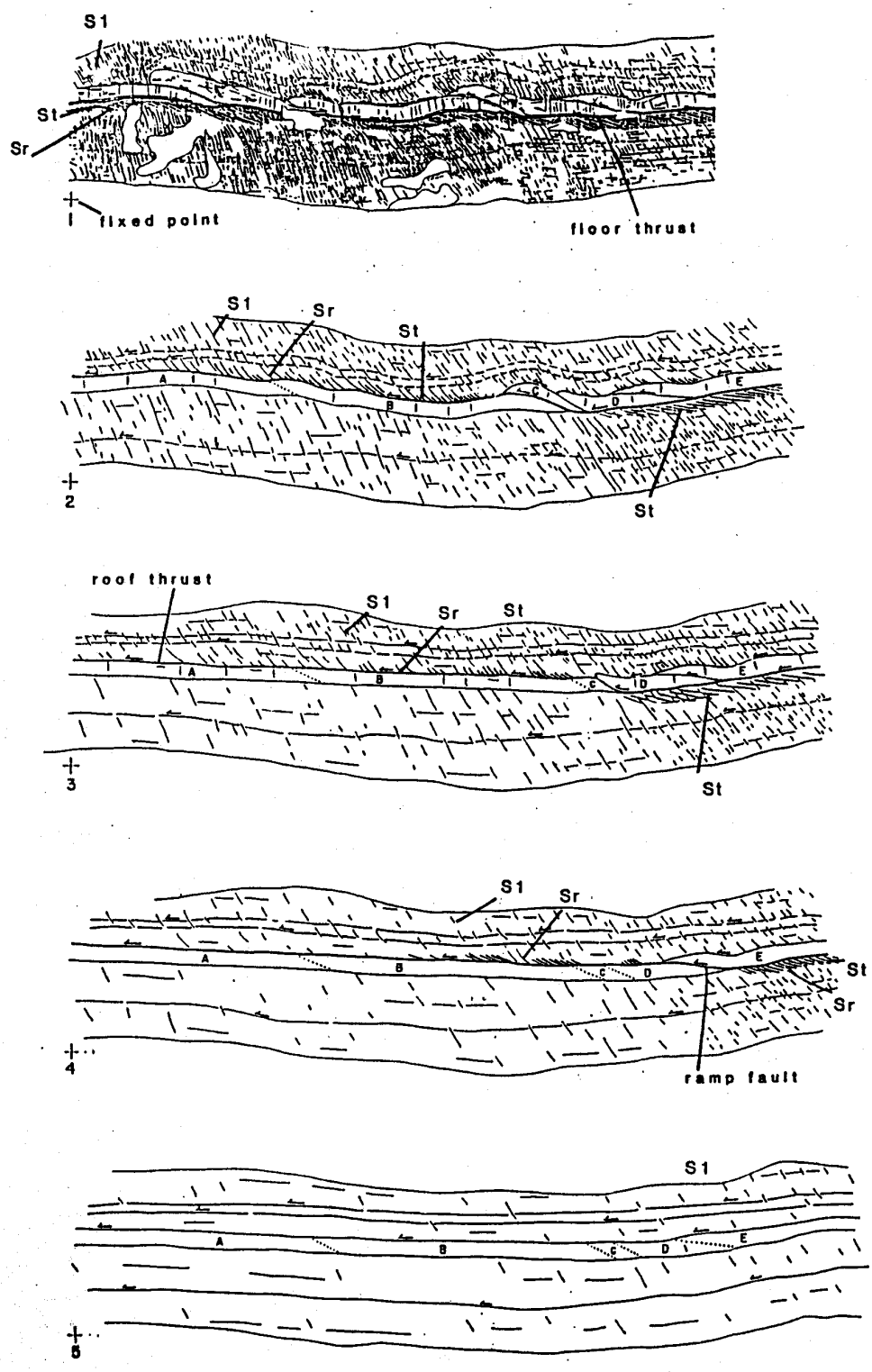


**RETRODEFORMED SECTION OF THE CUMBERLAND HEAD FORMATION**

Figure 8. Retrodeformation of the beam. Progressive pulling back of ramp thrust occurs from west to east accompanied by progressive decrease in cleavage development. From Stanley (1988).

**STOP 4: LESSOR'S QUARRY, A ROLFE STANLEY MEMORIAL OUTCROP.**
(N 44.64938°, W 73.32899°; NAD 83)

NO HAMMMERS PLEASE. There is plenty of loose material on the quarry floor to collect. Abundant fossils can be seen both in the walls of the quarry and in the loose debris. This is the second of two Rolfe Stanley Memorial Outcrops we will be visiting.

Lessor's Quarry exposes several bedding parallel and bedding cutting faults in the Glens Falls Limestone. The north wall displays several interesting features (Figure 9) including an out-of-sequence thrust that is both bedding parallel and bedding-cutting indicating that is preserves parts of its initial ramp and flat sections (labeled "Thrust Fault" in figure 9). It cuts an earlier folded thrust with fault splay and tip (labeled "Synformal Thrust Fault" in figure 9). The folding of the earlier thrust is thought to be the result of an unseen ramp beneath the quarry (Stanley, 1988); e.g. a fault bend fold similar to those seen in the roof thrusts at the "Beam". Since the younger through-going thrust cuts the earlier folded thrust, the younger thrust must be an out-of-sequence fault.

Also related to the younger out-of-sequence fault is the orientation of bedding in the block above the thrust. In the eastern part of the wall, bedding parallels the thrust, while in the middle parts of the north wall, bedding is truncated by the thrust. Then, in the western part of the wall, bedding returns to a parallel position (Figure 9). This suggests that the currently flat thrust in the middle of the wall, initially developed as a ramp, cutting bedding in the upper block. This part of the upper block was then transported off the ramp and onto a nearby flat section of fault, resulting in counterclockwise rotation of the upper block in this section. Note also, the spaced pressure solution cleavage in the upper block is rotated in a counterclockwise manner in the middle part of the wall, over the "ramp" section. Because the cleavage was rotated during movement, the fault must have evolved subsequent to cleavage development, consistent with its interpretation as an out-of-sequence fault (recall that the Highgate Falls Thrust also rotates cleavage).

Along the western wall, next to the entrance, is a steeply dipping fault surface decorated with smeared calcite where the upper block has been removed by quarry operations. It is abundantly lineated with slickenfibers; well-developed steps indicate an east-over-west sense of transport for the removed upper block.

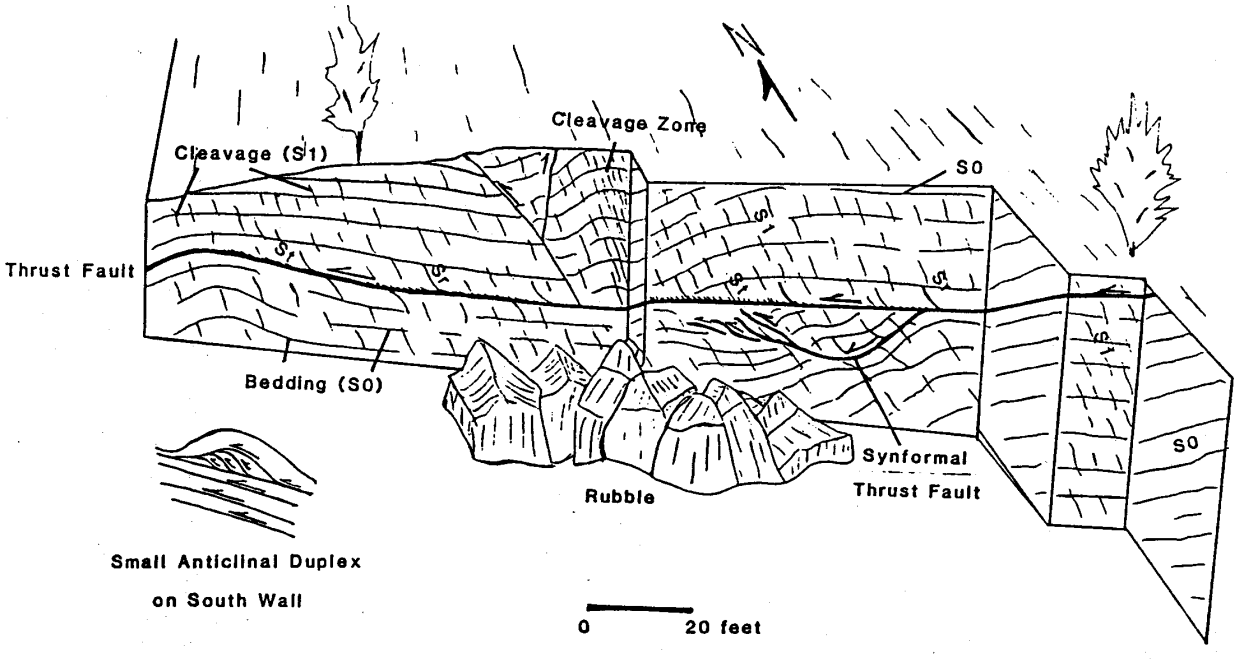


Figure 9. Lessor's Quarry, north wall. From Stanley (1988).

**END OF TRIP.**

**To return to Price Chopper Parking lot from Lessor's Quarry:**

| | | |
|---|---|---|
| | | Return to Sunset View Road. |
| 180.7 | 0.1 | Turn right onto Sunset View Road. |
| 181.3 | 0.6 | Turn right onto US Rt. 2 East. |
| 190.6 | 9.3 | Turn right onto I-89 South entrance ramp |
| 201.0 | 10.4 | Take Exit 13 to I-189 West |
| 202.2 | 1.2 | Take exit ramp to US Rt. 7. |
| 202.3 | 0.1 | Turn left onto US Rt. 7 South. |
| 221.3 | 19.0 | Turn right onto VT Rt. 22A South. |
| 229.1 | 7.8 | Turn right onto VT Rt. 17 West. |
| 237.5 | 8.4 | Cross bridge to NY. Continue on NY Rt. 185. |
| 241.6 | 4.1 | Turn left on to NY Rt. 9N South. |
| 246.2 | 4.6 | Turn right. Stay on Rt. 9N South. |
| 253.7 | 7.5 | Turn right onto NYS Rt. 74. |
| 271.1 | 17.4 | Turn left onto I-87 South entrance ramp. |
| 300.2 | 29.1 | Take Warrensburg Exit 23. |
| 300.5 | 0.3 | Turn right onto Diamond Point Road. |
| 300.6 | 0.1 | Turn left onto US Rt. 9 South. |
| 300.7 | 0.1 | Turn right onto Bakers Crossing. |
| 300.8 | 0.1 | Turn right onto Prosser Road. |
| 300.9 | 0.1 | Turn left into Price Chopper parking lot. |

## REFERENCES

Avramtchev, L. 1989. Carte des gîtes minéraux des Appalaches, re- gion des Basses-terres du Saint-Laurent et Estrie–Beauce. Ministère de L'Énergie et des Ressources, Québec, DV 87-19, map scale 1:250 000.

Charbonneau, J-M., 1980, Region de Sutton: Ministere de L'Energie et des Ressources DPV-681, 89 p., 1 pl.

Globensky, Y., et al., 1993, Lexique Stratigraphique Canadien, Région des Appalaches, des Basses Terres du Saint Laurent et des îles de la Madeleine: Ministere de l'Energie et des Ressources du Quebec, DV 91-23, 327 p

Haschke, M. R., 1994, The Champlain thrust fault system in northwestern Vermont—structure and lithology of the Taconic foreland sequence in the Highgate Center quadrangle [Unpublished M.Sc. thesis]: State University of New York at Albany, Albany, New York, 124 p., 3 pl.

Hayman, N. M., and Kidd, W. S. F., 2002, Reactivation of prethrusting, synconvergence normal faults as ramps within the Ordovician Champlain–Taconic thrust system: Geological Society of America Bulletin, v. 114, p. 476-489.

Landing, E., 1983, Highgate Gorge: Upper Cambrian and Lower Ordovician continental slope deposition and biostratigraphy, northwestern Vermont: Journal of Paleontology, v. 57, p. 1149-1187.

Lebel, D., and Kirkwood, D., 1998, Nappes and mélanges in the Quebec-Bellechasse area: Their regional tectonic and stratigraphic significance in the Humber zone: Geological Association of Canada/Mineralogical Association of Canada, Fieldtrip Guidebook, 64 p.

Mehrtens, C. J., and Dorsey, R. J., 1987, Stratigraphy and bedrock geology of the northwestern portion of the St. Albans quadrangle and the adjacent Highgate Center quadrangle, Vermont: Vermont Geological Survey Special Bulletin No. 9, 28 p., 2 pl.

Ratcliffe, N.M., Stanley, R.S., Gale, M.H., Thompson, P.J., and Walsh, G.J., 2011, Bedrock geologic map of Vermont: U.S. Geological Survey Scientific Investigations Map 3184, 3 sheets, scale 1:100,000.

Rowley, D. B., and Kidd, W. S. F., 1981, Stratigraphic relationships and detrital composition of the medial Ordovician flysch of western New England: Implications for the tectonic evolution of the Taconic orogeny: Journal of Geology, v. 89, p. 199-218.

Schoonmaker, A., 2005, Convergent and collisional tectonics in parts of Oregon, Maine, and the Vermont–Quebec border: [unpublished Ph.D. dissertation], University at Albany, State University of New York, Albany, New York, 218 p., 7 pl.

Shaw, A. B., 1958, Stratigraphy and structure of the St. Albans area, northwestern Vermont: Bulletin of the Geological Society of America, v. 69, p. 519-568, 1 pl.

St.-Julien, P., 1977, Geology of the Quebec City area, Guidebook for Geologic excursions A-4 and B-3: New England Intercollegiate Conference, Quebec City, p. A4-1—A4-32.

St.-Julien, P., and Hubert, C., 1975, Evolution of the Taconian orogen in the Quebec Appalachians: American Journal of Science, v. 275-A, p. 337-362.

Schoonmaker, A., and Kidd, W.S.F., 2007, A reappraisal of the allochthonous nature of the Rosenberg slice and Stanbridge Group of southern Quebec and northwestern Vermont, Canadian Journal of Earth Sciences, v. 44, p. 155-169.

Stanley, R.S., 1988, Foreland deformation as seen in western Vermont, Field Trip Guidebook, New York State Geological Association, 60th Annual Meeting, p. 45-78.

Stanley, R.S., and Ratcliffe, N.M. 1985, Tectonic synthesis of the Taconian Orogeny in western New England, Geological Society of America Bulletin, v. 96, p. 1227-1250.

# NEW VIEWS ON THE DEGLACIATION OF MT MANSFIELD

By

Paul Bierman, University of Vermont, Burlington, VT 05405
Lee Corbett, University of Vermont, Burlington, VT 05405
Stephen Wright, University of Vermont, Burlington, VT 05405
P. Thompson Davis, Bentley University, Waltham, MA 02452
Chris Halstead, University of Vermont, Burlington, VT 05405
Jeremy Shakun, Boston College, Chestnut Hill, MA 02467

## INTRODUCTION

Mt. Mansfield, the highest peak in Vermont, preserves evidence of Pleistocene glaciation including erratic boulders, striations, and ice-sculpted rock outcrops. Over the past several years, we have been collecting samples of bedrock and erratic boulders and using them for cosmogenic dating. Mapping of recessional sedimentary features including moraines and striations where bedrock crops out on the mountain, place these data in context. This part-day day trip will (weather permitting) travel to the top of the mountain by car and visit locations we have sampled while discussing the ages that resulted from these analyses. We will discuss evidence for ineffective erosion at the mountain peak (could there have been cold-based ice?). If time permits, we may examine ice marginal deposits in the valley resulting from ice channelized by the topography. For those who are interested, the trip will end with a tour of the Vermont cosmogenic clean labs now supported by as a community sample processing facility by the US NSF.

## SETTING

Mt. Mansfield (Figs. 1 and 2, elevation 1339 m a.s.l.) is Vermont's highest peak, located in the north-central part of the state, along the spine of the Green Mountains. Mt. Mansfield is ~35 km east of the Champlain valley and ~100 km west of the Connecticut River valley. The study area is underlain by rocks that contain sufficient quartz for analysis of *in situ* cosmogenic nuclides. The landscape in the study area is subalpine and alpine, dominated by conifers, with the highest elevations just above tree line. Following deglaciation, the summit has served as a high-elevation refuge for plants that still persist in the warmer modern climate and grow in alpine soils (Munroe et al., 2007).

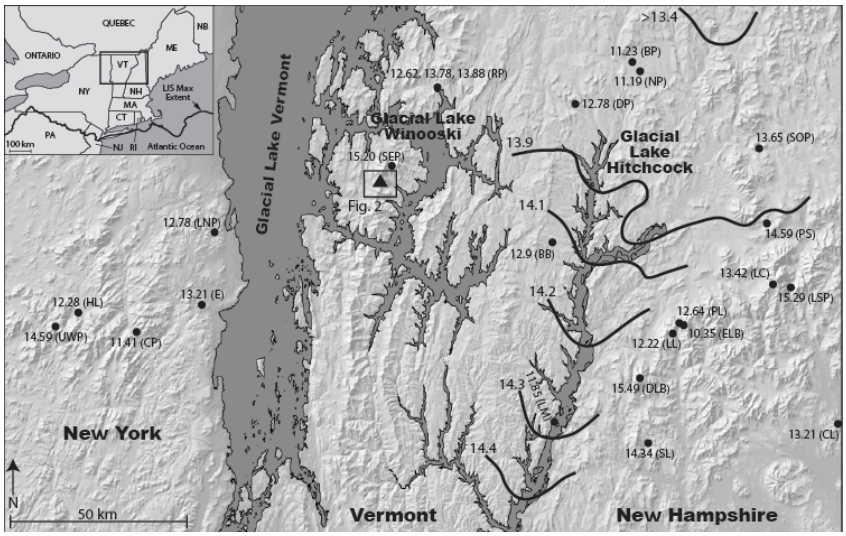


Figure 1. Generalized map of northern New York, Vermont, and New Hampshire showing previous age constraints (in ka) relevant to Mt. Mansfield's deglacial history. Ice margin positions based on glacial Lake Hitchcock varve chronology from Ridge et al. (2012) shown as thick black lines. Radiocarbon ages shown with black circles. Extent of glacial lakes are shown in light gray. Black box shows location of Figure 2. Mt. Mansfield is shown by the black triangle. Inset shows location of the study area.

Field observation reveals evidence of prior glaciation. Striations are visible on many bedrock surfaces and show multiple directions of ice flow including NW-SE along most of Mt. Mansfield's summit ridge, N-S in some lower elevation areas, and W-E in the valley south of Mt. Mansfield (Fig. 2). At lower elevations, bedrock outcrops are rounded and sculpted; however, at higher elevations, outcrops sometimes exhibit frost shattering. In areas where the mountain slopes are mantled by thick accumulations of till, such till frequently forms distinct step-like moraines (Fig. 2). Recent mapping has confirmed that these features are not cored by bedrock and do not show signs of mass movement (Wright, 2018). Continuous parallel flights of moraines are clearly visible on the LIDAR imagery where they gently slope into tributary valleys, with spacing between adjacent moraines typically ranging between 20 and 75 m.

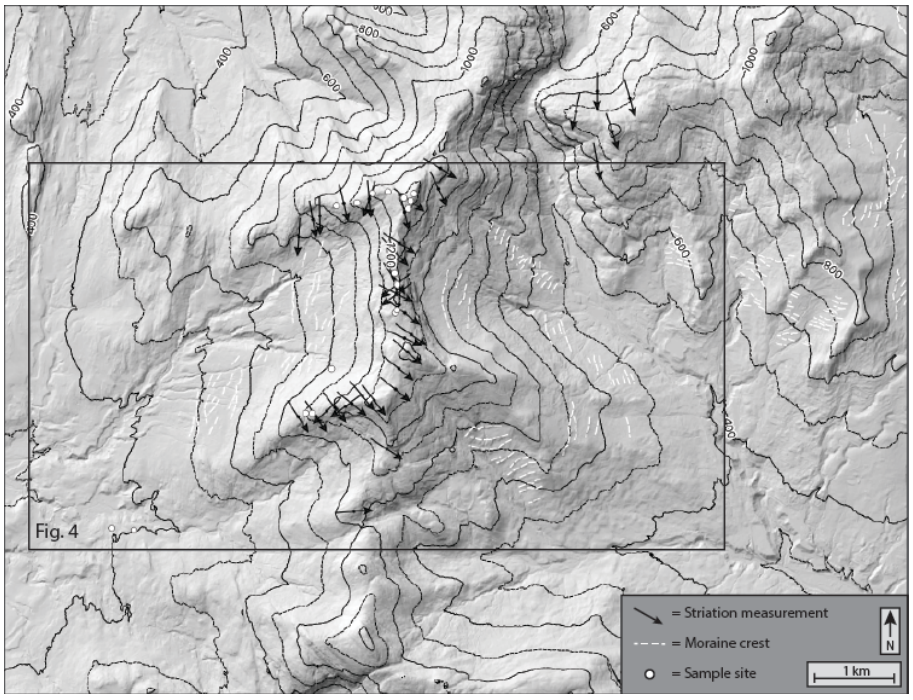


Figure 2. Shaded relief map of the Mt. Mansfield area based on LIDAR, with 100 m contours shown in black (LIDAR from the Vermont Center for Geographic Information, www.vcgi.vermont.gov). Thin arrows denote striation measurements and white dashed lines show mapped moraine crests. Sample sites are shown with white circles (refer to Figure 3 for sample names).

## PREVIOUS WORK

Mt. Mansfield has long been the subject of geologic inquiry, beginning with the work of Hitchcock et al. (1861). The occurrence of glacial striations (Hungerford, 1868) and erratic boulders on the summit ridge (Christman, 1959; Hitchcock et al., 1861) provided the initial evidence that even the highest elevations had been covered by a large, continental-scale ice sheet. While some postulated that large sediment ridges on Mt. Mansfield's east side were end moraines formed by an episode of cirque glaciation that post-dated regional glaciation (Wagner, 1970), others argued that steep valleys on the mountainside were formed prior to the LGM (Davis, 1999; Loso et al., 1998; Waitt and Davis, 1988) and that the ridges originally interpreted as end moraines of cirque glaciers near Mt. Mansfield were instead eskers formed beneath the retreating ice sheet (Wright et al., 1997).

The timing of deglaciation of the summit region was unknown prior to recent cosmogenic dating reported here. The only nearby age data come from Sterling Pond (SEP) ~4 km northeast of the summit and ~400 m lower in elevation (Fig. 1). Here, an organic radiocarbon measurement (hereafter organic $^{14}$C, to differentiate from *in situ* $^{14}$C) from bulk sediment at the base of a core yielded an age of 12760 ± 70 $^{14}$C yr BP (Lin, 1996), or 15100-15300 cal yr BP (1σ age range, all organic $^{14}$C ages have been recalibrated using Calib version 7.1 (Stuiver et al., 2015) and the IntCal13 calibration curve (Reimer et al., 2013)). This age, if correct, is a minimum limit for the timing of summit deglaciation because it is considerably lower in elevation (919 m) than the summit (1339 m) and would have still been buried by ice after Mt. Mansfield's summit became exposed as the ice thinned. However, bulk lake sediment organic $^{14}$C ages may be inaccurate. On one hand, there is an unknown lag time needed for vegetation to become

established and organic material enter the lake basin (Davis and Davis, 1980); on the other hand, bulk lake sediment ages are often too old because they contain recycled carbon (Davis et al., 1995) or are subject to hard water effects (Shotton, 1972). Several studies in Vermont have shown organic macrofossil ages to be hundreds of years younger than bulk sediment ages (Brown, 1999; Noren, 2002; Parris, 2003), likely because of carbon recycling and the sinking of macrofossils through unconsolidated pond-bottom material.

Chronologic data from the glacial lake valleys to the west and east of Mt. Mansfield (Ridge, 2004) provide context for the deglaciation of the study area. Because lakes in these valleys did not form until the valleys became ice-free, ages from the glacial lake sediments provide minimum limits for the deglaciation of Mt. Mansfield. To the west, the Champlain valley (Fig. 1) contained glacial Lake Vermont (Chapman, 1937; Rayburn et al., 2005; Ridge, 2004). Macrofossils from glacial Lake Vermont sediments have organic $^{14}$C ages of 10900 ± 75 $^{14}$C yr BP (Rayburn et al., 2007) and 11360 ± 115 $^{14}$C yr BP (Cadwell et al., 1991; Rayburn et al., 2007), yielding calibrated ages of 12710-12830 and 13100-13300 cal yr BP respectively (1σ age ranges). To the east, varve chronologies from glacial Lake Hitchcock sediments in the Connecticut River valley (Fig. 1) place the retreating LIS margin at the same latitude as Mt. Mansfield after 13900 cal yr BP (Ridge et al., 2012), following abandonment of the Littleton-Bethlehem moraine in northern New Hampshire (Thompson et al., 2017). Along the eastern border of the Green Mountains, varves from glacial Lake Winooski (Larsen, 1972, 1987), when correlated with the North American Varve Chronology (Ridge et al., 2012), indicate that the lake existed from ~14100 to 13820 cal yr BP (Larsen et al., 2003; Wright, 2018). The formation of Lake Winooski at ~14100 cal yr BP represents the most geographically proximal minimum limit for the deglaciation of Mt. Mansfield as constrained by glacial lakes.

In addition to information from glacial lakes, basal organic $^{14}$C ages from sediment cores of small, upland lakes and ponds in the northern half of Vermont, northeastern New York, and northern New Hampshire (Fig. 1) provide additional constraints for the timing of deglaciation (Ridge et al., 1999). However, due to the uncertainties discussed above, particularly the recycling of old carbon in bulk sediments (Davis et al., 1995) and the unknown lag time between deglaciation and organic sedimentation (Davis and Davis, 1980), basal sediment core ages vary widely. Ages from material at the bottoms of lake sediment cores range from 13000 to 9155 $^{14}$C yr BP (Bierman et al., 1997; Davis et al., 1980; Lin, 1996; McDowell et al., 1971; Munroe, 2012; Noren et al., 2002; Parris et al., 2010; Rogers et al., 2009; Spear, 1989; Spear et al., 1994; Sperling et al., 1989; Thompson et al., 1996; Whitehead and Jackson, 1990), yielding calibrated ages of 15490-10350 yr BP (Fig. 1). Compilations of radiocarbon ages from the northeastern United States, including those from New York, Vermont, New Hampshire, Massachusetts, and Maine, show a similarly wide spread of ages (Davis and Jacobson, 1985; Gaudreau and Webb, 1985).

## METHODS

We collected samples during 2015-2017 from 20 bedrock and boulder surfaces using a hammer and chisel. Samples span from 411 to 1305 m a.s.l. and are from Mt. Mansfield's lowlands, ridges, and summit. We avoided sampling surfaces that exhibited evidence of significant subaerial erosion and boulders that may have rolled. At each sample site, we used high-precision GPS to record latitude, longitude, and elevation; we measured thickness and shielding, and made observations about sample surface characteristics. We isolated quartz for *in situ* $^{10}$Be and $^{14}$C analyses at University of Vermont following the methods of Kohl and Nishiizumi (1992).

We calculated $^{10}$Be and $^{14}$C exposure ages with Version 3 of the online exposure age calculator formerly known as CRONUS Earth (Balco et al., 2008) and the regionally-calibrated northeastern North American production rate dataset (Balco et al., 2009). We implement "LSDn" scaling because it uses nuclide-specific equations that reflect the differences between $^{10}$Be and $^{14}$C production (Borchers et al., 2016; Lifton, 2016; Lifton et al., 2014). The calculated ages assume no nuclides inherited from previous exposure and no post-exposure erosion or shielding.

## AGE DATA

Background-corrected sample $^{10}$Be concentrations yield exposure ages of 12.9 ± 0.4 to 22.9 ± 0.5 ka (1σ analytical uncertainties, Figs. 3 and 4). In the one instance where we sampled bedrock (MM-02, 14.8 ± 0.3 ka) and boulder (MM-01, 14.5 ± 0.3 ka) surfaces in close proximity (at 1170 m a.s.l.), the two ages agree within 1σ internal uncertainties (Fig. 3). In general, exposure ages increase with elevation (Fig. 4); samples below ~1200 m a.s.l. form

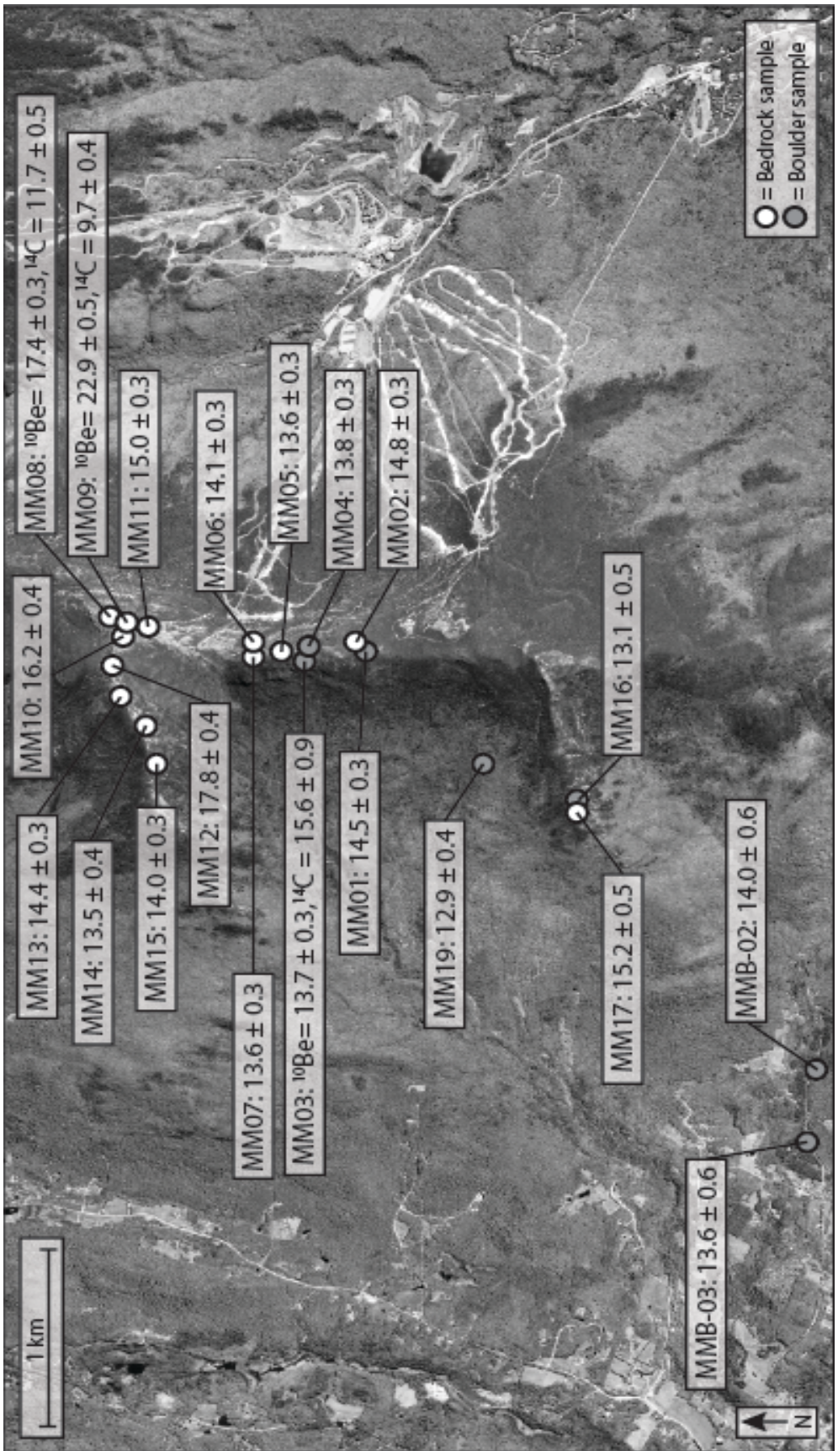


Figure 3. Satellite imagery (Google Earth) of the Mt. Mansfield area (see location context in Figs. 1 and 2). Sample locations are shown with white circles (bedrock) and gray circles (boulders). All ages in ka are $^{10}$Be unless otherwise specified; uncertainties are 1σ internal (analytical).

an overlapping population of ages (average 13.9 ± 0.6 ka, n = 15, 1SD) and samples above ~1200 m a.s.l. are older (15.0-22.9 ka).

Background-corrected in situ $^{14}C$ concentrations yield exposure ages of 9.7 – 15.6 ka (Figs. 3 and 4). For the lower-elevation boulder sample (MM-03, 1176 m a.s.l.), the $^{10}Be$ (13.7 ± 1.2 ka) and *in situ* $^{14}C$ (15.6 ± 2.5 ka) ages agree within 1σ external uncertainties (Fig. 3; we use external uncertainties here because of the differing production rate calibrations and scaling). Conversely, closer to the summit, in samples of bedrock, there are significant mismatches between the exposure ages generated with the two nuclides (MM-08, $^{10}Be$ 17.4 ± 1.5 ka, $^{14}C$ 11.7 ± 1.4 ka; and MM-09, $^{10}Be$ 22.9 ± 2.0 ka, $^{14}C$ 9.7 ± 1.0 ka). The $^{14}C$ ages are younger.

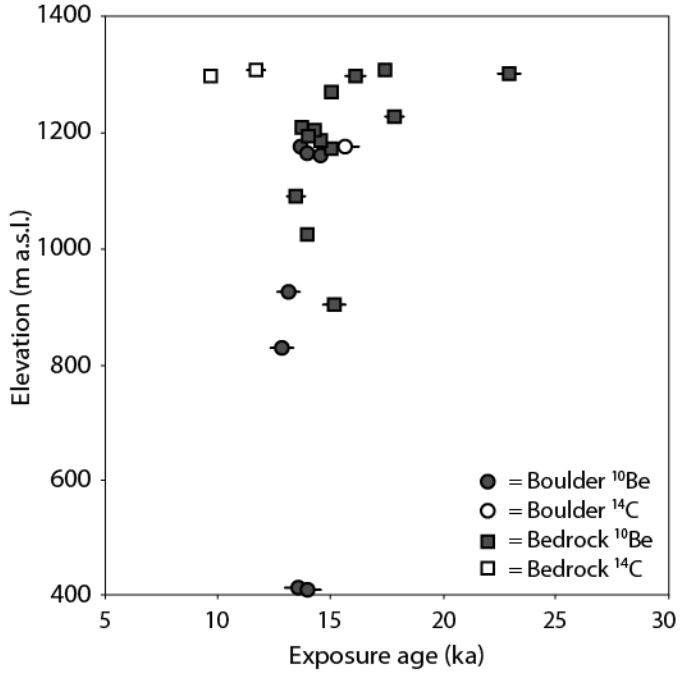


Figure 4. Exposure ages (calculated assuming no inherited nuclides and no post-burial shielding or erosion) shown against elevation. Round symbols show boulders and square symbols show bedrock; gray symbols show $^{10}Be$ and hollow symbols show *in situ* $^{14}C$. Error bars show 1σ internal uncertainties, which in many cases are smaller than the symbols.

## INTERPRETATION

Mt Mansfield's lower elevations (~400-1200 m a.s.l.) were deeply eroded by the LIS, yielding fresh, glacially sculpted landscapes following deglaciation. This erosion is evidenced by the agreement between bedrock and boulder exposure ages and is also suggested by the agreement between exposure ages generated with different nuclides on the same sample surface (Figs. 3 and 4). The agreement between $^{10}Be$ and $^{14}C$ ages indicates that at least several meters of rock were removed from exposed surfaces during the last glaciation, leaving behind minimal inherited $^{10}Be$ (the longer-lived nuclide) from pre-LGM exposure. The exposure ages at lower elevations therefore record the timing of exposure and yield an estimate of deglaciation at ~13.9 ± 0.6 ka ($^{10}Be$, n = 15, average, 1SD).

Data from Mt. Mansfield's uplands demonstrate that the geomorphic history at high elevations is more complicated than at lower elevations. The presence of two young *in situ* $^{14}C$ ages (11.7 and 9.7 ka, both from surfaces with older $^{10}Be$ ages) suggests that Mt. Mansfield's summit was shielded by ice, snow, and/or till for longer than lower elevation areas. These young exposure ages (as compared to the ~13.9 ka exposure ages at lower elevations) imply that bedrock surfaces at the highest elevations were isolated from nuclide production until several ka after the LIS margin had retreated from the region. The close agreement between $^{10}Be$ and *in situ* $^{14}C$ exposure

ages at a lower elevation site (sample MM-03) suggests that prolonged shielding was restricted to the summit region.

Post deglaciation shielding of samples collected from Mt. Mansfield's summit could be the result of one or more sheilding processes, including cover by thick snow, stagnant ice, and/or till. In the case of ice or snow, small snowfields or carapaces could have remained behind following rapid LIS thinning (although this is unlikely given how rapidly the ice sheet was losing mass at that time, Lambeck et al. (2014)) or could have regenerated. In the case of till, sediment cover could have existed for millennia following deglaciation, eventually eroding away to expose bedrock surfaces. Although there is abundant till on Mt. Mansfield's flanks, there is virtually no till on the summit today, so it was either never there or has been completely removed. Regardless of the shielding mechanism, the summit surfaces were ultimately exposed in the early Holocene (Figure 5), perhaps driven by regional warming also observed in paleoenvironmental proxies in nearby Sterling Pond (Lin, 1996), Nulhegan Pond, and Beecher Pond (Fig. 1; Munroe (2012)). If exposure of the summit occurred gradually, through slow melting of ice/snow or progressive stripping of till, then the bedrock surfaces we analyzed would have received a portion of their nuclide concentrations through thin cover and partial shielding; in that case, the *in situ* $^{14}$C ages represent maximum limits for the time at which bedrock surfaces became bare.

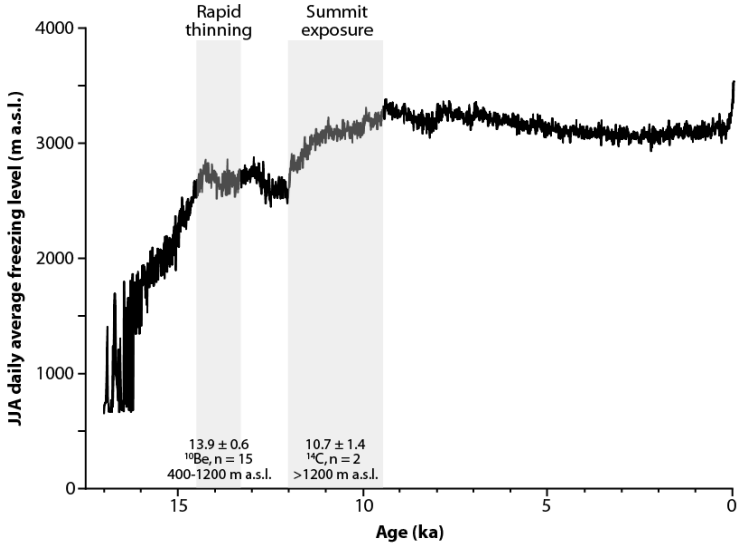


Figure 5. Simulated June/July/August daily average freezing level for 44°N 72°W from Liu et al. (2009), courtesy of F. He. Overlain in gray bars are inferences from the cosmogenic data described in the text.

Assuming the *in situ* $^{14}$C ages record the time of exposure of Mt. Mansfield's summit, then the $^{10}$Be concentrations must contain a large inventory of nuclides inherited from pre-LGM exposure (because $^{10}$Be is the longer-lived nuclide and decay during LGM burial was negligible). In that case, assuming an exposure time of 10.7 ka (the average of the two summit *in situ* $^{14}$C ages), the high-elevation surfaces are carrying an excess of ~4-12 ka of $^{10}$Be, or ~30-50% of their total nuclide concentrations. These old $^{10}$Be exposure ages do not represent early thinning of the LIS and exposure of Mt. Mansfield's summit at ~23 ka (the exposure $^{10}$Be age of bedrock surface MM-09) because the young *in situ* $^{14}$C ages preclude this possibility and because the ice margin was at its terminal position several hundred km south of the study area at that time (Balco et al., 2002; Corbett et al., 2017). Further, the heterogeneity of the high-elevation $^{10}$Be exposure ages is more indicative of variable sub-glacial erosion, which often creates a scattered population of ages (Briner et al., 2005), instead of early exposure, which would result in a single population of older exposure ages.

Significant inherited $^{10}$Be from pre-LGM exposure could persist in Mt. Mansfield's high elevations due to cold-based ice with limited erosive power (Kleman and Borgstrom, 1994) covering Vermont's highest topography and/or because the duration of ice flow over the summit was very short. The existence of cold-based Laurentide ice has been documented widely in the high latitudes (Briner et al., 2014; Briner et al., 2006; Corbett et al., 2016;

Margreth et al., 2016) and also in the contiguous United States, including the low elevations of Wisconsin (Bierman et al., 1999; Colgan et al., 2002) and the highest summits of Maine and New Hampshire (Bierman et al., 2015). In this case, the summit regions of Mt. Mansfield (and other mountains of the northeastern United States) may represent relict landscapes that were preserved, but not deeply eroded or reshaped, beneath LGM ice cover (Sugden, 1977, 1978; Sugden and Watts, 1977). The soils on the summit of Mt. Mansfield, which preserve evidence of significant contribution from dust (Munroe et al., 2007), may predate the Holocene if they were preserved subglacially. The presence of old, long-exposed soils is consistent with the observation that sediments from the Brown's River, which drains Mt. Mansfield's western flank, have appreciably higher meteoric $^{10}$Be concentrations than other river sediments in Vermont (Borg, 2010).

## ROAD LOG

The trip begins at the Stowe Mountain Resort parking lot; this is adjacent to the Toll Road up Mount Mansfield and reached from the Mountain Road (Route 108) in Stowe, VT. It is immediately adjacent to the Inn at the Mountain (https://earth.app.goo.gl/p4hZ95) and located at: 44.51069951, -72.76578428. We will consolidate vehicles (primarily using UVM vans) to reduce impact on the Mountain Road and because of limited parking at the summit. Trip limited to 30 people in total. NOTE: you must bring lunch, food, water and warm clothes; once we leave the parking lot there are no facilities on the mountain. The road is only open in the summer to vehicles and there is a charge for use. In the winter, it is used as a ski trail.

Start of driving trip, Toll Road, Mile 0 – Parking lot off of 108 at the base of the Toll Road. From here we will drive 4.8 miles up a steep, one lane, mostly dirt road.

End of driving trip, Toll Road, Mile 4.8 – Arrive at the parking lot at top of the road, elevation 1170 m asl. From here, we will walk along the ridge, weather permitting to a variety of sampled outcrops on the summit ridge trail. The trail is rough and rocky and not always well marked. Our journey and time spent on the ridge will depend on the weather which can be quite variable and potentially dangerous any time of year. The summit of Mt. Mansfield is 1339 m and about a 2 km walk each direction from the upper parking lot. We hope to be able to walk to the summit and return if the weather allows.

Since our route will depend on weather, we include below a table of GPS coordinates for sample sites allowing others to relocate within a meter of where we collected each sample.

**Table 1. Cosmogenic Sample Locations and Types**

| Sample | Latitude | Longitude | Elevation (m) | Category |
|---|---|---|---|---|
| MM-01 | 44.530322 | -72.817178 | 1164 | Boulder |
| MM-02 | 44.530622 | -72.816911 | 1172 | Bedrock |
| MM-03 | 44.533573 | -72.816966 | 1176 | Boulder |
| MM-04 | 44.533473 | -72.816888 | 1174 | Boulder |
| MM-05 | 44.534746 | -72.817298 | 1180 | Bedrock |
| MM-06 | 44.536081 | -72.817325 | 1197 | Bedrock |
| MM-07 | 44.536076 | -72.817382 | 1197 | Bedrock |
| MM-08 | 44.543693 | -72.814341 | 1305 | Bedrock |
| MM-09 | 44.542895 | -72.814863 | 1300 | Bedrock |
| MM-10 | 44.543201 | -72.815912 | 1297 | Bedrock |
| MM-11 | 44.542003 | -72.815257 | 1270 | Bedrock |
| MM-12 | 44.543891 | -72.818372 | 1226 | Bedrock |

| | | | | |
|---|---|---|---|---|
| MM-13 | 44.543708 | -72.820781 | 1174 | Bedrock |
| MM-14 | 44.542637 | -72.823174 | 1090 | Bedrock |
| MM-15 | 44.542317 | -72.826389 | 1025 | Bedrock |

Stop 1. Sample sites MM-01 and MM-02. This is a site where a boulder and a nearby bedrock outcrop were collected. Both return $^{10}$Be exposure ages that are similar within error of 14.5 and 14.8 ka, respectively. We will speak at this location about sampling strategy, the use of high precision GPS for sample location, and the utility of matched boulder/bedrock pairs to test for inherited nuclides.

Stop 2. Sample site MM-03. This erratic boulder has been known to science for nearly two centuries. Featured in the illustration pictured first Edward Hitchcock's *Report on the Geology of Vermont* (1861) and reproduced below along with Thom Davis's best vintage interpreation, it has a $^{10}$Be exposure age of 13.65 ka and a $^{14}$C exposure age that is older but within one standard deviation (15.6 ka). We will speak at this boulder about the implications of the dual isotope measurements for ice cover and deglacial history. Note that a nearby boulder (MM-04, 15 m away) gives a nearly identical $^{10}$Be age of 13.75 ka.

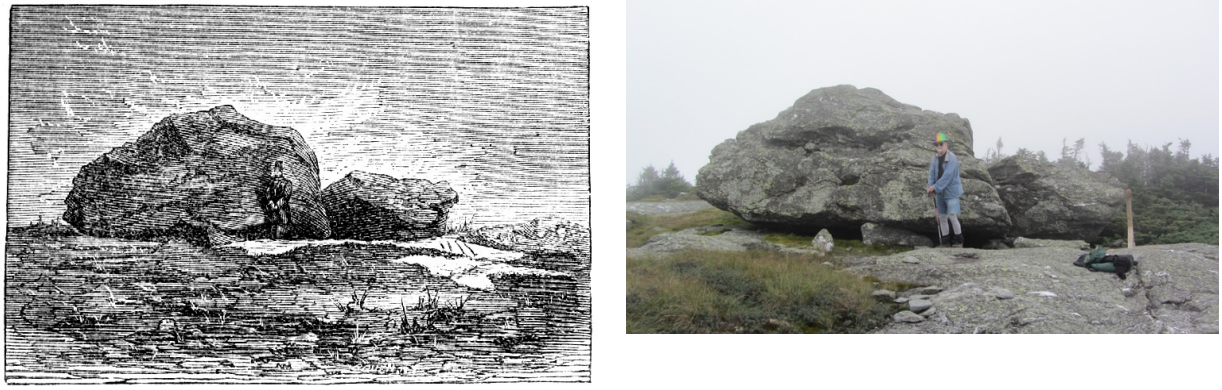

Figure 6. Sample site MM-03, then (1861) and now (2016).

Stop 3. MM-06 and -07. These are two bedrock samples collected very close to one another as a test of reproducibility. They have $^{10}$Be exposure ages of 14.1 and 13.6 ka. We will examine these sites closely and compare the weathering to that of the sites near the peak (Stop 4) which have higher, in some cases much higher $^{10}$Be exposure ages.

Stop 4. Sample sites MM-08, -09, -10, and -11. These are four bedrock samples sites near the summit of Mt. Mansfield ranging in elevation from 1270 to 1300 m asl. They have 4 of the 5 oldest exposure ages (15.2 – 22.9 ka) that we have measured on the mountain (the other being MM-12 on Sunset Ridge, about 50 m lower). These relatively high $^{10}$Be exposure ages imply ineffective glacial erosion and the inheriance of some nuclides from a prior period of surface or near-surface exposure. Two of the samples, MM-08 and MM-09 have also have in situ $^{14}$C exposure ages. These ages are much younger, 11.7 and 9.7 ka, respectively. We will talk at these sites about the need for some type of cover being present on the summit (till, ice, snow fields) after deglaciaion of the lower flanks of Mt. Mansfield at 13.9 ± 0.6 ka. After this stop, we will return to the vehicles and descend the Toll Road.

## REFERENCES CITED

Balco, G., Briner, J., Finkel, R. C., Rayburn, J. A., Ridge, J. C., and Schaefer, J. M., 2009, Regional beryllium-10 production rate calibration for late-glacial northeastern North America: Quaternary Geochronology, v. 4, no. 2, p. 93-107.

Balco, G., Stone, J. O., Lifton, N. A., and Dunai, T. J., 2008, A complete and easily accessible means of calculating surface exposure ages or erosion rates from $^{10}$Be and $^{26}$Al measurements: Quaternary Geochronology, v. 3, no. 3, p. 174-195.

Balco, G., Stone, J. O. H., Porter, S. C., and Caffee, M. W., 2002, Cosmogenic-nuclide ages for New England coastal moraines, Martha's Vineyard and Cape Cod, Massachusetts, USA: Quaternary Science Reviews, v. 21, p. 2127-2135.

Bierman, P. R., Davis, P. T., Corbett, L. B., and Lifton, N. A., 2015, Cold-based, Laurentide ice covered New England's highest summits during the Last Glacial Maximum: Geology, v. 43, no. 12, p. 1059-1062.

Bierman, P. R., Lini, A., Zehfuss, P., Church, A., Davis, P. T., Southon, J., and Baldwin, L., 1997, Postglacial Ponds and Alluvial Fans: Recorders of Holocene Landscape History: GSA Today, v. 7, no. 10, p. 1-8.

Bierman, P. R., Marsella, K. A., Patterson, C., Davis, P. T., and Caffee, M., 1999, Mid-Pleistocene cosmogenic minimum-age limits for pre-Wisconsinan glacial surfaces in southwestern Minnesota and southern Baffin Island: a multiple nuclide approach: Geomorphology, v. 27, no. 1, p. 25-39.

Borchers, B., Marrero, S., Balco, G., Caffee, M., Goehring, B., Lifton, N., Nishiizumi, K., Phillips, F., Schaefer, J., and Stone, J., 2016, Geological calibration of spallation production rates in the CRONUS-Earth project: Quaternary Geochronology, v. 31, p. 188-198.

Borg, J., 2010, Streambank stability and sediment tracing in Vermont waterways [MS: University of Vermont, 110 p.

Briner, J. P., Lifton, N. A., Miller, G. H., Refsnider, K., Anderson, R., and Finkel, R., 2014, Using in situ cosmogenic $^{10}$Be, $^{14}$C, and $^{26}$Al to decipher the history of polythermal ice sheets on Baffin Island, Arctic Canada: Quaternary Geochronology, v. 19, p. 4-13.

Briner, J. P., Miller, G. H., Davis, P. T., and Finkel, R. C., 2005, Cosmogenic exposure dating in arctic glacial landscapes: implications for the glacial history of northeastern Baffin Island, Arctic Canada: Canadian Journal of Earth Sciences, v. 42, p. 67-84.

-, 2006, Cosmogenic radionuclides from fjord landscapes support differential erosion by overriding ice sheets: Geological Society of America Bulletin, v. 118, no. 3/4, p. 406-420.

Brown, S. L., 1999, Terrestrial sediment deposition in Ritterbush Pond: Implications for Holocene storm frequency in northern Vermont [MS: University of Vermont, 180 p.

Cadwell, D. H., Connally, G. G., Dineen, R. J., Fleisher, P. J., Franzi, D. A., Fuller, M. L., Gurrieri, J. T., Haselton, G. M., Kelley, G. C., LaFleur, R. G., Muller, E. H., Pair, D. L., Rich, J. L., Sirkin, L. A., Young, R. A., and Wiles, G. C., 1991, Surficial geology map of New York.

Chapman, D. H., 1937, Late-glacial and postglacial history of the Champlain Valley: American Journal of Science, no. 200, p. 89-124.

Christman, R. A., 1959, Geology of the Mount Mansfield Quadrangle, Vermont: Bulletin No. 12 of the Vermont Geological Survey, p. 75.

Colgan, P. M., Bierman, P. R., Mickelson, D. M., and Caffee, M., 2002, Variation in glacial erosion near the southern margin of the Laurentide Ice Sheet, south-central Wisconsin, USA: Implications for cosmogenic dating of glacial terrains: Geological Society of America Bulletin, v. 114, no. 12, p. 1581-1591.

Corbett, L. B., Bierman, P. R., and Davis, P. T., 2016, Glacial history and landscape evolution of southern Cumberland Peninsula, Baffin Island, Canada, constrained by cosmogenic $^{10}$Be and $^{26}$Al: Geological Society of America Bulletin, v. 128, p. 1173-1192.

Corbett, L. B., Bierman, P. R., Stone, B. D., Caffee, M. W., and Larsen, P. L., 2017, Cosmogenic nuclide age estimate for Laurentide Ice Sheet recession from the terminal moraine, New Jersey, USA, and constraints on latest Pleistocene ice sheet history: Quaternary Research, v. 87, no. 3, p. 482-498.

Davis, M. B., Spear, R. W., and Shane, L. C., 1980, Holocene climate of New England: Quaternary Research, v. 14, p. 240-250.

Davis, P. T., 1999, Cirques of the Presidential Range, New Hampshire, and surrounding alpine areas in the northeastern United States: Geographie Physique et Quaternaire, v. 53, no. 1, p. 25-45.

Davis, P. T., and Davis, R. B., 1980, Interpretation of minimum-limiting radiocarbon ages for deglaciation of Mt. Katahdin area, Maine: Geology, v. 8, p. 396-400.

Davis, P. T., Dethier, D. P., and Nickmann, R., 1995, Deglaciation chronology and a late Quaternary pollen record from Woodford Bog, Bennington County, Vermont: Geological Society of America Abstracts with Programs, v. 27, no. 1, p. 38.

Davis, R. B., and Jacobson, G. L., 1985, Late glacial and early Holocene landscapes in northern New England and adjacent areas of Canada: Quaternary Research, v. 23, p. 341-368.

Gaudreau, D. C., and Webb, T., 1985, Late-Quaternary pollen stratigraphy and isochrone maps for the northeastern United States, *in* Bryant, V. M., and Holloway, R. G., eds., Pollen records of Late-Quaternary North American sediments, American Association of Stratigraphic Palynologists, p. 247-280.

Hitchcock, E., Hager, A. D., Hitchcock, E. J., and Hitchcock, C. H., 1861, Report on the Geology of Vermont: Descriptive, Theoretical, Economical, and Scenographical, Claremont, NH, Claremont Manufacturing Company.

Hungerford, E., 1868, Evidences of glacial action on the Green Mountain summits: American Journal of Science and the Arts, v. 45, no. 133, p. 1-5.

Kleman, J., and Borgstrom, I., 1994, Glacial land forms indicative of a partly frozen bed: Journal of Glaciology, v. 40, no. 135, p. 255-264.

Kohl, C. P., and Nishiizumi, K., 1992, Chemical isolation of quartz for measurement of in-situ-produced cosmogenic nuclides: Geochimica et Cosmochimica Acta, v. 56, no. 9, p. 3583-3587.

Lambeck, K., Rouby, H., Purcell, A., Sun, Y., and Sambridge, M., 2014, Sea level and global ice volumes from the Last Glacial Maximum to the Holocene: Proceedings of the National Academy of Sciences of the United States of America, v. 111, no. 43, p. 15296-15303.

Larsen, F. D., 1972, Glacial history of central Vermont, *in* Doolan, B. D., ed., New England Intercollegiate Geologic Conference Guidebook to Field Trips in Vermont, p. 297-316.

-, 1987, History of lakes in the Dog River Valley central Vermont, *in* Westerman, D. S., ed., New England Intercollegiate Geologic Conference Guidebook to Field Trips in Vermont, p. 213-237.

Larsen, F. D., Wright, S. F., Springston, G. E., and Dunn, R. K., 2003, Glacial, late-glacial, and postglacial history of central Vermont, Guidebook for the 66th Annual Meeting of the Northeast Friends of the Pleistocene, 62 p.:

Lifton, N., 2016, Implications of two Holocene time-dependent geomagnetic models for cosmogenic nuclide production rate scaling: Earth and Planetary Science Letters, v. 433, p. 257-268.

Lifton, N., Sato, T., and Dunai, T. J., 2014, Scaling in situ cosmogenic nuclide production rates using analytical approximations to atmospheric cosmic-ray fluxes: Earth and Planetary Science Letters, v. 386, p. 149-160.

Lin, L., 1996, Environmental changes inferred from pollen analysis and $^{14}$C ages of pond sediments, Green Mountains, Vermont [M.S.: University of Vermont, 133 p.

Liu, Z., Otto-Bliesner, B. L., He, F., Brady, E. C., Tomas, R., Clark, P. U., Carlson, A. E., Lynch-Stieglitz, J., Curry, W., Brook, E., Erickson, D., Jacob, R., Kutzbach, J., and Cheng, J., 2009, Transient simulation of last deglaciation with a new mechanism for Bølling-Allerød warming: Science, v. 325, no. 5938, p. 310-314.

Loso, M. G., Schwartz, H. K., Wright, S. F., and Bierman, P. R., 1998, Composition, morphology, and genesis of a moraine-like feature in the Miller Brook Valley, Vermont: Northeastern Geology and Environmental Sciences, v. 20, no. 1, p. 1-10.

Margreth, A., Gosse, J. C., and Dyke, A. S., 2016, Quantification of subaerial and episodic subglacial erosion rates on high latitude upland plateaus: Cumberland Peninsula, Baffin Island, Arctic Canada: Quaternary Science Reviews, v. 133, p. 108-129.

McDowell, L. L., Dole, R. M., Howard, M., and Farrington, R. A., 1971, Palynology and radiocarbon chronology of Bugbee Wildflower Sanctuary and Natural Area, Caledonia Country, Vermont: Pollen and Spores, v. XIII, p. 73-91.

Munroe, J. S., 2012, Lacustrine records of post-glacial environmental change from the Nulhegan Basin, Vermont, USA: Journal of Quaternary Science, v. 27, no. 6, p. 639-648.

Munroe, J. S., Farrugia, G., and Ryan, P. C., 2007, Parent material and chemical weathering in alpine soils on Mt. Mansfield, Vermont, USA: Catena, v. 70, p. 39-48.

Noren, A. J., 2002, A 13,000-year regional record of Holocene storms in the northeastern United States [MS: University of Vermont, 179 p.

Noren, A. J., Bierman, P. R., Steig, E. J., Lini, A., and Southon, J., 2002, Millennial-scale storminess variability in the northeastern United States during the Holocene epoch: Nature, v. 419, no. 6909, p. 821-824.

Parris, A. S., 2003, Holocene paleohydrology in the northeastern United States: a high resolution record of storms and floods [MS: University of Vermont, 141 p.

Parris, A. S., Bierman, P. R., Noren, A. J., Prins, M. A., and Lini, A., 2010, Holocene paleostorms identified by particle size signatures in lake sediments from the northeastern United States: Journal of Paleolimnology, v. 43, no. 1, p. 29-49.

Rayburn, J. A., Franzi, D. A., and Knuepfer, P. L. K., 2007, Evidence from the Lake Champlain Valley for a later onset of the Champlain Sea and implications for late glacial meltwater routing to the North Atlantic: Palaeogeography, Palaeoclimatology, Palaeoecology, v. 246, p. 62-74.

Rayburn, J. A., Knuepfer, P. L. K., and Franzi, D. A., 2005, A series of large, Late Wisconsinan meltwater floods through the Champlain and Hudson Valleys, New York State, USA: Quaternary Science Reviews, v. 24, no. 22, p. 2410-2419.

Reimer, P., Bard, E., Bayliss, A., Beck, J. W., Blackwell, P. G., Ramsey, C. B., Buck, C. E., Cheng, H., Edwards, R. L., Friedrich, M., Grootes, P. M., Guilderson, T. P., Haflidason, H., Hajdas, I., Hatte, C., Heaton, T. J., Hoffman, D. L., Hogg, A. G., Hughen, K. A., Kaiser, K. F., Kromer, B., Manning, S. W., Niu, M., Reimer, R. W., Richards, D. A., Scott, E. M., Southon, J. R., Staff, R. A., Turney, C. S. M., and van der Plicht, J., 2013, IntCal13 and Marine13 radiocarbon age calibration curves 0–50,000 years cal BP: Radiocarbon, v. 55, no. 4, p. 1869-1887.

Ridge, J. C., 2004, The Quaternary glaciation of western New England with correlations to surrounding areas, Developments in Quaternary Sciences, Volume 2B, Elsevier, p. 169-199.

Ridge, J. C., Balco, G., Bayless, R. L., Beck, C. C., Carter, L. B., Cean, J. L., Voytek, E. B., and Wei, J. H., 2012, The new North American varve chronology: A precise record of southeastern Laurentide Ice Sheet deglaciation and climate 18.2-12.5 kyr BP, and correlations with Greenland Ice Core records: American Journal of Science, v. 312, p. 685-722.

Ridge, J. C., Besonen, M. R., Brochu, M., Brown, S. L., Callahan, J. W., Cook, G. J., Nicholson, R. S., and Toll, N. J., 1999, Varve, paleomagnetic, and $^{14}C$ chronologies for Late Pleistocene events in New Hampshire and Vermont (U.S.A.): Geographie Physique et Quaternaire, v. 53, no. 1, p. 79-106.

Rogers, J. N., Fowler, B. K., McCoy, W. D., and Davis, P. T., 2009, Post-glacial mass wasting in Franconia Notch, White Mountains, New Hampshire, *in* Westerman, D. S., and Lathrop, A. S., eds., New England Intercollegiate Geologic Conference Guidebook to Field Trips in the Northeast Kingdom of Vermont and Adjacent Regions: Lyndonville, Vermont, p. 199-223.

Shotton, F. W., 1972, An example of hard water error in radiocarbon dating of vegetable matter.: Nature, v. 240, p. 460-461.

Spear, R. W., 1989, Late-Quaternary History of High-Elevation Vegetation in the White Mountains of New Hampshire: Ecological Monographs, v. 59, no. 2, p. 125-151.

Spear, R. W., Davis, M. B., and Shane, L. C. K., 1994, Late Quaternary History of Low- and Mid-Elevation Vegetation in the White Mountains of New Hampshire: Ecological Monographs, v. 64, no. 1, p. 85-109.

Sperling, J. A., Wehrle, M. E., and Newman, W. S., 1989, Mountain glaciation at Ritterbush Pond and Miller Brook, Northern Vermont, reexamined: Northeastern Geology, v. 11, no. 2, p. 106-111.

Stuiver, M., Reimer, P. J., and Reimer, R., 2015, CALIB Radiocarbon Calibration 7.1: calib.qub.ac.uk/calib/.

Sugden, D. E., 1977, Reconstruction of the morphology, dynamics, and thermal characteristics of the Laurentide Ice Sheet at its maximum: Arctic and Alpine Research, v. 9, no. 1, p. 21-47.

-, 1978, Glacial erosion by the Laurentide ice sheet: Journal of Glaciology, v. 20, no. 83, p. 367-391.

Sugden, D. E., and Watts, S. H., 1977, Tors, felsenmeer, and glaciation in northern Cumberland Peninsula, Baffin Island: Canadian Journal of Earth Sciences, v. 14, no. 12, p. 2817-2823.

Thompson, W. B., Dorion, C. C., Ridge, J. C., Balco, G., Fowler, B. K., and Svendsen, K. M., 2017, Deglaciation and late-glacial climate change in the White Mountains, New Hampshire, U.S.A.: Quaternary Research, v. 87, p. 96-120.

Thompson, W. B., Fowler, B. K., Flanagan, S. M., and Dorion, C. C., 1996, Recession of the Late Wisconsinan ice sheet from the northwestern White Mountains, N.H., *in* Van Baalen, M. R., ed., New England Intercollegiate Geologic Conference Guidebook to Field Trips in Northern New Hampshire and Adjacent Regions of Maine and Vermont: Cambridge, Massachusetts, Harvard University, p. 203-234.

Wagner, W. P., 1970, Pleistocene mountain glaciation, northern Vermont: Geological Society of America Bulletin, v. 81, no. 8, p. 2465-2470.

Waitt, R. B., and Davis, P. T., 1988, No evidence for post-icesheet cirque glaciation in New England: American Journal of Science, v. 288, p. 495-533.

Whitehead, D. R., and Jackson, S. T., 1990, The regional vegetation history of the High Peaks, Adirondack Mountains, New York: New York State Museum Bulletin, v. 478, p. 1-36.

Wright, S. F., 2018, Surficial geology and hydrogeology of the Bolton Mountain Quadrangle: Vermont Geological Survey, scale 1:24,000.

Wright, S. F., Whalen, T. N., Zehfuss, P. H., and Bierman, P. R., 1997, Late Pleistocene-Holocene history: Huntington River and Miller Brook valleys, northern Vermont, *in* Grover, T. W., Mango, H. N., and Hasenohr, E. J., eds., New England Intercollegiate Geologic Conference Guidebook to Field Trips in Vermont and adjacent New Hampshire and New York, p. C4: 1-30.

# IAPETAN RIFT–PASSIVE MARGIN TRANSITION IN NE LAURENTIA AND EUSTATIC CONTROL ON CONTINENTAL SLOPE OXYGENATION, TACONIC SLATE COLORS, AND EARLY PALEOZOIC CLIMATE

By

Ed Landing[1], New York State Museum, 222 Madison Avenue, Albany, NY 12230
Mark Webster[2], Department of the Geophysical Sciences, University of Chicago,
5734 South Ellis Avenue, Chicago, IL 60637
Email addresses: [1]ed.landing@nysed.gov, [2]mwebster@geosci.uchicago.edu

## INTRODUCTION

This excursion along the eastern margin of the New York Promontory was prepared for the combined meeting of the New England Intercollegiate Geological Conference and the New York State Geological Association (October 2018). Parts of this guide have been modified from reports by EL and MW and are so indicated. There are two purposes of the trip:

(1) The oldest rocks of the Taconic allochthon (originally deposited on the east Laurentian margin of the Iapetus Ocean and at least 75 km east of its present location) and coeval shelf margin rocks in the Green Mountain anticlinorium (not seen on this trip) indicate a surprisingly late persistence or rejuvenation of Iapetan rifting. Although Iapetan rifting began in the later Ediacaran, the oldest record of sedimentary rocks deposited on the middle Proterozoic basement of the Grenvillian orogen in NE Laurentia is late Early Cambrian, with immature sandstone (arkose) deposition continuing well into the Middle Cambrian in the eastern Ottawa-Bonnechere aulacogen (Landing et al., 2009, In press; Figure 1).

(2) The second purpose of this trip emphasizes the relationship of major eustatic changes to macroscale alternations in oxygenation on the east Laurentian continental slope as exhibited in the Lower Paleozoic of the Taconic allochthon. One take away from the trip is that formation-level, type 1 depositional sequences on the Cambrian–Ordovician shelf of eastern Laurentia are reflected by macroscale color alternations on the continental slope. Major eustatic rises and marine onlap of the cratons led to an increase in global insolation as reflective subaerial continental regions areas were inundated by shallow marine seas. These epeiric seas served as a heat sink, warmed the World Ocean, increased a key greenhouse gas (water vapor), all of which led to global temperature rise. Additional effects of high global temperatures include a decrease in storminess with decreased latitudinal temperature gradient as well as major intervals of deposition of organic-rich muds on the continental slope. Increased organic-rich mudstone deposition followed on the slope from the greater thickness and intensity of the mid-water low oxygen zone and in shallow shelf water with decreased oxygen solubility. Thus, high eustatic levels and consequent high global temperatures correlate with carbon sequestration and are the backdrop of the fossil fuel industries. This temperature increase is unrelated to changes in $pCO_2$ or other greenhouse gasses, and is termed "global hyperwarming" (Landing, 2002, 2007, 2012). "Global hyperwarming" is also pertinent to global climate in the near future with accelerated global warming with eustatic rise due to the melting of ice on land in the high mountains, Greenland and other North Atlantic islands, and Antarctica. (modified from Landing et al., 2007, p. 25)

## GEOLOGICAL CONTEXT

The route of this field trip helps emphasize the wealth of geologic history and geologic provinces that are displayed by the bedrock of eastern New York and eastern North America (Figure 1). The trip originates in Lake George village in middle Proterozoic basement of the southern Adirondacks (deformed and metamorphosed ca. 1.1 Ga in the Grenvillian orogeny) and ends in the Late Ordovician overthrust belt of the Taconic allochthon. This ca.

40 km W–E transect is comparable in geologic content to an excursion beginning in the Proterozoic of the Black Hills massif of South Dakota and ending in the Roberts Mountain allochthon in central Nevada.

By this analogy, the route (see geologic map in Fisher, 1984) passes out of the Proterozoic Adirondack basement south of Lake George; crosses the nearly flat-lying (albeit block-faulted) Laurentian Cambrian–Ordovician shelf of southern Warren and western Washington counties; then crosses N- and NE-trending faults that uplift the Proterozoic–Lower Paleozoic in the Whitehall area into a ridge comparable to the Rocky Mountain front range. The narrow belt of autochthonous Cambrian–Ordovician shelf sedimentary rocks just east of Whitehall and the Champlain Canal is comparable in position to the Paleozoics of the Great Basin. These Cambrian–Ordovician shelf rocks are thrusted upon themselves on a fault comparable to the Champlain thrust in the Whitehall area has an analog in the Sevier belt of central Utah. Finally, the transport of slope and rise facies of the Taconic allochthon onto Laurentia in the Late Ordovician–Early Silurian is analogous to the history and facies of the Devonian–Carboniferous Antler orogen of central Nevada–Idaho (Figure 2). (modified from Landing, 2002, p. B6-2, B6-3).

A more detailed geological history should note that the east Laurentian Early Paleozoic margin had re-entrants and promontories formed by the later Ediacaran break-up of Rodinia. Either this break up took place along a series of triple junctions with the opening of the Iapetus Ocean or along a series of rift segments offset by transform faults (see review in Webster and Landing, 2016, p. 195, 196). By either explanation, the fragmented NE Laurentian margin has the Newfoundland and New York promontories, Quebec Reentrant, and the Pennsylvania Reentrant (Figure 1).

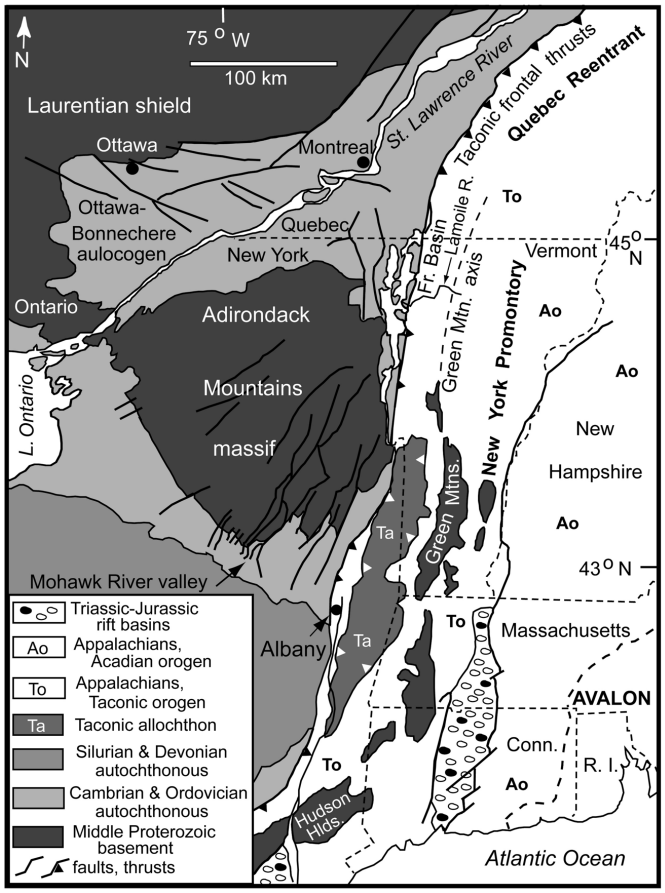


Figure 1. Geology of eastern New York and adjacent New England, Quebec, and Ontario. Figure emphasizes Ediacaran–earliest Cambrian rif features [active arms of Quebec Reentrant and New York Promontory and Ottawa–Bonnechere aulacogen failed arm] and from Mesozoic rifting that opened the Atlantic Ocean [“Trend of New York Bight” defined by SW- and E-trending active arms. North-trending failed arm formed Newark and Hartford basins]. Cretaceous coastal plain deposits of Long Island not shown. Modified from Hayman and Kidd (2002, fig. 1).

The rift–drift transition was late Early Cambrian (Landing, 2007, 2012; Landing et al., 2009, In press, Submitted), and is seen by a change from rift to shallow-marine sedimentary rocks in the Pinnacle Formation in NW Vermont (Cherichetti et al., 1998). Coeval feldspathic turbitites (Rensselaer and Bomoseen formations) are rift-related units further south (Figures 1, 2), where the rift–drift transition is marked by a change from the feldspathic sandstones of the Bomoseen into a muddy slope and rise. Coeval carbonates and siliciclastics were deposited on the slowly subsiding shelf. The passive margin ended with the Taconic orogeny and transport of slope–rise, trench-fill, and arc successions onto east Laurentia as the Taconian allochthons (Stop 5). This thrusting was accompanied by minor mafic volcanism,

of which the Stark's Knob mélange block near Schuylerville village provided the first evidence of volcanism on a subducting plate (Landing et al., 2003B). The outer (northern or western) allochthon slices (Figure 2) are weakly metamorphosed and have a coherent stratigraphy and the only fossils in the overthrusts (e.g., Zen, 1972). These features preserve and allow regional correlation of macroscale alternations in slope mudstones (modified from Landing, 2002, p. B6-2).

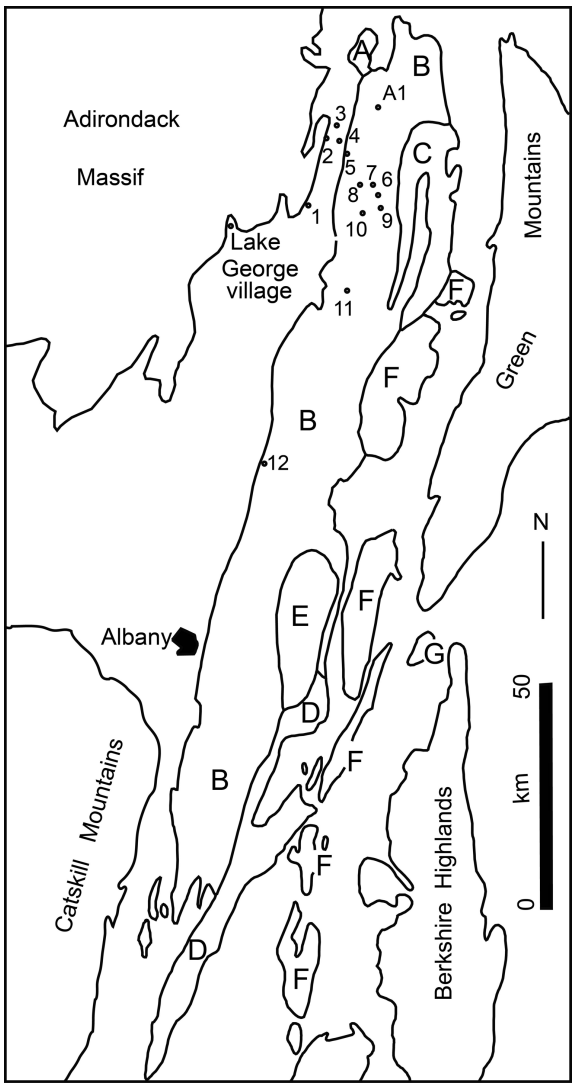


Figure 2— Generalized map showing Stops 1–12 and suggested Stop A1 at West Castleton (Appendix 1). Map shows succession of slices in the Taconic allochthon: A, Sunset Lake; B, Giddings Brook; C, Bird Mountain; D, Chatham; E, Rensselaer Plateau; F, Dorset Mountain–Everett; G, Greylock. Modified from Zen (1967).

## MACRO- AND MESOSCALE COLOR ALTERNATIONS IN THE TACONIC SUCCESSION

Siliciclastic mudstone colors in many rock successions, as well as the slates in the Taconian allochthons from New Jersey to western Newfoundland, are a proxy for changes in sea level, in climate, and in relative oxygenation of the mid-water mass on the continental slope. Macroscale alternations of black and green-dominated siliceous mudstones in the Cambrian–Ordovician in the external slices of the Taconian allochthons of New York and Québec (Figure 3; Stops 9, 12) reflect paleo-oceanographic changes. These macroscale alternations are 0.5–10.0 m-thick intervals of black mudstone, commonly pyritic and with thin- to locally thick-bedded limestone, that can be correlated between the Taconian overthrusts from eastern Pennsylvania to western Newfoundland. In addition, biostratigraphic study of fossils from the black mudstone alternations also allows each black mudstone to be correlated with a formation-scale depositional sequence on the Laurentian platform (Landing et al., 1992; Landing 2002, 2012, 2013A, 2013B; Figure 3). Thus, the black mudstones of the Schaghticoke dysoxic/anoxic interval on the Taconian slope (Stop 12) can be confidently correlated with the Tribes Hill Formation on the east Laurentian shelf.

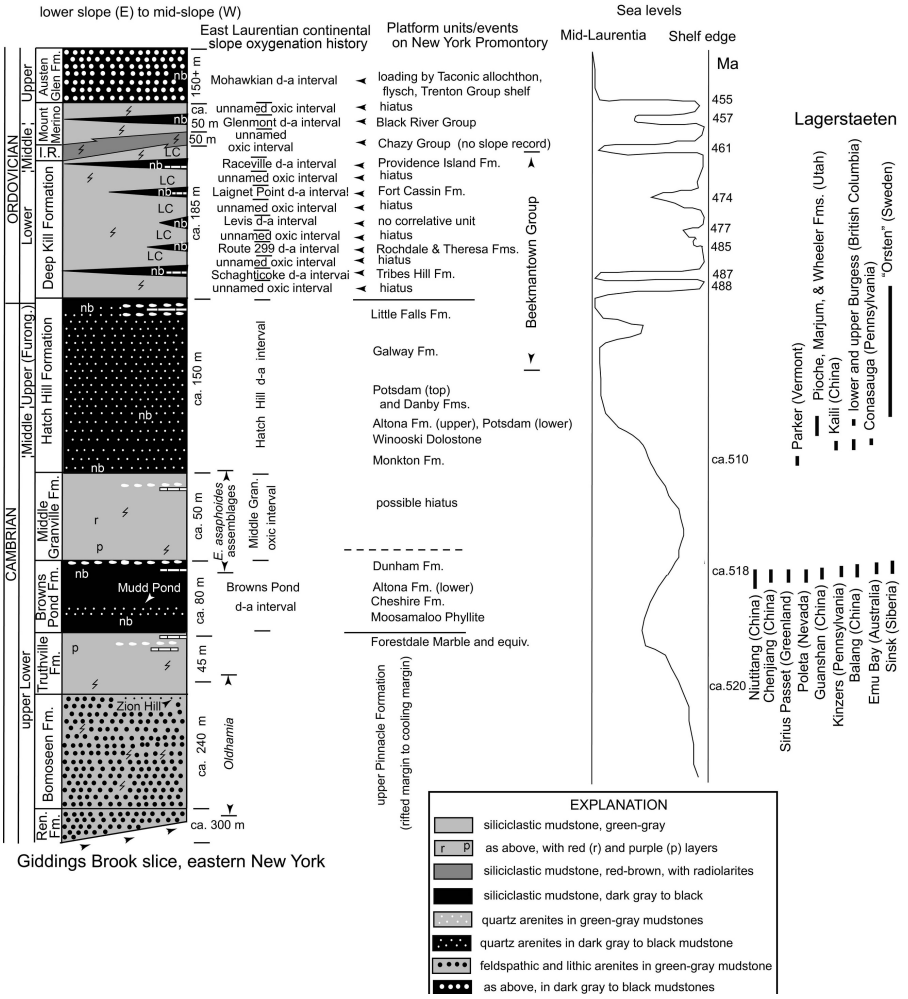


Figure 3. Stratigraphy of Giddings Brook slice, eastern New York–adjacent Vermont. Figure shows relationship of d/a black mudstones (Browns Pond and Hatch Hill formations and in Deep Kill Formation) and oxic slope facies to Laurentian shelf and global developments. After Landing (2012, fig. 1). "Ren." = Rensselaer Formation, which in the Giddings Brook slice is interbedded with the Bomoseen; d-a = dysoxic/anoxic; Gran., Granville. See stratigraphic nomenclature (Appendix 2)

Black organic-rich mud in the macroscale alternations was deposited on the upper and middle continental slope under a more intense and thicker dysaerobic to anoxic (d/a) slope water mass (Stops 6–10, 12). These d/a masses developed with sea-level rise, resultant climate amelioration (very warm "global hyperwarming" intervals), reduced oceanic circulation, and reduced srorminess with a decrease in latitudinal temperature gradients. Green (and purple and red) mud deposition reflect improved mid-water oxygenation, climate minima (icehouse/cool intervals), increased deep-water circulation; often have abundant sediment-surface and deep, probing traces; and very significantly, replace black mudstones in deeper waters of the lower continental slope (Landing and Benus, 1985; James and Stevens, 1986; James et al., 1988; Landing et al., 1992, 2002, 2007; Landing, 2007, 2012; Stop 6; Figure 4).

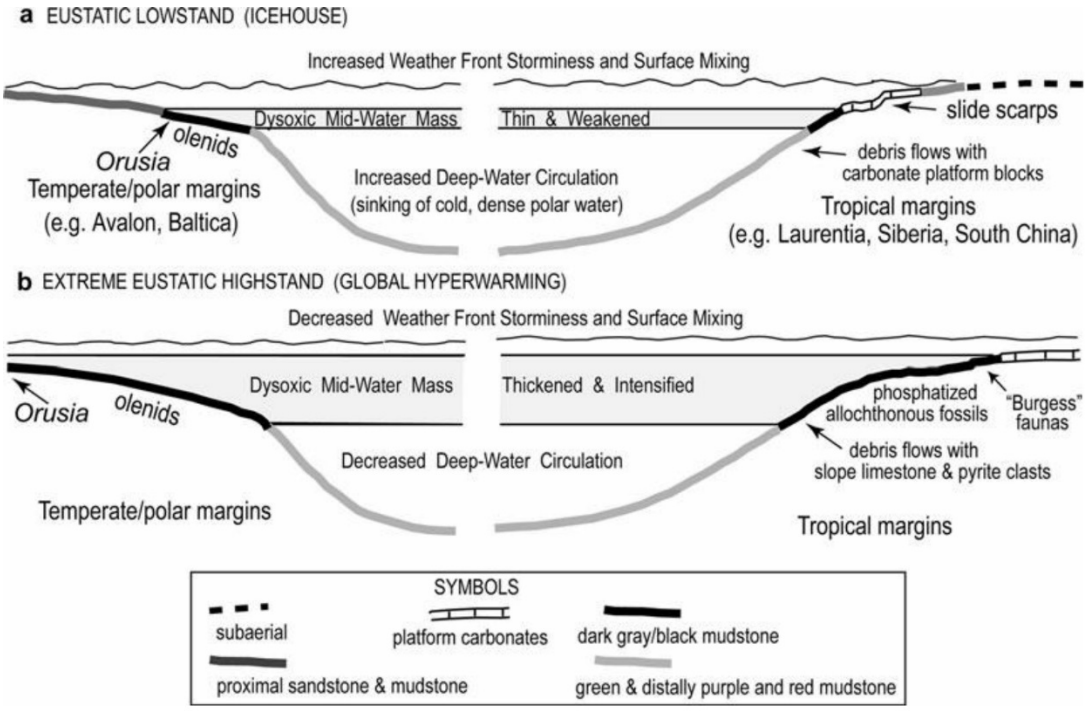


Figure 4. Global hyperwarming model for eustatic onlap (a) and offlap (b) litho- and biofacies patterns in tropical and higher latitude (respectively right and left sides of figures) paleocontinents in the Late Cambrian. Figure modified from Landing (2012, fig. 5).

Thin bedded limestones are characteristic in the black mudstones of macroscale alternations. They likely reflect, in part, off-shelf transport of carbonate from active and prograding carbonate platforms with sea-level rise and carbonate platform progradation, as well as with development of HST facies (Figure 4). However, the common occurrence of isolated to common carbonate nodules and amalgamated nodule beds that lack any fossil fragments or carbonate sand grains suggests that allochthonous (transported) carbonate is relatively insignificant as a component in the limestones in the black mudstones. Probably a much more important role in carbonate production was as a by-product of methanogenesis on the east Laurentian slope (e.g., Landing and Bartowski, 1996). Although black mudstones have relatively few trace fossils with low diversity, small sizes, and shallow penetration depths, the abundant trace fossils in green, purple, and red slates reflect higher bottom-water oxygen levels. Unfortunately, with exception of a limited number of reports (Landing et al., Submitted), trace fossils remain largely unstudied in the Taconian allochthons. The linkage of green and black mudstone deposition to sea-level fall and rise, respectively, and thus to shelf sequence stratigraphy, will be discussed on this trip.

The black mudstone and limestone intervals in macroscale alternations have supplied the majority of biostratigraphic information through the Taconic successions in NE Laurentia. This is because the limestones yield Cambrian macro- and microfaunas transported from the shelf margin (Landing and Bartowski, 1996; Landing et al., 2002; Landing et al., Submitted). Similarly, latest Cambrian–Ordovician black shales and limestones yield the majority of the graptolites (e.g., Ruedemann, 1902, 1903; Berry, 1960, 1962) and conodonts (Landing, 1976, 1977, 1993) known from the Taconic allochthons from New Jersey to western Newfoundland. Taconian black shale intervals are equated with unfavorable deep-ocean taphonomic conditions during global hyperwarming intervals—with higher preservation, and not higher production, of biologic materials transported into a deep-water environment largely devoid of larger organisms.

Although increased productivity of organic matter is commonly assumed as a way to produce organic-rich mudstones, there is no evident way in which organic productivity would significantly vary in the Cambrian–Ordovician. Subaerial organisms were limited in this interval and there is apparently no way to have marine productivity change significantly through this time. Indeed, with exception of the terminal Ordovician (Hirnantian Stage), no evidence for significant Early Paleozoic glaciation exists (e.g., Landing and MacGabhann, 2010; Landing, 2011). What this suggests is that dense cold waters generated at high latitudes and that are often regarded as significant to the generation of high productivity zones by upwelling did not exist in the Early Paleozoic. Thus, increased preservation of organic-rich mudstones rather than changes in productivity is seen as controlling the appearance of black mudstones on the middle continental slope. In addition, black mudstones accumulated in warm epeiric seas with limited oxygen in solution. On this trip, epeiric sea deposits with an interval of dark gray to black shales (Van Wie Member of the Tribes Hill Formation on the east Laurentian platform) will be seen (Stop 4, Figure 7).

The macroscale color alternations reflect sea-level and climate changes with an estimated periodicity of 3–5 m.y. (Landing et al., 1992, 2007; Landing, 2002). Shorter duration climate cycles in the Milankovich band are recorded by asymmetrical, mesoscale Logan cycles in green-dominated Taconian mudstones (Stop 11, Figure 9). Logan cycles are up to 5 m-thick mesoscale alternations, which because they show an upward decrease in organic content and a corresponding upward increase in carbonate content, are redox cycles known through the Phanerozoic (Landing and Benus, 1985; Landing et al., 1992, 2007; Landing, 2012, 2013A, 2013B). The significant feature of the macro- and mesoscale color alternations in Taconic slates is that continental slope facies appear to be more sensitive to recording climate changes than adjacent carbonate platform facies. (modified from Landing, 2002, B6-1, B6-2).

Black, organic-rich mud in the macroscale alternations were deposited on the upper and middle continental slope under a more intense and thicker dysaerobic to anoxic (d/a) slope water mass (Stops 6–10, 12). These d/a masses developed with sea-level rise, resultant climate amelioration (very warm "global hyperwarming" intervals), reduced oceanic circulation, and reduced srorminess with a decrease in latitudinal temperature gradients. Green (and purple and red) mud deposition reflect improved mid-water oxygenation, climate minima (icehouse/cool intervals), increased deep-water circulation; often have abundant sediment-surface and deep, probing traces; and very significantly, replace black mudstones in deeper waters of the lower continental slope (Landing and Benus, 1985; James and Stevens, 1986; James et al., 1988; Landing et al., 1992, 2002, 2007; Landing, 2007, 2012; Stop 6; Figure 4).

## ROAD LOG

**Mileage**

0.0 Depart Fort William Henry Resort parking lot. Turn right (South) onto Rte 9. Travel south on Rte 9 through village of Lake George kitsch. Small road cuts in Grenvillian Proterozoic gneiss at south end of village.
3.8 Intersection with Rte 149 at traffic light. Turn left (East).
5.3 At crest of low rise at south end of Proterozoic of French Mountain, note first view of high ridges in Taconic allochthon directly in front of vehicles.
6.5 Road sign shows vehicles are re-entering Adirondack Park.
8.0 Pass Queenbury Country Club on left. Underlying less resistant Cambrian–Lower Ordovician explains lack of relief.
8.9 Enter Washington County.
9.5 Low road cuts on left (North) in Grenvillian at south end of Sugar Loaf Proterozoic inlier.
10.5 Low road cuts in Grenvillian inlier east of Hadlock Pond fault.
13.1 Clear crest of hill and see spectacular view (if weather is clear) of N–S-trending ridges in Taconic allochthon across pastures developed on glacial outwash.
14.3 View to left (NE) of last (easternmost) ridge of Adirondacks east of Welch Hollow fault. East slope is nonconformity surface with lower Upper Cambrian Potsdam Formation eroded off.
14.8 Cross bridge over small creek with medium–massively bedded dolomitic limestone and hydrothermal replacement dolostone. The locally oolitic, thrombolitic, intraclast pebble facies exposed here are more suggestive of the Upper Cambrian Little Falls Formation, rather than the Lower Ordovician Tribes Hill

Formation (e.g., "Fort Edward Dolostone" [abandoned by Landing, 2003, 2012) as mapped by Fisher, 1984).

16.4 Enter village of Fort Ann.

17.4 Turn N (left) at T-junction in Fort Ann onto Rte. 4.

19.4 Pass ca. 1.0 mile of roadcuts in Proterozoic Hague gneiss on block uplifted by Welch Hollow fault.

20.3 Stop on east side of highway just south of north exit of Flat Rock Road. Walk ca. 50 m N to Stop 1.

**STOP 1: MIDDLE PROTEROZOIC–CAMBRIAN NONCONFORMITY AND RELATIONSHIP OF THIN LOWER PALEOZOIC SHELF SUCCESSION TO CONTINENTAL SLOPE OXYGENATION AND PALEOCLIMATE. (10 MINUTES)** (Stop 2 of Landing 2002; Stop 1.5 of Landing et al., 2007)

The stop shows several meters of east-dipping, medium–coarse grained, slightly dolomitic, brownish-weathering quartz arenite of the Potsdam Formation (Keeseville Member) with a basal quartz pebble conglomerate nonconformably overlying middle Proterozoic Hague gneiss. We are about 7 m below an upper Middle Cambrian trilobite-bearing horizon higher in the Keeseville with *Crepicephalus*, *Komaspidella*, and *Lonchocephalus* (Flower, 1964, p. 156; Landing et al., 2007, Stop 1.4).

This photogenic locality records the absence of ca. 600 million years of Earth history at this planar nonconformity. Further north in the Lake Champlain lowlands as the south flank of the Ottawa-Bonnechere aulocogen (OBa) is approached, the non-fossiliferous, feldspathic, often fluviatile facies of the lower Potsdam Formation (Ausable Member) appears under the Keeseville (Figures 1, 3). The oldest Paleozoic unit on the Grenville orogen in the OBa of northeastern New York and Adjacent Quebec is the Altona Formation—a thin (to 84 m-thick) heterolithic unit under the Ausable that includes lower wave-deposited feldspathic sandstones and red mudstones and a higher subtidal red-mudstone and sandstone with hydrothermal dolostones (compare Landing et al., 2009, In press, with Lowe et al., 2017, 2018; Figure 3).

Stop 1 emphasizes that the Lower Paleozoic of the eastern New York shelf is very thin by comparison with Great Basin and southern Canadian Rockies sequences (i.e., 100s of meters vs. several thousand meters). The ridge crest to the east is capped by the upper Little Falls Formation and only ca. 200 m of upper Middle–Upper Cambrian overlies the Grenvillian basement. Thin Lower Paleozoic successions occur in this region of New York and Vermont due to its location on the slowly subsiding New York Promontory rift-margin of Laurentia (Thomas, 1977; Williams, 1978). For this reason, this passive margin can be expected to record Early Paleozoic eustatic changes as type 1 erosive sequence boundaries (e.g., Landing et al., 2003A). For example, the Cambrian–Ordovician boundary is a type 1 sequence boundary everywhere on the New York and western Vermont shelf and across most of the Laurentian platform except parts of the Great Basin and Southern Oklahoma aulacogen (Landing, 1988A; Landing et al., 1996, 2003, In press).

The *Crepicephalus* Chron (a "Chron" is the age of a biostratigraphic "Zone") is a time in the late Middle Cambrian in which epeiric seas covered almost all of Laurentia except for the Trans-Continental Arch (e.g., Lochman-Balk, 1971), as well as major parts of other paleocontinents. Such an interval of high eustatic levels and high global insolation would have corresponded to a time of global hyperwarming, to d/a conditions on the Laurentian continental slope (i.e., part of the Hatch Hill Formation; Figure 3), and the probability of off-shelf transport of Potsdam sands and their deposition as part of the Hatch Hill lithofacies as seen at Stop 7. (modified from Landing et al., 2007, p. 30)

20.3 At end of Stop 1, continue north to Whitehall. Rte 4 roughly follows a topographic break corresponding to the Proterozoic–Cambrian nonconformity.

21.7–23.6 Grenville gneiss and intersection with Rte 22 on right (east); road is now Rte 4 and 22 (combined). Road cuts along Rte 22 east of Comstock State Prison are important sections through conodont-, cephalopod-, trilobite-bearing Lower Ordovician Tribes Hill (="Great Meadows Formation", abandoned), Rochdale (="Fort Anne Formation", abandoned), and Fort Cassin formations (Landing et al., 1988B, 2003, 2012, Appendix 2).

24.0 Dip slope at 10–12 O'Clock is nonconformity surface on middle Proterozoic.

26.5 Hill directly in front (north) of vehicle is Skene Mountain in Whitehall. This rock under this hill corresponds

to the entire terminal Middle–Upper Cambrian of the southern Lake Champlain Lowlands.

28.7 Enter Whitehall village.

29.3 At light in Whitehall, turn right (East) onto Rte 4. Drive across Champlain Canal and Wood Creek.

29.7 Rest stop at convenience store just before traffic light.

29.7 Turn left (north) at light onto William Street, drive through Whitehall village along the foot of Skene Mountain (Figure 5).

30.1 Stop sign, bear gently right (North) as William Street becomes North William Street.

30.2 Park next to bridge over lock on Champlain Canal. Stop 2 is the high road cut on the east side of North William Street.

**STOP 2. POTSDAM FORMATION ROADCUT.** (10 MINUTES).
(Stop 2 of Landing, 2002; Stop 2.1 of Landing et al., 2007)

Ca. 30 m of upper Potsdam (Keeseville Member) siliceous and dolomitic quartz arenite are exposed in the Whitehall area. Whitehall east of the Champlain Canal is on the Proterozoic, and the canal is cut in Potsdam sandstone (Figure 5). Herring-bone cross sets, dolomitic quartz arenite pebbles at the base of small channels/dunes, and U-shaped *Diplocraterion* burrows point to tide-influenced, high energy Potsdam facies at Stop 1. The upper Middle Cambrian Potsdam is overlain by lower Upper Cambrian dolomitic quartz arenites and quartzose dolostones of the Galway Formation higher on Skene Mountain (="Ticonderoga Formation," term abandoned, also mistakenly termed "Theresa Formation" in reports on eastern New York; Landing et al., 2003, In press). The top of Skene Mountain is upper, but not uppermost, Little Falls Formation limestone (Landing et al., 2010). (after Landing et al., 2007, p. 31)

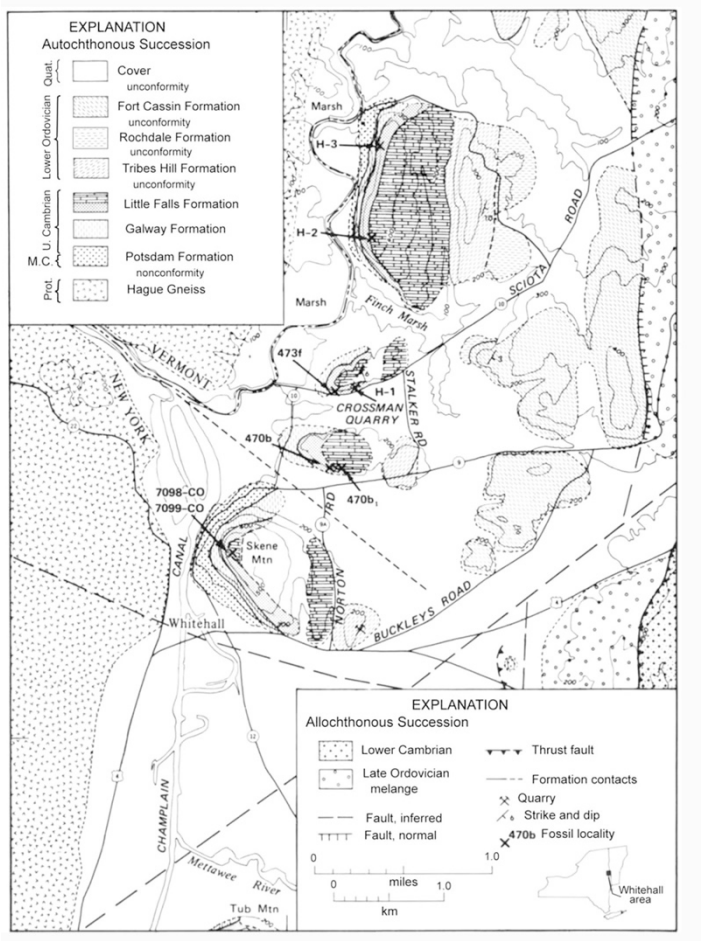


Figure 5. Geologic map of Whitehall area. Stop 2 is road cut at west base of Skene Mountain above; Stop 3, Crossman quarry; Stop 4, Rte 4 roadcut W of intersection with Buckleys Road. Contour interval 100 feet (ca. 30 m). Figure, stratigraphic nomenclature, and correlations modified from Taylor and Halley (1974, fig. 1).

30.2 At end of stop, continue north on North Williams Street; pass cuts in Potsdam Formation on the right.

30.6 Intersection with Doig Street (Washington Co. Rte 10) on left. Turn left (North).

31.2 Sharp turn to right (East); bear right on Washington Co. Rte 10.

31.6 Stop opposite old quarry on N side of Rte 10 or pull into track that enters middle of the quarry. Walk west ca. 40 m to white weathering, rounded road cut in massive dolostone at the base of the section. This cut will be inspected first, followed by a short walk to fallen blocks in the middle of the quarry, and finishing with a look at well preserved Upper Cambrian east Laurentian shelf facies at the east end of the quarry.

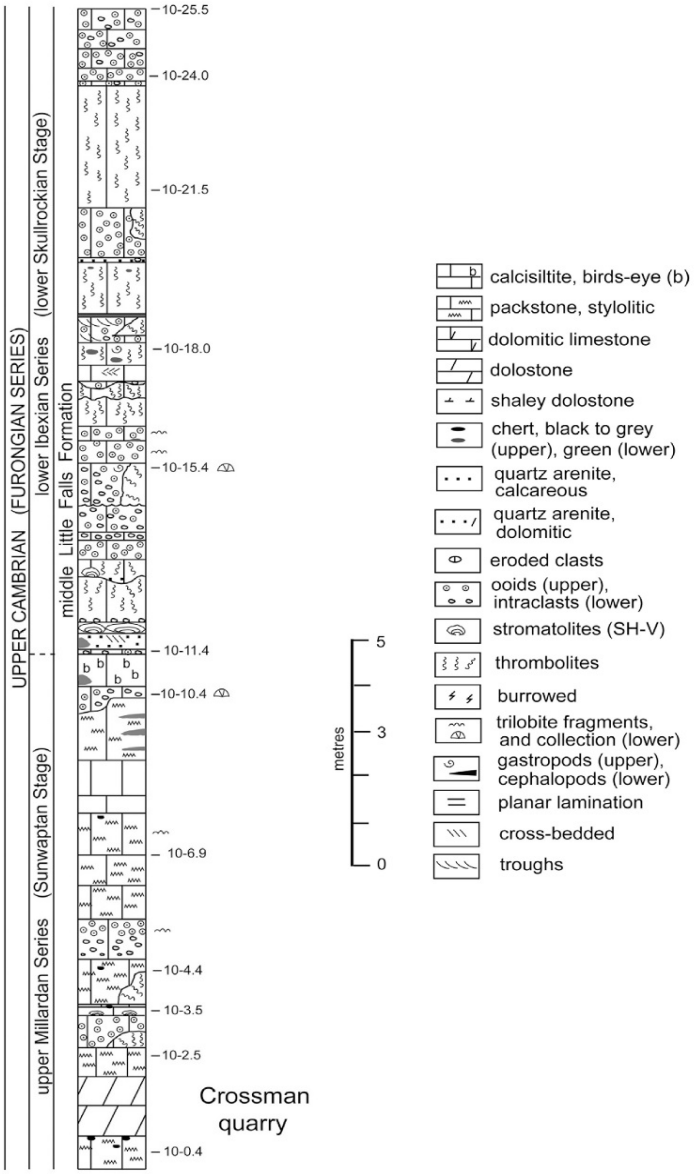


Figure 6. Cambrian stratigraphy at Stop 3 (Crossman quarry) just north of Washington County Rte 10. Conodont samples (meters above base of section) indicated by numbers to right of column (e.g., 10-10.4).

**STOP 3. CROSSMAN QUARRY: UPPER CAMBRIAN LITTLE FALLS FORMATION.** (20 MINUTES). (Stop 4 of Landing, 2007; Stop 2.3 of Landing et al., 2007)

NO HAMMERS! The eastern end of the quarry (Figure 5) shows ca. 18 m of medium- to massively bedded oolitic, stromatolitic, and thrombolitic limestones with 4 m of overlying calcareous quartz arenite. This shallow carbonate platform facies, represents Fisher's (1977) undefined "Warner Hill Limestone" member of the middle "Whitehall Formation" (abandoned designations). As commonly seen in Cambrian–Ordovician carbonate platform successions in eastern New York, hydrothermal dolomitization likely during the Late Ordovician Taconian orogeny has led to abrupt lateral and vertical changes from limestones with well preserved primary structures to dolostones without primary structures is seen in the Little Falls Formation at Stop 3 (see Collins-Wait and Lowenstein, 1994; Landing et al., 1996; Landing, 2007). The limestones are increasingly dolomitized with the loss of primary features in the western part of the quarry. In the western quarry, neomorphic dolostones predominate and have been termed the "Skene Dolostone"

(Wheeler, 1941) sensu Fisher (1977, 1984). These sucrosic "Skene" dolostones comprise the road cut opposite the western end of the quarry. Long term weathering of these dolostones yields buff-colored blocks that are present in the talus at the west end of Crossman quarry.

Well preserved primary carbonate structures appear in the middle part of the quarry. A photogenic block with a large, gray thrombolite capped by laminated thin, greenish weathering limestones with chert lenses and small SH-V stromatolites lies at the base of the cliff in mid-quarry.

A biostratigraphically important Late Cambrian trilobite assemblage appears ca. 3.5 m above the base of the eastern quarry wall (Taylor and Halley, 1974). A meter above this, the major trilobite replacement (biomere) that marks the Laurentian Upper, but not uppermost, Cambrian Sunwaptan Stage–Ibexian Series boundary is located at a lithofacies break that includes an intraclast pebble-ooid packstone bed (with the biomere boundary), an overlying quartz arenite, and a distinctive bed with SH-V and LLH-V stromatolites (Landing et al., 2010). Above this, a biofacies dominated by snails and other mollusks with rare trilobites and sparse euconodonts occurs in a thrombolite-dominated succession to the top of the quarry, and indicates a restricted, relatively near-shore environment (e.g., Westrop et al., 1995).

One purpose of Stop 3 is to show the lithology of non-dolomitized Upper Cambrian limestones of the Little Falls Limestone ("=Whitehall Formation," abandoned term; Landing et al., 2003A) for comparison with lithofacies of the overlying Tribes Hill Formation at Stop 4.

The second purpose of Stop 3 is to show the lithology of an extensive carbonate platform facies that extended in the Late Cambrian from eastern Laurentia and lenses out in coeval siliciclastic-dominated deposits of the Upper Mississippi Valley in western Wisconsin and Minnesota and passes west through the Black Hills and into western Laurentia. As the Late Cambrian was a time of particularly extensive epeiric seas and consequent global warming (e.g., Landing, 2010, 2011, 2012), it was also a time in which black shale deposits as those of the Hatch Hill Formation developed on the east Laurentian slope (Stop 7, 8). (modified from Landing, 2002, p. B6-7; Landing et al., 2007, p. 33, 34).

31.6 At end of Stop 4, continue east on Washington Co. Rte 10.

31.9 Intersection with Stalker Road, turn right (South). The first ridge to the east is the local top of the Cambrian–Ordovician passive margin carbonate platform (Middle Ordovician Providence Island Dolostone). A thrust relationship suggestive of the Champlain thrust further north brings the Potsdam Formation and younger Cambrian–Middle Ordovician units onto the Providence Island Dolostone. The second ridge to the east is the front of the Taconic allochthon, which overrides synorogenic, lower Upper Ordovician "Snake Hill Formation" flysch and Forbes Hill mélange (Fisher, 1984).

32.9 Stop sign at intersection with Washington Co. Rte. 9, turn right (West).

33.5 Intersection with Rte. 9a (Norton Road), turn left (south) on Norton Road and cross east end of Skene Mountain.

34.0 Intersection with Rte 4., turn left (East).

34.2 Stop at east end of high, whitish weathering road cut in Tribes Hill Formation. Although dominated by dolostone, this cut is only 0.3 km south on strike of identical, but non-dolomitized strata with well preserved primary depositional structures in the Tristates quarry (see Landing et al., 2003A; Kröger and Landing, 2007; for conodonts, trilobites, and cephalopods). Key stratigraphic divisions (Sprakers, Van Wie, and Wolf Hollow members) of the Tribes Hill Formation will be pointed out from the south side of Rte 4; only the uppermost Tribes Hill Formation (Canyon Road Member, highstand facies) is missing in the Rte 4 road cut, as well as in the Tristates quarry.

**STOP 4. RTE. 4: LOWER ORDOVICIAN (UPPER LOWER TREMADOCIAN) TRIBES HILL FORMATION.**
(20 Minutes)

This east-dipping section brackets most of the Tribes Hill Formation (="Great Meadows Formation," abandoned, of Fisher and Mazzulo, 1976, and "Spellman Formation," abandoned, of Fisher, 1968). Well preserved, dark grey limestones with primary structures in the Tristates quarry just 0.2 mi. to the north (see Landing, 2002, Stop 5; Landing et al., 2003), are replaced directly along strike by hydrothermal, whitish

dolostones at Stop 4. As detailed by Landing et al. (1996, 2003a, 2012) and Landing and Westrop (2006), the Tribes Hill Formation, with a uniform succession of four lithologically distinctive members, can be recognized in outcrops over about 12,000 square kilometers from Dutchess County, SE New York, through the lower Mohawk River valley of east-central New York, and north through the Lake Champlain lowlands. Just north of the New York-Quebec line near Ste-Clotilde, the Tribes Hill Formation has been termed the "Ste-Clotilde Member" (Landing et al., In press).

With exception of the Great Basin and the Southern Oklahoma aulacogen, the Cambrian–Ordovician boundary is an unconformity across the Laurentian craton (Landing, 1988, 2012; Landing et al., In press). Early, but not earliest, Ordovician (i.e., late early Tremadocian) eustatic rise led to the Stonehenge transgression (Taylor et al., 1992) across Laurentia with carbonate platform deposits reaching the Upper Mississippi Valley (Oneota Dolostone) and the Rocky Mountains (e.g., Manitou Formation). These onlap units form a type 1 depositional sequence, are about the same age, and have *Rossodus manitouensis* Zone conodonts. This depositional sequence unconformity is the contact of the Upper Cambrian Little Falls Formation and Tribes Hill, with some localities showing channels up to 2.0 m deep that are filled with Upper Cambrian carbonate blocks (Landing et al., 2003A).

*Rossodus manitouensis* Zone conodonts have been recovered from most outcrops of the Schaghticoke d/a interval in continental slope sequences in NE Laurentia (e.g., Landing et al., 1986). This means that the extensive deposits of the Stonehenge transgression correspond to intense continental slope d/a conditions, as would be expected by the global hyperwarming model (Figures 3, 4).

Figure 7. Stop 4: Hydrothermally dolomitized Tribes Hill Formation on north side of Rte 4 at the east end of the roadcut. Heavy black lines bracket Van Wie Member with regionally extensive storm beds (incraclast conglomerates) at base and middle of member and with thin gray shale laminae at this locality. Sprakers Member underlies Van Wie and Wolf Hollow overlies, Note massive thrombolites at top of section.

The three lower members of the Tribes Hill Formation are exposed at Stop 4 (Figure 7). These include the thinner bedded, silty, locally intraclast-rich limestones (now dolomitized) of the Sprakers Member (which includes Fisher and Mazullo's, 1976, "Winchell Creek Siltstone," abandoned).

The most interesting unit of the Tribes Hill is the Van Wie Member. Although the Van Wie is never more than about 1.5 m in thickness, it occurs throughout the outcrop belt of the Tribes Hill. In all sections where it is exposed, it invariably has a basal intraclast conglomerate (to 25 cm in thickness) and a middle, thinner intraclast bed. These beds are perfect time-markers and seem to represent major storm beds in a time when dark shale appears in the Tribes Hill Formation. The Van Wie Member is composed only of black shale to the south in Dutchess County (Landing et al., 2003A). To the north and west, the shale lightens and has more limestone/dolomitized limestone beds (e.g., Landing et al., 1996), as at Stop 4. This presence of organic rich shale and the indication of d/a conditions on the NE Laurentian shelf also

corresponds to the global hyperwarming model which predicts increased preservation (not increased production) of organic material in hot, oxygen-poor epeiric seas.

The Wolf Hollow Member (Fisher, 1954; = "Fort Edward Dolostone member" of Fisher and Mazullo, 1976; ="Kingsbury Limestone," abandoned of Fisher, 1984, Appendix 2) occurs above the Van Wie at the Rte 4 cut and is characterized by massive thrombolite buildups in all outcrop areas of the Tribes Hill Formation. These huge thrombolites can be seen in the upper part of the Rte 4 cut.

The highstand facies of the Tribes Hill is the Canyon Road Member (Landing et al., 1996). The Canyon Road features lower ooid wackestones and mollusk-rich carbonates above the Wolf Hollow thrombolites. Higher strata include sparsely fossiliferous carbonates with planar stromatolites and molds of gypsum and anhydrite crystals and nodules of the upper Canyon Road Member. However, the Canyon Road is absent in the Rte 4 and nearby Tristates quarry sections (Figure 5).

34.2 At end of Stop 4, continue east on Rte 4 across the railroad tracks. The low ridge in front of the vehicles is the front of the Taconic overthrust.
34.7 Turn right at Y-intersection at Fort Anne Antiques store onto County Rte 18, Pass cemetery on right which is on Taconic mélange under the Taconic master thrust.
36.2 Note low brownish outcrops on left (north) side of road. Stop on right side of road at top of low hill.

**STOP 5. TACONIC OVERTHRUST.** (10 MINUTES).

NO HAMMERS! This is primarily a stop for geological perspective as well as one of the best localities to photograph the base of the Taconic master thrust.

The sheared brownish sandstone at the east end of the roadcut is the upper Lower Cambrian Bomoseen Formation, which here forms the westernmost edge of the Giddings Brook slice. The ca. 2.0 m of thin-bedded, gray weathering, dark gray, fossiliferous limestone under the Bomoseen is a block of Upper Ordovician Glen Falls Limestone (Trenton Group, global Katian Stage) in what has been called the Forbes Hill mélange (Zen, 1961; Fisher, 1984).

A look to the west shows just how "compact" the geology of eastern New York is (Figure 1). As noted above, the Proterozoic basement of the Adirondack Mountains massif is analogous to the Black Hills in South Dakota; the block faulted, uplifted Proterozoic–Ordovician shelf succession in the southern Lake Champlain lowlands to the front of the Rocky Mountains; and the Taconic overthrust succession to the Nevada thrust belt.

36.2 At end of stop, continue east on County Rte. 18.
37.7 At four-way stop in hamlet of East Whitehall, turn right (South) on Co. Rte. 21. The cross road is in the Upper Cambrian part of the Hatch Hill Formation, with EL having found disarticulated olenid trilobites in a thin limestone bed on the east side of Rte. 21. This trilobite locality is ca. 50 m North of the intersection. After the intersection, drive South on strike along roadcuts in interbedded black shale and reddish (pyritic and dolomitic) weathering sandstone of anoxic/highly dysoxic Hatch Hill Formation (upper Lower Cambrian–lowest Ordovician).
38.8 After crossing creek at curve in road, pass more Hatch Hill Formation in road cut on right. After this point, the road swings east and crosses a large westerly overturned syncline in the Giddings Brook slice.
39.3 Greenish gray roadcut of Lower Ordovician Deep Kill Formation ("Poultney Formation" in many reports, abandoned designation, Landing, 2012).
40.5 At "sudden" Y-intersection, turn right (South) onto Holcombville Road. Drive south past low road cuts in black slates and thin sandsones in east-dipping, OVERTURNED upper Lower Cambrian Browns Pond Formation.
41.0 Overlook of Browns Pond to south.
41.5 Pass low roadcuts on east and west sides of Holcombville Road. These overgrown cuts comprise the upper part of the type section of the Browns Pond Formation of Kidd et al. *in* Fisher (1984), The southerly cut on the east side of the road includes black shale with thin, laminated sandstones that are almost devoid of fossils with exception of a large looping epichnial trace fossil. The northerly cut on the west side of the road

is a carbonate clast debris flow (Holcombville Member of Landing et al., Submitted) that forms the top of the Browns Pond Formation from Washington Co. to Dutchess County 160 km to the south. The pasture further west is underlain by slaty green mudstones of the Middle Granville Formation. These strata (Stop 3B and 3C of Rowley et al. (1979), Stop 8 of Landing, 2002, Stop 6.2 of Landing et al., 2007) will be better seen at Stop 6.

42.0 Stop at entrance to small newly reactivated quarry on west side of road. This stop consists of two parts. Do not descend into the quarry.

A sharp black–green mudstone transition (Browns Pond–Middle Granville formation contact; see Figure 3) is exposed at the top of the steep ramp that descends into the quarry. The Holcombville Member consists of thin limestones interbedded with black shale and capped by a massive calcareous sandstone debris flow at the top of the ramp. These strata are replaced ca. 50 m north along strike by fossiliferous, bedded turbiditic limestones that show fracturing and incipient transition into a debris flow.

The second part of this stop is an examination of the abundant trace fossils in oxic facies of the Middle Granville Formation. Bedding surfaces of the Middle Granville Formation are present on large blocks of green and red slate at the south end of the Holcombville quarry and in the hillock of scrap slate on the east side of the road. These bedding surfaces occur because of the local bedding plane-parallel cleavage. These bedding surfaces are crowded with shallow trace fossils that range up to several centimeters in diameter.

**STOP 6. LATE EARLY CAMBRIAN ANOXIC–OXIC–ANOXIC MACROSCALE ALTERNATIONS.** (30 MINUTES).
(Stops 6A and 6B of Landing et al., 2007)

**Browns Pond Formation and Holcombville Member**

The Holcombville Road quarry is an overturned section. It begins with 2.0 m of black siliciclastic mudstones with light gray, nodular lime mudstones. The black mudstones are capped by a 30–40 cm-thick, white weathering, light gray, conglomeratic pack- to grainstone composed of limestone sand–small intraclast pebbles and trilobite fragments with black phosphatic sand grains.

This ca. 2.4 m of section is the type locality of the Holcombville Member of the Browns Pond Formation (proposed in Landing et al., Submitted). This is the top of the Browns Pond Formation and the end of the late Early Cambrian Browns Pond d/a macroscale interval on the east Laurentian continental slope (Landing and Bartowski, 1996; Figure 3). The 30–40 cm-thick limestone thickens to 2.0 m about 50 m to the north where weathered cracks on the top surface of the unit show initial fracturing and formation of a debris flow. Micro- and macrofaunal elements of the lower *Elliptocephala asaphoides* assemblage (Lochman, 1956; Bird and Rasetti, 1968; Landing and Bartowski, 1996) occur in this top member of the Browns Pond Formation (E. Landing and M. Webster, unpub. data).

**Middle Granville Formation**

A very abrupt change into the gray-green mudstones of the Middle Granville Formation takes place right at the top of the 30–40 cm-thick limestone clast debris flow. The lower part of this greenish macroscale interval formed by the Middle Granville Formation has several beds of nodular lime mudstone. A thin limestone clast debris flow (less than 1.0 m-thick), which may be visible if the water level is low, is composed of slumped fragments of these nodular limestones. All of the thin Middle Granville Slate is exposed in the quarry. Several beds of purple slate in the Middle Granville Formation are present higher in the quarry.

**Hatch Hill Formation.**

A transitional interval from the Middle Granville Formation into the Hatch Hill Formation is seen in the west wall of the quarry, where the Middle Granville changes color into a grayish hue. Black, pyritiferous mudstones of the lower Hatch Hill Formation [i.e., the Hatch Hill interval, or terminal Lower Cambrian–lowest Ordovician dysoxic/anoxic macroscale interval (Landing *et al*., 2002)] appear ca. 5 m higher. Finally, beds of dolomitic quartz arenite characteristic of the Hatch Hill Formation are found not more than 10 m stratigraphically above the west wall of the quarry.

**Middle Granville Slate and Middle Granville oxic interval (MGOI)** (15 minutes)

**Trace fossils** Trace fossils are abundant in the red and green mudstones of the Middle Granville Formation. The crude retaining wall composed of large slate slabs at the south end of the Holcombville Road quarry and the large large pile of brownish red and minor green slate on the east side of the road came from the Holcombville Road quarry.

If the light is good, dense *Planolites* and large grazing traces up to 2 cm-wide can be seen on many of the bedding plane-parallel cleavage surfaces of the green and reddish slate. The abundance of burrows, which led to the general absence of primary depositional structures in the slate, and its reddish color (produced by traces of ferric iron) are consistent with deposition of the Middle Granville Slate under a more oxygenated slope-water mass than the underlying Browns Pond Formation. Evidence for skeletalized metazoans is not present in the reddish, purple, and green mudstones of the Middle Granville Formation. Either these metazoans were not present on the bottom, or their calcareous remains were dissolved away during diagenesis.

**MGOI** Landing *et al*. (2002) noted that the uppermost Lower Cambrian (upper but not uppermost *Olenellus* Zone) on the New York and Québec portions of the eastern Laurentian slope is composed of red and green siliciclastic mudstones. Unfortunately, Landing (2007, also Landing et al., 2007) equated this interval of improved oxygenation of slope waters with the presumed lowered sea-levels, cooler climates, and deeper circulation of oxygenated surface waters during Palmer and James' (1971) Hawke Bay regression. Subsequent sea-level rise and the re-establishment of dysaerobic slope facies (e.g., Hatch Hill Formation and Hatch Hill dysoxic/anoxic interval) took place in the terminal Early Cambrian (Landing et al., 2002).

This interpretation has been re-evaluated with the obvious fact that the lower *Elliptocephals asaphoides* assemblage of the upper Browns Pond and Middle Granville formations is not terminal Lower Cambrian (upper Dyeran Stage in Laurentia) but is best regarded as middle Dyeran. Thus, it is older than the "Hawke Bay regression" and the improved slope oxygenation represented by the Middle Granville Formation is now called the Middle Granville Oxic Interval (MGOI, Landing et al., Submitted; Figure 3). In the course of this re-evaluation, Landing et al. (Submitted) questioned the existence of a global "Hawke Bay regressive interval," restricted the "Hawke Bay" to its type area in NE Laurentia, and regarded it as epeirogenic in origin. They concluded that units such as the Hatch Hill Formation really reflect shore-line derived sand transport from Laurentia at a time of slowly rising sea levels that led to a global hyperwarming interval. In short, Early–Middle Cambrian boundary interval eustatic rise and climate amelioration led the development of a poorly oxygenated (hot) continental shelf in such widely separated areas as northern Vermont (Parker Slate) and eastern California (Mule Springs Formation) (Landing and Bartowski, 1996). (text modified from Landing et al., 2007, p. 64)

42.0 At end of stop, turn around and go north on Holcombville Road.
43.0 Turn left (west) onto Tanner Hill Road.
43.5 Park just before (east of) lowest exposed rocks on right (north) side of road. Walk uphill and examine east dipping (overturned) section in core of large syncline. Walk through section in Hatch Hill, Deep Kill, Indian River, and Mount Merino formations (Figure 3). Stop 7 ends just west of hill crest with re-appearance of Indian River Formation red mudstones on west limb of syncline.

## STOP 7. TANNER HILL ROAD: HATCH HILL D/ INTERVAL (LATE EARLY CAMBRIAN–EARLIEST ORDOVICIAN) THROUGH EARLY LATE ORDOVICIAN PALEOOCEANOGRAPHIC CHANGES ON THE EAST LAURENTIAN SLOPE

(30 MINUTES).
(Stops 6A and 6B of Landing et al., 2007)

**Hatch Hill Formation deposition.**

Dolomitic quartz arenites; conglomeratic sandstones; and interbedded, minor dark gray and black siltstones and shales of the Hatch Hill Formation form the lowest part of the section. (Remember that the section is overturned.) The medium- to massively bedded, coarse, lensing, conglomeratic sandstones and conglomerates of the lowest part of this interval have typically been compared to submarine channel-fill deposits in reports on Taconic geology (e.g. Keith and Friedman, 1977, 1978; Friedman, 1979; *Rowley et*

*al*., 1979). However, significant erosion at the base of purported channels and vertical stratigraphic successions characteristic of channels have never been described in the Taconic regions. These coarse-grained sandstones and conglomerates may simply be sand- and debris-sheets that originated at many places along the shelf–slope break and upper slope, and not from a persistent point source (submarine canyon head).

The sandstones of the Hatch Hill Formation become thinner-bedded and finer-grained higher in the section, and black mudstones become dominant. This entire interval with black mudstones up to an abrupt transition into the green-gray mudstones of the overlying Deep Kill Formation is the Hatch Hill Formation. The Hatch Hill records a long interval of persistent dysaerobic deposition on the east Laurentian continental slope (terminal Early Cambrian–lowest Ordovician [lowest Tremadocian] Hatch Hill dysoxic/anoxic interval) (see Landing, 1993; Landing *et al*., 2002).

However, the changes in relative oxygenation of slope waters through this long interval are admittedly poorly known at present. Indeed, the development of three important Upper Cambrian "Grand Cycles" on the northeastern Laurentian shelf (Chow and James, 1987) should have been accompanied by sea-level and climate fluctuations recorded by changes in relative oxygenation on the continental slope. One explanation for the lack of any apparent record for changes in relative oxygenation through this interval may be that the transport and deposition of the thick sandstones that characterize the lower Hatch Hill served to erode and obscure much of the record of relative oxygenation that is recorded elsewhere in the Taconic succession by mudstones of various colors. Even with a maximum estimated thickness of 200 m (Rowley et al., 1979), the 20 m.y. interval bracketed by the Hatch Hill Formation indicates that it is a condensed unit that may have a number of unconformities produced during the transport and deposition of thick sand sheets. These sand sheets may have been emplaced primarily during eustatic lows.

Sandstones disappear in the upper Hatch Hill in the Tanner Hill section. The upper Hatch Hill corresponds to the interval of earliest Ordovician d/a mudstone deposition that has been termed "Poultney A" (abandoned designation, Landing, 1988b) by Theokritoff (1959; Zen 1964).

**Deep Kill Formation.**

A sharp transition from the Hatch Hill Formation into the overlying green-gray mudstones of the Deep Kill Formation is present in the drainage ditch on the north side of Tanner Hill Road. Limited outcrop of the Deep Kill Formation likely explains the apparent absence of the black mudstone-limestone mesoscale intervals characteristic elsewhere of the formation (Figure 3).

**Indian River Formation**

The transition into the lowest synorogenic sediments of the Taconic allochthon is observable just west of the crest of the hill with the appearance of low outcrops of the red, thin (ca. 50 m) Indian River Slate. Fisher (1961) attributed the red color of the Indian River to off-slope transport of lateritic sediments produced on the platform during development of the Knox unconformity. However, the rapid development of bacterial films on sediment grains with their transport into marine regimes regularly leads during early burial to a grayish sediment color, and an alternative explanation for the color of the Indian River must be found.

Landing (1988b) noted three lines of evidence in proposing that the Indian River reflects very slow deposition on an oxygenated sea-floor and long sediment residence time at the sediment-water interface. These lines of evidence include: 1) occurrence of radiolarian cherts and thin volcanic ashes undiluted by background argillaceous sediment; 2) thorough burrow-homogenization of much of the unit; and 3) presence of large, up to 3 cm-wide burrowers that were active on a well-oxygenated bottom).

**Indian River Formation: oldest synorogenic deposit of Taconic orogeny and its age**

The cherty, red slaty mudstones of the Indian River Slate mark an important stage early in the Taconic orogeny. Landing et al. (1992) discussed comparable red mudstones in a number of orogens, where they always underlie green mudstones and higher flysch (e.g., Taconian allochthons from New York to western Newfoundland, southern Uplands of Scotland, Hercynian Rheinisches Schiefergebirge and Harz Mountains, and Jurassic of Japan).

These data suggest that red, cherty, oxygenated shales in collisional orogens reflect the following history: 1) passage of a peripheral bulge through passive margin successions; 2) consequent flexural uplift and restriction of sedimentation on the peripheral bulge to slowly deposited pelagic muds, radiolarian cherts, and thin volcanic ashes of the Indian River-type; and 4) final flexural down-warping and increased rates of deposition as sediment provenance changes to the emergent accretionary prism (initial cherty green mudstones of Mount Merino-type and overlying Austin Glen flysch). The transition into the green-dominated, synorogenic mudstones of the overlying Mount Merino and then into Austin Glen Formation flysch are present in the core of the Tanner Hill syncline north of the road.

The interpretation of the Indian River Formation as reflecting the first indication of the Taconian orogeny in continental slope facies seems also to explain why its color (red and minor green) is so distinct from other continental slope mudstones in the Taconics (Figure 3). Rather than being part of the "standard" black or green macroscale alternations that reflect eustatic and climate change by the hyperwarming model, the red color of this apparently condensed unit and presence of volcanic ashes suggest depositional controls associated with advance of the Taconic arc toward the Laurentian margin.

The age of the Indian River Formation can only be approximated because biostratigraphically useful fossils (e.g., graptolites, conodonts) have not been recovered from it—although it is possible that the radiolarians in the cherts (Ruedemann and Wilson, 1936) might allow correlation of the unit. Geochronologic dating of the ashes is certainly possible, although it has not been done.

The Indian River is likely upper Middle Ordovician (Darriwillian Stage). It is underlain by lower Middle Ordovician rocks (upper Dapingian Stage) of the Deep Kill Formation (Landing, 1976) and overlain by the lower Upper Ordovician (lower Sandbian Stage) Mount Merino Formation with *Nemagraptus gracilis* Zone graptolites (e.g., Berry, 1962).

44.0 End of Stop 7 is just west of hill crest, drive west on Tanner Hill Road.
44.5 Park on side of Tanner Hill Road at curve opposite intersection with unpaved road on left. Stop 8 is the black mudstone-rich road cut to the south.

**STOP 8. CAMBRIAN–ORDOVICIAN BOUNDARY INTERVAL IN DYSOXIC/ANOXIC HATCH HILL FORMATION**
(20 MINUTES)
(Stop 6.4 of Landing et al., 2007)

**Graptolite and conodont biostratigraphy**

As discussed above, the Cambrian–Ordovician boundary is a type 1 sequence boundary/unconformity across most of the Laurentian craton. However, stratigraphically unbroken Cambrian–Ordovician boundary intervals occur in successions marginal to NE Laurentia. This is the case in the upper Hatch Hill Formation in northern and southern localities in the Taconic allochthon (Landing, 1993). An understanding of the Cambrian–Ordovician boundary interval in the Taconics came from a re-examination of three supposed "Upper Cambrian" dendroid graptolite genera that had been repeatedly cited from Stop 8 (Berry, 1959, 1961; Bird and Rasetti, 1968; Fisher, 1984).

Examination of these specimens in the NYSM Paleontology Collection showed the assemblage was not Upper Cambrian because it is comprised exclusively of rhabdosomes of the earliest Tremadocian form *Rhabdinopora flabelliformis praeparabola* Erdtmann, 1982 (Landing, 1993). This monospecific, lowest Tremadocian dendroid assemblage was relocated in a shaly interval (42.9–43.4 m) near the top of this cut on Tanner Hill Road (Figure 22). Twelve samples were processed for conodonts, but only a sample at 22.8 m yielded conodont elements—an upper Sunwaptan Stage fauna [*Eoconodontus notchpeakensis* Zone with *E.* (*E.*) *alisoniae* Landing, 1983; *E.* (*E.*) *notchpeakensis* (Miller, 1969); *Proconodontus muelleri* Miller, 1969]. These limited biostratigraphic data indicate that the base of the Ordovician lies in the interval 22.8 to 42.9 m, an interval without any evident stratigraphic break or lithofacies change (Figure 8).

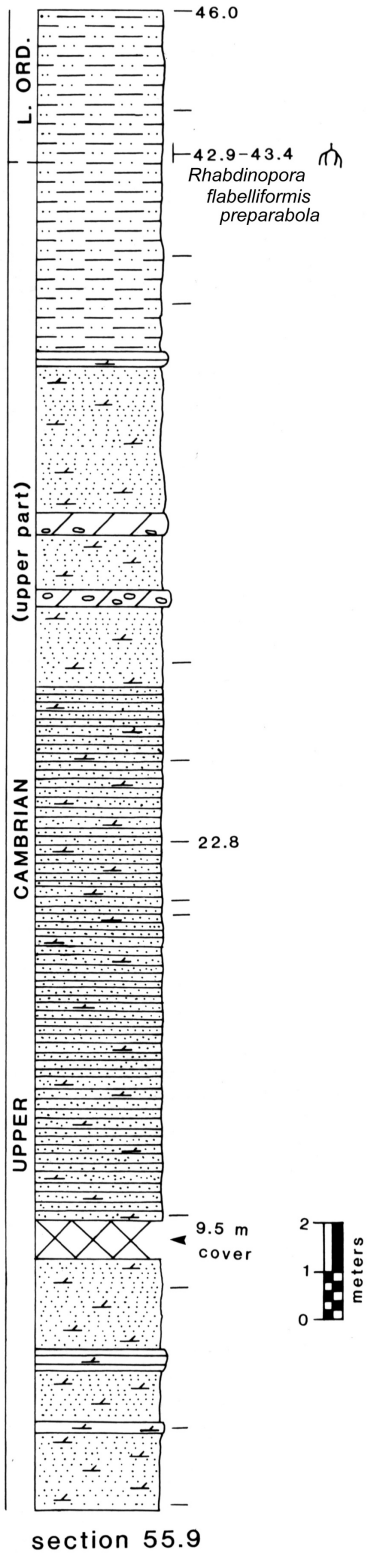


Figure 8. Cambrian–Ordovician boundary at Stop 8

**Lithostratigraphy and regional comparisons**

The Stop 8 succession in the upper Hatch Hill Formation is dominated by thin- to medium-bedded dolomitic quartz arenites and dark gray silt shales with debris flows with pebble-sized dolomitic sandstone clasts. By comparison, bedded limestones and carbonate clast debris flows dominate the Cambrian–Ordovician boundary interval at a locality approximately 160 km south in the southern Taconics near Hudson, New York (Landing, 1993)**.** As in the late Early Cambrian (Landing and Bartowski, 1996), southern localities in the Giddings Brook thrust seem to have occupied a somewhat higher position on the continental slope and have more prominent bedded limestones and carbonate clast debris flows (Landing, 1993).

The presence of black mudstones of the Hatch Hill d/a interval through the boundary interval obviously does not seem to follow the global hyperwarming model. Perhaps the explanation lies with erosion of boundary interval strata across most of the Laurentian craton with eustatic fall that was not latest Cambrian but earliest Ordovician.

44.5 At end of Stop 8, reverse vehicles and drive back to Holcombville Road.

45.5 Intersection with Holcombville Road, turn right (south).
47.5 Intersection with DeKalb Road, turn left (east).
48.5 Intersection with Steel Bridge Road, turn right (south).
49.0 Intersection with Rte 22A, make hard left onto dangerous curve.
49.5 Cross Mettawee River.
50.0 Drive by Stop 9, a high roadcut on left side of Rte. 22A.
50.25 Turn right on asphalt road (Butler Road) and park. Walk back to Stop 9.

**STOP 9. RACEVILLE: EARLY MIDDLE ORDOVICIAN DYSOXIC/ANOXIC INTERVAL**
(15 MINUTES)
(Stop 11 of Landing, 2002)

This vertically dipping section shows a black mudstone-limestone, d/a macroscale alternation in the lower (northern) part of the section and overlying greenish-gray, siliciclastic mudstone without limestone intercalations. The ca. 2 m-thick interval of interbedded limestone and black mudstone is repeated three times in the northern half of the roadcut with the northernmost and central repetitions comprising a faulted antiform and the southern repetition fault bounded.

Most of the limestone in the lower part of the section consists of fine-grained, argillaceous lime mudstones that appears to have resulted from diagenetic remobilization of fine-grained carbonate and/or methanogenic production of nodular diagenetic carbonate. Acid dissolution of these limestones yields conodonts (e.g., *Histiodella* species) indicative of the highest (lower Middle Ordovician, lower Whiterockian) black mudstone-limestone macroscale alternation of the Deep Kill Formation (Landing et al., 1992; Landing, 2012; Figure 3). The climate maximum, eustatic high, and resultant interval of intensified dysaerobic slope water recorded by the Raceville cut is equated with earliest Middle Ordovician (Whiterockian) eustatic rise across Laurentia and with deposition of such units as the Providence Island Dolostone (Figure 3). (modified from Landing, 2002, p. B6-14)

50.25 At end of Stop 9, walk back to Butler Road parking area. Return south on Rte 22A.
53.0 Enter Middle Granville.
56.0 Intersection with Rte 22, turn right (NW) on Rte 22.
59.0 Enter village of North Granville.
59.25 Turn right (north) onto Upper Turnpike at general store in North Granville.
59.5 Cross single lane bridge on Mettawee River; park immediately north of the bridge. Walk east for ca. 0.6 km on dirt track that follows the Mettawee River. Descend to river bank at east side of ruins of a small mill(?) foundation. Stop 10 features an overturned (east-dipping), almost completely exposed section from the base of the Middle Granville through the Browns Pond Formation and down into the upper Bomoseen Formation.

**STOP 10. BEST EXPOSED TACONIC SECTION: BROWNS POND AND BOMOSEEN FORMATIONS ON METTAWEE RIVER**
(90 MINUTES)
(Stop 5A of Rowley et al., 1979)

**Overview**

An exception to the limited outcrops typical of the Taconics is the almost completely exposed succession that extends along the Mettawee River. This is an overturned (ca. 30° E) Cambrian–Ordovician succession in the Giddings Brook slice (Jacobi, 1977; Rowley et al., 1979). It was measured stratigraphically downward (i.e., upstream) from a horizon low in the Middle Granville Formation. Sample horizons are recorded as meters below the top of the section (e.g., Mett-neg 29.0; Figure 9).

The Lower Cambrian (Bomoseen–base of Middle Granville formations; Figure 9) extends upstream from the falls over the Bomoseen Formation to 0.6 km east of the Upper Turnpike bridge. The Mettawee River section is on the SE margin of Theokritoff's (1964) map area, but he mapped the interval between the Bomoseen and Hatch Hill formations as green and purple green slates, although an intervening black slate unit is prominent in this interval (Figure 3). Subsequently, Jacobi (1977; also Rowley et al., 1979) mapped this unit of black siliciclastic mudstone and limestone within the Bomoseen–Hatch Hill interval.

This black unit is the Browns Pond Formation (Jacobi, 1977; Kidd et al. *in* Fisher, 1984). Recognition of the Browns Pond Formation as distinct from the lithologically similar, higher Hatch Hill is important for mapping purposes (Rowley et al, 1979; Fisher, 1984) and demonstrates that the two formations represent temporally distinct intervals of strong d/a on the east Laurentian continental slope. This has implications for regional and global geological and climatic history (Landing, 2000, 2007, 2012; 2013A, B).

The Mettawee River section received little early paleontological attention. Walcott (1912, p. 188, USNM locality 21a) reported a linguloid brachiopod and trilobites he identified as "*Olenellus*?", "*Ptychoparia* sp.", and "*Microdiscus connexus* (Walcott)" from a "limestone below the first fall of Mettawee River, above the North Granville bridge…" but did not illustrate the specimens and gave limited provenance information. Without modern study, Walcott's (1912) identifications only indicate a Laurentian late Early Cambrian (Waucoban) age. This fauna could have come from any Lower Cambrian unit in the section as high as the lower Hatch Hill Formation (Figure 3).

The turbiditic limestones and thin debris flows at the top of the Browns Pond Formation (Holcombville Member of Landing et al., Submitted) earlier yielded the oldest acid-resistant microfossils from the southern Taconic allochthon (Landing and Bartowski, 1996). This suggested that older limestones and calcareous clast debris flows exposed through the Browns Pond and extending down into the upper Truthville Formation (Figures 3, 9) on the Mettawee River might have biostratigraphically significant faunas that could provide an upper age bracket on the origin of the east Laurentian passive margin in offshore facies, and also a bracket on the earliest d/a interval on the east Laurentian continental slope.

**Lithofacies and sediment provenance**

Most of the Browns Pond and Truthville formations on Mettawee River are a low energy facies of planar laminated mudstone and scattered mm-thick sandstones. The succession demonstrates for the first time that the Browns Pond is dominated by thin (cm- to several mm-thick), argillaceous lime mudstone-rich distal turbidites that may have sand- to rare granule-sized clasts of black lime mudstone. A near lack of trace fossils in the Browns Pond (noted below; also Landing, 2012) suggests the substrate was low in oxygen and metazoans were probably rare. The most abundant body fossils are echinoderm sclerites that comprise a few thin lenses and small ripples (to 1 cm-high) and were likely washed off the east Laurentian shelf or upper slope (horizons Mett-neg 112.5; -neg 62.5, -neg 28.5; Figure 9).

Decollement surfaces in the middle Browns Pond (Figure 9) suggest rapid deposition and easterly transport of weakly compacted mudstone. Weak compaction, soft mud at the sediment–water interface, and low oxygen bottom waters that led to black, organic-rich mud deposition (Landing, 2012) with locally abundant pyrite (Figure 9) suggest that Browns Pond and Truthville shelly fossils are allochthonous (e.g., Thayer, 1983).

Carbonate clast debris flows occur in the Truthville and Browns Pond. The clasts are fine grained, dark colored, and laminated and were locally derived, and not from an Iapetus Ocean-facing shelf or upper slope. Thus, debris flows clasts in the Browns Pond and Truthville yield limited skeletal fossils.

As proposed earlier (Landing, 2007, 2012, 2013a, b), the succession of the Mudd Pond Member quartzite and late Early Cambrian age of the uppermost Browns Pond (Landing and Bartowski, 1996) suggest these units are the slope equivalent of the shelf Cheshire Formation (quartz sandstone tidalite) and Dunham Formation (now dolostone-dominated) (Figures 3, 9). This lithologic correlation and the soft, strongly d/a substrate

**Trace fossils and bottom water oxygenation**

*Planolites* burrows at the base of thin sandstones of the upper Bomoseen persist into the Truthville Formation where they appear at the base of a few thin sandstone laminae (Figure 9). The Browns Pond has

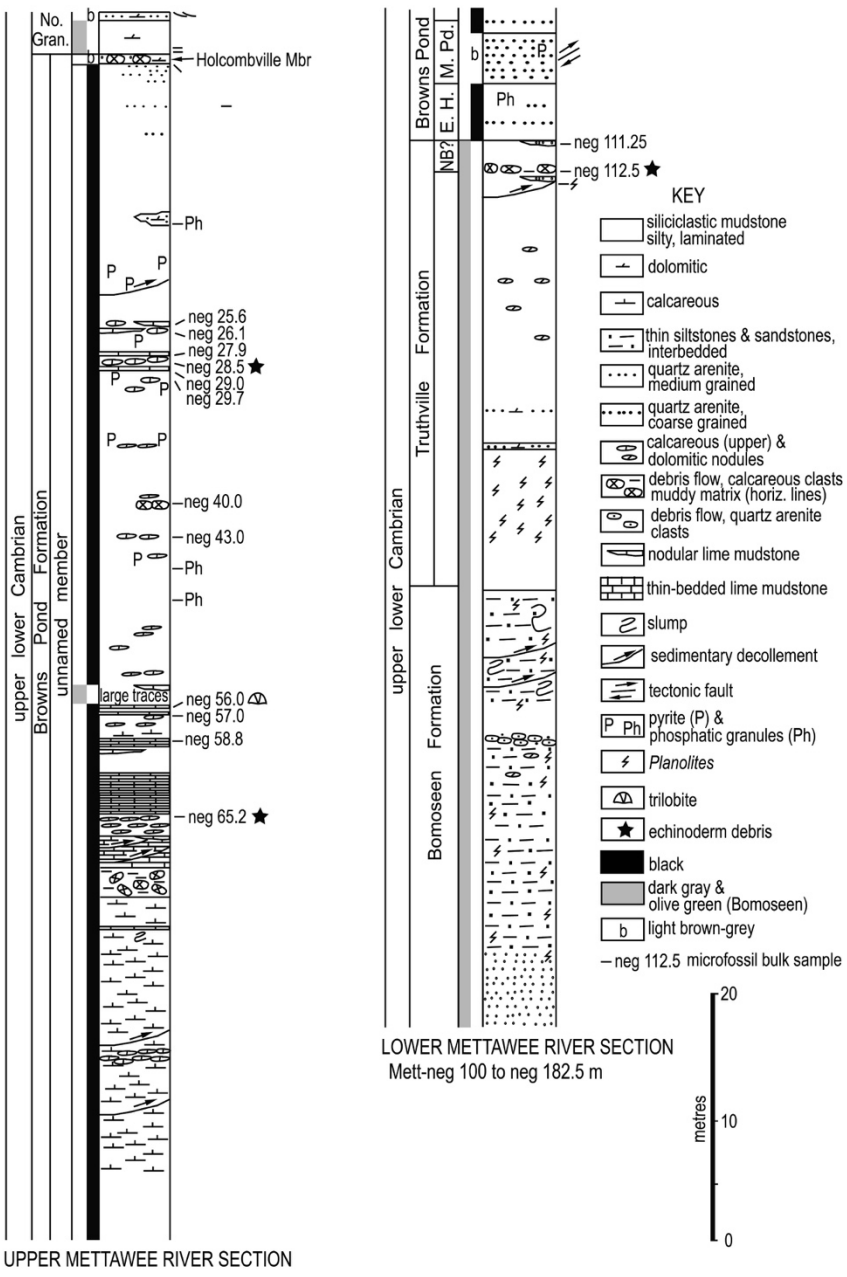


Figure 9. Section along the Mettawee River downstream from the falls on the Bomoseen Formation to c. 0.6 km upstream from the Lower Turnpike bridge at North Granville village, N.Y. Abbreviations: E.H., Eddy Hill Member; M. Pd., Mudd Pond Member; No. Gran., North Granville Formation.

of the Browns Pond would mean that the abundant, fine-grained carbonate component of bedded carbonates and secondarily transported debris flows came off the Dunham shelf (Figure 3) and that much of the fossil debris was similarly transported.

rare trace fossils with a few *Planolites* at Mett-neg 71.6 to Mett-neg 82 m on bedding surfaces and in slabbed sections.

Most of the Browns Pond Formation lacks any traces, which is consistent with it's interpretation as a strongly d/a facies (Landing, 2007, 2012, 2013A, B). The only large traces found in our study are black anastomosing forms limited to an interval of green weathering, medium grey mudstone (Mett-neg 55.0 to Mett-neg 56.5) that records a more oxic time on the sea floor (e.g., Landing, 2012). The large traces suggest *Megagrapton* Książkiewicz, 1968, a distinctive graphoglyptid known from large polygonal nets with common right angle branches (e.g., Książkiewicz, 1970). However, recent analysis of graphoglyptids (Fan et al., 2018) shows that *Megagrapton* actually has burrow segments intersecting at a variety of angles and thus allows a tentative assignment of the Browns Pond traces to "*Megagrapton*?" These large traces are not restricted to a bedding surface; they are endichnial and the product of a burrowing organism.

Ichnofossils of the Taconic allochthon have not received modern study, and the Browns Pond specimens can only be compared with the spartan original description and illustration of *Fucoides flexuosus* Emmons, 1844. They were compared with specimens in the NYSM Paleontology Collection that were collected from the "Cambrian roofing slates" in the vicinity of Middle Granville village that have been assigned to Emmon's ichnospecies. Both the Browns Pond and Middle Granville specimens have been tentatively assigned to *Megagrapton*? *flexuosus* (Landing et al., Submitted). Walcott (1890, p. 603) complicated an understanding of Taconic Cambrian ichnofossils by synonymizing all previously named,

elongate taxa with the thin (i.e., thread-like) looping trace *Helminthoidichnites* Fitch, 1850. This synonymy meant that the much wider looping traces of the genotype *Gordia marinus* Emmons, 1844, became *H. marinus* (Emmons, 1844). Walcott (1890, pl. 52) illustrated large and anastomosing traces comparable to those from Mettawee River as *H. marinus*?

**Late Early Cambrian age of syrift and passive margin (Truthville–lower Hatch Hill Formation)**

A significant "younging" of the oldest units deposited along the margin of the New York Promontory (Figure 3) is indicated by re-evaluation (Landing et al., Submitted) of the biostratigraphic information on mineralogically immature, likely synrift deposits in the Taconic allochthon (i.e., Rensselaer and Bomoseen formations). In addition, small skeletalized faunas appear below and persist through the Browns Pond d/a interval to provide an upper age bracket (late Early Cambrian; middle Dyeran Age in Laurentia) on the rift–passive margin transition along the New York Promontory.

Reactivation of rifting or persistence of rifting into the late Early Cambrian (late Dyeran) and into the middle Middle Cambrian is suggested by the first marine transgression of the Ottawa-Bonnechere aulacogen and the coeval, on-strike subsidence of the Franklin Basin on the northwest Vermont shelf (Landing, 2007, 2012, 2013A, B; Landing et al., 2009, In press; Webster and Landing, 2016; Figure 1). The occurrence of *Oldhamia*-bearing trace fossil assemblages from the Rensselaer and Bomoseen formations comports with Dyeran and not Ediacaran or earliest Cambrian rifting and production and accumulation of immature sediments on the Iapetus-facing margin of the New York Promontory, as well as the Quebec Reentrant and Newfoundland Promontory. Recent study (Herbosch and Vaniers, 2011) shows that the trace fossil *Oldhamia* is biostratigraphically useful and not a form that could range even down into the Ediacaran. Indeed, *Oldhamia* is known worldwide from strata that are no older than the late Early Cambrian, and its occurrence in the Rensselaer and Truthville formations thus brackets the transition in NE Laurentia from a rifted margin in the late Early Cambrian in the Taconics of New York and Quebec (see Swett and Narbonne, 1993; Landing et al., Submitted) and western Newfoundland (Lindholm and Casey, 1990).

The trilobite *Olenellus* from the Cheshire Formation has been reported as the oldest body fossil on the northeast Laurentian passive margin (Osberg, 1969; Allen et al., 2010). However, *Olenellus* was actually reported to occur much below the Cheshire in chemically immature (synrift) arkoses at Clarksburg Mountain, northwest Massachusetts (Walcott, 1888). The Clarksburg Mountain rocks with purported *Olenellus* were mapped as "Cheshire" by Ratcliffe et al. (1993) with the "Cheshire" claimed to nonconformably overlie gneisses in southern Vermont and adjacent Massachusetts (e.g., Rankin et al., 1989; Hatcher, 2010; Allen et al., 2010). However, Walcott's (1888) *Olenellus* report is from rocks that occur only ca. 30 m) above the nonconformity with middle Proterozoic gneisses. This occurrence in conglomeratic arkoses brought to the "Mendon Formation" (Brace, 1953, p. 33; Skehan, 1961), and now best assigned to the Pinnacle Formation (Landing, 2007, 2012, 2013a, b; Webster and Landing, 2016; Figure 3). Walcott's (1888) supposed *Olenellus* specimen was never illustrated and a search of the USNM collections by MW did not lead to its recovery. Thus, a presently unidentified trilobite has been found in the oldest synrift sedimentary rocks on what became the NE Laurentian shelf, with the trilobite indicating a late Early Cambrian (Epoch 2) correlation comparable to that of the oldest known rocks (i.e., Rensselaer or Bomoseen formations) of the Taconic allochthon. This generalized correlation supports the conclusion that Iapetan rifting persisted or was re-established on the NE Laurentian margin in the late Early Cambrian.

Higher Mettawee River strata provide information on post-synrift deposits on the continental slope of NE Laurentia. The age of these deposits are provided by fossils from the Mettawee River section and other localities. The middle Dyeran *Elliptocephala asaphoides* assemblage spans the upper Browns Pond–lower Hatch Hill formations. This assemblage brackets the d/a intervals known from these two formations and the more oxic strata of the Middle Granville Formation (Landing and Bartowski, 1996; Landing 2012; Figure 3). The Mettawee River section shows that small skeletalised taxa known from the *E. asaphoides* assemblage persist lower through the Browns Pond and into the relatively oxic facies of the upper Truthville Formation (Landing et al., Submitted).

The likely sediment source of the carbonate-rich Browns Pond Formation and its fossils was the Dunham Formation on the eastern shelf of the New York Promontory (Figure 3). This slope–shelf

correlation accords with correlation of the Mudd Pond Member quartzite with Cheshire Formation tidalites on the shelf (Landing, 2007, 2012). This correlation of shelf and continental slope units would make the lowest calcareous mudstones of the Browns Pond Formation equivalent to the shelf-margin Moosalamoo Phyllite that underlies the oldest NE Laurentian carbonate platform carbonates (Forestdale Marble; Figure 3).

These correlations mean that a significant amount of rift–passive margin rocks on the NE Laurentian shelf (Pinnacle–Dunham) and slope (Rensselaer–Browns Pond) are lower and middle Dyeran. This remarkable history of events that took place in the earlier Dyeran is actually incomplete as the Middle Granville Formation (and Middle Granville Oxic Interval, or MGOI), its shelf-equivalent HST, and the lowermost Hatch Hill Formation, are all middle Dyeran (upper *Elliptocephala asaphoides* assemblage interval). Thus, reestablishment of reduced slope water circulation and deposition of dysoxic/anoxic mudstones of the lower Hatch Hill Formation beginning in the middle Dyeran in the Taconics of eastern New York and adjacent Vermont are significantly older than the upper Forteau and lower Hawke Bay formations (upper Dyeran) of western Newfoundland.

The MGOI is proposed as replacement for the earlier named "Hawke Bay Oxic Interval" in theTaconics by Landing (2012; "HBOI" abandoned by Landing et al., Submitted). Correlation of the lower Hawke Bay Formation in western Newfoundland as upper Dyeran means that it is the lower, but not lowermost, part of the lengthy Hatch Hill d/a interval (middle Dyeran to lowermost Ordovician; Landing 2012) that really correlates with the Hawke Bay Formation and "events" (Landing et al., Submitted). As concluded by the latter authors, the designation "Hawke Bay Events" ("HBE") should probably be limited to NE Laurentia where a comparable rifting history that persisted into or was reinitiated in the late Early Cambrian along the Newfoundland and New York promontories and included similar, likely coeval, lower passive margin successions (Bradore–Hawke Bay and Cheshire–Monkton formations).

The paradigm that the Hawke Bay Events necessarily featured major eustatic regression and an interregionally extensive unconformity should be questioned as noted by Nielsen and Schovsbo (2015) who regarded the "Hawke Bay regression" in Baltica as an epeirogenetic event. Similarly, Knight et al. (2017) also suggested that the "type" Hawke Bay Event unit, the Hawke Bay Formation in western Newfoundland may also be the record epeirogenic activity, not eustatic changes. Indeed, available evidence can be used to interpret the Hawke Bay Formation not as a regressive sedimentary unit but as an HST lithosome. By this proposal, the Hawke Bay, and possibly Monkton Formation in NE Vermont, were deposited either during an interval of reduced rate of sea-level rise and development of a shallow-water siliciclastic by-pass shelf with significant offshore transport of shoreline-derived quartz sand (Landing et al., Submitted). The qualification "local epeirogenic uplift" is appropriate in NE Laurentia as approximately coeval (upper Dyeran–Middle Cambrian) deposits of the Parker Formation in NW Vermont that are correlated with the Hawke Bay Formation record an abrupt and continuing epeirogenic foundering of the Franklin Basin and at least the eastern part of the Ottawa-Bonnechere aulocogen (Landing et al., 2009; Webster & Landing, 2016). (modified from Landing et al., Submitted)

59.5 At end of Stop 10, turn around and return to North Granville.

59.75 Turn right (west) at intersection with Rte. 22.

62.0 Intersection with Rte. 40, turn left (south) on Rte 40. The ridge to the left (east) of Rte 40 is formed of more resistant rocks at the western edge of the Taconian allochthon. The SSW trend of Rte 40 from this point to just north of Troy follows the front of the allochthon and edge of the Giddings Brook slice. Rte 40 meanders back and forth from the edge of the allochthon and onto erosionally less resistant, structurally underlying Upper Ordovician "Snake Hill" synorogenic flysch and wildflysch (see Landing et al., 2003b; English et al., 2006) and, in the area of Middle Falls, onto Lower and Middle Ordovician shelf carbonates.

63.0 High road cut on left (east) is in overturned Deep Kill Formation. The road cut shows repetitions of meter-scale Logan cycles that are relatively tectonized (faulted). Better preserved Logan cycles will be seen at Stop 11. This road cut is Stop 12 of Landing (2002).

78.0 Stop at T-junction in Argyle village, turn left (south) and continue on Rte 40.

80.0 Stop on edge of Rte 40 close to ca. 10 m-high cut with prominent banded slaty mudstones (Logan cycles) on left (east) side of road. CAUTION! Traffic can be heavy so cross road after discussion only with care.

No hammers on this superb locality, take pictures only. When examining road cut, stay close to the steel barrier or walk inside the barrier and hug the rocks.

**STOP 11. LOGAN CYCLES IN THE DEEP KILL FORMATION: MESOSCALE CYCLES IN THE MILANKOVITCH BAND.**
(15 MINUTES)

This is one the most assessible and well preserved outcrops that shows the color and lithologic alternations characteristic of Logan cycles (Landing and Benus, 1985; Landing et al., 1992) in the Lower–lower Middle Ordovician Deep Kill Formation. NO HAMMERS AT THIS STOP!

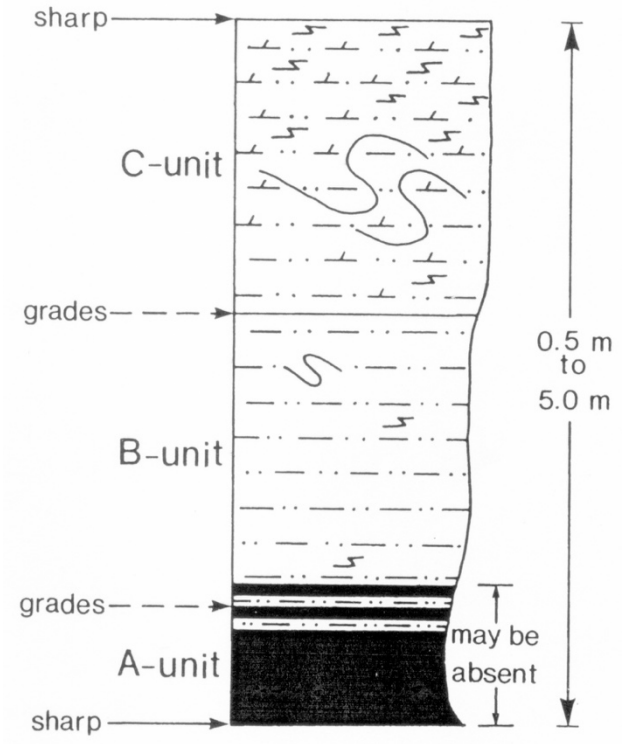


Figure 10. Stop 11: internal stratigraphy of Logan cycles (mesoscale cycles). Contacts with under- and overlying Logan cycles are "sharp;" transitions between units A–C of a Logan cycle are transitional ("grades"). Modified from Landing et al. (1992, fig. 8).

The road cut lies close to the leading (west) edge of the Taconic allochthon and Giddings Brook slice. The section is overturned and dips gently to the east. The utility of Logan cycles (Figure 10) in geological field work is that the upward transition of muddy intervals provides tops-sense in successions that otherwise lack much in the way of primary structures. Thus, successions with ABCABC, BCBC, or ABABABCABC, etc. alternations can be invariably used to determine tops-sense in a "monotonous" mudstone or slate sequence because A-units form the base of tripartite Logan cycles and C-units form the top.

About six Logan cycles are present in this ca. 8 m-thick section. Most of the cycles are BC cycles, and lack the lower black mudstone that appears in many, but not all, Logan cycles (Figure 10). The buff-weathering, dolomitic C-intervals are often the thickest part of the Logan cycles at Stop 11 and grade imperceptibly down into greenish B-intervals. Several of the Logan cycles show the abrupt upward transition from the C-interval into the black mudstone (A-unit) of the overlying Logan cycle.

Well preserved Logan cycles that extend through a completely exposed section through the Floian Stage at the leading edge of the Taconian allochthon at Levís, Québec, appear to have an average duration of less than 100 k.y. (Landing et al., 1992). EL's experience is that only the more proximal parts of Laurentian slope successions (i.e., the Levis area in Québec and the central and southern Giddings Brook slice in eastern New York) show Logan cycles, while more distal successions are comprised of completely oxic mudstones with green, purple, and red color.

Logan cycles should be seen as potentially economically significant as they comprise the dominant depositional motif in the deeper-water, organic-rich, Miocene petroleum source rocks on the southern margin of the Mediterranean (Landing et al., 1992). However, the rocks of the Giddings Brook slice record a much higher burial temperature, with euconodont elements typically opaque black in color and showing a C.A.I. (Color Alteration Index) of 4.0, which means that any organic materials have been transformed into graphite (e.g., Landing, 1976, 1993).

80.0 At end of Stop 11, continue south on Rte 40.

87.6 Pass by intersection with Bald Mountain Road on right. The old Bald Mountain limestone quarry was developed in a giant block of white weathering, massive limestone with a mollusk-dominated fauna (e.g., Cushing and Ruedemann, 1914, p. 75–80). This macrofauna and conodonts (E. Landing, unpub. data) indicate a late Early Ordovician (Floian) age, and allows interpretation of the Bald Mountain limestone as a massively bedded block of Fort Cassin Formation torn off the outer carbonate platform by Taconian thrusting. The block lies under the Taconic masterthrust in early Late Ordovician wildflysch (see Zen, 1967, p. 31, 32, 36).

88.5 Enter village of Middle Falls.

89.5 Turn left (south) on Rte 40. For the next several miles, Early Ordovician carbonate platform units under the Taconic allochthon are exposed in low cuts along the east side of Rte 40.

92.1 Note cut in vertical beds of lower Trenton Group (Upper Ordovician, Katian) limestones and thin interbedded black mudstones along east side of road and opposite wide dirt pull-off on west side of road. This is a good place to bring class trips, as it provides a panorama that includes the Devonian of the Catskill High Peaks to the southwest, the Proterozoic Grenvillian of the southernmost Adirondacks to the west, and the Lower Cambrian of the Taconic allochthon on the hill crest immediately east. In addition, the Upper Ordovician "Knox unconformity" can be investigated at the very north end of the outcrop. The "Knox unconformity" is seen at the contact of relatively proximal, brachiopod-dominated limestones of the Trenton Group with underlying, brown weathering dolostones (age presently undetermined, possibly early Middle Ordovician and referable to the Providence Island Dolostone).

103.3 Stop light, continue straight on combined Rte 40 and 67 into village of Schaghticoke.

104.2 Turn right on curve immediately after red brick church and park in Hoosick River overlook parking area. Until recently, the rocks in Schaghticoke gorge below the dam could be accessed by walking downslope under the Rte 40 bridge. Unfortunately, the response to drinking parties and a few drownings has meant that an iron fence has been put along the gorge, and this makes access difficult. What will be done for Stop 12 will be a photographic overlook downstream from the eastern part of the bridge. Two areas on the north bank and on the upstream side of the island in the middle of the Hoosick where black mudstones of the Schaghticoke dysoxic/anoxic interval crop out can be seen. After this, CAREFULLY cross the bridge roadway, and the same Schaghticoke d/a interval can be seen tectonically repeated several times from a viewpoint directly down from the NE end of the bridge.

**STOP 12. SCHAGHTICOKE GORGE: LATE EARLY TREMADOCIAN DYSAEROBIC INTERVAL.**
(40 MINUTES).
(Stop 13 of Landing, 2002).

The section appears to comprise a tectonically isolated slice at the leading edge of the Taconic allochthhton and Giddings Brook slice. This is the type section of the upper lower Tremadocian (Lower but not lowermost Ordovician) "Schaghticoke Shale" (term abandoned by Landing, 1988b, and grouped as the lowermost part of the Deep Kill Formation).

Schaghticoke gorge features the structural duplication of a thin (ca. 4 m) black mudstone-limestone macroscale alternation in greenish-gray slaty mudstones. Graptolites from the black mudstones (Ruedemann, 1903) are representative of the lower Ordovician Matane faunas known along the leading edges of the Taconian allochthons in Québec. Unfortunately conodonts from limestones in the Schaghticoke d/a interval in the Hoosick River gorge are limited to stratigraphically long-ranging protoconodonts (Landing, 1976; E. Landing unpublished data). The lithology of this middle–upper Tremadocian black shale-limestone macroscale alternation is remarkably similar to the coeval (based on graptolites) black shale-limestone macroscale alternation exposed for 400 km along the south shore of the St. Lawrence River in Québec and which yields *Rossodus manitouensis* Zone conodonts (Landing et al., 1986). The Schaghticoke d/a interval of climate maximum and intensified dysaerobia on the Taconic continental slope and elsewhere along the Laurentian margin (Landing, 2012) is equated with the eustatic rise and the Stonehenge transgression (Taylor et al., 1992) that led to deposition of the Tribes Hill Formation as a type 1 depositional sequence (Stop 4).

104.2 At end of stop, continue south on Rte 40.

104.9 Turn right (west) at intersection with Rte 67 and continue driving west.
119.0 Drive through village of Malta, NY, on Rte 67.
120.0 Rte 67 intersects Northway (U.S. Interstate 87), take entrance ramp (Exchange 12) to north. Most of route is on low-lying terrane developed on Late Ordovician Utica Formation (black mudstone with abundant graptolites). A few miles south of Lake George village, note road cuts in middle Proterozoic Grenvillian orogen (Adirondack basement).
141.0 Exit Northway at Exit 22 (Lake George village and Fort William Henry), end of trip.

## ACKNOWLEDGMENTS

Grateful appreciation for access is given to the property owner at Mettawee River (Stop 10, Liz XXX) and to the quarry company at the Holcolmville Road quarry (Stop 6, Hilltop Slate of Middle Granville, NY, via David Lundy). Recent work in the Taconic slate belt was funded, in part, by NSF Research Grant EAR Integrated Earth Systems 1410503 to MW. Text for this field trip guide is modified from Landing (2002, 2007) and Landing et al. (2007, Submitted).

## REFERENCES

Allen, J.S., Thomas, W.A., and Lavoie, D., 2010. The Laurentian margin of northeastern North America: *in* Tollo, R.P., Bartholomew, M.J., Hibbard, J.P., and Karabinos, P.M. (eds.), From Rodinia to Pangaea: the lithotectonic record of the Appalachian region. Geological Society of America, Memoir 206, pp. 71–90.

Berry, W.B.N., 1959. Graptolite faunas of the northern part of the Taconic area: *in* Zen, E. (ed.), Stratigraphy and structure of west-central Vermont and adjacent New York. Guidebook for the 51st Annual Meeting of the New England Intercollegiate Geological Conference, October 17, 18, 1959, Rutland, Vermont, pp. 61–70.

Berry, W.B.N., 1960. Graptolite fauna of the Poultney Slate: American Journal of Science, 259, 223–228.

Berry, W.B.N., 1962. Stratigraphy, zonation, and age of Schaghticoke, Deepkill, and Normanskill shales, eastern New York: Geological Society of America Bulletin, 73, 695–718.

Bird, J. M., and Rasetti, F., 1968. Lower, Middle, and Upper Cambrian faunas in the Taconic sequence of eastern New York: stratigraphic and biostratigraphic significance: Geological Society of America, Special Paper 113, 66 p.

Bonham, L.D., 1950. Structural geology of the Hoosick Falls area, New York–Vermont, in relation to the theory of the Taconic overthrust: Unpublished Ph.D. dissertation, University of Chicago, 111 p.

Brace, W.F., 1953. The geology of the Rutland area, Vermont: Vermont Geological Survey, Bulletin 6, 124 p.

Brett, K.D., and Westrop, S.R., 1996., Trilobites of the Lower Ordovician (Ibexian) Fort Cassin Formation, Champlain Valley region, New York State and Vermont: Journal of Paleontology, v.70, 408–427.

Chierenzelli, L., Doolan, B. & Mehrtens, C., 1998. The Pinnacle Formation: a late Precambrian rift valley fill with implications for Iapetus rift basin evolution: Northeastern Geology and Environmental Sciences, v. 20**,** 175–185.

Chow, N., and James, N.P., 1987. Cambrian Grand Cycles: a northern Appalachian perspective: Geological Society of America Bulletin, v. 98, 418–429.

Clarke, J.M., 1903. Classification of the New York series of geological formations: New York State Museum, Handbook 19, 55 p.

Collins-Wait, D., and Lowenstein, T.K., 1994. Diagenesis of Cambro-Ordovician Beekmantown Group carbonates, southern Lake Champlain valley: Geological Society of America, Abstracts with Programs, v. 26 (3), 11, 12.

Craddock, J.C., 1957, Stratigraphy and structure of the Kinderhook quadrangle, New York, and the "Taconic klippe": Geological Society of America Bulletin, v. 68, 675–724.

Cushing, H.P., and Ruedemann, R., 1914. Geology of Saratoga Springs and vicinity: New York State Museum Bulletin, v. 169, 177 p.

Dale, T.N., 1899. The slate belt of eastern New York and western Vermont: U.S. Geologic al Survey Annual Report 19, 153–300.

Emmons, E., 1844.The Taconic System based on Observations in New-York, Massachusetts, Maine, Vermont and Rhode-Island: Carrol and Cook, Printers, Albany, 68 p.

English, A.M., Landing, E., and Baird, G.C., 2006. Snake Hill—reconstructing Taconic foreland basin litho- and biofacies from a giant mélange block in eastern New York, USA: Palaeogeography, Palaeoclimatology, Palaeoecology, v. 242, 1200–1220.

Erdtmann, B.-D., 1982. A re-organization and proposed phylogenetic classification of planktic Tremadoc (Early Ordovician) dendroid graptolites: Norsk Geologisk Tiddskrift, v. 62, 121–145.

Ethington, R.L., and Clark, D.L., 1981. Lower and Middle Ordovician conodonts from the Ibex area, western Millard County, Utah: Brigham Young University Geology Studies, v. 28, 155 p.

Fan, R.-Y., Gong, Y.-M., and Uchmann, A., 2018. Topological analysis of graphoglyptid trace fossils, a study of microbenthic solitary and collective animal behavior in the deep sea environment: Paleobiology, v. 44, 306–325.

Fisher, D.W., 1961. Stratigraphy and structure in the southern Taconics (Rensselaer and Columbia counties, New York): *in* LaFleur, R.L. (ed.), Guidebook to field trips, New York State Geological Association, 33rd Annual Meeting, Troy, NY, pp. D10–D27.

Fisher, D.W., 1968. Geology of the Plattsburgh and Rouses Point quadrangles, New York and Vermont: New York State Museum, Map and Chart Series, 10, 37 p.

Fisher, D.W., 1977. Correlation of Hadrynian, Cambrian, and Ordovician rocks in New York State. New York State Museum, Map and Chart Series, 25, 75 p.

Fisher, D. W., 1984., Bedrock geology of the Glens Falls–Whitehall region, New York: New York State Museum, Map and Chart Series, 35, 58 p.

Fisher, D.W., and Hansen, G.F., 1951, Revisions in the geology of Saratoga Springs, New York, and vicinity. American Journal of Science, v. 249, 795–814.

Fisher, D.W., and Mazzulo, S.J., 1976. Lower Ordovician (Gasconadian) Great Meadows Formation in eastern New York: Geological Society of America Bulletin, v. 87, 1143–1158.

Fitch, A., 1850., A historical, topographical and agricultural survey of the County of Washington. Parts 3–5: New York Agricultural Society Transactions, v. 9, 753–944.

Flower, R. 1964., The nautiloid order Ellesmeroceratida (Cephalopoda): New Mexico Bureau of Mining and Mineral Resources, Memoir 12, 234 p.

Flower, R., 1968, Fossils from the Fort Ann Formation: New Mexico Institute of Mining and Technology, Memoir 22, p. 29–34.

Friedman, G.M., 1979. Sedimentary environments and their products, shelf, slope, and rise of Proto-Atlantic (Iapetus) Ocean, Cambrian and Ordovician Periods, eastern New York State: *in* Friedman, G.M. (ed.), Guidebook for field trips. New York State Geological Association, 51st Annual Meeting, and New England Intercollegiate Geological Conference 71st Annual Meeting, pp. 47–86.

Hatcher, R.D., Jr., 2010. The Appalachian orogen: a brief summary: *In* Tollo, R.P., Bartholomew, M.J., Hibbard, J.B, and Karabinos, P.M. (eds.), From Rodinia to Pangaea: the lithotectonic record of the Appalachian region. Geological Society of America, Memoir 206, pp. 1–19.

Hayman, NW., and Kidd, W.S.F., 2002. The Champlain thrust system in the Whitehall–Shoreham area: influence of pre- and post-thrust normal faults on the present thrust geometry and lithofacies distribution: *in* McLelland, J., and Karabinos, P. (eds.), Guidebook for field trips in New York and Vermont. New England Intercollegiate Geological Conference, 94th Annual Meeting, and New York State Geological Association, 74th Annual Meeting, Lake George, New York, pp. A7-1–A7-27.

Herbosch, A., and Verniers, J., 2011. What is the biostratigraphic value of the ichnofossil *Oldhamia* for the Cambrian: a review: Geologica Belgica, v.14, 229–248.

James, N.P., and Stevens, R.K., 1986. Stratigraphy and correlation of the Cambrian–Ordovician Cow Head Group, western Newfoundland: Geological Survey of Canada, Bulletin 366, 143 p.

James, N.P., Knight, I., Stevens, R.K., and Barnes, C.R., 1988. Trip B1. Sedimentology and paleontology of an Early Paleozoic continental margin, western Newfoundland: Fieldtrip Guidebook. Newfoundland Geological Association-Mineralogical Association of Canada-Canadian Association of Petroleum Geologists, 121 p.

Jacobi, L.D., 1977. Stratigraphy, depositional environment and structure of the Taconic allochthon, central Washington County, New York: Unpublished MSc. Thesis, State University of New York at Albany, 191 p.

Keith, A., 1932, Stratigraphy and structure of northwestern Vermont: Washington Academy of Science Journal, v. 22, 357–379, 393–406.

Keith, B.D., and Friedman, G.M., 1977. A slope–fan–basin–plain model, Taconic sequence, New York and Vermont: Journal of Sedimentary Petrology, v. 47, 1220–1241.

Keith, B.D., and Friedman, G.M., 1977. A slope–fan–basin–plain model, Taconic sequence, New York and Vermont: *in* Curtis, D.M. (ed.), Environmental problems in ancient sediments. Society of Economic Paleontologists and Mineralogists, Reprint Series, v. 6, pp. 178–199.

Knight, I., Boyce, W.D., C. B. Skovsted, C.B, and Balthasar, U., 2017. The Lower Cambrian Forteau Formation, southern Labrador and Great Northern Peninsula, western Newfoundland: lithostratigraphy, trilobites and depositional setting: Government of Newfoundland and Labrador, Department of Natural Resources, Geological Survey, Occasional Papers, 2017-01, 72 p.

Kröger, B., and Landing, E., 2007. The earliest Ordovician cephalopods of eastern Laurentia—ellesmerocids of the Tribes Hill Formation, eastern New York. Journal of Paleontology, v. 81, 841–857.

Kröger, B., and Landing, E., 2010. Early Ordovician community evolution with eustatic change through the middle Beekmantown Group, northeast Laurentia**:** Palaeogeography, Palaeoclimatology, Palaeoecology, v. 294, 174–188.

Książkiewicz, M., 1968. O niektórych problematykach z fliszu Karpat Polskich (Częśź III): Polska Towarzystu Geologii, Rocznik, v. 38, 3–17.

Książkiewicz, M., 1970. Observations on the ichnofauna of the Polish Carpathians: *in* Crimes, T.P., and Harper, J.C. (eds.), Trace Fossils, Geological Journal, Special Issue 3, pp. 283–343.

Landing, E., 1976. Early Ordovician (Arenigian) conodont and graptolite biostratigraphy of the Taconic allochthon, eastern New York: Journal of Paleontology, v. 50 614–646.

Landing, E. 1977. "*Prooneotodus*" *tenuis* (Müller, 1959) apparatuses from the Taconic allochthon, eastern New York: construction, taphonomy, and the protoconodont "supertooth" model: Journal of Paleontology, v. 71, 1072–1084.

Landing, E. 1988a. Cambrian–Ordovician boundary in North America: revised Tremadocian correlations, unconformities, and "glacioeustasy": *in* Landing, E. (ed.), The Canadian Paleontology and Biostratigraphy Seminar, Proceedings. New York State Museum Bulletin, v. 462, pp. 48–58.

Landing, E. 1988b. Depositional tectonics and biostratigraphy of the western portion of the Taconic allochthon, eastern New York State: *in* Landing, E. (ed.), The Canadian Paleontology and Biostratigraphy Seminar, Proceedings. New York State Museum Bulletin, v. 462, pp. 96–110.

Landing, E. 1993. Cambrian–Ordovician boundary in the Taconic allochthon, eastern New York, and its interregional correlation: Journal of Paleontology, v. 67, 1–19.

Landing, E., 2002. Early Paleozoic sea levels and climates: new evidence from the east Laurentian shelf and slope: *in* McLelland, J., and Karabinos, P. (eds.), Guidebook for Fieldtrips in New York and Vermont, New England Intercollegiate Geological Conference, 94th Annual Meeting, and New York State Geological Association, 74th Annual Meeting, Lake George, NY, pp. C6-1–C6-22.

Landing, E., 2007. Ediacaran–Ordovician of east Laurentia—geologic setting and controls on deposition along the New York Promontory: *in* Landing, E. (ed.), Ediacaran–Ordovician of east Laurentia—S. W. Ford Memorial Volume. New York State Museum Bulletin, v. 510 pp. 5–24.

Landing, E., 2011. No Late Cambrian ice in Laurentia. GSA Today, v. 21. doi:10.1130/G113C.1, p. e19

Landing, E., 2012. Time-specific black mudstones and global hyperwarming on the Cambrian–Ordovician slope and shelf of the Laurentia palaeocontinent: Palaeogeography, Palaeoclimatology, Palaeoecology, v. 367–368, 256–272.

Landing, E., 2013a. Extended Abstract—The Great American Carbonate Bank in northeast Laurentia: its births, deaths, and linkage to continental slope oxygenation (Early Cambrian–Late Ordovician): *in* Derby, J.R., Fritz, R.D., Longacre, S.A., Morgan, W.A., and Sternbach, C.A. (eds.), The Great American Carbonate Bank, essays in honor of James Lee Wilson: the geology and economic resources of the Cambrian–Ordovician Sauk Megasequence of Laurentia. American Association of Petroleum Geologists Bulletin, v. 98, pp. 253a–260a.

Landing, E., 2013b. The Great American Carbonate Bank in northeast Laurentia: its births, deaths, and linkage to continental slope oxygenation (Early Cambrian–Late Ordovician): *in* Derby, J.R., Fritz, R.D., Longacre, S.A., Morgan, W.A., and Sternbach, C.A. (eds.), The Great American Carbonate Bank, essays in honor of James Lee Wilson: the geology and economic resources of the Cambrian–Ordovician Sauk Megasequence of Laurentia. American Association of Petroleum Geologists Bulletin 98, pp. 451–490.

Landing, E., and Bartowski, K. E., 1996. Oldest shelly fossils from the Taconic allochthon and late Early Cambrian sea-levels in eastern Laurentia: Journal of Paleontology, v. 70, 741–761.

Landing, E., and Benus, A.P., 1985. The Levis Formation: passive margin slope processes and dynamic stratigraphy in the western area: *in* Riva, J.F. (ed.), Field Trips Guidebook. Canadian Paleontology and Biostratigraphy Seminar, Ste. Foy, Quebec. Université Laval Press, Ste. Foy, pp. 1–11.

Landing, E., and MacGabhann, B.A., 2010. First evidence for Cambrian glaciation provided by sections in Avalonian New Brunswick and Ireland—additional data for Avalon–Gondwana separation by the earliest Palaeozoic: Palaeogeography, Palaeoclimatology, Palaeoecology, v. 285, 174–185.

Landing, E., and Westrop, S.R., 2006. Early Ordovician faunas, stratigraphy, and sea-level history of the middle Beekmantown Group, northeastern New York: Journal of Paleontology, v. 80, 958–980.

Landing, E., Benus, A.P., and Whitney, P. R., 1992. Early and early Middle Cambrian continental slope deposition: shale cycles and sandstones in the New York Promontory and Quebec Reentrant region: New York State Museum Bulletin, v. 474, 40 p.

Landing, E., Geyer, G., and Bartowski, K.E., 2002. Latest Early Cambrian small shelly fossils, trilobites, and Hatch Hill dysaerobic interval on the east Laurentian continental slope: Journal of Paleontology, v. 76, 285–303.

Landing, E., Westrop, S.R., and Van Aller Hernick, L. 2003A. Uppermost Cambrian–Lower Ordovician faunas and Laurentian platform sequence stratigraphy, eastern New York and Vermont: Journal of Paleontology, v. 77, 78–98.

Landing, E., Pe-Piper, G., Kidd, W.S.F., and Azmy, K., 2003B. Tectonic setting of outer trench slope volcanism: pillow basalt and limestone in the Ordovician Taconian orogen of eastern New York: Canadian Journal of Earth Sciences, v. 40, 1173–1187.

Landing, E., Amati, L., and Franzi, D. A., 2009. Epeirogenic transgression near a triple junction: the oldest (latest Early–Middle Cambrian) marine onlap of cratonic New York and Quebec: Geological Magazine, v. 146, 552–566.

Landing, E., Franzi, D.A., Hagadorn, J.W., Westrop, S.R., B. Kröger, B, and Dawson, J., 2007. Cambrian of east Laurentia: field workshop in eastern New York and western Vermont: *in* Landing, E. (ed.), Ediacaran–Ordovician of east Laurentia—S. W. Ford Memorial Volume. New York State Museum Bulletin, v. 510, pp. 25–80.

Landing, E., Westrop, S.R., Kröger, B., and English, A.M., 2010. Left behind—extinction and a relict trilobite fauna in a Cambrian–Ordovician boundary succession (northeast Laurentian platform, New York): Geological Magazine, v. 148, 529–557. doi:10.1017/S0016756810000019

Landing, E., Westrop, S.R., Adrain, J., and Kröger, B., 2012. Early Ordovician (Tremadocian) eustasy and biotas on a tropical passive margin—Tribes Hill–Rochdale formations in eastern Laurentia (New York and adjacent Vermont): Geological Magazine, v. 149, 93–123.

Landing, E., Salad Hersi, O., Amati, L., Westrop, S.R., and Franzi, D.A. In press. Early Paleozoic rifting and reactivation of a passive-margin rift: Insights from detrital zircon provenance signatures of the Potsdam Group, Ottawa graben by Lowe et al. (2018, GSA Bulletin, v. 130, no. 7/8, p. 1377–1396). COMMENT: Geological Society of America Bulletin.

Landing, E., Webster, M., Andreas, A., and Bowser, S.S., Submitted. Late Early Cambrian persistence of Iapetan rifting, continental slope anoxic–oxic intervals, and "Hawke Bay Events" in NE Laurentia: (to) Geological Magazine.

Lindholm, R.M., and Casey, J., 1990. The distribution and possible biostratigraphic significance of the ichnogenus *Oldhamia* in the shales of the Blow Me Down Brook Formation, western Newfoundland: Canadian Journal of Earth Sciences, v. 27, 1270–1287.

Lochman, C., 1956. Stratigraphy, paleontology, and paleogeography of the *Elliptocephala asaphoides* strata in Cambridge and Hoosick quadrangles, New York: Geological Society of America Bulletin, v. 67, 1331–1396.

Lochman-Balk, C., 1971. The Cambrian of the craton of the United States: *in* Holland, C.H. (ed.), Cambrian of the New World. Wiley-Interscience, New York, pp. 79–167.

Lowe, D.G., Arnott, R.W.C., Nowlan, G.S., and McCracken, A.D., 2017. Lithostratigraphic and allostratigraphic framework of the Cambrian–Ordovician Potsdam Group and correlations across early Paleozoic southern Laurentia: Canadian Journal of Earth Sciences, v. 54, p. 550–585, https//doi.org/10.1139/cjes-2016-0151.

Lowe, D.G., Arnott, R.W.C., Chiarenzelli, J.R., and Rainbird, R.H., 2018. Early Paleozoic rifting and reactivation of a passive-margin rift: insights from detrital zircon provenance of the Potsdam Group, Ottawa graben: Geological Society of America Bulletin, doi: 10.1130/B31749.1, 21 p.

Miller, J.F., 1969. Conodont fauna of the Notch Peak Limestone (Cambro-Ordovician), House Range, Utah. Journal of Paleontology, v. 43, 413–439.

Nielsen, A.T., and Schovsbo, N.H., 2015. The regressive Early–Mid Cambrian 'Hawke Bay Event' in Baltoscandia: epeirogenic uplift in concert with eustasy: Earth-Science Reviews, v. 151, 288–350.

Osberg, P.H. 1969. Lower Paleozoic stratigraphy and structural geology, Green Mountain–Sutton Mountain anticlinorium, Vermont and southern Quebec: *in* Kay, G.M. (ed.), North Atlantic Geology and Continental Drift: A Symposium on the Origin of the Atlantic Ocean. American Association of Petroleum Geologists, Memoir 12, pp. 687–700.

Palmer, A.R., and James, N.P., 1980. The Hawke Bay event: a circum-Iapetus regression near the Lower–Middle Cambrian boundary: *in* Wones, D.R. (ed.), The Caledonides in the USA. Department of Geological Sciences, Virginia Polytechnic Institute and State University, Memoir 2, pp. 15–18.

Potter, D.B., 1972, Stratigraphy and structure of the Hoosick Falls area, New York–Vermont, east-central Taconics: New York State Museum, Map and Chart Series 19, 71 p.

Rankin, D.W., Drake, A.A., Jr., Glover, L., III, Goldsmith, R., Hall, L.M., Murray, D.P., Ratcliffe, N.M., Read, J.F., Secor, D.T., Jr., and Stanley, R.S., 1989. Pre-orogenic terranes. Chapter 2: *in* Hatcher, R.D., Jr., Thomas, W.A., and Viele, G.W. (eds.), The Appalachian-Ouachita orogen in the United States. Geological Society of America, Geology of North America, F-2, pp. 7–100.

Ratcliffe, N.M., Potter, D.B., and Stanley, R.S., 1993. Bedrock geologic map of the Williamstown and North Adams quadrangles, Masssachusetts and Vermont, and part of the Cheshire quadrangle, Massachusetts: U. S. Geological Survey, Miscellaneous Publications, Map 1-2369.

Ratcliffe, N.M., Stanley, R.S., Gale, M.H., Thompson, P.J., and Walsh, G.J., 2011. Bedrock geologic map of Vermont, scale 1:100,000. United States Geological Survey Scientific Investigations, Map 3184, 3 sheets.

Rodgers, J., 1937, Stratigraphy and structure in the upper Champlain Valley: Geological Society of America Bulletin, v. 48, 1573–1586.

Rowley, D. M., Kidd, W. S. F. and Delano, L. L., 1979. Detailed stratigraphic and structural features of the Giddings Brook slice of the Taconic allochthon in the Granville area: *in* Friedman, G.M. (ed.), Guidebook, Joint Annual Meeting of the New York State Geological Association and New England Intercollegiate Geological Conference, Rensselaer Polytechnic Institute, Troy, N. Y., pp. 186–242.

Ruedemann, R., 1902. The graptolite (Levis) facies of the Beekmantown Formation in Rensselaer County, New York: New York State Museum Bulletin, v. 52, 546–575.

Ruedemann, R., 1903. The Cambric *Dictyonema* fauna in the slate belt of eastern New York: New York State Museum Bulletin, v. 227–228, p. 116–130.

Ruedemann, R., 1929. Note on *Oldhamia* (*Murchisonites*) *occidens* (Walcott): New York State Museum Bulletin, v. 281, 47–51.

Ruedemann, R., 1942. *Oldhamia* and the Rensselaer Grit problem: New York State Museum Bulletin, v. 327, 47–51.

Ruedemann, R., and Wilson, T.Y., 1936. Eastern New York cherts: Geological Society of America Bulletin, v. 47, 1535–1586.

Schuchert, C., 1937. Cambrian and Ordovician of northwestern Vermont: Geological Society of America Bulletin, v. 48, 1001–1078.

Skehan, J. W., 1961. The Green Mountain anticlinorium in the vicinity of Wilmington and Woodford, Vermont: Vermont Geological Survey, Bulletin 17, 159 p.

Sweet, W., Ethington, R.L., and Barnes, C.R., 1971. North American Middle and Upper Ordovician conodont faunas: *in* Sweet, W., and Bergström, S. (eds.), Symposium on Conodont biostratigraphy. Geological Society of America, Memoir 127, pp. 163–193.

Swett, N.L., and Narbonne, G.M., 1993. Occurrence of the Cambrian trace fossil *Oldhamia* in southern Québec: Atlantic Geology, v. 29, 69–73.

Swinnerton, A.C., 1922. Geology of a portion of the Castleton, Vermont, quadrangle: Unpublished Ph.D. dissertation, Harvard University, 262 p.

Taylor, J.F., Repetski, J.E., and Orndorff, R.C., 1992. The Stonehenge transgression: a rapid submergence of the central Appalachian basin in the Early Ordovician: *in* Webby, B.D., and Laurie, J.R. (eds), Global Perspectives on Ordovician Geology. Balkema, Rotterdam, pp. 409–418.

Taylor, M.E., and Halley, R.B., 1974. Systematics, environment, and biogeography of some Late Cambrian and Early Ordovician trilobites from eastern New York State: U.S. Geological Survey. Professional Paper 834, 38 p.

Thayer, C.W., 1983. Sediment-mediated biological disturbance and the evolution of marine benthos: *in* Tevesc, M.J.S., and McCall, P.L. (eds.), Biotic interactions in Recent and fossil benthic communities, Topics in Geobiology, v. 3, pp. 480–627.

Theokritoff, G., 1959.Stratigraphy and structure of the Taconic sequence in the Thorn Hill and Granville quadrangles: *in* Zen, E. (ed.), New England Intercollegiate Geological Conference, 51st Annual Meeting, Rutland, pp. 53–58.

Theokritoff, G., 1964. The Taconic stratigraphy in northern Washington County, New York: Geological Society of America Bulletin, v. 75, 171–190.

Theokritoff, G., 1981. Early Cambrian faunas of eastern New York State--taphonomy and ecology: *in* Taylor, M.E. (ed.), Short Papers for the Second International Symposium on the Cambrian System. USGS Open File Report 81-743, pp. 228–230.

Thomas, W.A., 1977. Evolution of Appalachian–Ouachita salients and recesses from reentrants and promontories in the continental margin: American Journal of Science, v. 277, 1233–1278.

Ulrich, E.O., and Cushing, H.P., 1910, Age and relationships of the Little Falls Dolostone (Calciferous) of the Mohawk Valley. New York State Museum Bulletin, v. 140, 97–140.

Walcott, C.D., 1888. The Taconic system of Emmons: American Journal of Science, Third Series, v. 35, 229–242.

Walcott, C.D., 1890. The fauna of the Lower Cambrian or *Olenellus* Zone: U.S. Geological Survey, Tenth Annual Report 1888–1889, pp. 509–763.

Walcott, C.D., 1912. Cambrian Brachiopoda: U. S. Geological Survey Monograph, 51**,** 1235 p.

Webster, M., and Landing, E., 2016. Geologic context, biostratigraphic significance, and systematic revision of late early Cambrian olenelloid trilobites from the Parker and Monkton formations, northwestern Vermont: Australasian Palaeontological Memoirs, v. 49, 193–240. ISSN 2205-8877

Welby, 1961, Bedrock geology of the central Champlain Valley of Vermont: Vermont Geological Survey, Bulletin 14, 296 p.

Westrop, S.R., Trembley, J.V., and Landing, E., 1995. Declining importance of trilobites in Ordovician nearshore communities: dilution or displacement?: Palaios, v. 10, 75–79.

Wheeler, R.R., 1942. Cambrian–Ordovician boundary in the Adirondack-border region. American Journal of Science, v. 240, 518–524.

Williams, H., 1978. Tectonic lithofacies map of the Appalachian orogen: Map 1, Memorial University of Newfoundland, St. John's.

Wilmarth, M.G., 1938, Lexicon of geologic names of the United States (including Alaska): U.S. Geological Survey, Bulletin 896, 2396 p.

Zen, E. 1961. Stratigraphy and structure at the north end of the Taconic Range in west-central Vermont: Geological Society of America Bulletin, v. 72, 292–338.

Zen, E. 1964. Taconic stratigraphic names: definitions and synonyms: U. S. Geological Survey. Bulletin 1174, 95 p.

Zenger, D.H., 1981, Stratigraphy and petrology of the Little Falls Dolostone (Upper Cambrian), east-central New York: New York State Museum, Map and Chart 34, 138 p.

## APPENDIX 1

### STOP A1: "WEST CASTLETON FORMATION" TYPE SECTION IS HATCH HILL FORMATION

**Location**

Stop A1 features the completely exposed core of the Scotch Hill syncline (Figure 11) on the north side of Scotch Hill Road at the hamlet of West Castleton, Vermont. This photogenic section is located between Glen Lake and Lake Bomoseen. This section with two thick intervals of thin-bedded dolomitic quartz arenite (lower to 3.75 m and upper 1.3 m thick) is complemented by two overgrown road cuts just to the south on the east side of Scotch Hill Road. The more northerly road cut is 30 m north of the intersection of Scotch Hill Road and Corvell Road (unpaved) and exposes 5.5 m of east-dipping black shale and thin, lenticular, cross-laminated, orange-weathering dolomitic sandstones. The sandstones comprise ca. 30% of the short section. The second section extends for 300–500 m south of the intersection of Corvell and Scotch Hill roads and includes ca. 5.0 m of black shale and thin bedded, cross-laminated, orange-weathering dolomitic sandstones (ca. 50% of section).

**Purpose**

As it is relatively distant from the other stops of field trip A5 further south, this important locality could not be accommodated into the trip schedule but should be visited by the participants at another time.

**Problems with the "West Castleton Formation" (abandoned)**

Zen (1961) proposed the "West Castleton Formation" based on the, then probably much better exposed, road cut on Scotch Hill Road south of the hamlet of West Castleton. As the rocks in the road cut strike directly into the syncline only a short distance north at West Castleton, the synclinal succession is obviously also "West Castleton Formation." The syncline in "West Castleton" is immediately underlain by purple and red slates (Zen, 1961, pl. 3, fig. 2 caption) that have yielded an *Elliptocephala asaphoides* assemblage from an interval of thin bedded limestones (Schuchert, 1937, p. 1038). The road cut has not yielded fossils, although Swinnerton (1922) noted but did not illustrate a purported *Olenellus*.

Figure 11. Stop A1: Lower Hatch Hill Formation in core of Scotch Hill syncline, north side of Scotch Hill Road between Glen Lake and Lake Bomoseen at hamlet of West Castleton, Vermont. Although traditionally assigned to the type "West Castleton Formation" (designation abandoned by, e.g., Landing, 1988b, etc.), the thick intervals of dolomitic quartz arenite sandstones in the lower and middle parts of the dark gray to black slatey mudstone-dominated outcrop, the persistence of thin dolomitic sandstones to the top of the outcrop, and the significant proportions of dolomitic quartz sandstones lower in the type section demonstrate the lithologic similarity with characteristic Hatch Hill Formation facies throughout the western Taconic allochthon. In addition, immediately underlying strata consist of green to red siliciclastic slates with fossiliferous limestones (*Elliptocephala asaphoides* assemblage) that are comparable to the Middle Granville Formation that underlies the Hatch Hill Formation throughout the western Taconic allochthon.

The red and green slates with a limestone interval below the "West Castleton" show the "West Castleton" is underlain by the rocks identical in lithology and with the same fauna as the Middle Granville Formation (Stop 6). The presence of these red and green slates just under the "West Castleton" in the core of the Scotch Hill syncline indicates that the type section of the "West Castleton" is low in the formation and is late Early Cambrian. It should be noted that most of the northern part of Scotch Hill Road before the easterly curve at Glen Lake follows along the Middle Granville–"West Castleton" contact.

What seems to have developed from Zen's (1961) description of the West Castleton is a seeming belief in the dominance of black siliciclastic mudstones in the formation (e.g., Potter, 1971, Ratcliffe et al., 2011), although substantial amounts of dolomitic quartz arenite occur in the unit both in the currently observable rock in the road cuts and in the core of the Scotch Hill syncline (Figure 11, also "Location" above)).

This presence of dolomitic sandstones in the "West Castleton" type section makes the formation quite similar lithologically to the Hatch Hill Formation, which Theokritoff (1959) described as consisting of black mudstones and interbedded orange weathering (dolomitic) sandstones. Given this lithologic similarity, the "key" distinction between the Hatch Hill and "West Castleton" seems to have been a belief that the former was Upper

Cambrian and the latter Early Cambrian (Zen, 1964, see descriptions of the two formations)—a mistaken distinction that is essentially maintained in the Vermont Geologic Map (Ratcliffe et al., 2011).

Indeed, Theokritoff's (1959) "Late Cambrian" graptolites have been reevaluated and show that the upper Hatch Hill in the northern and southern Taconics is lowest Ordovician (Stop 8; Landing, 1993). Similarly, the succession at Judson Point, Columbia County, eastern New York (Bird and Rasetti, 1968), shows that a Hatch Hill-type facies extends down into the upper *Elliptocephala asaphoides* assemblage interval and extends upward through the middle Middle Cambrian at Judson Point. Recent investigation of the succession at and further south along strike of Judson Point (by EL) shows that this Hatch Hill-type facies is underlain by green mudstones with thin limestones and a carbonate clast debris flow at a locality 935 m SSE from the base of the Judson Point section. This locality lies the recently bulldozed (Spring 2018) entrance road into No. 164 Southers Road. The presence of a lower *Elliptocephala asaphoides* assemblage (i.e., Landing and Bartowski, 1996) in the thin limestones in green mudstone represents the upper Middle Granville Formation and records an identical succession to that at West Castleton.

Rowley et al. (1979, p. 197) first began a tentative re-evaluation of the distinction of the Hatch Hill and "West Castleton Formation" by noting that the "distinction (of the formations) is marginal" and suggesting that the "West Castleton" "may be better regarded as a facies of the Hach Hill." Subsequently, Landing (1988b, 1993, 2002, 2007) synonymized the "West Castleton" with the Hatch Hill—a repeated nomenclatural decision and evaluation not reflected in any way in the Geologic Map of Vermont (Ratcliffe et al., 2011). Thus, the Hatch Hill Formation and Hatch Hill d/a interval represent a long-term (late Early Cambrian–earliest Ordovician) interval with organic-rich mudstone deposition on the east Laurentian continental slope (e.g., Landing et al., 2002).

The other problem with the "West Castleton Formation" is that two somewhat similar d/a mudstone-rich intervals exist in the Taconic succession, and lithologic similarity has led to long-term confusion of the Browns Pond Formation with the Hatch Hill/"West Castleton" in the Taconics. However, careful mapping and good outcrops allows distinction of the Browns Pond and Hatch Hill by the former's appearance a short stratigraphic distance above the Bomoseen Formation (Stop 9) and the presence of Dale's (1899) green and red "Cambrian roofing slates" (i.e., Middle Granville Formation and upper "Bull Formation" of the Vermont Geologic Map) between the two black mudstone intervals (e.g., Stop 6). The invariable presence of the red and green slates precludes any statement that the Browns Pond is "interbedded" with the "West Castleton" (Ratcliffe et al., 2011).

This reliance on stratigraphic succession as an important aid in distinguishing the Browns Pond and Hatch Hill/"West Castleton" formations has allowed a re-evaluation of Bonham (1950) and Lochman's (1956) localities with *Elliptocephala asaphoides* assemblages in the central Taconics (see Potter, 1972, appendix 4). All of these localities occur in successions that include the underlying Bonoseen Formation and are thus referable to the Browns Pond Formation, and not to the Hatch Hill/"West Castleton." The conclusion, as in Landing (1988b) is that "West Castleton Formation" must be abandoned in favor of the coeval and lithologically identical Hatch Hill Formation.

**In appreciation**

Jim and Bunny Whitman genially gave permission to examine the synclinal succession in the back yard of their cottage. The property has been owned by the Whitman family back to Jim's grandparents, Mary and Jim Larkin. Jim Larkin was a slate quarryman of Welsh descent.

## APPENDIX 2

**Revisions in Stratigraphic Nomenclature—Cambrian–Ordovician Platform**

**Tectonic setting and stratigraphic nomenclature**. A very uniform upper Middle Cambrian–Lower Ordovician lithostratigraphy occurs in authochthonous sequences on the north and west sides and to the south of the Lake Champlain lowlands in southern Quebec and SE Ontario and adjacent New York. This succession is also present in the parautochthonous Champlain slice in west-central Vermont and easternmost New York (e.g., Fisher, 1984; Figures 1, 3). This frankly "layer cake" lithostratigraphic succession was deposited after down-faulting and submergence of the mouth of the Ottawa-Bonnechere aulacogen (OBa) beginning in the late Early Cambrian with deposition of the Altona Formation through the middle Middle Cambrian. Altona deposition was followed by deposition of the fluviatile arkoses of the Ausable Member of the Potsdam Formation in the OBa and as far south as the central Lake Champlain lowlands.

Following Ausable Member deposition, marine transgressions took place across a depositional surface with minimal, essentially 0°, depositional slope across the Grenville basement and across the Ausable Member in the OBa and northern Lake Champlain lowlands. This post-Ausable depositional setting meant the final establishment of the post-rifting passive margin and deposition of mineralogically mature quartz sandstones (Keeseville Member of the Potsdam Formation) and overlying Beekmantown Group with lower quartz sand- and carbonate-rich (Galway Formation) and higher dominantly carbonate deposits of the higher Beekmantown Group (Little Falls–Providence Island formations). As now interpreted, the carbonate-dominated units of the Beekmantown Group are separate type 1 depositional sequences that comprise formation-level units with uniform member-level lithostratigraphy, characteristically formation-distinct macro- and microfossil assemblages (trilobites, cephalopods, gastropods, conodonts), and likely are separated from each other by hiatuses of longer duration than the time represented by each formation (e.g., Landing, 2007, 2012; Kröger and Landing, 2010)

A confusing stratigraphic nomenclature for the shelf succession has obscured the regional extent of lithic units and the simple pre-Taconic orogeny evolution of this stretch of the New York Promontory (Figure 12). In part, this complexity, with an unnecessarily large number of named lithostratigraphic units, reflects casual stratigraphic practices that featured naming units without designation or description of type sections, detailed lithic characteristics, or specified upper or lower contacts. These contacts were often changed arbitrarily, and lateral correlations were commonly established by assertion rather than by biostratigraphic or lithostratigraphic analyses (Figure 12, see discussion below of Tribes Hill Formation). An additional problem resulted from hydrothermal dolomitization during the Taconic orogeny that resulted in quite rapid lateral transitions from limestones with well preserved depositional fabrics to dolostones that lack much in the way of primary fabric (Stops 3, 4)—a situation compounded by a seeming "need" to give the coeval non-dolomitized and dolomitized intervals separate formal lithostratigraphic names (see Little Falls Formation, below). In a number of cases, observance of stratigraphic naming procedures (e.g., North American Commission on Stratigraphic Nomenclature [NACSN], 2005) meant that units, as formations, were subdivided into a number of formations with the name of the subdivided formation assigned to one of the parts (i.e., undesirable restiriction by the NACSN)

Synonymous units that essentially differ because that occur in different map areas or in map areas studied by different workers without a broader experience in the region's field geology have persisted in the literature by a sort of scholasticism. This unquestioning regard for the older literature somehow did not allow revisions or any consideration of the synonymization of identical lithostratigraphic units. Thus, Fisher (1954) and Fisher and Mazzulo (1976) used distinctive stratigraphic names, Tribes Hill Formation and "Great Meadows Formation," for the same unit (Tribes Hill) in the Mohawk River valley and southern Lake Champlain lowlands ("Great Meadows"), while using "Gailor Dolomite" (Fisher and Hansen, 1951) for identical strata in the Saratoga, NY, area just about midway between the Mohawk and Lake Champlain regions (Landing and Westrop, 2006) . The contacts of lithologic untis were often changed arbitrarily, and lateral correlations were commonly established by assertion rather than by biostratigraphic or lithostratigraphic analyses (Figure 12).This complexity also reflects the proposal of different names for lithologically identical, laterally continuous, and coeval and, thus, synonymous units in New York and Vermont. A lack of consideration of much of the available literature, as in the recently updated Vermont geologic map (Ratcliffe et al., 2011), means that a uniform stratigraphic nomenclature that should have been applied to the Vermont–New York shelf still does not exist in widely available publications.

**Potsdam, Galway, Little Falls, Galway, "Ticonderoga" (abandoned), and "Whitehall" (abandoned) formations.** Landing et al. (2009, In press) have discussed the nomenclature of the Potsdam Formation and limited it to the grade of "formation" and not "group," and detailed that Potsdam Formation deposition did not persist either on the NE Laurentian shelf or in the Ottawa-Bonnechere aulacogen into the Early Ordovician (e.g., Lowe et al., 2017, 2018). An error on the revised Vermont Geologic Map (Ratcliffe et al., 2011, legend) limits the range of the Potsdam to the "Upper Cambrian," although the unit ranges only into the middle Upper Cambrian and its upper part (Keeseville Member) is upper Middle Cambrian at its base (Stop 1, this report). [It might also be noted that the correct age of the Monkton Formation in Vermont has always been late Early Cambrian (late Dyeran) and not "Middle Cambrian" as on the revised Vermont Geologic Map (Ratcliffe et al., 2011, legend)].

Rodgers (1937) proposed "Whitehall Formation" for a temporally-defined, carbonate-dominated, lowest Ordovician unit in the Lake Champlain Lowlands (Fig. 2). His "Whitehall" overlay an unfossiliferous, but presumably, Upper Cambrian interval referred to the Little Falls Formation of Clarke (1903) in the Lake Champlain

Lowlands. However, the "Whitehall" and Little Falls Formations unconformably underlie the Tribes Hill Formation in the Lake Champlain Lowlands and Mohawk Valley, respectively, and both "units" are now known to range only into the uppermost Cambrian. The "Whitehall" ranges into the uppermost *Cordylodus proavus* Zone (Landing et al., 2003), and the Little Falls in the Mohawk valley ranges into the middle *C. proavus* Zone (Landing et al., 1996).

The Little Falls Formation has always been regarded as a carbonate-dominated (now largely hydrothermally dolomitized; Stop 3, this report) unit that overlies a mixed dolostone and quartz arenite "transitional facies" (i.e., the Galway Formation of Fisher and Hansen, 1951) above Potsdam Formation quartz arenites in the Mohawk valley (e.g., Wilmarth, 1938, p. 1194–1196; Zenger, 1981). Similarly, the "Whitehall" overlies the mixed dolostone and quartz arenite facies of a purported "Ticonderoga Formation" (J. Rodgers *in* Welby, 1961; abandoned by Landing et al., 2003A; a junior synonym of Galway Formation in Figure 12), and the latter overlies the Potsdam in the Lake Champlain lowlands. These data on lithologic composition, upper and lower contacts, and age support Ulrich and Cushing's (1910) recognition of the Little Falls Formation (="Whitehall Formation," abandoned) and the replacement of "Ticonderoga" (abandoned) by Galway Formation in the Lake Champlain lowlands. Unfortunately, the status of the "Ticonderoga Formation" (abandoned) does not seem to have been considered, and the term "Ticonderoga Formation" still appears on the revised Vermont Geologic Map (Ratcliffe et al., 2011).

**Tribes Hill, "Cutting" (abandoned), and "Great Meadows" (abandoned) Formation.** Ulrich and Cushing's (1910) and Wheeler's (1942) proposal of a unified stratigraphic nomenclature to the Upper Cambrian–Lower Ordovician of the Mohawk valley and southern Lake Champlain lowlands showed a great appreciation for the lateral continuity of stratigraphic units on the New York Promontory. Although dismissed without adequate discussion by Fisher and Mazzullo (1976, p. 1443), Ulrich and Cushing's and Wheeler's recognition of the Tribes Hill Formation extending from the Mohawk River into the Lake Champlain lowlands is appropriate.

The "Cutting/Great Meadows Formation" (terms abandoned; Landing et al., 1988A; Landing, 2002, 2007, 2012) of the Lake Champlain lowlands rests unconformably on latest Cambrian carbonates and forms a deepening–shoaling sequence in the *Rossodus manitouensis* Zone. These relationships are identical to those of the coeval Tribes Hill Formation in the Mohawk River valley (see Landing et al., 1996). The vertical facies succession in the "Cutting/Great Meadows" is also identical to that of the Tribes Hill in the Mohawk valley so that the same member-level nomenclature is appropriate (Stop 4, this report; discussed below). These lithologic correspondences mean that "Cutting Formation" and "Great Meadows Formation" must be abandoned for the older synonymous term "Tribes Hill Formation," a well published stratigraphic reevaluation not present in the revised Vermont Geologic map (Ratcliffe et al., 2011, legend), with the latter not noting that there is a type 1 sequence boundary at the base of the Tribes Hill Formation that is the trans-Laurentian shelf Cambrian–Ordovician boundary (e.g., Landing et al., In press). The revised Vermont Geologic Map shows the "Whitehall Formation (designation abandoned) ranging into the lowest Ordovician, without incorporating then available bio- and lithostratigraphic work that shows the top of the Little Falls Formation as Upper, but not uppermost Cambrian, both in eastern New York and on the Vermont side of Lake Champlain (Landing et al., 2003A, 2007, 2010). [The Cambrian–Ordovician boundary unconformity also extends into deeper water facies, and the revised Vermont Geologic Map (Ratcliffe et al., 2011) incorrectly shows the Gorge Formation of the Franklin Basin extending into the Lower Ordovician, while a Gorge–Highgate Formation succession without an intervening unconformity is incorrect (e.g., Landing et al., 2007)]

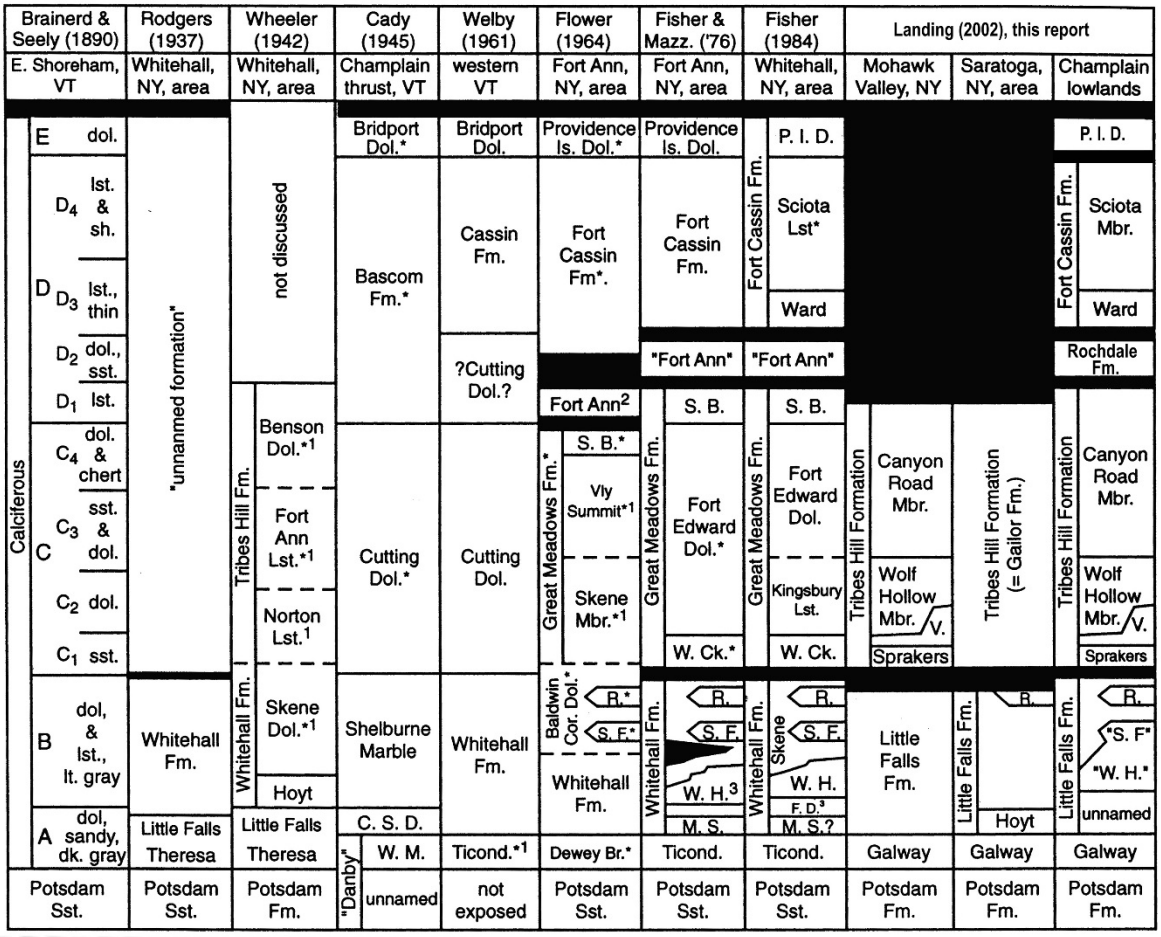


Figure 12. Upper Cambrian–Middle Ordovician stratigraphic nomenclature of the Laurentian platform, eastern New York and western Vermont. Cambrian–Ordovician boundary is hiatus between the Little Falls and Tribes Hill formations. *Paraprioniodus costatus-Chosonodina rigbyi-Histiodella holodentata* Interval conodonts (Ethington and Clark, 1981, = Fauna 4 of Sweet et al., 1971) through Providence Island Formation (E. Landing, unpub. data) indicates Beekmantown Group extends into Middle Ordovician. International agreement means that overlying strata of Chazy, Black River, and Trenton groups are Upper Ordovician, and the "Knox unconformity" is the lower bracket of the Upper Ordovician. Symbols: asterisk (*) is first proposal of stratigraphic name; superscripts 1–3 are abandoned units by 1—inadequate location of type section, description of lithology, or contacts, 2—no type section, lithologic description, or contacts provided, 3—unit is synonym of earlier named unit; quotation marks, for reasons 1–3 unit not recognized in this report. Abbreviations: Bridport Dol., Bridport Dolostone, abandoned; C. S. D., Clarendon Springs Dolostone, abandoned; Dewey Br., Dewey Bridge Dolostone, abandoned; F. D., Finch Dolostone, abandoned; M. S., Mosherville Sandstone, abandoned; P. I. D., Providence Island Dolostone; R., Rathbunville School Limestone, Ri., Ritchie Limestone, abandoned; S.B., Smith Basin Limestone, abandoned; S.F., "Steves Farm Limestone," informal designation; Ticond., Ticonderoga, abandoned; V, Van Wie Member; W. Ck., Winchell Creek, designation abandoned; W. H., Warner Hill Limestone, designation abandoned; W. M., Wallingford Member. Figure modified from Landing (2002, fig. 2) and Landing et al. (2003A, fig. 2).

**Members of the Tribes Hill Formation.** Landing et al. (1996) proposed the Sprakers Member for lower Tribes Hill strata that extend upward from the unconformity with the Little Falls Formation to a shale-dominated reentrant (Van Wie Member of Landing et al., 1996) under the cliff-forming Wolf Hollow Member of Fisher (1954). The Sprakers changes laterally from intertidal carbonates and overlying wave-deposited fossil grainstones and calcisiltites in the western Mohawk valley into micro-cross-laminated silty dolostones and fine-grained dolomitic sandstones in the east (Landing et al., 1996, fig. 2, Hoffmans section). The Sprakers Member at Hoffmans is lithologically similar to Fisher and Mazzullo's (1976) "Winchell Creek Siltstone."

Dark shales with lenticular intraclast and calcisiltite beds of the thin (ca. 1.5 m) Van Wie Member mark the maximum highstand of Tribes Hill deposition in the Mohawk valley (Landing et al., 1996; Landing, 1998). Similar, dark, pyritiferous silt shale and lenticular dolomitic sandstones with bidirectional (wave-generated) cross beds in the upper "Winchell Creek Siltstone" at Tristates Quarry and Comstock (Stops 5, 7) are referred herein to the Van Wie Member (Figure 2). The Tribes Hill is thicker in the Lake Champlain lowlands (e.g., 69 m at Comstock vs. 30 m in the Mohawk valley), and the stratigraphic distance from the top of the Van Wie to the lowest thrombolites is also somewhat more [4.5 m and 10 m at Tristates Quarry and Comstock (Fig. 3) vs. 1.0–4 m in the Mohawk valley; Landing et al., figs. 2, 3]. Interestingly, a lenticular quartz arenite dune in the middle Van Wie at Comstock and Tristates Quarry seems to correspond to the intraclast pebble storm bed in the middle Van Wie in the Mohawk valley (Landing et al., 1996, figs. 2, 3).

Recognition of the Sprakers and Van Wie members as divisions of the lower–middle "Winchell Creek Siltstone" (Fisher and Mazzullo, 1976; abandoned herein) means that a Winchell Creek-type facies reappears above the Van Wie and is transitional into the cliff-forming, thrombolitic facies in the middle Tribes Hill. Fisher (1962b; Fisher and Mazzullo, 1976) referred the carbonate-rich interval of the middle–upper "Great Meadows" to a "Fort Edward Dolostone" member without designating a type section in the Middle Ordovician flysch terrane of the Fort Edward, NY, area. Fisher (1984) later "undesirably restricted" (see North American Stratigraphic Commission, 1983) the "Fort Edward" by separating out the lower thrombolitic interval as a "Kingsbury Limestone" and retaining "Fort Edward" for the remainder. This restriction created an objective homonym of "Fort Edward" in Fisher's (1977, 1984) own publications.

Thrombolites appear only in the upper Wolf Hollow Member in the Mohawk valley (Landing et al., 1996). This highstand facies is now recognized above the Van Wie Member in the Lake Champlain lowlands (Figure 2). The Wolf Hollow Member is recognized as the senior synonym of the upper "Winchell Creek", "Kingsbury," and "Fort Edward" Members (all units abandoned) in the Lake Champlain lowlands, where it extends from the top of the Van Wie to the top of the thrombolite build-ups, as in the Mohawk valley.

The Canyon Road Member (Landing et al., 1996), which is the upper member of the Tribes Hill Formation in the Mohawk valley, includes lower intraclast-fossil hash beds and higher evaporitic dolostones above the highest Wolf Hollow thrombolites (Landing et al., 1996). A similar, carbonate-dominated, aggradational or progradational highstand facies is marked in the Lake Champlain lowlands by replacement of Wolf Hollow thrombolite build-ups by overlying ooid wackestones and higher, mollusk-rich lime mudstone. This lime mudstone is Flower's (1968a) "Smith Basin Limestone" (see Stop 7 discussion). The most appropriate stratigraphic designation for the entire supra-thrombolite, carbonate-dominated interval of the upper Tribes Hill Formation in the Mohawk valley and Lake Champlain lowlands is "Canyon Road Member." "Smith Basin Limestone" is regarded as an informal submember for the massive lime mudstone unit of the uppermost Canyon Road Member in the Lake Champlain lowlands.

**Rochdale Formation.** Regional litho- and biostratigraphic work indicates that the Rochdale Formation extends through the Lake Champlain lowlands south into southern Dutchess County, New York (Landing et al., 2012). Rochdale Formation, first named for Rochdale, NY, replaces "Fort Ann Formation" (designation abandoned) as a carbonate-dominated, middle Lower Ordovician (late Tremadocian) type depositional sequence. This second Early Ordovician depositonal sequence in the Lake Champlain lowlands that unconformably overlies the Tribes Hill Formation and unconformably underlies the Ward Siltstone member of the upper Lower Ordovician Fort Cassin Formation (see Fisher, 1984; Brett and Westrop, 1996; Landing et al., 2012). The designation "Fort Ann" previously abandoned) is continued in use on the revised Vermont Geologic Map, the unit is not represented as a distinct depositional sequence, and its age is mistakenly given as "Arenigian" (now Floian) by Ratcliffe et al. (2011, legend).

The checkered history of "Fort Ann" (Figure 12) includes its proposal as an undescribed middle member of the Tribes Hill Formation (Wheeler, 1942), and its redefinition (Flower, 1968b) as a formation above the Tribes Hill (i.e., "Great Meadows") Formation in the Lake Champlain lowlands. Thus, "Fort Ann" is an objective homonym of itself (!) in several important early publications that sought to establish a uniform stratigraphic nomenclature in the Lake Champlain lowlands. No type section was ever designated for the "Fort Ann," and it should be noted that Fort Ann village itself is built on Late Ordovician flysch.

**Upper Beekmantown Group** The two upper formations of the Beekmantown Group are the Fort Cassin and overlying Providence Island formations, which extend (under various names) from Dutchess County, SE New York, through the Lake Champlain lowlands, and into the Montreal–Ottawa areas of the Ottawa-Bonnechere aulacogen. Each formation is a separate type 1 depositional sequence with the lower Ward Member (fine sandstones) of the Fort Cassin unconformably overlying the Rochdale Formation. The Fort Cassin is a middle to upper Lower Ordovician (Floian) unit. In turn, the lower Middle Ordovician Providence Island Formation (defined on Providence Island in Vermont but referred to by a junior synonym as "Bridport Dolostone," designation abandoned, on the Vermont Geologic Map by Ratcliffe et al., 2011) unconformably overlies the Fort Cassin as a type 1 depositional sequence as the uppermost unit of the Beekmantown Group; it yields lower Llanvirnian conodonts.

The Providence Island Formation is unconformably overlain by the Chazy Group, with the unconformity defining the trans-Laurentian Middle–Late Ordovician boundary at the Sauk–Tipeecanoe Megasequence boundary (see summaries in Brett and Westrop, 1996; Landing, 2007, 2012; Landing and Westrop, 2006; Landing et al., 2007; Landing et al., 2012; Figure 3). The Vermont Geologic Map (Ratcliffe, 2011, legend) does not incorporate the depositional sequence history and unconformities through the upper Beekmantown, shows the upper Fort Cassin as Middle Ordovician (Llanvirnian) although trilobites and published conodont work limits the formation to the middle Lower Ordovician (Brett and Westrop, 1996; Landing and Westrop, 2006), and does not show the Providence Island Formation as a regionally extensive unit.

**Revisions in Stratigraphic Nomenclature—Taconic Allochthon**

A dismaying number of stratigraphic names has been generated for Cambrian–Ordovician units along the ca. 200 km length of the Taconic allochthon from Sudbury, Vermont, to Beacon, near Poughkeepsie, New York (see Zen, 1964). In part, this practice has been a natural consequence of problems involving correlation into the more highly metamorphosed higher (and eastern) thrust slices. However, it is unfortunate, in particular, that separate nomenclatural schemes exist for the northern, central, and southern parts of the Giddings Brook slice (see Zen, 1964; Fisher, 1977) because adequate outcrops and biostratigraphic controls allow reconstruction of the stratigraphic succession and detailed correlations along the length of the slice.

The tectonic history of the Giddings Brook succession (i.e., rift margin feldspathic quartz and lithic arenites [latest Precambrian?–Early Cambrian Rensselaer Formation], Early Cambrian–Middle Ordovician passive margin slope deposits that record sea-level and paleo-oceanographic changes correlateable for long distances along along the slope [Stops 8–13], and progressive evidence for convergence beginning in the Middle–Upper Ordovician [Indian River–Austin Glen formations, Stop 9] led to a uniform stratigraphy that can be recognized in the Sunset Lake, Giddings Brook, and Bird Mountain slices (Landing 1988b). In general, the lithostratigraphic scheme outlined by Rowley et al. (1979) in the northern part of the Giddings Brook slice is appropriate for the external slices. Two exceptions to this scheme were noted by Landing (1988b):

**Deep Kill Formation and its synonyms.** "Deep Kill Formation" (Ruedemann, 1902) is the senior synonym for the "Schaghticoke Shale" (Ruedemann, 1903; Stop 13); "Poultney Slate" (Keith 1932), particularly "Poultney B and C" of Theokritoff (1959; Zen, 1967); and "Stuyvesant Falls Formation" (Craddock, 1957; Fisher, 1961, 1962). Although Fisher (1961) incorrectly argued that Ruedemann (1902) defined the Deep Kill as a biostratigraphic unit from what is now known to be two slices at the sole of the Taconic master thrust, Ruedemann (1919), Ruedemann and Cook (1930) and Ruedemann et al. (1942) emphasized the "Deep Kill Shale" as a greenish-gray mudstone-dominated, lithologic and map unit of Early Ordovician age (now known to range into the early Middle Ordovician; Landing, 1976) in the central and southern Taconics.

As noted in this field trip and in Landing et al. (1992), the Lower Ordovician, macroscale black shale-limestone–green shale alternations at the type section of the Deep Kill Formation, are recognizeable in "Poultney B and C" and the "Stuyvesant Falls." Considerable confusion has always attended mapping of the black mudstone-dominated interval termed "Poultney A" by Theokritoff (1959; see Zen, 1964, p. 65; Stop 8). Its definition was primarily biostratigraphic, with the assignment of this black shale-limestone interval as a lowest "Poultney Shale" "member" solely on the basis of its Early Ordovician age. "Poultney A" is not distinguishable from the upper "Germantown Formation" and "West Castleton Formation" (Zen, 1964, p. 65), and the latter three units have been abandoned and synonymized with the Hatch Hill Formation (Landing 1988b).

**Austin Glen and "Pawlet" Formations.** A second problem is posed by names applied to the Upper Ordovician synorogenic flysch because interpreted tectonic setting has influenced nomenclature. "Pawlet Formation" has been used in the northern Taconics (e.g., Rowley et al., 1979) to refer to flysch in stratigraphic continuity with the allochthonous Taconic sequence, and "Austin Glen" has been preferred for coeval "parauthchthonous"? or allochthonous flysch at the leading edge of the allochthon (Potter, 1972; Fisher, 1977). Lithologic similarity of this medium- to massively-bedded arenite-dominated unit within and along the leading edge of the allochthon and the onset of its deposition late in the early Late Ordovician (upper *Nemagraptus gracilis* Chron) lead to the conclusion that Austin Glen Formation is a senior synonym of "Pawlet Formation" (abandoned designation; Landing, 1988a).

**Browns Pond, Hatch Hill, "West Castleton," and "Bull" formations.** As discussed in Appendix 1, the type section of the "West Castleton Formation" can be confidently referred to the Hatch Hill Formation, with most fossiliferous outcrops of the "West Castleton" in New York now understood to be referable to the Browns Pond Formation. These conclusions have been earlier detailed (e.g., Landing, 1993, 2007, 2012; Landing et al., 2007), but the revised Vermont Geological Map (2011, legend) incorrectly maintains use of the "West Castleton Formation" (abandoned) as a mapping unit in Vermont, and by implication in the Taconic succession of eastern New York.

It should also be emphasized that recognition (Rowley et al., 1979) and later formal naming of the black mudstones of the Browns Pond Formation as a unit under the red and green "Cambrian roofing slates," or Middle Granville Formation (Kidd et al. *in* Fisher, 1984), means that the traditional "Bull Formation" (*fide* Ratcliffe et al., 2011) actually includes three formations: the Truthville, the Browns Pond, and the Middle Granville formations. For this reason, the "Bull Formation" must be abandoned as a mapping unit, and "Bull Formation" (abandoned) should not appear on the revised Geologic Map of Vermont.

**Geology of the Copper-Kiln Landslide: a glimpse into the Marcy massif detachment zone**

By

Regan, S.P.[1], Dept of Geosciences, University of Alaska, Fairbanks, Fairbanks AK 99775
Guevara, V.E.[2], Dept of Geosciences, Skidmore College, Saratoga Springs NY 12866
Drauschak, T.[2], Dept of Geosciences, Skidmore College, Saratoga Springs NY 12866
Chiarenzelli, J.R.[3], Dept of Geology, St. Lawrence University, Canton NY 12230
Gaschnig, R.M.[4], Env, Earth and Atmospheric Sciences, University of Massachusetts , Lowell, Lowell MA 01854

## INTRODUCTION

The Mesoproterozoic Grenville Province of eastern North America is a classic Proterozoic orogenic belt that formed over a protracted period resulting in the assembly of Rodinia (Hoffman, 1988). Despite the routine interpretation that the Grenville Province exposes the orogenic infrastructure of modern collisional orogens, the Grenville is unique from Phanerozoic orogenic belts, as anorthosite and related mafic rocks comprise >20% of the exposed region (Fig. 1a; Corriveau et al., 2007). This is in stark contrast to all Phanerozoic orogens, which lack massif-type anorthosite, let alone in such quantities or volumes (Ashwal, 1994; 2010). Owing to a high rheologic strength resulting from exceptionally coarse grain sizes, high temperatures of crystallization, and relatively low density, it follows that anorthosite complexes may have had a profound impact on the thermal and structural architecture of the Grenville Province as a whole.

The Adirondack Mountains in northern New York are a Mesozoic domical uplift of Grenvillian basement and form the southern extension of the contiguous Grenville Province (Fig. 1b; Roden-Tice et al., 2000). The region has served as a testing ground for petrologic inquiry and new analytical techniques for decades (Kemp, 1898; Buddington, 1939; Postel, 1954; Valley and O'Neil, 1982; Bohlen, 1985; Spear and Markussen, 1997; Bonamici et al., 2015; Quinn et al., 2017; among many others). The Adirondack Mountains contain several anorthosite complexes including the Marcy massif, the Oregon dome, and Snowy Mountain dome. The Marcy anorthosite massif (Mm) is a 3000 $km^2$ classic Proterozoic-type anorthosite complex underlying the majority of the High Peaks region of the Adirondack Park in northern NY, and is thus an excellent place to study the impact of volumetrically abundant anorthosite on the orogenic infrastructure of the Grenville Province.

In late August, 2011, Tropical Storm Irene catalyzed over 40 landslides in the High Peaks region (Mackenzie, 2017). The highest concentration of landslides occurred within the eastern High Peaks area, and provide an unprecedented window into the internal compositional heterogeneity and structural complexity within the relatively undeformed Marcy massif (Chiarenzelli et al., 2015). As a companion to a 2015 NYSGA field trip (Chiarenzelli et al., 2015), which focused on the Bennies Brook slide on the northwestern slope of Lower Wolfjaw Mountain, we looked at a landslide in proximity to the northern margin of the Marcy massif. The Copper-Kiln (or Cooper-Kill) landslide occurred north of Wilmington near Whiteface Mountain, and combined with detailed 1:24,000-scale mapping along the southeastern margin of the Marcy massif, provide insight into how the anorthosite behaved during the polyphase metamorphic and structural evolution of the Adirondack Mountains.

## BACKGROUND

The Grenville Province of North America records evidence for multiple accretionary phases followed by a collisional tectonic phase lasting from 1080 – 980 Ma referred to as the Grenvillian Orogeny (Rivers, 2008). The Adirondack region dominantly formed during the Shawinigan orogeny, which ended with extensive Anorthosite-Mangerite-Charnockite-Granite (AMCG) plutonism (McLelland et al., 2004). The Adirondack region is divided into the amphibolite-facies Adirondack lowlands and granulite-facies Adirondack highlands (Fig 1b; Selleck et al., 2005). Separated by the southwest-striking, northwest-dipping, Carthage-Colton shear zone, the Adirondack highlands preserve evidence for experiencing granulite-facies metamorphism during the Ottawan phase of the Grenvillian Orogeny (*referred to as Ottawan orogeny here;* McLelland et al., 2001), which is absent in the adjacent

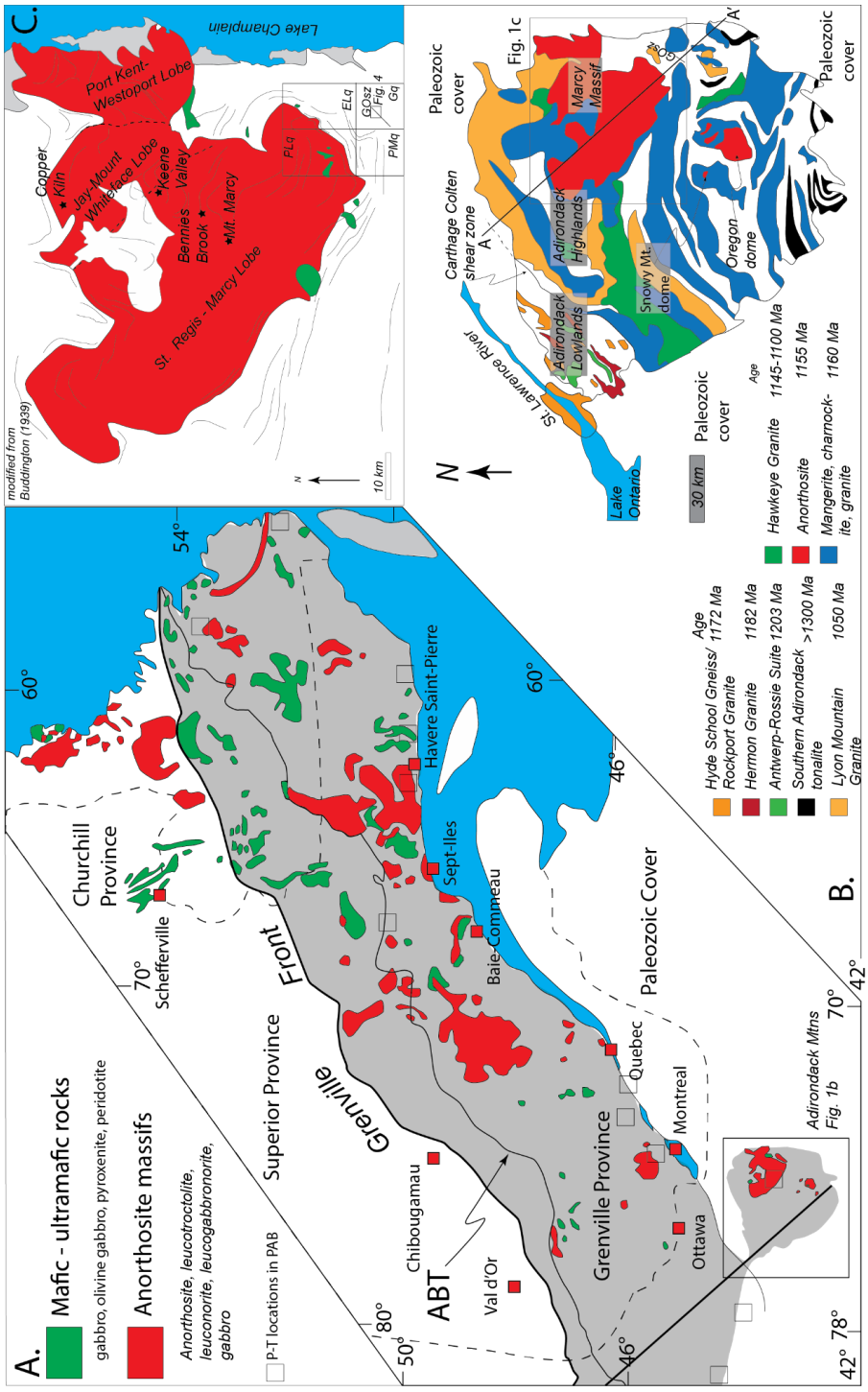


Figure 1: A) Schematic map of the Mesoproterozoic Grenville Province showing the distribution of massif-type anorthosite bodies (ABT: allochthon boundary thrust; modified from Corriveau, 2007); B) Generalized geologic map of the Adirondack region displaying the distribution of igneous suites (modified from McLelland et al., 2004); C) Detailed map of the Mm with foliation form lines from Balk (1931; modified by Buddington, 1939) – Location of Copper-Kiln slide on *northwestern margin of the Jay-Mt Whiteface lobe*.

lowlands. Structural and geochronologic data from the Carthage Colton shear zone indicate that it accommodated top down to the northwest (normal) motion juxtaposing orogenic lid rocks too high in the crust to have undergone regional penetrative tectonism during the Ottawan phase of the Grenville Orogeny adjacent to middle crustal rocks of the Adirondack highlands (Selleck et al., 2005; Bonamici et al., 2011; 2015). Motion along the Carthage Colton shear zone occurred at ca. 1040 Ma, interpreted to reflect collapse of overthickened crust at the end of the Ottawan orogeny (Selleck et al., 2005).

Evidence for extensional collapse in the Adirondack Mountains is widespread and been the focus of substantial work. The Carthage-Colton shear zone is the best studied feature exhibiting extensional deformation and delineates the boundary between Adirondack highlands and lowlands (Selleck et al., 2005). The East Adirondack shear zone to the south and east of the Marcy massif is also interpreted to reflect orogenic collapse and accommodated top – down to the southeast deformation at ca. 1040-1020 Ma (Wong et al., 2011). However, this feature has only been identified in several road outcroppings, and it does not correspond to a major thermal discontinuity as does the Carthage-Colton shear zone. Also associated with extensional collapse is the voluminous emplacement and crystallization of leucogranitic to syenitic rocks collectively referred to as the Lyon Mountain granite (LMG; Postel, 1954; Chiarenzelli et al., 2017). The LMG rims the Marcy massif and intruded along mylonitic zones in the Carthage Colton shear zone (Selleck et al., 2005). It is undeformed and cross cuts regional granulite-facies tectonic fabrics, providing a minimum age of tectonism. Decades of detailed U-Pb zircon geochronology has confirmed late Ottawan emplacement of the LMG, with U-Pb zircon crystallization ages of individual samples spanning from 1062 – 1038 Ma (Chiarenzelli et al., 2017; *and references therein*). Of particular interest are numerous iron oxide-apatite deposits hosted by the Lyon Mountain granite, which have a controversial origin ranging from completely magmatic (Lupulsecu et al., 2017) to entirely metasomatic (Valley et al., 2009; 2011). The degree of albitization associated with all ore occurrences demands a metasomatic component, but the role and origin of fluids in concentrating ore materials in the LMG remains enigmatic.

**Petrogenesis of the Adirondack AMCG suite**

Within the Adirondack highlands, the largest suite of plutonic rocks belong to the ca. 1160-1140 Ma anorthosite-mangerite-charnockite-granite (AMCG) suite (Fig. 1b; McLelland et al., 2004; Hamilton et al., 2004), which are, collectively, a hallmark of the Grenville Province and Proterozoic anorthosite complexes as a whole. Zircon geochronology (McLelland et al., 2004) suggests that members of this suite are coeval, but not necessarily comagmatic, in which anorthosite and mafic varieties of the suite are derived from fractional crystallization of asthenospheric-derived mafic parent (Regan et al., 2011), and quartz-bearing endmembers are derived from lower crustal anatexis (McLelland et al., 2004; Hamilton et al., 2004). Furthermore, based on timing constraints, anorthosite, and associated MCG, magmatism corresponds to the final stages of Shawinigan orogenesis, which set the stage for lithospheric foundering and asthenospheric upwelling catalyzing the formation of anorthosite at the base of the crust (Valentino et al., 2018).

The AMCG suite of the Adirondack region has been host to numerous stable and radiogenic isotopic tracer studies, including Oxygen in zircon (Valley et al., 19934); Hafnium in zircon (Bickford et al., 2010); Oxygen in contact zone minerals (Valley and O'Neil, 1982), and Oxygen in plagioclase feldspar (Morrison and Valley, 1989; Peck et al., 2010a), and whole rock separates (Peck et al., 2010). Oxygen isotopes in zircon display uniformly elevated $\delta O^{18}$ values from 8.0 – 11.0 ‰ (Valley et al., 1993; Peck et al., 2010a). Values for AMCG rocks in the Adirondack Mountains are anomalously high compared to most other AMCG suites in the Grenville, except for the Morin Massif, which preserves similarly high $\delta O^{18}$ values (Peck et al., 2010a). The deviations of these two complexes were preliminarily interpreted as having been contaminated by oceanic lithosphere, in contrast to other anorthosite massifs (Peck et al., 2010a). Furthermore, Hf isotopic measurements in zircon display uniform $\varepsilon_{Hf(Tc)}$ (Tc = time of crystallization) throughout the entire suite, which plot between contemporaneous CHUR (chondritic uniform reservoir) and depleted mantle (Bickford et al., 2010). Therefore, much of the isotopic characteristics of the Mm are analytically identical to those of coeval granitoid rocks, which may be a function of relatively low residence time of granitic source rocks (Peck et al., 2010a).

A suite of gabbronorite rocks, commonly referred to as coronitic metagabbros, occur as satellite plutons exposed along the edges of the Mm (Buddington, 1939; McLelland and Chiarenzelli, 1988; McLelland et al., 2004; Regan et al., 2011), with a minority internal to it, and share a similar U-Pb crystallization age (McLelland and Chiarenzelli, 1988; McLelland et al., 2004). They contain a higher $\varepsilon_{Nd(Tc)}$ than the surrounding Mm (Regan et

al., 2011), and mantle like $\delta O^{18}$ values (6.0 ‰; Valley et al., 1993), suggesting that they did not undergo the contamination present within the Mm. Whole rock major and trace element geochemistry and Nd isotopic evidence was discussed in Regan et al. (2011) and demonstrates that the suite of gabbronorites is permissible as the parental magma for the Mm. These data collectively suggest that the Mm experienced hybridization and batholith-wide contamination by and with the granitoid counterparts during or after the parental magma had become isotopically isolated.

**Constraints on metamorphism in the Adirondack highlands**

The Adirondack highlands have been host to classic thermobarometric studies (Bohlen et al., 1985) and forward petrologic modelling (Spear and Markussen, 1997; Storm and Spear, 2005). However, until recently, distinguishing effects of Shawinigan vs Ottawan orogenies remained problematic. Initially, based on exchange thermometry, Bohlen et al (1985) suggested that paleoisotherms were centered on the Marcy anorthosite massif and Oregon Dome (Fig. 1b), which also corresponded to zircon recrystallization textures above the 725°C paleoisotherm (Chiarenzelli et al., 1993). Spear and Markussen (1997) performed systematic thermobarometric analysis and petrogenetic modelling on anorthositic rocks from the northern Marcy massif, and acquired peak P-T conditions of 0.8 GPa and > 800°C corresponding to garnet-absent pyroxene recrystallization, followed by cooling and exhumation. Storm and Spear (2005) performed a similar analysis on a suite of metapelitic rocks in the southern Adirondack Mountains, which yielded similar P-T results interpreted by the authors to suggest that the "bulls-eye" pattern of Bohlen et al (1985) was not a robust estimate of peak temperatures.

In-situ zircon geochronology from anorthosite-series rocks was performed and presented in Peck et al. (in press). Samples were acquired from the southeastern margin of the Mm, but similar petrologic textures were observed in a suite of samples from the northern margin of the Mm presented in Spear and Markussen (1997). Zircon associated with garnet coronae around ilmenite were targeted as the ilmenite would provide Zr during retrograde metamorphism from a garnet-absent peak assemblage (Spear and Markussen, 1997; Peck et al., in press). Analyses suggested coronae growth, which post dates deformation in most places, occurred from ca. 1060 – 1040 Ma, overlapping considerably with the emplacement of the Lyon Mountain granite (Chiarenzelli et al., 2017). In-situ zircon dating from a suite a quartzites near the sample locality of Storm and Spear (2005) was performed by Peck et al. (2010). Their study indicates that local anatexis and metamorphic zircon growth occurred at c. 1180-1135 Ma, synchronous with the Shawinigan Orogeny (Peck et al., 2010b). Therefore, although the thermobarometric constraints suggest similar peak metamorphic conditions across the Adirondack highlands, ambiguity remains over the timing of P-T conditions retrieved from any rock sample in the absence of robust petrochronologic constraints, . It is clear that AMCG rocks near the Marcy massif underwent granulite-facies metamorphism during the Ottawan orogeny. However, these data also suggest that the "bulls-eye" pattern (Bohlen et al., 1985) may represent Ottawan paleoisotherms, and that conditions calculated by Storm and Spear (2005) represent Shawinigan conditions overprinted by an Ottawan thermal disturbance.

**The Marcy massif: a historic perspective**

The Adirondack anorthosites have been studied for over a century (Kemp, 1898; Ailling, 1932). Although rocks belonging to the series are highly variable in texture and composition, they are generally lumped into two separate units, or facies (Kemp, 1898; Buddington, 1939). The Whiteface-facies is predominately composed of gabbroic anorthosite to anorthositic gabbro and fine to medium-grained anorthosite and other intrusive units like jotunites, ferrodiorites, and gabbros. The Marcy-facies (or megacrystic Anorthosite) is composed of coarse to pegmatitic anorthosite with blue-gray andesine and subordinate labradorite (Miller, 1919). Composition and grain size aside, the most obvious differences between the two facies are the spatial distribution and degree of deformation of each unit. The relatively finer-grained Whiteface-facies is generally found at or near the margin of the Marcy Anorthosite massif and commonly contains a strong protomylonitic to mylonitic fabric. This was originally interpreted as a km-scale chill zone around the core of Marcy-facies Anorthosite (Kemp, 1898). This idea has not been developed or rigorously tested, but is the best model to explain the spatial variations in anorthosite texture. The contact between the two facies is gradual, and often composed of interlayered rock with characteristics of each, referred to as the "transitional zone" by Buddington (1939).

Buddington (1939; after Balk, 1931) separated the Mm into three lobes (Fig. 1c): the St. Regis- Marcy (Cushing, 1907; Ailling, 1919; Balk, 1931), the Jay-Mount Whiteface (Buddington, 1939), and the Port-Kent – Westport (Balk, 1931; Buddington, 1939). Fig. 1c is modified from Buddington (1939; after Balk, 1931). Each lobe has a Marcy-facies core wrapped by deformed Whiteface-facies, indicating that the three may be three distinct structural domes of the same batholith. Tectonites, including the heterogeneous Whiteface-facies, parallel the margin of the Mm (Balk, 1931) suggesting that rocks deformed around the Mm during regional deformation and metamorphism. Based on in-situ zircon geochronology, the age of this phase of tectonism is interpreted to be c. 70 Ma younger than the crystallization of the Mm and related rocks (Peck et al., in press).

The emplacement mechanism of the Mm and massif-type anorthosite in general remains the subject of debate (Meyers et al., 2008). One of the foundational problems central to this debate is the emplacement depth of massif-type anorthosite. Petrologic evidence for a polybaric origin for the Mm is widespread. High Al opx megacrysts suggest crystallization over 1.0 GPa (Bohlen and Essene, 1978). However, the presence of monticellite and depleted $\delta O^{18}$ values within the contact zone of the Mm require a shallower emplacement depth (Valley and O'Neil, 1982; Clechenko et al., 2002), consistent with orthopyroxene compositions from Marcy-facies anorthosite (Spear and Markussen, 1997). However, within extensional settings, meteoric water has been demonstrated to be capable of penetrating depths > 20 km. Florence et al. (1995) interpreted moderate pressure and high temperature metamorphism (P: 0.37 – 0.64 GPa and T: 700°-770°C) within the western Adirondack Mountains to have been synchronous with AMCG magmatism based on macro and microstructural relationships with proximal nelsonite dikes.

## STRUCTURE OF THE MARCY MASSIF

The Mm exhibits vastly different deformation styles from its interior to its margins. The following section describes the structures within the Mm, at the margins of the Mm, the differences between them, and their implications for the deformational history of the Mm.

### Deformation within the Marcy massif

The Mm is a vast region of undeformed, coarse-grained to pegmatitic anorthosite. However, parts of the interior Mm preserve evidence for localized deformation in the form of cm-scale granulite to amphibolite-facies shear zones, often corresponding to rheologic heterogeneities (Chiarenzelli et al., 2015). Detailed structural work on the Bennies and Wolfjaw Brook landslides will be described in detail here, but similar features have been observed in other locations throughout the Mm, including Cascade, Big Slide, Saddleback, Algonquin, Wright, and Hurricane Mountains. For more information on the Bennies Brook landslide please refer to Chiarenzelli et al. (2015), but detailed descriptions of other landslides are currently unavailable.

The reactivated Bennies Brook landslide formed during Tropical Storm Irene in 2011. It is positioned on the northwest slope of Lower Wolfjaw Mountain (Mackenzie, 2017). There are predominately two orientations of shearing exposed along the landslide with variable, but broadly consistent shear sense (Fig. 2). Both sets of shear zones are (sub)vertical with weakly developed subhorizontal mineral stretching lineations. Typically, NNW-SSE oriented shear zones contain dextral kinematic indicators and ESE-WNW oriented shear zones display a sinistral shear sense. Where seen interacting, the two generations of shear zones are mutually off-setting, suggesting a conjugate origin. A small set of pegmatitic gabbro dikes are slightly deformed, but oriented in a NE-SW orientation. The localized nature of shearing in a variety of mediums paired with systematic orientation of shear zones with antithetic kinematics indicates that strain was predominately coaxial internal to the Mm (Cavalcante and Fossen, 2017; Regan et al., in review).

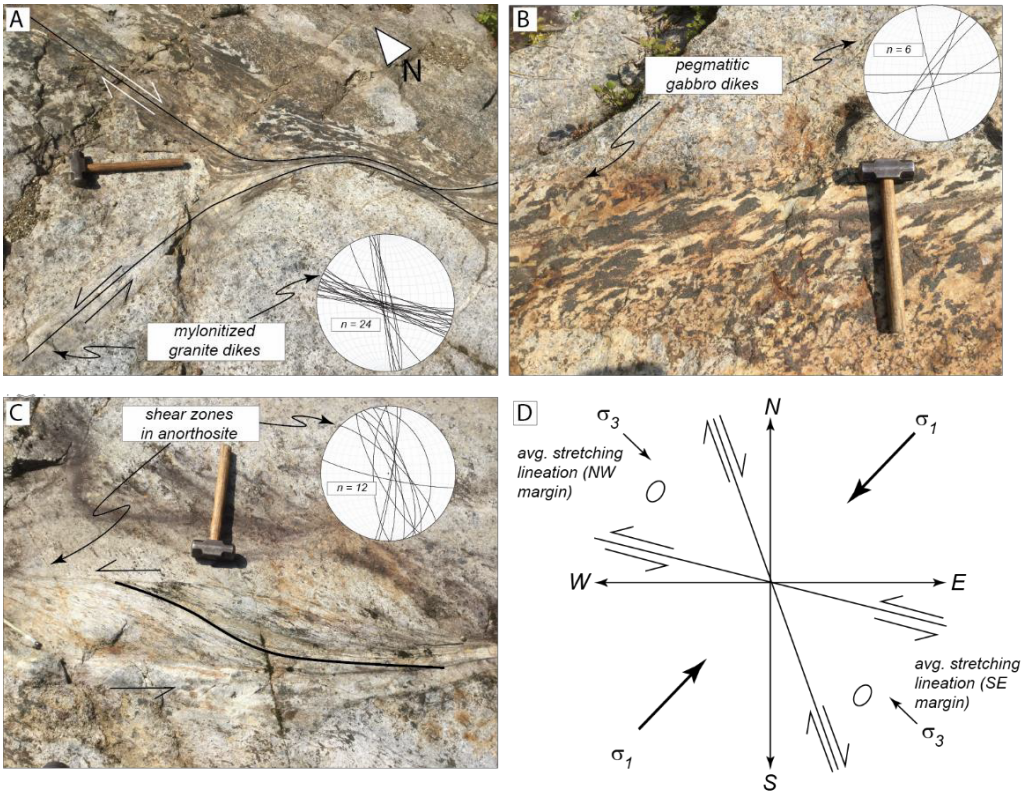


Figure 2: Representative photographs of the Bennies Brook landslide (for more information see Chiarenzelli et al. 2015). A) Mutually off-setting shear zones with antithetic kinematics suggesting a conjugate origin; B) Internaly strained pegmatitic gabbro dike with dextral shear sense; C) localized sinistral shear zone in anorthosite; D) schematic diagram of conjugate relationships from Bennies Brook slide with stretching lineation averages from margin rocks discussed herein labeled.

**Deformation along the margin of the Marcy massif**

As noted in Balk (1931) and Buddington, (1939), fabric trajectories parallel the contact of the Mm with surrounding country rock. 1:24,000 scale mapping along the southeastern margin of the Mm, focused on the structural setting and distribution of IOA-deposits hosted by the Lyon Mountain granite (Chiarenzelli et al., 2017), has produced new structural constraints on fabrics parallel to the margin of the Mm. At its southeastern margin, the Mm is rimmed by a variably thick zone of fine-grained (Whiteface- facies) gabbroic anorthosite (0.25 - > 1.0 km; Kemp, 1898), that generally displays a strong foliation and mineral stretching lineation. Isolated regions internal to the Mm have km-scale patches of deformed gabbroic anorthosite, interpreted as extensional klippe of the marginal package of rocks. These marginal rocks referring to the package of strongly deformed rocks rimming the anorthosite (anorthosite and country rock) contain granulite progressing to amphibolite facies metamorphic assemblages, and dip moderately to the southeast, away from the Mm. The boundary of the anorthosite, and host tectonites, are folded by open, upright folds shallowly plunging to the east-southeast. This generation of folds ($F_3$ of Regan et al. (2015)) is associated with plutons of the Lyon Mountain granite and may have facilitated its emplacement (Chiarenzelli et al., 2017).

Structural analysis of marginal rocks provides new insight into the geometry and kinematics of the Mm (Fig. 3). Stereonet analysis of foliation measurements form a girdle with a principal β-axis of 26° to 146° (n = 479). Stretching lineation measurements girdle about the mean foliation (045°, 25°; n = 111) with a mean orientation parallel with the calculated β-axis derived from foliation measurements (Fig. 3b). Consistent kinematic indicators

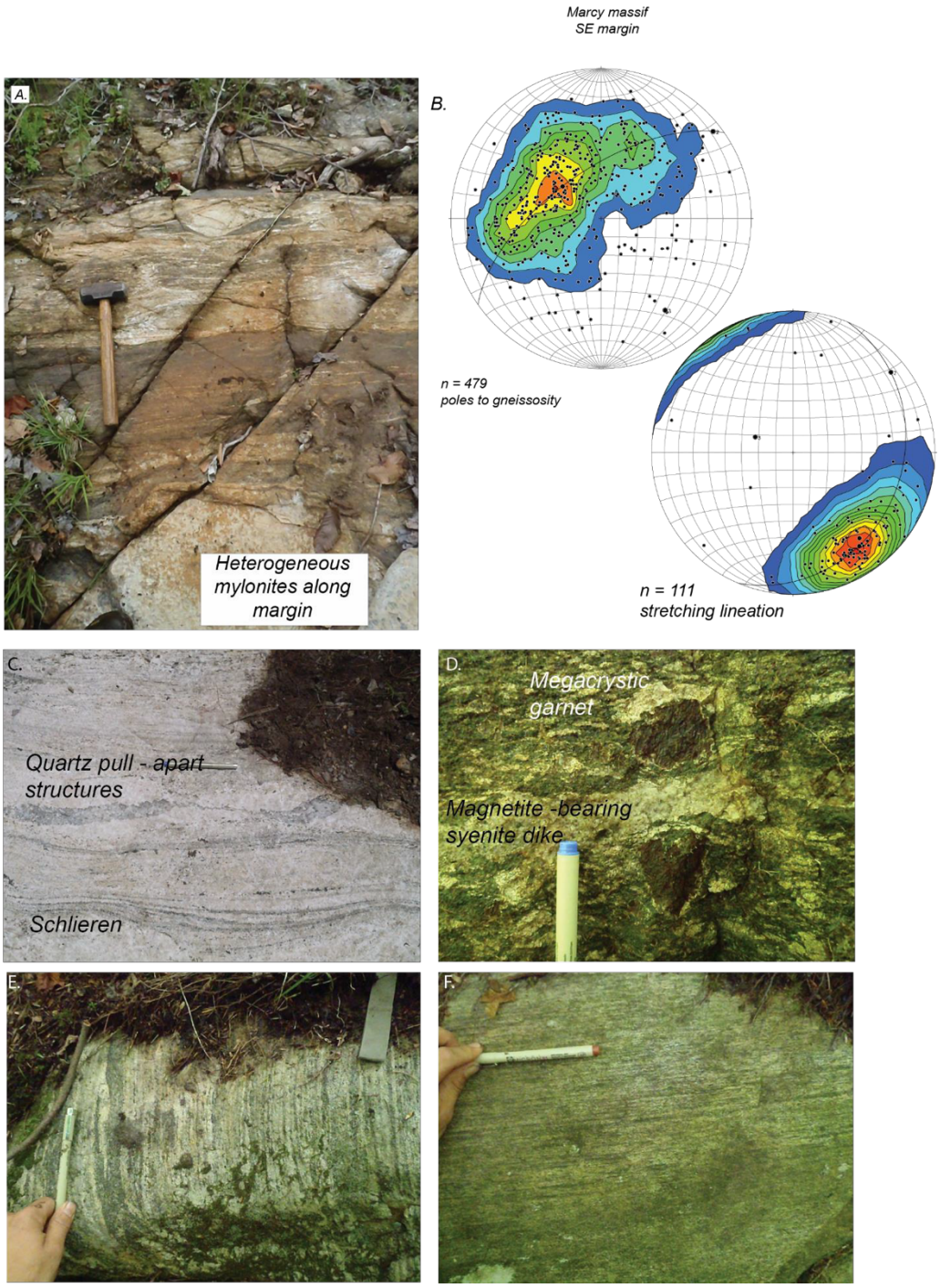


Figure 3: Representative field photographs and structural summary of marginal rocks along the SE margin of the Mm. A) Heterogeneous mylonites in the Whiteface-facies anorthosite; B) lower hemisphere projections of structural elements, upper left: poles planes of foliations, lower right: stretching lineation measurements; C) well-layered Lyon Mountain granite with quartz pull-apart structures and schlieren; D) syenite dike cross-cutting ferrodiorite within the marginal package of rocks with megacrystic gore-mtn type garnet present adjacent to the contact (for more information see McLelland and Selleck, 2011); E) strongly deformed gabbroic anorthosite; D) mylonitized gabbroic rock in marginal shear zone

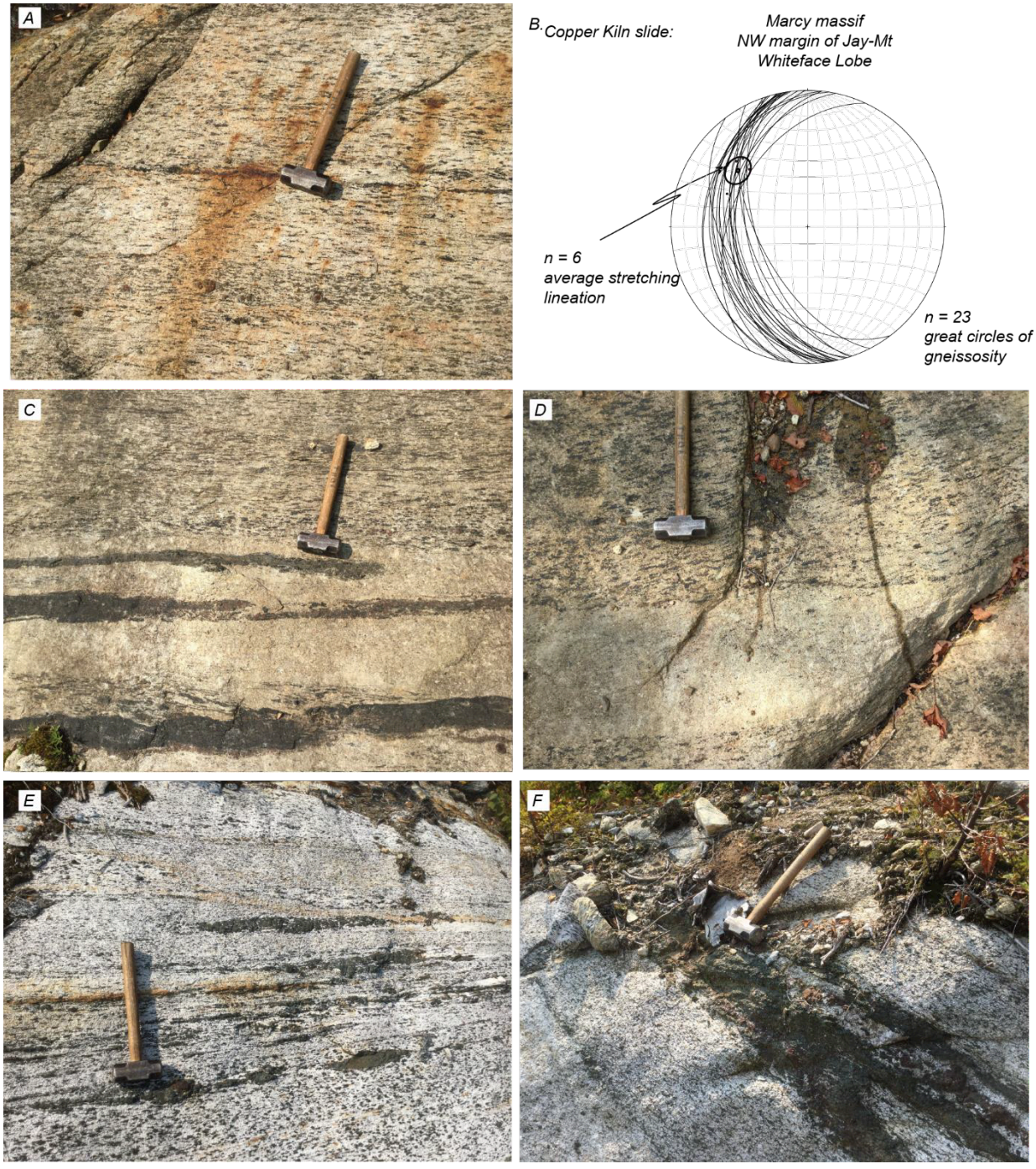


Figure 4: Representative field photographs and structural summary of the Copper-Kiln landslide. A) Strongly deformed gabbroic anorthosite with garnet porphyroblasts; B) lower hemisphere projection of foliation measurements (great circles) and stretching lineations; C) leucogranitoid sheet with preserved and relatively undisturbed mafic layers; D) leucogranitoid sheet with obliquity between host rock gneissosity and intrusive contact; E) strongly deformed gabbroic anorthosite with abundant dismembered calc-silicate xenoliths; F) Strongly deformed skarn rock xenoliths in protomylonitic gabbroic anorthosite

suggest oblique-normal shear sense of top-down to the southeast. Syn- to post-kinematic metamorphic assemblages consisting of hornblende ± garnet ± clinopyroxene ± orthopyroxene are interpreted to record peak- to post peak-metamorphic conditions. Evidence of post-kinematic metamorphism is generally preserved as coronae, and within marginal rocks, garnet envelopes lineated orthopyroxene and hornblende. These data suggest that deformation occurred during peak Ottawan metamorphic conditions within the Adirondack highlands (Spear and Markussen, 1997), and that the anorthosite behaved as a rigid body during granulite-facies deformation and subsequent leucogranite plutonism synchronous with regional cooling and decompression (Spear and Markussen, 1997; Chiarenzelli et al., 2017; Regan et al., in review). In-situ U-Th-total Pb geochronology of syn-kinematic monazite corroborates these interpretations, constraining the timing of deformation within the Mm detachment zone from 1070-1060 Ma (Regan et al., in review).

The Copper-Kiln landslide is located north of Wilmington, NY, within 2 km of the northwestern margin of the Jay-Mt. Whiteface lobe within the Mm (Fig 1c). It exposes over 0.5 km of continuous bedrock exposure. The landslide exposes deformed heterogeneous gabbroic anorthosite of the Whiteface facies (Fig. 4a). With increasing elevation there are abundant screens of dismembered and strongly deformed calc-silicate xenoliths of varying composition including skarns with wollastonite, garnet, and diopside. All rocks exposed along the landslide have a nearly constant foliation of 172°, 42° (RH rule; Fig. 4b), and a variably developed mineral stretching lineation plunging 34° to 309°. Kinematics are difficult to identify on the landslide and give varying senses, but overall a reverse/sinistral sense of shear is interpreted based on exposures closer to the actual margin of the Mm. There are abundant, but cryptic, leucogranite and syenite sills preserving subtle obliquity with host rock gneissosity (Fig. 4c,d). They are similar in color and texture on the weathered surface, making them difficult to see. Locally, these late intrusive rocks fill in boudined gabbro layers within the gabbroic anorthosite, suggesting emplacement during deformation; however the relatively fine grain sizes and internally undeformed state suggests a late syn- to post-kinematic relationship (McLelland et al., 2001).

## ANALYTICAL DATA

### Geochronology

Sample CKS-1 is a syenitic sill that is subconcordant to the dominant foliation in the northeastern lobe of the Marcy massif. Several of these intrusions are exposed in the Copper Kiln slide. We dated zircon in this sill via laser ablation inductively coupled mass spectrometry (LA-ICPMS) in order to: 1) determine the timing of leucogranitoid intrusion into the Marcy massif, and 2) place a minimum constraint on the timing of fabric development in this part of the Marcy massif. Mineral separation and mounting were performed at the University of Arizona and cathodoluminescence (CL) imaging was done at Middlebury College. Isotopic and trace element analyses of zircon were performed at the University of Massachussetts – Lowell on an Agilent 7900 quadrupole ICP-MS with a Teledyne CETAC LSX-213 laser ablation system using a 30 $\mu$m spot size.

Zircon grains from this sample take the form of either: 1) euhedral, oscillatory-zoned grains, or 2) xenocrystic (~1150 Ma) cores surrounded by euhedral, pointy overgrowths with oscillatory zoning (Fig. 5). We interpret the overgrowths to have grown directly from a melt during emplacement and crystallization of the syenite sill. Out of 40 analyses, 15 analyses from both oscillatory zoned grains and euhedral pointy overgrowths were "concordant" (e.g. overlapping within 2σ uncertainty). Some of these analyses gave spuriously high Ti and LREE concentrations, which we interpreted to be contaminated by inclusions. The 11 concordant analyses of inclusion-free zircon (based on trace element concentrations) give a weighted mean $^{207}Pb/^{206}Pb$ age of 1043 ± 20 Ma (MSWD = 2.3), and a Concordia upper intercept age of 1045 ± 20 Ma (MSWD = 1.5; Fig. 5). These dates are consistent with the syenite sills intruding the Marcy anorthosite during orogenic collapse and widespread intrusion and crystallization of the Lyon Mountain granite at c. 1050 Ma (e.g. Chiarenzelli et al., 2017), and place a minimum age constraint on deformation in the northeastern part of the Marcy massif.

We used the Ti in zircon thermometer (Watson et al., 2006) to place constraints on crystallization temperature of the sill. Ti concentrations range from 5.5 to 15.6, giving a range of Ti in zircon temperatures (assuming $a_{TiO2} = 0.8$, and $a_{SiO2} = 1$) of 712 ± 3 to 813 ± 13 °C, with a weighted average of 726 ± 13 °C. We note here that our values for $a_{TiO2}$ and $a_{SiO2}$ to calculate temperature are conservative maxima, as the timing of zircon crystallization relative to quartz and Ti-bearing phases from the melt is unknown. The zircon crystallization

temperatures derived here are thus minima, as decreased $a_{TiO2}$ or $a_{SiO2}$ would serve to increase apparent temperature. These temperatures are similar to those estimated from granulite facies metamorphic assemblages within the Marcy Massif (e.g. Spear and Markussen, 1997) that developed at c. 1040-1050 Ma (Peck et al., in press). The lack of obvious chilled margins in the sill and minimally retrogressed granulite-facies assemblages in the adjacent gabbroic metaanorthosite suggest intrusion into hot (> 700 □C) subsolidus crust of the Marcy Massif at 1045 ± 20 Ma.

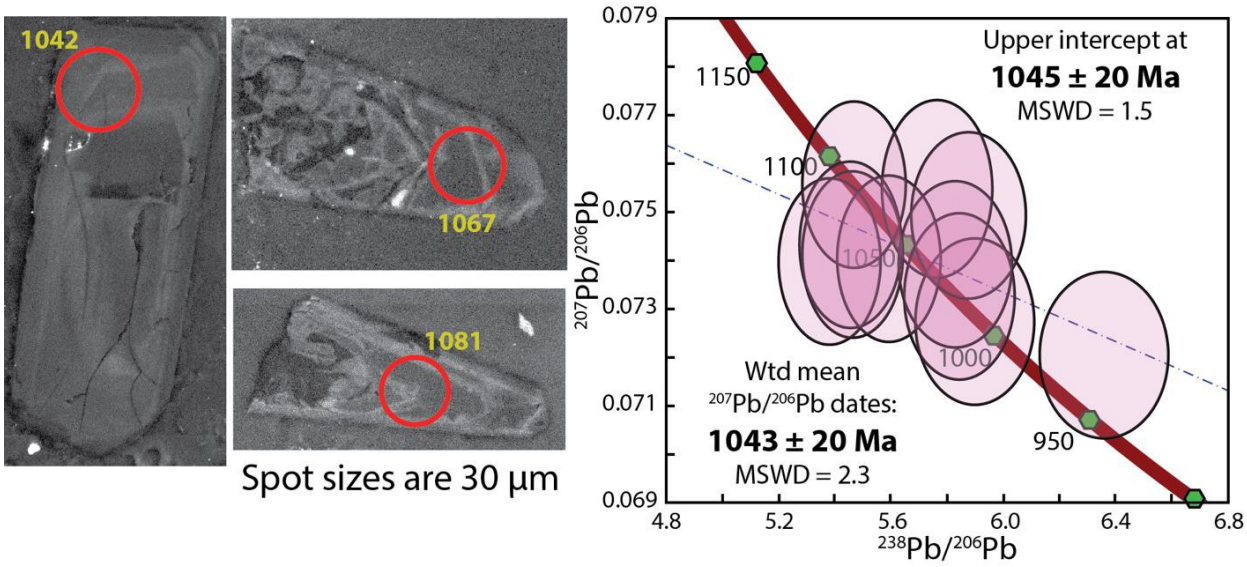


. Figure 5: Geochronology summary for U-Pb zircon data discussed in text. Sample of leucogranitoid sheet

## INTERPRETATIONS

The Mm is rimmed by a thick zone of high grade tectonites that preserve evidence of progressive strain parallel to, and around, the rigid anorthosite body at ca. 1060-1040 Ma. Lower hemisphere

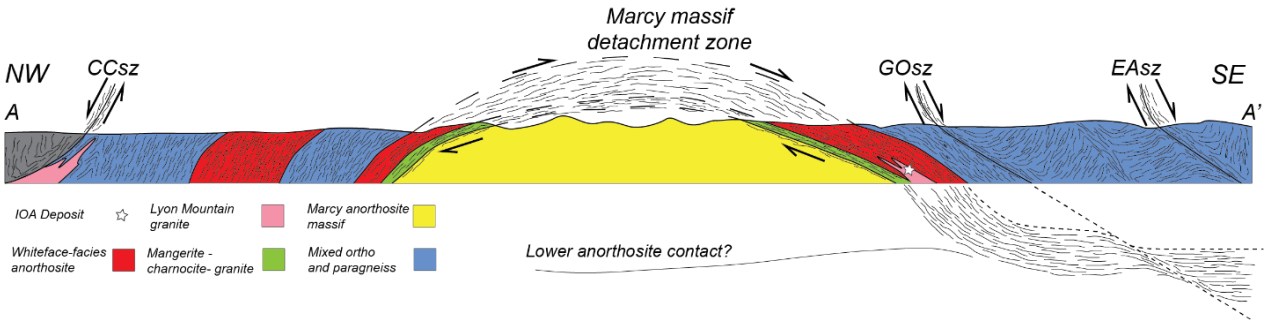


Figure 6: Schematic cross section labeled on Fig. 1b of the Adirondack Mountains with new structural and kinematic data taken into account. The Mm is draped by a southeast-directed, domed, detachment which likely formed during initial extension of the Adirondack highlands during peak metamorphic conditions within the Mm.

projections of the localized conjugate shear systems internal to the Mm suggest a least compressive stress orientation of NW-SE, which is where stretching lineations defined by granulite-facies mineral assemblages from the southern and northern margin plot. We interpret this to suggest that deformation of the margins of the Mm occurred at granulite-facies conditions. Evidence that strain was coaxial within the core of the Mm and subsimple along the margin suggests that the Mm partitioned (sub)simple components of shear along the margin. Therefore, strain was not only localized along the margin, but also partitioned around the 3000 $km^2$ Mm. Kinematic indicators from the southeastern margin of the Mm suggest top-down and to the southeast relative motion, whereas along the northern margin of the Mm, shear-sense indicators indicate top-up to the southeast relative motion. Fig. 6 shows a schematic cross section of the Adirondack Mountains with the new structural information taken into account, and shows that the Mm is draped by a domed, SE-directed detachment, referred to here as the Marcy massif detachment zone.

The Mm detachment zone shares many of the geometric features of other well documented extensional gneiss domes and metamorphic core complexes from the Grenville Province (Busch et al., 1999; Rivers and Schwertdner, 2015; Dufrechou, 2017). However, the core is predominately composed of undeformed, but metamorphosed anorthosite, and hence is referred to as a metaigneous dome. Similarly, the Morin anorthosite is draped by a domed extensional shear zone (Soucy La Rouche et al.,, 2015; Defrechou, 2017). Monazite and zircon geochronology firmly establish the timing of deformation within the Mm detachment zone to 1070-1060 Ma, with local evidence for even younger deformation (Peck et al., in press). This immediately pre-dates more localized and bivergent extensional structures to the NW and SE of the Mm, like the Carthage-Colton shear zone (Selleck et al., 2005), the East Adirondack shear zone (Wong et al., 2011), and the Grizzle Ocean shear zone (Regan et al., in review). We interpret the Mm detachment zone to have initially formed at granulite-facies metamorphic conditions and at the onset of structural collapse of the southern Grenville orogeny.

The Lyon Mountain granite is an extensive leucogranitic suite that rims the Mm, and hosts abundant Fe-oxide – apatite deposits of current economic interest (Long et al., 2010; Valley et al., 2010; 2011; Chiarenzelli et al., 2017). Emplacement of the Lyon Mountain granite coincides with extensional collapse along the Carthage-Colton shear zone and East Adirondack shear zone (Selleck et al., 2005; Wong et al., 2011). Near the margin of the southeastern Mm, the Lyon Mountain granite forms numerous plutonic bodies that are associated with late and open folds, which likely accommodated protracted emplacement (Chiarenzelli et al., 2017), including hinges of the detachment zone fabric. Notably, the IOA deposits hosted by the LMG appear to correspond to relict hinge regions within the pluton, and are generally within several km of the Mm itself. Leucogranite and syenite sills within the gabbroic anorthosite exposed along the Copper-Kiln landslide are interpreted as relatively early Lyon Mountain granite intrusions that utilized the detachment fabric to ascend, and may mark the last gasp of motion along the detachment. Therefore, the Mm detachment zone initiated at granulite-facies pressure- temperature conditions, and as doming occurred, strain was localized into bivergent shear zones on both sides of the Mm detachment zone. During continued collapse, folding of the Mm detachment zone facilitated the emplacement of the Lyon Mountain leucogranite (Chiarenzelli et al., 2017).

Evidence for fluid flow within the Mm detachment zone is preserved in multiple rock types and mineral assemblages. IOA deposits hosted by the Lyon Mountain granite are associated with extensive sodic alteration, which is generally within several km of the margin of the Mm. Gore Mountain megacrystic garnet, the New York state mineral, has been interpreted as the result of metasomatic reactions catalyzed by leucogranite and pegmatite intrusions within AMCG lithologies, most of which are in relatively close proximity to the Mm. Lastly, Valley and O'Neil (1982) recognized low $\delta O^{18}$ values in calc-silicate lithologies adjacent and enclosed within anorthosite, interpreted to require a shallow emplacement. Subsequent work by Clechenko et al. (2003) demonstrated that zoned garnet within these lithologies also contain a low $\delta O^{18}$ signal interpreted to require surficial water interaction during Mm crystallization and emplacement. However, given the abundant independent lines of evidence for fluid flow within the detachment, it seems possible that the apparent interaction with meteoric water may instead have occurred during Ottawan collapse. These observations suggest that the Mm detachment zone facilitated magmatic and fluid flow from various sources ranging from magmatic to potentially surficial, and thus may have provided an ideal location for classic Adirondack ore deposits to have formed.

## CONCLUSIONS

The Mm detachment zone is a thick shear zone that envelopes the Marcy anorthosite massif in the Adirondack Highlands. It was active during peak metamorphic conditions within the Adirondack highlands, and specifically within the Mm. The shear zone formed during onset of extensional collapseof the southern Grenville Province during final assembly of Rodinia at ca. 1070 Ma. Recognition of domed extensional structure surrounding the Mm helps explain numerous outstanding questions in Adirondack geology, including the distribution of major ore deposits, the geometry of late syn-extensional leucogranitic bodies, existing thermobarometric work, and geochronology. We welcome lively discussion on the outcrop and hope everyone enjoys the rocks

## ACKNOWLEDGEMENTS

The authors would like to extend a special thanks to Dr. Bruce Selleck who originally recognized the importance of extensional deformation in the Adirondack Mounatins. Without his groundbreaking work and good humor, the work presented in this field trip would never have been possible. First author acknowledges Paul and Mary-Lloyd Borroughs for constant patience, support, hospitality, and amazing company during years of field work in the eastern Adirondack Mountains. Ray Coish and Will Amidon are thanked for their assistance with CL imaging and preliminary LA-ICPMS analyses of zircon.

**ROAD LOG**

Carpooling is required! Parking at the trailhead is extremely limited. To consolidate vehicles, meet in the parking lot at Wilmington Town Beach at Lake Everest, Wilmington, NY at 9:00 am. If possible, please carpool from the Lake George area with others who are staying there for the weekend. From the Wilmington Town Beach, we will carpool to the trailhead, which is located c. 5.9 km to the northwest, at the intersection of Bonnieview and John Bliss Road.

0.0 – 0.1: Depart Wilmington town beach on Bowman Lane, take right on Bonnieview Rd

0.1 – 3.4: Arrive at Copper-Kiln (or Cooper – Kill) trailhead, parking on west side of Rd (left side if headed north). Some parking on shoulder .

Hike for approximately two miles on the trail (gradual up hill) until a sharp left hand turn is reached with piled up down trees. We will stop and drink some water and introduce the region here. Follow the trip leader to the landslide (down hill to the north). There will be some scrambling to get to the first outcrop over the outwash.

**Stop 1: Deformed gabbro and gabbroic anorthosite**

(UTM: 0592904 4920688)

The first stop is not connected by continuous exposure to the rest of the slide. It is located in the outwash of the landslide. The pavement outcrop exposes deformed gabbroic anorthosite and gabbroic gneiss. There is very minor obliquity between the contact between the two lithologies and penetrative gneissosity indicating that a higher angle relationship may have been progressively rotated into parallelism. There is abundant syn-kinematic hornblende +/- biotite at this outcrop consistent with decompression from peak granulite-facies metamorphism during shear.

Figure 7: Stop 2 view down the landslide from the beginning of continuous exposure

**Stop 2: Bottom of the Copper-Kiln landslide**

(UTM: 0592531 4920764)

The base of the landslide composed of gabbroic anorthosite to fine-grained anorthosite with diffuse contacts. Coarse orthopyroxene porphryoclasts are aligned in the predominant foliation and rimmed by hornblende. Several garnet porphyroblasts are present, but almost entirely replaced with randomly oriented hornblende. The predominant foliation dips moderately to the west northwest. There are also two Neoproterozoic mafic dikes approximately 10 cm wide.

**Stop 3: Subconcordant leucogranite to syenite intrusions in anorthosite**
(UTM: 0592455 4920760)

*Figure 8: Concordant leucogranitoid sheet in strongly deformed gabbroic anorthosite*

Along the landslide there are abundant meter-scale subconcordant syenite to leucogranitic sills, preserving varying degrees of obiquity with host rock gneissosity. They are difficult to spot at first as they weather to a pale gray/pink and are initially difficult to distinguish from recrystallized anorthosite. The dikes contain minimal evidence for high degrees of strain, but the extent of post kinematic annealing still remains problematic. However, the preservation of perthitic textures, and subhedral and isolated mafic minerals, we interpret minimal subsolidus strain to have occurred subsequent to intrusion. They lack the very recognizeable mesoscopic fabrics contained in surrounding anorthosite to gabbroic anorthosite gneisses. This dike was analyzed for U-Pb zircon geochronology and Ti in zircon thermometry. Based on results discussed above, we interpret the leucogranitoids to be members of the Lyon Mountain ferroan leucogranite suite (Chiarenzelli et al., 2017), and to have been emplaced synchronous with extensional collapse of the Adirondack Highlands (Regan et al., in review). The Mm detachment zone may have aided in their initial emplacement as seen here.

As we continue walking up the slide, there will be countless opportunities to discuss the relationships of the leucogranitoid sheets and host rocks. A Google Earth file of all data available on NYSGA website with all measurements, locations, photographs, and descriptions.

**Stop 4: Skarn near top of landslide**
(UTM: 0592202 4920693)

As the landslide steepens and we approach the headwall, you will notice an increase in the number of pods, screens, and partially digested and subsequently deformed calc-silicate xenoliths. Xenoliths range in scale from cm-scale to several meters in thickness and display a varied mineralogy of garnet, diopside, wollastonite, dolomite, titanite, among others. Titanite can be seen in hand sample and is the root beer colored mineral in the calc-silicate lithologies. Thick quartz-veins several cm in thickness are also common in this package of rocks.

## REFERENCES

Ailling, H.L., 1919, Geology of the Lake Clear region, New York State Museum, Bulletin 207-208. Ailling, H.L., 1932, The Adirondack anorthosite and its problems: The Journal of Geology, v. 40, p. 193-237

Ashwal, L.D., 2010, The temporality of anorthosite: Canadian Mineralogist, v. 48, p. 711-728. Balk, R., 1931, Structural geology of the Adirondack anorthosite. Zeirschrift fur Kristallographie, Mineralogie and Petrographie, v. 41, p. 308-434.

Bickford, M.E., McLelland, J., Mueller, P., Kamenov, G.D., and Neadle, M., 2010, Hafnium isotopic compositions of zircon from Adirondack AMCG suites: implications for the petrogenesis of of anorthosites, gabbros, and granitic members of the suites: The Canadian Mineralogist, v. 48, p. 751-761

Bohlen, S.R., Valley, J.W., and Essene, E.J., 1985, Metamorphism in the Adirondacks: Petrology, pressure and temperature: Journal of Petrology, v. 26, p. 971 – 992.

Bohlen, S.R., and Essene, E.J., 1978, Igneous pyroxenes from metamorphosed anorthosite massifs: Contributions to Mineralogy and Petrology, v. 65, p. 433-442

Bonamici, C.E., Kozdon, R., Ushikuba, T., and Valley, J.W., 2011, High-resolution P-T-t paths from $\delta O^{18}$ zoning in titanite: a snapshot of late-orogenic collapse in the Grenville of New York: Geology, v. 39, p. 959-962.

Bonamici, C.E., Fanning, C.M., Kozdon, R., Fournelle, J.H., and Valley, J.W., 2015, Combined oxygen-isotope and U-Pb zoning studies of titanite: New criteria for age preservation: Chemical Geology, v. 398, p. 70-84.

Buddington, A.F., 1939, Adirondack igneous rocks and their metamorphism: Geological Society of America Memoirs, v. 7, p. 1-343.

Busch, J.P., Mezger, K., and van der Pluijm, B.A., 1997, Suturing and extensional reactivation in the Grenville orogeny, Canada: Geology, v. 25, n. 6, p. 507-510.

Chiarenzelli, J., Selleck, B., Lupulescu, M., Regan, S., Bickford, M.E., Valley, P., and McLelland, J., 2017. Lyon Mountain Ferroan Leucogranite Suite: Response to Collision, Thickened Crust, and Extension in the Core of the Grenville Orogen: *GSA Bulletin,* v. 129, no. 11/12, p. 1472-1488.

Chiarenzelli, J.R., and McLelland, J.M., 1993, Granulite facies metamorphism, paleoisotherms, and disturbance of the U-Pb systematics of zircon in anorogenic plutonic rocks from the Adirondack highlands: Journal of Metamorphic Geology, v. 11, p. 59-70

Chiarenzelli, J., Lupulescu, M., Regan, S., Valentino, D., and Reed, D., 2015, The Bennies Brook Slide: A window into the core of the Marcy Anorthosite: Field Trip A-1, New York State Geological Association, Plattsburgh, New York, September 12-13, 27p.

Chiarenzelli, J., Regan, S., Peck, W., Selleck, B., Baird, G. and Shrady, C., 2010, Shawinigan magmatism in the Adirondack Lowlands as a consequence of closure of the Trans-Adirondack back-arc basin: Geosphere, v. 6, p. 900-916.

Clechenko, C.C. and Valley, J.W., 2003, Oscillatory zoning in granet from Willsboro wollastonite skarn, Adirondack Mts, NY: a record of shallow hydrothermal processes preserved in a granulite-facies terrane: Journal of Metamorphic Geology, v. 21, p. 771-784.

Corriveau, L., Perreault, S., Davidson, A., 2007, Prospective metallogenic settings of the Grenville Province Mineral deposits of Canada: a synthesis of major deposit-types, district metallogeny, the evolution of geological provinces, and exploration methods; by Goodfellow, W D (ed.); Geological Association of Canada, Mineral Deposits Division, Special Publication no. 5, 2007 p. 819-847

Dufrechou, G., 2017, Aeromagnetic signature of an exhumed double dome system in the SW Grenville Province (Canada): Terra Nove, v. 00, p. 1-9.

Florence, F.P., Darling, R.S., Orrell, S.E., 1995, Moderate pressure metamorphism and anataxis due to anorthosite intrusion, western Adirondack highlands, NY: Contributions to Mineralogy and Petrology, v. 121, p. 424-436.

Hamilton, M.A., McLelland, J.M., and Selleck, B.W., 2004, SHRIMP U/Pb zircon geochronology of the anorthosite-mangerite-charnockite-granite suite, Adirondack Mountains, NY: Ages of emplacement and metamorphism, in Tollo, R.P., Corriveau, L., McLelland, J.M., and Bartholomew, M.J., eds., Proterozoic Tectonic Evolution of the Grenville Orogen in North America: Geological Society of America Memoir 197, p. 337–355.

Kemp, J.F., 1898, Geology of the Lake Placid Region: New York State Museum Bulletin, v. 21, 68 p.

Long, K.R., Van Gosen, B.S., Foley, N.K., and Cordier, D., 2010, The principal rare earth element deposits of the United States – A summary of domestic deposits and a global perspective: U.S. Geological Survey Scientific Investigations Report, 2010-5220, 96 p.

Lupulescu, M.V., Hughes, J.M. Chiarenzelli, J.R., and Bailey, D.G., 2017, Texture, crystal structure, and composition of fluorapatites from Iron oxide – apatite (IOA) deposits, eastern Adirondack Mountains, New York: The Canadian Mineralogist, v. 55, p. 399-417.

Mackenzie, K.B., 2017, Adirondack landslides: history, exposures, and climbing: in B. Selleck and J. Chiarenzelli (eds), Adirondack Journal of Environmental Sciences, v. 21, p. 167 – 193.

McLelland, J.M., Bickford, M.E., Hill, B.H., Clechenko, C.C., Valley, J.W., and Hamilton, M.A., 2004, Direct dating of Adirondack massif anorthosite by U-Pb SHRIMP analysis of igneous zircon: Implications for AMCG complexes: Geological Society of America Bulletin, v. 116, p. 1299– 1317.

McLelland, J. and Chiarenzelli, J., 1989, Age of xenolith-bearing olivine metagabbro, eastern Adirondack Mountains, New York: Journal of Geology, v. 97, p. 373-376.

McLelland, J.M. and Selleck, B.W., 2011, Megacrystic Gore Mountain-type garnets in the Adirondack Highlands: age, origin, and tectonic implications: GSA Bulletin, v. 7, p. 1194-1208.

McLelland, J., Hamilton, M., Selleck, B., McLelland, J., Walker, D., and Orrell, S., 2001, Zircon U-Pb geochronology of the Ottawan Orogeny, Adirondack highlands, New York; regional and tectonic implications: Precambrian Research, V. 109, p. 39-72.

Meyers, J.S., Voordouw, R.J., and Tettelaar, T.A., 2008, Proterozoic anorthosite–granite Nain batholith: structure and intrusion processes in an active lithosphere-scale fault zone, northern Labrador: Canadian Journal of Earth Sciences, v. 45, p. 909-934.

Miller, W.J., 1919, Geology of the Lake Placid Quadrangle: New York State Museum Bulletin, n. 211-212.

Morrison, J. & Valley, J.W. (1988): Contamination of the Marcy anorthosite massif, Adirondack Mountains, N.Y.: petrologic and isotopic evidence. Contributions to Mineralogy and Petrology, v. 98, p. 97-108.

Peck, W.H., Bickford, M.E., McLelland J.M., Nagle, A.N., and Swarr, G.J., 2010, Mechanism of metamorphic zircon growth in a granulite-facies quartzite, Adirondack highlands, Grenville Province, New York: American Mineralogist, v. 95, p. 1796-1806.

Peck, W.H., Selleck, B.W., Regan, S.P., Howard, G.E., and Kozel, O.O., in press, In-situ dating of metamorphism in Adirondack anorthosite: American Mineralogist, v. 133.

Porter, R.C., Fouch, M.J., and Schmerr, N.C., 2014, Dynamic lithosphere with the Great Basin: Geochemistry, Geophysics, Geosystems, v. 15, p. 1128-1146.

Postel, A. W., 1952, Geology of Clinton County magnetite district, New York. Geological Survey Professional paper 237.

Quinn, R., Kitajima, K., Nakashima, D., Spicuzza, m., and Valley, J., 2017, Oxygen isotope thermometry using quartz inclusions in garnet: Journal of Metamorphic Geology, v. 35, p. 231-252.

Regan, S.P., Chiarenzelli, J.R., McLelland, J.M., and Cousens, B.L., 2011, Evidence for an enriched asthenospheric source for coronitic metagabbros in the Adirondack Highlands: Geosphere, v. 7, no. 3, p. 694-709

Regan, S.P., Geer, P.S., Walsh, G.J., Aleinikoff, J.N., Baird, G.B., Valley, P.M., Williams, M.L., Jercinovic, M.J., and Grover, T.W., 2015, Precambrian Geology of the Eagle Lake quadrangle, Essex County, NY: New York State Geological Association field conference, p. 30-59.

Regan, S.P., Walsh, G.J., Williams, M.L., Chiarenzelli, J.R., Toft, M., and McAleer, R., in review, Syn-collisional exhumation of hot middle crust in the Adirondack Mountains: implications for extensional orogenesis in the southern Grenville Province: submitted to Geosphere.

Rivers, T. 2008. Assembly and preservation of lower, mid, and upper orogenic crust in the Grenville Province—Implications for the evolution of large, hot, long-duration orogens. Precambrian Research 167:237–59.

Rivers, T., 2011, Upper-crustal orogenic lid and mid-crustal core complexes: signature of a collapsed orogenic plateau in the hinterland of the Grenville Province: Canadian Journal of Earth Science, v. 49, p. 1-42.

Rivers, T., Culshaw, N., Hynes, A., Indares, I., Jamieson, R., and Martignole, J., 2012, The Grenville Orogen – a post LITHOPROBE perspective: Chapter 3 in Tectonic Styles in Canada: the LITHOPROBE perspective, edited by JA Percival, FA Cook, and RM Clowes, Geological Association of Canada, Special paper n. 49, p. 97-236.

Rivers, T., and Schwerdtner, W.M., 2015, Post – peakevolution of the Muskoka domain, western Grenville Province: ductile detachmentzone in a crustal-scale metamorphic core complex: Geoscience Canada, v. 42, p. 403-436.

Roden-Tice, M.K., Tice, S.J., and Schofield, I.S., 2000, Evidence for differential unroofing in the Adirondack Mountains, New York State, determined by apatite fission track thermochronology: Journal of Geology, v. 108, p. 155-169.

Schwerdtner, W.M., Rivers, T., Tsolas, J., Waddington, D.J., Page, S., and Yang, J., 2016, Transtensional origin of multi-order cross-folds in a high-grade gneiss complex, southwestern Grenville Province: formation during post-peak granitational collapse: Canadian Journal of Earth Sciences, v. 53, p. 1511-1538.

Selleck, B., McLelland, J.M., and Bickford, M.E., 2005, Granite emplacement during tectonic exhumation: The Adirondack example: Geology, v. 33, p. 781-784.

Soucy La rouche, R., Gervais, F., Tremblay, A., Crowley, J.L., and Rutter, G., 2015, Tectono-metamorphichistory of the eastern Taureau shear zone, Maurici area: Quebec: implications for the exhumation of the mid-crust in the Grenville Province: Precambrian Research, v. 257, p. 22-46.

Spear and Markussen, 1997, Mineral zoning, P-T-X-M phase relations and metamorphic evolution of some Adirondack granulites: Journal of Petrology, v. 38, p. 757-783.

Storm, L., and Spear, F., 2005, Pressure, temperature, and cooling rates of granulite facies migmatitic metapelites from the southern Adirondack highlands, New York: Metamorphic Geology, v. 23, p. 107 – 130.

Valentino, D.W., Chiarenzelli, J.R., and Regan, S.P., in press, Spatial and temporal links between accretionary orogenesis and massif anorthosite intrusion, southern Grenville Province, New York, U.S.A., Journal of Geodynamics

Valley, J.W. and O'Neil, J.R. (1982) Oxygen isotope evidence for shallow emplacement of Adirondack anorthosite. Nature, v. 300, p. 497–500.

Valley,J.W,Chiarenzelli,J.R. & McLelland,J.M., 1994, Oxygen isotope geochemistry of zircon: Earth and Planetary Science Letters, v. 126, p. 187-206.

Valley, P.M., Hanchar, J.M., and Whitehouse, M.J., 2011, New insights on the evolution of the Lyon Mountain Granite and associated kiruna-type magnetite apatite deposits, Adirondack Mountains, New York State: Geosphere, v. 7, n. 2.

Valley, P.M., Hanchar, J.M., and Whitehouse, M.J., 2009, Direct dating of Fe oxide-(Cu-Au) mineralization by U/Pb zircon geochronology: Geology, v. 37, p. 223–226, doi: 10.1130/G25439A.1.

Whitney, D.L., Teyssier, C., Rey, P., and Buck, W.R., 2013, Continental and oceanic core complexes: Geological Society of America Bulletin, v. 125, p. 273-298.

Williams, M.L., Karlstrom, K.E., Dumond, G., and Mahan, K.H., 2009, Perspectives on the architecture of continental crust from integrated field studies of exposed isobaric sections: In Crustal sections from the western North American Cordillera and Elsewhere: Implications for Tectonic and Petrologic Processes, R.B. Miller and A.W. Snoke (eds), Geological Society of America Special Paper, p. 219-241.

Wong, M.S., Williams, M.L., McLelland, J.M., Jercinovic, M.J. and Kowalkoski, J., 2011, Late Ottawan extension in the eastern Adirondack Highlands: Evidence from structural studies and zircon and monazite geochronology: GSA bulletin, v. 124, n. 5-6, p. 857 – 869.

# THE PISECO LAKE SHEAR ZONE: A SHAWINIGAN CRYPTIC SUTURE IN THE SOUTHERN ADIRONDACK MOUNTAINS, NEW YORK

By

David W. Valentino, Department of Atmospheric and Geological Sciences, SUNY Oswego, Oswego, NY 13126
Jeffrey R. Chiarenzelli, Department of Geology, St. Lawrence University, Canton, NY 13617
Email addresses: david.valentino@oswego.edu, jchiaren@stlawu.edu

## ABSTRACT

Highly deformed Piseco granitic gneisses occur in an arching east-west transpressional ductile shear zone (Piseco Lake shear zone) that spans the width of the exposed southern Adirondacks. The highly deformed granitic gneisses have restricted silica content, are metaluminous, alkali-calcic to calc-alkalic, continental arc trace element signatures. These granitic rocks intruded supracrustal gneisses resulting in extensive Shawinigan partial melting. The Piseco Lake shear zone (20-30 km wide) formed in this belt of granitic rocks and correlate with a pronounced arcuate-shaped high magnetic anomaly. The magnetic anomaly extends well beyond the exposed Adirondack basement window.

The shear zone is 20-30 km wide and is believed to be the location of a cryptic suture because it occurs between the Adirondack Highlands (underlain primarily by anorthosite and related granitic rocks, AMCG suite) and the Southern Adirondack Terrane (underlain by calc-alkaline tonalitic arc rocks) (Valentino et al., in press). Within the shear zone, the original megacrystic granite contains lineated quartz and rodded feldspar aggregates up to a meter long in places. Along the axis of the shear zone there are thick (1-2 km), subvertical zones of granitic L-S and L-tectonites. The northern domain of the zone is defined by large foliation domes that are cored by L-tectonite. The southern limbs of the domes steepen toward the south and merge with a wide zone (up to 15 km) of steeply dipping granitic mylonite. Overall, the shear system (domes and steep mylonite zone) forms the core of a region of intense ductile deformation with left-lateral kinematic indicators and subhorizontal E-W ribbon lineations.

The Piseco granitic suite are highly deformed suture-stitching arc plutons that intruded within a sinistral, oblique-convergent, shear system in the deep crust during the Shawinigan orogeny. This is ductile shear zone is the most continuous and largest in the entire Adirondack massif. The shear zone, associated granitic rocks, and the magnetic anomaly abruptly trends toward the south in the eastern Adirondacks. Just beyond this location, the magnetic anomaly appears to be truncated by a branch of the NY-AL magnetic lineament. Following the trace of the magnetic anomaly toward the west, suggests that the shear zone continues for a considerable distance beyond the Adirondack window. It's magnitude, in addition to the magnitude and extend of the associated magnetic anomaly, suggests that the Piseco shear zone penetrates the Moho.

The current field trip is an update on our very long research project, and it's geared toward an undergraduate student audience. All field locations were picked to accommodate large student groups. Sampling is generally prohibited by NYS law in the Adirondack Park, and we encourage future instructors to help preserve the field locations presented herein by showing and discussing, and not removing the spectacular bedrock features. Note that the field guide included here in was pirated and modified from the Friends of the Grenville field conference run by D. Valentino, J. Chairenzelli, D. Piaschyk, L. Williams and R. Peterson in 2008.

## INTRODUCTION

The Adirondack Mountains are a relatively recently uplifted (Roden-Tice and Tice, 2005), domal exposure of Mesoproterozoic high-grade gneisses that are part of the contiguous Grenville Province (Figure 1). Sharing many similarities to nearby rocks in Ontario and Quebec, and Grenville basement inliers in the Appalachians (McLelland et al., 2010), the rocks exposed in the Adirondacks record processes in the deep crust related to a series of orogenic events collectively known as the Grenville Orogenic Cycle (McLelland et al., 1988). Undergoing deformation spanning a period of over 250 million years (ca. 1250-1000 Ma), the Grenville Province of Laurentia is a small part of a world-wide system of orogenic belts whose assembly led to the eventual formation of the supercontinent Rodinia.

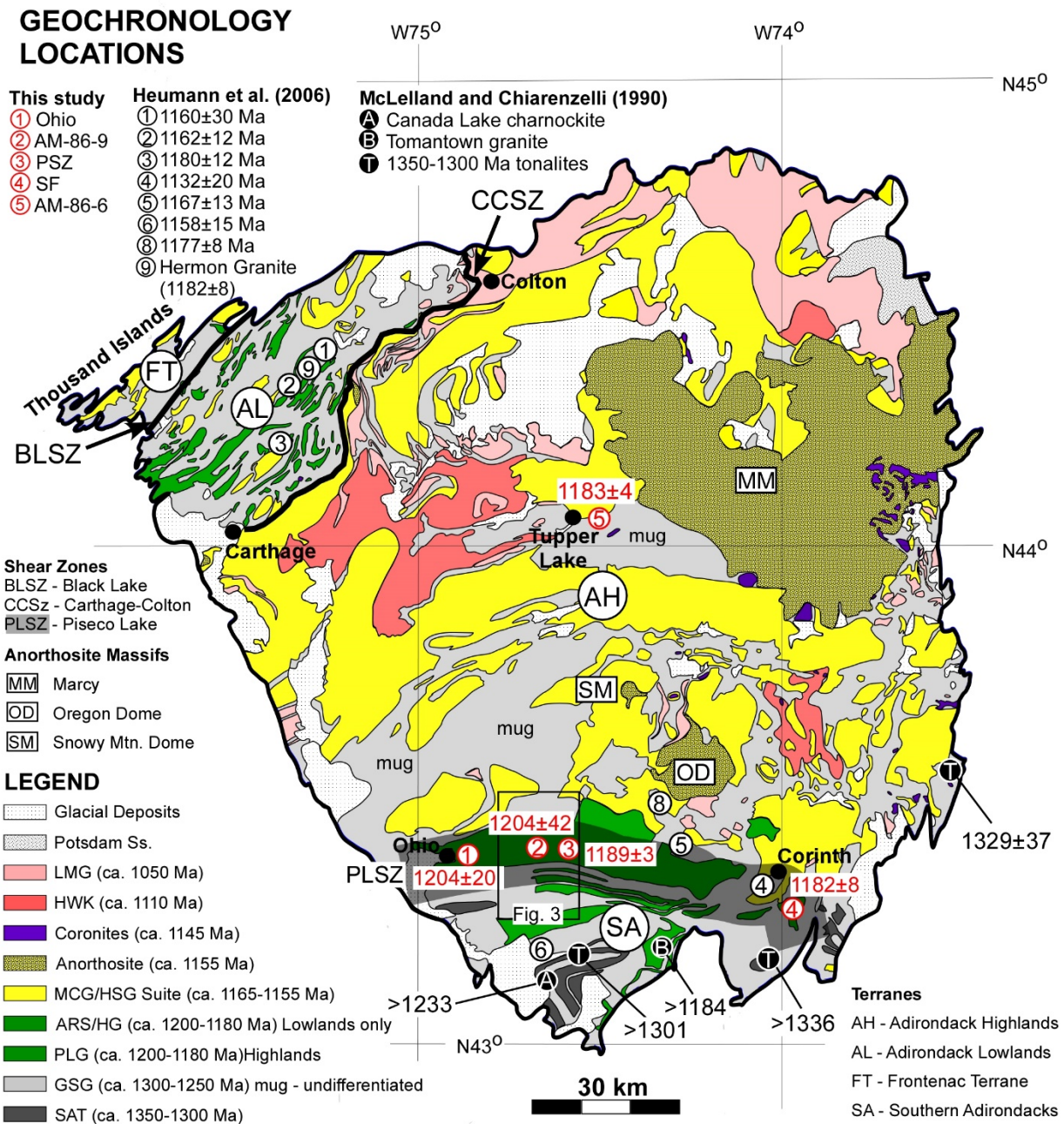


Figure 1. Simplified geological map showing rock suites (from Valentino et al. – in press): ARS – Antwerp-Rossie suite; GSG – metasedimentary rocks of the Grenville Supergroup; HG – Hermon granitic gneiss; HSG – Hyde School gneiss; HWK – Hawkeye granite; LMG – Lyon Mountain granite; MCG – Mangerite-charnockite-granite suite (granitoid part of AMCG suite); mug- mixed metasedimentary and metaigneous rocks that are most likely correlative with GSG; PLG – Piseco Lake gneisses; SAT – Southern Adirondack tonalite suite. U-Pb zircon analysis results (red circles – this study; white circles – Heumann et al., 2006; black circles – McLelland and Chiarenzelli, 1990). Numbered red circles (1-5) are geochronology locations for this study. Location of Figure 3 show as thin black rectangle.

The Adirondacks have been subdivided into the Lowlands and Highlands based on difference in metamorphic grade, predominance of supracustal verses metaigneous rocks, and topography. The Carthage-Colton shear zone in the northwestern Adirondacks (Geraghty et al., 1981; Wiener, 1983), is the boundary between these terranes. The

shear zone displays evidence of one or more ductile, high-grade events, as well as, later brittle remobilization and intrusion by leucogranites (Selleck et al., 2005). It has been interpreted as a late, brittle, normal fault accommodating orogenic collapse and, although the earlier ductile history is obscured, thrust and strike-slip kinematics have been noted (Baird and MacDonald, 2004; Wiener, 1983). Traditionally, lithologic similarities with the Central Metasedimentary Belt in Canada has led to inclusion of the Adirondack Lowlands as part of this terrane; whereas, the Adirondack Highlands has been equated to the Central Granulite Terrane of Quebec, again based on lithologic similarities and metamorphic grade. More recently Rivers (2008) has proposed orogen-wide subdivisions based on geochronology, and metamorphic and structural data. He suggested that the Adirondacks were part of a terrane accreted during the Shawinigan Orogeny (ca. 1140-1200 Ma) and subsequently were part of the orogenic lid; part of a medium to low pressure belt of allochthonous rocks that lack the widespread deformation that occurred elsewhere during the Ottawan Orogeny (ca. 1020-1080).

Tectonic models in the South-Central Grenville Province suggest that southeastern margin of Laurentia (present coordinates) has been the site of subduction and accretionary processes for much of the period between 1200-1500 Ma (Carr et al., 2000; Hanmer et al, 2000; Rivers and Corrigan, 2000). Part of this pre-orogenic history includes a period of back-arc, failed rift spreading in the Central Metasedimentary Belt (Dickin and McNutt, 2007) and the opening of a marginal sea within the current location of the Trans-Adirondack Back-arc Basin (Chiarenzelli et al., 2012). This began ca. 1300 Ma and was terminated by the Elzevirian Orogeny at ca. 1240 Ma. The continental arc developed along the leading edge of Laurentia (ca.1300-1350 Ma) was dismembered and dispersed by this subsequent rifting. Fragments of this arc are now found in Ontario, Quebec, the Green Mountains of Vermont, and in the Southern and Eastern Adirondacks, and were accreted to Laurentia during the Shawinigan Orogeny (Figure 1). Collectively these rocks have been called the Dysart-Mt. Holly Complex (Hanmer et al., 2000) after locations in Ontario and Vermont, respectively. The ca. 1300-1350 Ma tonalitic rocks in the Southern Adirondacks (McLelland and Chiarenzelli, 1990) and the Green Mountains of Vermont (Ratcliffe et al., 1991) are considered part of this arc or arcs.

## THE PISECO GRANITOID AND SHEAR SYSTEM

The Piseco granitoid suite (Figure 2), located in the southern Adirondacks, was originally thought be part of a basement complex to the Adirondack supracrustal sequence (McLelland and Isachsen, 1986), and were later characterized as granitic members of the AMCG suite (McLelland et al., 1988; 2004; Hamilton et al., 2004). Most recently, evidence supports an independent origin, and slightly older age for these rocks, which are exclusively found within, and along strike, of the highly tectonized Piseco shear zone (Valentino et al., in press). Their ubiquitous high strain prohibits detailed characterization of primary textures at most locations. However, the bulk mineralogy and detailed geochemistry, in addition to very large recrystallized mineral aggregates suggest that these rocks were predominantly igneous, megacrystic, and associated with arc Shawinigan plutononism (Valentino et al., in press).

In contrast to the dominant northeast structural trends throughout most of the Grenville Province, the south-central Adirondack Highlands structural grain is predominantly east-west (Figure 2), including the belt of Piseco granitoids. Across strike, where the overlying Paleozoic cover rocks have been stripped away, this region is greater than ~150 km wide and displays general parallelism of geologic contacts, fold axes, compositional layering, strike of foliation, the trend of mineral elongation lineations and substantial (~5-10 km wide) zones of mylonite. Several large (>20 km across) structural domes, cored by rheologically rigid anorthosite, lie within the zone (Chiarenzelli et al., 2000; Gates et al., 2004; Valentino et al., 2004; Valentino et al., 2008), and kinematic investigations indicate that this zone is dominated by left-lateral transpressive shear (Chiarenzelli et al., 2000; Gates et al., 2004; Valentino et al., 2008). There are a number of large-scale features, such as drag folds and rotated giga-scale clasts (i.e. Snowy Mountain anorthosite body), which are consistent with the abundant meso- and micro-scale kinematic indicators including S-C fabrics, shear bands, and rotated porphyroclasts of various minerals (Gates et al., 2004). Here we designate this east-west striking, broad zone of gneisses as the Central Adirondack Shear System (CASS), and the crust-scale structures of the CASS are interpreted as the consequence of transpressional modification of earlier recumbent folds, analogous to those exposed in the Adirondack Lowlands (Chiarenzelli et al., 2000). The CASS is superimposed on rocks that contain widespread granulite-facies mineral assemblages, deformed migmatitic gneisses, and substantial volumes of supracrustal rocks, all supporting earlier history of compressional tectonism as described above. However, discrete mylonite zones within the CASS were shown to contain retrograde deformation fabrics, with some containing fabric forming greenschist facies minerals, such as biotite, chlorite and muscovite (Price et al.,

2003; Valentino et al., 2008). These relationships suggest that structural activity within the CASS outlasted high-grade conditions and continued through denudation, uplift and cooling of the central Adirondacks. It was previously proposed that the locus of deformation within the CCAS, the Piseco Lake shear zone, marks the boundary of oblique-slip convergence between the southeastern margin of Laurentia and the Southern Adirondack arc terrane (Gates et al. 2004; Valentino et al., 2008).

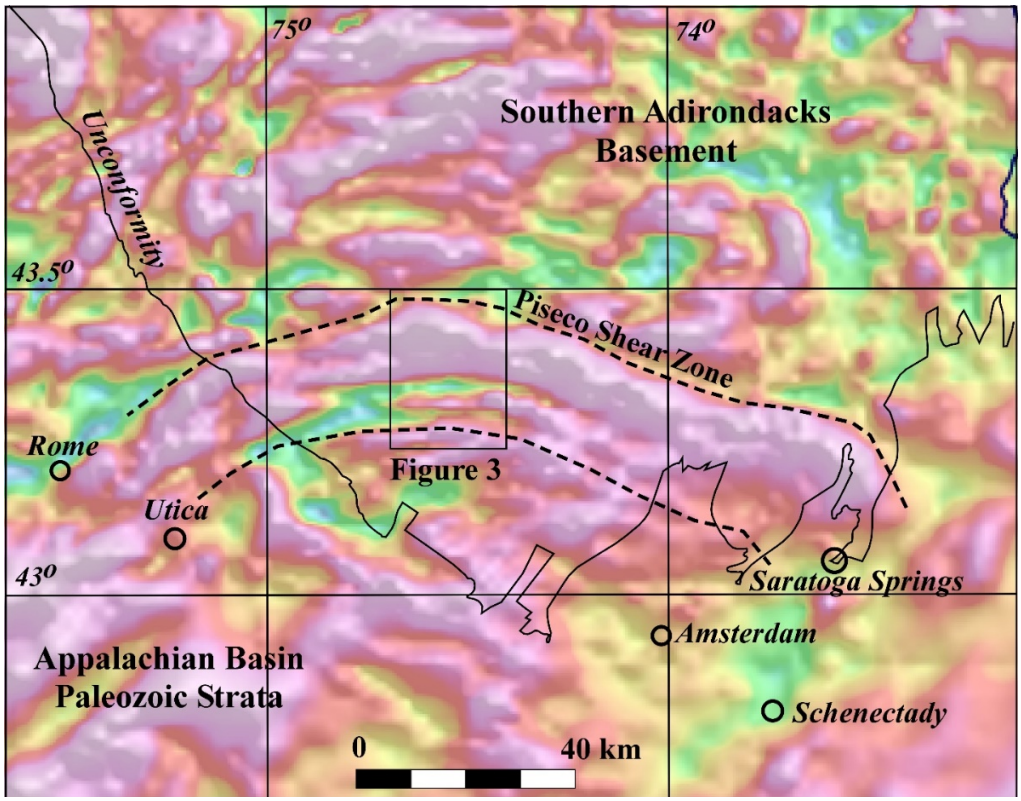


Figure 2. Magnetic anomaly map of the southern Adirondack region. Location is shown on Figure 1.

**The Piseco Lake Shear Zone**

Several discrete ductile shear zones occur within the CASS (Gates et al., 2004; Valentino et al., 2008; Weimer et al., 2001), with the Piseco shear zone as the most continuous and largest spanning the entire 120 km width of the Adirondack massif and upward of 30 km wide (Figures 2 and 3). A prominent magnetic anomaly correlates with the Piseco Lake shear zone (PLz) and it appears that the zone extends well beyond the exposed limits of the Adirondack massif (Figure 2). Strong deformation in the area surrounding Piseco Lake was first noted by Cannon (1937). Fakundiny (1996) and Fakundiny et al. (1994) proposed a fundamental structural discontinuity in this area based largely on geomorphological criteria and the trace of the Prospect Fault (Valentino et al., 2012). In addition, fundamental lithologic differences have been noted across the boundary as AMCG rocks are rare or absent to the south, whereas tonalitic rocks (ca.1300-1350 Ma) of the Southern Adirondack arc terrane have not been recognized north of it. The PLz is developed in a suite of granitoids (Piseco Lake Granitoids – PLG) that span the width of the Adirondack massif outcrop belt, but more importantly the belt strongly correlates with the pronounced linear magnetic anomaly.

The PLz is defined by spectacular L-S, L>S and L-tectonites developed in the Piseco granitoids, with an east-west arching trend. This trend continues smoothly to the eastern margin of the Adirondack Dome, where before plunging beneath Paleozoic cover rocks to the east at Spier Falls on the Hudson River, where the lineation and foliation gradually transitions to a north-south orientation defining a broad (10's of km) open vertical fold. The PLz comprises parallel structural domains that developed contemporaneously: 1) a broad (10-15 km wide) tabular steeply dipping zone of granitic mylonite (southern domain); 2) a series of flanking upright (5-10 km wide) foliation

domes (northern domain) (Cannon, 1937; Glennie, 1973; McLelland, 1984; Wiener et al., 1984). There is no apparent structural discontinuity between the foliation of the southern mylonite zone and the foliation in the dome region. As well, lineations are consistent in orientation and defined by the same minerals within both domains. Collectively, these structural domains make up a zone of ductile deformation that is upward of 30 kilometers wide, crossing the exposed width of the boundary between the Central and Southern Adirondacks.

**The Southern Domain – Shear Zone**

There is a well-defined textural transition that occurs in variably deformed granitoids in the southern limit of the PLz. From south to north, the granitic rocks exhibit moderately deformed megacrysts of K-feldspar, well developed mylonite with remnant K-feldspar grains (~5-10 mm in diameter) and finally domains of ultramylonite (Valentino et al., 2008). Penetrative foliation is defined by dynamically recrystallized quartz, K-feldspar and plagioclase, and alignment of micas. Rocks within the zone are made of fine-grained aggregates of these minerals in strong alignment. Locally there are 2-6 cm long K-feldspar megacrysts and/or porphyroclasts preserved which are consistent with a plutonic origin. Pegmatitic and aplitic layers provide evidence of strong transposition of primary contacts (Piaschyk et al., 2005; Valentino et al., 2008). Rocks with steeply dipping penetrative mylonitic fabric persist over an across strike distance of more than 10 km, eventually merging with the highly deformed granitoids in the northern domes. Lineations in this zone are subhorizontal and defined by dynamically recrystallized quartz, K-feldspar, plagioclase, and accessory mafic minerals such as hornblende, biotite or chlorite. Shear sense indicators are abundant and occur at the meso- and microscopic scale. K-feldspar megacrysts form Type I S-C fabrics, σ- and δ- porphyroclasts and domino-structures (Figure 4). Where the L-S fabrics are well developed, consistently the shear sense indicators are sinistral across the entire 10 km wide zone of the southern domain.

**Northern Domain – Dome**

Penetrative foliation and lineations define several upright antiformal domes (Cannon, 1937; Glennie, 1973; Weiner et al., 1984; Valentino et al., 2012) that flank the north side of the steeply dipping mylonite zone (southern domain). These domes have subhorizontal arching axes that trend approximately 110º in the east, 090º in the central region, and 080º in the west. The largest of these domes occurs in the vicinity of Piseco Lake. The foliation on the dome limbs dips moderately with mineral elongation lineations that trend at 110º and plunge about 10º eastward. In the crest of the domes, foliation is not well developed and penetrative lineations are defined by mineral rods, rods of mineral aggregates, and mineral ribbons. Lineations in the domes are intensely developed, and in many places the linear fabric is dominant over the weak foliation (L>>S) with grain aggregate aspect ratios upward of 60:1, in the L-parallel and S-perpendicular plane, as originally noted by McLelland (1984). Some rocks, of considerable thickness ~1-2 km, in the core of the domes lack foliation altogether and are true L-tectonites. Microscopic examination showed that the lineations are defined by dynamically recrystallized ribbons and rods of quartz, K-feldspar, plagioclase, in addition to streaks of magnetite, biotite, chlorite and occasionally muscovite (Valentino et al., 2008).

Like the rocks in the southern domain, shear-sense indicators are abundant in the dome rocks that are not dominated by L-tectonite. They include Type I S-C mylonite, σ - and δ -porphyroclasts of K-feldspar, and asymmetric polymineralic tails around porphyroclasts (Figure 4). These kinematic indicators reveal a consistent sinistral-shear sense on both the north- and south-dipping L-S tectonite domains of the domes.

**Magnetic Anomalies**

The magnetic anomaly map of North America (U.S.G.S. – Mineral Resources Online Spatial Data) has an interesting distribution of high and low anomalies in the Adirondack region that roughly correlate with major metaigneous and metasedimentary rock bodies (Figure 2). The corresponding magnetic anomaly for the anorthosite bodies is low, while vast regions underlain by charnockitic gneiss express high anomalies. Regions of the Adirondacks with substantially thick sequences of supracrustal rocks generally have low magnetic anomaly signatures, similar to the anorthostie bodies. Magnetic anomaly patterns in the Adirondack lowlands are parallel to the overall northeastern striking geologic structures that control the geographic distribution of various metaigneous and metasedimentary rock bodies. Within the Adirondack Highlands, the northern region can be characterized as having magnetic anomalies with a nebulous, or unorganized, structural pattern, most likely the result of the vast anorthosite bodies that make up the Mount Marcy massif.

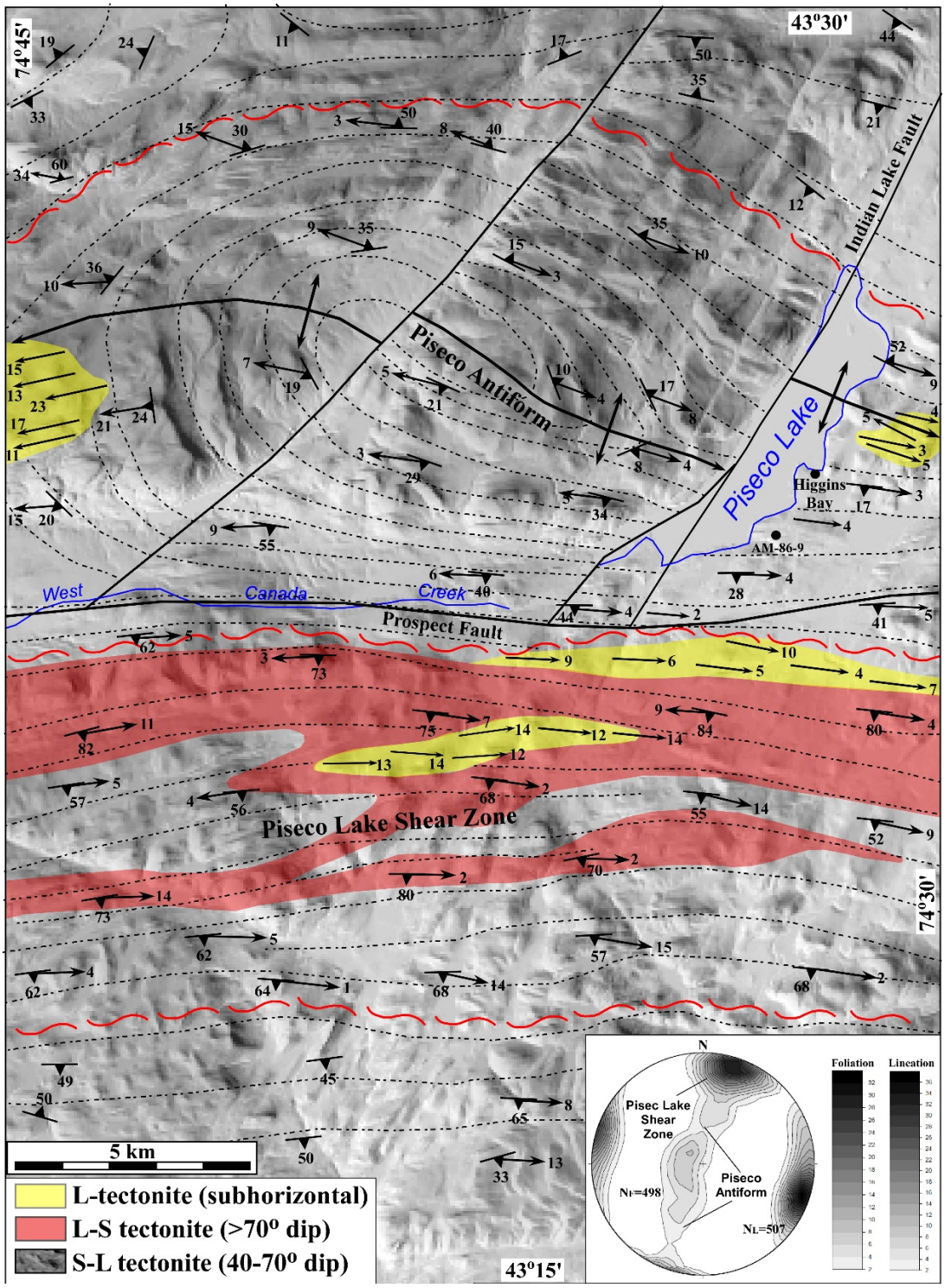


Figure 3. Simplified structural geology map for the Piseco Lake shear zone and dome plotted on a gray-scale digital elevation model. Location is shown on Figure 2. Inset shows lower hemisphere contour stereogram for poles to foliation and lineation data collected in the mapped region. Note that the lineation data is a composite plot for both the antiform and shear zone domains; foliation is designated separately. The sinuous dashes show the approximate boundaries of the Piseco Lake shear zone in this area. The axis of the Piseco antiform is shown in addition to Mesozoic faults (heavy black lines) that offset the antiform axis near Piseco Lake (Valentino et al., 2012).

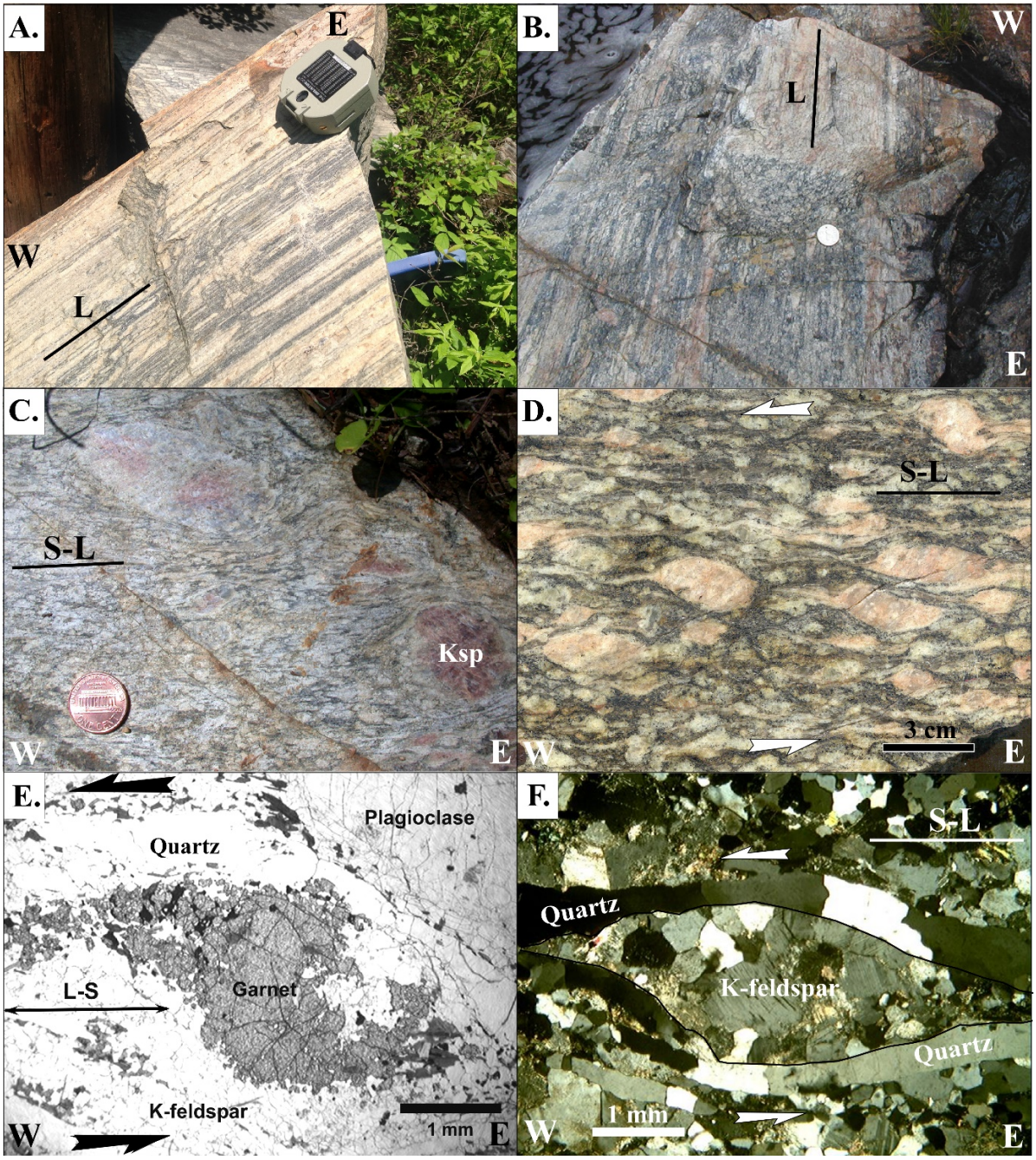


Figure 4. Examples of deformation fabrics in the Piseco shear zone. A. Strongly lineated granitic mylonite from the southern flank of the structural dome near Piseco Lake. B. Tectonite dominated by mineral aggregate elongation lineations from the core of the dome. C. Well developed granitic mylonite from the southern steeply dipping shear zone. D. Augen mylonite with relict K-feldspar megacrysts forming asymmetric σ-porphyroclasts on the northern flank of the dome. E. Photomicrograph of asymmetric garnet enveloped in quartz ribbons, and recrystallized K-feldspar and plagioclase (ppl). F. Photomicrograph of highly deformed granitic gneiss from the Piseco shear zone (xpl) displaying polygonal grains of dynamically recrystallized K-feldspar and quartz ribbons. The aggregate of K-feldspar (center) is surrounded by quartz ribbons and the overall shape forms a recrystallized asymmetric sigma-porphyroclast.

With the exception of small anorthosite bodies with ovoid low magnetic anomalies, the structural pattern of anomalies in the central and southern Adirondacks is strikingly regular and trends roughly east-west parallel to the structures of the Central Adirondack Shear System (Chiarenzelli et al., 2000; Gates et al., 2004; Valentino et al., 2008). One of the most pronounced high magnetic anomalies extends unbroken across the entire exposed width of the southern Adirondacks, forming a broad open arch that curves to a north-south trend in the east and appears to be sharply truncated near Saratoga Spring, NY. This anomaly extends west of the Adirondacks where it bifurcates and continues beneath the Appalachian basin of central NY. This high magnetic anomaly has the most structural continuity for any anomaly associated with the exposed basement geology, and it directly correlates with the highly deformed Piseco granitoid suite and related shear system (McLelland and Isachsen, 1986; McLelland et al., 1988; 2004; Gates et al., 2004; Hamilton et al., 2004; Valentino and Chiarenzelli, 2008).

## ORIGIN OF THE PISECO LAKE GRANITOIDS

The limited compositional range, megacrystic texture, coarse grain-size, and large volume of the Piseco Lake granitoids suggest they are an intensely deformed and deep-seated suite of granitic plutons. The occurrence of deformed and transposed cross-cutting aplites and pegmatites is in concert with this interpretation (Piaschyk et al., 2005; Price et al., 2003). Previous U-Pb zircon studies (McLelland et al., 1988; Valentino et al., in press) confirm that the granitic precursors were intruded into the region by at least 1155 Ma and likely earlier (ca. 1200 Ma). The work of Heumann et al. (2006) has suggested that highly deformed paragneisses in contact with the Piseco Lake granitoids underwent anatexis and zircon and monazite growth from 1160-1180 Ma. If the Piseco Lake granitoids provided some, or all, of the heat that facilitated the melting, a significant volume of melt/heat must have been present by 1180 Ma. This is consistent with our preliminary zircon studies previously published (Valentino et al., in press), indicating intrusion prior to AMCG plutonism at ca. 1155-1165 Ma and likely at ca. 1200 Ma.

The fabric in the Piseco Lake granitoids and surrounding mylonitic pssamitic/pelitic gneisses, and hence the gross structure of the shear zone itself, can be tied to zircon and monazite growth during high-grade ductile deformation and melting during the waning phase of the Shawinigan Orogeny (Heumann et al, 2006). This is emphasized by the lack of younger “Ottawan” zircons in many of the paragneiss localities in the northwestern, central, and southern Adirondacks studied by Heumann et al. (2006) and in mylonitic gneiss analyzed for this study. Zircons younger than 1080 Ma are nearly absent, indicating minimal, if any, zircon growth during the Ottawan Orogeny along the Piseco Lake Shear Zone; but volumetrically significant metamorphic zircon growth occurred throughout the Shawinigan Orogeny. This in turn provides further evidence that the gross crustal architecture of the Central and Southern Adirondack Region and Central Adirondack Shear System was developed during the Shawinigan Orogeny. The Piseco Lake granitoids provide direct evidence of the processes at work in the deep crust and likely, upper mantle, just prior to and during, the Shawinigan Orogeny. In essence they, and their intense deformation, set the stage for the voluminous AMCG intrusions that followed (Valentino et al., in press).

The kinematic studies on all scales from microscopic to megascopic (Chiarenzelli et al., 2000; Gates et al. 2004; Valentino et al., 2008) indicate left-lateral motion focused along the shear zone and domes developed in the Piseco Lake granitoids. The focus of this intensive deformation, between two distinct terranes, has led to the conclusion that it demarcates a cryptic suture (Chiarenzelli et al., 2011; 2010a; Valentino et al., in press. Antiformal domes and the counterclockwise rotation of rigid anorthosite bodies (Chiarenzelli et al., 2000; Gates et al., 2004) suggest bulk crustal flow throughout the CASS region, as do vertical zones of L-tectonite and rocks with pronounced linear fabrics. Taken together these observations are consistent with the intrusion of a voluminous suite of suture-stitching plutons of arc affinity within a sinistral, oblique-convergent, ductile shear system during the Shawinigan orogeny.

## TECTONIC MODEL

Any tectonic model proposed to explain the origin and deformation of the Piseco Lake granitoids must take into consideration their field relations, age, geochemical and isotopic trends, intense deformation, kinematics, geophysical signature, and the geologic context of the region. Various lines of evidence presented in Valentino et al. (in press) and summarized herein, suggest that the granitoids are the deformed roots of a continental batholith which developed just prior to, and during, the Shawinigan Orogeny and preceded voluminous AMCG plutonism.

Paleogeographically, the plutonic protoliths of the gneisses appear to represent the product of northward subduction of oceanic crust beneath the Southern Adirondack arc, Trans-Adirondack Back-Arc basin, and the

southeast edge of Laurentia, believed to be coincident with the Black Lake Shear Zone at this time (Chiarenzelli et al., 2010b; Wong et al., 2012; and Peck et al. 2004; 2013). Telescoping of this basin during closure led to massive shortening and collapse of the basin and attendant SW-directed thrusting and nappe formation. However, the dominant fabric, which overprints early events, was left-lateral plastic deformation related to oblique collision. The imprint of this late Shawinigan event is recorded at all scales from microscopic kinematic features to "mega" porphyroclasts and elongate structural domes (Chiarenzelli et al., 2000; Gates et al., 2004; Valentino et al., 2008) to a regional subhorizontal lineation.

AMCG plutonism began during the waning stages of Shawinigan orogenesis (Valentino et al., in press). This can be seen in the Marcy anorthosite massif where large, relative intact bodies of meta-anorthosite are cut by thin (1-2 cm) garnet-pyroxene shear zones, many with an E-W orientation (Hecklau et al., 2014). Intrusive boundaries, along coarse-gabbroic pegmatites and fine-grained granitic sheets, are often zones of intense strain. This suggests the meta-anorthosite body, although rigid and resistant to ductile deformation in general, underwent ductile deformation along heterogeneities. Coronitic metagabbros, thought to be the parental magmas from which anorthosite was derived via fractional crystallization (Regan et al., 2011), may provide a lower limit on regional ductile deformation associated with the Shawinigan Orogeny. Coronites display a wide range of deformational and metamorphic features ranging from equant bodies with pristine coronitic textures to elongate, curvilinear belts of garnetiferous amphibolite. In many instances garnetiferous amphibolites retain a small core of coronitic metagabbro that survived deformation (Lagor et al., 2013). Dating of one coronitic metagabbro from Dresden Station yielded an age of 1144+/-7 Ma via U-Pb zircon methods (McLelland and Chiarenzelli, 1989) and extends the range of ages generally attributed to the AMCG suite (ca. 1155-1165 Ma) to at least 1144 Ma. This age overlaps the age of 1151+/-9 Ma for monazite growth in the pelitic gneisses intruded by the Dresden coronitic metagabbro (Grover et al., 2013), indicating the growth of high-grade minerals in compositionally appropriate rocks during intrusion of the coronites.

The transition from arc magmatism represented by the Piseco Lake granitoids to intrusion by anorthosite massifs and cogenetic granitic rocks (AMCG suite) occurred within a relative short period of time; at most several tens of millions of years (Figure 5). This spatial and temporal link suggests that intense deformation associated with the Piseco Lake granitoids was the kinematic trigger for AMCG magmatism. Most models for AMCG rocks invoke for slab detachment or delamination, but few details are known. One possible explanation presented by Valentino et al. (in press) and favored here is that highly oblique subduction and orogeny-parallel deformation may have contributed to detachment and delamination. Shear stress may have reactivated old crustal weaknesses (transform-faults) and/or created tears that propagated into the descending slab and lower plate, resulting in splitting and fragmentation of the rigid lithosphere. Catastrophic failure of this type would allow rapid ascent of asthenospheric mantle, decompressional partial melting of the asthenosphere, and subsequent melting of underlying crustal rocks. Given left-lateral kinematics documented, the progressive closure of the ocean basin the foci of asthenospheric rise and production of AMCG magmatic rocks would propagate from west to east.

An analog for this model would incorporate aspects of the Andean margin where subducting slabs of different age and density behave as independent lithospheric "tiles". These tiles are separated by oceanic fracture zones, subducting at different rates and angles beneath South America, and control the distance between the magmatic arc and trench. In combination with highly oblique convergence, the oceanic fracture zones between these "tiles" would serve as inherent zones of weakness ultimately causing catastrophic tears in the subducting lithospheric plate. A similar scenario involving tearing and propagation of a subducting slab undergoing buckling is currently occurring along the Puerto Rican trench (Meighan and Pulliam, 2013; Meighan et al., 2013).

This tectonic model would not be complete without discussing the proximity of the Piseco shear zone to the New York-Alabama magnetic anomaly lineament (NY-AL), an anomaly that defines a major basement boundary that crosses eastern Laurentia (Steltenpohl et al., 2010). The origin of the anomaly is not definitively known, however, recent researchers have suggested that the linear nature of the anomaly is associated with an intracrustal transcurrent shear system with either dextral or sinistral displacement. Between northwestern Georgia and northeastern Pennsylvania, the NY-AL lineament trends without deviating about 046°, a distance greater than 1000 km (Figure 5). With an easterly change in trend of 15-20°, the lineament is shown to continue northeast and include the Catskill magnetic high extending from northeastern Pennsylvania to the Vermont-Massachusetts border region (Figure 6A). This trend crosses the Scranton gravity high, proposed to be a Neoproterozoic rift basin (Rankin, 1976; Hawman and Phinney, 1992). However, if the 046° trend of the >1000 km long NY-AL lineament is projected into

southern New York, it would correspond to the western margin of the Scranton gravity high (Figure 6B), in addition to the apparent truncations of a series of magnetic high anomalies, including the Piseco anomaly, and by association the granitoids and shear zone. Based on the transcurrent deformation associated with the PLz, we propose the zone to be a splay off of the major crustal boundary that is manifest as the NY-AL magnetic lineament (Steltenpohl et al., 2010).

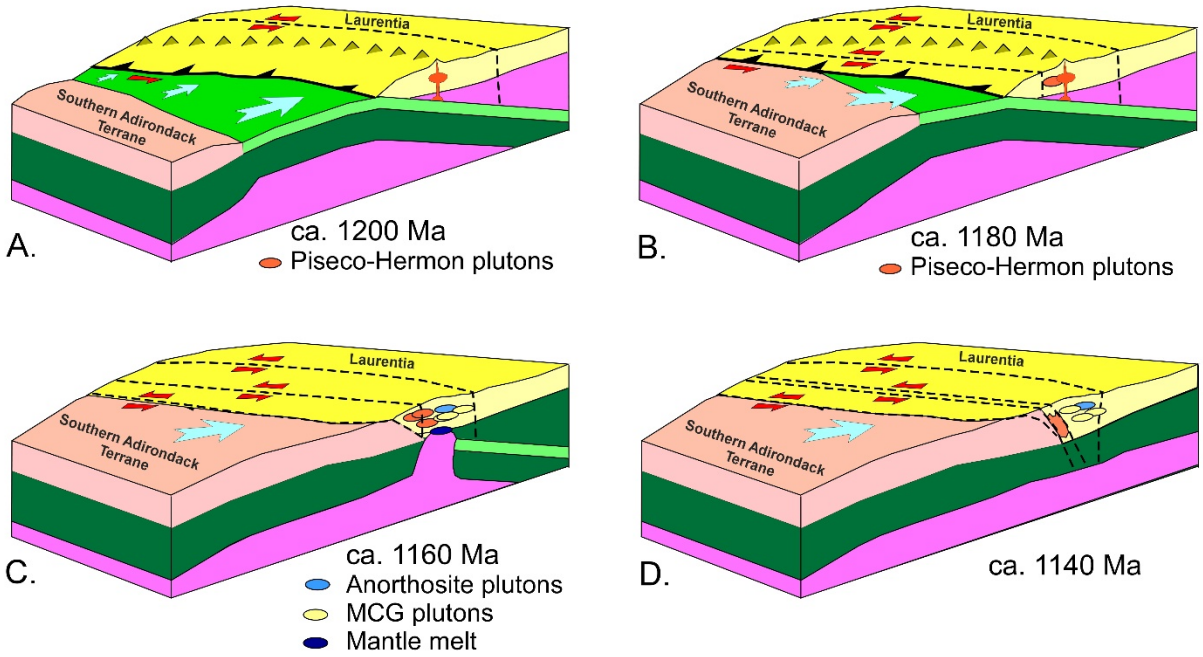


Figure 5. Tectonic model depicting the oblique subduction, subsequent oblique collision and sinistral transform boundary that forms on the granite-stitched suture between the Southern Adirondack Terrane and the Adirondack Highlands (Laurnetia). Refer above for details.

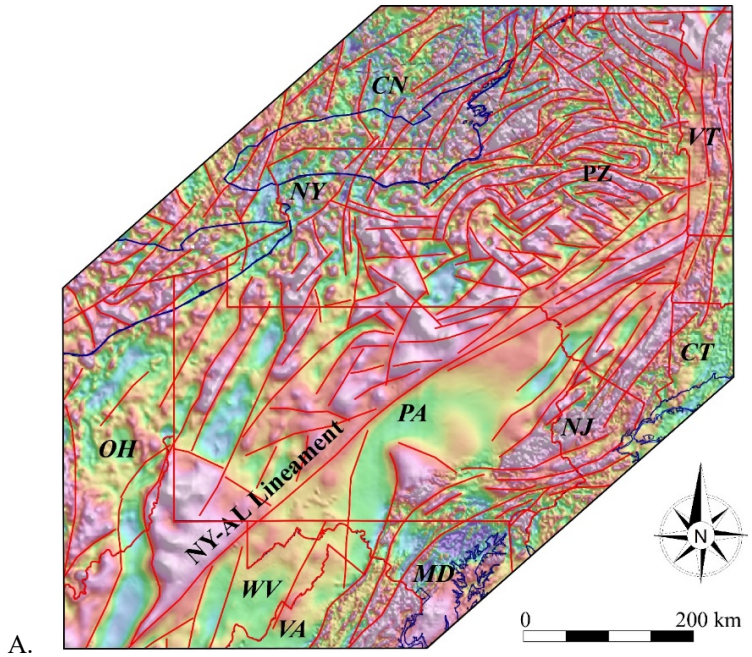

B.

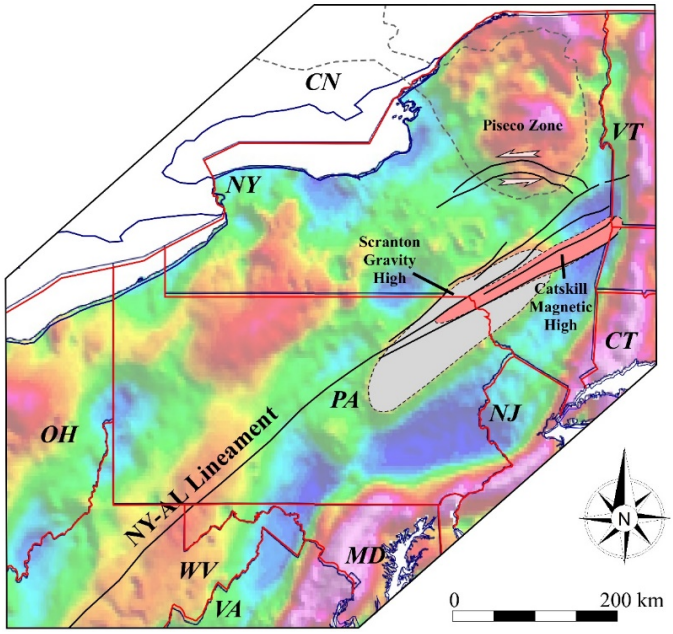


Figure 6. (A) Magnetic and (B) gravity anomaly maps with interpreted lineaments. The New York-Alabama lineament (NY-AL) is labeled along with the Scranton gravity high and the Catskill magnetic high. Outline of the Adirondacks is represented by the dashed line and the Piseco Lake shear zones (PZ) is shown with shear sense arrows (Maps from USGS respository online).

## ROAD LOG

Assemble in the parking lot at the Charlie John's market located the intersection of Route 8 and Route 30 in the village of Speculator, New York (Starting Point on map below). From this point the trip heads north on Route 30 to the first stop.

Mileage:
0.0 Assembly point
1.7 Stop 1: Park on the wide shoulder on the east side of Route 30. The outcrop is on the west side of the road, the traffic is light but fast, so be very careful crossing the road.

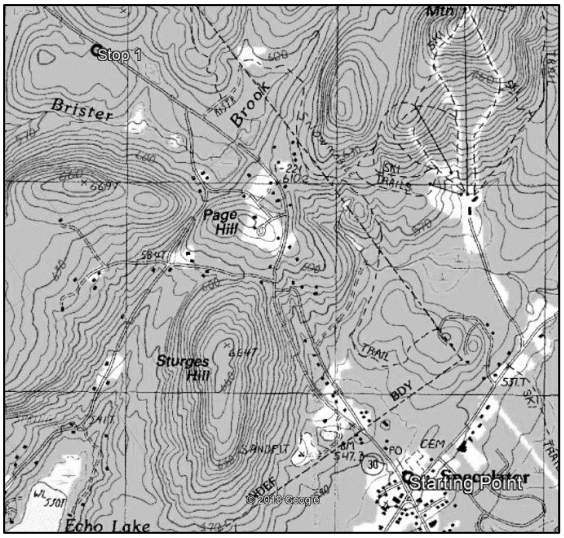

**STOP 1: Supracrustal rocks of the Adirondack Highlands, just north of the Piseco Lake shear zone (18T 549883 m E, 4818851 m N)**

There are several rock types that can be observed at this outcrop, along with the contacts and primary compositional layering. The northern ¼ of the outcrop consists of garnet amphibolite, the next ~ ¼ of the outcrop is calc-silicate gneiss and the southern ½ is fine-grained quartzo-feldspathic gneiss locally interlayered with highly folded marble (Figure 7). Complex sheath folds with sub-horizontal tight, isoclinal and sheath folds of foliation and compositional layers dominate the rock, particularly in the gneiss (trend to 110º). Excellent views of the folds are seen on top of the southern part of the outcrop. The contacts between the rock types are also folded in similar fashion. Matrix minerals define lineations that are E-W and subhorizontal, but are variable in orientation due to folding. Overall, the diverse lithologies and style of deformation are typical for the supracrustal rocks located north of the Piseco Lake grantioids. At this point, note that primary compositional layering is preserved at this outcrop.

Figure 7. Photograph of folded quartzo-feldspathic gneiss and marble (recessed part of outcrop). Note the stalk of grass for scale.

From Stop 1, proceed north to a safe place to turn around, and return to the intersection of Route 30 and Route 8 in the village of Speculator.

Mileage:
3.4 Turn west on Route 8 in the Village of Speculator.
5.4 First roadcut on right is highly lineated granitic gneiss in the margin of the PLsz.
12.2 Intersection with Old Piseco Road in Piseco, NY.
13.3 Park on north side of Route 8 at the low roadcut for Stop 2.

**STOP 2A-D: L-S and L>S fabrics in the Piseco dome – driving traverse**

**Stop 2A: 18T 540256 m E, 4808187 m N**
**Stop 2B: 18T 537957 m E, 4809931 m N**
**Stop 2C: 18T 534370 m E, 4805562 m N**
**Stop 2D: 18T 536919 m E, 4804838 m N**

The Piseco Lake shear zone includes the northern foliation domes that merge with the steeply dipping shear zones to the south. This series of field stops shows variations in the attitude and type of fabrics that occur in the core of the dome at Piseco Lake. Stops 2A to 2D are a driving traverse around Piseco Lake, the type location of

the Piseco antiform. At all of these localities, dynamically recrystallized feldspars and quartz form spectacular ribbon- and rod-shaped mineral lineations (McLelland, 1984), in addition to accessory biotite and magnetite. In many places, the alignment of ribbons forms the foliation in this outcrop. Individual quartz-ribbons have aspect ratios upward of 60:1. At Stop 2A, the foliation is weakly to moderately developed, and dips shallowly southward at the eastern part of the outcrop, but is steeply dipping at the western end of the outcrop. The transition between these different foliation attitudes is difficult to determine because the intensity of the foliation is variable. Lineations are penetrative on all scales, and consistent in attitude (Trend: 110°; Plunge: 05°). Stop 6A occurs on the southern flank of the map-scale dome portion of the Piseco antiform. At the western end of the outcrop there are rods of amphibolite (10-30 cm diameter) within the granitic gneiss.

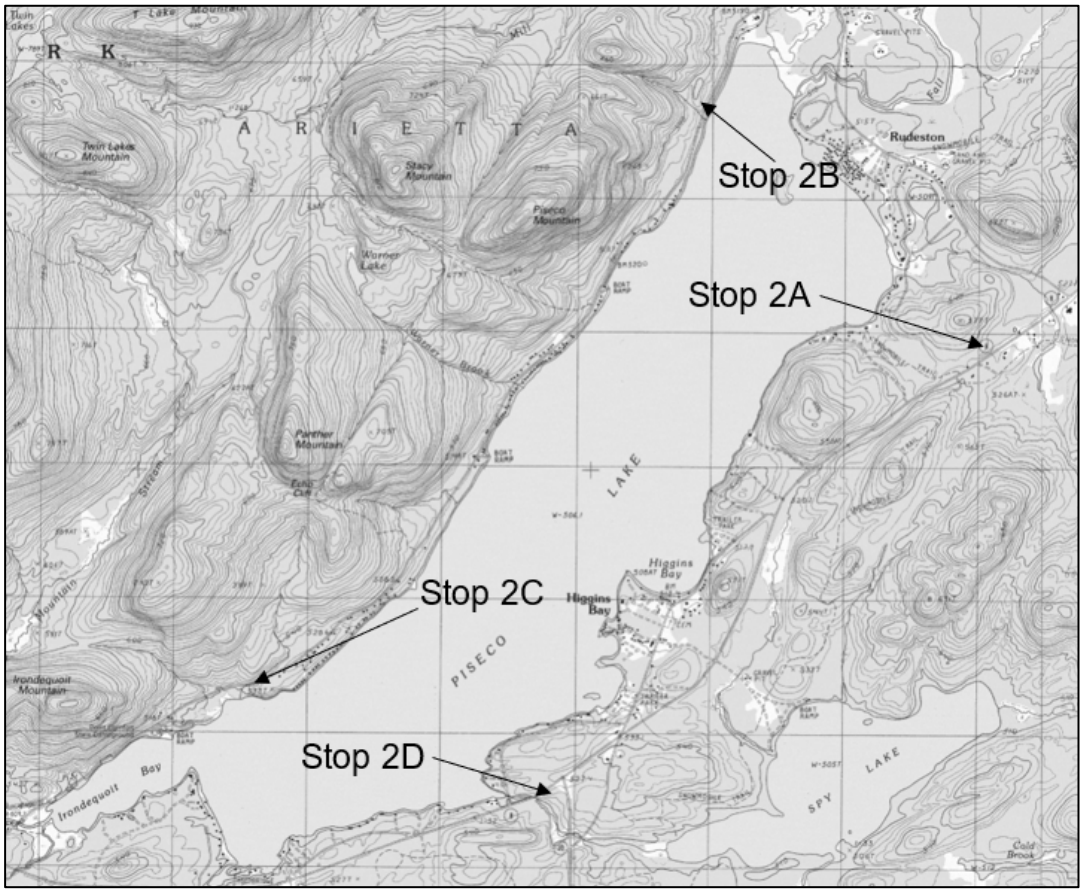


There is an apparent Mesozoic fault that traces down the western side of Piseco Lake and has locally displaced parts of the Piseco dome (Figure 3). At Stop 2B, again the foliation is weakly developed with a penetrative shallowly plunging lineation. However, the foliation, where it can be observed, dips northerly. As you drive southwest along the western side of Piseco Lake, note that the foliation gradually shallows and then dips southerly. There are several outcrops that can be observed where this transition in foliation attitude occurs. The rock fabrics at Stop 2C are similar to those at Stops 2A and 2B, but again the variably developed foliation dips toward the south. Stop 2D is located at the intersection of Rts. 8 and 10, and the folation and lineation is penetrative.

Common to all of these field stops is that biotite and sometimes chlorite blades form microscopic lineations and foliation parallel to the macroscopic structure. Rare grains of hypersthene have been found, but they always have well developed overgrowth textures that include biotite and chlorite. The biotite and chlorite are the most abundant index minerals in the granitic gneiss, and suggest the deformation was last active under low- to moderate- metamorphic conditions, although probably began at much higher conditions to account for the relict grains of hypersthene.

Mileage:
13.3 Turn around and proceed east on Rt. 8 about 0.5 mile. west on Rt. 8.
13.8 Turn north and follow the road around Piseco Lake to Stops 2B and 2C.
22.7 At the intersection with Rt. 8, turn east and proceed about 2.9 miles.
23.6 Turn south onto Rt. 10 and park for Stop 2D. Proceed south on Rt. 10 about 1.2 miles.
24.8 Turn west onto Powley Road (becomes a gravel road) and continue 4.9 miles.
29.7 Park where Powley Road traverses through the Notch.

**STOP 3: Steeply dipping mylonite zone of the southern PLsz (18T 530638 m E, 4799018 m N)**

Along Powley Road, depending on the time of year and the amount of road maintenance, there are a sub-continuous series of pavement exposures located in the road bed, as well as in the gutter on the east (northeast-bound) side of the road. Due to the nature of this location, the extent of the exposed rock at this stop changes yearly, so some or all of the rock described here may be viewable depending upon the time of the season in which the stop is visited (best later in the summer). The best exposures occur along the road between West and East Notch Mountains.

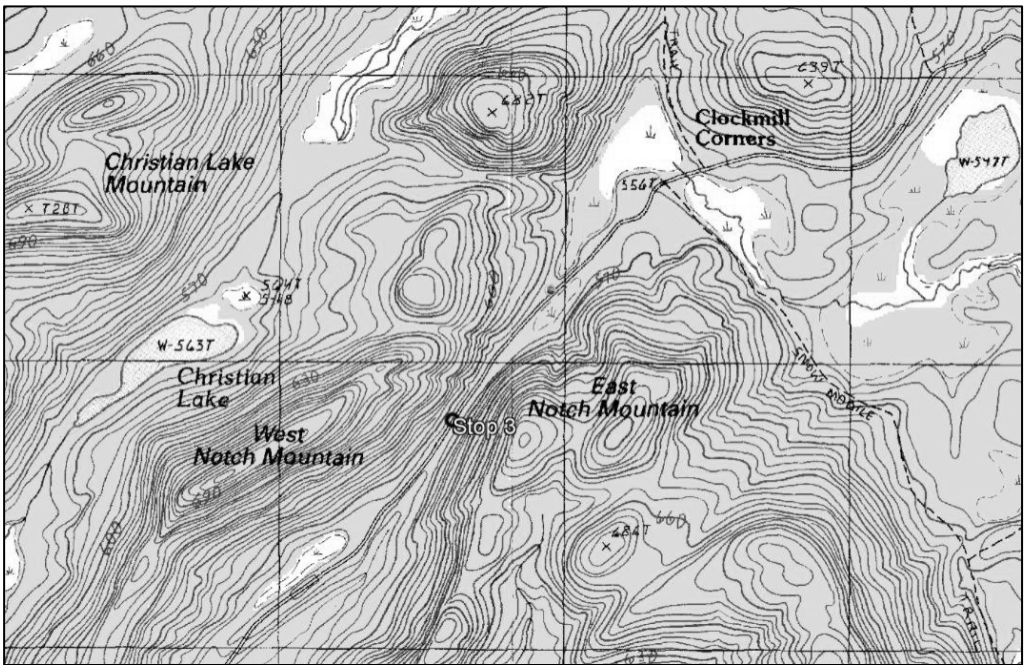


All rocks in this region are very similar in mineral content, and vary only in detail with regard to mineral percentage and fabric type and intensity. The rock is dominantly granitic gneiss with intense subhorizontal to shallowly plunging mineral elongation lineation that trends on average about 095 º, with steeply dipping generally east-west striking foliation. Both fabric elements are defined by ribbons of quartz, and ribbons of aggregate feldspar and quartz (generally 1-5 cm long depending upon grain size). Intensity of the fabric varies across strike at the 50 cm scale, with local layers of significantly coarser-grained fabrics (grains up to 1 cm in diameter). There are also places where the foliation intensity varies as seen at the field stops around Piseco Lake. Rare amphibolite bodies that are 10's of cm thick occur within the granitic gneiss. Shear sense indicators are abundant in the granitic rocks and consistently show sinistral shear sense.

Mileage:

35.7 Continue south on Powley Road about 6 miles and park. Outcrops are located along the bank of East Canada Creek.

**STOP 4: Southern extent of steeply dipping mylonite (18T 527500 m E, 4790961 m N)**

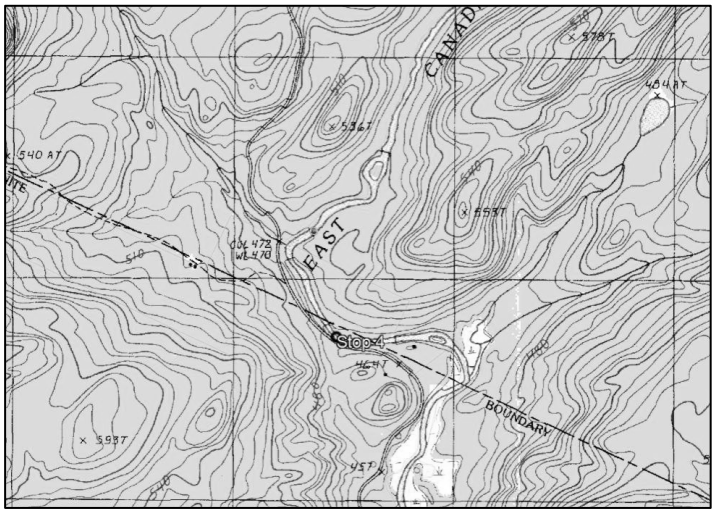


Here the granitic gneiss fabrics contain both a penetrative foliation and lineation. The foliation is steeply dipping and strikes about east-west. Mineral elongation lineation defined by linear aggregates of quartz and feldspar are subhorizontal. The extent of readily available bedrock exposure diminishes south of this location, so this may be the southern-most exposure of the Piseco Lake shear zone. Note that this location is about 21 kilometers across strike from the northern side of the Piseco dome where the pronounced lineation occurs.

Mileage:

46.6 Turn around and proceed back to the intersection of Powley Road and Rt. 10, about 10.9 miles.
47.8 Continue north on Rt. 10 about 1.2 miles to the intersection with Rt. 8.
59.9 Turn west onto Rt. 8 and drive 12.1 miles to Moorehouseville.
61.5 Turn north onto Fayle Road, proceed north. Cross a one lane wood bridge and drive to an opening in the trees at the end of Fayle Road. Park and hike to the west about 350 meters to the west end of the small linear hill.

**STOP 5: L>>S and L-tectonite in the core of the Piseco antiform (18T 518563 m E, 4805631 m N)**

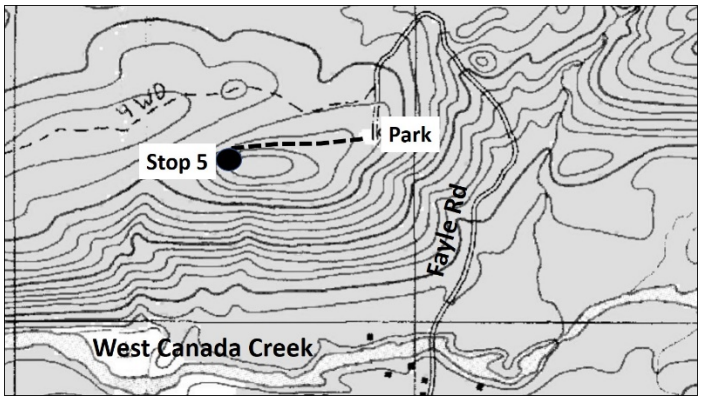


Excellent outcrops on the northwestern side of a small hill just west of the parking area. Follow the dirt road to a path through the woods, and then head up hill to the south to the outcrops. This outcrop of granitic gneiss contains domains of L>S and L>>S. The L>S domains contain large and numerous σ-type shear sense indicators, some δ-type are present but are much less frequent. The porphyroclasts are large about 1-3 cm and the recrystallized porphyroclastic material is often wrapped with a quartz ribbons. The interpreted shear sense is low-angle and left lateral. The foliation strikes east-west and dips gently to the south. Return to the vehicles by

following the path. At this point the trip is over. Retrace your trip to Route 8. If you are headed back to Lake George, then follow Route 8 back to Speculator, NY, then turn south on Route 30.

End of trip.

## ACKNOWLEDGMENTS

We would like to thank the many students and staff of the SUNY Oswego Geology Research Field Program whose field work and research efforts helped make this field trip possible. Special thanks to Damian Piaschyk, Lindsay Williams, Rachel Price and Robert Peterson. Chiarenzelli would like to thank the James S. Street Fund at St. Lawrence University for partial support of the analytical work discussed herein.

## REFERENCES CITED

Baird, G. B., and MacDonald, W. D., 2004. Deformation of the Diana Syenite and Carthage-Colton Mylonite Zone: implications for timing of the Adirondack Lowlands deformation. in Tollo, R. P., Corriveau, L., McLelland, J., and Bartholomew, M. J., eds., Proterozoic Tectonic Evolution of the Grenville Orogen in North America: Geological Society of America Memoir 197, p. 285-297.

Cannon, R.S., Jr., 1937. Geology of the Piseco Lake Quadrangle. New York State Museum Bulletin, no. 312, 107p.

Carr, S.D., Easton, R.M., Jamieson, R.A., and Culshaw, N.G., 2000, Geologic transect across the Grenville orogen of Ontario and New York: Canadian Journal of Earth Sciences, v. 37, p. 193-216.

Chiarenzelli, J., Hudson, M., Dahl, P., and deLorraine, W. D., 2012. Constraints on deposition in the Trans-Adirondack Basin, Northern New York: Composition and origin of the Popple Hill Gneiss: Precambrian Research, v. 214-215, p. 154-171.

Chiarenzelli, J. R., Valentino, D. W., Thern, E., and Regan. S., 2011, The Piseco Lake Shear Zone: A Shawinigan Suture (abstract): Geological Association of Canada, v. 34, p. 40.

Chiarenzelli J., Regan, S., Peck, W., Selleck, B., Baird, G. and Shrady, C., 2010a. Shawinigan Magmatism in the Adirondack Lowlands as a Consequence of Closure of the Trans-Adirondack Back-Arc Basin: Geosphere, v. 6, p. 900-916.

Chiarenzelli, J., Lupulescu, M., Cousens, B., Thern, E., Coffin, L., and Regan, S., 2010b. Enriched Grenvillian Lithospheric Mantle as a Consequence of Long-Lived Subduction Beneath Laurentia: Geology, v. 38, p. 151-154.

Chiarenzelli, J., Valentino, D., and Gates, A., 2000. Sinistral transpression in the Adirondack Highlands during the Ottawan Orogeny: strike-slip faulting in the deep Grenvillian crust. Abstract presented at the Millenium Geoscience Summit GeoCanada 2000, Calgary, Alberta May 29-June 1st.

Dickin, A.P. and McNutt, R.H., 2007, The Central Metasedimentary Belt (Grenville Province) as a failed back-arc rift zone: Nd isotope evidence: Earth and Planetary Science Letters, v. 259, p. 97-106.

Fakundiny, R. H. 1986. Trans-Adirondack Mountains Structural Discontinuities. In Proceedings of the Sixth International Conference on Basement Tectonics, edited by M. J., Jr. Aldrich, and A. W. Laughlin, pp. 64-75. International Basement Tectonics Association, Salt Lake City, Utah.

Fakundiny, R. H., Yang, J., and Grant, N. K. 1994. Tectonic Subdivisions of the Mid-Proterozoic Adirondack Highlands in Northeastern New York: Northeastern Geology, v. 16, p. 82-93.

Gates, A., Valentino, D., Chiarenzelli, J., Solar, G., and Hamilton, M., 2004. Exhumed Himalayan-type syntaxis in the Grenville Orogen, northeastern Laurentia: Journal of Geodynamics, v. 37, p. 337-359.

Geraghty, E. P., Isachsen, Y. W., and Wright, S. F. 1981. Extent and character of the Carthage-Colton mylonite zone, northwest Adirondacks, New York. U.S. Nuclear Regulatory Commission, NUREG/CR-1865, 83 p.

Glennie, J. S., 1973. Stratigraphy, structure, and petrology of the Piseco Dome area, Piseco Lake 15' quadrangle, southern Adirondack Mountains, New York (Ph.D. thesis). Syracuse, New York, Syracuse University, 45 pp.

Hamilton, M.A., McLelland, J.M., and Selleck, B.W., 2004. SHRIMP U/Pb zircon geochronology of the anorthosite-mangerite-charnockite-granite suite, Adirondack Mountains, NY: Ages of emplacement and metamorphism, *in* Tollo, R.P., Corriveau, L., McLelland, J.M., and Bartholomew, M.J., eds., Proterozoic Tectonic Evolution of the Grenville Orogen in North America: Geological Society of America Memoir 197, p. 337–355.

Hanmer, S., Corrigan, D., Pehrsson, S., and Nadeau, L., 2000. SW Grenville Province, Canada: the case against post-1.4 Ga accretionary tectonics: Tectonophysics, v. 319, p. 33-51.

Hawman, R.B. and Phinney, R.A.,1992. Structure of the crust and upper mantle beneath the great valley Allegheny Plateau of eastern Pennsylvania, 1, Comparison of linear inversion methods for sparse wide-angle reflection data, Journal of Geophysical Research, v. 97, p. 371–391.

Hecklau, S., MacKenzie, K., and Chiarenzelli, J., 2014. Geological investigation of Bennies Brook Landslide, Lower Wolfjaw Mountain, Adirondack High Peaks Region (abstract): NE Geological Society of America Abstracts with Programs, v. 46, p. xx.

Heumann, M.J., Bickford, M.E., Hill, B.M., McLelland, J.M., Selleck, B.W., and Jercinovic, M.J., 2006. Timing of anatexis in metapelites from the Adirondack lowlands and southern highlands: A manifestation of the Shawinigan orogeny and subsequent anorthosite-mangerite-charnockite-granite magmatism: Geological Society of America Bulletin, v. 118, p. 1283-1298.

McLelland, J. M., 1984. Origin of ribbon lineation within the Southern Adirondacks, U.S.A.: Journal of Structural Geology, v. 6, p. 147-157.

McLelland, J. and Chiarenzelli, J., 1989. Age of a xenolith-bearing olivine metagabbro, Eastern Adirondack Mountains, New York. Journal of Geology, v. 97, p. 373-376.

McLelland, J. M. and Chiarenzelli, J. R., 1990. Geochronological studies of the Adirondack Mountains, and the implications of a Middle Proterozoic tonalite suite, *in* Gower, C., Rivers, T., and Ryan, C., eds., Mid-Proterozoic Laurentia-Baltica: Geological Association of Canada Special Paper 38, p. 175-194.

McLelland, J. and Isachsen, Y., 1986, Geologic synthesis of the Adirondack Mountains and their tectonic setting within the Grenville of Canada, *in* Moore, J., Baer, A., and Davidson, A., eds., The Grenville Province: Geological Association of Canada Special Paper 31, p. 75–95.

McLelland, J.M., Selleck, B.W., and Bickford, M.E., 2010. Review of the Proterozoic evolution of the Grenville Province, its Adirondack outlier, and the Mesoproterozoic inliers of the Appalachians, *in* Tollo, R.P., Bartholomew, M.J., Hibbard, J.P., and Karabinos, P.M., eds., From Rodinia to Pangea: The Lithotectonic Record of the Appalachian Region: Geological Society of America Memoir 206, p. 1–29.

McLelland, J., Chiarenzelli, J., Whitney, P., and Isachsen, Y., 1988. U-Pb zircon geochronology of the Adirondack Mountains and implications for their geologic evolution: Geology, v. 16, p. 920-924.

Meighan, H. E., Pulliam, J., Brink, U., Lopez-Venegas, A. M., 2013. Seismic evidence for a slab tear at the Puerto Rico trench, Journal of Geophysical Research: Solid Earth, v. 118, iss. 6, p. 2915-2923.

Meighan, H. E. and Pulliam, J., 2013. Seismic anisotropy beneath the northeastern Caribbean: implications for subducting North American lithosphere, Bulletin de la Societe Geologique de France, v. 184, Iss. 1-2, p. 67-76.

Peck, W., Selleck, B., Wong, M., Chiarenzelli, J., Harpp, K., Hollocher, K., Lackey, J., Catalano, J., Regan, S., and Stocker, A., 2013. Orogenic to post-orogenic (1.20–1.15 Ga) magmatism in the Adirondack Lowlands and Frontenac terrane, southern Grenville Province, USA and Canada: Geosphere, v. 9, p. 1637-1663.

Peck W. H, Valley J. W., Corriveau L., Davidson A., McLelland J., and Farber, D.A ., 2004, Oxygen-isotope constraints on terrane boundaries and origin of 1.18-1.13Ga granitoids in the southern Grenville Province. *in* Proterozoic tectonic evolution of the Grenville orogen in North America, Tollo RP, Corriveau L, McLelland J, and Bartholomew MJ, eds.: Boulder, Colorado, Geological Society of America Memoir 197, p. 163-182.

Piaschyk, D., Valentino, D.W., and Solar, G.S., 2005. Variations in L- and S-tectonite on the northern boundary of the Piseco Lake shear zone, western Adirondack mountains, New York. *in* Valentino, D.W. (ed.), Guidebook for Field Trips for the Annual Meeting of the New York State Geological Association, v. 77**,** Trip B2, 20p.

Price, R., Valentino, D., Solar, G., and Chiarenzelli, J., 2003. Greenschist facies metamorphism associated with the Piseco Lake shear zone, Central Adirondacks, New York (abstract): Northeast Geological Society of America Abstract with Programs, Halifax, Nova Scotia, v. 35, p. 22.

Rankin,D.W.,1976. Appalachian salient and recesses: late Precambrian break-up and the opening of the Iapetus Ocean, Journal of Geophysical Research, v. 81, p. 5605–5619.

Regan, S.P., Chiarenzelli, J.R., McLelland, J.M., and Cousens, B.L., 2011. Evidence for an enriched asthenospheric source for coronitic metagabbros in the Adirondack Highlands: Geosphere, v. 7, no. 3, p. 694-709.

Rivers, T., 2008. Assembly and preservation of lower, mid, and upper orogenic crust in the Grenville Province – Implications for the evolution of large hot long-duration orogens: Precambrian Research, v. 167, p. 237-259.
Rivers, T. and Corrigan, D., 2000, Convergent margin on southeastern Laurentia during the Mesoproterozoic: tectonic implications: Canadian Journal of Earth Sciences, v. 37, p. 359-383.

Roden-Tice, M. K. and Tice, S. J., 2005. Regional-scale mid-Jurassic to Late Cretaceous unroofing from the Adirondack Mountains through central New England based on apatite fission-track and (U-Th)/He thermochronology: Journal of Geology, v. 113, p. 535-552.

Selleck, B.W., McLelland, J.M., and Bickford, M.E., 2005. Granite emplacement during tectonic exhumation: The Adirondack example: Journal of Geology, v. 33, p. 781-784.

Steltenpohl, M. G., Zitez, I., Horton, J. W., Jr., and Daniels, D. L., 2010. New York-Alabama lineament: A buried right-slip fault bordering the Appalachains and mid-continent North America, Geology, v. p. 38, no. 6, p. 571-574.

United State Geological Survey, 2017. Magnetic Anomaly Maps and Data for North America, Mineral Resources Online Spatial Data, https://mrdata.usgs.gov/magnetic/

Valentino, D., Chiarenzelli, J., Hewitt, E., and Valentino, J., 2012. Applications of water-based magnetic gradiometry to assess the geometry and displacement for concealed faults in the southern Adirondacks Mountains, New York, U.S.A.: Journal of Applied Geophysics, v. 76, p. 109-126.

Valentino, D., Chiarenzelli, J., Paaschyk, D., Williams, L., and Peterson, R., 2008. The Southern Adirondack Sinistral Transpressive Shear System: *in* Friends of the Grenville (FOG) Field Trip 2008, D. Valentino and J. Chiarenzelli (eds.), September 28th, Indian Lake, New York, 56p.

Valentino, D. W., Chiarenzelli, J. R. and Regan, S., in press. Spatial and temporal links between Shawinigan accretionary orogenesis and massif anorthosite intrusion, southern Grenville province, New York, U.S.A., Journal of Geodynamics.

Wiener, R.W., 1983. Adirondack Highlands-Northwest Lowlands 'boundary': A multiply folded intrusive contact with associated mylonitization: Geological Society of America Bulletin, v. 94, p. 1081-1108.

Wong, M. S., Peck, W. H., Selleck, B. W., Catalano, J. P., Hochman, S. D., and Maurer, J. T., 2011, The Black Lake shear zone: A boundary between terranes in the Adirondack Lowlands, Grenville Province, Precambrian Research, v. 188, p. 57-72.

# FAULT SYSTEMS OF THE TACONIC FORELAND; WHITEHALL, NY TO WEST HAVEN, VERMONT [ALL KINDS OF FAULTS!]

William S.F. Kidd, formerly of Geological Sciences, University at Albany, Albany, NY 12222
Stephen S. Howe, Atmos. & Environmental Sciences, University at Albany, Albany, NY 12222
Chul Lim, formerly of Geological Sciences, University at Albany, Albany, NY 12222
Email address: wkidd@albany.edu

## INTRODUCTION AND SUMMARY

Map-influencing faults of all displacement kinds are observed in the anomalously narrow Taconic orogenic foreland belt in the region where it crosses the New York - Vermont border between Whitehall, NY and West Haven, VT. Outcrop and map evidence for the relative age and displacement of these faults can be seen on this trip. In general, transported Cambro-Ordovician rocks of the continental shelf/platform and of the off-shelf strata in the Taconic Allochthon are affected by thrust faults of a range of ages relative to development of folding and cleavage in particular rock packages. The thrusts all predate large-scale strike-parallel east-side-down normal faulting, in most places in the area to be visited apparently localised, in a large displacement (1000m or more), on one such fault, the Mettawee River Fault. The youngest of the fault sets consist of cross-strike, strike-slip faults, mostly ENE- to NE-trending, some of which have mappable apparent left-lateral displacement, cutting thrusts and the normal fault. Movement on the strike-slip fault system at West Haven was accompanied in this area by fluids shown by our measurements of fluid inclusion homogenization to have been at temperatures sufficiently high to be most likely of Ordovician (Taconic) age. These oblique faults probably had a prior history as components of a trench forebulge normal fault system; they may have influenced at that time and perhaps also earlier the sedimentation on the Laurentian continental shelf, and therefore they may have been localised by an old inherited fracture/fault system in the underlying Grenville basement of this area. More generally, forebulge normal fault scarp topography, whose development mostly predated thrust arrival at any position, are perhaps also responsible for the repeated detachment and stacking of thin slices of the medial Ordovician limestones of the uppermost carbonate shelf which are extensively developed in the area of this field trip. The lower contacts of these slices show evidence of thrust fault transport, and do not support a model of large-scale olistostromal origin. Because the trip is confined to the area affected by thrusts, we will not see unmodified forebulge-type normal faults in autochthonous basement and platform strata, but they occur just to the west along southernmost Lake Champlain. And there are other kinds of fault affecting geological maps of the area which may be mentioned during the trip.

## STRATIGRAPHIC CONSIDERATIONS

The stratigraphy defined in the autochthonous Cambro-Ordovician shelf strata near Whitehall (Fisher, 1985) includes: basal clastics (Potsdam sandstone, Ticonderoga dolomitic sandstone); massive dolostones (Whitehall formation, which include a limestone unit, Warner Hill limestone); a second sequence of mixed carbonate and clastic units (Great Meadows formation; which includes Winchell Creek arenite/siltstone, Fort Edward dolostone, & Smiths Basin limestone); a second mostly dolostone unit (Fort Ann formation; which includes many impersistent thin limestones); and a second sequence of mixed carbonates and clastics (Fort Cassin formation; which includes the Ward siltstone, Sciota limestone, & the Providence Island dolostone). The more distinctive of the lithic units are readily mappable and traceable in the gently-dipping section of autochthonous strata along the whole length of the area of this field trip.

In the transported Champlain system thrust sheets, however, things are not so readily separated. Hayman & Kidd, (2002a) maintained, and we agree, that the stratigraphy to use within the Champlain system thrust sheets is best kept simple – a basal quartzite, an overlying dolomitic section, capped by a Chazy and younger limestone section. The middle of this simple sandwich largely contains massive (and monotonous) dolostones; very locally in Vermont, distinctive units (a thin (<10 meters) limestone, and a siltstone horizon) can be found within them. This massive dolostone with a few discontinuous and thin limestone horizons, in the Shoreham Thrust sheet in the area of the field trip, must be a distal facies of some part of the autochthonous succession near Whitehall. We call this the Providence Island facies as almost all of it most closely resembles descriptions of the Providence Island unit in the

Whitehall succession, but we do not mean to imply any age constraint by this purely lithostratigraphic label. Only the base of the Pinnacle Thrust sheet is seen north of the latitude of Whitehall in the area of the trip, and it consists of quartzites and dolostones equivalent to part of the Potsdam, and perhaps of the Ticonderoga units of the Whitehall autochthonous strata.

Taconic units of the northern Allochthon in the area of the field trip are all slates with exceptions for arenites contained in the Hatch Hill, thicker limestone breccias and an arenite of the Browns Pond, and cherts of the Mt Merino.

The medial Ordovician grey shales and silty shales of the area are an orogenic flysch deposit; syn-orogenic clastic materials shed from the active Taconic orogen to the east. In the area of the field trip, coarser clastic materials are quite uncommon, compared with the area around Albany and farther south. Most of the material to be seen on this trip, deposited originally over subsiding shelf rocks, was deformed by overriding thrust sheets, and transported to some (unknown) extent; much of it is now melange in the sense it contains a characteristic pervasive lenticular fracturing/"cleavage", termed phacoidal by some. The exception is in the northern area of the trip, around West Haven, where well-cleaved grey slates with silty laminae in places outcrop extensively, and are called Hortonville (Zen, 1967); these are probably a lithological equivalent to the medial Ordovician grey shale and melange farther south. We think from their structural condition that they should be regarded as a (western) part of the Taconic Allochthon, and that they are likely to have been significantly thrust-transported.

## SOME ASPECTS OF THE FAULT SYSTEMS AND TECTONIC SETTING

This field trip visits outcrops of the Champlain thrust system which was responsible for large (>80 km) thrust transport of the shelf section carried by it around Burlington; the thrust system projects to depth and thus is dynamically related to the overlying Taconic thrusts, and collectively forms a decollement beneath the Green Mountain crystalline core of the Taconic orogen (Rowley, 1982).

The Cambrian-early Ordovician strata of the Taconic Allochthon were first identified by Bird and Dewey (1970) as continental rise and middle Ordovician foredeep sedimentary facies, with refinements placing them in the setting of an island arc-passive continental margin collision made by subsequent work (Rowley et al., 1979; Rowley and Kidd, 1981; Bosworth and Rowley, 1984). This requires a restoration of these rocks to their depositional site as far-traveled tectonically rooted thrusts such as are found in modern arc-continent collisions (Rowley and Kidd, 1981). A more recent contribution (MacDonald et al 2017) proposes that the western margin of the Taconic orogen is merely a rear-arc fold-thrust belt, consequent on older subduction/collision event(s) farther east.

The simplest model of such a foreland thrust system predicts a forward-propagating system where thrusts young to the west. However, relationships of thrusts found in the Taconic foreland require at least some late deformation (Zen, 1972; Rowley and Kidd, 1981; Stanley and Ratcliffe, 1985). One explanation for late deformation derives from observations of outcrop structures, fabrics, and map patterns in the Taconic foreland requiring at least one out-of-sequence thrust towards the front of the Taconic thrust system. This thrust was (perhaps awkwardly) named the Taconic Frontal Thrust due to its position at the western front of the Taconic Allochthon near Whitehall, NY (Bosworth et al., 1988).

The Taconic Frontal Thrust cuts the Taconic Basal Thrust, the thrust responsible for the initial transport of the rise-facies Taconic sequence (Bosworth and Rowley, 1984). Most of the deformational patterns at both the outcrop and map scale can be explained with this model of Middle Ordovician forward propagating thrusting, with a component of out-of-sequence thrusting, the latter perhaps in part of the Acadian rather than the Taconic orogenic event (Zen, 1972; Hames et al., 1991; Chan and Crespi, 2001).

A key structure in understanding the geology of the exceptionally narrow Taconic thrust belt in the area of this field trip is the Mettawee River Fault, first recognised by Fisher (1985), a late strike-parallel eastward-downthrow normal fault that significantly truncates all the thrusts of the Champlain Thrust system. A consequence of the Mettawee River Fault is that it eliminates Champlain thrust slices from map view, by an amount which varies along its trace (Fig 1). Evidence for normal faulting and inferences of its age found by Lim et al (2005) in the Taconic thrust melange belt and on the frontal Taconic fault near Troy, NY suggests that these, and the Mettawee River

Fault, are more probably Ordovician (Taconic) rather than Acadian structures. Lim and Kidd (2008) suggested the change to extension from shortening was a result of a propagating breakoff of the subducted lithospheric slab.

The middle Ordovician outer trench slope was the site of normal faulting, between the synconvergence flexural forebulge and the trench (Cisne et al, 1982; Bradley and Kusky, 1985; Bradley and Kidd, 1991). Hayman and Kidd, (2002a,b) proposed that these prethrusting faults localised many of the along- and across- strike lithic unit changes within the Champlain system thrust sheets. On this trip, faults of this origin (near West Haven) are inferred to have interacted with at least one thrust of the Champlain thrust system, but subsequent components of both strike-slip and dip-slip displacement on the oblique faults have further complicated the relationships.

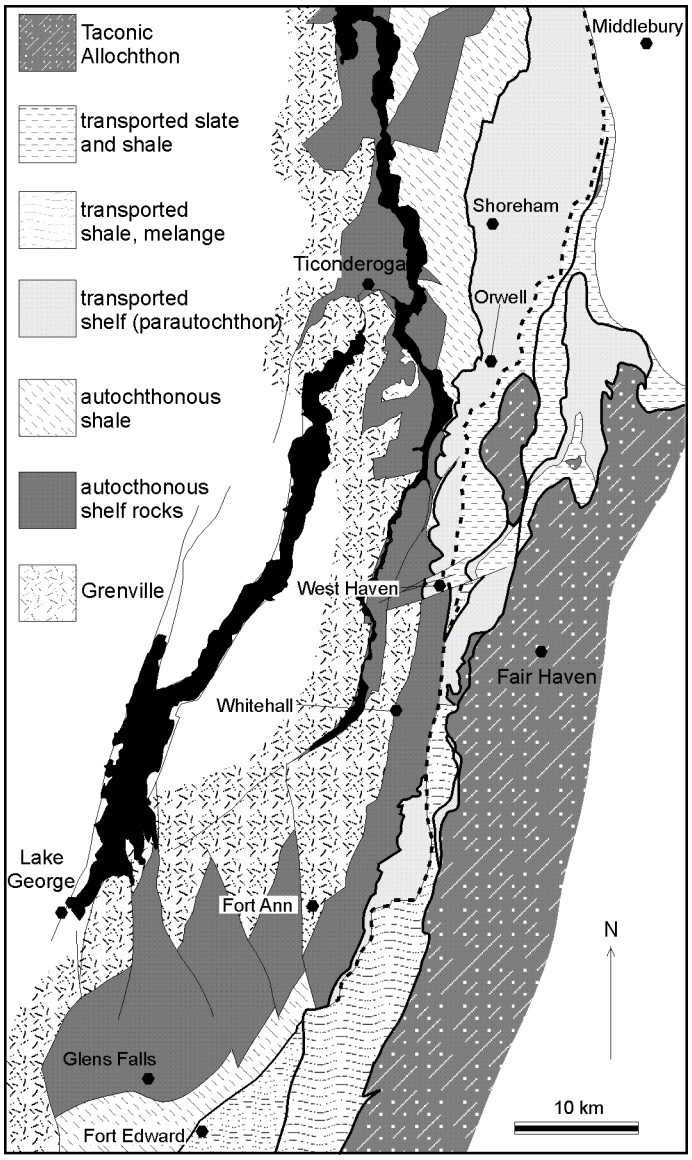


Figure 1. Regional map of west-central Vermont to the upper Hudson River valley of New York illustrating the trace (thicker lines) of the Champlain thrust system. The Mettawee River Fault (thick dashed line) places deformed and low grade metamorphosed shale and flysch, and to the north of Whitehall, imbricated upper shelf carbonates, against the transported shelf (parautochthon). South of the disappearance of the transported shelf, the western thrusts of the Champlain thrust system climb into the melange belts of the Hudson Valley flysch and melange (Kidd et al, 1995); it is unclear exactly where in this belt the trace of the Mettawee River Fault runs. Diagram modifed from Hayman & Kidd (2002a).

## VEIN FLUID INCLUSIONS AND FLUID TEMPERATURES

Fluid inclusions in veins associated with faults can give information about the contemporary fluid temperatures, and may constrain the possible source(s) of the fluids from which the veins grew. The temperature information, in the absence of geochronological data, may also permit a constraint to be placed on the age of the veins and the associated faulting. Lim et al (2005) reported on the structural history and fluid inclusions of calcite and quartz-calcite veins associated with thrust and later cross-cutting but strike-parallel normal sense faults in the Ordovician melange west of the Taconic Allochthon (see Fig. 2). In the NY Capital Region near Albany, both the thrust and the younger normal-sense veins have fluid homogenization temperature ranges (280-190C) significantly higher than those in nearby Devonian Helderberg Limestones affected by Acadian thrusts (most are 130-100C, max. 170C). The inference is that the veins and associated faults in the Ordovician melange of the NY Capital Region, including those immediately adjacent to the western bounding fault of the Taconic Allochthon, are all Ordovician-age structures. The absence of any original normal-sense veins cutting thrusts in the Helderberg thrust belt tends to support this interpretation. All inclusions from veins in the Ordovician melange have low salinity, consistent with a metamorphic fluid source at greater depth down-dip to the east in or under the Taconic thrust prism.

Only thrust sense veins were observed and sampled in Ordovician melange north of the NY Capital Region, and these show (Fig. 2) somewhat lower homogenization temperature ranges, apparently declining to the north, to about 190-220C at the Mettawee River locality of Stop 1A of this trip, and to about 150-210C in the slates adjacent to the Mettawee River Fault exposed near West Haven at stop 6B of this trip. Note that these are still well above the typical 100-130C homogenization temperatures found in samples from the Acadian Helderberg thrust belt near Albany.

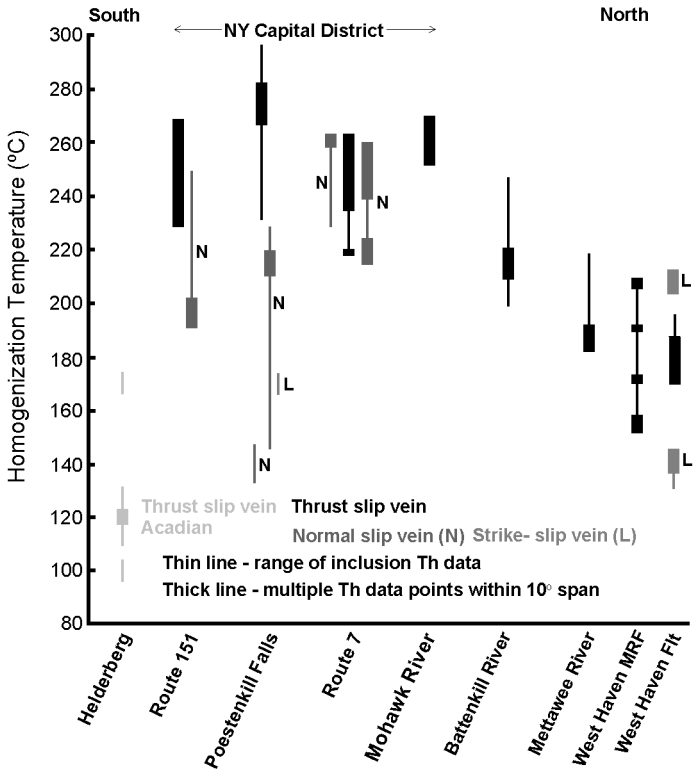


Figure 2. Fluid inclusion homogenization temperature ranges for veins of the Taconic foreland thrust belt, mostly from Ordovician melange. Thrust-sense veins shown black; normal-sense veins shown dark grey (N); strike-slip left lateral veins shown medium-grey (L). Compiled from data in Lim et al (2005), with addition of West Haven Fault.

After finding the outcrop at West Haven (stop 7A of this trip) where N-S striking probable thrust-sense calcite veins in the limestone are offset by ~E-W left-lateral strike-slip veins, we sampled these, and measured fluid inclusion homogenization temperatures. The summarised results are included in Fig 2, and temperatures for the older veins of 170-195C fall within in the range found for thrust-sense veins nearby in the outcrop of stop 6B. Temperatures for the cross-cutting strike-slip veins yielded two groups of restricted temperature ranges, with two different samples having homogenization temperatures ~205-215C, and one other sample ~135-145C. Interpretation of the lower temperature range might be that it is from younger vein growth after introduced hot fluids had cooled; or that they are secondary inclusions formed after the rocks had cooled significantly. However, the higher range above 200C found in two samples, which we suggest constrains the initial fluid temperature along the strike-slip fractures, we think is good, or at least suggestive evidence that these veins are Ordovician. Although we do not have measurements from veins of normal sense outside the NY Capital Region, we do observe that the Mettawee River normal Fault cuts all thrusts of the Champlain Thrust system, in the area of this field trip. The WSW-ENE strike-slip faults cut the Mettawee River Fault (Fig 8; stops 6B, 7C), so we suggest that all faults seen on this trip, including these, are Ordovician (and Taconic) structures.

## ACKNOWLEGEMENTS

Parts of this field guide and some of the stops visited are derived from text and figures in Bosworth and Kidd (1985) - for stops 1A, 1B, 4, and 5; some other parts derive from text and figures in Hayman and Kidd (2002a) - for stops 1A and 6A and 6B; the material descriptions for the other stops are new.

Detailed geological mapping that contributes to understanding of this area and the fault structures in it can be found in several theses and dissertations completed in the Geological Sciences at SUNY Albany; Louise (Delano) Jacobi (1977); David Rowley (1979, 1983); Christof Steinhardt (1983); Jennifer Granducci (1995); Nick Hayman (1997), as well as unpublished maps by Pan Yun and Ed Rodgers. In addition, undergraduate students participating in the Albany field mapping course over many years helped by locating outcrops and in identifying some key localities. Maps made by Steve Tice and John Moss near Whitehall were particularly helpful, and participants in the course in 1998-2001, 2005 and 2006 helped in untangling the geology nearer West Haven. Permission by numerous landowners to enter their properties is greatly appreciated and in particular the owners of the Book Farm are thanked for allowing numerous visits over many years. The current owners of Coggman Creek Farm at West Haven are also thanked for permitting us to drill samples from the unique outcrop near their house.

## ROAD LOG AND STOP DESCRIPTIONS

**Assembly Point** – Fort William Henry parking lot, Lake George Village, Saturday, 13th October, 2018, 8.30 am. If more convenient to meet at Stop 1, arrive there no later than 9am.

### MILEAGE

| Miles | Incr. | Directions |
|---|---|---|
| 0.0 | 0.0 | Intersection US Rte 9 and NY Rte 149 about 4 miles south of Lake George Village NY. Go east on Rte 149. |
| 11.7 | 11.7 | Intersection NY Rte 149 and US Rte 4, Fort Ann NY; turn left onto Rte 4 northbound. |
| 15.5 | 3.8 | Intersection (with light) US Rte 4 and NY Rte 22 at Comstock NY; turn right onto Rte 22. |
| 19.7 | 4.2 | Intersection NY Rte 22 and NY Rte 40 (to right); Sheehan Rd Ext (to left); turn left. |
| 19.9 | 0.2 | Go 0.2 mile to end of Sheehan Rd Ext; intersection with Grey Goose Rd and Upper Turnpike; turn part left onto Upper Turnpike. |
| 20.9 | 1.0 | Go 1.0 miles to gravel parking area on right [43.470907, -73.369207] - **Stop 1** |
| | | Walk down the path from the center of the east side of the parking area to the outcrop at the river [43.471240, -73.368354]. |

**Caution - If wet, the path down can be slippery since it passes through well-rounded fluvial pebble gravel and underlying lake clays; the sloping bedding surfaces of the carbonate outcrops at this locality can also be treacherous in places. Poison ivy occurs here**

## STOP 1A: METTAWEE RIVER FAULT AT THE TYPE LOCALITY

[NO HAMMERS OR SAMPLING PLEASE - NY DEC REGULATIONS]

The carbonates here along the west bank of the river are mapped by Fisher (1985) as early Ordovician Providence Island Formation, and dip about 10-20 degrees east; they are the upper part of a thrust-transported section above the Comstock (= Pinnacle) Thrust. The lowest part of the section here consists of dolostones; the upper 4 meters contains limestone beds; we think it is possible that the part of the section containing limestones is either basal Chazy or Black River. These show some bedding surfaces with well-developed ripples, and small mudcracks, and selectively dolomitized burrows. Local meter-scale folding of periclinal geometry affects these beds near this end of the section. Across the river at this point, you can see the dark mid-Ordovician non-calcareous shales which are there partly disrupted with phacoidal melange-type fabric. In the low cliff, a gently east-dipping planar vein of fibrous quartz cuts the deformed shales; the vein has top to west, thrust sense of shear. Walk north along the west bank of the Mettawee River on the mostly dolostone outcrop. About 170 meters north [43.473241; -73.368196], dark highly deformed mid-Ordovician shales extend from the east bank across the river to an almost complete section at the small rapids. Depending on the streamflow, it may or may not not be possible to examine the shale closely. The contact of the deformed shale with the dolostone beds at the west side of the stream is not quite fully exposed (even at the lowest water we have seen, there is a gap of 10 cm or so), but is clearly sharp, and parallel with bedding in the dolostones. This is somewhat surprising, for a contact which maps out a short distance to the north as a sharp fault that unquestionably truncates this and other lower units of the carbonate shelf stratigraphy, as well as the major thrust fault which duplicates this sequence (see the map of Fisher, 1985). Also surprising, for a fault that must have substantial normal sense displacement, is the fact that most or all quartz fiber slickensides in the shale here give thrust sense of displacement. We could infer either that the normal fault mapped to the north passes east of this outcrop within the shale belt, or west within the transported shelf carbonate section (of course badly exposed in that particular place), or that the motion is confined to a surprisingly narrow zone along the contact; the full exposure at Stop 6B suggests the latter possibility is more likely than one might be inclined to think based on this outcrop at Stop 11 alone.

Walk back to the south end of the carbonate outcrop on the west bank of the river [43.471240, -73.368354]. If the water is high or it is raining, Stop 1B will be omitted. If conditions permit, scramble along the west bank to the south, and through the scrub along the west side of the old mill race cut at the waterfall, then walk south along the west bank of the river for about 1 km.

## STOP 1B: DEFORMED FLYSCH AND MELANGE BELOW CONTACT WITH TRANSPORTED CHAZYAN SHELF CARBONATES, IN THE BANKS OF THE METTAWEE RIVER

The Mettawee River here provides a superb series of exposures (location in Fig 3) that cross from parautochthonous shelf carbonates (mostly dolostones) at the access point, south past the waterfall (43.470990; -73.367826) through alternating zones of flysch-type dark shales, and shale melange, to a large sliver of Chazyan carbonate (mostly limestones, starting at 43.462450; -73.362534) (Fig. 3). The eastern part of the carbonate sliver is poorly exposed in the river, but mapping demonstrates that this fault contact (the Taconic Frontal Fault) cuts obliquely across Taconic stratigraphy and large-scale fold axial traces, and is therefore a post-slaty cleavage generation structure (Fig. 3).

The allochthonous carbonate at this locality and along the western edge of the Allochthon in general has been interpreted and shown on a published map by Fisher (1985) as blocks-in-shale (i.e., olistoliths) rather than as coherent fault slivers. This locality (and stop 5) provide excellent examples to test these two alternative hypotheses. The carbonate/melange contact exposed in the woods across the river here can be walked for nearly 2 kilometers as a continuous, unbroken structure along strike, with internal fold axes in the carbonates approximately parallel to the general contact trend (Selleck and Bosworth, 1985, Plate 1A).

The carbonate must be in the form of a large, probably composite sheet. Minor secondary disruption near its margins is undoubtedly present (of structural and perhaps sedimentary causes), but we maintain that the origin of this and other km-(length)-scale carbonate sheets adjacent to the Allochthon was by detachment of thin slices from the top part of the underthrusting shelf rocks and their incorporation to and imbrication at the base of the advancing thrust pile. We think based on our mapping of all this belt north to West Haven that it is highly misleading to describe the geometry of the large carbonate bodies along the western edge of the Allochthon as "blocks-in-shale", and that it is most unlikely that they arose as primary sedimentary slump features (further discussed in Rowley and Kidd, 1982).

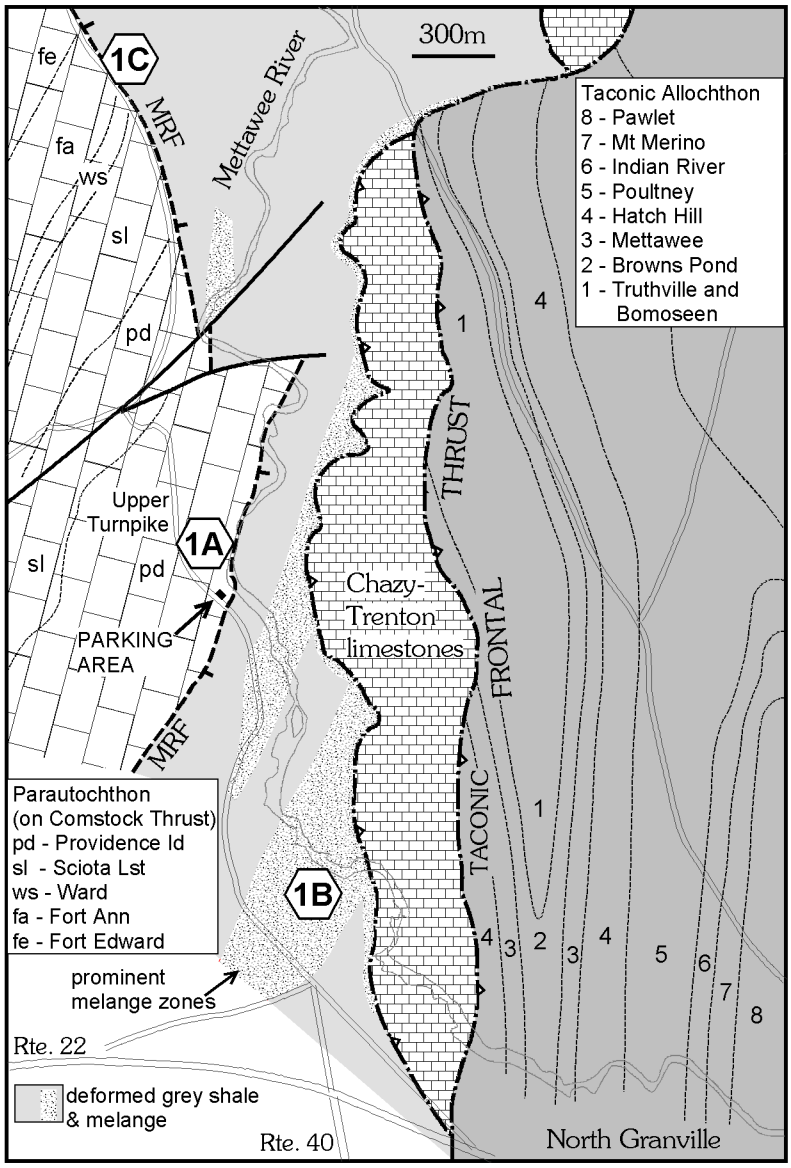


Figure 3. Geological map of the vicinity of the Taconic Frontal Thrust near the Mettawee River northwest of North Granville, NY, showing locations of stops 1A, 1B, and 1C. Geology modified after Selleck and Bosworth (1985); units in the parautochthonous shelf from Fisher (1985).

Walk back to the parking area.

22.3 1.4 Turn right out of parking area, go north 1.4 miles on Upper Turnpike, park on right side of road where it reaches its highest point [43.489336, -73.375452] - **Stop 1C**.

***Please stay on the road and its margins; we do NOT have permission to enter the field or woods here***

**STOP 1C: METTAWEE RIVER FAULT ALONG UPPER TURNPIKE**

Two outcrops of shale melange occur a short distance into the field to the east, where outcrop on the west side of the road and into the woods adjacent exposes dolostones of the Cambro-Ordovician shelf (here Fort Ann Fm according to Fisher, 1985; see Fig. 3). These outcrops demonstrate the existence of the Mettawee River Fault as an east side down normal fault and closely constrain its position.

| | | |
|---|---|---|
| 24.3 | 2.0 | Continue another 2.0 miles on Upper Turnpike, park on right side of road about 150 meters before a low point in the road and a sharp left curve just beyond<br>[43.515749, -73.382460] - **Stop 2** |

**STOP 2: POTSDAM/TICONDEROGA ARENITES AND THE COMSTOCK (PINNACLE) THRUST.**

In low roadside exposure on the west side of the road gently-dipping Upper Cambrian sandstones can be seen, mapped by Fisher (1985) as Ticonderoga and upper Potsdam Formations. The map shows they can be systematically traced for 9 kilometers to the south and, for a shorter distance, to the northeast of this place. Along with the overlying carbonate shelf sequence they demonstrate a major thrust duplication of almost the whole thickness of the local Cambro-Ordovician continental shallow marine platform/shelf sequence. The thrust carrying these strata was termed the Comstock Thrust by Fisher (1985); it climbs rapidly at a lateral ramp 9 km south of this locality (see Fig. 4, and Hayman & Kidd, 2002a; Stop 12) and can be traced a further 11 km carrying limestones of the uppermost part of the Ordovician shelf sequence before it climbs again, into the shale-melange belt, near Smiths Basin.

This small outcrop is not photogenic, and the thrust itself is not exposed here (exposures of it have been found in the woods to the west and southwest), but the map demonstrates its reality, and also that it and the sheet of shelf strata it carries are cut and truncated by the Mettawee River Fault (normal, east side down). Limestones of medial Ordovician age form a low outcrop at the sharp corner in the road to the north, and a larger outcrop on the other side beyond, and are shown by Fisher as Isle La Motte Formation (= Middlebury limestones) and form the foot wall of the Comstock Thrust here. It is probable that the original thrust relationship has been modified at this location by a later ENE-trending fault, but this does not significantly change the basic overthrust relationship.

Hayman & Kidd (2002a, b) provide reasons why this thrust should be specifically identified structurally as the southern extension of the Pinnacle Thrust exposed near Shoreham VT, but it is also helpful to understand that this thrust is the lowest (westernmost) thrust of the overall Champlain Thrust system in this area from Whitehall south to Fort Ann; lower components seen in Vermont (Shoreham Thrust; Main Champlain Thrust) die out southward with their displacements transferred upward along lateral ramps.

| | | |
|---|---|---|
| 26.3 | 2.0 | Continue on Upper Turnpike (at 1.7 miles cross Mettawee River bridge) to intersection with Washington Co. Rte 12, stop sign, turn right. |
| 27.4 | 1.1 | Go 1.1 miles on Rte 12 to intersection with Beckett Road, turn left. |
| 29.0 | 1.6 | Go to intersection with stop sign at Washington Co. Rte 18; turn left (watch out for fast traffic from either direction). |
| 29.3 | 0.3 | Go about 0.25 mile - park on right [43.538499, -73.347383] - take care not to get mired in the ditch; turn on hazard flashers; watch for fast traffic before exiting vehicle;<br>walk about 150m west to roadside outcrop on north side [43.539244, -73.348779] - **Stop 3**. |

**Warning - poison ivy occurs on this outcrop, and most abundantly in the road verge in front of it**

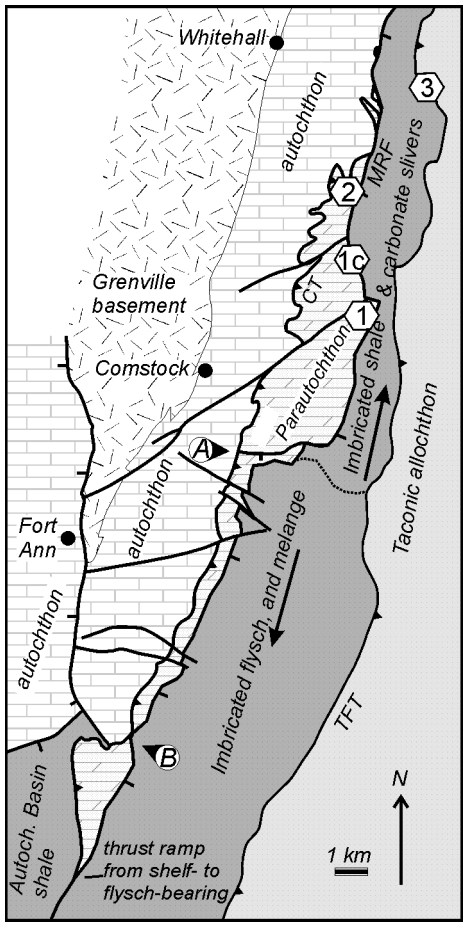


Figure 4. Geological map of the Taconic foreland between Smith's Basin and Whitehall, NY, showing locations of stops 1, 2, and 3, and the trace of thrusts and normal faults between the Taconic frontal thrust (TFT) and the autochthonous Cambro-Ordovician shelf sequence. At the points marked with labeled triangles, the westernmost thrust of the Champlain system (Comstock Thrust - CT) climbs section abruptly (A), and changes footwall lithology (B), across faults with normal sense slip prior to thrusting. MRF - Mettawee River (normal) Fault. Geology modified after compilation by Fisher (1985); diagram from Hayman and Kidd (2002a).

## STOP 3: FRONTAL FAULT OF THE TACONIC ALLOCHTHON AS A POST-CLEAVAGE THRUST

This outcrop (location shown on Fig. 4) is one of a very few places where the western fault contact of rocks of the main Taconic Allochthon is fully exposed; you will see three of them on this field trip. The roadcut exposes cleaved arenites and siltstones belonging to the early Cambrian/latest preCambrian Bomoseen unit of the Taconic Allochthon stratigraphy (a member of the Bull Fm. of Zen, 1967). A gently east-dipping fault contact on a meter or less thickness of dark phacoidal melange-fabric shale is present, although it may require a small amount of digging to complete the exposure. Below the shale, fine-grained medial Ordovician limestones (Glens Falls/Orwell) dipping gently eastward form the western part of the outcrop. The limestones map as a thin (c.10m.) slice above a much larger thickness of medial Ordovician shale and shale melange exposed to the west. This is the same relationship inferred in the Mettawee River section at Stop 1B, although there a different and younger Taconic rock unit locally maps adjacent to the fault. Note that the cleavage in the Bomoseen dips moderately to steeply east and must be truncated by the more gently east-dipping fault. This relationship is consistent with the oblique truncation of map-scale tight-isoclinal folds and their axial traces at the fault in this region, folds to which this cleavage is an axial surface fabric. Bomoseen arenites and siltstones are typically greenish chloritic colours, but in this

exposure they are grey to dark grey, particularly near the fault contact with dark medial Ordovician shales affected by phacoidal melange-fabric cleavage. We think that fluid hydrocarbons migrating in the fault channel while it was active penetrated into the lowest Taconic rocks here and (now dehydrogenated carbon) are the cause of the colour difference. The low-angle attitude of the fault exposed here (and shown by local detailed mapping into the stream just to the north) suggests it is a thrust.

Near Troy, NY, in the gorge of the Poestenkill, sense of shear evidence suggests that the more steeply-dipping fault exposed there is an east-side-downthrown normal fault which has cut and displaced the original Taconic thrust contact (Lim & Kidd, 2008). Similarly, a large roadcut on NY route 9G west of Hudson, NY exposes a sharp vertical fault contact that is also probably a normal fault. Such post-thrust normal faulting is also seen in calcite veins developed within the Ordovician melange terrain of the NY Capital District (Lim et al, 2005), and in the Mettawee River Fault seen at stops 1, 6B, and 7C on this trip (the trace of which projects well to the west of this locality; see Fig. 4). In this outcrop and more generally in the northern part, however, we think that an older thrust relationship is preserved at the western margin of the Taconic Allochthon, with the transport at this place being post-folding and cleavage development in the Taconic Allochthon strata.

| | | |
|---|---|---|
| 29.7 | 0.4 | Continue west for 0.4 mile on Washington Co. Rte 18 to intersection with Beckwith Road; turn right. |
| 30.7 | 1.0 | Go to stop sign at intersection with US Rte 4; cross over (very carefully - fast traffic) onto Washington Co. Rte 9B. |
| 31.2 | 0.5 | Go to intersection at stop sign with Washington Co. Rte 9. Turn left. |
| 31.4 | 0.2 | About 0.1 mile cross railroad tracks; at 0.2 mile turn right onto Carlton Road at triangular intersection. |
| 32.1 | 0.7 | Go about 0.7 mile and park on right just before intersection with Lanphere Lane (on left) [43.575141, -73.347418] - **Stop 4** |

**STOP 4: FOLDED THRUSTS OF TACONIC ALLOCHTHON SLATES (PLUDE'S QUARRY).**

Locality marked on Fig. 6. Plude's Quarry (Fig. 5) provides another of the few known exposures of Taconic Allochthon continental rise rocks lying upon the underlying melange/flysch sequence. Along Carlton Road the shales and minor thin silty wackes of the Taconic flysch are broken into a phacoidal melange fabric, seen in the lowest part of the western face of the outcrop. Going up the western outcrop face, a contact of this material overlain by slates with a planar slaty cleavage can be found. This is the Taconic Frontal Fault, again; but mapping by us (as shown in Fig. 6) clearly demonstrates that here, this fault, and the immediately underlying carbonate slice (not exposed in this outcrop), are folded on a map scale. Higher up the outcrop face, harder greyish-green slates contain thin fine-grained ribbon arenites and are consequently identified as belonging to the Poultney Formation of the Taconic Allochthon sequence. In the northern outcrop face of the old quarry, the regional slaty cleavage in those rocks passes down into the grey slates without arenites, that are above grey "shales" with phacoidal melange fabric at the western base of this face. The Poultney rocks above are clearly folded with the slaty cleavage as an axial surface fabric. A previous description of this outcrop (Bosworth and Kidd, 1985), suggested that there is an older, folded (thrust) fault, crossed by the slaty cleavage, that occurs between the Poultney slates above, and the grey slates below, and that this structure may be of the same generation as the early, folded, "Taconic Basal Thrust" of Rowley and Kidd (1981). The gray slates in this interpretation would be a transported constituent of the Middle Ordovician flysch ("Hortonville" lithology). Alternatively, but perhaps less likely, they might be an arenite-poor section of the Poultney unit and that no significant fault occurs at this contact internal to the rocks showing slaty cleavage in this outcrop. What do you think?

In either case, the local geological map shows that the fault expressed by melange fabric at the lower western side of the quarry is also folded, but this fault structure is not required to pre-date or overlap in time the cleavage affecting Taconic Allochthon rocks. The underlying limestone slice that is also affected by folding shows a solution cleavage, variably developed; while this is plausibly the product of the local strain that transported and folded the limestones, this does not mean that it is the same age as the slaty cleavage expressed in the Poultney slates in the quarry. This solution cleavage is more likely to have

developed later in the overall Taconic imbrication/transport sequence, just before or during the transport of the shelf limestone, and after the thrust emplacement of the Taconic Allochthon above the limestone.

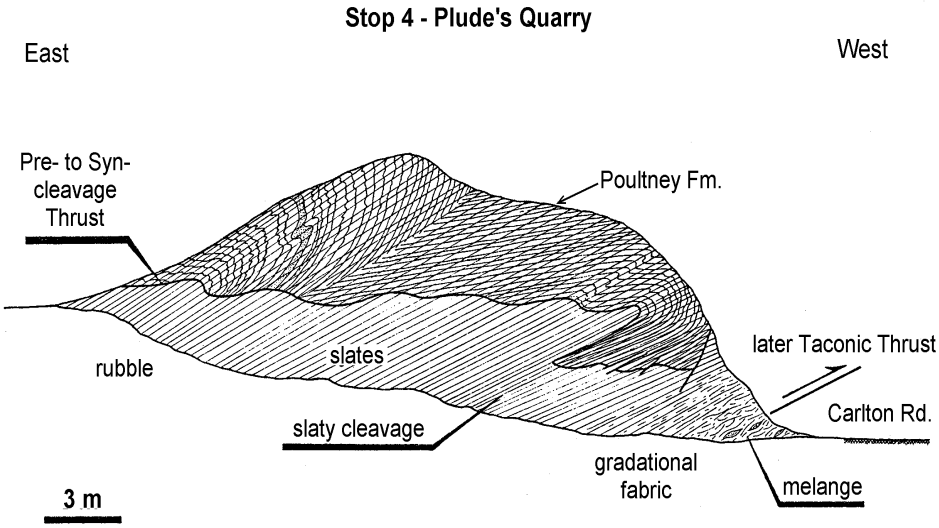


Figure 5. Western most thrust carrying Taconic Allochthon slates, exposed in face of Plude's Quarry, Stop 4; location marked on Fig. 6). The geological map (Fig. 6) shows that this thrust, marked by shale melange, and an underlying limestone thrust slice, are folded locally on a large scale. In the quarry, allochthonous Poultney Formation slates overlie grey slates along a contact which may be an older thrust, affected by folding and cut by the slaty cleavage. It is possible that the grey slates are also part of the Poultney (and that there is no early thrust), but they more closely resemble an Ordovician flysch lithology ("Hortonville"). If this identification is correct, the contact cannot be stratigraphic, but would have to be a largely pre-slaty cleavage thrust, with thrusting and folding perhaps in part synchronous, as the amplitude of the fold in the thrust surface in the easternmost anticline is less than the amplitude in the folded Poultney. Slightly modified from Bosworth & Kidd (1985).

| | | |
|---|---|---|
| 32.8 | 0.7 | Continue on Carlton Road 0.7 mile to intersection with Westcott Road; turn left. |
| 33.9 | 1.1 | Go to end of Westcott Road at stop sign intersection with Co Rte 11; turn left. |
| 34.0 | 0.1 | Park on right about 100 meters down the road [43.592398, -73.344854]; walk another 50 meters down to outcrop on the north side [43.592133, -73.345231] - **Stop 5** |

**Warning - be cautious about where you step up to the rock face - in places, large blocks are visibly detached, and may be very unstable**

**STOP 5: THRUST OF MEDIAL ORDOVICIAN LIMESTONES OVER SHALY MELANGE**

Locality indicated on Fig. 6. Carbonate exposures such as this one form lenticular belts bounded by medial Ordovician shales and shale melange (flysch) in a zone near this vicinity up to a few kilometers wide between the western edge of the Taconic Allochthon and the eastern edge of gently east-dipping, unfolded strata that rest with intact unconformable relationship on crystalline Grenville basement (such as those exposed along Rt 4 just east of Whitehall, and on Warner Hill visible a few kilometers due west of this locality). Where contacts are exposed, such as here, evidence for faulted lower contacts of limestone over shale are seen. In particular, the underside of the limestone is coated with fibrous vein-type slickensides, the lineation plunging ~120º close to down-dip. Truncation of stratification in the limestone is seen locally. An abundance of veins in the limestone within about 50cm of the thrust surface suggests hydrofracturing and high fluid pressures during thrusting. A crude, lenticular cleavage in the underlying shales is deflected adjacent to the fault surface. A small horse of shale, isolated above the main thrust surface by a duplex mechanism, can be seen about half way along the exposure of the thrust (Fig. 7).

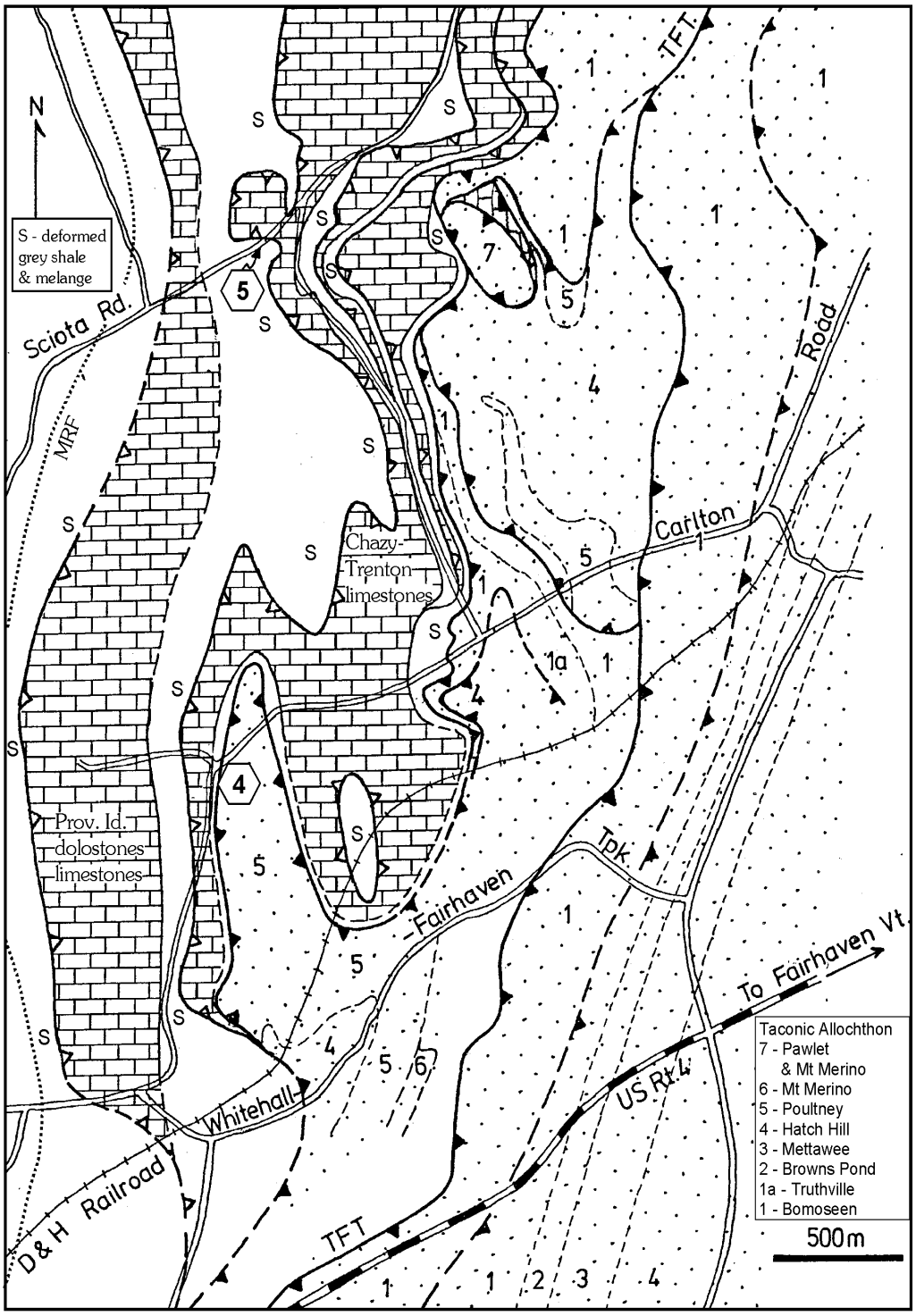


Figure 6. Geological map of the Taconic foreland fold and thrust belt northeast of Whitehall, NY, showing locations of stops 4, and 5, and the trace of thrust faults between the Taconic Frontal Thrust (TFT) and the Mettawee River (normal) Fault (MRF). Geology mapped by W. Kidd; modified from the versions shown in Bosworth & Kidd (1985), and Bosworth et al (1988).

Towards the western limit of the overlying carbonate sheet a detached sliver of carbonate about a meter long lies in the cleaved shale just below the prominent fault surface. This may be a structurally detached

piece or (less likely because of its shape) an olistolith. Similar lozenge-shaped pieces of medium-grained graywacke up to about 1/2 m long occur sparingly in the phacoidally-cleaved shale in the western part of the cut. Slickensided surfaces suggest that they too are products of structural disruption ("structural slicing"), although an olistolithic origin for these small objects cannot be discounted.

The shale and siltstone is locally bedded, with minor folds in part of the outcrop. Most is pervasively disrupted by the phacoidal cleavage whose microstructural character, with abundant evidence for shear offsets, is clearly related to faulting (Bosworth and Vollmer, 1981; Bosworth, 1982, 1984). This carbonate and other exposures like it are shown on the New York State geological map and by Fisher (1985) as giant olistolithic blocks. We find this interpretation of the outcrops to be unconvincing and prefer an interpretation, as shown on Fig. 6, where the carbonates and stratigraphically overlying shales form thin thrust sheets accreted beneath the Taconic Allochthon. Demonstrable tight folds and internal duplex faults within these carbonate sheets account for the many places where stratigraphic continuity is disrupted within them.

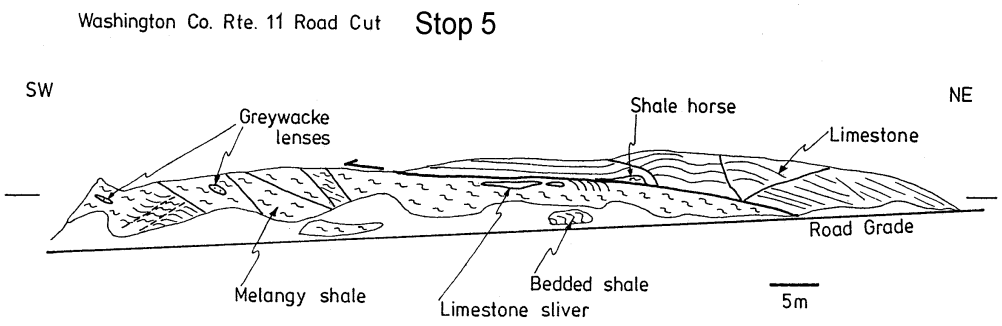


Figure 7. Profile exposed in road cut on north side of Washington County Route 11, 0.35 mile east of intersection with Sciota Road. Location marked on Fig. 6. Ordovician Isle La Motte (Middlebury) limestone thrust over medial Ordovician melangy shales. Diagram from Bosworth & Kidd (1985).

34.3 0.3 Continue down Washington Co. Rte 11 to intersection with Washington Co. Rte 10; turn right.
38.6 4.3 Go north on Washington Co. Rte 10;
at 2.5 miles cross (slowly) Poultney River Bridge, NY-Vermont border; road becomes Book Road
at 3.2 miles pass Book Farm;
at 4.3 miles park on right on grass verge [43.645701, -73.347671]; dirt road intersects on left.

Lunch stop may involve driving or walking detour on dirt road to Book's pond and picnic area (~0.3 miles each way; not included in road log).

Roadside outcrop about 160m walk south along Book Road [43.644500, -73.348832] - **Stop 6A**
and
Outcrop in woods and streambed about 500m walk ENE through the field to the east of the road [43.647590, -73.341250] - **Stop 6B**

**STOP 6A: SHOREHAM THRUST EXPOSURE ON BOOK ROAD**

In the center portion of this roadcut exposure, grey-black non-calcareous shale (mid-Ordovician) up to 1 meter thick, with a pronounced phacoidal cleavage indicative of large shear strain, occurs below a sharp contact with highly fractured massive dolostones ("Providence Island" lithology). This is the Shoreham Thrust, and mapping of the surrounding area (Fig. 8) shows unequivocally that it is here the westernmost thrust in the Champlain System - in other words that the "Main Champlain", or Orwell Thrust farther north

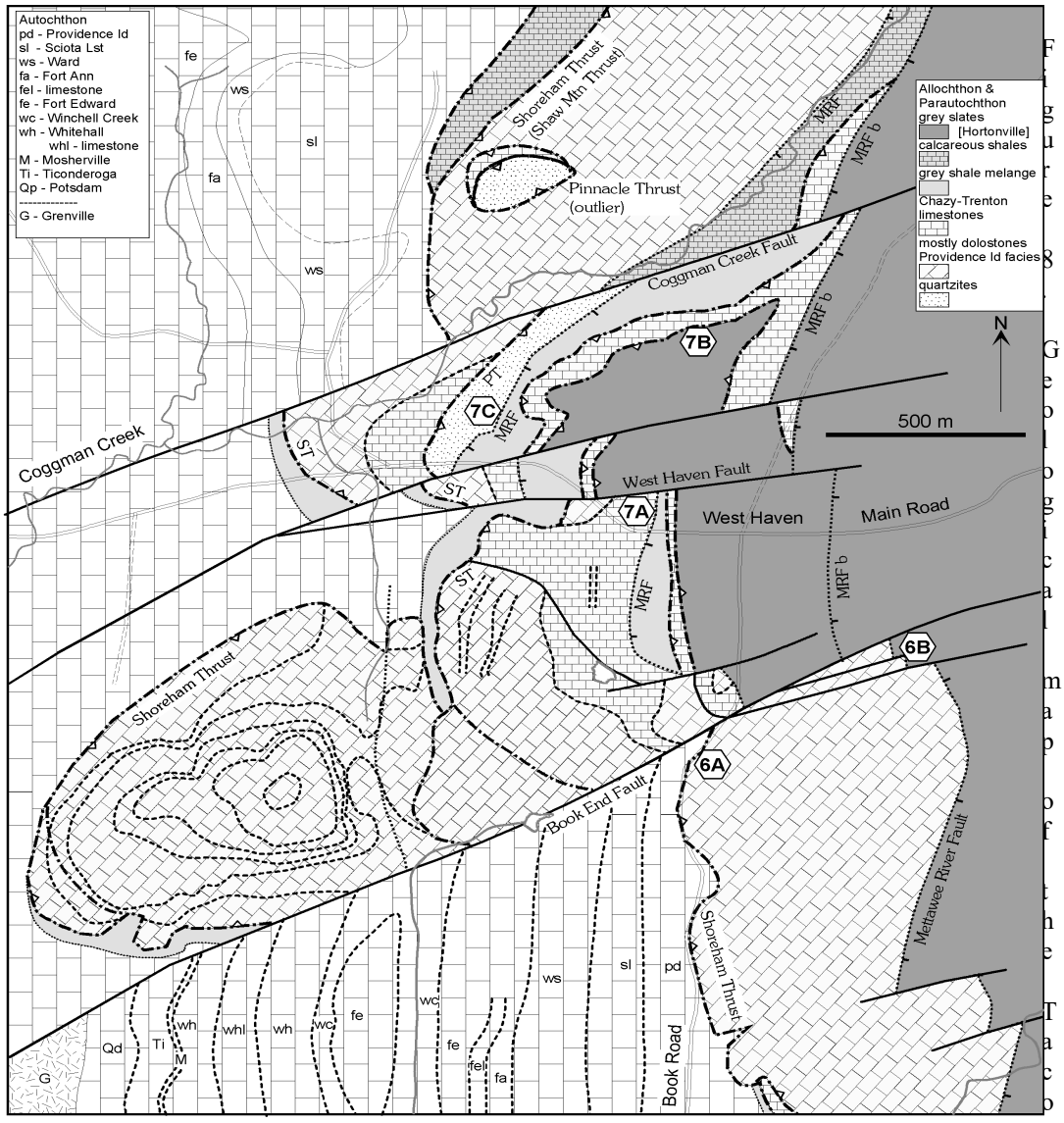


Figure 8. Geological map of the Champlain Thrust system in the foreland fold and thrust belt at West Haven, VT showing locations of stops 6A and 6B; and 7A, 7B, and 7C. The trace of thrust faults of the Champlain Thrust system crossing this map are the Shoreham Thrust (ST), and the Pinnacle Thrust (PT). Local exposure of the thrust carrying allochthonous grey slates (Hortonville) is found at stop 7B. The Mettawee River (normal) Fault (MRF) is exposed at stop 6B; this fault is interpreted to split into two strands north of the left-lateral Book End Fault. The dissection of the thrusts by the MRF and the younger strike-slip faults make the local geology exceptionally complex. Geological mapping, compilation and interpretation by W. Kidd, including information from Steinhardt (1983), and Granducci (1995).

has disappeared (Hayman and Kidd, 2002a, b). To the south across the Vermont-New York border, near the Poultney River, the Shoreham Thrust also disappears, first because it is truncated by the Mettawee River normal Fault, although minor folding and incipient ramps can be detected in shelf rocks at its expected position in a outlier which occurs east of Whitehall. A major WSW-ENE cross-fault (the Book End Fault) passing north of this outcrop at stop 6A cuts and displaces the autochthonous shelf section and the Champlain Thrust System stack, crossing Book Road at the parking spot. The Shoreham Thrust is offset by this structure with an apparent left lateral displacement of about 2 kilometers. Two other faults like this one pass through the next valley north near West Haven hamlet. These cross faults are discussed in the description of Stops 6B and 7 below.

**STOP 6B: METTAWEE RIVER FAULT NEAR WEST HAVEN**

ASK PERMISSION AT BOOK FARM BEFORE ENTERING - find Book Farm along Book Road 1.1 miles south of specified parking place

From parking place, enter field on east by walking between the two fences, opening the gate if necessary (and closing it behind you) - please do not climb over it or the fence. Follow the grassed-over track into the edge of the woods (about 100 meters), then along the edge of the woods (about another 200 meters), then angle down the crest of a low ridge in the meadow (about another 100 meters) to the edge of the woods crossing the low ridge. Outcrop of fractured tan-weathing dolostone ("Providence Island" lithology) is found just inside the woods at this point.

Use the sketch map below to navigate and understand the geology from this point on. About 60 meters east of the first dolostone outcrop, in the bed of the stream near the south end of the small ravine, dark slates ("Hortonville"), of presumed mid-Ordovician age, are exposed in contact with the dolostones [43.647590, -73.341250] . This contact is clearly a steep (60º) east-dipping fault, truncating the moderately east- dipping thick bedding in the dolostones, and the cleavage in the slates. Given the regional context, with no thick dark slates occurring west of this point, but rather the carbonates of the Shoreham Thrust slice, then the underlying autochthonous Cambro-Ordovician "Whitehall facies" shelf sequence, with Potsdam sandstone/quartzite at its base lying unconformably on Grenville basement, this fault must be a normal fault, and is in fact the Mettawee River Fault first proposed by Fisher (1985) in New York. It is the only complete exposure of this fault, although our mapping demonstrates that it runs continuously from the Mettawee River (stop 1A) north through this locality at least as far north as the latitude of Shoreham, VT, and all along this length it truncates regionally the thrust stack of the Champlain Thrust System.

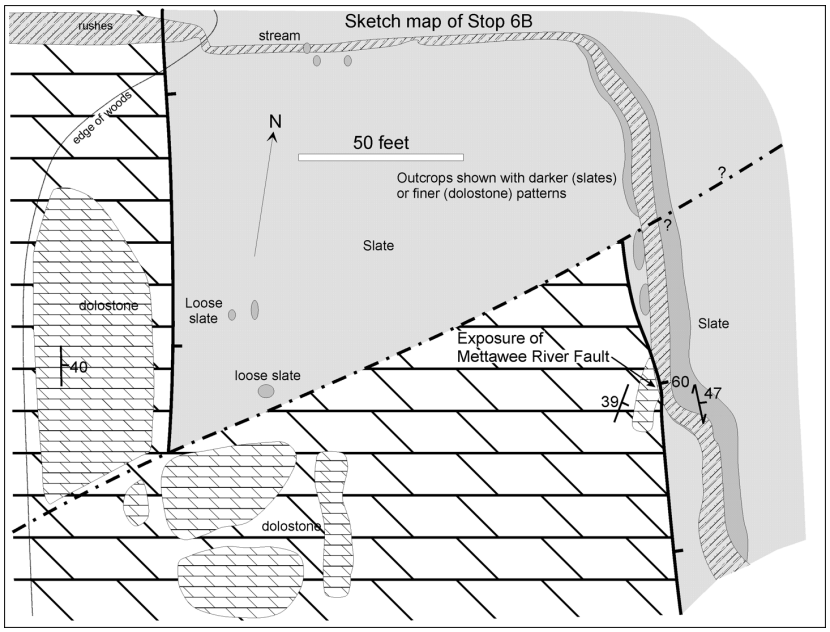


Figure 9. Outcrop and geologic map of Stop 6B – exposure of the Mettawee River Fault near West Haven, VT. Diagram from Hayman & Kidd (2002a).

We suspect that it extends significantly farther north and south than this, but there is a lack of clear truncation of components of the Champlain Thrust System beyond these extents. One reason for suspecting a larger along-strike extent is the minimum displacement, which can be constrained from cross-sections, and which demand at least 1000 meters of throw, and perhaps more than 1500 meters. This fault cuts out large, significant parts of the Champlain Thrust stack, and is one of the main reasons why previous attempts failed to trace the major thrust faults of the System southward. What age is this normal fault? We have no

direct younger age limit in the mapped area, other than the observation that it is cut and displaced by the WSW-ENE faults which also cut the Shoreham Thrust. In fact this set of local outcrops (see Fig. 9 sketch map) shows that relationship directly, with a smaller splay of the larger WSW-ENE fault displacing in an apparent left-lateral sense the dolostone-slate contact (the Mettawee River Fault).

Evidence to be shown in the outcrop of the next stop (Stop 7A) demonstrates that these apparent strike-slip offsets on the WSW-ENE faults are from actual strike-slip displacement; discussion of the age and origin of this youngest faulting type and orientation is included with Stop 7A.

39.0 0.4 Continue north on Book Road to crossroads intersection with Main Road at West Haven; turn left.
39.1 0.1 Go west 0.1 mile on Main Road and park on right on road verge before driveway to Coggman Creek Farm (red barn); do not block any access, please. [43.651369, -73.349745].
**Stops 7A, B and C**. (all walking).
[7A 43.65216, -73.35094]; [7B 43.65738, -73.34863]; [7C 43.654645, -73.356594]

ASK PERMISSION AT THE FARMHOUSE TO VISIT THIS OUTCROP AND THE OUTCROP OF STOP 7B. DO NOT GO TO THE OUTCROP UNLESS YOU HAVE PERMISSION. NO HAMMERS ALLOWED.

At the barns, follow the track west 50 meters to the low lying limestone outcrop surfaces.

## STOP 7A: VEINS AND LEFT-LATERAL STRIKE-SLIP FAULTING IN LIMESTONE AT WEST HAVEN

On the main part of the outcrop, abundant calcite veins of two generations can be seen. The older set strike about N-S and mostly dip moderately to very steeply east. Their displacement sense is not particularly significant for this field trip, and is undetermined in most cases, but east-over-west thrust sense has been seen, as well as some strike-slip component in places, of dextral sense. The significant vein set for our purpose is the one striking between E-W and WSW-ENE, which in all cases cut N-S veins, and can be shown in a number of examples to displace subvertical instances in a sinistral sense. From this outcrop, the only one around West Haven where we have found this evidence, we infer that the apparent displacements on the WSW-ENE faults mapped here resulted from real left-lateral strike-slip displacement, not entirely from steeply directed north-side-down slip cutting gently-moderately east-dipping strata and thrust faults.

We sampled by drilling short cores of some of the veins in this outcrop, and looked for suitable fluid inclusions in doubly polished sections to measure fluid homogenization temperatures, and freezing temperatures, to determine the salinity for the fluids forming the veins. Refer to the vein fluid inclusion discussion in the introduction for overview and details. To summarise the essential point: low salinity fluid inclusions having homogenization temperatures up to 205-215C were found in the younger WSW-ENE veins having left-lateral strike-slip offset. Fluids in the fractures at burial depth when the veins formed would have been above this temperature, the amount depending on the depth, which we do not know. However, by comparison with results from Ordovician (Taconic) and Devonian (Acadian) vein fluid inclusions in the Albany area, we think this temperature is high enough to be indicative of an Ordovician age. Devonian veins (thrust sense only) from the Acadian foreland fold and thrust belt there are distinguishably lower, most around 120-130C. We are not aware of any reason to suppose that Acadian fluids are likely to have been significantly hotter in western Vermont compared with the Albany area, and we note an absence of both strike-parallel normal faults and WSW-ENE cross-faults cutting the Acadian Helderberg fold-thrust belt. So we think the WSW-ENE faults crossing the Taconic foreland thrust belt in this area are strike-slip faults (at least in their later/last slip episodes), and Ordovician (Taconic) in age, and are the youngest of the sets of structures of the Taconic event.

Whether they are Ordovician, or younger, what is their tectonic origin? Thrust faults are easy to understand in the context of the Taconic arc-continent convergence (Bird and Dewey, 1970), and strike-parallel normal faults in that general context similarly have modern exemplars, both of pre-thrusting origin from slab-pull on the downgoing lithosphere (Schoonmaker et al, 2005), and extension late in and/or after convergence from slab detachment (Davies & Blanckenburg, 1995) or regional stress removal by large-

scale plate boundary reorganisation. Strike-parallel strike-slip faults also are no problem to accommodate by strain partitioning of plate motion (McCaffrey, 1996). Cross-strike strike-slip faults of small displacement, on the other hand, are usually secondary linking structures (tear faults) for thrust (or perhaps with oblique slip for normal fault systems), and these commonly also serve as fault segment delimiters for earthquake slip zones. We think this may be the explanation for these WSW-ENE faults in the Taconic foreland but there is a problem; there are no known contemporary thrust or normal faults of the right relative age, nor any of a compatable slip direction! The WSW-ENE faults cut the Mettawee River normal fault, which itself cuts the youngest thrust in the Champlain Thrust stack. Even if we are wrong about the age constraint inferred from the fluid inclusion minimum temperature, the Acadian thrust slip direction for this sector of the northern Acadian Appalachians is also not towards WSW. Perhaps there could be small displacement blind thrust segments in the flat-lying platform sediments of the Taconic foreland, with WSW-directed slip, that would be the very last activity of the Taconic orogen, and to which these strike-slip faults form tear fault linking structures?

There are other features of the geology apparently associated with the West Haven cross-fault zone that we have noted: a) the abrupt change in the medial Ordovician strata across it from non-calcareous shales occurring to the south, to significant thicknesses of calcareous shales (Cumberland Head and Stony Point Fms) to the north. In addition, b) changes in thickness of the early Ordovician Ward Siltstone appear to be associated with this zone, and perhaps also with other faults of this orientation near and south of Whitehall. The implication is that these faults have developed using older fractures in the basement, and that these older structures also may have influenced subsidence patterns and deposition of sediments of the shelf both before and during the approach of the Taconic thrust stack.

Also, c) the map complexity near West Haven implies that the Shoreham Thrust interacted with an already fault-displaced irregular floor, from normal faulting on these oblique structures before the thrust stack interacted with it; it is admitted that inadequate outcrop and want of 3-D information prevent any clear demonstration of this. However, the same structural history inferred here can be observed if you visit outcrop adjacent to the Split Rock Point Fault [44.267592; -73.337305] near Westport NY where normal displacement on the NE-striking fault is expressed by the juxtaposition of Grenville gneisses and medial Ordovician calcareous shales; the dipping shales bent up by the normal-sense shear strain are cut by calcite veins showing clear evidence of strike-slip displacements, of both dextral and sinistral sense.

From the barns, walk north across the fields to the edge of the woods where a small stream bed (often dry) enters the woods [43.65678, -73.34888]. Follow the track into the woods on the west side of the stream bed; where the slope increases, the stream bed exposes continuous outcrop in a small cliff (a waterfall when the stream is running) and the banks and bed of the stream above and below.

## STOP 7B: FLAT-LYING THRUST FAULT OF TACONIC SLATES OVER CALCAREOUS SHALES AND LIMESTONES SOUTH OF COGGMAN CREEK

The small waterfall cliff, and the stream bed above, expose grey slates with a well-developed, moderately east-dipping cleavage. At the base of the small cliff, these slates rest on a practically flat thrust fault carrying them over dark calcareous shales. These calcareous shales pass down into limestones which form the rest of the outcrop in the stream bed and on the valley walls adjacent. The limestones are medial Ordovician Glens Falls, Orwell, and perhaps Middlebury equivalents, similar to those seen at stop 3, 5, and 7A (but are, we think - see map of Fig. 8 - not part of the same thrust slice as at stop 7A). The transported slates possess a well-developed planar slaty cleavage and so in a structural sense belong with the Taconic Allochthon. Their lithology, the same seen at stop 6B, monotonous, slightly silty, pale to medium grey slate, with thin silty laminations seen in some places, has been given the name Hortonville Slate by Zen (1967) in the area of the main Taconic Allochthon to the east. It is probably a medial Ordovician-age deposit, a facies of the orogenic flysch clastics accompanying the Taconic convergence, but significantly farther-transported than the melange, shales and turbidites of the Hudson Valley. Along structural strike, to the NNE near Benson, these rocks adjoin the Sunset Lake slice of the Taconic Allochthon, and we regard them as an enlarged addition/extension of the Sunset Lake slice. If this interpretation is valid, then the thrust exposed here is essentially another exposure of the western marginal fault of the Taconic Allochthon.

*If you are using this field guide independently, you need to return to the Main Road at West Haven, go west along the road 0.3 mile, and ask permission at the house on the north side of the road to visit the outcrop of Stop 7C. If permission is obtained, the outcrop is about 150 meters north of the house.*

If permission was previously obtained, return from Stop 7B to the edge of the woods and walk west along the edge for about 450 meters, passing limestone outcrops in the woods extending from near stop 7B until reaching the point where the ridge crest starts descending towards the west and enters the woods. Down the slope to the north at this point, the last limestone outcrop occurs above an exposure of dark melange-fabric shale just below it, showing that the thrust at the base of this limestone sheet runs here. From the point on the ridge, go approximately southwest contouring around the ridge end, and descend slightly into another (usually dry) streambed running roughly west.

**STOP 7C: METAWEE RIVER FAULT AND QUARTZITES OF THE PINNACLE THRUST WEST OF WEST HAVEN**

See Fig 8 for location and geological surroundings. Exposures of dark partly melange-fabric shale occur intermittently in the bed and low bank of the stream to just before a sharp increase in the gradient over a rock ledge exposing well-lithified quartz arenites/quartzites. Below these, down stream, dolostones also outcrop. These arenites are part of the Potsdam/Ticonderoga unit of the Cambro-Ordovician shelf sequence, lying above the (here unexposed) Pinnacle Thrust, and must be separated from the melangy shales seen a few feet upstream by the principal strand of the Mettawee River Fault.

These quartzites also outcrop on the crest of the hill across Coggman Creek to the north, where they form an isolated erosional outlier of the Pinnacle Thrust, which overlies mainly dolostones of the Shoreham (locally termed Shaw Mountain) Thrust. We think the quartzite exposures near Root Pond a few kilometers to the northeast also form isolated remnants of the Pinnacle Thrust sheet, and that isolation by truncation of the Mettawee River normal Fault is a key to understanding their relationships, as it is for the similar occurrences of such quartzites in the same structural setting all the way from here at Stop 7C to Whitehall NY, where they can be shown to continue in the hanging wall of the Comstock thrust, as seen at Stop 2.

Walk back up the ridge on the north side of the stream to the field, and thence back to the barns at the Coggman Creek (old Richardson) Farm.

**END OF TRIP.**
**To return to Lake George:**

| | | |
|---|---|---|
| 42.6 | 3.5 | Turn around; go east on Main Road. At 0.1 mile pass Book Road intersection; 1.0 mile pass Best Road intersection (on left); 1.4 miles pass Stage Road intersection (on left; Main Road here takes sharp turn to right); 2.2 miles cross Hubbardtown River bridge; 2.7 miles pass Hackadam road intersection (on right); 3.5 miles stop sign intersection with Vermont Rte 22A. Turn right. [*For Burlington and other northern destinations using I-89, turn left*] |
| 45.0 | 2.4 | Go 2.4 miles south on Vermont Rte 22A to entrance ramp for US Rte 4 West; turn right up the ramp, join Rte 4 westbound. [*For Rutland and points eastern, go under the Rte 4 bridge and take the eastbound ramp*] |
| 53.2 | 8.2 | At 1.7 miles Vermont-NY border at Poultney River; at junction at light in Whitehall with NY Rte 22, turn left. |
| 63.8 | 10.6 | Follow US Rte 4 south10.6 miles to intersection at light in Fort Ann with NY Rte 149; turn right onto Rte 149. |
| 75.5 | 11.7 | Follow NY Rte 149 to intersection at light with US Rte 9 - end of log; turn right and go ~4 miles to Lake George Village [*For Albany, and points south and west, turn left, go 0.7 miles on Rte 9 to the second light, (Rte 23 intersection); turn right, go 0.2 mile to ramp entrance on left for I-87 south*]. |

**REFERENCES**

Bird, J. M., and Dewey, J. F., 1970, Lithosphere plate-continental margin tectonics and the evolution of the Appalachian orogen: Geological Society of America Bulletin, 81, 1031-1060

Bosworth, W., 1982. Evolution and structural significance of master shear zones within the parautochthonous flysch of eastern New York: Vermont Geology, v.2 (Symposium on Taconic Geology), 6-13.

Bosworth, W., 1984. The relative roles of boudinage and "structural slicing" in the disruption of layered rock sequence: J. Geol., v.92, 447-456

Bosworth, W. and Vollmer, F.W., 1981. Structures of the medial Ordovician flysch of eastern New York: deformation of synorogenic deposits in an overthrust environment. J. Geol., v.89, 551-568.

Bosworth, W. and Rowley, D.B., 1984. Early obduction-related deformation features of the Taconic Allochthon: analogy with structures observed in modern trench environments. Geol. Soc. Amer. Bull., v.95, 559-567

Bosworth, W., and Kidd, W.S.F., 1985. Thrusts, melanges, folded thrusts, and duplexes in the Taconic Foreland. pp. 117-146 in Lindemann, R.H., (editor) Field Trip Guidebook, 57th Annual Meeting, New York State Geological Association, 27-29 September 1985, Skidmore College, Saratoga Springs, NY.

Bosworth, W., Rowley, D. B., Kidd, W. S. F., and Steinhardt, C., 1988, Geometry and style of post-obduction thrusting in a Paleozoic orogen: the Taconic Frontal Thrust System: Journal of Geology, v. 96, p. 163-180.

Bradley, D. C., and Kidd, W. S. F., 1991, Flexural extension of the upper continental crust in collisional foredeeps: Geological Society of America Bulletin, v. 103, p. 1416-1438.

Bradley, D. C., and Kusky, T. M., 1986, Geologic evidence for the rate of plate convergence during the Taconic arc - continent collision: Journal of Geology, v. 94, p. 667-681.

Chan, Y.-C., Crespi, J. M. and Hodges, K. V. 2001, Dating cleavage formation in slates and phyllites with the 40Ar/39Ar laser microprobe: an example from the western New England Appalachians, USA: Terra Nova, v 13.

Cisne, J. L., Karig, D. E., Rabe, B. D., and Hay, B. J., 1982, Topography and tectonics of the Taconic outer trench slope as revealed through gradient analysis of fossil assemblages: Lethaia, v. 15, p. 229-246.

Davies, J.H., and von Blanckenburg, F., 1995, Slab breakoff; A model of lithosphere detachment and its test in the magmatism and deformation of collisional orogens: Earth and Planetary Science Letters, v. 129, p. 85–102.

Jacobi, Louise D. 1977. Stratigraphy, Depositional Environment and Structure of the Taconic Allochthon, Central Washington County, New York. Unpublished MSc. thesis, State University of New York at Albany.193pp +ix +2p. abstract; 4 folded plates (map, sections, stratigraphy) online at http://www.atmos.albany.edu/geology/webpages/ldelano.html

Fisher, D. W., 1985. Bedrock geology of the Glens Falls-Whitehall region, New York: New York State Museum Map and Chart Series, v. 35.

Granducci, J.L., 1995. Stratigraphy and structure at the southern end of Lake Champlain in Benson, Vermont. Unpublished MSc. thesis, State University of New York at Albany. 106 pp., +xi; 2 folded plates (maps); online at http://www.atmos.albany.edu/geology/webpages/granduci.html

Hames, W.E., Tracy, R.J., Ratcliffe, N.M., and Sutter, J.F., 1991, Petrologic, structural, and geochronologic characteristics of the Acadian metamorphic overprint on the Taconian Zone in part of southwestern New England: American Journal of Science, v. 291, 887-913.

Hayman, N.W., 1997. Pre-thrust normal faults and post-tectonic micas in the Taconic Range of west-central Vermont. Unpublished MSc. thesis, State University of New York at Albany. 179 pp., +xiii; 3 folded plates (maps); online at http://www.atmos.albany.edu/geology/webpages/nhaymana.html

Hayman, N.W., and W.S.F. Kidd, 2002a. The Champlain Thrust System in the Whitehall- Shoreham area: influence of pre- and post-thrust normal faults on the present thrust geometry and lithofacies distribution. Field trip A7, pages7-1 to 7-24 in McLelland, J.M., amd Karabinos, P., (editors) Guidebook for Fieldtrips in New York and Vermont. New England Intercollegiate Geological Conference 94th Annual meeting, and New York State Geological Association 74th Annual meeting, Lake George, NY, September 27th-29th, 2002. Skidmore College, Saratoga Springs

Hayman, N. M., and Kidd, W. S. F., 2002b, Reactivation of prethrusting, synconvergence normal faults as ramps within the Ordovician Champlain–Taconic thrust system: Geological Society of America Bulletin, v. 114, p. 476-489.

Jacobi, Louise D. 1977. Stratigraphy, Depositional Environment and Structure of the Taconic Allochthon, Central Washington County, New York. Unpublished MSc. thesis, State University of New York at Albany.193pp +ix +2p. abstract; 4 folded plates (map, sections, stratigraphy); online at http://www.atmos.albany.edu/geology/webpages/ldelano.html

Kidd, W.S.F., Plesch, A., and Vollmer, F.W., 1995, Lithofacies and structure of the Taconic flysch, mélange, and allochthon, in the New York Capital District, in Garver, J.I., and Smith, J.A., eds., Field Trip Guide for the 67th Annual Meeting of the New York State Geological Association: Union College, Schenectady, NY, p. 57–80

Lim, C., Kidd, W.S.F., and Howe, S.S., 2005. Late shortening and extensional structures and veins in the western margin of the Taconic Orogen (New York to Vermont) J. Geol., 113, 419–438.

Lim, C., and Kidd, W.S.F., 2008. Foreland zone faults and veins related to along-strike propagation of slab breakoff at the end of the Taconic orogeny. Geological Society of America Abstracts with Programs, 40 (2), 29.

MacDonald, F.A., Karabinos, P.M., Crowley, J.L., Hodgin, E.B., Crockford, P.W., and Delano, J.W, 2017. Bridging the gap between the foreland and hinterland II: geochronology and tectonic setting of Ordovician magmatism and basin formation on the Laurentian margin of New England and Newfoundland. Amer. J. Sci., 317, 555–596.

McCaffrey, R. 1996. Slip partitioning at convergent plate boundaries of southeast Asia. In: Hall, R. & Beundell, D. J. (eds) Tectonic Evolution of Southeast Asia, Geological Society of London Special Publications, 106, 3-18.

Ratcliffe, N.M., Stanley, R.S., Gale, M.H., Thompson, P.J., and Walsh, G.J., 2011, Bedrock geologic map of Vermont: U.S. Geological Survey Scientific Investigations Map 3184, 3 sheets, scale 1:100,000.

Rowley, D.B., 1980. Complex Structure and Stratigraphy of Lower Slices of the Taconic Allochthon Near Middle Granville, New York. Unpublished MSc. thesis, State University of New York at Albany. 258pp., +xv.; 3 folded plates (maps); online at http://www.atmos.albany.edu/geology/webpages/rowleyms.html

Rowley, D.B., 1983. Operation of the Wilson Cycle in western New England during the Early Paleozoic: with emphasis on the stratigraphy, structure, and emplacement of the Taconic Allochthon. Unpublished PhD dissertation, State University of New York at Albany. 602pp. (2 volumes), +xxvi; 4 folded plates (maps);online at http://www.atmos.albany.edu/geology/webpages/rowleyph.html

Rowley, D. B., 1982, New methods for estimating displacements of thrust faults affecting Atlantic type shelf sequences: with an application to the Champlain Thrust, Vermont: Tectonics, v. 1, p. 369-388.

Rowley, D. B., and Kidd, W. S. F., 1981, Stratigraphic relationships and detrital composition of the medial Ordovician flysch of western New England: Implications for the tectonic evolution of the Taconic orogeny: Journal of Geology, v. 89, p. 199-218.

Rowley, D.B. and Kidd, W.S.F., 1982. Stratigraphic relationships and detrital composition of the medial Ordovician flysch of western New England: implications for the tectonic evolution of the Taconic Orogeny: a reply to Rodgers. J. Geol., v.90, 219-226.

Rowley, D.B., Kidd, W.S.F., and Delano, L.L., 1979. Detailed stratigraphic and structural features of the Giddings Brook Slice of the Taconic Allochthon in the Granville area. pp. 186-242 in Friedman, G.M., (ed.) NY State Geol. Assoc. and NEIGC Guidebook, RPI, Troy, NY.

Schoonmaker, A., Kidd, W.S.F., and Bradley, D.C., 2005, Foreland-forearc collisional granitoid and mafic magmatism caused by lower-plate lithospheric slab breakoff: The Acadian of Maine, and other orogens: Geology, v. 33, p. 961– 964

Selleck, B. and Bosworth, W., 1985. Allochthonous Chazy (Early Medial Ordovician) Limestones in eastern New York, tectonic and paleoenvironmental interpretations. Amer. J. Sci., v.285, 1-15.

Stanley, R.S., and Ratcliffe, N.M., 1985, Tectonic synthesis of the Taconian orogeny in western New England: Geological Society of America Bulletin, v. 96, p. 1227-1250.

Steinhardt, C.K., 1983. Structure and Stratigraphy of West Haven, Vermont. Unpublished MSc. thesis, State University of New York at Albany. 167 pp., +x; 4 folded plates (maps) ; online at http://www.atmos.albany.edu/geology/webpages/steinhar.html

Zen, E.-An, 1967, Time and space relationships of the Taconic allochthon and autochthon: Geological Society of America Special Paper, v. 97, 107pp.

Zen, E.-An, 1972, Some Revisions in the Interpretation of the Taconic Allochthon in West-Central Vermont: Geological Society of America Bulletin, v. 83, p. 2573-2588.

# NEW INSIGHTS INTO GLACIAL LAKES VERMONT AND ALBANY

By

John A. Rayburn[1], Dept. of Geology, SUNY New Paltz, New Paltz, NY 12443
David J. DeSimone[2], DeSimone Geoscience Investigations, Petersburg, NY 12138
Amy B. Frappier[3], Department of Geosciences, Skidmore College, Saratoga Springs, NY 12866
Email addresses: [1]rayburnj@newpaltz.edu, [2]hawkeye272david@yahoo.com, [3]afrappie@skidmore.edu

## INTRODUCTION

The first comprehensive study of the proglacial lakes in the Hudson and Champlain Valleys was published by J.B. Woodworth in 1905 (NYSM Bulletin 84). He noted that "*Lake Albany doubtless began on the south in the waters standing in front of the retreating ice sheet prior to the opening of the Mohawk outlet of the great glacial lakes to the west. As soon as the ice retreated in the valley to a position north of Albany and the drainage of Lake Iroquois came into the Hudson Valley Lake Albany properly came into existence*". While glacial lacustrine sediments in the Champlain Valley were originally attributed by Upham (1889), Baldwin (1894), Peet (1904), and others to be a separate Glacial Lake Champlain, Woodworth notes that its confines were somewhat larger and proposed the name of Glacial Lake Vermont, and that to the south it was certainly confluent with Glacial Lake Albany as he defined. "*The outlet of theses ice-dammed waters at this early stage of confluence across the present divide of the Hudson and Champlain basins is a matter which concerns the interpretation of Lake Albany on the south and is considered in that connection. Lake Vermont may be said properly to have come into existence when in consequence of a local lowering of waters south of Fort Edward a discharge began across a barrier into the Hudson Valley to the south.*"

While Woodworth (1905) only described one Lake Albany level, he noted under Lake Vermont that there were the Quaker Springs, Coveville, and Fort Edward levels. Of these, Woodworth stated that "*The question of the outlets of Lake Vermont ... has not been completely exploited as yet by field work*". The Fort Edward level outlet, better defined by Chapman (1932) as the Fort Ann outlet (see also DeSimone et al., 2008 NEFOP Field Guide Stop "Chapman's Potholes"), is the only one that truly meets his definition of Lake Vermont. Although Chapman recognized several separate Fort Ann levels, only the lowest of these may actually have been confined north of the Champlain-Hudson divide. Woodworth and later Fairchild (1917), Stoller (1922), and Chapman (1937), suggested that the Coveville level threshold is represented by a channel overhanging the Hudson River near Coveville, NY. There are two significant problems with this hypothesis however: 1) the bedrock that this channel is formed in is generally too soft to have withstood the estimated steady-state discharge of the pro-glacial lake and 2) more recent mapping demonstrates that Coveville level strandlines exist south of this location.

## GLACIAL LACUSTRINE SEDIMENTATION

The large glacial meltwater reservoirs of glacial Lakes Albany and Vermont were aligned north-south along the Hudson and Champlain valleys of eastern New York (Fig. 1). Although separately defined, they were actually separate stages of the same reservoir, but because of a continuously receding northern margin and dropping levels caused by changes due to threshold variation, generally recognized as "Lake Albany" when primarily located in the Hudson Valley, and "Lake Vermont" when primarily located in the Champlain Valley. The separate levels of these lakes are also recognized by sub-stage names. There is some disagreement in the literature about the name when the body of the lake was primarily straddled across the Hudson-Champlain basin divide. This configuration has occasionally been recognized as "Lake Quaker Springs" or the Quaker Springs level of Lake Albany.

Sedimentation into the glacial lake was significant, coming either from the melting Laurentide ice, or from significant fluvial systems developing to the east and west of the lake. In the deeper areas along the axis of the Hudson and Champlain Valleys this resulted in sometimes hundreds of meters of clay or clay/silt varved deposits. These deposits, where exposed in the Hudson Valley following the complete drawdown of the glacial lake, later became the source material for brick manufacturing and within the exposed walls of these brickyards Antevs (1922, 1928) was able to make his measurements and correlations that began the high-resolution chronology for the lake.

In the Champlain Valley, these thick fine-grained deposits remain submerged in the deepest locations under modern day Lake Champlain (cf. Cronin et al., 2008). Shallower water sand and silt deposits are also often preserved as varves where they accumulated below wave-base. Broad shallow water lacustrine sands are evident in areas where the water was too shallow to preserve annual variation in sedimentation. These areas are now often expressed as dune fields, such as the large region of mostly parabolic dunes in the Albany Pine Bush and points north through Saratoga County.

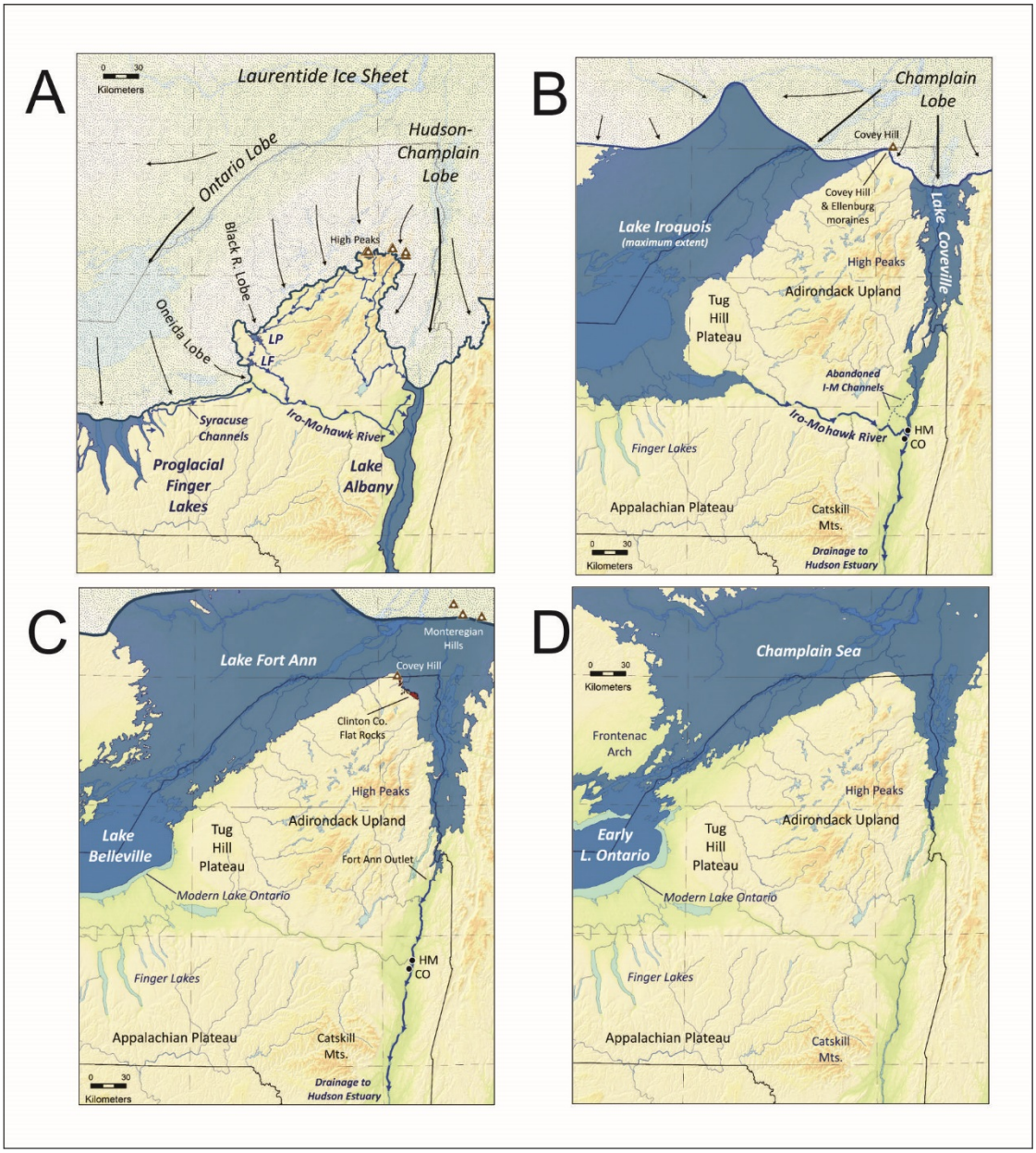


Figure 1. Development of glacial lakes Albany (A), Iroquois (B), Vermont (B&C) and the Champlain Sea (D). From Franzi et al. (2016).

Glacial lacustrine shoreline features include deltas, beach berms, and beach scarps. Of these, the deltas are the most prevalent and often easiest to locate (Figure 2). Large complex deltas are found in all major alluvial inputs to the valleys such as the Saranac, Ausable, Boquet, Winooski, Batten Kill, Hoosic, and Mohawk Rivers. The

complexity of these deltas is primarily due to the progressive lake stage lowering which would initiate incision into the existing delta surface and deposition in equilibrium with the new level, sometimes along the edge of the delta and sometimes farther down-valley depending on the relative base level drop and the gradient of the valley floor. Smaller stranded deltas associated with creeks or streams have also been preserved but are sometimes harder to locate. Stranded beach berms can be found where there was less of a direct alluvial influence, a source of coarse material to rework, and sufficient fetch or current across the lake to generate the berm. Examples of these are easily seen along the eastern shoreline north of Troy, NY where the lake was quite wide and a primary west wind (in agreement with the parabolic dune morphology) allowed waves to act on thick glacial fluvial deposits. Beach scarps form under similar conditions, but where the sediments are cohesive fine-grained material.

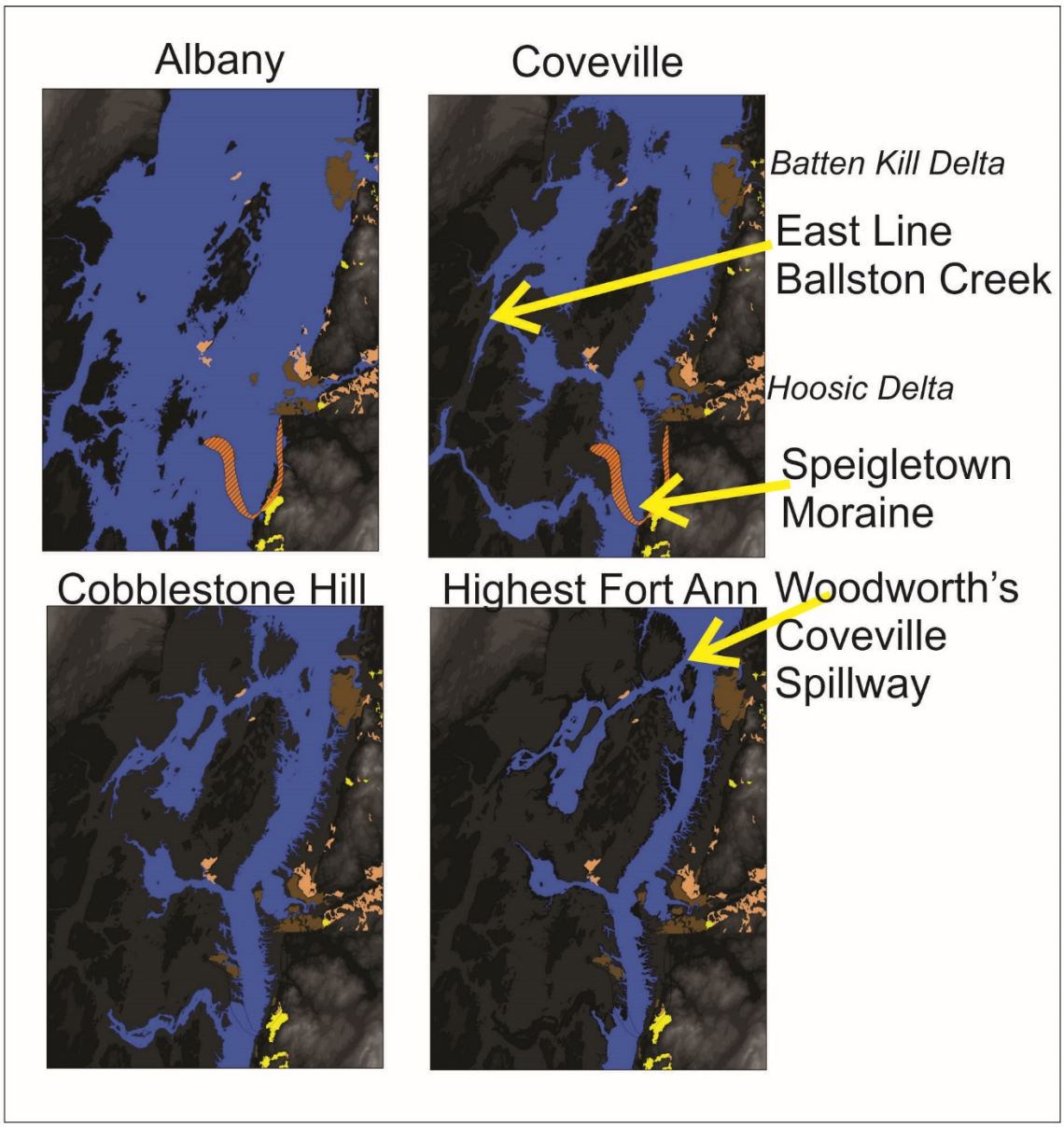


Figure 2: GIS models of lake levels in the Hudson Valley between Glens Falls and Troy. Mapped surficial geology from Schock (1963) and DeSimone (2016). Representation of the original full extent of the Speigletown kame moraine complex is estimated for Albany and Coveville levels.

Care must be taken, however when mapping lacustrine sediments in the Hudson and Champlain valleys to note the elevation, position in the valley, and relation to ice margin indicators before assigning the deposit to a level

of Lake Albany or Lake Vermont. Glacial ice either behaving as a lobe around an upland, or melting in the uplands before the lowlands, is likely to trap meltwater in the lateral upland valleys as an isolated smaller and higher elevation glacial lake (cf. Franzi et al, 2016). These smaller lakes, dammed from the main valley by ice and controlled by local thresholds, may be significantly large, deep, and long lived to produce lacustrine features similar in scale to what might be expected by the main valley lake at that location. These lacustrine deposits will eventually be incised when the ice dam melts away but a significant area of stranded lacustrine deposits are likely to remain. The result in the Hudson and Champlain valleys is that those lacustrine deposits will pre-date the main valley deposits immediately adjacent, and the shoreline elevations will be higher, due to the local threshold.

## ICE MARGIN INDICATORS

We might conveniently distinguish between ice margin indicators typically found in upland tributary regions from the Hudson-Champlain lowlands. In the uplands, mapping ice margins often relies upon recognition of kame moraines, heads of outwash, kame deltas and less common till moraines. Identification of ice margins across the interfluves between tributary valleys has traditionally been much harder. However, the advancement in the use of Lidar hillshade maps has made inroads and turned often problematic correlations between tributaries into more confident correlations (Barclay, 2018). Kame moraines have been most helpful in the region adjacent to the middle Hudson lowland of this trip. Indeed, the term kame moraine was defined by Taylor (1903) during his mapping of the Hoosic River drainage basin in the early decades of the 20$^{th}$ century. Kame moraines have been more frequently identified than other upland ice marginal deposits in the Taconic Highlands and southwestern Vermont.

Hudson-Champlain lowland ice margins are most readily identified by kame deltas sourced from subglacial meltwaters that may be preserved isolated on the lowland floor surrounded but not completely buried by deeper water fine grained lacustrines. As an example, Schock (1963) mapped the Troy North 7.5 minute quadrangle and identified 2 adjacent kame deltas with different topset elevations. Kame moraines and kame terraces deposited along the junction of the lowland and uplands are another example of ice marginal deposits mappable in the Hudson lowland. LaFleur (1965) mapped these through the Troy 15 minute quadrangle along the shoreline of Lake Albany. Schock also mapped a portion of a now recognized kame moraine-kame terrace complex that is Stop 6 on this field trip. The largest mappable band of kame moraine in the field trip portion of the Hudson lowland is the Glen Lake kame moraine, a complex deposit that likely formed as the ice margin fronting Lake Albany receded over time while holding steady at the kame moraine (Connally and Sirkin, 1969; DeSimone & LaFleur 2008). Tributaries feeding from uplands into the lowland glacial lakes may have deposited a delta against a receding ice front but recognition of the ice marginal component of the delta may be difficult especially after the delta has been incised due to lowering lake levels. The ice marginal component may no longer be recognizable as a portion of the landscape but can only be found through stratigraphic analyses.

## ICE MARGIN AND LAKE LEVEL HISTORY

Early Lake Albany levels and thresholds in the southern and mid-Hudson valley are complex and have been most recently investigated by Stanford (2009). He suggested that early lake Albany was dammed by a moraine at the Hudson Narrows between Staten Island and Brooklyn sending discharge into Long Island Sound controlled by a bedrock exposure at Hell Gate in the East River. When ice retreat reached Kingston, NY about 150 km north, catastrophic drainage of the upland glacial Lake Wallkill (cf. Peteet et al., 2009) breached the moraine causing incision into the moraine and lake bottom resulting in an unstable threshold that worked its way north creating progressively lower levels of Lake Albany. He suggests that this would have been relatively fast initially, but later limited by marine incursion into the valley during the late stages of Lake Albany and the early stage of Lake Vermont. Previously, LaFleur (1979, NYSGA trip) suggested the uplifting lake bottom may have controlled Lake Albany. The relative rates of sea level rise and differential isostatic adjustment would have induced continued incision until Lake Vermont stabilized in the bedrock threshold at Fort Ann, NY.

This study will incorporate only glacial lacustrine levels from measured strandlines between the confluence of the Hudson and Mohawk Rivers at Cohoes, NY and Canada. All strandlines were measured using GPS for

surface location and barometric altimeter for elevation. [Some data previously published in Rayburn (2004), DeSimone (2006) and DeSimone et al. (2008).] In Figure 3, all strandlines at elevations that suggest levels of Lake Albany are colored blue with the lowest in black. All strandlines suggesting levels of Lake Vermont are in orange. The highest elevation Champlain Sea strandlines are in green. All strandlines that can be shown to correspond to isolated higher elevation lakes, or are of uncertain origin, are identified as "other". The levels are correlated with a best fit linear function.

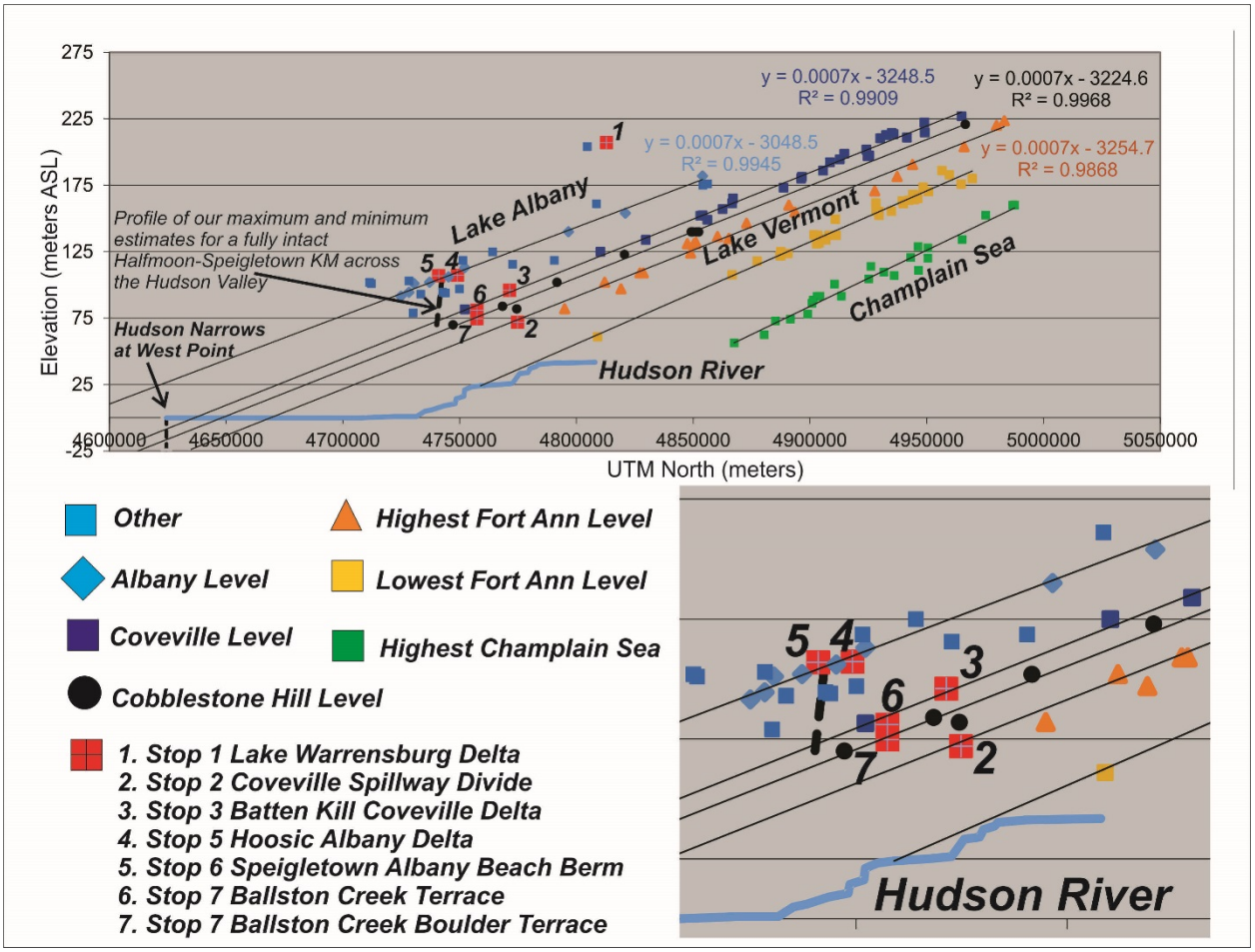


Figure 3. Glacial lacustrine strandline data with best fit linear trend lines to the major levels. Strandlines discussed in field stops are identified in red.

The data suggest that the highest Lake Albany level in the northern Hudson Valley is likely controlled in the southern Hudson Valley and may have been stable until the ice margin reached into the southern Champlain Valley. The northern most data point is the Forestdale, Vermont delta as originally mapped by Chapman (1932). At this location there may have been a significant lake level drop and grounding of the ice margin given the very large and clearly ice contact deltaic deposits on the Coveville Level at Street Road, NY and Brandon, VT. A projection of the Coveville level down-valley reaches the bedrock narrows of the central Hudson Valley at West Point, NY. There may have been a relatively stable threshold at/near this location because the Coveville level was stable for more than 300 years (Gonda & Rayburn, 2018). The next level below the Coveville level is the Cobblestone Hill level and may be associated with the Lake Iroquois flood along the ice margin at Covey Hill on the New York-Quebec border that redirected Lake Iroquois discharge from the Mohawk River valley to the northern end of Lake Champlain (Rayburn et al., 2005, 2011; Franzi et al., 2016). A prominent boulder bar at the Altona Flatrock north

of Plattsburgh, NY confirms an immediate lake level drop associated with this catastrophic flood event (Rayburn et al., 2005).

Neither the Coveville level nor the Cobblestone Hill level, however, can be traced as far south as the Mohawk River confluence. In fact it has been demonstrated that base level for the Mohawk River must have been at the Hudson River channel while it still produced discharge from glacial Lake Iroquois (Wall *in* DeSimone et al., 2008). The knick point of Cohoes Falls at the distal end of the valley is graded to the Hudson River channel and has migrated more than 2 km up valley, yet the modern day Mohawk River discharge does not appear to have eroded the soft shale/graywacke mélange knick point during more than 250 years of human observation (Wall i*n* DeSimone et al 2008). Wall (1995) calculated the paleodischarge of the IroMohawk River. Therefore the threshold for the Coveville level must be north of Cohoes, NY. Given that the southernmost identified Coveville strandline is along the Hoosic River, this limits the geographical area for the threshold to a few quadrangles between the Hoosic and Mohawk Rivers.

It is apparent that following the Lake Iroquois outburst flood, the lake level was very unstable and likely incised through the glacial and lacustrine sediment filling the valley as it fell through the Cobblestone Hill level and through multiple "Fort Ann" levels. Note that only the highest (dark orange) and lowest (light orange) Fort Ann level strandlines are shown in Figure 2. The channel called "The Cove" at Coveville, which Chapman (1932) had suggested was possibly the Coveville level threshold is actually at Fort Ann level and may likely be a remnant of this incision in the soft mélange bedrock or of some flow out of the Saratoga Lake basin region. It's not until the threshold migrates to the stronger crystalline Precambrian rock at Fort Ann, NY does it stabilize and remain constant until the ice margin exposes a direct route to the sea through the St. Lawrence (Rayburn et al., 2005; Franzi et al., 2016).

## MOHAWK DISTRIBUTARY CHANNELS

If the northern Hudson Valley was sufficiently dammed by a huge kame moraine between Halfmoon and Speigletown, then discharge from the Coveville level would have to be up along the east or west flanks of the valley (Fig. 2). One likely possibility is a series of channels on the west side. These channels include the Ballston Lake Channel and Round Lake, Drummond Creek Channel, and the Kayderosseras Creek Channel. Although these channels had originally been suggested to be distributary channels for the IroMohawk River (Fig. 4; Stoller, 1911), it is conceivable that they could be later used in the reverse flow direction for Coveville level discharge. The elevation of the highest point of these channels at East Line, NY could, within measurement error, serve as a threshold for the Coveville level. For this to be true, there should be evidence to support this reversal of flow, and exposure of a sufficiently stable rock outcrop at the threshold elevation. Field investigation confirms the findings of Stoller (1911) suggesting that these channels we formed by discharge coming from the Mohawk River. No bedrock other than the soft mélange composed of shale with very little greywacke was found in the channels. The abundant stream terraces cut into the bedrock of the Ballston Creek channel between the Lake Albany the modern stream levels indicate that these channels incise rapidly and easily with falling base level (see Stop 7).

Falling Albany waters toward Coveville through levels previously identified that were not likely stable lakes such as Albany II and Quaker Springs may have contributed the lowering base level needed to initiate this erosion. This is a brief window of time when features lower than Albany but higher than Coveville form. The East Line to Anthony Kill and Drummond Kill to Fish Creek erosion may have occurred as base levels fell ***below*** Coveville but ***before*** the IroMohawk flow completely subsided. We traditionally envision that turning the Iromohawk off as if with a switch with flow going to the Champlain lowland and that event triggered the breach of the Coveville dam. Yet, must this be a cause and effect occurrence? Might the Coveville dam have been breached by IroMohawk flow and for a time the lake level lowered as the lake floor was incised…much the same as Stanford envisions for Lake Albany. The distributary channels formed as flow used all of the distributary channels - Stoller was correct for the most part. Then, the level stabilized at Cobblestone Hill but that was really only an interim when flow switched off the IroMohawk. Continued erosion of the lake floor to a stable Fort Ann level ensued controlled by hard bedrock.

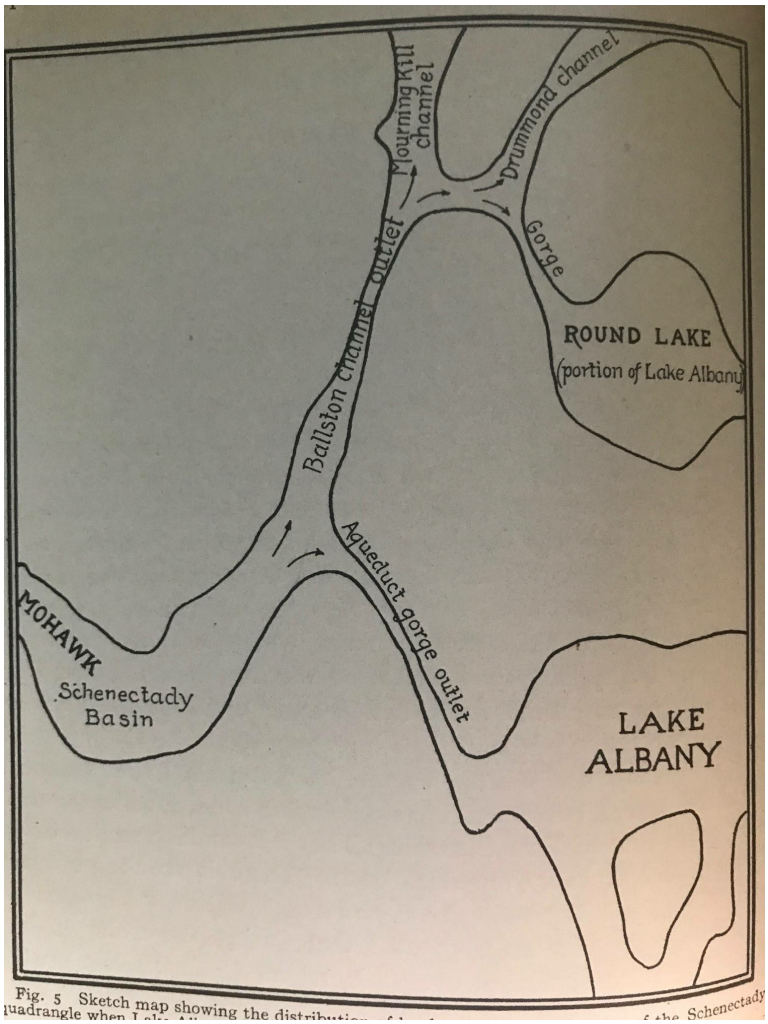


Fig. 5 Sketch map showing the distribution [illegible] quadrangle when [illegible] of the Schenectady

Figure 4. The IroMohawk distributary channels from Stoller (1911)

**ROAD LOG**

Assemble in the McDonald's parking lot west of Northway (Interstate 87) Exit 23 in Warrensburg. All roads for this trip are paved except for private drives into sand and gravel pits. This route is designed to be as efficient as possible between stops. Several alternate but more time consuming routes exist and provide a much better sense of regional geology, but our plan is to maximize discussion time at each stop.

**Mileage**

| | | |
|---|---|---|
| Start | | 3632 Main St. Warrensburg: Warrensburg McDonalds Parking Lot off Northway (87) Exit 23. |
| 0 | 0 | Right onto (West) US 9 |
| 0.3 | 0.3 | Left across Judd Bridge then Right onto River Street (NY 418) |
| 3.6 | 3.9 | Turn left to follow NY 418 |
| 3.0 | 6.9 | Park in pull-off on the left at the Thurman town line |
| End | | 5359-5377 Warrensburg Rd. Stony Creek |

**STOP 1: GLACIAL LAKE WARRENSBURG**

Along the upper Hudson between Luzerne and Warrensburg, the bluffs expose fine sand terraces, till, and bedrock. A few locations preserve elevated deltas and varved clays, in horizontal orientation and tilted large-scale

slump blocks. Glacial Lake Warrensburg was named and mapped by Miller (1911, 1914), who inferred a single long, narrow ice-dammed glacial lake that integrated lacustrine features from Corinth in the south (Stoller's 1916 moraine-dammed Lake Corinth) through Warrensburg and into the upper Hudson and Schroon valleys north of North Hudson (Lake Pottersville, Miller 1914), including the Paradox Lake valley east of Ticonderoga. Figure 5 shows Miller's 1925 general map of the paleo-lake extent (dashed line indicates a Hudson-Champlain ice margin). Lake Warrrensburg must be older than the terrace at the Luzerne ice margin (Hanson, 1977). We infer that Lake Warrensburg flooded the Hudson-Schroon Valley north of Luzerne for a brief ~few-century period, beginning with the ice blockage around ~15.3-15.1ka.

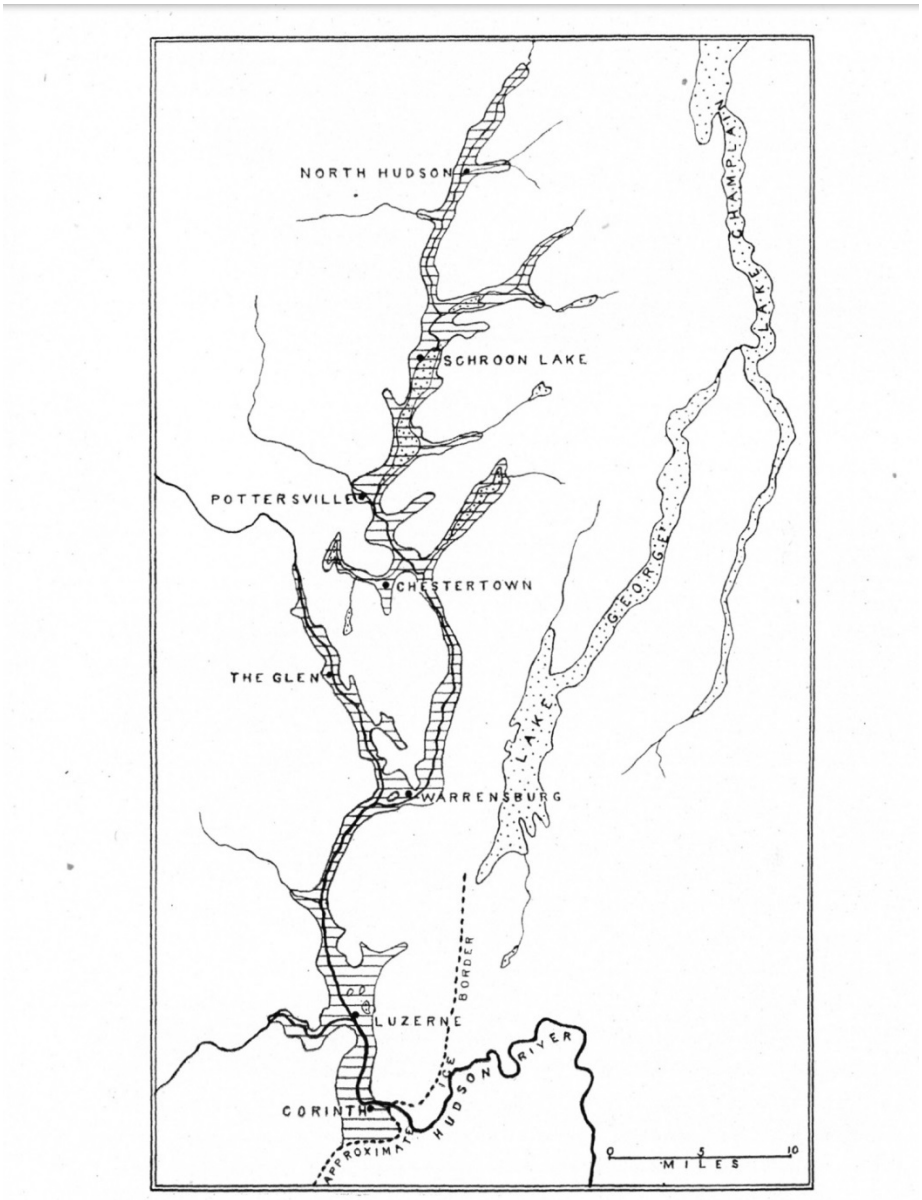


FIGURE 1.—*Map showing Extent of Glacial Lake Warrensburg*
The lined area indicates the location of the lake in southeastern Adirondack region of New York State.

Figure 5. Extent of Glacial Lake Warrensburg from Miller (1925)

Miller (1925) reports a graduated level of lacustrine deltas and sand plains, from 208 masl at Corinth to 300 m at Deadwater Pond about 110km to the north. He gives a slope estimate for the entire lake of 4.5 feet per mile, or

about about 1 m/1.16 km. Miller locates the lake outlet between the ice and the Palmertown range highland pass "cut by a stream of large volume" near South Corinth. When the ice front retreated past Corinth into the Lake George valley, the upper Hudson outlet eroded below 194m, shifting flow to the east at Corinth through the Hudson valley into Lake Albany, or down the Kayaderosserass to the Milton delta. Lake Warrensburg presumably drained by ~14.7ka to 14.8ka, during retreat of the ice blockade in the Bølling-Alleröd.

In 2011-12, 2015-16, and 2017-18, undergraduate teams in Amy Frappier's Honors *Paleoclimatology Practicum* course have investigated GL Warrensburg varves using a series of short Ridge-style cores from a horizontal varve deposit overlain by a flat massive fine sandy unit several meters thick. The overlying unit is very silty, coarsening-upwards, and contains a kettle bog. Recent field observations of the varve deposits in this area by R.H. Lindemann, Frappier and students, and John Rayburn, indicate that varves can be found in protected locations in the upper terraces, along the banks of the Hudson, and into the river channel. The varve deposits form characteristically steep slopes, and are prone to slumping where undercut by stream incision. Our discontinuous varve cores from our upper terrace site reveal large ~10cm-scale and small ~1-2cm-scale varve sequences (Brill et al., 2012; Nolan et al., 2018). At least one low-sedimentation rate period a few decades in length occurring between ~1-decade-long intervals when annual deposition was higher (Khan et al, 2016). The data are insufficient to determine whether this general sequence relates to glacial melting directly, or to hydroclimate fluctuations at regional or watershed scale that may integrate glacial melting and postglacial sedimentary redistribution processes. Longer, more continuous varve records from this and other sites in the lake basin may help to resolve this and other questions related to deglaciation of the upper Hudson Valley.

Figure 6: John Rayburn investigates a tilted slump block with a Glacial Lake Warrensburg varve sequence incised by the Hudson River. Erosion of the outcrop has accentuated the grain-size contrast, revealing larger, possibly annual-scale summer layers, and smaller-scale sub-annual events.

Rock flour, silt, and fine sand deposited in Lake Warrensburg was most likely sourced, at least in part, from valley glacier outwash in the adjacent Adirondack highlands, rather than solely from the Laurentide ice sheet. This suggests that GL Warrensburg varve sequences are likely to reflect high-altitude local conditions in the upper Hudson/eastern Adirondack region, particularly in the southern and western Hudson parts of the paleo-lake basin. Whether these varve sequences can be successfully cross-dated to the NAVC remains to be seen, but recovering longer sequences are essential (Nolan et al, 2018). Varves in the tilted slump block (Fig. 6 above) provide a promising target for future work, and additional field scouting further north may reveal additional sites where varves are preserved, including sites with the potential for local pro-glacial conditions that may be sensitive to larger-scale Laurentide ice dynamics. The differing sensitivities of the southern/western and northern/eastern reaches of Glacial Lake Warrensburg present opportunities for future investigations of this interesting interval of deglaciation in the eastern Adirondacks.

En route to Stop 1, we pass by a typical elevated sand terrace in Warrensburg at ~720 ft (Fig. 7). Stop 1 offers roadside access to a Lake Warrensburg delta perched on the Western flank of the Hudson Valley. Topset beds with rounded river cobbles evident in the upper section are mostly obscured by grain flows down the exposed section. The delta clearly exposes tilted foreset beds (Fig. 8). Their southerly dip indicates flow from up-valley, rather than from a lateral tributary. Known varve exposures found below the sand unit outcrop just 1km downstream on the eastern side of the Hudson in the lee of a riverbend, but are not accessible by car. Split varve cores will be available for inspection along with the exposed delta, as we discuss the emerging picture of how Lake Warrensburg fits into the regional deglaciation history.

Figure 7: Lake Warrensburg sand terrace on the west side of the Schroon River Pond dam.

Figure 8: Foreset beds dipping southwest (left) and bottomset beds (right) in the Lake Warrensburg delta terrace at the Thurman town line.

**Mileage**

| | | |
|---|---|---|
| Start | | |
| 6.9 | 6.9 | Retrace route to Warrensbrug McDonalds |
| 0.1 | 7 | Continue to intersection with Diamond Point Rd and turn left. |
| 0.1 | 7.1 | Turn right onto 87 South |
| 15.5 | 22.6 | ***Northway Rest Area for optional restroom stop*** |
| 7.6 | 30.2 | Take Exit 16 to Ballard Rd |
| 0.2 | 30.4 | Turn left (East) onto Ballard Rd. |
| 2.1 | 32.5 | Continue across Rt. 50 following Taylor, Coldbrook, and Rugg Rd. |
| 3.3 | 35.8 | Keep Right onto NY 32 South |
| 3.3 | 39.1 | Turn Left onto Co Rd. 42 (Lock 5, Hudson Crossing Park) |
| 0.3 | 39.4 | Turn right into Parking area |
| End | | County Rd. 42, Schuylerville - Hudson Crossing Park |

**STOP 2: THE COVE AT COVEVILLE**

Woodworth suggested that the fully prograded Batten Kill delta into the Hudson Valley may have dammed lower lake levels, forcing discharge through the uplands onto the western uplands (Fig. 2). The flow would therefore have been forced between Bacon Hill and Northumberland and across a divide into the Fish Creek channel at Grangerville (Fig 9). From there it would follow the channel to Victory Mills, but then continue southeastwards and re-enter the Hudson Valley at the rock ledge at The Cove. His justification for this morphology is that "*The cove at Coveville in its relation to this hanging valley shows clearly that a large stream at one time flowed southward over*

*the wall of the gorge at this place into the main gorge of the Hudson river, and was arrested after a slight amount of cutting had been accomplished*". Chapman (1932) sites Woodworth (1905), and further states that "*At Coveville, where the southern end of this channel overhangs the Hudson River by more than a hundred feet, is a rock ledge which acted as the controlling threshold for the waters during the Coveville stage of Lake Vermont*".

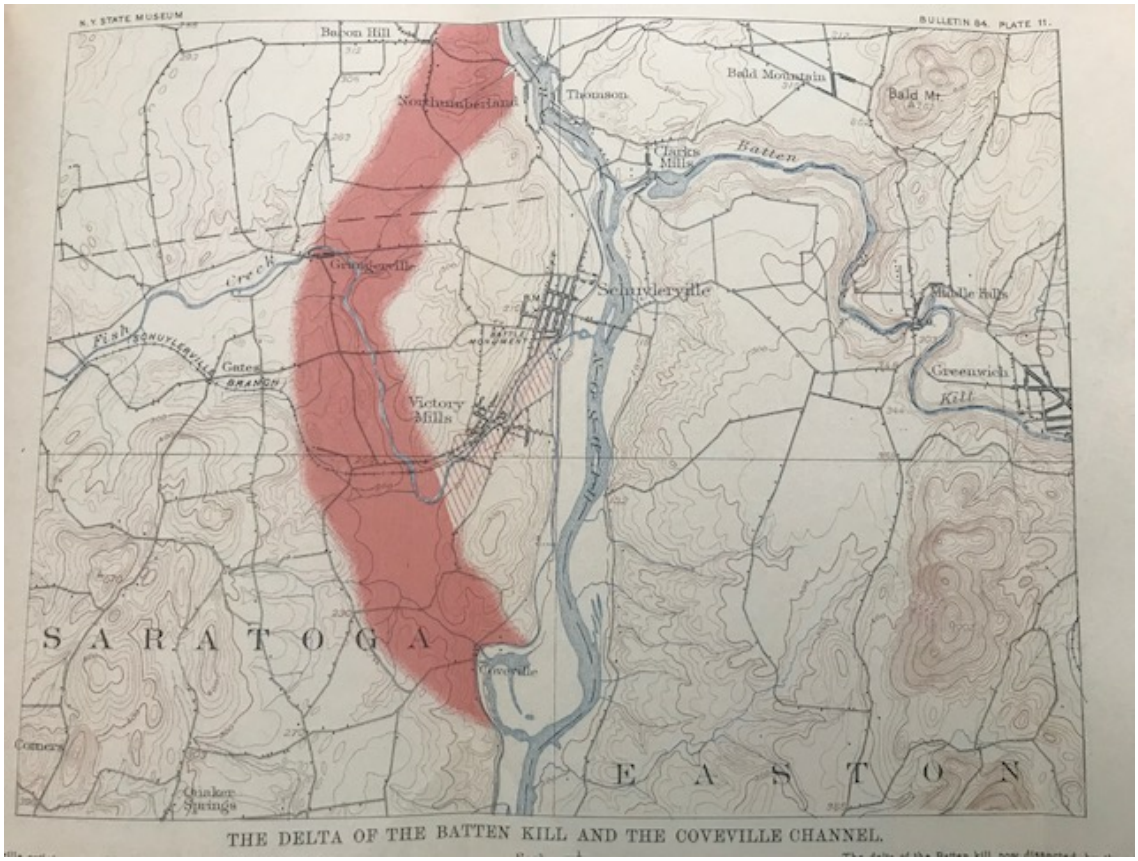


Figure 9. Proposed Coveville Spillway around the Batten Kill delta valley fill from Woodworth (1905)

There are several circumstances which strongly argue against the Coveville threshold being located in any part of this channel, however. The primary observation is that no part of this channel is at the Coveville elevation level. The highest modern divide elevation just off Grange Hall Road correlates to the highest Fort Ann level (Fig 3), and The Cove incision is only a little lower than the lowest Fort Ann level. Secondly, the bedrock type along the channel path is not sufficiently strong to have held up to steady state Coveville phase discharges. While some rock at the northern end of the channel is allochthonous (Starks Knob, for example), the primary rock type through the rest of the area is a weak shale that demonstrates significant incision in equilibrium with modern base level and discharges. Since the Coveville stage remained constant and steady for hundreds of years until the catastrophic discharge associated with the breakout of Lake Iroquois at Covey Hill, the threshold for this lake must be elsewhere. The formation of Woodworth's channel was more likely caused quickly by lake levels falling below the Coveville level with abandonment occurring as the discharge more easily cut through the Batten Kill delta and lacustrine deposits in the main Hudson channel. The Cove itself may just be an abandoned meander bend formed by Fort Ann level discharge through the valley.

**Mileage**

| | | |
|---|---|---|
| Start | | |
| 0.3 | 0.3 | Retrace route to NY 32 (US 4) and turn left (South) |
| 0.8 | 1.1 | Turn left onto NY 29 |
| 2.3 | 3.4 | Turn left into parking lot of The Ice Cream Man |
| End | | 417 NY 29, Greenwich |

**STOP 3: BATTEN KILL DELTA**

One of the most well preserved deltaic landforms can be seen where the Batten Kill joins the Hudson River across the valley from Schuylerville. An excellent road traverse is to follow Rte 29 east from Schuylerville. Once across the Hudson River, the road rises moderately and climbs from bottomset beds through foreset beds to a large, delta topset flat. Minor drainage ditch exposures reveal the sediment of the delta that generally fines upward and reflects the pro-gradational nature of the landform. In 2008, the FOP trip (DeSimone et al., 2008) visited an active sand and gravel pit in the topsets and upper foresets but that pit is now long closed and well vegetated. A walking traverse along Windy Hill Road would give students an opportunity to follow the delta fore-slope and examine the sediment in drainage ditches.

An altimeter determined elevation of the topsets places them at 96m (315ft) correlating to the Coveville lake level (Fig. 3). Woodworth first recognized this beautiful delta does not fall on a Lake Albany water plane. Subsequent detailed surficial mapping by DeSimone confirmed Woodworth's placement of the delta on a lower lake level. The important factor here is that Woodworth first had the foresight to recognize a major delta was correlative to a lake level lower than Albany. A short distance farther east in Greenwich there is a remnant of a higher deltaic surface that records deposition in a 115m (380ft) lake, a level that would place it on an Albany II water plane. This is the highest deltaic surface recognized from mapping along the Batten Kill and it does not fall on the highest level of Lake Albany as correctly noted by Woodworth. Either a higher delta has been removed by erosion or Lake Albany lowered before ice retreat opened the Batten Kill valley.

**Mileage**

| | | |
|---|---|---|
| Start | | Retrace route to NY 32 |
| 2.3 | 2.3 | Turn left (South) onto NY 32 (US 4) |
| 0.2 | 2.5 | Turn left to follow NY 32 (Horicon/Gates Ave) |
| 2.6 | 5.1 | Turn left onto Hathaway Rd. |
| 1.3 | 6.4 | Turn left onto Coveville Rd. |
| 0.6 | 7 | Turn right (South) onto US 4 |
| 4.3 | 11.3 | Turn right onto Phillips Rd. (Saratoga National Battlefield) |
| 2.4 | 13.7 | Continue on Phillips/Saratoga National Battlefield Rd. to parking lot. |
| End | | Saratoga National Historic Park |

**STOP 4: THE SARATOGA NATIONAL HISTORIC PARK (Lunch Stop)**

The short drive from Route 4, the old Colonial river road, up along the Kroma Kill to the park visitors center basically followed a transect perpendicular to the river. We went from flood plain alluvium up through a thick deep water glaciolacustrine clay section deposited in Glacial Lake Albany at its different levels. The fine grained lake silt and clay is capped along the flat river bluffs by a thin layer of lake sand deposited in the shallower waters of the last true lake in this section of the valley, Lake Coveville. We ascended to the gently rolling terrain at the top of the road where we parked and are in an area of generally thin till with rock outcrop.

Your vista from the terrace and lawn of the visitors center embraces a wonderful perspective across the Hudson Valley that is the consequence of both pre-glacial bedrock erosion that established the general geomorphology and Pleistocene glacial erosion and deposition that left the valley infilled with sediment (Fig. 10).

Subsequent Late Pleistocene and Holocene erosion carved into the sediment and bedrock and left the landscape we see today.

Figure 10: Looking east across the Hudson Valley from the Saratoga National Historic Park

The underlying bedrock topography and the more obvious glacial geomorphology were responsible for the terrain over which the 2 Battles of Saratoga were fought in September and October 1777. A single image is provided here to summarize the impacts of the geologic history on the battles (DeSimone 2016) and both bedrock and surficial geologic maps of the 4 quadrangles encompassing the SNHP will be available to view and discuss during lunch (DeSimone 2015a, 2015b). The maps are digitally published and those interested in the data layers can find them from the National Park Service and/or see the notations at the bottom of both maps.

The generation of the two maps is the result of a long, eight-year desire that finally came about in 2014-2015. DeSimone represented the Vermont Geological Survey at a two-day meeting held at UMass in 2007 to discuss the status of mapping in regional Park Service properties. Bruce Heise and Tim Connors represented the National Park Service (NPS). When the SNHP came up for discussion, DeSimone volunteered that most of the park had already been mapped by students of Bob LaFleur during the late 1970s. Eric Hanson (1977, 1980) mapped in the Mechanicville, Schaghticoke and Quaker Springs quadrangles, Jack Dahl (1978) mapped in the Mechanicville and Schaghticoke quadrangles, and DeSimone mapped the Schuylerville quadrangle (1977, 1985). DeSimone suggested it should be an easy task to finish a map of the park. Fast forward to late 2014; Bruce and Tim contacted DeSimone to see if he was interested in doing the project. However, the surprise was they wanted a map of the 4 quadrangles, not just the park and there were little funds to do much, if any field work (Fig. 11). In early 2015, they indicated they also wanted a bedrock map of the 4 quadrangles. The result is the 2 maps you have to view. Both maps largely represent compilations with editing on DeSimone's part. Meshing the surficial maps together and field checking the contacts consumed nearly all of the allotted field time. Map units were re-designated in an updated fashion with some compromises and simplifications for clarity. Both printed maps were intended to be wall hangers for the SNHP staff and the text on the maps was intended to be educational to the non-geologist.

The bedrock map is work by Kidd, Plesch, and Vollmer (1995), Rickard (unknown date), Landing et al. (2003), Fisher et al. (1970), and a beautiful hand colored map of the Schuylerville 15-minute quadrangle attributed

by Rickard to Reudemann (unknown date). My role was to compile and edit the data, merge and extrapolate contacts and convert map units in older terminology to those of Kidd et al (1995). DeSimone chose to add pre-glacial bedrock channels to this map using data from Dineen and Hanson (1983) and Bruehl (1969) with extensions from both data sources.

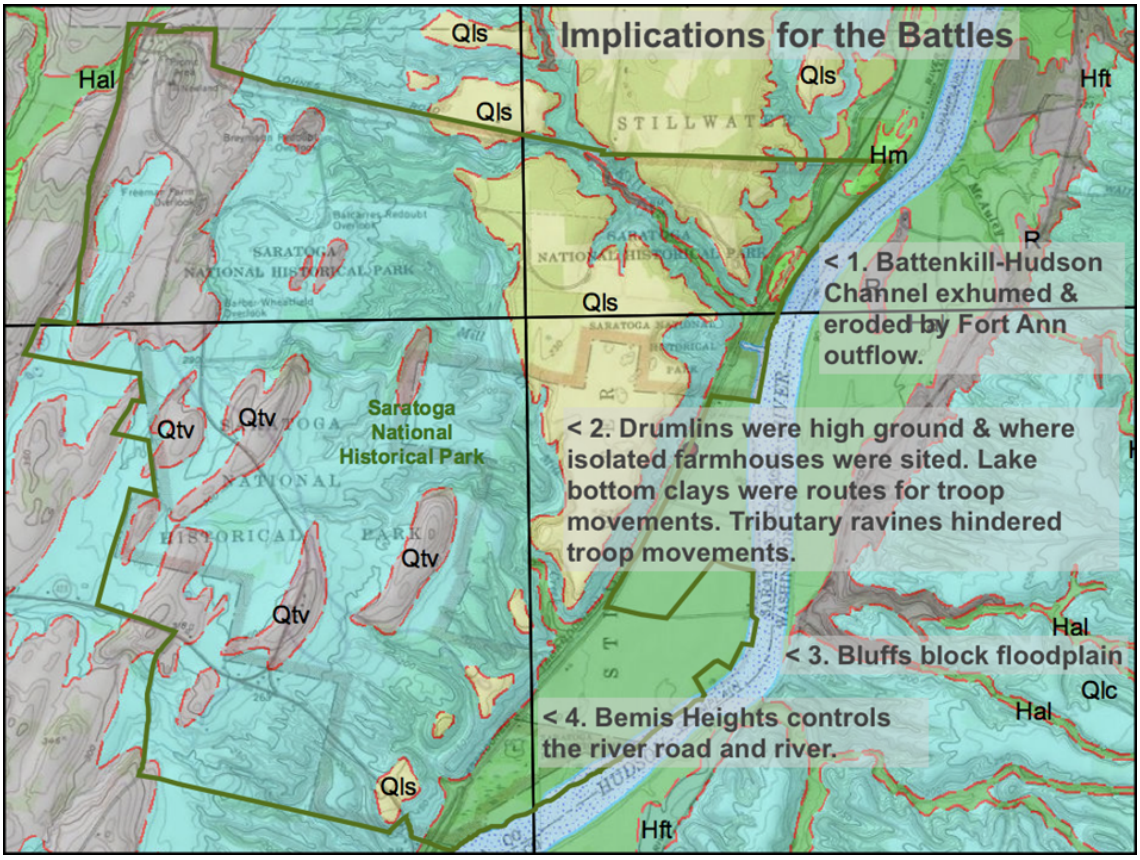


Figure 11. The geology had a hand in dictating the battle tactics.

The lunch view has the gently rolling to sloping till terrain of the visitors center giving way to the clay flats that were farm fields in 1777. The park has tried to maintain the vegetative cover as close to what it was during 1777. The Hudson Valley Lake Albany shoreline is both in the near distance and in the middle distance across the valley where the land slopes up abruptly into the Taconic highlands with the highest summit in view being Willard Mountain, a local ski area. That break in slope approximates the Lake Albany shoreline and follows Route 40 where we'll drive after lunch. The track of Route 40 also largely coincides with the trace of the Taconic Frontal Thrust or TFT as seen on the bedrock map. On a clear day, the view extends into the far distance where the summit ridge of the Green Mountains is visible.

**Mileage**

| | | |
|---|---|---|
| Start | | Retrace route to US 4 |
| 2.4 | 2.4 | Turn right (South) on US 4 |
| 4.9 | 7.3 | Turn left onto Stillwater Bridge Rd. (Rt. 125) |
| 4.7 | 12 | Turn right onto Main St. (Rts. NY 40 & 67) |
| 1.5 | 13.5 | Turn right onto Farm to Market Rd. (NY Rt. 67) |
| 1.1 | 14.6 | Turn at gravel pit entrance |
| End | | 895 Farm to Market Rd., Schaghticoke |

**STOP 5: HOOSIC DELTA**

The Hoosic River and the Batten Kill are two large Hudson River tributaries that drain the Taconic Mountains along the east side of the valley. From the Batten Kill, we proceeded south along Rte 40 following the shoreline of Glacial Lake Albany and also largely following the trace of the Taconic Frontal Thrust or Emmons's Line. A very distinct lowland to upland break in slope is present.

We continued south to the junction of Rte 40 and Rte 67W and turned west to head back toward the Hudson River. We drove across several of the four readily distinguishable deltas of the Hoosic River deposited into different glacial lake levels. Each succeeding delta breached the older, higher delta. The expression of the deltas as landforms is harder to discern. However, this trip stop lets you see some deltaic sediment stratigraphy. There are two pits across the road from each other and at the time of this writing, we cannot know for certain which pit we can get access to on the day of the trip. Both pits are fairly small and if they are working in them, there will be no permission granted.

The sediment exposed is largely medium to fine sand with predominantly horizontal thin beds, some ripple laminations and no evident ice contact deformation. The sand beds are overlain by variably thick pebble gravel beds with medium to coarse sand. The pebble gravels are cross bedded with some cut and fill structures. The pebble gravels truncate the underlying sand beds. At the smaller pit on the north side of Rte 67, the gravel beds are thin and some of the topsoil has been removed from the exposed face. The original thickness of the gravel facies cannot be determined. At the larger pit on the south side of Rte 67, the gravel facies appears to be intact in the high wall of the pit beneath the more mature vegetation. Here, the pebble gravel facies is approximately 2m thick.

The elevation of the flat top of the landform in the south side pit is 107m (350ft) using the topographic map spot elevation. The pit has been excavated into an isolated terrace within the 107m (350ft) Hoosic delta (Fig. 3). The north side pit was excavated into a lower 98-99m (325ft) Hoosic delta. The largest preserved fragment of the Hoosic deltas has an extensive topset plain between the 113-118m (370-390ft) elevations. A lower terrace of the Hoosic River that may be deltaic lies at 82m (270ft).

**Mileage**

| | | |
|---|---|---|
| Start | | Retrace to route to NY Rt. 40 |
| 1.1 | 1.1 | Turn right (South) on NY Rt. 40 |
| 5.7 | 6.8 | Turn right at gravel pit entrance |
| End | | 449 NY 40, Troy |

**STOP 6: SPEIGLETOWN KAME MORAINE & STRANDLINE**

This large pit with multiple open excavations exists in the Speigletown kame moraine-kame terrace (Fig. 12). The entrance to the operation is from NY Rte 40. Route 40 follows the old Mahican Indian trail later used as a Colonial coach road. The road generally follows the eastern shoreline of Glacial Lake Albany. Along this route from the Batten Kill south to the Hoosic River and continuing south to the pit, your drive follows the glacial lake shoreline. The shore face is sometimes veneered with beach sand overlying finer grained sediments. The Fane pit began decades ago at the road level. The landform is a kame terrace here that caps bedrock sometimes visible in deeper excavations. Across the road from the pit entrance, shale bedrock is exposed. The depositional environment was that of a classic kame terrace deposited between the Hudson-Champlain ice and the valley wall. The deeper parts of the pit reveal sedimentation from subglacial meltwaters that represent an esker distributing sediment into a subaqueous fan. There are remnants of ice contact sand and gravel deposits that can be seen north of Rte 142, west of Rte 40 and continuing down to toward the Hudson River in Pleasantdale. However, these are not shown on the 1963 surficial map of Schock. Mr. Fane reports hunting along trails leading down to the river and finding a large area of gravel buried by the silt-clay. In contrast, the kame terrace likely received sediment from a meltwater and meteoric water stream following the ice margin. Indeed, some of the sediment may be from the Hoosic River to the north as ice still blocked the river outlet.

Figure 12. Sands and gravels from large flow events along the east valley wall.

Beach sand and even pebble gravel caps the sequence and will be our first vantage point in the pit along the power line. There is a pocket of silt-clay below the beach berm that may represent a small pond behind a sand spit. This is one of the finest sections of Lake Albany beach preserved in a still rural setting. Look across to the road bordering the south face of the pit and you can see the beach profile. The berm here is exceptionally high and this appears to be a natural feature, not built up at all for the power line construction.

Wander to the deepest excavations in the pit. Excavations have reached bedrock at least locally capped with a veneer of till. Ground water seeps out along the base of the gravel and sand as further downward infiltration of ground water is inhibited by the comparatively impermeable till and bedrock. The deeper portions of the pit reveal subaqueous fan sand and gravel. Previously, we could observe arched anti-form bedding from a classic esker. Finer grained lacustrine sediments have an on-lap relationship to the ice contact sediments indicating the quieter water facies were deposited after retreat of the ice removed the source of the proximal gravel and sand facies. One can think of the subglacial meltwater source as a fire hose discharging water and sediment from beneath the glacier into the bottom of Lake Albany. The point source of sediment deposits coarse grained sediment in one locale while adjacent areas have finer grained sediment. The fire hose analogy works if you think of the hose spraying sediment first in one direction and then in another.

We'll work our way up section toward the east where the sediment is interpreted to have been cascading from the kame terrace environment into the deeper lake waters. Slope instabilities and debris flows must have been common. At any given moment, the pit face may show soft sediment deformation, load deformation and evidence of subaqueous sediment flows. Nearshore sediments in the higher parts of the pit truncate and overlie an ice contact facies composed of interbedded gravel and sand with typical ice contact deformation.

**Mileage**

| | | |
|---|---|---|
| Start | | Retrace route to Stop 5 |
| 6.8 | 6.8 | Follow NY Rt. 67 West through Mechanicville to Maltaville |
| 11.1 | 17.9 | At the second traffic circle take the first exit (North) onto US 9/NY 67 |
| 0.9 | 18.8 | At the following second traffic circle take the third exit (West) to follow NY 67 |
| 1.7 | 20.5 | Turn left onto East Line Rd. |
| 0.5 | 21 | Turn left into Shenantaha Park entrance |

| | | |
|---|---|---|
| 0.3 | 21.3 | Turn into Parking Lot |
| End | | 3 Horseshoe Bend, Ballston Spa |

**STOP 7. BOULDER MORAINE & LAG TARRACE IN BALLSTON CREEK CHANNEL AT SHENANTAHA CREEK PARK**

This last stop takes us to the Shenantaha Park on the Round Lake quadrangle that was most recently mapped by Hanson (1977b). A possible alternative to the Fish Creek/Coveville channel as a threshold and discharge channel for the Coveville level is a drainage divide at East Line between the Morning Kill, Drummond Creek, and Ballston Creek. Besides being at an elevation consistent with the Coveville level it would provide a threshold and drainage network that would effectively control the Coveville level if the main Hudson Valley were dammed between Speigletown and Halfmoon (Fig. 2). This network together with the Ballston Lake channel is all part of the Mohawk distributary channel network and may have been earlier formed in equilibrium with both northward discharge from the IroMohawk as well as southward discharge from glacial Lake Warrensburg. Early investigation of this system was published by Stoller (1911) who inferred that: "*A flood of waters once swept northward through Ballston channel, dividing in the vicinity of East Line into three currents which pursued the several courses described above. The time in glacial history when this took place was subsequent to the general disappearance of the ice and also subsequent to the stage of maximum development of Lake Albany*" (Fig 4). Stoller (1916) recognized the southern end of a lake that he named Lake Corinth that the Hudson River drained via Kayderosseras Creek southward into Lake Albany forming the Milton delta (Fig. 13). However at 125m (410ft) it is significantly above the Albany water plane (Fig 3) and may actually represent a separate higher-elevation ice marginal lake.

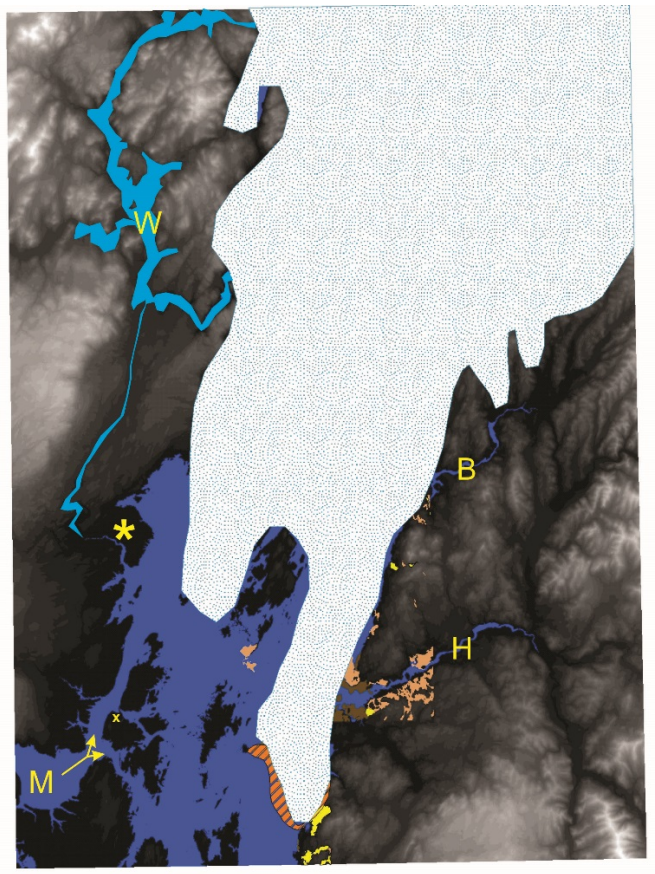


Figure 13. GIS model of Lake Albany level with the ice margin at Speigletown and Lake Warrensburg discharge forming a delta at Milton. M: IroMohawk discharge into Lake Albany, W: Lake Warrensburg, *: Milton Delta, H: Hoosic Valley, B: Batten Kill Valley, x: Location of Stop 7. Representation of the original full extent of the Speigletown kame moraine complex in orange.

The much larger extent of Lake Corinth was recognized by Miller (1925) and renamed Lake Warrensburg (Stop 1), and that its existence must have been caused by ice damming the modern Hudson channel east of Corinth. It is possible that when the ice was farther south than depicted in Figure 13 the western region of the Hudson Valley including Milton and the distributary channels was confluent with a higher elevation glacial lake in the Mohawk Valley. Northward recession of the ice margin would subsequently drain this lake to Albany level allowing Mohawk Valley discharge directly into Lake Albany through the distributary channels. Eventual ice margin retreat to Glens Falls would open the modern upper Hudson channel to Lake Albany completely draining Lake Warrensburg.

For the distributary channels to form the threshold and drainage route for the Coveville level around the Speigletown moraine (Fig. 2) they would require flow southward through the Morning Kill and/or Drummond Creek channels, and/or westward drainage through the Ballston Creek channel to Ballston Lake to the Mohawk Valley. This would in turn necessitate that the IroMohawk flow directly eastward to the Hudson Valley through its modern channel at Cohoes rather than the distributary channels. It would also necessitate a bedrock exposure of significant strength to withhold steady state discharge from Lake Coveville. These conditions lead to a series of problems. First, like Woodworth's proposed Coveville outlet, the local exposed bedrock is a weak shale/greywacke mélange that demonstrates easy incision to base level even under modern discharge conditions. Second, like Stoller, we observe no southward flow indicators in the channels and only very strong eastward flow indications in the Ballston Creek channel. This includes an imbricated boulder terrace (also recognized by Stoller, 1911) near the head of the Ballston Creek channel that could only have resulted from strong eastward flow towards Round Lake (Fig. 14).

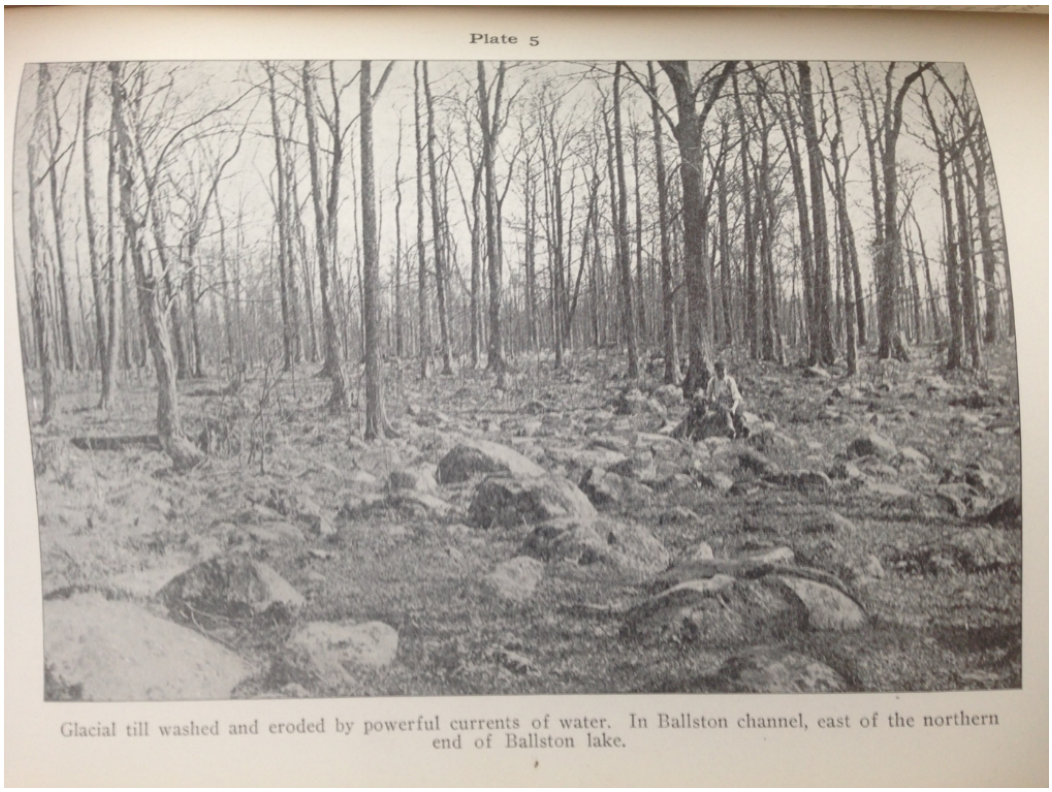
Plate 5

Glacial till washed and eroded by powerful currents of water. In Ballston channel, east of the northern end of Ballston lake.

Figure 14. Boulder terrace formed into a moraine near the head of the Ballston Creek channel. Imbrication indicates eastward flow through the channel towards Round Lake. (From Stoller, 1911)

On the positive side, however we have evidence that the IroMohawk must have been flowing directly eastward through the modern channel at least at the very end of the Coveville Phase. As stated in the introduction, the base level for Cohoes Falls which clearly migrated back through the shale-rich mélange from the Hudson Valley is at Hudson River level, and that discharges only on the scale of the IroMohawk could have caused this knick point

migration. This now under-fit falls is apparently frozen in time with the reversal of drainage of Lake Iroquois at Lake Iroquois into Lake Vermont causing it to drop from Coveville level to Cobblestone Hill and Fort Ann levels (Rayburn et al., 2005; Franzi et al., 2007; DeSimone et al., 2008; Franzi et al., 2016). Interestingly there are a number or terraces carved into the shale of the Ballston Creek channel ranging in elevation from Coveville level at the head of the channel Shenantaha Creek Park near East Line down to through the Fort Ann levels and below to the east, suggesting that this channel was at baseline equilibrium with Lake Albany and Lake Vermont (Fig 15). Also the imbricated boulder moraine surface along the creek at the edge of the park correlates to Cobblestone Hill level, suggesting that it may have been the Lake Iroquois breakout flood that caused the lagged surface in the boulder moraine and that flow was eastward into the Hudson Valley at this location.

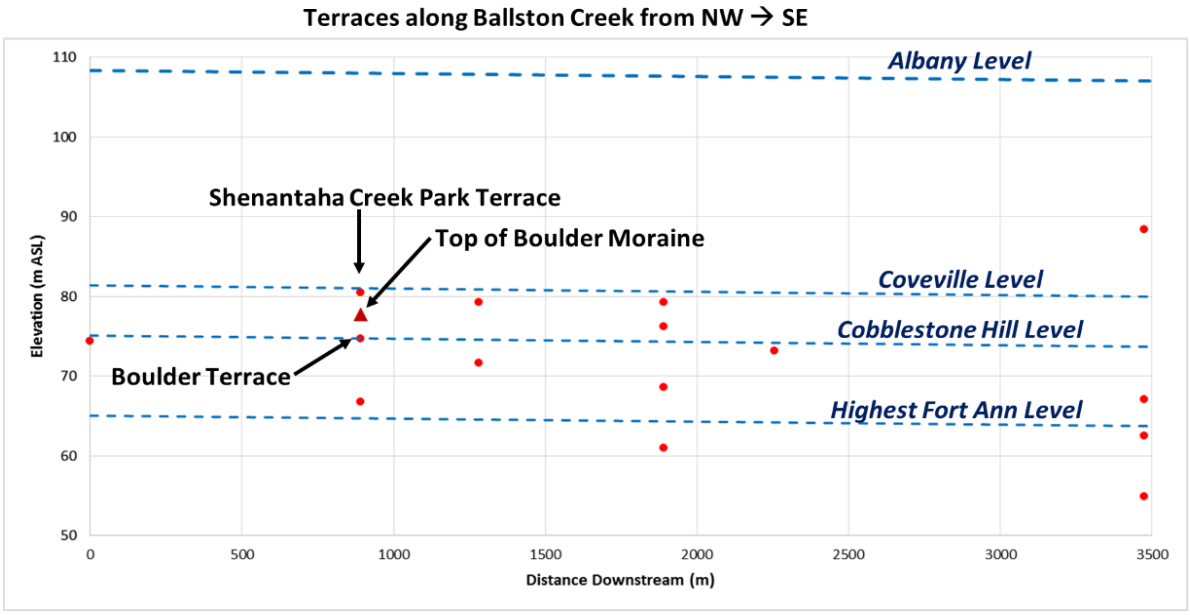


Figure 15. Altimeter determined elevations of terraces and the top of a moraine in the Ballston Creek channel compared with glacial lake levels in the Hudson Valley.

**ACKNOWLEDGEMENTS**

We would like to thank and acknowledge Eric Hanson and Gary Wall for their discussions and insights into the glacial geology of this part of the Hudson Valley. We would also like to acknowledge the geology students at Skidmore College who put so much effort into the exploration of glacial Lake Warrensburg.

**REFERENCES**

Antevs, E., 1922: The recession of the last ice sheet in New England. American Geographical Society Research Series 11, 120 pp.

Antevs, E., 1928: The last glaciation, with special reference to the ice sheet in northeastern North America. American Geographical Society Research Series 17, 292 pp.

Baldwin, S.P., 1894. Pleistocene History of the Champlain Valley. Am. Geol. 13: 170-184.

Barclay, D.J., 2018. Deglacial Ice Margins in the Finger Lakes Region of Central New York. Geological Society of America Abstracts with Programs. Vol. 50, No. 2, doi: 10.1130/abs/2018NE-311170.

Brill, M., Leverone, T., Loehr, C., Pinkey-Drobnis, A. D., and Frappier, A. 2012. Varve chronology from Glacial Lake Warrensburg: A preliminary study of a forgotten glacial lake near Warrensburg, NY. Geological Society of America Abstracts with Programs, Vol. 44, No. 2, p. 99, Abstract 41-4.

Bruehl, D. H., 1969. Bedrock topography of the Albany to Lake George area, New York: NY State Department of Transportation, open file 1:62,500 maps.

Chapman, D.H., 1932. Late Glacial and Post-glacial History of the Champlain Valley. American Journal of Science. 34: 89-124.

Connolly. G.G., and Sirkin, L.A., 1969. Deglacial history of the Lake Champlain-Lake George lowland: NYSGA Guidebook, 41st annual meeting, Trip I, 20p.

Cronin, T.M., Manley, P., Brachfield, S., Manley, T., Willard, D.A., Guilbualt, J-P., Rayburn, J.A., Thunell, R., Berke, M., 2008. Impacts of post-glacial lake drainage events and revised chronology of the Champlain Sea episode 13-9 ka. Palaeogeography, Palaeoclimatology, Palaeoecology, 262, 46-60.

Dahl, J., 1978. Surficial geologic map of the northern half of the Schaghticoke, NY, 1:24,000 quadrangle: NY State Geological Survey, open file map 2gk1296.1 .

DeSimone, D. J., 1977. Glacial geology of the Schuylerville quadrangle, NY: Rensselaer Polytechnic Institute, Master's thesis with 1:24,000 map.

DeSimone, D. J., 1985. The Late Woodfordian history of southern Washington County, NY: Rensselaer Polytechnic Institute, Doctoral dissertation with maps.

De Simone, D.J., 2006. Strandline features in the Hudson-Champlain region reveal water planes which tilt at 4.0 ft/mi: GSA Abstracts with programs, NE sectional meeting, March 2006.

DeSimone, D.J., 2015a. Bedrock Geologic Map of Saratoga National Historical Park and Vicinity, New York: National Park Service publication, map & text.

DeSimone, D.J., 2015b. Surficial Geologic Map of Saratoga National Historical Park and Vicinity, New York: National Park Service publication, map & text.

DeSimone, D.J., 2016. Surficial & Bedrock Maps of the Saratoga National Historical Park Generated for Archaeological & Educational Purposes: NE-GSA Abstracts with Programs, Mt. Washington, NH.

De Simone, D.J., and La Fleur, R.G., 1985. Glacial geology and history of the northern Hudson basin, NY and VT: NYSGA guidebook to field trips, trip A-10, p. 82-116.

DeSimone, D. J., and LaFleur, R. G., 2008. Deglacial history of the upper Hudson region: NY State Geological Association, Guidebook to Field Trips, 80th annual meeting, Trip 4, p. 35-56.

De Simone, D.J, Wall, G.R., Miller, N.G., Rayburn, J.A., Kozlowski, A.L., 2008. Glacial geology of the northern Hudson through southern Champlain lowlands: Friends of the Pleistocene, Guidebook to field Trips, 71st annual meeting.

Dineen, R. J., and Hanson, E. L., 1983. Bedrock topography and glacial deposits of the Colonie Channel between Saratoga Lake and Coeymans, NY: NY State Museum, Map & Chart Series #37, 1:62,500 maps.

Fairchild, H.L., 1917. Post-glacial features of the upper Hudson Valley. NYS Mus. Bull. 195, 22p.

Fisher, D. W., et al, 1970. Geologic map of New York, Hudson-Mohawk sheet: NY State Museum, Map & Chart Series #15, 1:250,000 map.

Franzi, D.A., Ridge, J.C., Pair, D.L., DeSimone, D.J., Rayburn, J.A., Barclay, D.J., 2016. Post Valley-Heads deglaciation of the Adirondack Mountains and adjacent lowlands. Adirondack Journal of Environmental Studies 21, 119-146.

Gonda, N.J., Rayburn, J.A., 2018. Cross-correlation of Glacial Lake Vermont Varve Sections in New York and Vermont. In: Program with Abstracts, Geological Society of America Northeastern Section Meeting, 2018.

Hanson, E.L., 1977a. Late Woodfordian drainage history in the lower Mohawk Valley: RPI MS thesis.

Hanson, E. L., 1977b, Surficial geologic map of the Round Lake, NY, 1:24,000 quadrangle: NY State Geological Survey, open file map 2100.384.

Hanson, E. L., 1980. Surficial geologic map of the Quaker Springs, NY, 1:24,000 quadrangle: NY State Geological Survey, open file map 2gk881.

Hanson, E. L., 1977, and Dahl, J., 1978. Surficial geologic map of the Mechanicville, NY, 1:24,000 quadrangle: NY State Geological Survey, open file map 2gk680.

Khan, T., Thieringer, P., Outterson, A., Bullis, C., Lovejoy, C., Mccully, E., Nitkin, E., Carames, J., Sidor, L., Kilgore, M., Ng-Yow, R., and Frappier, A. B. 2016. A continued analysis of the Glacial Lake Warrensburg varve chronology. Poster presentation 39-6. NEGSA Annual Meeting, 21-23 March, 2016, Albany, NY. Geological Society of America Abstracts with Programs. Vol. 48, No. 2. DOI: 10.1130/abs/2016NE-272619.

Kidd, W. S. F., Plesch, A., Vollmer, F. W., 1995. Lithofacies & structure of the Taconic flysch, melange & allochthon in the NY Capital District: NY State Geological Association, Guidebook to Field Trips, 67th annual meeting, p. 57-80.

La Fleur, R.G., 1979. Deglacial events in the eastern Mohawk-northern Hudson lowland: NYSGA Guidebook to field trips, 51st annual meeting, p.326-350.

La Fleur, R.G., 1965. Glacial geology of the Troy, NY, quadrangle: NYS Museum and Science Service, Map and Chart series #7.

Landing, E., et al, 2003. Tectonic setting of outer trench slope volcanism: pillow basalt and limestone in the Ordovician Taconian orogen of eastern New York: Canadian Journal of Earth Sciences, vol. 40, p. 1173-1187.

Miller, W.J., 1911. Preglacial course of the upper Hudson River. Bul. of the Geol. Soc. of Am. 22:185-186.

Miller, W.J., 1914. Geology of the North Creek Quadrangle, New York. NYS Mus. Bul. 170: 69-73.

Miller, W.J., 1925. Remarkable Adirondack glacial lake. GSA Bulletin 36: 513-520.

Nolan, K., Cristiano, J. Mundi, C., Casarella, D., Wall, B., Hudziak, S.X., Deutsch, E., Janigian, L., Frappier, A., 2018. Expanding the varve chronology: More preliminary results from Glacial Lake Warrensburg, Hudson Valley, NY. Geological Society of America Abstracts with Programs. Vol. 50, No. 2, doi: 10.1130/abs/2018NE-311170.

Peet, C.E., 1904. Glacial and Post-glacial Histories of the Hudson and Champlain Valleys. Jour. Geol. 12:415-469, 617-660.

Peteet, D., Rayburn, J.A., Menking, K., Robinson, G., Stone, B., 2009. Deglaciation in the southeastern Laurentide sector and the Hudson Valley – 15,000 years of vegetational and climate history - Trip 4; ; In: NYSGA Annual Meeting Guidebook, 2009, p. 4.1 - 4.18.

Rayburn, J.A., 2004. Deglaciation of the Lake Champlain Valley New York and Vermont and Its possible effects on North Atlantic climate change. Ph.D. Dissertation, Binghamton University, 158 p.

Rayburn, J. A., Cronin, T. M., Franzi, D. A., Knuepfer, P. L. K., & Willard, D. A. 2011. Timing and duration of North American glacial lake discharges and the Younger Dryas climate reversal. Quaternary Research, 75(3): 541–551.

Rayburn, J. A., Franzi, D. A., & Knuepfer, P. L. K. 2007. Evidence from the Lake Champlain Valley for a later onset of the Champlain Sea and implications for late glacial meltwater routing to the North Atlantic. Palaeogeography, Palaeoclimatology, Palaeoecology, 246(1): 62–74.

Rayburn, J. A., Knuepfer, P. L. K., & Franzi, D. A. 2005. A series of large, Late Wisconsinan meltwater floods through the Champlain and Hudson Valleys, New York State, USA. Quaternary Science Reviews, 24(22): 2410–2419.

Ruedemann, R., unknown date. Bedrock geologic map of the Schuylerville, NY, 1:62,500 quadrangle: NY State Geological Survey, open file map 1g1372.

Rickard, L. V., unknown date. Bedrock geologic map of the Schuylerville, NY, 1:62,500 quadrangle: NY State Geological Survey, open file map 1g1645.1 .

Schock, R. N., 1963. Geology of the Pleistocene sediments, Troy North quadrangle: RPI MS thesis.

Stanford, S. D. 2009. Onshore record of Hudson River drainage to the continental shelf from the late Miocene through the late Wisconsinan deglaciation, USA: synthesis and revision. Boreas, 39(1): 1–17.

Stoller, J.H., 1911. Glacial geology of the Schenectady quadrangle: NYS Museum Bulletin 154.

Stoller, J.H., 1916. Glacial geology of the Saratoga quadrangle: NYS Museum Bulletin 183.

Stoller, J.H., 1918. Glacial geology of the Cohoes quadrangle: NYS Museum Bulletin 215.

Stoller, J.H., 1922. Late Pleistocene history of the lower Mohawk and middle Hudson region: GSA Bulletin, vol. 33, p. 515-526.

Taylor, F.B., 1903. The correlation and reconstruction of recessional ice borders in Berkshire County, Massachusetts: Journal of Geology, vol. 11, p323-364.

Upham, W., 1889. Glaciation of the Mountains in New England and New York. Am. Geol. 4:165-174, 205-216.

Wall, G. R., 1995. Postglacial drainage in the Mohawk River Valley with emphasis on paleodischarge and paleochannel development: Doctoral dissertation, Rensselaer Polytechnic Institute, Troy, New York, 352p.

Woodworth, J.B., 1905. Ancient water levels of the Champlain and Hudson valleys: NYS Museum Bulletin #84, 265p.

# THE CHEEVER AND MINEVILLE IRON OXIDE-APATITE (IOA) DEPOSITS

Marian V. Lupulescu [1], Research & Collections, New York State Museum, Albany NY
Jeffrey R. Chiarenzelli [2], Dept. of Geology, St. Lawrence University, Canton NY
David G. Bailey [3], Geosciences Dept., Hamilton College, Clinton NY
Sean P. Regan [4], Dept. of Geology, University of Alaska, Fairbanks, AK
Jared W. Singer [5], Earth and Environmental Sciences, RPI, Troy, NY

E-mail address: [1]marian.lupulescu@nysed.gov; [2]jchiarenzelli@stlawu.edu; [3]dbailey@hamilton.edu; [4]sregan5@alaska.edu; [5]singej2@rpi.edu

## INTRODUCTION

The iron deposits of New York State were an important source for the U.S. iron industry during the nineteenth and twentieth centuries. The main component of the ore was magnetite; it was accompanied in some deposits by hematite, with gangue minerals such as feldspar, quartz, amphibole, and fluorapatite. Most of the medium-to high-grade magnetite ore was mined underground.

Iron mining in New York State has a long history. There are two main regions where iron mining was developed, the Hudson Highlands in the south, and the Adirondack Mountains in the north. After more than a century of iron production, Smock (1889) completed the first report on the iron ores of New York State and the first classification based on a "geologico-geographical arrangement." His classification included almost all the iron occurrences known at that time and all the major ore types (magnetic iron, hematite, limonite, and carbonates).

The iron deposits from the Adirondack Mountains (Figure 1) can be divided into two major types: (a) iron oxide – apatite (IOA) deposits, and b) titanium iron oxide deposits. The most significant IOA deposits are those associated with the A-type Lyon Mountain Granite (gneiss), the Benson Mines magnetite-sillimanite-garnet ores, and the Jayville and Clifton magnetite ± vonsenite deposits, all of which are in St. Lawrence County. The most significant Ti-Fe oxide deposits are those found at Tahawus in association with rocks of the Anorthosite-Mangerite-Charnockite-Granite (AMCG) suite (nelsonites associated with gabbroic anorthosite), and smaller occurrences at Split Rock ("cumberlandite"), Craig Harbor (hornblendite), Tunnel Mountain (gabbro), all in Essex County, and the Port Leyden nelsonites in Lewis County.

The IOA deposits of the eastern Adirondacks display many similarities with Kiruna-type iron deposits. The IOA deposits found in Scandinavia, the Americas, Russia, Iran, Australia, and China, vary in age from Archean to Pleistocene (Williams et al. 2005), are all associated with volcanic to subvolcanic rocks, and were intensely metasomatized (Harlov 2016 and references therein). Their origin is strongly debated by modern researchers, but three hypotheses prevail: (a) primary igneous origin altered by secondary hydrothermal replacement (Sillitoe and Borrows 2002); (b) igneous derivation by liquid immiscibility (Nyström and Henriquez 1994; Naslund et al. 2002; Chen et al. 2010; Tornos et al. 2016); (c) flotation of silica melt-derived magnetite microlites (Knipping et al. 2015).

During this trip we will visit two IOA deposits, the Cheever Mine located north of Port Henry, and the # 21 mine at Mineville (Essex County) where we will examine the mineral composition of the ore, the contact with the host rock, the petrographic features of the host, and discuss the geochemistry, geochronology, and origin of the deposits. Both were significant iron producers but are also widely known for the association of REE-bearing apatite, and the exquisiteness of the magnetite crystals that can be seen today in many museums around the world. The mining history of the Mineville-Port Henry district is well presented by Farrell (1996) and summarized by Lupulescu and Pyle (2008) in their report for the NYSGA Annual Meeting at Lake George.

New data and comments for this field trip improve and bring new knowledge to the prior field trips offered by NYSGA in 2008 (Mineville) and 2015 (Cheever). Some parts of the text are comparable with those from Lupulescu and Pyle (2008) and Lupulescu et al. (2015) field guides.

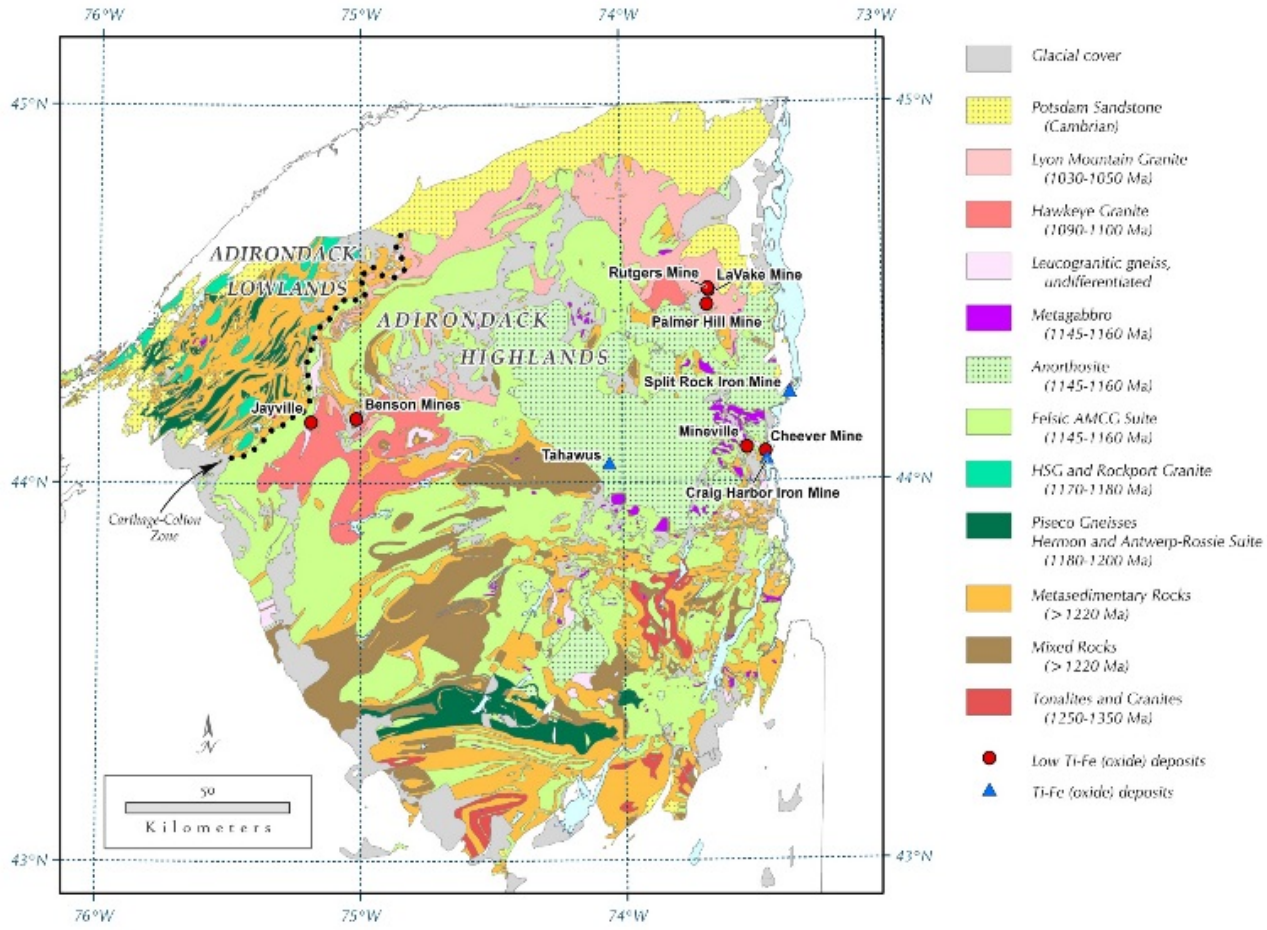


Figure 1. Distribution of IOA and Fe-Ti oxide deposits in the Adirondacks.

## GENERAL GEOLOGY

The Adirondacks are in the Mesoproterozoic Grenville Province situated between the Archean Superior Province and the Paleozoic rocks of the Appalachian Orogen. The Grenville Province is characterized by large volumes of massif anorthosite and related rocks (Anorthosite-Mangerite-Charnockite-Granite or AMCG suite) that are abundant in the Adirondack Highlands where they were intruded toward the end of the Shawinigan Orogeny (ca. 1140-1165 Ma).

The Grenville Province was shaped by three orogenies: (a) Elzevirian (1245-1220 Ma); (b) Shawinigan (1200-1140 Ma); and Grenvillian (1090-980 Ma). The Grenvillian Orogeny is considered to include the Ottawan (1090-1020 Ma) and Rigolet (1010-980 Ma) pulses (Rivers 2008). The extent of deformation and metamorphism associated with each of these events varies geographically and division of the Grenville into the monocyclic and polycyclic belts (Rivers, 1989).

The Adirondacks have been subdivided into the Adirondack Highlands (AH) and Lowlands (AL), based on lithology and metamorphic grade. In the Adirondack Region the Lowlands do not record the latter two events, while in the Highlands both the Shawinigan and Ottawan events are noted (Chiarenzelli et al. 2011). The boundary between the AH and AL is known as the Carthage-Colton shear zone. The AH is characterized by the intrusion of the AMCG suite and granulite-facies metamorphism. The AMCG members are rare in the AL where the rocks reached the upper amphibolite facies metamorphic grade during the Shawinigan Orogeny.

The IOA deposits are found only in the Adirondack Highlands. The Mineville-Port Henry mining district is in the eastern Adirondacks between the Marcy anorthosite massif and Lake Champlain. This region contains

metasedimentary rocks, anorthosite, gabbro, leucogranitic rocks of the Lyon Mountain granite, and pegmatites. The magnetite-apatite deposits cross-cut all lithologies except the late pegmatites and are typically associated with hydrothermally-altered rocks of the Lyon Mountain granite (Valley et al. 2011). The Lyon Mountain granite is a regionally extensive rock unit hosting varied iron deposits across the eastern and northern areas of the Adirondacks. Chiarenzelli et al. (2017) interpreted it as a ferroan granite formed during the extension and collapse of an elevated plateau after the cessation of the Ottawan Orogeny.

While widely distributed throughout the northern half of the Adirondack Highlands the Lyon Mountain Granite also serves as the host rock for the iron deposits. It often shows chemical alteration near the ore dominated by quartz-albite assemblages thought to represent hydrothermal alteration during and/or after ore emplacement (Valley et al. 2011). While the spatial relationship between IOA ore and the Lyon Mountain Granite is well known, the possible genetic relationship is less clear.

Although complications exist from xenocrystic zircon, geochronological study of the Lyon Mountain Granite over the last three decades indicates that it was intruded between 1030-1070 Ma throughout the Highlands, with peak emplacement between 1040-1050 Ma (Figure 2). Numerous samples of IOA ore in the eastern Adirondack Highlands have also been dated by zircon and yield a range of ages from ca. 1040 to 980 Ma; leading some workers (Valley et al., 2010; Valley et al. 2011) to conclude that the ore has a long and complicated history including alteration, remobilization, and that it was possibly intruded at several times. The ages substantiate field relations where planar dike/sill-like bodies cross-cut the Lyon Mountain Granite. Abundant generations of monazite and apatite and other radiogenic minerals have been documented by Lupulescu et al. (2017). It should be noted that in Mineville and elsewhere the IOA ore is cross-cut by a widespread suite of pegmatites yielding ages between 1020-1040 Ma (Lupulescu et al. 2011).

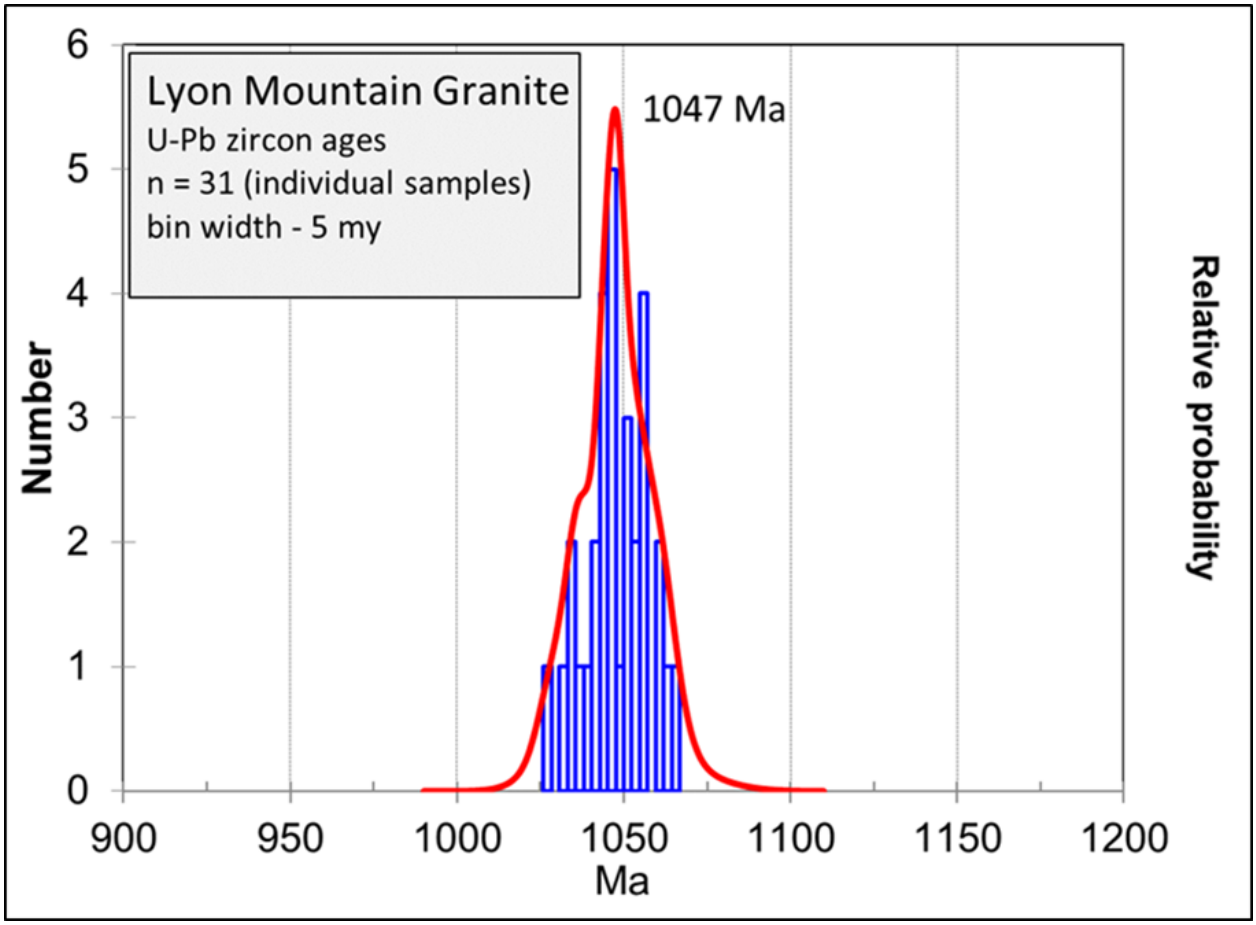


Figure 2. Distribution of ages of the Lyon Mountain Granite throughout the Adirondack Highlands (after Chiarenzelli et al. 2018)

## ROAD LOG

The field trip starts at the Port Henry Boat Launch Site at 8:30 AM. The site is at the intersection of Dock and Velez lanes in Port Henry, Essex County. There is no problem to find the meeting place, Port Henry is a small town and the access to the site is from Rt. 22. No need for carpooling, there is enough parking space at both sites

**Stop 1. CHEEVER MINE. Location coordinates: N 44° 04' 43.5"; W 73° 27' 14.3"**

The Cheever Mine is located above Lake Champlain north of the village of Port Henry. The ore strikes approximately north-south, dipping toward the west. The old mine workings are preserved as several trenches that follow the ore body for more than 0.5 km. The local bedrock geology consists of rocks of the Grenville Supergroup (marble and pelitic gneiss), coronitic gabbro, amphibolite, and pink to green variably altered rocks of the Lyon Mountain granite.

The metasedimentary rocks are represented by marbles containing folded and disrupted lenses of calc-silicates and gneisses. The coronitic metagabbro is spatially associated with the leucocratic rocks containing the magnetite-apatite ore. A similar situation can be seen at the Barton Hill mines at Mineville. The nature of the contact (tectonic vs. intrusive) is not obvious, being obscured by recent alluvium and cover in both cases. The coronitic metagabbro from Cheever mine is sheared toward the contact with the leucocratic rocks which contain quartz, albite, pyroxene, +/- microcline. Lenses of mafic rocks containing pyroxene, amphibole, fluorapatite, and magnetite can be found in the tailings (the underground works are not accessible).

The coronitic metagabbro occurs in massive or layered form. The massive form contains plagioclase "clouded" with spinels, pyroxenes, garnet and annite. Both ortho- and clinopyroxene grains are present, and most display tiny elongated exsolution lamellae of other pyroxenes and ilmenite as the result of the sub-solidus re-equilibration during slow cooling. Rare grains of ilmenite and pyrrhotite pepper the rock. The coronitic metagabbro contains some layered facies with the same composition as the massive variety.

The footwall rock which hosts the ore is a granitic rock composed predominantly of quartz and albite. Minor phases are grains of relict clinopyroxene (largely replaced by chlorite), zircon (some grains are partially metamict), and magnetite with ilmenite lamellae. The hanging wall rock contains more relict pyroxenes than the footwall, and the magnetite/ilmenite grains are rounded and, in places, associated with pyroxene replaced by chlorite. In other areas, the rock displays a gneissic texture with alternating "bands" of quartz and albite, and pyroxene, amphibole, annite, magnetite, ilmenite, and rare grains of apatite and pyrrhotite (altered to goethite). Exsolution textures within the pyroxenes are common. This rock grades into a microcline, albite, quartz, pyroxene, amphibole, and ilmenite-rich gneiss. The ore-hosting rocks are undeformed (this observation is supported by field and microscopic study) and contain pyroxene, and in places rounded, droplet-looking, grains of magnetite and or ilmenite.

The rocks have high concentrations of $Na_2O$ (3.48 wt.% in the metagabbro, to 6.31 wt.% in the footwall leucogneiss); $K_2O$ varies from 0.36 % in the footwall rock to 3.63 % in the highest stratigraphic unit of the hanging wall leucogneiss. All rocks display normative "hypersthene". The rocks are enriched in REEs and have steep profiles, like those from Mineville.

The magnetite-fluorapatite ore at the Cheever Mine exists as dikes / sills that have sharp contacts with the host rock. The ore contains abundant magnetite, fluorapatite, and augitic pyroxene. Other mineral phases present include ilmenite, titanite rimming magnetite, zircon, monazite-Ce, stillwellite-Ce, allanite-Ce, and thorite. The amphibole tremolite is very rare, and mostly is the result of the low temperature interaction of clinopyroxene, quartz, and later fluids. A relatively F-rich (1. 19 to 1.58 wt.%) amphibole with blue pleochroism under plane polarized light seems to be the last igneous mineral in the succession. Rare spinel phases were exsolved along the {111} crystallographic planes of the large magnetite grains. Lupulescu et al. (2017) interpreted the fluorapatite textures as result of the intense metasomatism; the products of the metasomatic reactions are monazite-(Ce) and allanite-(Ce) (Figure 2). The fluorapatite grains display high REE concentrations, especially heavy REEs and Y (Lupulescu et al. 2017). A detailed overview of the geology of the Cheever mine is in the report for the NYSGA Annual Meeting 2016 (Lupulescu et al. 2015).

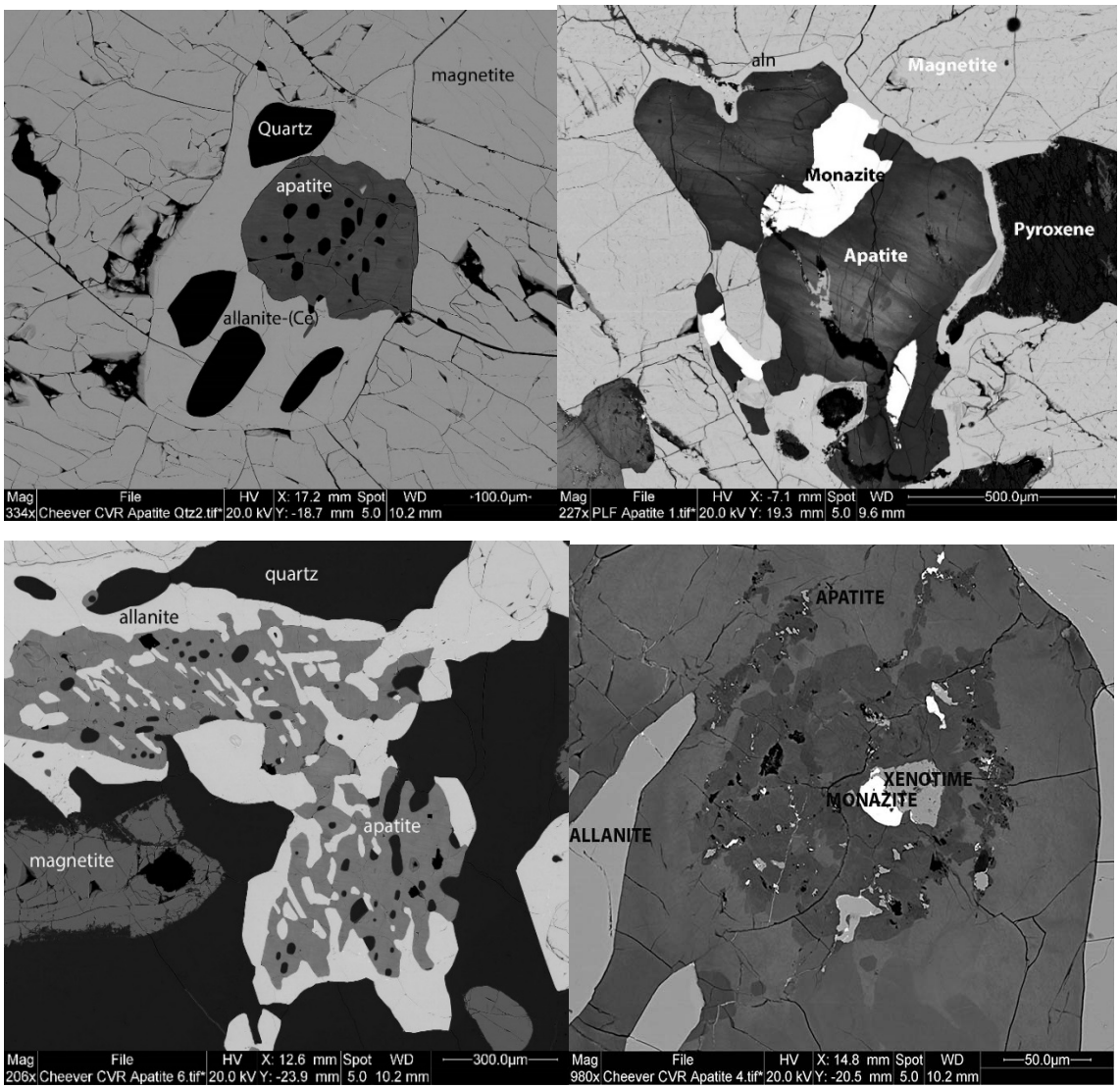


Figure 3. Textures of fluorapatite in the Cheever IOA deposit. Metasomatic reactions between REEs-bearing fluorapatite and fluids produced monazite-(Ce), allanite-(Ce), and xenotime-(Y).

The field relations and results of samples of the Lyon Mountain Granite collected for U-Pb zircon geochronology at the Cheever mine are shown in Figure 4. At these localities zircon xenocrysts were absent in several of the samples and ranged in age up to 1242 Ma where present. Lyon Mountain Granite samples range in age from 1040-1066 Ma in concert with ages obtained from numerous samples of the unit throughout the Highlands, suggesting multiple intrusive events along a magmatic conduit or fault. Note that the Lyon Mountain Granite is intruded by a gabbroic rock. The ore sample here yielded a sparse population of zircons, interpreted as igneous in origin, whose age was 1033.6±2.9 Ma.

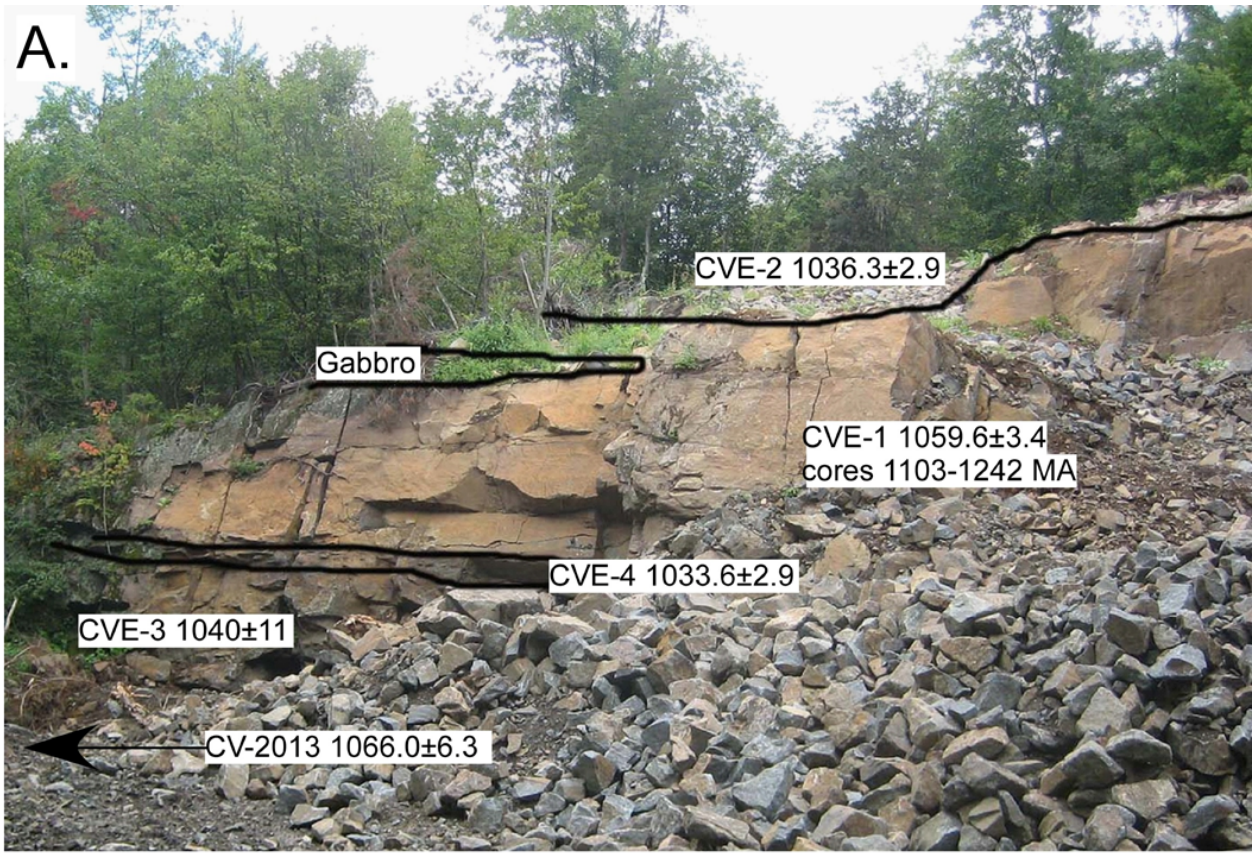


Figure 4. Existing quarry face at the Cheever Mine showing the samples collected for U-Pb zircon geochronological study and the results. Sample CVE-4 is from the ore horizon. Sample CV-2013 is located about 50 m south of the quarry face. Sample CV-7 is located approximately 300 m southeast of the quarry face and yields an age of 1043.9±4.1 Ma. After Chiarenzelli et al. (2018).

**Stop 2. MINEVILLE. Location coordinates: N 44º 05' 22.5"; W 73º 31' 30.5"**

The host rocks at the Mineville mines have both mafic and felsic compositions and display igneous features. The metasedimentary rocks from the area include marbles, calc-silicates, and gneisses that structurally overly the igneous sequence. One of the first researchers at the Mineville mines, Kemp (1908), described the host rocks as "augite syenites and related types" with granite and diorite compositions being the "related types." Alling (1925) suggested an igneous and sedimentary origin for the various protoliths that were later metamorphosed during the Grenville orogenic cycle. Buddington (1939) considered the composition of the host rocks as a petrographic hybrid between granite and metasedimentary or metagabbroic rocks. McKeown and Klemic (1956), using the maps of the Republic Steel geologists, described a structural sequence of metamorphic rocks, starting with a basal metagabbro (Kemp's mafic syenite) followed by the magnetite ore and granite gneiss from the "Old Bed", passing into a diorite, then to gabbroic rocks and the associated magnetite ore of the "Harmony Bed".

Our observations show that the first unit above the magnetite-apatite ore in the hanging wall is a pinkish rock that compositionally grades from granite to syenite. Above this unit, there is a leucocratic granite, which is in turn overlain by amphibolite (Figure 3A). The foot wall is a gabbro intruded by two sheets of leucocratic granite and a pegmatite (Figure 3B).

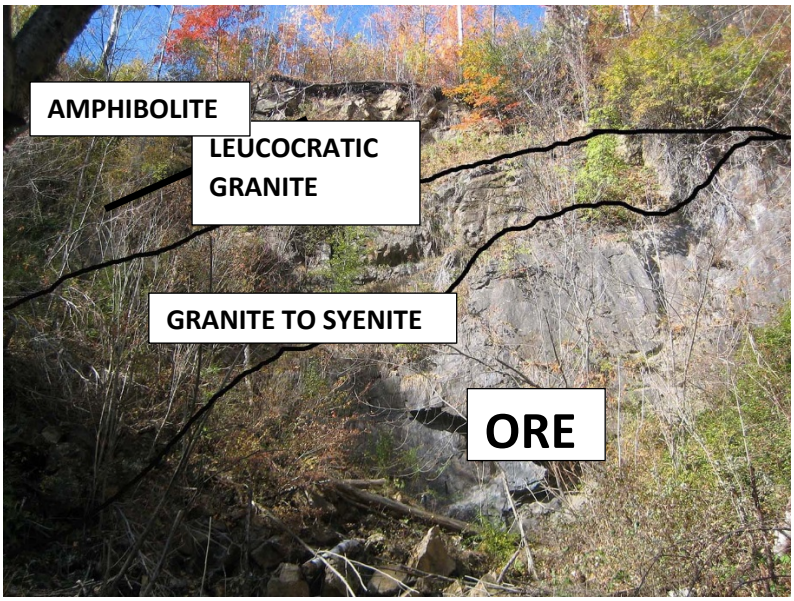


Figure 3A. Succession of rock units in the hanging wall at the # 23 mine, Mineville.

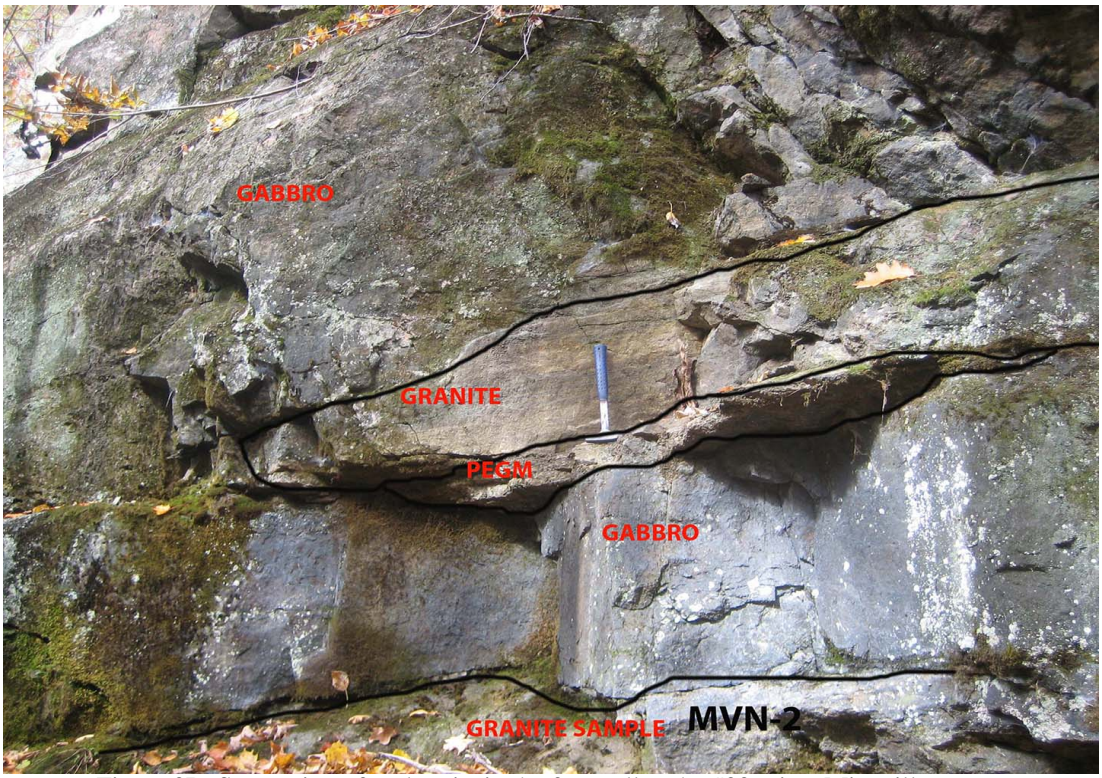


Figure 3B. Succession of rock units in the footwall at the #23 mine, Mineville.

The main minerals that were identified at Mineville in association with the ore are: magnetite, hematite (martite), fluorapatite, stillwellite-(Ce), allanite-(Ce), monazite-(Ce), edenite, actinolite, ferro-actinolite, scapolite, titanite, and zircon and dolomite, smoky quartz, calcite in late veins, and ilmenite and titanian hematite as tiny disseminations in the host rock. Micron-size mineral phases of secondary thorite, allanite-(Ce), parisite, and monazite-(Ce) in some apatite crystals were recognized under the polarizing microscope and by SEM – EDS in thin/polished sections. Bastnaesite-(Ce) and lanthanite-(Ce) previously reported by McKeown and Klemic (1956),

and Blake (1858), respectively, were found as very rare and tiny crystals based on the electron microprobe data (Figure 4A). A detailed mineralogy of the Mineville deposit was presented in the report for the NYSGA Annual Meeting 2008 (Lupulescu and Pyle 2008).

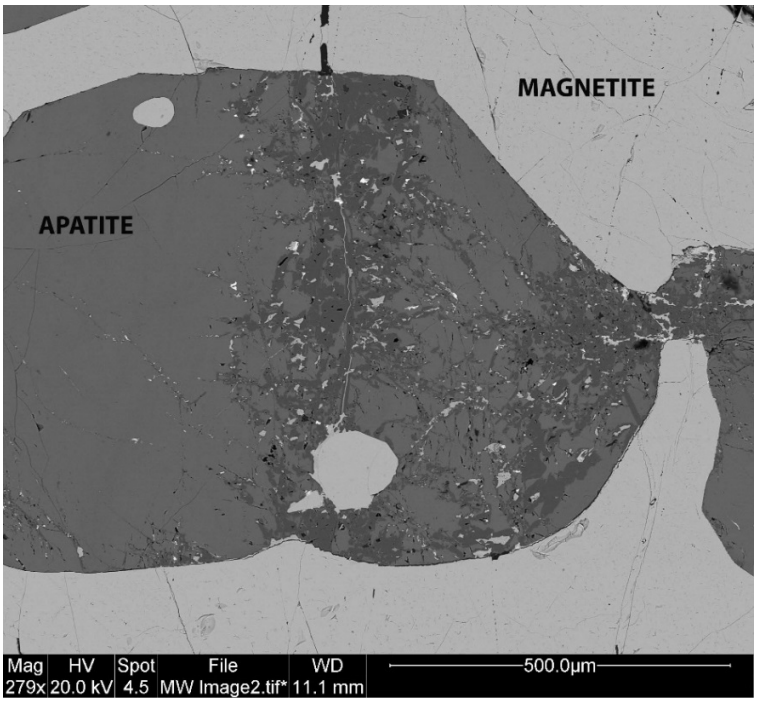


Figure 4A. BSE image of a metasomatic texture of an apatite crystal. The apatite is fractured, reacted with the invading fluids, and generated secondary REEs-bearing mineral phases. The new formed phases are too tiny to be positvely identified.

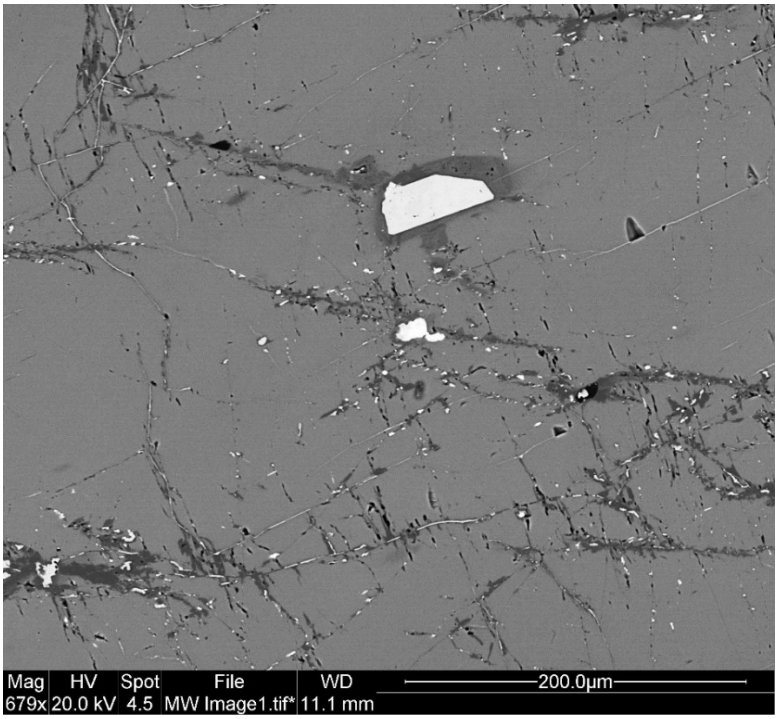


Figure 4B. BSE image of a metasomatized apatite crystal. The bright large crystal is bastnaesite-(Ce).

Fluorapatite from the Mineville deposit contains high concentrations of LREEs and especially HREEs. According to Molycorp estimation in 1980, the 5 million cubic meter tailings (Figure 5) contain "8-9 million kilograms of $Y_2O_3$ with an average grade of 0.12 wt.% $Y_2O_3$ and 0.6 wt.% REO" (Mariano & Mariano 2012).


Figure 5. View of the Mineville tailings from Google Earth (Credit: David Tewksbury-Hamilton College).

## MEETING LOCATION

The field trip starts at the Port Henry Boat Launch Site. The site is at the intersection of Dock and Velez lanes in Port Henry, Essex County.

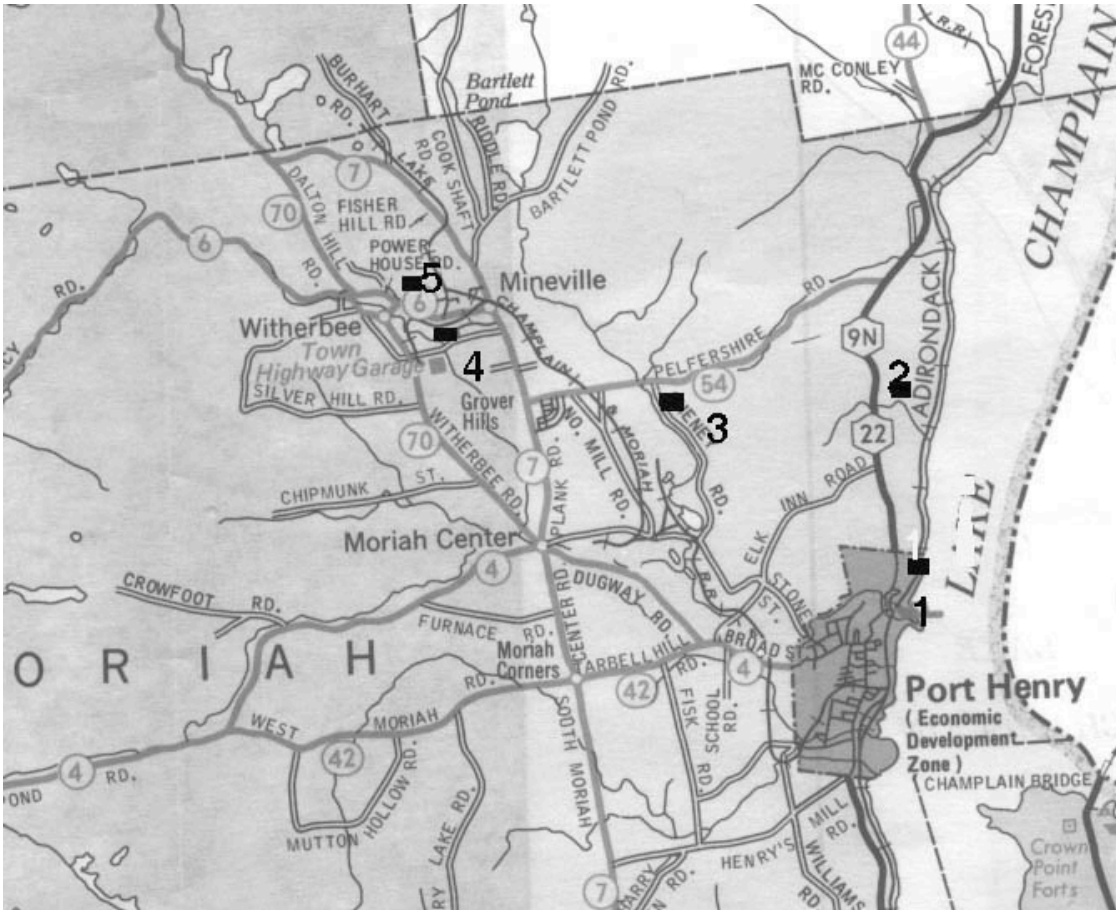


Figure 6. Location map of the Cheever and Mineville IOA deposits and neighboring mines (1. Craig Harbor Mine; 2. Cheever Iron Mine; 3. Pelfshire iron Mine; 4. Mineville group of mines; 5. Barton Hill group of mines). We will visit only the Cheever (2) and Mineville (4) mine.

## ACKNOWLEDGEMENTS

The authors are grateful to Mr. Anthony and John Real for granting access to their Cheever property and Mr. Paul Trombley for providing help while visiting the Mineville area.

## REFERENCES

Alling, H. L., 1925, Genesis of the Adirondack magnetites. Economic Geology, v. 20, p. 335 - 363.

Blake, W. P., 1858, Lanthanite and allanite in Essex County, N. Y., Am. J. Sci. p.245.

Buddington, A. F., 1939, Adirondack igneous rocks and their metamorphism. Geol. Soc. Am. Memoirs, 7.

Chen, H., Clark, A. H. and Kyser, T. K., 2010, The Marcona magnetite deposit, Ica, south-central Peru: a product of hydrous, iron-oxide-rich melts? Econ. Geol. 105, 1441-1456.

Chiarenzelli, J., Selleck, B., Lupulescu, M., Regan, S., Bickford, M. E., Valley, P., and McLelland, J, 2017, Lyon Mountain ferroan leucogranite suite: Magmatic response to extensional thinning of overthickened crust in the core of the Grenville orogen. GSA Bull., https:// doi .org /10 .1130 /B31697.1

Chiarenzelli, J., Valentino, D., Lupulescu, M., Thern, E., and Johnston, S., 2011. Differentiating Shawinigan and Ottawan Orogenesis in the Central Adirondacks: Geosphere, v. 7, p. 2-22.

Farrell, P., 1996, Through the Light Hole, North Country Books, Utica, N. Y., 245 p.

Harlov, D. E., 2015, Apatite: a fingerprint for metasomatic processes. Elements 11, 171-176.

Knipping, J. L., Bilenker, L. D., Simon, A. C., Reich, M., Barra, F., Deditius, A. P., Lundstrom, C., Bindeman, I., and Munizaga, R., 2015, Giant Kiruna-type deposits form by efficient flotation of magmatic magnetite suspension. Geology 43:7, 591-594.

Lupulescu, M. V., Hughes, J. M., Chiarenzelli, J. R., and Bailey, D. G., 2017, Texture, crystal structure, and composition of fluorapatites from iron oxide-apatite (IOA) deposits, eastern Adirondack Mountains, New York. Can. Mineral., **55**, 399-417.

Lupulescu, M., and Pyle, J., 2008, Mining history, mineralogy and origin of the gneiss (granite)-hosted Fe-P-REE and Fe oxide and gabbro-hosted Ti-Fe- oxide deposits from the Mineville-Port Henry region, Essex County, NY. New York State Geological Association Fieldtrip Guide Book for the 80th Annual Meeting, Lake George, New York, p.117-129.

Lupulescu, M., Chiarenzelli, J., Bailey, D., and Regan, S., 2015, The magnetite-fluorapatite ores from the eastern Adirondacks, New York: Cheever mine. In "Geology of the Northeastern Adirondack Mountains and Champlain–St. Lawrence Lowlands of New York, Vermont and Québec" New York State Geological Association, 87th Annual Meeting State University of New York at Plattsburgh, Plattsburgh.

Lupulescu, M.V., Chiarenzelli, J.R., Pullen, A.T., and Price, J.D., 2011, Using pegmatite geochronology to constrain temporal events in the Adirondack Mountains: Geosphere, v. 7, p. 23-39.

Mariano, N. A. and Mariano, A. Jr., 2012, Rare earth mining and exploration in North America. Elements 8, 369-376.

McKeown, F. A., and Klemic, H., 1956, Rare – earth – bearing apatite at Mineville, Essex County, New York, U. S. Geol. Surv. Bull. 1046 – B, 23 p.

Naslund, H. R., Henriquez, F., Nyström, J. O., Vivallo, W., and Dobbs, F. M., 2002, Magmatic iron ores and associated mineralization: examples from the Chilean High Andes and Coastal Cordillera. *In* Hydrothermal Iron Oxide Copper-Gold & related Deposits: A Global Perspective (Porter, T. M. Ed.), **2**, 207-226. PGC Publishing, Adelaide.

Nyström, J. O. and Henriquez, S., 1994, Magmatic features of iron ores of the Kiruna type in Chile and Sweden. Ore textures and magnetite geochemistry. Econ. Geol. 89, 820-839.

Rivers, T., 2008, Assembly and preservation of lower, mid, and upper orogenic crust in the Grenville Province—Implications for the evolution of large hot long-duration orogens. Precambrian Research 167, 237–259.

Rivers, T., Martingole, J. Gower, C., and Davidson A., 1989, New tectonic divisions of the Grenville Province, Southeast Canadian Shield: Tectonics, v. 8, p.63-84.

Sillitoe, R. H. and Burrows, D. R., 2002, New field evidence bearing on the origin of the El Laco magnetite deposit, northern Chile. Econ. Geol. 97, 1101-1109.

Smock, J. C., 1889, First report on the iron mines and iron-ore districts in the State of New York, Bulletin of the New York State Museum of Natural History, No. 7, 70 p.

Tornos, F., Velasco, F. and Hanchar, J. M., 2016, Iron-rich melts, magmatic magnetite, and superheated hydrothermal systems: The El Laco deposit, Chile. Geology 44:6, 427-430.

Valley, P. M., Hanchar, J. M., and Whitehouse, M. J., 2010, Direct dating of Fe oxide-(Cu-Au) mineralization by U/Pb zircon geochronology. Geology 37.3, 223-226.

Valley, M. P., 2011, Fluid alteration and magnetite-apatite ore mineralization of the Lyon Mountain Granite: Adirondack Mountains, New York State. PhD Thesis, Memorial University of Newfoundland, 304 p.

Williams, P. J., Barton, M. D., Johnson, D. A., Fontbote, L., DeHaller, A., Mark, G., Oliver, N. H. S., and Marschick, R., 2005, Iron oxide copper-gold deposits, geology, space-time distribution, and possible modes of origin. Econ. Geol. 100, 371-405.

# GEOLOGY OF THE NORTHERN TACONIC ALLOCHTHON: STRAIN VARIATION IN THRUST SHEETS, BRITTLE FAULTS, AND POSTRIFT DIKE EMPLACEMENT

by

Jean Crespi, Jennifer Cooper Boemmels, and Jessica Robinson
Geosciences, University of Connecticut, Storrs, CT 06269

## INTRODUCTION

This field trip has three purposes: (1) to present a synthesis of structural and strain data for the Taconic slate belt, which lies in the northern part of the Giddings Brook thrust sheet in the Taconic allochthon, (2) to present an analysis of fault-slip data for postcleavage faults in the region, and (3) to present the results of work on mafic dikes in the Taconic lobe of the New England–Québec igneous province. The stops have been selected to illustrate the along-strike variation in structure and strain, to show representative postcleavage faults, and to include dikes in a variety of orientations. The data presented at the stops cover a region that extends for about 60 km along strike in the Giddings Brook thrust sheet, from Hubbardton, Vermont, in the north to Salem, New York, in the south (Figs. 1 and 2).

Emplacement of the Taconic allochthon took place during the Early to Late Ordovician Taconic orogeny. In the northeastern United States, the Taconic orogeny has traditionally been interpreted as resulting from the collision of a west-facing volcanic arc with the eastern margin of Laurentia (Bird and Dewey, 1970; Rowley and Kidd, 1981; Stanley and Ratcliffe, 1985). In this interpretation, emplacement of the Taconic allochthon occurred in a proforeland setting. New geochronological data, however, indicate that the orogeny involved several phases (Karabinos et al., 1998, 2017; Macdonald et al., 2014, 2017). During the first phase, a west-facing volcanic arc built on peri-Gondwanan basement collided with a fragment of a hyperextended eastern Laurentian margin. During the second phase, this composite ribbon terrane collided with Laurentia proper. Slab breakoff and a reversal of subduction polarity resulted in the establishment of an east-facing volcanic arc. During the third and final phase, the Taconic allochthon was emplaced. In this revised interpretation, emplacement of the Taconic allochthon occurred in a retroarc setting.

The eastern North American margin developed after Paleozoic contractional tectonics culminated in the formation of Pangea. Early Mesozoic rifting of Pangea was accompanied by the development of a system of rift basins of Late Triassic and Late Triassic–Early Jurassic age and by massive outpourings of basalt of the ~201 Ma central Atlantic magmatic province (CAMP). The extension direction during rifting was generally northwest–southeast (Withjack et al., 2012). In the northeastern United States, CAMP dikes trend northeast–southwest, consistent with the extension direction for rifting. Postrift magmatic bodies include the plutons and sheet intrusions of the Early Cretaceous New England–Québec (NEQ) igneous province (McHone, 1984; McHone and Butler, 1984). The origin of these intrusives has long been debated. They may be related to passage of the Great Meteor hotspot (Morgan, 1972; Sleep, 1990), edge-driven convection (Matton and Jébrak, 2009), opening of the North Atlantic Ocean (McHone and Butler, 1984), delamination of overthickened crust, or some combination of these mechanisms.

## VARIATION IN STRUCTURE AND STRAIN IN THE NORTHERN GIDDINGS BROOK THRUST SHEET

In the 1970s and 80s, Bill Kidd and students at SUNY Albany produced detailed bedrock geologic maps of the Taconic slate belt (available at www.atmos.albany.edu/geology/webpages/SUNYATaconicGeologicalMaps.html). Together with the Bedrock Geologic Map of Vermont (Ratcliffe et al., 2011), these maps show that (1) regional-scale structures within this part of the northern Giddings Brook thrust sheet curve to define a salient and recess and (2) the thrust sheet plunges gently to the south such that shallower structural levels are exposed along strike from north to south. As a result, the Taconic slate belt provides opportunities to understand the way strain varies around map-view curves in orogenic belts and with distance from the base of a thrust sheet.

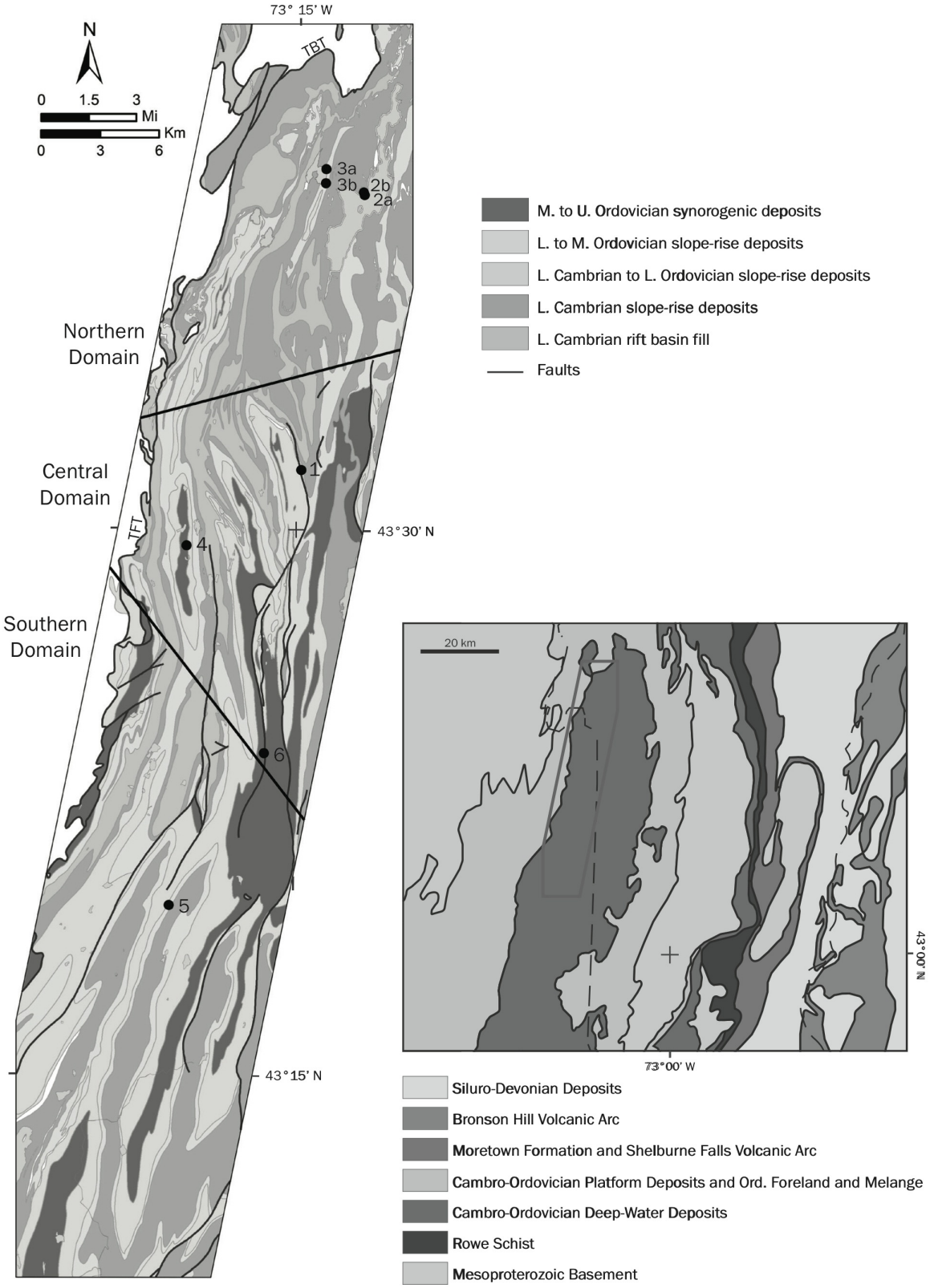


Figure 1. Bedrock geologic map of Taconic slate belt in northern part of Giddings Brook thrust sheet showing structural domains and field trip stops (modified from Ratcliffe et al. (2011); location map modified from Hibbard et al. (2006)).

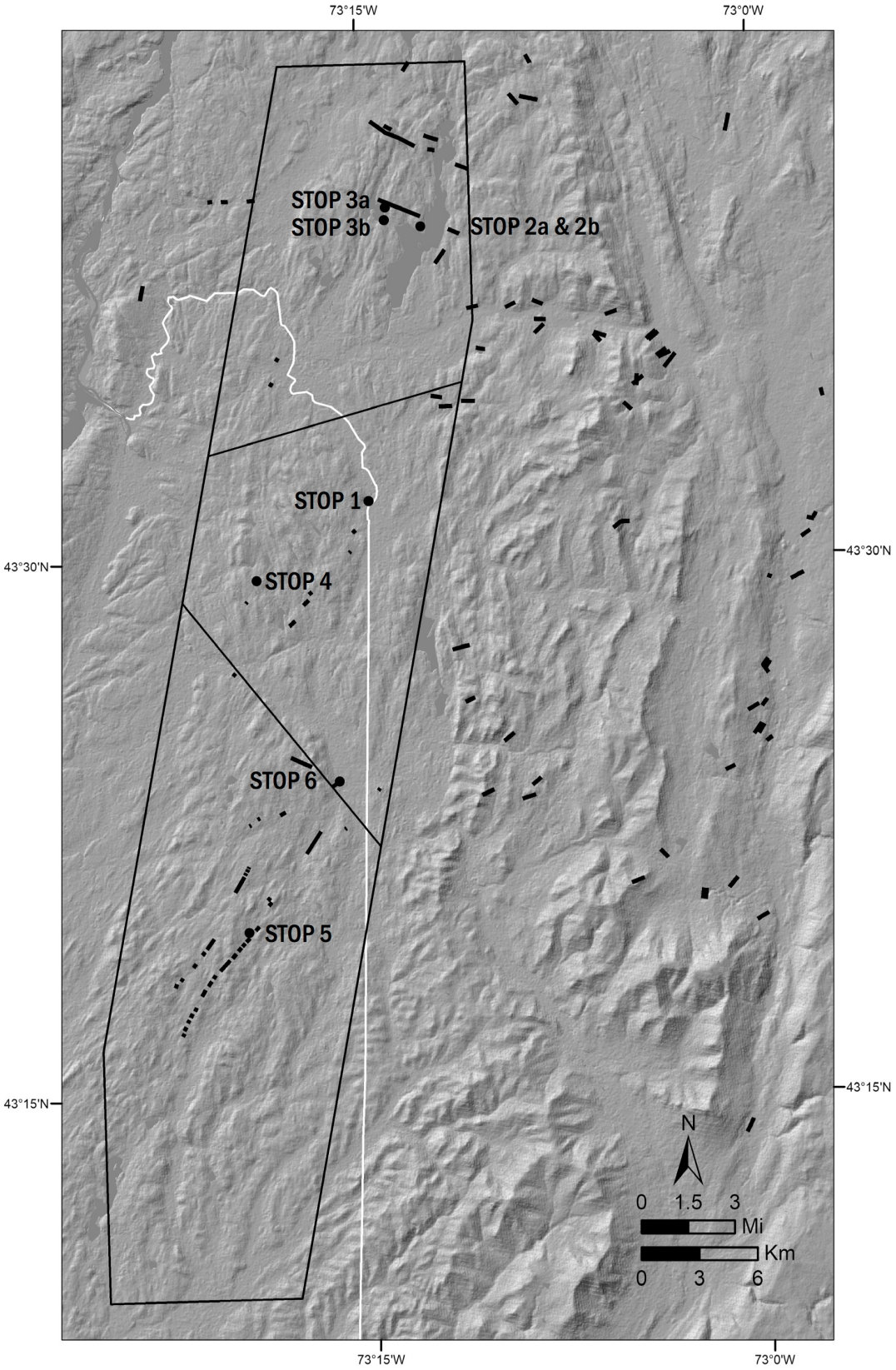


Figure 2. DEM of northern Taconic allochthon and vicinity showing dikes in Taconic lobe of NEQ igneous province and field trip stops (modified from Dale (1899), Fisher (1985), and Ratcliffe et al. (2011)).

The salient and recess are defined mainly by variations in the trend of the axial traces of regional-scale folds (Fig. 1). In Vermont, the axial traces trend north-northeast–south-southwest, parallel to the overall trend of the Taconic allochthon. Across the state border to the south in New York, the axial traces have north-northwest–south-southeast trends. Further south in New York, the axial traces return to north-northeast–south-southwest trending. This curvature delineates a salient in the north and a recess in the south.

A plunge to the south for the northern part of the Giddings Brook thrust sheet is indicated by the along-strike variation in age of exposed stratigraphic units and by the mapped location of the trace of the Taconic Basal thrust. The oldest unit of the Taconic sequence in the Giddings Brook thrust sheet, Cambrian (?) rift clastics of the Bomoseen Member of the Nassau Formation, is more extensively exposed in the north than in the south. In addition, the youngest units, synorogenic strata of the Middle to Upper Ordovician Indian River, Mount Merino, and Pawlet/Austin Glen formations, are not present in the north but are extensively exposed in the south. The trace of the Taconic Basal thrust forms the northern boundary of the Giddings Brook thrust sheet, consistent with the plunge direction given by the along-strike variation in age of exposed stratigraphic units. The variation in age of exposed stratigraphic units together with the total thickness of the Taconic sequence indicates a plunge to the south of about 1° to 2°.

We have recognized three main structural domains and one subdomain in the Taconic slate belt (Fig. 1). The northern limb of the salient forms the northern domain. The shared limb of the salient and recess forms the central domain. The southern limb of the recess forms the southern domain. The subdomain, which we refer to as the high strain subdomain, occupies a small area of the shared limb of the salient and recess on the eastern edge of the central domain. All three domains and the high strain subdomain contain evidence for top-to-west-northwest noncoaxial flow during slaty cleavage development, and we interpret slaty cleavage development as part of a continuum of deformation related to emplacement of the Taconic allochthon during the Taconic orogeny. Other aspects of the cleavage-related strain, however, are distinct in each domain/subdomain. The northern and southern domains are characterized by dip-slip thrusting, with the strain magnitude and degree of fiber asymmetry higher in the structurally lower northern domain. The central domain, in contrast, has been interpreted as a region of inclined transpression (Crespi et al., 2010). The high strain subdomain is distinct from the central domain because it is characterized by dip-slip thrusting in addition to a higher strain magnitude. Stop 1 of this field trip is in the high strain subdomain. Stops 2 and 3 are in the northern domain. Stops 4 and 5 are in the central domain and southern domain, respectively. Stop 6 lies near the boundary between the central and southern domains.

## TACONIC LOBE OF THE NEW ENGLAND–QUÉBEC IGNEOUS PROVINCE

Drawing from a reconnaissance map produced by C.D. Walcott of Burgess Shale fame, T. Nelson Dale published the first bedrock geologic map of the entire Taconic slate belt (Dale, 1899). The map broadly differentiates Lower Cambrian and Lower Silurian (Ordovician) rocks of different compositions and shows the location and orientation of igneous dikes, now interpreted to belong to the NEQ igneous province.

The igneous dikes in the Taconic slate belt lie in the Taconic lobe (Fig. 2), the southernmost of three lobes on the western edge of the NEQ igneous province (McHone and Butler, 1984). The Taconic lobe differs from the Monteregian Hills lobe in southern Québec and the Burlington lobe in northern Vermont in that the dikes in the Taconic lobe show a wide range in orientation with a dominant north-northeast–south-southwest trend. The dikes in the Monteregian Hills lobe generally trend west-northwest–east-southeast, except where they form radial patterns around Early Cretaceous intrusive stocks, and the dikes in the Burlington lobe generally trend east–west (McHone, 1978). The Taconic lobe also differs from the Monteregian Hills lobe in that NEQ plutons are rare in the Taconic lobe. The Monteregian Hills lobe, in contrast, contains ten stocks that form a linear belt oriented parallel to the overall trend of the NEQ dikes in the lobe (McHone, 1984).

Most of the radiometric dates for the intrusives in the Taconic lobe are K–Ar ages. The dates are summarized in McHone and McHone (1993) and Eby and McHone (1997). Two dikes have been dated, both lying in the Taconic allochthon, and these yielded ages of 113 ± 4 Ma and 108 ± 4 Ma. These dikes trend east-northeast–west-southwest

and north-northeast–south-southwest. The Cuttingsville igneous complex in the Green Mountain massif and a nearby andesitic breccia yielded ages of 97 ± 8 Ma to 108 ± 1 Ma and 101 ± 2 Ma, respectively. The only $^{40}Ar/^{39}Ar$ date from NEQ intrusives in the Taconic lobe is a 100 ± 0.3 Ma age for the Cuttingsville igneous complex (Hubacher and Foland (1991) as referenced in McEnroe (1996)). These ages are younger for the most part than those obtained from intrusives in the Burlington and Monteregian Hills lobes (Foland et al., 1986; Bailey et al., 2017).

The NEQ intrusives in the Taconic lobe have received much less attention than the NEQ intrusives in the Burlington and Monteregian Hills lobes. We are currently obtaining new geochemical and geochronological data for the Taconic lobe intrusives to better define the similarities and differences between the three lobes and to improve understanding of the role of the NEQ igneous province in the postrift evolution of the eastern North American margin. We will examine NEQ dikes at Stops 3, 5, and 6 of this field trip.

## POSTCLEAVAGE FAULTS

Mesoscale faults that postdate slaty cleavage development are relatively common in the Taconic slate belt. The orientation of many of these faults has been influenced by the orientation of slaty cleavage, the faults reactivating cleavage surfaces or striking parallel to but dipping more steeply than cleavage. The faults may also reactivate bedding surfaces, and, in some cases, they reactivate folded bedding such that the overall direction of fault slip is parallel to the fold hinge line. Other mesoscale, postcleavage faults in the Taconic slate belt, however, do not show evidence of having formed along preexisting surfaces.

Most of the mesoscale, postcleavage faults in the Taconic slate belt are normal faults or oblique- and strike-slip faults with a component of normal displacement. Faure et al. (1996, 2006) analyzed normal faults along strike in the Québec Appalachians and attributed the faults to two main extensional events: Late Triassic–Early Jurassic rifting of Pangea involving the separation of eastern North America and northwestern Africa and Early Cretaceous rifting of Pangea involving the separation of Labrador and Greenland. Paleostress analysis of faults interpreted as related to the former yielded east–west and northwest–southeast trends for the minimum compressive stress (Faure et al., 2006). Paleostress analysis of faults interpreted as related to the latter yielded an early phase of northeast–southwest extension and a later phase of north–south extension contemporaneous with emplacement of the intrusive bodies in the Monteregian Hills lobe of the NEQ igneous province (Faure et al., 1996). Separation of the normal faults into two main extensional events is facilitated in the Québec Appalachians by the difference in orientation for the minimum compressive stress indicated by the trends of CAMP and NEQ dikes.

Lim et al. (2005) analyzed mesoscale normal faults in the mélange belt west of the Taconic allochthon and attributed the faults to gravitational collapse of the Taconic orogenic wedge. The faults crosscut both the phacoidal cleavage in the mélange and postcleavage reverse faults related to slip along the Champlain thrust. They may or may not contain vein material. Crosscutting relations suggest the normal faults with vein material predate the normal faults without vein material. The normal faults are thought to have formed shortly after Taconic convergence ceased because fluid inclusions in the vein material yielded homogenization temperatures similar to or slightly lower than those obtained from fluid inclusions in vein material along the reverse faults and because the relatively high homogenization temperatures are inconsistent with an origin during a subsequent tectonic event.

The mesoscale, postcleavage normal faults in the Taconic slate belt may have formed during gravitational collapse of the Taconic orogenic wedge, during Late Triassic–Early Jurassic rifting of Pangea, and/or during emplacement of the Early Cretaceous dikes in the Taconic lobe of the NEQ igneous province. A gravitational collapse origin is supported by the Taconic allochthon lying closer to the hinterland of the Taconic orogenic wedge than the mélange belt to the west of the Taconic allochthon. A Late Triassic–Early Jurassic rifting origin is supported by evidence for rift-related normal faults several hundred kilometers west of the coast in the Québec Appalachians (Faure et al., 2006). An NEQ origin is supported by dike-fault crosscutting relations. In particular, a north-northeast-trending dike in the Taconic allochthon to the east of the Taconic slate belt is cut by a normal fault (Zen, 1972). The dike has yielded a hornblende K–Ar age of 108 ± 4 Ma (Zen, 1972; McHone and McHone, 1993).

Our analyses of mesoscale, postcleavage normal faults, oblique-slip faults, and strike-slip faults in the Taconic slate belt show that they are broadly consistent with east–west to northwest–southeast extension. Although NEQ dikes in the Taconic slate belt trend west-northwest–east-southeast and east–west, we have not identified normal faults indicative of north-northeast–south-southwest or north–south extension. We will examine mesoscale, post-cleavage faults at Stops 1, 4, and 6 of this field trip.

## ROAD LOG

Meet on Sunday, October 14 at 8:30 a.m. at Stop 1 (43° 31.610'N, 73° 14.835'W). Park in the parking lot for the Ole Hampton House Tavern at 110 Campbell Lane in Hampton, New York. The restaurant does not have a sign other than "Free Pizza," "Band Sat. Night," or the like. It is located on the northeast corner of the intersection of County Road 18A and Campbell Lane. Park on the side of the parking lot near the trees away from the restaurant. Bring lunch and water. The lunch stop for this trip is at Glen Lake boat launch, and there is no place nearby to purchase lunch. Most of the stops are a short walk over relatively even terrain from the parking areas. One of the stops involves a scramble up a pile of slate rubble at the end of a short uphill walk into an abandoned quarry, and another stop is reached via a three-quarter mile round-trip walk in the woods on a relatively level portion of a marked hiking trail. Restrooms are available at the Stewart's Shops in Poultney (near Stop 1) and in Fair Haven (on the drive to Stop 2 and on the drive to Stop 4). Be prepared to catch up with the group on your own if you stop to use the restroom.

**Mileage**

0.0 Parking area for Stop 1. Stop 1 (43° 31.610'N, 73° 14.835'W) is the roadcut on either side of Co. Rd. 18A.

**STOP 1. HIGH STRAIN SUBDOMAIN (POULTNEY/DEEP KILL FORMATION).** 43° 31.610'N, 73° 14.835'W. (1 HOUR).

This exposure of the Lower to Middle Ordovician Poultney/Deep Kill Formation was created in the mid 1990s when County Road 18A was constructed to improve road traffic safety. The strata lie on the overturned limb of a regional-scale syncline and in the immediate footwall of the out-of-sequence Middle Granville thrust. Our analysis of the orientations of slaty cleavage and the stretching lineation and of syntectonic fibers places the exposure in the high strain subdomain on the eastern edge of the central domain.

Slaty cleavage strikes north-northeast and dips moderately east-southeast, and the stretching lineation plunges approximately down the dip of slaty cleavage. Syntectonic fibers associated with slaty cleavage development are curved in *XZ* sections consistent with top-to-west-northwest noncoaxial flow. The fibers yield stretch values for the *X* direction of about 2.2–2.3. They also record a small amount of extension in the *Y* direction. The central domain, in contrast, is characterized by north-northwest strikes for slaty cleavage, a moderately raking stretching lineation, and lower stretch values for the *X* direction.

Many mesoscale folds are present in the exposure (Fig. 3). They are unusual because the hinge lines plunge moderately to steeply southeast. Hinge lines of folds in the Taconic slate belt are typically subhorizontal to gently plunging, and, in the central domain, the plunge direction is south-southeast. The bedding-cleavage intersection lineation also plunges to the southeast although not as steeply as the fold hinge lines. This difference is likely because the mesoscale folds are mostly in the middle of the exposure and the bedding-cleavage intersection lineation was measured at the ends of the exposure where bedding is planar. The folds in the exposure are also asymmetrical such that they have an S shape when viewed down plunge.

The fold geometry can be explained by initial development of parasitic folds and subsequent rotation of the hinge lines of the parasitic folds toward the stretching lineation. The S-shaped fold asymmetry is consistent with an origin as parasitic folds on the overturned limb of a west-vergent, regional-scale fold. In addition, the orientation of

Figure 3. Photograph of asymmetric folds in middle of roadcut on northeast side of County Road 18A at Stop 1. View is to northeast.

the hinge lines is consistent with an initial gentle south-southeast plunge and counterclockwise rotation toward the downdip stretching lineation during top-to-west-northwest noncoaxial flow. This interpretation implies that this area was a long-lived region of high strain, the folds starting to rotate during folding and continuing to rotate during slaty cleavage development. The Middle Granville thrust may be a late-stage expression of this high strain zone.

Mesoscale, postcleavage faults in the strata typically contain laminated veins with well-developed steps. Some of the faults have formed along folded surfaces, a good example lying on the northeast side of County Road 18A near the middle of the exposure (Fig. 4). These faults are normal faults on the long limbs of the folds and reverse faults on the short limbs of the folds. Slip was subparallel to the hinge lines. In the example in Figure 4, the outer part of the fold has moved up relative to the inner part of the fold, and the striae show a systematic variation in orientation around the fold such that they are closer to exactly parallel to the hinge line in the hinge.

0.0 Turn left out of the parking area for Stop 1 onto Campbell Ln.
0.0 At the stop sign, turn right onto Co. Rd. 18A.
0.0 Pass Stop 1.
0.2 At the stop sign, turn right onto NY-22A.
3.0 Cross into Vermont. NY-22A becomes VT-22A.
4.5 VT-22A merges with VT-4A/Main St.
4.7 Pass the Fair Haven town green.
4.8 Keep to the right to continue on VT-4A/Main St.
5.2 At the 4-way stop, continue straight onto Dutton Ave.
5.6 Cross over US-4.
5.7 Dutton Ave. becomes Scotch Hill Rd.
9.0 Scotch Hill Rd. becomes West Castleton Rd.
9.6 Pass Stop 3b.

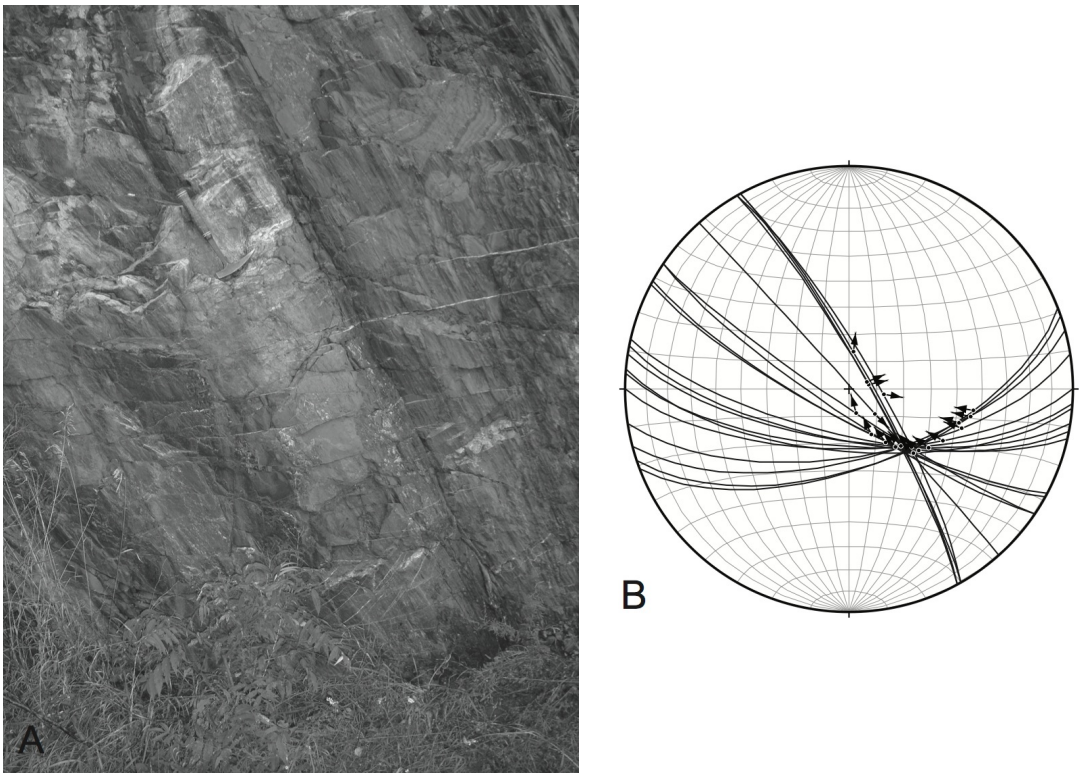


Figure 4. (A) Photograph of fold at Stop 1 (fold in bottom right of Fig. 3). View is to north-northwest. Handle of hammer is parallel to hinge line. (B) Stereonet of bedding-parallel faults in fold in (A). Great circles—fault planes; dots—striae; arrows—motion of hanging wall. Equal-area, lower-hemisphere projection.

9.6 Keep to the right to stay on the paved road (West Castleton Rd.).

9.8 Intersection of West Castleton Rd., Cedar Mountain Rd. (to the left), and the entrance to Bomoseen State Park (straight ahead). Turn left onto Cedar Mountain Rd. (dirt road).

11.0 Park at the entrance to Cedar Point quarry. Do not block access to the white house. Stop 2a (43° 39.185'N, 73° 12.525'W) is located a short distance from the start of the path into Cedar Point quarry, and Stop 2b (43° 39.255'N, 73° 12.555'W) is located at the top of the slate pile at the end of the path into the quarry.

The walk into Cedar Point quarry is relatively easy until the last part which involves climbing up a pile of slate rubble. Walk up the path to Stop 2a, which is to the right of the path near the beginning of the path. Continue walking up the path. At the Y, bear left onto a relatively level part of the path (do not take the uphill path to the right). At the end of the path, climb the pile of slate rubble to Stop 2b. Return to the path and follow it back to the entrance to the quarry.

**STOP 2. NORTHERN DOMAIN (METTAWEE SLATE/MIDDLE GRANVILLE SLATE).** 43° 39.185'N, 73° 12.525'W and 43° 39.255'N, 73° 12.555'W. (1 HOUR 15 MINUTES).

Cedar Point quarry exposes the hinge zone of a north-northeast-trending, regional-scale syncline. The folded strata belong to the Lower Cambrian Mettawee Slate/Middle Granville Slate, a purple and green slate that contains reduction spots useful for strain analysis. The quarry lies in the northern domain where slaty cleavage strikes north-northeast and dips gently east-southeast and where the stretching lineation plunges approximately down the dip of slaty cleavage. Here, slaty cleavage is overprinted by a crenulation cleavage, which becomes the dominant cleavage to the east of the approximate longitude of Lake Bomoseen and Lake St. Catherine. Although this crenulation cleavage is locally present in the Taconic slate belt, it does not appear to affect the orientation of slaty cleavage. In the northern domain, where the crenulation cleavage is more common than in the central and southern domains, the

mean orientation of slaty cleavage for sites without a crenulation cleavage is essentially the same as the mean orientation of slaty cleavage for sites with a weakly to moderately developed crenulation cleavage.

At Stop 2a, the concave side of a folded bedding surface is visible through the graffiti. The intersection of the axial planar slaty cleavage with bedding indicates the hinge line of the syncline is gently plunging, which is typical of folds in the Taconic slate belt. At Stop 2b, the convex side of a folded bedding surface and the profile plane of the syncline are visible. The tight to isoclinal nature of the syncline is typical of folds in the Taconic slate belt.

Reduction spots are common in the slabs in the slate pile at Stop 2b. Two types of reduction spots are present: those with irregular shapes and those that are elliptical. The latter have been measured and reported on by Wood (1974), Hoak (1992), and Goldstein et al. (1995). The reduction spots here and elsewhere in the Taconic slate belt plot in the flattening field of a Flinn plot, and Goldstein et al. (1995) interpreted their horizontal distribution on a Flinn plot as indicating the slates underwent a minimum of 55% volume loss during slaty cleavage development. Our strain data for the northern domain from strain fringes around pyrite framboids in black slates are not consistent with the reduction spot data. The strain fringes do not show fiber growth in the *Y* direction, and so we infer plane strain deformation for slaty cleavage development. In addition, the strain fringe data yield internally consistent data when combined with the orientation of slaty cleavage if constant volume is assumed. The 2.28 mean stretch value for the *X* direction obtained from strain fringes for the northern domain gives a strain ratio for the *XZ* plane of 5.2 for constant volume and a strain ratio for the *XZ* plane of 10.4 for 50% volume loss. These values can be plotted on an $R_{XZ}$ versus $\theta'$ graph for simultaneous simple shear and volume change (Fossen and Tikoff, 1993) using the 28° mean dip of slaty cleavage in the northern domain and an appropriate dip for the Giddings Brook thrust sheet. We use a thrust sheet dip of 5° east, giving a $\theta'$ value of 23°. A value of 5.2 for $R_{XZ}$ results in the northern domain plotting close to the curve for simple shear, which is by definition a constant volume deformation. A value of 10.4 for $R_{XZ}$ results in the northern domain plotting in the volume gain field, which is at odds with the 50% volume loss assumption used to obtain $R_{XZ}$.

0.0 Return along Cedar Mountain Rd. to the intersection of Cedar Mountain Rd., West Castleton Rd., and the entrance to Bomoseen State Park.

1.2 Intersection of Cedar Mountain Rd., West Castleton Rd., and the entrance to Bomoseen State Park. At the stop sign, turn right onto West Castleton Rd.

1.3 At the Y, bear right onto Moscow Rd. (dirt road).

1.3 At the intersection, keep to the right to continue on Moscow Rd. toward Glen Lake boat launch.

1.4 Turn right into the parking area for Glen Lake boat launch and park. Walk back a short distance along Moscow Rd. to Glen Lake boat launch. Stop 3a (43° 39.885'N, 73° 13.980'W) is located on Glen Lake Trail about 10 minutes (~0.35 miles) from the trailhead. To access Glen Lake Trail, walk past the boulder barrier at the boat launch. Stop 3b (43° 39.500'N, 73° 13.995'W) is located in the backyard of the camp on West Castleton Rd. where the road passes Glen Lake. Stop 3b is a no-hammer stop.

Glen Lake Trail (visit vtstateparks.com/assets/pdf/bomoseentrailmap.pdf for a copy of the trail map) is well marked with blue trail blazes, and the walk to Stop 3a is relatively easy with little elevation change, the occasional fallen tree, and some irregular terrain where the trail passes over exposed tree roots. About 7 minutes (~0.25 miles) from the trailhead, the trail splits shortly after passing a foundation. Take the right fork, which passes on the east side of a cellar hole. The left fork follows the water's edge and is not the main trail. About 10 minutes (~0.35 miles) from the trailhead, the trail climbs up a small ridge. A hemlock tree with a girth of about 2 m and a blue trail blaze stands at the top of the ridge. The south-southwest side of the Bomoseen dike is exposed in the vicinity of this tree. Continue to follow the trail as it descends into a small valley to the north of the ridge. The valley is before the trail bends downhill to the left. Walk off trail just upslope from the valley floor to where a recently fallen tree has exposed the north-northeast side of the Bomoseen dike. Return to the trail and follow it downhill to the right. Rubble next to the trail of the dike and wall rock marks the dike-wall rock contact on the north-northeast side of the dike. Follow the trail up-

hill back to the valley floor and walk off trail to the east-southeast toward Moscow Rd. Several exposures of the dike and of the wall rock to the south-southwest of the dike are present in this area. Return to the trail and follow it back to the trailhead.

Walk back along Moscow Rd. and West Castleton Rd. to Stop 3b.

Return to Glen Lake boat launch. Lunch. Note the outcrops of the Poultney/Deep Kill Formation, which are on the gently dipping, upright limb of the Scotch Hill syncline.

**STOP 3. BOMOSEEN DIKE AT GLEN LAKE (STOP 3A), NORTHERN DOMAIN (POULTNEY/DEEP KILL FORMATION) (STOP 3B), AND LUNCH.** 43° 39.885'N, 73° 13.980'W and 43° 39.500'N, 73° 13.995'W. (2 HOURS).

The exposure of the Bomoseen dike at Stop 3a consists of several small and discontinuous outcrops of the dike between the eastern shore of Glen Lake and Moscow Road. Outcrops of the wall rock (West Castleton Formation on the Bedrock Geologic Map of Vermont (Ratcliffe et al., 2011) and Poultney and Hatch Hill formations on Rowley's map of the Lake Bomoseen area (Rowley, 1983, Plate 1)) are also present.

The Bomoseen dike was named by McHone and McHone (1993) for an exposure of the dike on VT-30 along the eastern shore of Lake Bomoseen. The dike appears on Dale's map of the Taconic slate belt (Fig. 5) (Dale, 1899) and is reproduced on Fowler's map of the Castleton area (Fowler, 1950, Plate II) and on the Bedrock Geologic Map of Vermont (Ratcliffe et al., 2011). It trends west-northwest–east-southeast and is relatively wide and long compared to other NEQ dikes in the Taconic lobe.

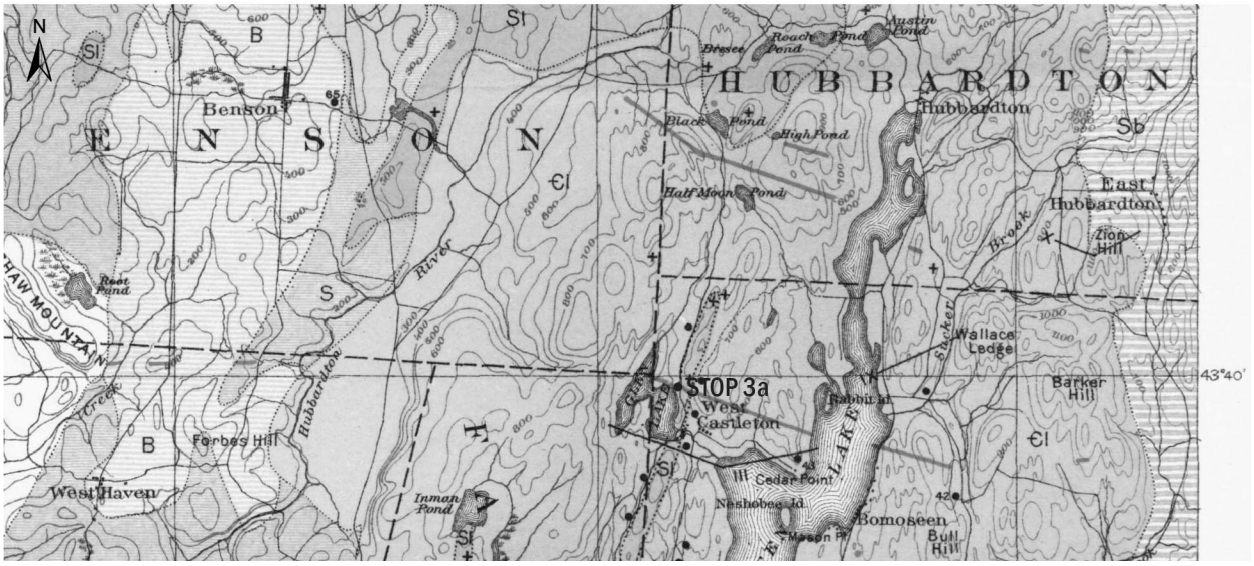


Figure 5. Portion of Dale's map of Taconic slate belt (Dale, 1899) showing location of Stop 3a. Map scale is 1:115,385.

McHone and McHone (1993) reported a width of 12 m for the Bomoseen dike at the VT-30 exposure (the entire width of the dike is no longer preserved). Our observations of the dike at the Glen Lake exposure give a comparable width. The location of the dike-wall rock contact on the north-northeast side of the dike can be located fairly closely on the trail by the change from dike rubble to slate rubble. A sample we collected from the southern side of the exposure of the dike closest to Moscow Road contains the dike-wall rock contact on the south-southwest side of the dike.

The Bomoseen dike is shown as extending continuously for nearly 5 km on Dale's map of the Taconic slate belt (Dale, 1899). In addition to the Glen Lake and VT-30 locations, the Bomoseen dike is well exposed along North Road.

Of interest at Stop 3a is the well-developed pencil cleavage in the wall rock adjacent to the dike-wall rock contact on the north-northeast side of the dike. This pencil cleavage has been formed by the intersection of the well-developed slaty cleavage with closely spaced dike-parallel fractures.

The exposure of the Scotch Hill syncline at Stop 3b (Fig. 6) is one of the best-known exposures in the Taconic slate belt. It lies in the northern domain. Slaty cleavage forms a divergent cleavage fan with the overall orientation of slaty cleavage similar to the mean orientation of slaty cleavage in the northern domain. Because sampling is prohibited at the exposure, the orientation of the stretching lineation was not determined, and the characteristics of strain fringes around subspherical core objects were not assessed.

Figure 6. Photograph of exposure of Scotch Hill syncline at Stop 3b. View is to northeast.

The folded strata, which belong to the Poultney/Deep Kill Formation, contain two sets of veins, one that predates folding and one that formed at the same time as folding. A subhorizontal, north-northeast-trending fold axis for the Scotch Hill syncline is shown by both the pole to the best-fit plane to the poles to bedding and by the bedding-cleavage intersection lineation at the exposure (Figs. 7A and 8A). The poles to slaty cleavage lie on the best-fit plane to the poles to bedding (Fig. 7A). The prefolding veins are similarly oriented throughout the fold, and their poles do not plot on the best-fit plane to the poles to bedding (Fig. 7B). The synfolding veins lie in a range of orientations, and their poles plot on the best-fit plane to the poles to bedding (Fig. 7B).

The prefolding veins are long, thin, and planar (Fig. 8B–D). They are commonly boudined (Fig. 8B), and they are crosscut by the synfolding veins (Fig. 8C, D). The synfolding veins have a less uniform morphology but are commonly short, thick, and sigmoidal (Fig. 8C–F). They are either boudined or folded depending on the angle between the vein and slaty cleavage. Synfolding veins that are especially thick, however, do not appear deformed. Although the prefolding veins appear approximately parallel to slaty cleavage on the profile plane of the fold, their noncoaxiality with the fold can be seen on west-northwest-facing bedding surfaces on the subvertical limb of the fold. The trace of cleavage on the bedding surfaces is subhorizontal whereas the trace of the prefolding veins plunges to the south. The coaxiality of the synfolding veins with the fold can also be seen on these surfaces. Both the trace of cleavage and the trace of the synfolding veins are subhorizontal (Fig. 8A).

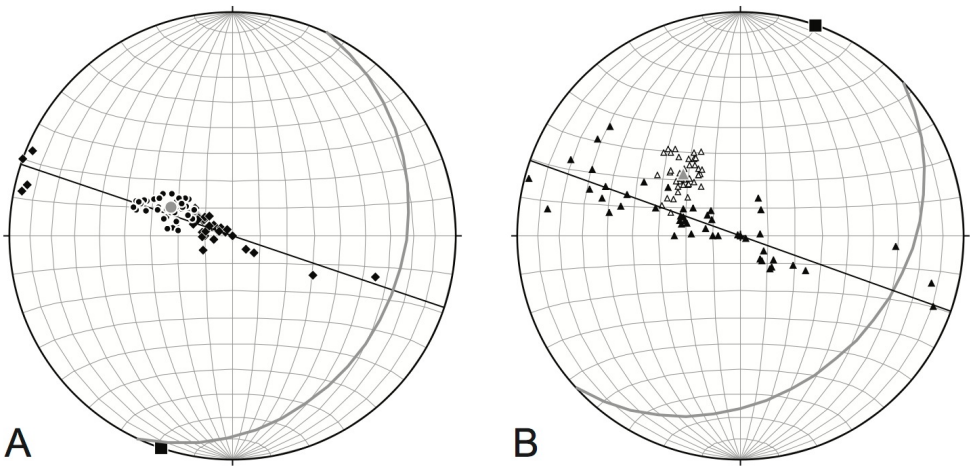


Figure 7. Stereonets of (A) bedding and slaty cleavage and (B) prefolding and synfolding veins at Stop 3b. Small black diamonds—poles to bedding; small black dots—poles to slaty cleavage; large gray dot—mean pole to slaty cleavage; small white triangles—poles to prefolding veins; small black triangles—poles to synfolding veins; large gray triangle—mean pole to prefolding veins; gray great circle—mean slaty cleavage in (A) and mean prefolding veins in (B); black great circle—best-fit plane to poles to bedding in (A) and best-fit plane to poles to synfolding veins in (B); large black square—fold axis given by pole to best-fit plane to poles to bedding in (A) and fold axis given by pole to best-fit plane to poles to synfolding veins in (B). Equal-area, lower-hemisphere projections.

The asymmetry of the synfolding veins is consistent with flexural folding. On the gently dipping limb of the fold, the synfolding veins are commonly irregularly shaped, but a large vein has a classic sigmoidal shape, the S shape when viewed to the north-northeast indicating thrust sense of shear (Fig. 8E). On the subvertical limb of the fold, the synfolding veins are commonly sigmoidal, the Z shape when viewed to the north-northeast indicating west-side-up sense of shear (Fig. 8F). These opposite senses of shear are as predicted for flexural folding with a pinned fold hinge. The mystery of the prefolding veins having similar orientations on the two limbs of the fold despite being prefolding is solved when shearing related to flexural folding is applied to their orientation. The change in orientation of the prefolding veins from limb rotation was essentially offset by the change in orientation from flexural-folding-related shearing within the bedding layers.

0.0 Turn left out of the parking area for Stop 3 onto Moscow Rd.
0.0 At the Y, bear right and continue on Moscow Rd.
0.1 At the yield sign, turn right onto West Castleton Rd.
0.1 Pass Stop 3b.
0.7 West Castleton Rd. becomes Scotch Hill Rd.
4.0 Scotch Hill Rd. becomes Dutton Ave.
4.1 Cross over US-4.
4.5 At the 4-way stop, continue straight onto VT-4A/N. Main St.
4.9 Pass the Fair Haven town green.
5.2 Turn right to continue on VT-4A/Prospect St.
6.6 At the stop sign/traffic light, turn left onto US-4.
6.8 Cross into New York.
8.7 Turn left onto Co. Rd. 21.
10.9 At the stop sign, continue straight on Co. Rd. 21.
12.7 Bear right onto Holcombville Rd.
14.4 Turn right onto Tanner Hill Rd.

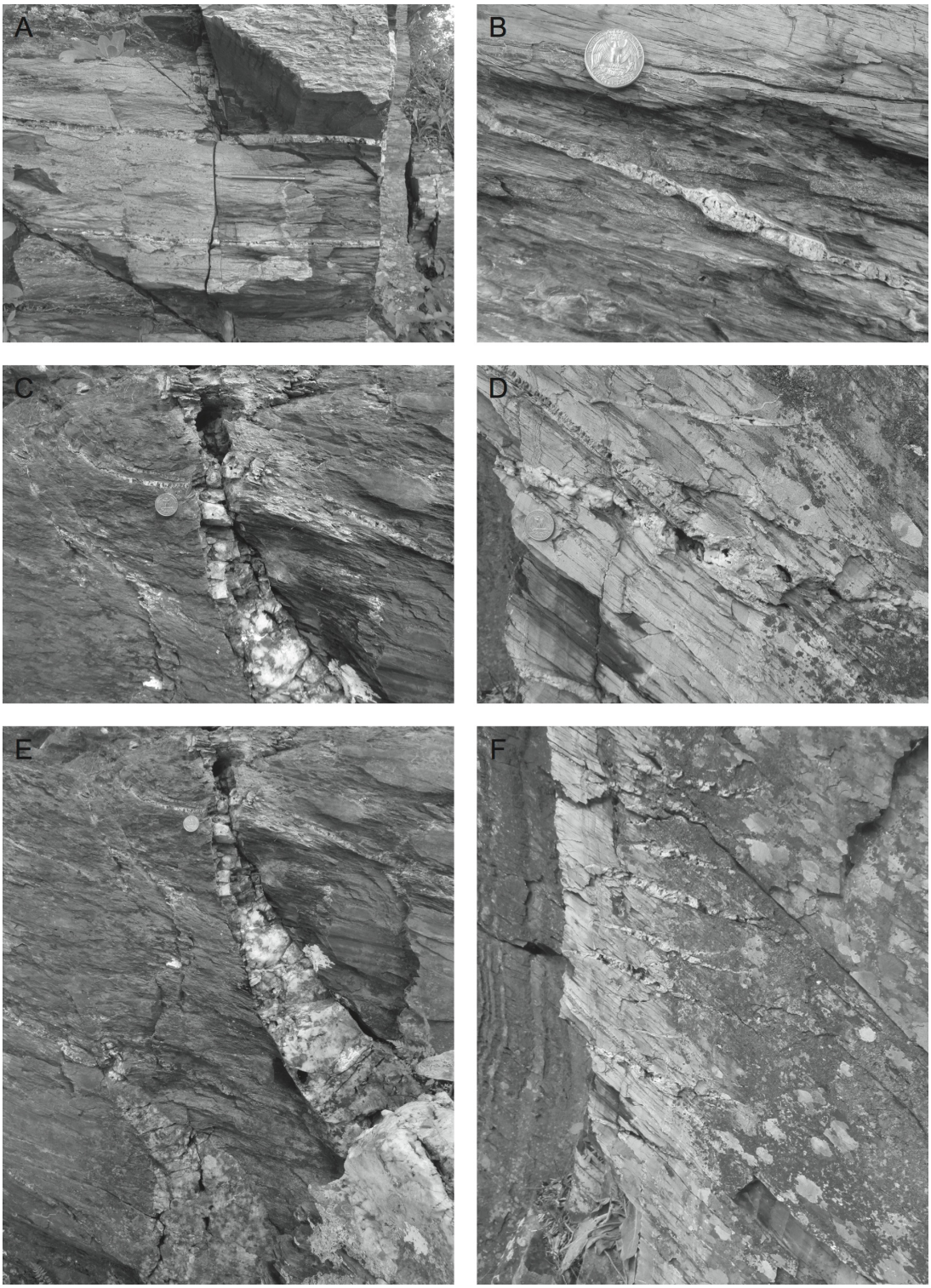


Figure 8. Photographs of structural features at Stop 3b. (A) Bedding surface on subvertical limb of fold. Pencil is horizontal and parallel to intersection of slaty cleavage on bedding and intersection of synfolding veins on bedding. (B) Prefolding vein on gently dipping limb of fold. (C) Crosscutting relation of prefolding and synfolding veins on gently dipping limb of fold. (D) Crosscutting relation of prefolding and synfolding veins on subvertical limb of fold. (E) S-shaped synfolding vein on gently dipping limb of fold. (F) Z-shaped synfolding veins on subvertical limb of fold. View is to east-southeast in (A). View is to north-northeast in (B)–(F).

15.1 Park on the shoulder on the northeast side of Tanner Hill Rd. Stop 4 (43° 29.515'N, 73° 19.125'W) is the quarry immediately east of the parking area and the exposures along the road in the vicinity of the parking area.

**STOP 4. CENTRAL DOMAIN (INDIAN RIVER–PAWLET/AUSTIN GLEN FORMATIONS).** 43° 29.515'N, 73° 19.125'W. (45 MINUTES).

The bedrock geology along Tanner Hill Road was mapped by Jacobi (1977) and is described in Rowley et al. (1979) and Landing (2002). The road transects the Tanner Hill syncline, and, although many of the exposures are small, the stratigraphic succession is readily observed and contacts between units are easily located. Exposures on the west limb of the syncline are somewhat inaccessible because of a new maple sugaring operation.

The small quarry immediately east of the parking area for this stop is in the Middle Ordovician Indian River Formation, a red slate interpreted as the oldest synorogenic unit in the Giddings Brook thrust sheet (Landing, 2002, 2012). Macdonald et al. (2017) dated a sample from a half-meter thick silicified layer of green slate in this quarry using LA-ICPMS and CA-IDTIMS. Zircon grains interpreted to be of primary volcanic origin and in the youngest population obtained by LA-ICPMS analysis yielded a CA-IDTIMS age of 466.06 ± 0.21 Ma.

Stop 4 lies in the central domain between the Taconic Frontal thrust and the Lee Road fault. The syncline extends for the length of the Taconic slate belt, the axial trace trending north-northeast–south-southwest in the northern and southern domains and north–south in the central domain. Folds between the Lee Road fault and Middle Granville thrust in the central domain have axial traces that trend north-northwest–south-southeast. The anomalous orientation of the fold axial traces is interpreted to be a result of the central domain having undergone inclined transpression (Crespi et al., 2010). Consistent with such a three-dimensional deformation, the stretching lineation is not downdip, and the strain fringes record extension in the *Y* direction. Moreover, in addition to the top-to-west-northwest sense of shear given by fibers in strain fringes in the *XZ* plane throughout the Taconic slate belt, fibers in strain fringes in the central domain are locally curved in the *XY* plane, the sense of curvature indicating sinistral shear.

Mesoscale, postcleavage normal faults are present in the exposures along Tanner Hill Road, most commonly in the Indian River Formation. Some of the faults contain laminated quartz and chlorite veins, but most lack fault-zone vein material, most likely because the faults are weathered. Faults with thick panels of laminated quartz and chlorite veins and well-developed steps can be found in out-of-place blocks in the quarries on either side of Tanner Hill Road. Although some faults are parallel to slaty cleavage, most strike parallel to but dip more steeply than cleavage (Fig. 9). The angle between the faults and slaty cleavage is on average about 10°–15°.

0.0 Continue on Tanner Hill Rd.
0.6 Intersection of Tanner Hill Rd., Truthville Rd., and Welch Rd. (to the right). Continue straight onto Truthville Rd.
2.6 At the stop sign, continue straight on Truthville Rd.
3.7 At the stop sign, continue straight onto Co. Rd. 12.
3.9 At the stop sign, turn right to continue on Co. Rd. 12A.
4.2 At the stop sign, turn right onto NY-22.
5.2 Bear left onto Co. Rd. 17.
5.8 At the stop sign, turn left onto NY-40.
12.0 At the traffic light, turn left onto NY-149.
15.8 Turn right onto Searles Rd. (dirt road).
16.6 At the stop sign, continue straight onto Liebig Rd.
16.8 View to the east of the Taconic Range and Green Mountains.
19.2 Turn right onto Big Burch Hill Rd.
19.4 Turn left onto Bardin Rd. (dirt road). Bardin Rd. is incorrectly labeled on Google Maps and Google Earth. Bardin Rd. is the road between Liebig Rd. to the east and "Bardin Rd." (a driveway) to the west.

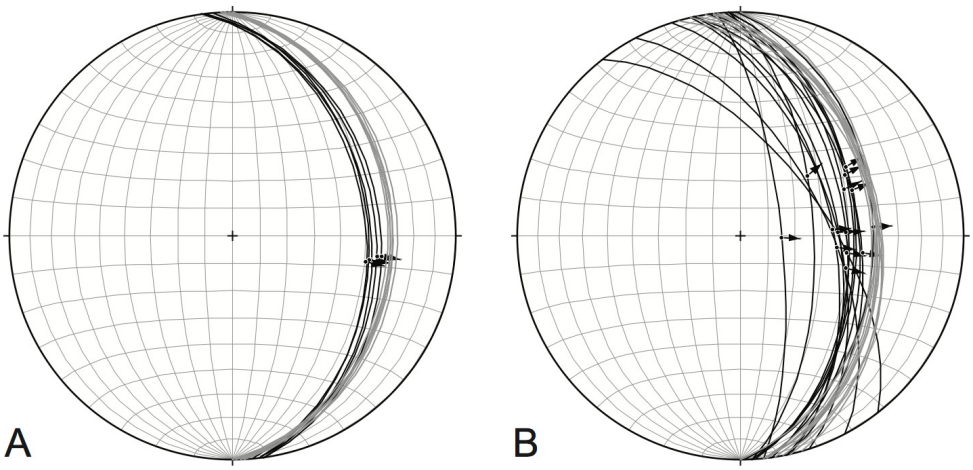


Figure 9. Stereonets of postcleavage faults and slaty cleavage in exposures of Indian River Formation along Tanner Hill Road. (A) Upright limb and (B) overturned limb of Tanner Hill syncline. Black great circles—fault planes; dots—striae; arrows—motion of hanging wall; gray great circles—slaty cleavage. Equal-area, lower-hemisphere projections.

19.4 Park along the west side of Bardin Rd. Walk a short distance along Bardin Rd. to the large bend in the road. Stop 5 (43° 19.630'N, 73° 19.670'W) consists of the small roadcuts along the west side of Bardin Rd. and various outcrops in the woods immediately west of Bardin Rd.

**STOP 5. SOUTHERN DOMAIN (HATCH HILL FORMATION) AND BARDIN DIKE.** 43° 19.630'N, 73° 19.670'W. (45 MINUTES).

This exposure of the Lower Cambrian to Lower Ordovician Hatch Hill Formation consists of interbedded black slate and quartz arenites. Subvertical bedding is visible in the small roadcut on the north side of the large bend in Bardin Road, and subhorizontal bedding is visible in the small roadcut on the south side of the large bend in Bardin Road. Subvertical to steeply east-dipping and subhorizontal bedding is visible in the outcrops in the woods immediately west of Bardin Road. The exposure lies on the upright limb of a regional-scale syncline on Shaw's map of portions of the Granville, Hartford, Hebron, and Pawlet townships (Shaw, 1984) and on the overturned limb of a regional-scale syncline on the Bedrock Geologic Map of Vermont (Ratcliffe et al., 2011). The bedding-cleavage relations at the exposure indicate a north-northeast-trending anticlinal hinge between the area with subvertical to steeply east-dipping bedding and the area with subhorizontal bedding. This anticline is parasitic to the regional-scale fold.

The characteristics of Stop 5 are typical of the southern domain. Slaty cleavage strikes north-northeast and dips about 30° east. The stretching lineation is about down the dip of slaty cleavage. Syntectonic fibers associated with slaty cleavage development are generally straight in *XZ* sections. Where they exhibit subtle curvature, the sense of curvature is consistent with top-to-west-northwest noncoaxial flow. The fibers yield a mean stretch value for the *X* direction of 1.6 and a mean stretch value for the *Y* direction of 1.1. The main differences between the southern and northern domains are that the fibers in the southern domain are not as curved as they are in the northern domain and that the stretch values for the *X* direction in the southern domain are not as high as they are in the northern domain. These differences are consistent with the southern domain lying at a higher structural level, i.e., farther from the base of the Giddings Brook thrust sheet, than the northern domain.

An igneous dike, which we have named the Bardin dike, lies in the hinge zone of the anticline indicated by the bedding-cleavage relations at the exposure (Fig. 10). This dike together with many of the other dikes/dike segments in the southern part of the Taconic lobe was mapped in 1895 by Florence Bascom, a pioneer in the advancement of women in geology. Bascom's work contributed to Dale's efforts to map the Taconic slate belt, and the dikes that she mapped appear on Dale's map of the Taconic slate belt (Dale, 1899). The Bardin dike is about 2 m wide. Its trend is

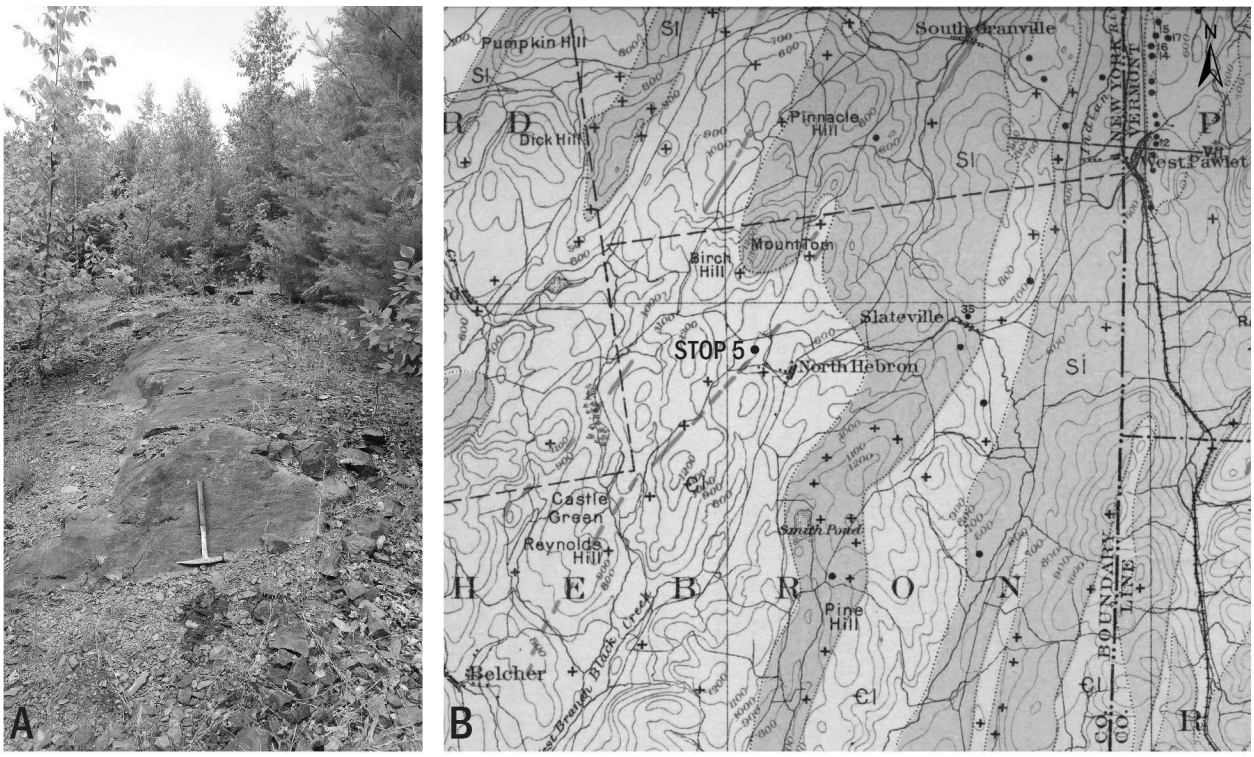


Figure 10. (A) Photograph of Bardin dike at Stop 5. View is to south-southwest. (B) Portion of Dale's map of Taconic slate belt (Dale, 1899) showing location of Stop 5. Map scale is 1:115,385.

subparallel to the axial traces of the regional-scale folds in the southern domain and to the axial trace of the local anticline that it has intruded. Like the Bomoseen dike, a well-developed pencil cleavage is present in the wall rock adjacent to the dike. It can be observed on both sides of the dike and has been formed by the intersection of the well-developed slaty cleavage with closely spaced dike-parallel fractures. Bascom's mapping shows the Bardin dike as one of a series of discontinuous dike segments that extends for about 12 km from Belcher, New York, to South Granville, New York (Fig. 10).

0.0 Continue on Bardin Rd.
0.3 Turn left at the T intersection onto Little Burch Hill Rd. (dirt road).
0.5 Bear right onto Liebig Rd.
0.8 At the stop sign, turn left onto Co. Rd. 31.
1.3 Turn left onto Co. Rd. 28.
4.8 At the stop sign, continue straight onto NY-149.
6.6 At the traffic light, turn left onto NY-149/NY-22.
6.7 Bear left to continue on NY-22.
7.0 Park on the shoulder on the northeast side of NY-22. Stop 6 (43° 23.825'N, 73° 16.150'W) is the roadcut on the northeast side of NY-22.

**STOP 6. CENTRAL DOMAIN/SOUTHERN DOMAIN BOUNDARY (MOUNT MERINO FORMATION) AND GRANVILLE DIKE.** 43° 23.825'N, 73° 16.150'W. (30 MINUTES).

This exposure of the Middle to Upper Ordovician Mount Merino Formation changes from interbedded black slate and chert in the northwestern part of the exposure to mainly chert in the southeastern part of the exposure. Slaty cleavage, which is well developed in the northwestern part of the exposure, dips moderately east, and bedding is subvertical. The exposure lies on the upright limb of a regional-scale anticline on Kidd's map of the Lee Road area

(Kidd, 1976)/Fisher's map of the Glens Falls–Whitehall region (Fisher, 1985) and on the Bedrock Geologic Map of Vermont (Ratcliffe et al., 2011). The bedding-cleavage relations here, however, indicate the exposure is on an overturned limb. This implies the strata are on the limb of a fold that is parasitic to the regional-scale fold.

Stop 6 lies near the boundary between the central and southern domains where the trend of the fold axial traces changes from north-northwest–south-southeast in the central domain to north-northeast–south-southwest in the southern domain. Slaty cleavage strikes slightly east of north and dips moderately east. The stretching lineation is about down the dip of slaty cleavage. We have not analyzed syntectonic fibers at this location.

A narrow igneous dike lies near the southeastern end of the exposure. This dike does not appear on Dale's map of the Taconic slate belt (Dale, 1899). It is shown, however, on Kidd's map of the Lee Road area (Kidd, 1976) and is reproduced on Fisher's map of the Glens Falls–Whitehall region (Fisher, 1985). We have named this dike the Granville dike. It is about 25 cm wide and has been mapped for a distance of about 0.4 km.

Like the Bardin dike, the Granville dike is one of a number of northeast-trending dikes/dike segments in the southern part of the Taconic lobe. These dikes have the same general trend in the southern domain, where the structural grain trends north-northeast–south-southwest, and in the central domain, where the structural grain trends north-northwest–south-southeast. Thus, while the dikes generally follow the structural grain in the southern domain, they cut across it in the central domain. The northeast-trending Granville dike cuts across the structural grain, but this is not immediately apparent at Stop 6 because both the dike and bedding are subvertical and because the orientation of bedding is difficult to see in three dimensions in the chert layers next to the dike. About 2 m to the northwest of the dike, bedding strikes about 035–040 (Fig. 11). Because the dike is slightly magnetic and somewhat curved, we used the orientation of dike-parallel fractures in the vicinity of the dike as a proxy for the orientation of the dike. These fractures strike about 060–075 (Fig. 11), which is oblique to bedding and similar to the 055–060 trend of the dike shown on Kidd's map of the Lee Road area (Kidd, 1976). The oblique relation between the Granville dike and the structural grain is readily seen on Kidd's map of the Lee Road area (Kidd, 1976)/Fisher's map of the Glens Falls–Whitehall region (Fisher, 1985) where the dike is shown cutting across the contact between the Indian River and Mount Merino formations (Fig. 11).

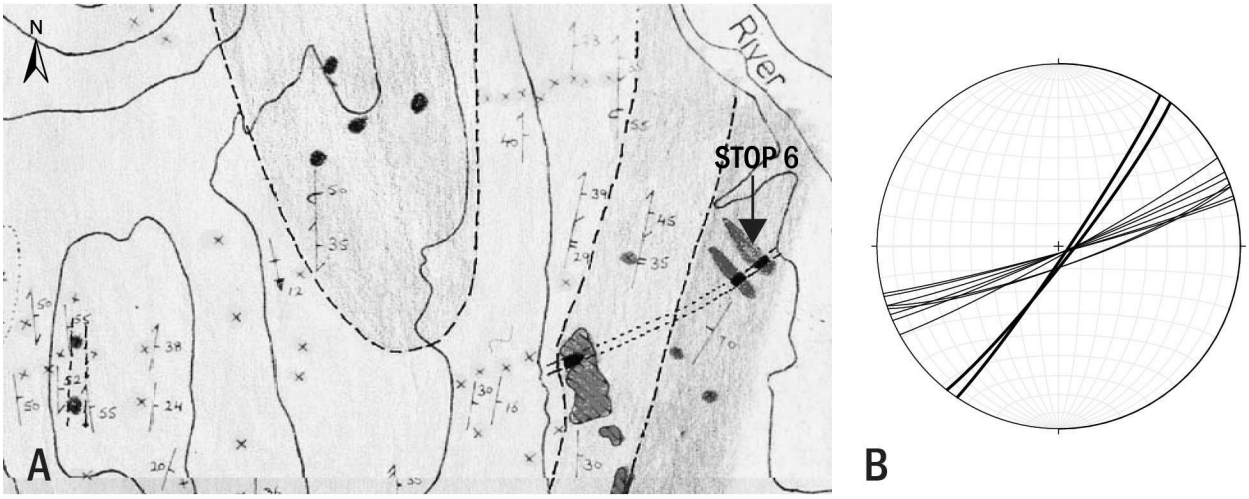


Figure 11. (A) Portion of bedrock geologic map of Lee Road area (Kidd, 1976) showing location of Stop 6. Stratigraphic units outward from core of anticline—Hatch Hill Formation, Poultney/Deep Kill Formation, Indian River Formation, Mount Merino Formation; black areas within parallel dotted lines—Granville dike. Map scale is 1:12,000. (B) Stereonet of bedding and dike-parallel fractures at Stop 6. Thick great circles—bedding; thin great circles—dike-parallel fractures. Equal-area, lower-hemisphere projection.

Several brittle faults are present in this exposure. They are either oblique to both bedding and slaty cleavage or parallel to bedding.

## REFERENCES CITED

Bailey, D.G., Lupulescu, M., Chiarenzelli, J., and Traylor, J.P., 2017, Age and origin of the Cannon Point syenite, Essex County, New York: Southernmost expression of Monteregian Hills magmatism?: Canadian Journal of Earth Sciences, v. 54, no. 4, p. 379–392, https://doi.org/10.1139/cjes-2016-0144.

Bird, J.M., and Dewey, J.F., 1970, Lithosphere plate-continental margin tectonics and the evolution of the Appalachian orogen: Geological Society of America Bulletin, v. 81, no. 4, p. 1031–1060, https://doi.org/10.1130/0016-7606(1970)81[1031:LPMTAT]2.0.CO;2.

Crespi, J.M., Underwood, H.R., and Chan, Y.-C., 2010, Orogenic curvature in the northern Taconic allochthon and its relation to footwall geometry, *in* Tollo, R.P., Bartholomew, M.J., Hibbard, J.P., and Karabinos, P.M., eds., From Rodinia to Pangea: The lithotectonic record of the Appalachian region: Geological Society of America Memoir 206, p. 111–122, https://doi.org/10.1130/2010.1206(06).

Dale, T.N., 1899, The slate belt of eastern New York and western Vermont: U.S. Geological Survey Annual Report 19, pt. 3, p. 153–307.

Eby, G.N., and McHone, J.G., 1997, Plutonic and hypabyssal intrusions of the Early Cretaceous Cuttingsville complex, Vermont, *in* Grover, T.W., Mango, H.N., and Hasenohr, E.J., eds., Guidebook for the 89th Annual Meeting of the New England Intercollegiate Geological Conference: Castleton, Vermont, Castleton State College, p. B2-1–B2-16.

Faure, S., Tremblay, A., and Angelier, J., 1996, State of intraplate stress and tectonism of northeastern America since Cretaceous times, with particular emphasis on the New England–Québec igneous province: Tectonophysics, v. 255, no. 1–2, p. 111–134, https://doi.org/10.1016/0040-1951(95)00113-1.

Faure, S., Tremblay, A., Malo, M., and Angelier, J., 2006, Paleostress analysis of Atlantic crustal extension in the Québec Appalachians: The Journal of Geology, v. 114, no. 4, p. 435–448, https://doi.org/10.1086/504178.

Fisher, D.W., 1985, Bedrock geology of the Glens Falls–Whitehall region, New York: New York State Museum Map and Chart Series 35, scale 1:48,000, 3 sheets, 58 p. text.

Foland, K.A., Gilbert, L.A., Sebring, C.A., and Chen, J.-F., 1986, $^{40}Ar/^{39}Ar$ ages for plutons of the Monteregian Hills, Québec: Evidence for a single episode of Cretaceous magmatism: Geological Society of America Bulletin, v. 97, no. 8, p. 966–974, https://doi.org/10.1130/0016-7606(1986)97<966:AAFPOT>2.0.CO;2.

Fossen, H., and Tikoff, B., 1993, The deformation matrix for simultaneous simple shearing, pure shearing, and volume change, and its application to transpression-transtension tectonics: Journal of Structural Geology, v. 15, no. 3–5, p. 413–422, https://doi.org/10.1016/0191-8141(93)90137-Y.

Fowler, P., 1950, Stratigraphy and structure of the Castleton area, Vermont: Vermont Geological Survey Bulletin 2, 83 p.

Goldstein, A., Pickens, J., Klepeis, K., and Linn, F., 1995, Finite strain heterogeneity and volume loss in slates of the Taconic allochthon, Vermont, U.S.A.: Journal of Structural Geology, v. 17, no. 9, p. 1207–1216, https://doi.org/10.1016/0191-8141(95)00022-6.

Hibbard, J.P., van Staal, C.R., Rankin, D.W., and Williams, H., 2006, Lithotectonic map of the Appalachian orogen, Canada–United States of America: Geological Survey of Canada "A" Series Map 2096A, scale 1:1,500,000, 2 sheets, https://doi.org/10.4095/221912.

Hoak, T.E., 1992, Strain analysis, slaty cleavage, and thrusting in the Taconic slate belt: Northeastern Geology, v. 14, p. 7–14.

Hubacher, F.A., and Foland, K.A., 1991, $^{40}Ar/^{39}Ar$ ages for Cretaceous intrusions of the White Mountain magma series, northern New England, and their tectonic implications: Geological Society of America Abstracts with Programs, v. 23, p. 47.

Jacobi, L.D., 1977, Stratigraphy, depositional environment, and structure of the Taconic allochthon, central Washington County, New York [M.S. thesis]: Albany, New York, State University of New York at Albany, 191 p.

Karabinos, P., Samson, S.D., Hepburn, J.C., and Stoll, H.M., 1998, Taconian orogeny in the New England Appalachians: Collision between Laurentia and the Shelburne Falls arc: Geology, v. 26, no. 3, p. 215–218, https://doi.org/10.1130/0091-7613(1998)026<0215:TOITNE>2.3.CO;2.

Karabinos, P., Macdonald, F.A., and Crowley, J.L., 2017, Bridging the gap between the foreland and hinterland I: Geochronology and plate tectonic geometry of Ordovician magmatism and terrane accretion on the Laurentian margin of New England: American Journal of Science, v. 317, no. 5, p. 515–554, https://doi.org/10.2475/05.2017.01.

Kidd, W.S.F., 1976, Geology of the Lee Road area, Granville, New York: http://www.atmos.albany.edu/geology/webpages/SUNYATaconicGeologicalMaps.html (August 2018).

Landing, E., 2002, Early Paleozoic sea levels and climates: New evidence from the east Laurentian shelf and slope, *in* McLelland, J., and Karabinos, P., eds., Guidebook for the 94th Annual Meeting of the New England Intercollegiate Geological Conference and the 74th Annual Meeting of the New York State Geological Association: Lake George, New York, p. B6-1–B6-22.

Landing, E., 2012, The great American carbonate bank in eastern Laurentia: Its births, deaths, and linkage to paleooceanic oxygenation (Early Cambrian–Late Ordovician), *in* Derby, J.R., Fritz, R.D., Longacre, S.A., Morgan, W.A., and Sternbach, C.A., eds., The great American carbonate bank: The geology and economic resources of the Cambrian–Ordovician Sauk megasequence of Laurentia: American Association of Petroleum Geologists Memoir 98, p. 451–492, https://doi.org/10.1306/13331502M983502.

Lim, C., Kidd, W.S.F., and Howe, S.S., 2005, Late shortening and extensional structures and veins in the western margin of the Taconic orogen (New York to Vermont): The Journal of Geology, v. 113, no. 4, p. 419–438, https://doi.org/10.1086/430241.

Macdonald, F.A., Ryan-Davis, J., Coish, R.A., Crowley, J.L., and Karabinos, P., 2014, A newly identified Gondwanan terrane in the northern Appalachian Mountains: Implications for the Taconic orogeny and closure of the Iapetus Ocean: Geology, v. 42, no. 6, p. 539–542, https://doi.org/10.1130/G35659.1.

Macdonald, F.A., Karabinos, P.M., Crowley, J.L., Hodgin, E.B., Crockford, P.W., and Delano, J.W., 2017, Bridging the gap between the foreland and hinterland II: Geochronology and tectonic setting of Ordovician magmatism and basin formation on the Laurentian margin of New England and Newfoundland: American Journal of Science, v. 317, no. 5, p. 555–596, https://doi.org/10.2475/05.2017.02.

Matton, G., and Jébrak, M., 2009, The Cretaceous peri-Atlantic alkaline pulse (PAAP): Deep mantle plume origin or shallow lithospheric breakup?: Tectonophysics, v. 469, no. 1–4, p. 1–12, https://doi.org/10.1016/j.tecto.2009.01.001.

McEnroe, S.A., 1996, North America during the Lower Cretaceous: New paleomagnetic constraints from intrusions in New England: Geophysical Journal International, v. 126, no. 2, p. 477–494, https://doi.org/10.1111/j.1365-246X.1996.tb05304.x.

McHone, J.G., 1978, Distribution, orientations, and ages of mafic dikes in central New England: Geological Society of America Bulletin, v. 89, no. 11, p. 1645–1655, https://doi.org/10.1130/0016-7606(1978)89<1645:DOAAOM>2.0.CO;2.

McHone, J.G., 1984, Mesozoic igneous rocks of northern New England and adjacent Québec: Geological Society of America Map and Chart Series MC-49, scale 1:690,000, 1 sheet, 5 p. text.

McHone, J.G., and Butler, J.R., 1984, Mesozoic igneous provinces of New England and the opening of the North Atlantic Ocean: Geological Society of America Bulletin, v. 95, no. 7, p. 757–765, https://doi.org/10.1130/0016-7606(1984)95<757:MIPONE>2.0.CO;2.

McHone, J.G., and McHone, N.W., 1993, Field guide to Cretaceous intrusions in the northern Taconic Mountains region, Vermont: Vermont Geology, v. 7, p. 1–27.

Morgan, W.J., 1972, Deep mantle convection plumes and plate motions: American Association of Petroleum Geologists Bulletin, v. 56, no. 2, p. 203–213, https://doi.org/10.1306/819A3E50-16C5-11D7-8645000102C1865D.

Ratcliffe, N.M., Stanley, R.S., Gale, M.H., Thompson, P.J., and Walsh, G.J., 2011, Bedrock geologic map of Vermont: U.S. Geological Survey Scientific Investigations Map 3184, scale 1:100,000, 3 sheets, https://doi.org/10.3133/sim3184.

Rowley, D.B., 1983, Operation of the Wilson cycle in western New England during the early Paleozoic: with emphasis on the stratigraphy, structure, and emplacement of the Taconic allochthon [Ph.D. thesis]: Albany, New York, State University of New York at Albany, 602 p.

Rowley, D.B., and Kidd, W.S.F., 1981, Stratigraphic relationships and detrital composition of the medial Ordovician flysch of western New England: Implications for the tectonic evolution of the Taconic orogeny: The Journal of Geology, v. 89, no. 2, p. 199–218, https://doi.org/10.1086/628580.

Rowley, D.B., Kidd, W.S.F., and Delano, L.L., 1979, Detailed stratigraphic and structural features of the Giddings Brook slice of the Taconic allochthon in the Granville area, *in* Friedman, G.M., ed., Guidebook for the 51st Annual Meeting of the New York State Geological Association and the 71st Annual Meeting of the New England Intercollegiate Geological Conference: Troy, New York, Rensselaer Polytechnic Institute, p. 186–242.

Shaw, W.J., 1984, Geological map of portions of Granville, Hartford, Hebron townships, Washington County, New York, and Pawlet Township, Rutland County, Vermont: http://www.atmos.albany.edu/geology/webpages/SUNYATaconicGeologicalMaps.html (August 2018).

Sleep, N.H., 1990, Monteregian hotspot track: A long-lived mantle plume: Journal of Geophysical Research, v. 95, no. B13, p. 21,983–21,990, https://doi.org/10.1029/JB095iB13p21983.

Stanley, R.S., and Ratcliffe, N.M., 1985, Tectonic synthesis of the Taconian orogeny in western New England: Geological Society of America Bulletin, v. 96, no. 10, p. 1227–1250, https://doi.org/10.1130/0016-7606(1985)96<1227:TSOTTO>2.0.CO;2.

Withjack, M.O., Schlische, R.W., and Olsen, P.E., 2012, Development of the passive margin of eastern North America: Mesozoic rifting, igneous activity, and breakup, *in* Roberts, D.G., and Bally, A.W., eds., Regional Geology and Tectonics: Phanerozoic Rift Systems and Sedimentary Basins: Amsterdam, The Netherlands, Elsevier, p. 301–335, https://doi.org/10.1016/B978-0-444-56356-9.00012-2.

Wood, D.S., 1974, Current views of the development of slaty cleavage: Annual Review of Earth and Planetary Sciences, v. 2, p. 369–401, https://doi.org/10.1146/annurev.ea.02.050174.002101.

Zen, E-an, 1972, Some revisions in the interpretation of the Taconic allochthon in west-central Vermont: Geological Society of America Bulletin, v. 83, no. 9, p. 2573–2588, https://doi.org/10.1130/0016-7606(1972)83[2573:SRITIO]2.0.CO;2.

# A TRAVERSE THROUGH THE SUTURE ZONE BETWEEN LAURENTIA AND THE MORETOWN TERRANE IN NORTHWESTERN MASSACHUSETTS

Paul Karabinos, Department of Geosciences, Williams College, Williamstown, MA 01267, pkarabin@williams.edu
Francis A. Macdonald, Department of Earth Science, Webb Hall, UC Santa Barbara, Santa Barbara, CA 93106, francism@geol.ucsb.edu
James L. Crowley, Department of Geosciences, Boise State University, Boise, ID 83725, jimcrowley@boisestate.edu

## ABSTRACT

U-Pb dates on magmatic and detrital zircon from samples in the hinterland of the Taconic orogen place new constraints on the timing and plate tectonic geometry of terrane accretion and magmatic arc activity. The Moretown terrane, a Gondwanan-derived exotic block, extends from the Rowe Schist-Moretown Formation contact in the west to the Bronson Hill arc in the east. Arc-related plutonic and volcanic rocks formed above an east-dipping subduction zone under the western leading edge of the Moretown terrane from approximately 500 to 470 Ma, until it collided with hyperextended distal fragments of Laurentia, represented by the Rowe Schist. Magmatic arc rocks formed during this interval are primarily located in the Shelburne Falls arc, although some rocks that formed above the early east-dipping subduction zone are located in the northern part of the Bronson Hill arc to the east. Metasedimentary rocks in the Shelburne Falls arc contain detrital zircon derived from mixing of Gondwanan, Laurentian, and arc sources, suggesting that the Moretown terrane was proximal to Laurentia by 475 Ma. Explosive eruptions at 466 to 464 Ma preserved in the Barnard Volcanic Member of the Missisquoi Formation in Vermont and as ash beds in the Indian River Formation in the Taconic allochthons may record slab-breakoff of subducted lithosphere following collision of the Moretown terrane with distal Laurentian crustal fragments. Between 466 and 455 Ma a reversal in subduction polarity lead to a west-dipping subduction zone under Laurentia and the newly accreted Moretown terrane. Magmatic arc rocks in the Bronson Hill arc formed above this west-dipping subduction zone along the eastern trailing edge of the Moretown terrane at approximately 455 to 440 Ma. The western boundary of Ganderia in New England is east of the Bronson Hill arc, buried beneath Silurian and Devonian rocks deformed during the Acadian orogeny.

## INTRODUCTION

Before plate tectonic theory was applied to the Appalachians (e.g. Bird and Dewey, 1970; St. Julien and Hubert, 1975), and even before absolute radiometric ages were available, three major orogenies were recognized based on paleontological constraints on deformed rocks below angular unconformities: the Ordovician Taconic, the Devonian Acadian, and the Pennsylvanian to Permian Alleghenian orogenies. During the 1970s and 1980s, it was common for geologists working in western New England to ascribe deformation to either the Taconic or Acadian orogenies. This simplified view of early Paleozoic tectonism held that the Taconic orogeny resulted from the collision of Laurentia with a '*Taconic arc*' (for example, Rowley and Kidd, 1981; Stanley and Ratcliffe, 1985) and that the Acadian orogeny marked the collision of a Gondwanan-derived microcontinent called Avalonia (for example, Rast and Skehan, 1993). The Alleghenian orogeny occurred when the main Gondwanan continent arrived in the Late Paleozoic, and it was believed to have only affected rocks in southeastern New England (for example, Quinn and Moore Jr, 1968).

Detailed work in New England and in the Canadian Appalachians, where oceanic tracts, arcs, and Gondwanan-derived microcontinents are better preserved, has resulted in a much more intricate and complex history of arc and microcontinent accretion, reversals in subduction polarity, and intermittent back-arc rifting (for example, Van Staal et al., 1998; Zagorevski et al., 2008). More recent tectonic syntheses have expanded the number of orogenies to the Taconic, Salinic, Acadian, Neoacadian, and Alleghenian, and some of these involve multiple phases (for example, Van Staal and Barr, 2012). Gondwanan-derived microcontinents now include the Moretown terrane (Macdonald et al., 2014), Ganderia (Van Staal et al., 1998), Avalonia (Rast and Skehan, 1993), and Meguma (Schenk, 1997, White and Barr, 2010). Furthermore, we now know that Alleghenian deformation affected rocks as far west as the Bronson Hill arc and Connecticut Valley Trough in western Massachusetts (for example, Robinson et

al., 1992). The expanding geochronological database in the northern Appalachians suggests that the Laurentian margin was continuously active from approximately 475 to 270 Ma.

Hibbard et al. (2006) mapped the suture between peri-Laurentian and peri-Gondwanan terranes in the New England Appalachians along the western margin of the Bronson Hill arc (Fig. 1). This interpretation required that the Shelburne Falls arc (Fig. 1) formed on a Laurentian-derived microcontinent as proposed for the Dashwoods block in Newfoundland (Waldron and van Staal, 2001), and that the Bronson Hill arc formed on the western leading edge of Ganderia (Hibbard et al., 2006). Based on detrital zircon data from the Moretown Formation in Massachusetts and Vermont, Macdonald et al. (2014) and Karabinos et al. (2017) argued that the suture between Laurentia and Gondwanan-derived terranes is located approximately 50 km further west along the contact between the Rowe Schist and the Moretown Formation, which is characterized by a high concentration of mafic and ultra-mafic lenses, interpreted as remnants of subducted oceanic lithosphere. Because the evidence for a Gondwanan source for the metasedimentary rocks came from the Moretown Formation, we called this newly identified Gondwanan-derived block the Moretown terrane.

The relocation of the suture has some important tectonic implications for the deep crustal structure of the New England Appalachians. 1) It requires that the Shelburne Falls arc formed on Gondwanan-derived crust rather than Laurentian crust. 2) Instead of the Bronson Hill arc having formed above an east-dipping subduction zone on the western leading edge of Ganderia, we suggested that it formed above a west-dipping subduction zone along the eastern trailing edge of the Moretown terrane after a reversal in subduction polarity. 3) If the Moretown terrane is distinct from Ganderia, the suture between these two Gondwanan-derived terranes must be located somewhere under the Silurian-Devonian rocks of the Central Maine basin (Fig. 1).

The focus of this trip is the evidence for a plate suture between Laurentia and a Gondwanan-derived microcontinent, the Moretown terrane, proposed by Macdonald et al. (2014) and Karabinos et al. (2017). In Massachusetts, this suture coincides with the boundary between the Rowe Schist and the Moretown Formation. There is nothing cryptic about this suture; it is characterized by a dramatic difference in sediment source as revealed by detrital zircon populations, and is characterized by a high concentration of mafic and ultramafic lenses, which we interpret as remnants of oceanic crust and mantle from an east-dipping subduction zone. It also coincides with a sharp 10 to 15 km decrease in depth to MOHO from the Laurentian margin to the Moretown terrane (Li et al., 2018). We will also discuss evidence suggesting that much of the 475 Ma arc magmatism in the Shelburne Falls arc occurred in close proximity to Laurentia even though the arc was built on the Gondwanan-derived Moretown terrane.

## GEOLOGIC FRAMEWORK

### *The Laurentian Margin*

***Rifting and Mesoproterozoic Basement Rocks***- The Neoproterozoic breakup of Rodinia created a south-facing rifted margin on Laurentia at approximately 20° S latitude (Torsvik et al., 2012). The age of rifting in western New England is constrained by 570 to 555 Ma volcanic and plutonic rocks (Kumarapeli et al., 1989; Walsh and Aleinikoff, 1999). Remnants of the rift shoulders are found as structural inliers in the Berkshire and Green Mountain massifs, located in western Massachusetts and Vermont (fig. 1), which are composed of ca. 1400 to 950 Ma Mesoproterozoic to Early Neoproterozoic para- and ortho-gneiss that are correlated with the Grenville Province of Canada and the Adirondack Mountains of New York (Karabinos et al., 2008; Karabinos and Aleinikoff, 1990; Ratcliffe and Zartman, 1976; Zen et al., 1983).

***The Dalton Formation*** (Neoproterozoic to Cambrian) in western Massachusetts and Vermont was deposited unconformably on Mesoproterozoic basement of the Berkshire and Green Mountain massifs. The Dalton Formation is compositionally and texturally immature and displays large lateral facies and thickness variations, which reflect deposition in an active rift environment (Allen et al., 2010; Williams and Hiscott, 1987). The Dalton Formation is exposed along the western margins of the Berkshire and Green Mountain massifs, and the lowest unit is a quartz-pebble conglomerate that lies above basement gneisses (fig. 1). Stratigraphically above the conglomerate, the Dalton Formation includes meta-arkose and graphitic phyllite, which is stratigraphically below the Cambrian Cheshire Quartzite (Landing, 2012).

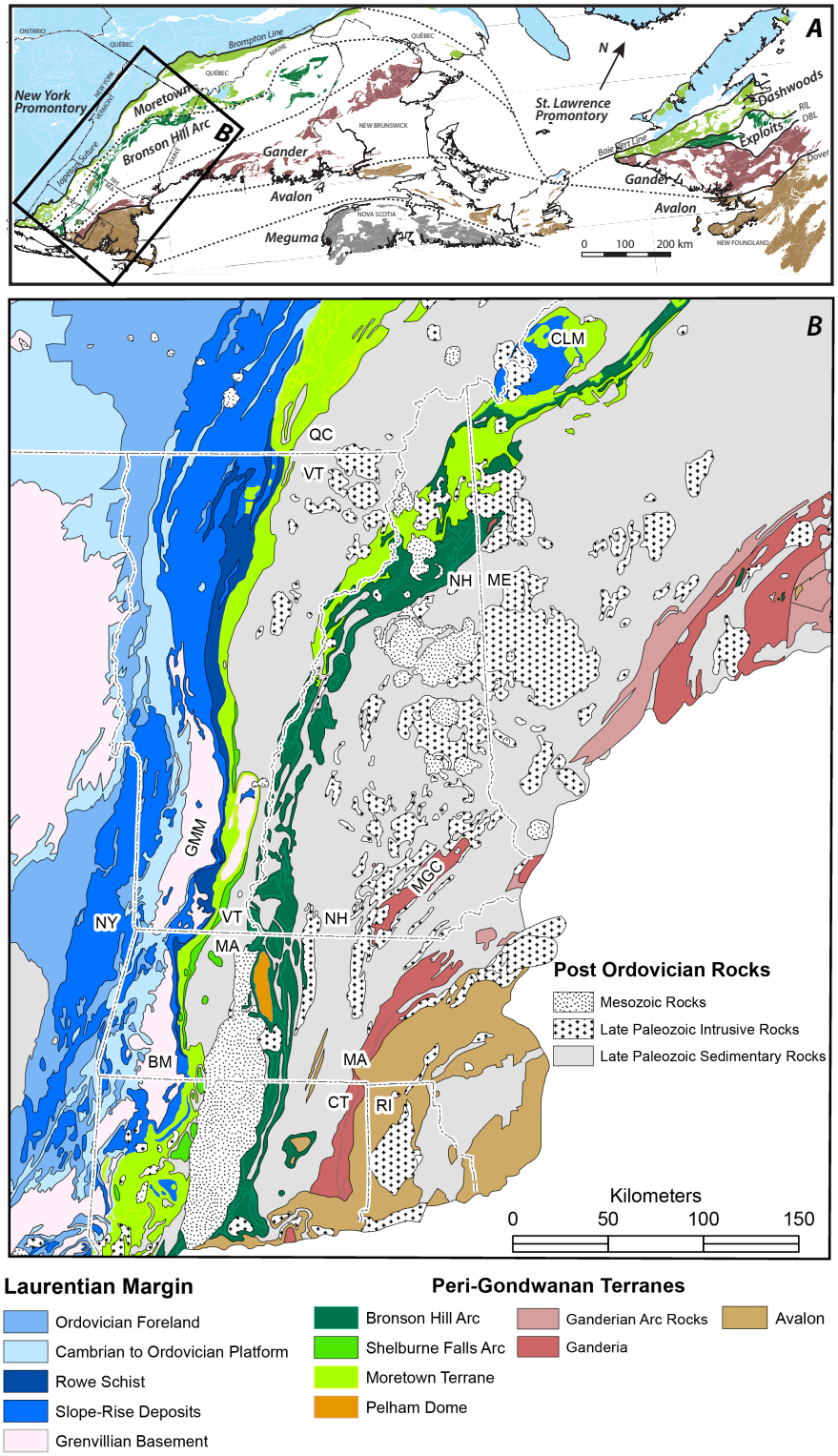


**Fig. 1. (A) Tectonic map of the Appalachians modified from Hibbard et al. (2006). Outline shows location of more detailed tectonic map of New England in 1B. (B) Tectonic map of New England modified from Hibbard et al. (2006). Abbreviations are: BM- Berkshire massif, CLM- Chain Lakes massif, GMM- Green Mountain massif, MGC- Massabesic Gneiss Complex. (C) Location map of samples collected for LA-ICPMS detrital zircon analysis. Units use the same colors and patterns as shown in figure 1B.**

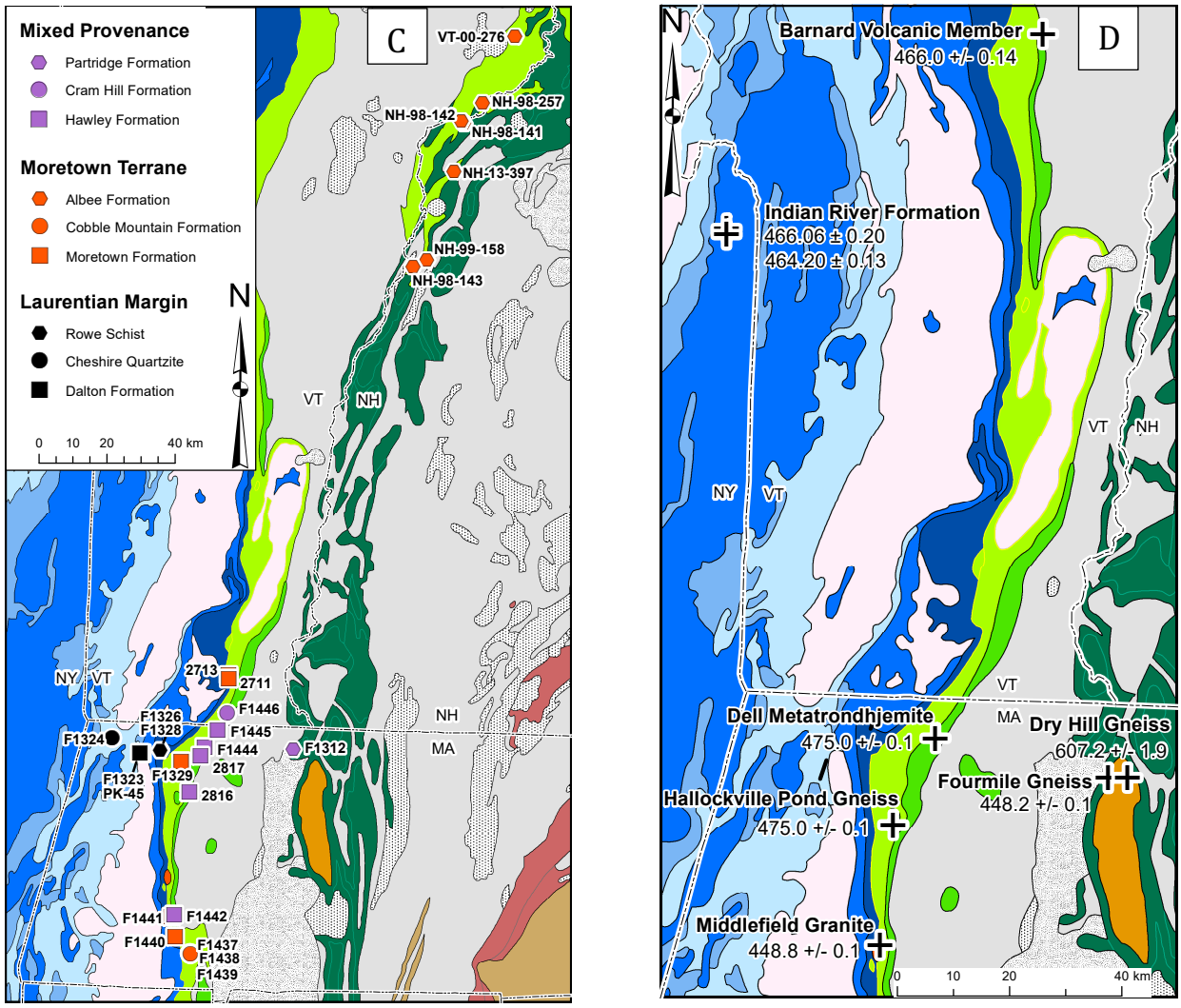


**Fig. 1, cont. (D) Location map of samples dated by U-Pb zircon CA-IDTIMS. Units use the same colors and patterns as shown in figure 1B. (E) Schematic diagram of Neoproterozoic to Ordovician rocks involved in the Taconic orogeny of New England. Laurentian deformed margin units based on Zen and other (1983), Doll et al. (1961), and Ratcliffe et al. (2011). Western and Eastern cover sequences stratigraphy is modified from Karabinos (1988). Peri-Gondwanan realm units, and detrital zircon provenance indicators from Macdonald et al. (2014) and this study. Bronson Hill arc ages from Tucker and Robinson (1990) and Moench and Aleinikoff (2003).**

***The Cheshire Quartzite*** was deposited as a mature quartz arenite in a stable shelf environment and it marks the transition from the rift to drift phase of the opening of the Iapetus Ocean (Allen et al., 2010; Williams and Hiscott, 1987).

***Shelf Carbonate Rocks***- Continued tectonic stability of the Laurentian margin to the Early Ordovician is recorded by the extensive Early Paleozoic carbonate platform preserved throughout the Appalachians. Now metamorphosed to dolomitic and calcitic marble, with interbedded quartzite units, these rocks include the Stockbridge Formation in Massachusetts and the Vermont Valley sequence. The Mesoproterozoic basement gneisses of the Berkshire and Green Mountain massifs, together with the clastic cover rocks, were thrust westward over the Early Cambrian to Early Ordovician carbonate platform margin (Zen et al., 1983; Karabinos, 1988; Ratcliffe et al., 2011).

***Distal Margin of Laurentian-*** Outboard of the Laurentian continental shelf, an Ediacaran to Early Ordovician of deeper-water sequence has been interpreted to record deposition on the continental slope and rise (Rowley and Kidd, 1981). These rocks are now preserved in the older units of the Taconic klippen west of the Green Mountain and Berkshire massifs and the Hoosac Formation and Rowe Schist east of the massifs (figs. 1 and 2; Karabinos, 1988; Rowley and Kidd, 1981; Stanley and Ratcliffe, 1985).

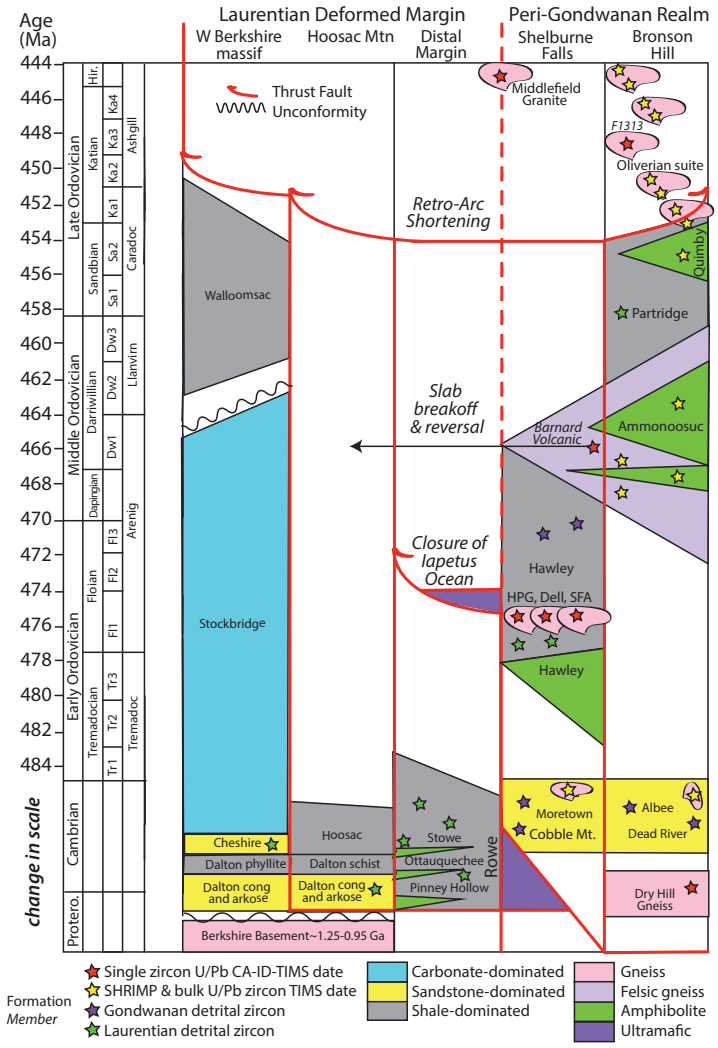


**Fig. 2. Time-space diagram of Neoproterozoic to Ordovician rocks involved in the Taconic orogeny in New England. Laurentian deformed margin stratigraphy based on Karabinos (1988), Zen et al. (1983), and Doll et al. (1961). Peri-Gondwanan realm stratigraphy based on Macdonald et al. (2014), Tucker and Robinson (1990), and Moench and Aleinikoff (2003). HPG- Hallockville Pond Gneiss, Dell- Dell Metatrondhjemite, SFA- Shelburne Falls arc.**

***The Rowe Schist*** is a quartz-rich schist correlated with the Pinney Hollow, Stowe, and Ottauquechee Formations in Vermont by Stanley and Ratcliffe (1985). These rocks may have formed on hyper-extended Laurentian crust, and been separated fom the Laurentian passive margin by the Taconic Seaway (Macdonald et al., 2014; Waldron and van Staal, 2001). Walsh and Aleinikoff (1999) reported a 571 ± 5 Ma U-Pb zircon age for a meta-felsite from the Pinney Hollow Formation from Vermont, but the age of the other units is not constrained by radiometric dating. The youngest detrital zircon grains from the Rowe Schist are Neoproterozoic to Cambrian (585 ± 30, 566 ± 19, 560 ± 29, 536 ± 27 Ma, Macdonald et al., 2014), placing an approximate lower limit on the age of deposition (fig. 3). The structurally lower part of the Rowe Schist is predominantly non-graphitic, whereas the upper part is typically graphitic. Mafic and ultramafic lenses are common in the Rowe Schist, especially near its upper contact with the Moretown Formation (Chidester et al., 1967).

***Gondwanan-Derived Exotic Units***

Ordovician and older rocks east of the Rowe Schist formed within the Iapetus Ocean or on Gondwanan-derived microcontinents.

***The Moretown Formation*** occurs immediately east of the Rowe Schist (fig. 1). In Massachusetts and in Vermont it was mapped as an Ordovician unit (Doll et al., 1961; Ratcliffe et al., 2011; Zen et al., 1983), and interpreted by Rowley and Kidd (1981) and Stanley and Ratcliffe (1985) as a forearc deposit of the '*Taconic arc*'. It is a light gray to buff, fine-grained pinstriped granofels and schist, and contains numerous mafic layers 1 to 3 m thick. The mafic layers originated as tholeiitic basalt or basaltic-andesite that formed either during crustal extension above an Early Ordovician east-dipping subduction zone or above a Late Ordovician to Silurian west-dipping

subduction zone (Coish et al., 2011). Locally, the mafic layers contain 1 to 5 mm plagioclase crystals in the center and aphanitic crystals near one or both margins, suggesting that some of the mafic layers are dikes with chilled margins. Macdonald et al. (2014) demonstrated that detrital zircon in the Moretown Formation was derived from Gondwanan sources, and suggested a Cambrian age for the unit. The Cambrian age assignment of Macdonald et al. (2014) is inconsistent with the interpretation that the Moretown Formation formed as an Ordovician forearc deposit (Rowley and Kidd, 1981; Stanley and Ratcliffe, 1985).

***Ultramafic Lenses-*** Both the Rowe Schist and Moretown Formation host numerous ultramafic lenses near their contact (Chidester et al., 1967; Ratcliffe et al., 2011; Zen et al., 1983), consistent with the interpretation that this contact is a major suture zone similar to the Birchy Complex in Newfoundland (van Staal et al., 2013). In northern Vermont the equivalent contact between rocks formed on or near the Laurentian margin and the Moretown Formation also contains lenses of ultramafic rocks and rare mafic schist preserving evidence for Early Ordovician blueschist metamorphism (Laird et al., 1984). Continuing north across the Canadian border, this contact is marked by the Mont-Orford, Lac-Brompton, Asbestos, and Thetford-Mines ophiolites (Tremblay et al., 2009; Tremblay and Pinet, 2016). The west vergence of faults and folds in this zone of concentrated ultramafic rocks and evidence for high-pressure metamorphism has been used as critical evidence for an east-dipping subduction zone prior to the Taconic collision of Laurentia with an arc terrane (for example, Rowley and Kidd, 1981; Stanley and Ratcliffe, 1985).

***The age of suturing*** of the Rowe Schist-Moretown Formation contact is constrained by the Middlefield Granite in Middlefield, Massachusetts (figs. 1D and 1E). The Middlefield Granite intruded both the Rowe Schist and Moretown Formation at their contact but is not offset by motion along this major suture zone. Furthermore, xenoliths of pelitic and mafic schist in the Middlefield granite contain a folded schistosity, indicating that they were deformed prior to intrusion (Karabinos and Williamson, 1994). Thus, the CA-IDTIMS age of 444.8 $\pm$ 0.1 Ma for this pluton (Macdonald et al., 2014) indicates that Taconic displacement along this major suture ended before 445 Ma, while arc magmatism was active to the east in the Bronson Hill arc and to the south in western Connecticut (Sevigny and Hanson, 1993, 1995).

***Cobble Mountain Formation***- Metasedimentary units correlated with the Moretown Formation include the Cobble Mountain Formation in southwestern Massachusetts (Stanley and Hatch, 1988) and the Albee Formation in northeastern Vermont and adjacent New Hampshire (Doll et al., 1961). The Cobble Mountain Formation outcrop belt begins in southwestern Massachusetts, near the southern-most exposures of the Moretown Formation, and continues into Connecticut (Zen et al., 1983; Rodgers, 1985). The Cobble Mountain Formation was mapped as an Ordovician unit, and was considered by Stanley and Hatch (1988) as a facies equivalent of the Moretown Formation. It is dominated by quartz, feldspar schist, but the lithology is variable.

***The Albee Formation*** outcrop belt is located in northeastern Vermont (Doll et al., 1961; Ratcliffe et al., 2011). The Albee Formation is a light gray quartzite and feldspathic quartzite with interbedded slate, phyllite, or schist, depending on the grade of metamorphism. Micaceous quartzite commonly displays a distinctive pinstripe texture, similar to the Moretown Formation. Correlative rocks occur in adjacent New Hampshire (Lyons et al., 1997), where Moench et al. (1995) mapped them as Dead River Formation, following the convention of Osberg et al. (1985), who reassigned rocks originally mapped as Albee Formation in Maine to the Dead River Formation. The age of the Albee Formation is constrained to be older than a 492.5 $\pm$ 7.8 Ma intrusive tonalitic sill (U-Pb zircon SHRIMP age) east of West Bath, New Hampshire (Rankin et al., 2013).

***The Neoproterozoic Dry Hill Gneiss*** is exposed in the core of the Pelham dome in the Bronson Hill arc (fig. 1). It is a microcline-biotite and microcline-hornblende gneiss containing microcline megacrysts, and interpreted as a metamorphosed alkali rhyolite (Zen et al., 1983). Tucker and Robinson (1990) reported a TIMS upper intercept age of 613 ± 3 Ma, which they interpreted as the eruption age, and a lower intercept age of 289 ± 4 Ma, which they attributed to Alleghenian metamorphism. The Neoproterozoic age of the Dry Hill Gneiss suggests a Gondwanan affinity (Hodgkins, 1985). Aleinikoff et al. (1979), and Wintsch et al. (1990) suggested that the core of the Pelham dome, along with the Willimantic dome in Connecticut, were the western-most exposures of Avalonia in New England. Evidence presented by Macdonald et al. (2014) demonstrated that the Moretown Formation includes metasedimentary rocks with Gondwanan provenance, and raises the possibility that the Dry Hill Gneiss is basement to the Moretown terrane.

***Ordovician Arc-Related Units***

***The Hawley Formation*** is exposed east of and structurally above the Moretown Formation. Equivalent units in Vermont include the Barnard Volcanic, Whetstone Hill, and Cram Hill Members of the Missisquoi Formation of Doll et al., 1961. The Hawley Formation in Massachusetts contains diverse rocks types studied by Jon Kim for his doctoral dissertation. The formation is mostly mafic schist and gneiss, which have island arc tholeite, mid-ocean ridge basalt / back arc-basin basalt, and boninitic geochemical characteristics (Kim and Jacobi, 1996). The Legate Hill Brook Metadacite and the intrusive Dell Metatrondhjemite have arc or fore-arc geochemical signatures (Kim and Jacobi, 1996). The Hawley Formation contains a western and eastern belt of graphitic pelitic schist, a quartz-rich granofels, and layers of volcanoclastic garnet-hornblende schist (garbenschiefer) derived from interlayered mafic and pelitic schist. The Hawley Formation also includes the Charlemont Mafic Intrusive Suite, which Kim and Jacobi (1996) suggested formed during an episode of Ordovician back-arc extension. Kim and Jacobi (1996) observed that amphibolites from the eastern portion of the Moretown Formation are geochemically similar to mid-ocean ridge basalt found in the Hawley Formation, and that trondhjemites and mafic sills from the Shelburne Falls dome (Collinsville Formation) are geochemically similar to the Dell Metatrondhjemite and boninites in the Hawley Formation, respectively. Although the boninitic geochemistry of mafic rocks in the Hawley Formation has been used as evidence for formation in a forearc setting (for example Kim and Jacobi, 1996), it is also compatible with an intra-arc extensional environment, as suggested by the geochemistry of the Charlemont Mafic Intrusive Suite.

Macdonald et al. (2014) presented a CA-IDTIMS U-Pb zircon age for the intrusive **Dell Metatrondhjemite** of 475.5 ± 0.2 Ma (fig. 1D), thus constraining the Hawley Formation to be at least this old. The age of the Dell Metatrondhjemite is in excellent agreement with U-Pb zircon ages for rocks in the Shelburne Falls and Goshen domes presented by Karabinos et al. (1998), and along with the geochemical data described above, firmly links the Hawley Formation to the Shelburne Falls arc. Further, the Dell Metatrondhjemite age is very similar to the 475.0 ± 0.1 Ma U-Pb zircon age for the **Hallockville Pond Gneiss** (fig. 1D), which intruded the Moretown Formation (Karabinos and Williamson, 1994; Macdonald et al., 2014).

***The Collinsville Formation of the Shelburne Falls Arc***- On its eastern margin, the Hawley Formation is structurally overlain by Silurian and Devonian formations of the Connecticut Valley trough (Hatch, 1988; fig. 1). Several domes in the Connecticut Valley trough expose the Collinsville Formation (of Zen et al., 1983; Rodgers, 1985), which are composed of 475 to 470 Ma arc-related bimodal mafic and felsic plutonic rocks (Karabinos et al., 1998). Karabinos et al. (1998) also dated samples of the Barnard Volcanic Member of the Missisquoi Formation (of Doll et al., 1961) in Vermont that range in age from 475 to 470 Ma. Older felsic plutons dated between 502 to 483 Ma have been reported from southern Vermont (Aleinikoff et al., 2011). Together, the Hallockville Pond Gneiss, the Hawley and Collinsville Formations in Massachusetts and the Barnard Volcanic Member in Vermont preserve a record of a magmatic arc, the Shelburne Falls arc of Karabinos et al. (1998) that formed on the Moretown terrane (Macdonald et al., 2014). The common occurrence of arc-related rocks in the time interval 475 to 470 Ma suggests that a significant tectonic event triggered widespread magmatism in the Shelburne Falls arc at this time.

***Arc Rocks in Southwestern Connecticut***- The Moretown terrane and the Shelburne Falls arc continue southward into western Connecticut (fig. 1) where Sevigny and Hanson (1993, 1995) reported U-Pb zircon ages of 454 to 438 Ma from small intrusive bodies belong to the Brookfield plutonic suite and the Newtown, Harrison, and Beardsley Gneisses, which they suggested formed in a Late Ordovician to Early Silurian arc along the eastern Laurentian margin. Although no 485 to 465 Ma arc-related rocks have been reliably dated in southwestern Connecticut, it is important to note that the 454 to 438 Ma gneisses intruded older arc-related rocks of the Collinsville Formation that, according to Sevigny and Hanson (1993, 1995), were already deformed during an early Taconic event. Thus, older arc-related rocks, possibly coeval with 475 to 470 Ma rocks dated in Massachusetts and Vermont, must exist in southwestern Connecticut, although overprinting by high-grade Acadian metamorphism has made it difficult to date them.

***The Bronson Hill Arc***- East of the Connecticut Valley trough and the Mesozoic Basin, Ordovician meta-igneous rocks are also preserved in structural domes (Thompson et al., 1968; Hibbard et al., 2006; fig. 1). Tucker and Robinson (1990) presented precise U-Pb zircon TIMS ages from rocks in the Bronson Hill arc in central Massachusetts and southern New Hampshire. Late Ordovician plutonic rocks of the Swanzey, Pauchaug, Monson, and Fourmile Gneisses range in age from 454 +3/-2 to 442 +3/-2 Ma. In addition, they dated rhyolite from the upper

member of the Ammonoosuc Volcanics at 453 ± 2 Ma, and from the Partridge Formation at 449 +3/-2 Ma. Tucker and Robinson (1990) demonstrated that the plutonic and volcanic rocks have overlapping ages. More importantly, they highlighted the problem that Late Ordovician arc-related rocks in the Bronson Hill belt are younger than the classic Taconic deformation and metamorphism recognized in western New England. The authors offered strikingly different proposals to explain the age discrepancy. Tucker suggested that the Bronson Hill arc collided with an already assembled "*Taconia*", and that the Taconic orogeny resulted from collision of Laurentia with an older arc, possibly represented by the "*Ascot-Weedon-Hawley-Collinsville terrane*". In contrast, Robinson suggested that the Ascot-Weedon and Hawley-Collinsville sequences are not sufficiently distinct nor are they definitely older than rocks in the Bronson Hill arc, and he proposed the existence of a single arc system. Karabinos et al. (1998) showed that rocks in the Hawley-Barnard-Collinsville sequence are significantly older than lithologically similar rocks in the Bronson Hill arc studied by Tucker and Robinson (1990), and they argued that the younger arc rocks formed after a reversal in subduction polarity after collision of the Shelburne Falls arc with the Laurentian margin.

North of the area studied by Tucker and Robinson (1990), Valley et al. (2015) reported new U-Pb zircon SHRIMP ages from the Bronson Hill arc in west central New Hampshire of 475 ± 5, 466 ± 8, 460 ± 3, 454 ± 3, 450 ± 4, 448 ± 5, and 445 ± 7 Ma. They suggested that the overlap between older and younger arc rocks in the Shelburne Falls and Bronson Hill arcs can best be explained by a single long-lived arc.

Lyons et al. (1986) presented U-Pb zircon ages from the Highlandcroft Plutonic Suite in northern New England ranging from ca. 453 ±±± 4 to 443 ± 4 Ma, similar to ages reported to the south by Tucker and Robinson (1990). Moench and Aleinikoff (2003) also dated arc-related volcanic and plutonic rocks in the 456 ± 3 to 442 ± 4 Ma range, in northern New England, but they also discovered older 469 ± 2 and 467 ± 4 Ma plutons and suggested that the older plutons intruded the lowermost Ammonoosuc Volcanics near the type locality of the formation. Uppermost Ammonoosuc Volcanics gave ages of 465 ± 6 and 461 ± 8 Ma. Moench and Aleinikoff (2003) also dated a younger series of felsic volcanics in the Quimby Formation at 443 ± 4 Ma. They suggested that the older volcanic and plutonic rocks formed above an older east-dipping subduction zone and that the younger Quimby Formation and the Highlandcroft and Oliverian Plutonic Suites formed after a reversal in subduction polarity.

Gerbi et al. (2006a) studied rocks in the Chain Lakes massif in Maine and presented U-Pb zircon TIMS ages of 477 +7/-5 Ma for the Boil Mountain Complex, and U-Pb SHRIMP ages of 472 ± 6 Ma for the Skinner Pluton and 443 ± 3 Ma for the Attean Pluton. Gerbi et al. (2006b) presented detrital zircon SHRIMP ages from rocks in the Chain Lakes massif that indicate a Laurentian source for the detritus. The presence of both Early and Late Ordovician plutons in this part of the Bronson Hill arc is similar to the segment studied by Moench and Aleinikoff (2003). Two rocks were sampled for detrital zircons, the McKenney Stream and Sarampus Falls facies. The provenance of the detrital grains is convincingly Laurentian, but because the age of these rocks is poorly constrained, it is possible that they were deposited after collision with Laurentia.

Working in the southern part of the Bronson Hill arc in Connecticut, Aleinikoff et al. (2007) reported U-Pb zircon SHRIMP ages of 456 ± 6 Ma for the Boulder Lake Gneiss, 449 ± 4 Ma for the Middletown Formation, and 459 ± 4 Ma for the Higganum Gneiss from the Killingworth dome. Pb and Nd isotopic geochemistry of these rocks suggests that rocks of the Killingsworth complex in the dome resulted from mixing of more radiogenic (high $^{207}Pb/^{204}Pb$ and intermediate $\varepsilon_{Nd}$) Gondwanan terrane sources and less radiogenic (low $^{207}Pb/^{204}Pb$ and low $\varepsilon_{Nd}$) Laurentian components, whereas rocks of the Middletown complex were derived from mixing of more radiogenic rocks and primitive (low $^{207}Pb/^{204}Pb$ and high $\varepsilon_{Nd}$) material (Aleinikoff et al., 2007). They identified Ganderia as the Gondwanan component, but at the time of their study the existence of a more westerly Gondwanan-derived crustal fragment, the Moretown terrane (Macdonald et al., 2014), was unknown. Aleinikoff et al. (2007) suggested that the Killingworth complex (mixing of Gondwanan and Laurentian components) formed above an east-dipping subduction zone on the western margin of Ganderia, and that the Middletown complex (mixing of Gondwanan and more primitive components) formed to the east in a back-arc rift environment.

Detailed accounts of Appalachian orogenesis in the Canadian Appalachians have been presented recently for Quebec (Tremblay and Pinet, 2016), New Brunswick (van Staal et al., 2016), and Newfoundland (van Staal et al., 2007; van Staal and Baar, 2012). These authors provide valuable summaries of the geochronological data base that constrains the timing of arc magmatism and accretion of terranes to the Laurentian margin. As discussed in Karabinos et al. (2017) fundamental questions remain concerning terrane affinity, and the timing of collision of

terranes with the Laurentian margin, and continuity of terranes and boundaries between the New England and Canadian Appalachians.

## METHODS

Siliciclastic units and igneous rocks were sampled for U-Pb zircon geochronological studies. All zircon populations were first analyzed by laser ablation inductively coupled plasma mass spectrometry (LA-ICPMS). Igneous samples and critical detrital zircon populations were then picked off the mounts for chemical abrasion isotope dilution thermal ionization mass spectrometry (CA-IDTIMS). The detailed methods used for LA-ICPMS and CA-TIMS dating of zircon can be found in Karabinos et al. (2017).

## GEOCHRONOLOGY RESULTS

Detailed descriptions of individual samples can be found in the Appendix following the Road Log.

## INTERPRETATIONS OF GEOCHRONOLOGY

***Dalton Formation, Cheshire Quartzite, and Rowe Schist***- The detrital zircon age spectra found in the Dalton Formation samples (fig. 3) indicate that grains derived locally from the underlying 960 Ma Stamford Granite Gneiss dominate the population. Typically, major 960 Ma peaks are not observed in detrital zircon age spectra from Laurentian samples (for example Cawood and Nemchin, 2001; Macdonald et al., 2014). The age spectrum from the Dalton Formation matrix sample, F1323, includes numerous grains of more common igneous rocks found in the Grenville basement rocks of the Adirondack Mountains and the Berkshire and Green Mountain massifs (Aleinikoff et al., 2011; Karabinos et al., 2008; Karabinos and Aleinikoff, 1990; McLelland et al., 2010).

Detrital zircon age spectra from the Cheshire Quartzite and from the Rowe Schist (fig. 3) are dominated by 1050 to 1200 Ma grains typical of igneous rocks from the Grenville orogeny (Cawood and Nemchin, 2001). Minor components include late Neoproterozoic grains, possibly derived from rift volcanic rocks (Kumarapeli et al., 1989), older Mesoproterozoic grains similar in age to ca. 1350 Ma Elzevirian trondhjemitic gneisses in the Green Mountain massif (Ratcliffe et al., 1991), and minor peaks at 1.5, 1.85, and 2.7 Ga.

The restricted age range of the detrital zircon population of the Dalton Formation and the immaturity of the sedimentary protolith suggest a local source for the detritus. The Cheshire Quartzite population is much more diverse and typical of the Grenville province of eastern North America (Cawood and Nemchin, 2001), as expected for a mature quartzite. In contrast, the great diversity in detrital zircon ages from the Rowe Schist, in particular sample F1328, is consistent with deposition in a distal continental margin setting offshore from Laurentia, where along shore currents transported far-travelled zircons.

***Moretown Formation***- All five samples of the Moretown Formation (fig. 4) display prominent peaks in the 500 to 800 Ma age range, atypical of detritus derived from Laurentia, but typical of Gondwanan sediments (for example, Fyffe et al., 2009). Minor peaks in the interval 1.0 to 1.3 Ga are present in the Moretown samples, but subordinate to the Neoproterozoic peaks. In contrast, zircon grains in the 550 to 700 Ma age range are rare in Neoproterozoic to Cambrian sediments derived from Laurentia, and peaks in the 1.0 to 1.2 Ga range dominate the spectra. The dominant Neoproterozoic age peak in the detrital zircon populations corresponds to widespread arc plutonic and volcanic rocks common on Gondwanan crustal fragments in the Appalachians (Fyffe et al., 2009). Macdonald et al. (2014) also suggested that the Moretown Formation is a Cambrian unit based on the youngest detrital zircon grains (514 Ma) dated by TIMS, and the oldest intrusive rocks (496 and 502 Ma, Aleinikoff et al., 2011) found in outcrops that Macdonald et al. (2014, 2015) interpreted as likely Moretown Formation correlatives in southern Vermont.

***Cobble Mountain Formation***- The Neoproterozic peaks that dominate Moretown Formation samples are only a minor component of the Cobble Mountain Formation detrital zircon population. The Cobble Mountain Formation detrital zircon age spectra are characterized by peaks at 1500 to 1600 Ma, 1700 to 1800 Ma, and 1300-1400 Ma, consistent with an Amazonian (Strachan et al., 2007) or West African (Bradley et al., 2015) sediment source. The contrast in detrital zircon characteristics between the Moretown and Cobble Mountain Formations calls into question the correlation of these units by Stanley and Hatch (1988). Nonetheless, the age spectra of the Cobble Mountain Formation samples indicate a Gondwanan rather than a Laurentian source.

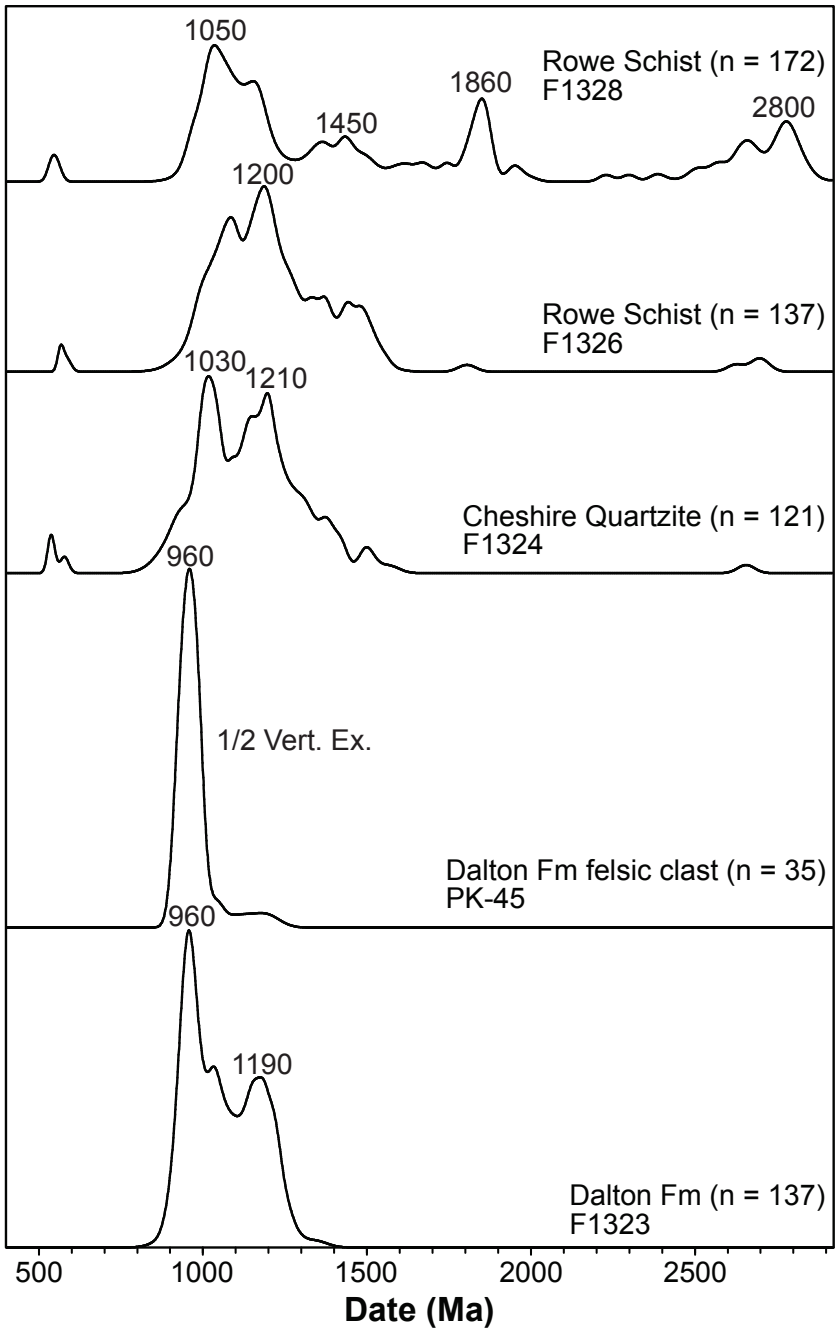


**Fig. 3. Detrital zircon normalized probability density plots of samples from Laurentian margin deposits. Locations are shown in figure 1C.**

***Albee Formation***- Five of the seven samples of the Albee Formation have the most prominent peaks in the interval 600 to 630 Ma (fig. 4). One (NH-98-158) has the most prominent peak at 1200 Ma with strong peaks at 530 and 630 Ma. The same six samples also have prominent peaks at 1.5 to 1.6 Ga. One sample of the Albee Formation, VT-98-257, bears a striking resemblance to the Cobble Mountain Formation detrital zircon populations (fig. 4) with a dominant peak at 1.5 Ga and another peak at 1.7 Ga. One Albee Formation sample, NH-13-397, for which there are only 50 grains analyzed, is quite similar to the Moretown Formation detrital zircon populations (fig. 4). The remaining five samples combine the characteristics of the Moretown and Cobble Mountain Formations detrital zircon data, except that they also contain robust peaks at 1.2 to 1.3 Ga, and minor peaks in the 800 to 1000 Ma range.

The age spectra shown in figure 4 are compatible with the interpretation that the Albee Formation is part of the Moretown terrane located east of the Connecticut Valley trough (fig. 1). The somewhat more diverse zircon populations in the Albee Formation may reflect a more cosmopolitan provenance in this part of the Moretown terrane.

***Hawley Formation***- The Hawley Formation is at least slightly older than the 475 Ma intrusive Dell Trondhjemite (Macdonald et al., 2014). This age constraint, in conjunction with the presence of two Ordovician detrital zircon grains in F1442 (460 ± 22 and 469 ± 18 Ma) and twenty detrital zircon grains in sample F1444 (weighted mean date of 474 ± 12 Ma) (fig. 6), indicates that the sedimentary component of the Hawley Formation was deposited during peak magmatic activity in the Shelburne Falls arc.

We interpret the detrital zircon age spectra from samples 2816, 2817, F1446, and F1507 to represent a mixing of detritus from both Laurentian and Gondwanan sources. Sample 2817 (n = 123) (figs. 1 and 6) is dominated by a sharp 950 Ma peak approximately coeval with the Stamford Granite Gneiss exposed in the Green Mountain and Berkshire massifs (Karabinos and Aleinikoff, 1990). Sample 2816 (n = 84) (figs. 1 and 6) is dominated by peaks at 1000 and 1100 Ma, but also contains a prominent peak at 550 Ma uncharacteristic of Laurentian derived sediments. Sample F1446 (n = 121) (figs. 1 and 6) is from the Cram Hill Formation in southern Vermont, on strike with the eastern graphitic schist belt in the Hawley Formation, the so-called Sanders Brook Black Slate of Kim and Jacobi (1996). The probability plot for this sample is diverse and complex. The most prominent peak is 1300 to 1400 Ma, similar in age to the ca. 1350 Ma Elzevirian trondhjemitic gneisses in the Green Mountain massif reported by Ratcliffe et al. (1991), but also similar to 1300 to 1400 Ma peaks in two of the three Cobble Mountain Formation samples. There are also significant peaks at 1500 to 1600 and 1700 to 1800 Ma, similar to peaks in the Cobble Mountain Formation samples (fig. 6). There is a broad peak between 1.0 to 1.2 Ga, and less prominent peaks at 600, 800. We interpret the age spectrum to reflect mixed Laurentian and Gondwanan sources, similar to the Cobble Mountain Formation, for the detritus. Sample F1507 (n = 109) (figs. 1 and 6) is dominated by peaks at 960, 1050, and 1170 Ma, but contains a significant peak at 580 Ma.

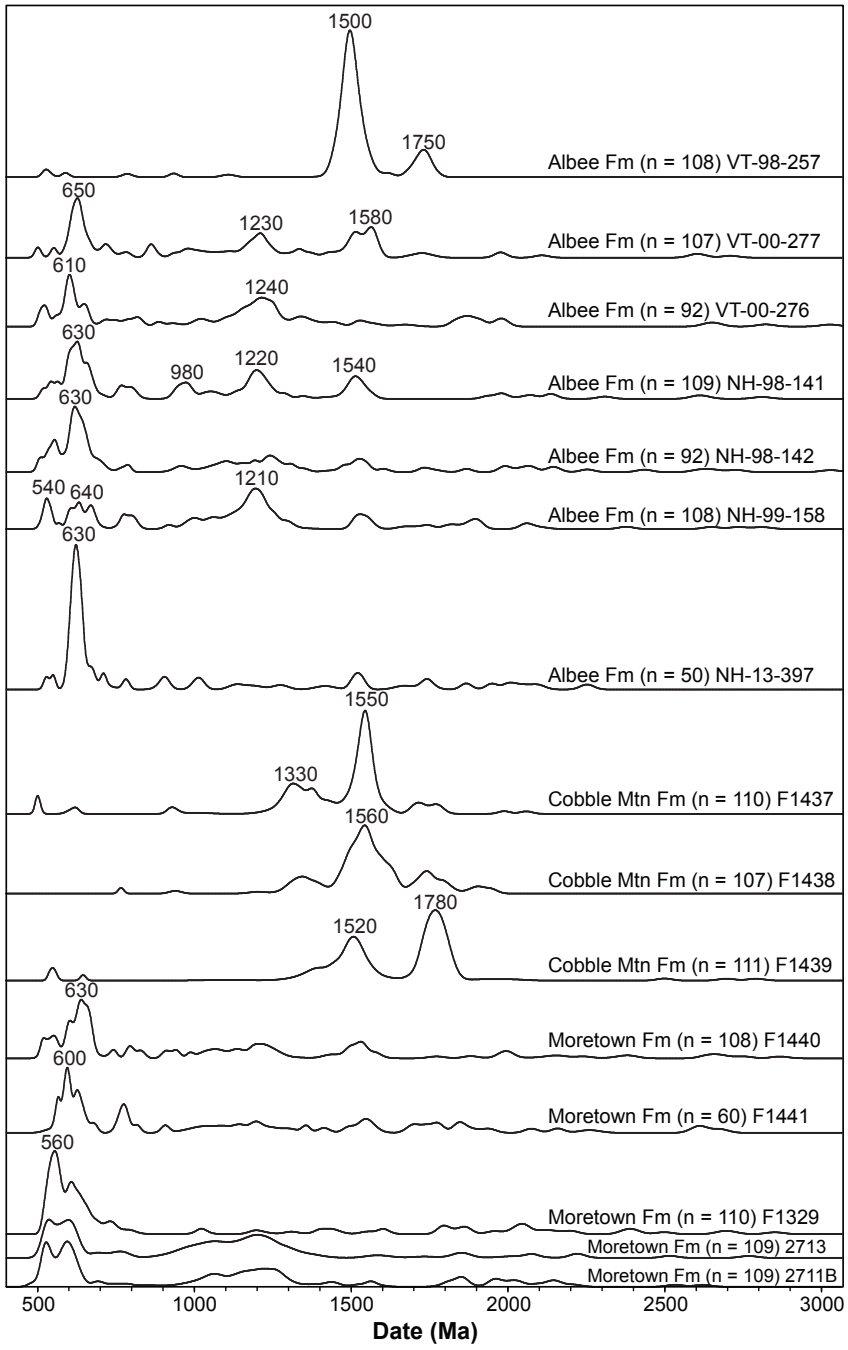


**Fig. 4. Detrital zircon normalized probability density plots of samples interpreted to come from units belonging to the Gondwanan-derived Moretown terrane. Locations are shown in figure 1C.**

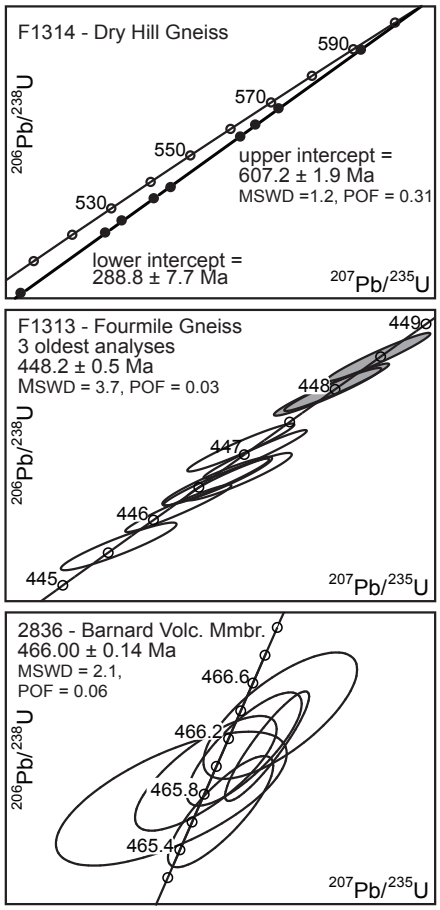


**Fig. 5. Concordia plots from single grains and fragments of zircon analyzed by chemical abrasion-thermal ionization mass spectrometry. Locations are shown in figure 1D.**

To summarize, our data suggest that the metasedimentary units of the Hawley Formation were deposited during the Early Ordovician (approximately 475 Ma) and that the sediments received detritus from Laurentian and Gondwanan sources, and from coeval magmatic rocks. Thus, we argue that the collision between the Rowe Schist and the Moretown terrane-Shelburne Falls arc must have occurred at about this time.

***Barnard Volcanic Member of the Missisquoi Formation***- The CA-IDTIMS date of 466.00 ± 0.14 Ma (fig. 5) for sample 2836 is younger than the 471.4 ± 3.7 Ma age reported by Karabinos et al. (1998) for a sample of the Barnard Volcanic Member near the base of the more than 1 km thick sequence of felsic gneiss at the type locality of the unit (Richardson, 1924). The 466 Ma age of the Barnard Volcanic Member is indistinguishable from the age of an ash layer from the Indian River Formation in the Giddings Brook thrust sheet of the Taconic allochthons (Macdonald et al., 2017). The thick sequence of felsic igneous rocks that make up the Barnard Volcanic Member may preserve a volcanic center or a magma chamber that supplied volcanic eruptions of ash to the Laurentian margin, and the timing of these eruptions may coincide with slab breakoff following collision of the Moretown terrane with Laurentia.

***Partridge Formation***- Our small detrital zircon yield (24 grains) from sample F1312 suggests that the Partridge Formation received grains from Ordovician arc magmatism, as well as Laurentian and Gondwanan sources (fig. 6). Merschat et al. (2016) presented detrital zircon data from two sample of the Partridge Formation in New Hampshire. The samples contain Mesoproterozoic zircon dates typical of Grenvillian rocks from Laurentia, as well as 1.6 to 1.8 and 2.5 to 2.8 Ga grains likely derived from Laurentian mid-continent sources, and Neoproterozoic grains that are typical of peri-Gondwanan sources (Merschat et al., 2016). Some of the 1.6 to 1.7 Ga grains may also have been sourced from the Cobble Mountain or Albee Formations (see fig. 4). These detrital zircon ages provide critical evidence that the Bronson Hill arc was proximal to Laurentia when arc magmatism was active in the Late Ordovician. Detritus from a Gondwanan source also appears to be represented in the Partridge Formation.

Harwood and Berry (1967) described *C. bicornis* graptolites from the Partridge Formation in New Hampshire, which were later reclassified as *N. gracilis* by Riva (1974), thus establishing a Sandbian age (458.4 ± 0.9 to 453.0 ± 0.7 Ma, Gradstein et al., 2012) for this part of the Partridge Formation. Tucker and Robinson (1990) presented a U-Pb zircon TIMS age of 449 +3/-2 Ma for a volcanic bed from the Partridge Formation in Massachusetts (fig. 7).

The Partridge Formation is an important component of the Bronson Hill arc, and the detrital zircon age spectra indicate that the arc formed in close proximity to Laurentia. A mixed Laurentian-Gondwanan source of detrital zircons in the Partridge Formation is consistent with Bronson Hill magmatism on the eastern trailing edge of the Moretown terrane, but not consistent with magmatism on the western leading edge of Ganderia during its transit through the Iapetus ocean before its Early Silurian collision with Laurentia as proposed by Hibbard et al. (2006).

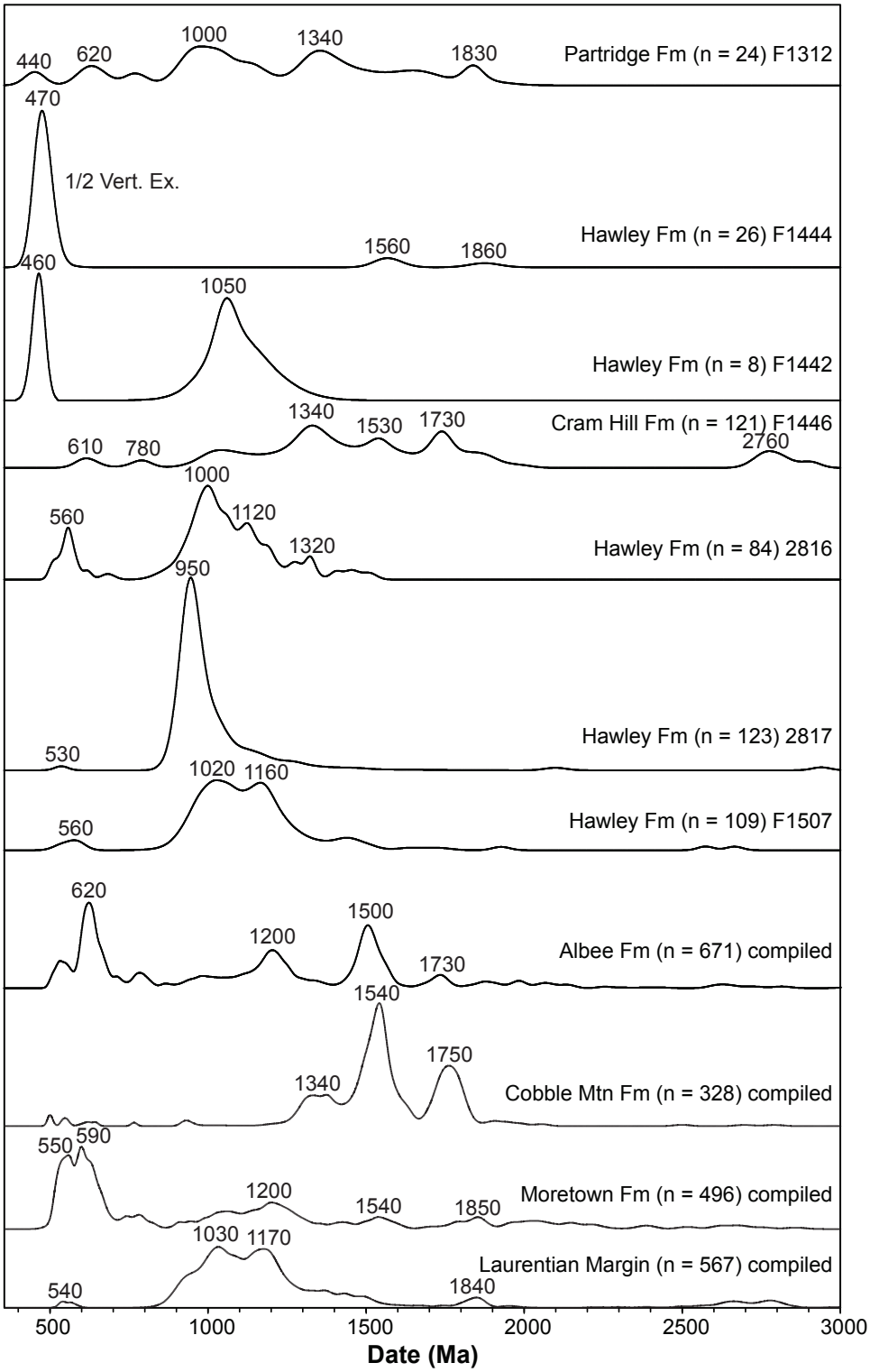


**Fig. 6. Detrital zircon normalized probability density plots of samples interpreted as having a mixed Laurentian and Gondwanan provenance. Locations are shown in figure 1C.**

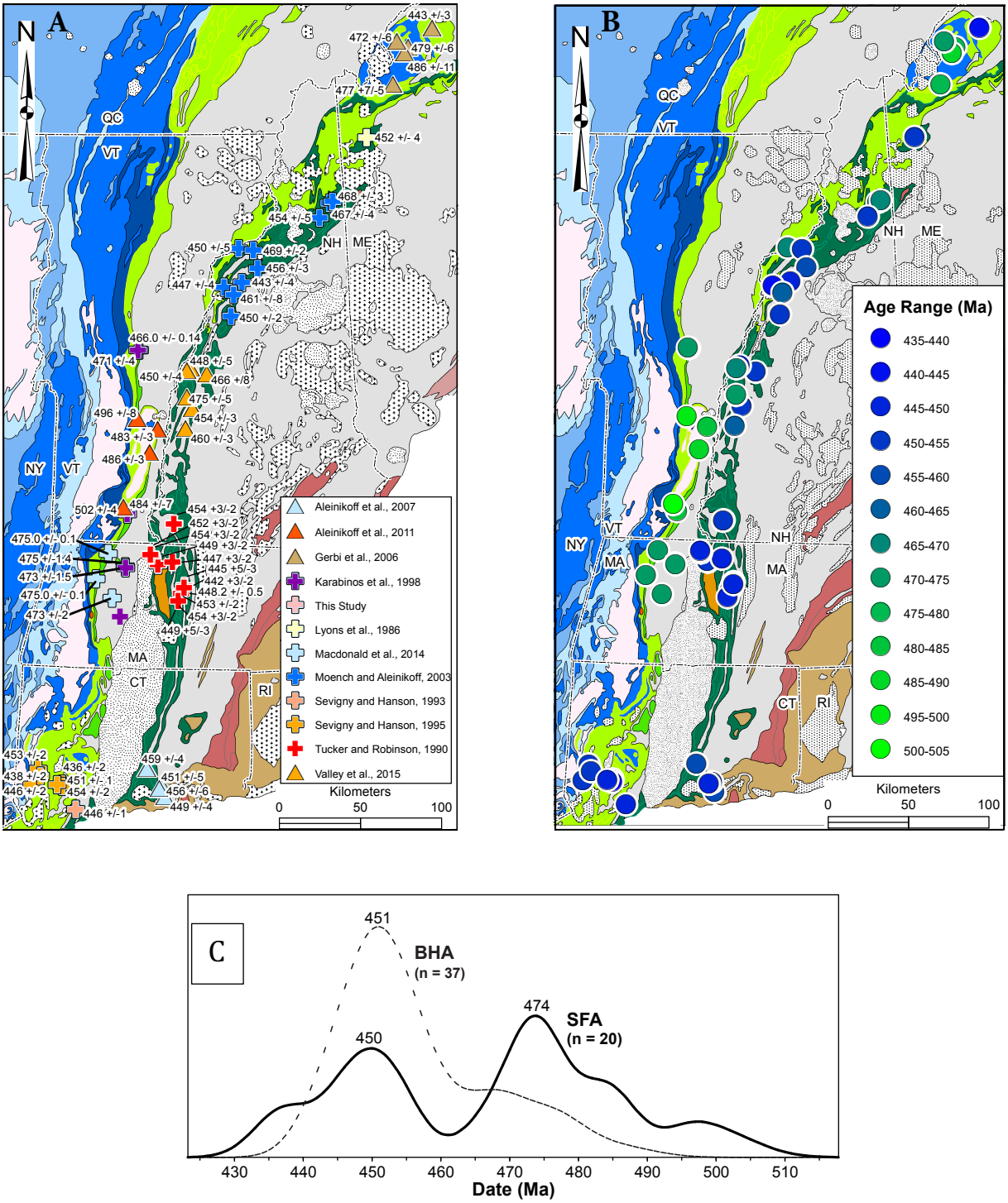


**Fig. 7. (A) Tectonic map of New England showing the locations of dated rocks in the Shelburne Falls and Bronson Hill arcs. Triangles are SHRIMP U-Pb zircon ages and pluses are TIMS U-Pb zircon ages. References give data sources. Ages are in Ma. Units use the same colors and patterns as shown in figure 1B. (B) Tectonic map of New England showing the location of dated rocks in the Shelburne Falls and Bronson Hill arcs in 5 m.y. intervals. Units use the same colors and patterns as shown in figure 1B. (C) Normalized probability plot for U-Pb igneous crystallization ages for rocks from the Bronson Hill arc (BHA- dashed curve) and from the Shelburne Falls arc (SFA- solid curve). Locations of dated samples and references are shown in (A).**

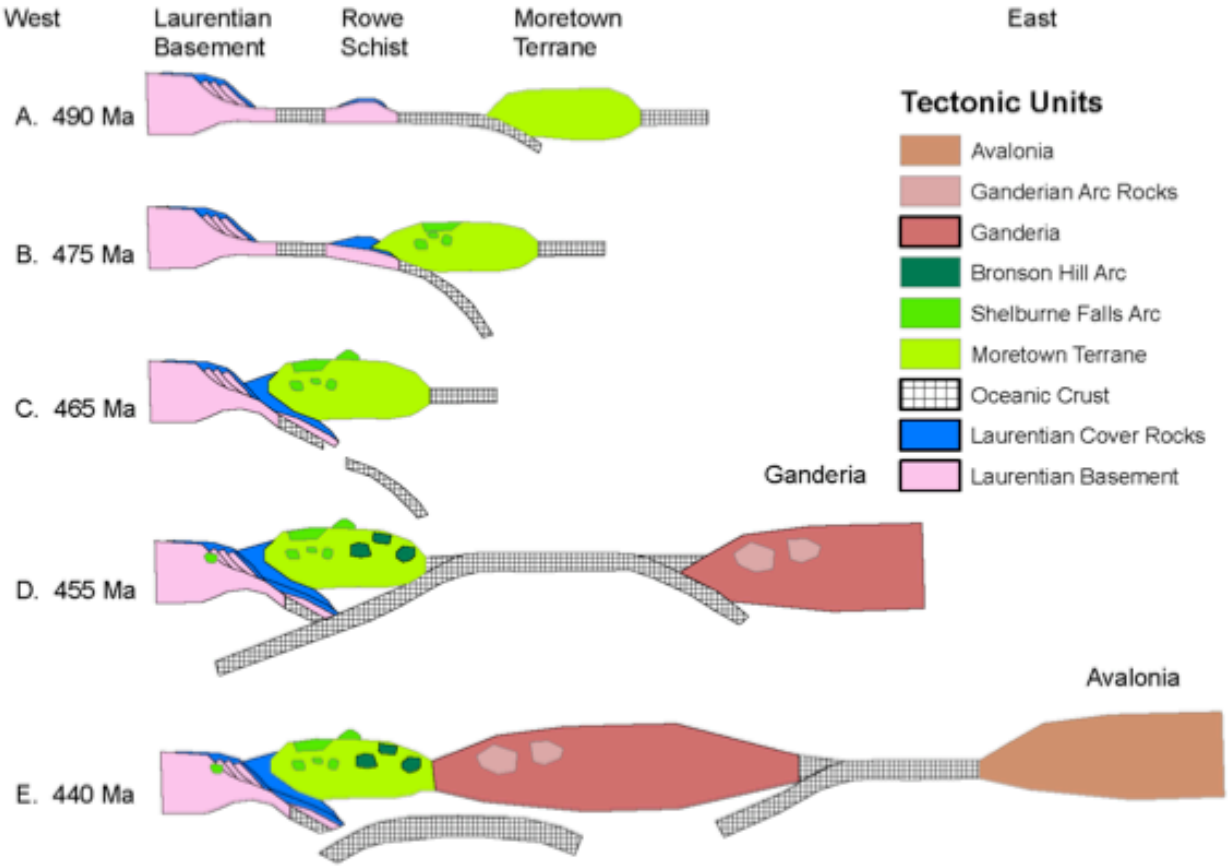


**Fig. 8. Schematic cross-sections showing the early Paleozoic tectonic evolution of the New England Appalachians.**

## DISCUSSSION

### *The Suture between Laurentia and Gondwanan-derived Terranes*

Macdonald et al. (2014) used detrital zircon data to demonstrate that the contact between the Rowe Schist and Moretown Formation in Vermont and western Massachusetts is the suture between Laurentia and Gondwanan-derived crust. The Moretown Formation was previously interpreted as a forearc deposit to the Taconic arc (Rowley and Kidd, 1981; Stanley and Ratcliffe, 1985), but it contains no Ordovician zircons, which would presumably be common in a Taconic forearc deposit. Instead, the Moretown Formation is dominated by zircon grains derived from Neoproterozoic arcs, similar to Gondwanan-derived terranes studied elsewhere (Fyffe et al., 2009). Lenses of amphibolite and altered ultramafic rocks are especially common near the Rowe Schist-Moretown Formation contact (Chidester et al., 1967; Zen, 1983; Ratcliffe et al. 2011) consistent with the interpretation that the boundary represents a major suture between Laurentia and Gondwanan-derived crust.

Geologic evidence suggests that the suture formed when the Moretown terrane collided with distal elements of Laurentia above an east-dipping subduction zone. Folds and thrust faults in this zone consistently record west vergence, and evidence for high-pressure metamorphism, including remnant blueschist occurrences, has been reported by Laird et al. (1984). The 505 to 473 Ma $^{40}Ar/^{39}Ar$ metamorphic dates from amphibolites near the suture zone (Laird et al., 1984; Castonguay et al., 2012) record exhumation and cooling of rocks from the Iapetan oceanic realm of the Laurentian plate. Further, numerous $^{40}Ar/^{39}Ar$ cooling ages between 471 and 460 Ma from rocks in the Laurentian rift-drift succession and the Rowe Schist record cooling from metamorphic temperatures (Tremblay and

Pinet, 2016; Castonguay et al., 2012; Laird et al., 1984; Whitehead et al., 1996) after collision of Laurentia and the Moretown terrane. Most importantly, there is no record of Early Ordovician arc magmatism in rocks of Laurentian affinity that would be expected if an Early Ordovician subduction zone had dipped westward under the Laurentian margin.

A critical problem that requires further investigation is that there is no record of Early Ordovician deformation, foreland basin deposits, or air-fall tephras on the Laurentian carbonate platform to the west. As discussed in Macdonald et al. (2017), unconformities within the Early Ordovician carbonate sequence may reflect tectonic activity outboard to the east, but was not dragged down into a subduction zone during this early phase of the Taconic orogeny. Thus, Karabinos et al. (2017) suggested that the collision occurred outboard of the Laurentian passive margin, perhaps east of an intervening Taconic Seaway (fig. 8). It is important to keep in mind that the current thrust geometry and close proximity of the carbonate platform sequence in the footwall and the Taconic thrust sheets and basement massifs in the hanging wall is the likely the result of post-Taconic, Salinic and/or Acadian thrusting (Karabinos et al., 2008; Webb et al., 2018).

Zircon data from the Hawley Formation, which is an integral component of the Shelburne Falls arc, suggest that the Moretown terrane and its active arc were close enough to Laurentia by 475 Ma to receive detritus from the Grenville orogen. The age of the Hawley Formation is constrained by the time of intrusion of the Dell Metatrondhjemite at 475 Ma, and the youngest, Ordovician, detrital zircon grains in two of our sample (F1442 and F1444, fig. 5). Together these data point to an Early Ordovician age for the Hawley Formation. Detrital zircon data from four of our samples (2816, 2817, F1446, F1507, fig. 6) provide evidence for a mixed Laurentian-Gondwanan provenance for metasedimentary units in the Hawley Formation. The mixed provenance suggests that by 475 Ma the Shelburne Falls arc, which was built on the Moretown terrane, was proximal to the Laurentian margin. Thus, the collision between the Rowe Schist and the Moretown terrane and the subsequent magmatism in the Shelburne Falls arc must have occurred outboard of the passive Laurentian margin, yet close enough for metasedimentary rocks of the Hawley Formation to have incorporated Laurentian detritus.

***Extent of the Moretown Terrane***

Macdonald et al. (2014) demonstrated that the Moretown terrane extends from western Massachusetts to northern Vermont. Our detrital zircon data from the Albee Formation suggest that the Moretown terrane extends as far eastward as the Bronson Hill arc in northern New Hampshire (figs. 1 and 8). Our data from the Cobble Mountain Formation in southwestern Massachusetts, together with Wintsch et al. (2015, 2016) data from several formations in western Connecticut suggests that the Moretown terrane continues southward in western New England into Connecticut (fig. 1). Stanley and Hatch (1988) interpreted the Cobble Mountain Formation as a facies equivalent of the Moretown Formation in southern Massachusetts. Our zircon data indicate that the Cobble Mountain Formation had a Gondwanan provenance, but that its source was different than the Moretown Formation; it may be an older unit or have received sediment from a different drainage system. The Albee Formation was correlated with the Moretown Formation by Doll et al. (1961), and our detrital zircon data are consistent with this interpretation. The detrital zircon population from one of our samples of Albee Formation (VT-98-297, fig. 4) bears a striking resemblance to the Cobble Mountain Formation. The zircon population from another sample (NH-13-397, fig. 4) is very similar to those from the Moretown Formation. Other Albee Formation samples have age peaks similar to both the Moretown and Cobble Mountain Formations (fig. 4). Furthermore, the age of the Albee Formation is constrained to be older than the SHRIMP U-Pb zircon 492.5 ± 7.8 Ma age of an intrusive tonalite (Rankin et al., 2013), similar to the Cambrian age constraint placed on the Moretown Formation by felsic intrusive rocks (Aleinikoff et al., 2011; Macdonald et al., 2014).

Both the Moretown and Albee Formations are likely Cambrian in age (Macdonald et al., 2014, Rankin et al., 2013). The similarity in detrital zircon populations between the Albee Formation and the Moretown and Cobble Mountain Formation (fig. 4) supports the interpretation that the Moretown terrane extends as far east as the Bronson Hill arc. Furthermore, evidence from detrital zircon extracted from the Partridge Formation, discussed next, indicates a Laurentian provenance for Ordovician sediments deposited on the Bronson Hill arc (fig. 8).

***Paleogeogeography of the Bronson Hill Arc***

The Bronson Hill arc, shown as the eastern arc in figure 1B, extends from southern Connecticut through central Massachusetts and western New Hampshire into Maine. It was interpreted as the '*Taconic arc'* that collided

with Laurentia above an east-dipping subduction zone during the Taconic orogeny by Rowley and Kidd (1981) and Stanley and Ratcliffe (1985). Karabinos et al. (1998) argued that the Shelburne Falls arc, the western arc in figures 1B, 7, and 9, collided with Laurentia above an older east-dipping subduction zone, and that the Bronson Hill arc formed above a west-dipping subduction zone after a reversal in subduction polarity. Karabinos et al. (1998) further suggested that the Shelburne Falls and Bronson Hill arcs formed on a rifted Laurentian-derived ribbon continent, analogous to Dashwoods in Newfoundland (Waldron and van Staal, 2001). Macdonald et al. (2014) demonstrated that the Shelburne Falls and Bronson Hill arcs formed on Gondwanan-derived crust, the Moretown terrane. Hibbard et al. (2006) interpreted the Bronson Hill arc as the western leading edge of Ganderia. Several studies have also suggested that the Bronson Hill arc is a more complex composite arc that contains multiple arc tracts that formed at different times in different places (Aleinikoff et al., 2007; Karabinos, 2008; Dorais et al., 2011).

As shown in figure 7, the New Hampshire and Maine portions of the Bronson Hill arc contain ca. 485 to 465 Ma arc rocks coeval with rocks in the Shelburne Falls arc. This overlap in ages of arc rocks led Ratcliffe et al. (1999) and Valley et al. (2015) to suggest that the rocks in the western and eastern arc tracts are part of a single long-lived arc. Another interpretation is that there is some spatial overlap in rocks that formed above the older east-dipping and younger west-dipping subduction zones (Karabinos et al., 1998, 1999; Moench and Aleinikoff, 2003; Macdonald et al., 2014).

One sample of the Partridge Formation in Massachusetts (figs. 1C, 6) with a limited number of zircon grains (n = 24) contains some Ordovician grains, and appears to have mixed Laurentian and Gondwanan sources. Merschat et al. (2016) presented detrital zircon data from two samples of the Partridge Formation in New Hampshire and concluded that the sediment was derived from both Laurentian and peri-Gondwanan sources, but that the Laurentian source dominated the zircon population. Thus, the detrital zircon evidence from the Partridge Formation provides critical evidence that the Bronson Hill arc was proximal to Laurentia during arc magmatism by approximately 450 to 455 Ma (Tucker and Robinson, 1990), when the Partridge Formation (Harwood and Berry, 1967; Riva, 1974) was deposited.

This constraint on the paleogeography of this portion of the Bronson Hill arc leads us to the interpretation that the ca. 455 to 440 Ma arc-related plutonic and volcanic rocks in central Massachusetts and New Hampshire formed on the eastern margin of the already accreted Moretown terrane above a west-dipping subduction zone after a reversal in subduction polarity (fig. 8).

***Subduction Polarity Reversal***

We suggest that the Moretown terrane collided with distal Laurentian fragments at approximately 475 Ma. Because oceanic lithosphere was no longer available to the east-dipping subduction zone after collision, we argue that younger ca. 455 to 440 Ma plutonic and volcanic rocks in the Bronson Hill arc are more likely the product of magmatism above a west-dipping subduction zone under Laurentia and the newly accreted Moretown terrane (fig. 8). The initiation of the younger west-dipping subduction zone must have followed slab breakoff and the subsequent reversal in subduction polarity. Slab breakoff may coincide with the 466 Ma explosive eruption recorded in the Barnard Volcanic Member and in coeval ashes in the Indian River Formation in the Taconic allochthons (Macdonald et al., 2017). Because, detrital zircon data from the Partridge Formation indicate that the Bronson Hill arc formed close enough to Laurentia to receive its detritus, it is unlikely that this segment of the Bronson Hill arc was separated from Laurentia by significant tract of oceanic lithosphere.

Sevigney and Hanson (1993, 1995) proposed that the Brookfield Plutonic Suite and the Newtown, Harrison, and Beardsley Gneisses (454 to 438 Ma) in southwestern Connecticut (fig. 7) form the plutonic roots of a Late Ordovician to Early Silurian magmatic arc that formed above a west-dipping subduction zone on the Laurentian margin. Sevigny and Hanson (1993, 1995) also noted that the younger plutons intruded older rocks of the Collinsville Formation, which had already been deformed during an earlier Taconic event. The Collinsville Formation is a likely correlative with Early Ordovician rocks in the Shelburne Falls arc in Massachusetts and Vermont. The data and interpretations presented by Sevigny and Hanson (1993, 1995) are consistent with a reversal in subduction polarity.

Dated ashes in the Mohawk Valley in New York contain zircon grains with inherited cores of likely Grenvillian origin (Macdonald et al., 2017), further suggesting that a west-dipping subduction zone was established under Laurentia before the ca. 453 Ma age of the oldest of these ash deposits.

***Is the Moretown Terrane Distinct from Ganderia?***

Hibbard et al. (2006) showed the boundary between peri-Laurentian and peri-Gondwanan terranes, the Red Indian Line of Williams et al. (1988), on the west margin of the Bronson Hill arc in New England, and suggested that the Bronson Hill arc forms the western leading edge of Ganderia. Macdonald et al. (2014) demonstrated that the suture zone between Laurentia and peri-Gondwanan terranes is further west at the Rowe Schist-Moretown Formation contact, and our new data indicate that the Moretown terrane extends east to the Bronson Hill arc. We suggest that the Moretown terrane is a peri-Gondwanan fragment distinct from Ganderia. If the Moretown terrane and Bronson Hill arc are not part of Ganderia, the Late Ordovician west-dipping subduction zone proposed by Karabinos et al. (1998) and Macdonald et al. (2014) could have been just east and outboard of the Bronson Hill arc. If this interpretation is correct, the boundary between the Moretown terrane and Ganderia would be buried under Silurian to Devonian rocks in the Central Maine terrane.

If the Moretown terrane and Bronson Hill arc are part of Ganderia, however, the west-dipping subduction zone would have to be east and outboard of the Massabesic Gneiss Complex in New Hampshire (fig. 1B), which has been identified as part of Ganderia (Hibbard et al., 2006, Dorais et al., 2012; van Staal et al., 2016). Also, if the Moretown terrane and Ganderia are equivalent, it implies that Ganderia reached the Laurentian margin much earlier than the time proposed by van Staal et al. (2009) and van Staal and Barr (2012), and blurs the distinction between the Taconic and Salinic orogenies. Alternatively, these terranes were not continuous ribbon continents and reflect the collision of two distinct microcontinents.

***Taconic Composite Magmatic Arc***

Based on the evidence and arguments presented above, we suggest that the peri-Gondwanan Moretown terrane was the foundation of a composite magmatic arc. Arc magmatism above an east-dipping subduction zone produced Late Cambrian to Early Ordovician plutonic and volcanic rocks found mostly in the western Shelburne Falls arc (figs. 1, 7, and 8) until the Moretown terrane collided with distal hyper-extended Laurentian crust at approximately 470 Ma. After collision and slab break-off, a reversal in subduction polarity led to the initiation of a younger west-dipping subduction zone. Slab breakoff may be recorded by explosive eruptions at 466 preserved in the Barnard Volcanic Member and ashes in the Indian River Formation in the Taconic allochthons. Alternatively, the 466 eruptions may reflect initiation of west-dipping subduction (figs. 1, 7, and 8). In either case, we suggest that the west-dipping subduction zone must have been established before the onset of major magmatic activity in the eastern Bronson Hill arc at 454 Ma (Tucker and Robinson, 1990). As shown in figure 7, there is some spatial overlap in the age of arc-related rocks in the western and eastern arcs as previously defined. Thus, the terms Shelburne Falls arc and Bronson Hill arc, which have been used to describe different geographic areas, are better thought of as distinguishing arc magmatism above two different subduction zones. For example, there is clearly significant overlap in older and younger arc ages in the New Hampshire portion of the Bronson Hill arc (Moench and Aleinikoff, 2003; Valley et al., 2015; fig. 7). Although we believe that the evidence for a reversal in subduction polarity during Taconic orogenesis is compelling, and that the model we present here can explain many observations in western New England, it is important to acknowledge that the strict *spatial* distinction between an older Shelburne Falls arc and a younger Bronson Hill arc is not viable (Karabinos et al., 1999).

## CONCLUSIONS

1. Based on detrital zircon analysis, we suggest that the western boundary of the Gondwanan-derived Moretown terrane is the Rowe Schist-Moretown Formation contact, and that the eastern boundary is located in the Bronson Hill arc.

2. Magmatic arc rocks in the Shelburne Falls arc ranging in age from ca. 500 to 470 Ma formed above an east-dipping subduction zone on the western, leading edge of the Moretown terrane.

3. By 475 Ma the Moretown terrane and the Shelburne Falls arc were proximal to Laurentia; meta-sediments in the Hawley Formation, part of the Shelburne Falls arc, were receiving detritus from Laurentia. Collision between the Moretown terrane and distal elements of Laurentia, represented by the Rowe Schist was either in progress or about to begin. This is consistent with numerous $^{40}Ar/^{39}Ar$ cooling ages between 471 and 460

Ma from rocks in the Laurentian rift-drift succession and the Rowe Schist that record cooling from metamorphic temperatures (Tremblay and Pinet, 2016; Castonguay et al., 2012; Laird et al., 1984; Whitehead et al., 1996) after collision of Laurentia and the Moretown terrane.

4. Suturing of the Moretown-Rowe contact was complete by the time of intrusion of the Middlefield Granite at 448.8 ± 0.1 Ma in Massachusetts and the Brookfield Plutonic Suite at 454 ± 2 Ma in Connecticut (Sevigny and Hanson, 1995).

5. The Early Ordovician collision of the Moretown terrane with distal Laurentian crust left the Laurentian passive margin undeformed, suggesting that an oceanic tract separated the collision zone from the carbonate platform.

6. Slab-breakoff of subducted lithosphere occurred after the 475 Ma collision of the Moretown terrane with the Rowe Schist, but before the initiation of west-dipping subduction. It is possible that slab-breakoff is recorded by the explosive eruption in the Barnard Volcanic Member at 466 Ma, which was likely the source for ash beds in the Indian River Formation in the Taconic allochthons.

7. A reversal in polarity created a west-dipping subduction zone under the Laurentian margin and the newly accreted Moretown terrane. We propose that abundant 455 to 440 Ma magmatic arc rocks in the Bronson Hill arc formed above this west-dipping subduction zone, and that the arc formed along the eastern, trailing edge of the Moretown terrane.

8. The western boundary of Ganderia, represented by the Massabesic Gneiss Complex in New England, is east of the Bronson Hill arc buried under Silurian and Devonian meta-sediments deformed during the Acadian orogeny.

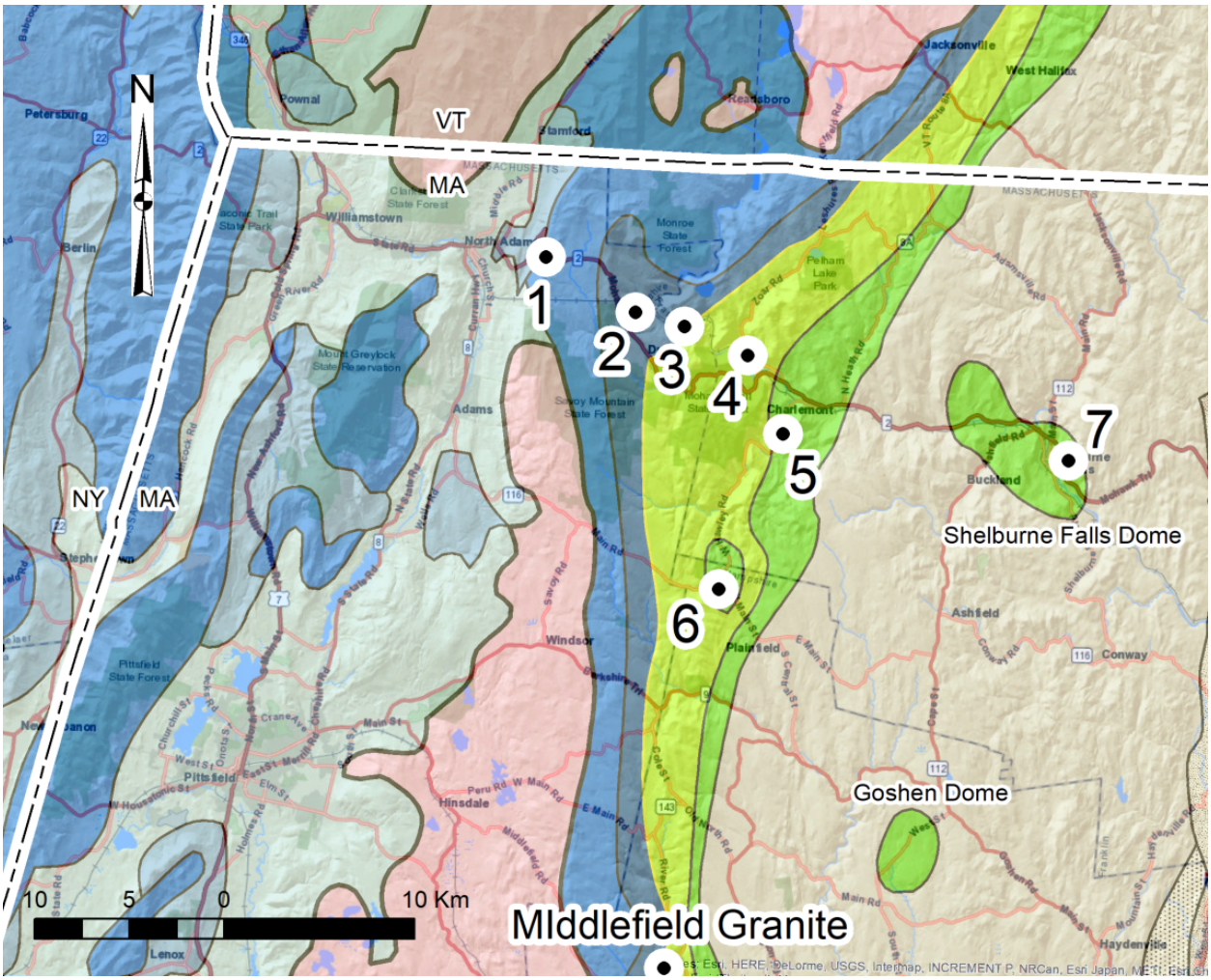


**Figure 9. Index map showing field trip stops. See Fig. 1 for legend.**

**ROAD LOG**

Meet on Sunday, October 14, 2018. 9:00 am at the old Wigwam and Western Summit Gift Shop (now closed) on Route 2 east of downtown North Adams and 0.8 miles uphill from the Golden Eagle Restaurant at Hairpin Turn. There is extra parking 100 m east at the trailhead for the Hoosac Range trail. The view to the west includes, from south to north, Mount Greylock, the Taconic Crest, and the southern end of the Green Mountains. Note that it is about two hours by car from Lake George to North Adams.

| Miles | | Directions |
|---|---|---|
| 0.0 | 0.0 | The Wigwam and Eastern Summit Gift Shop**.** |

**Stop 1- View to west and Hoosac Schist.** The gift shop has been closed for a while, but the platform next to it still provides a nice view of Mount Greylock (south), the Taconic Crest (distant ridge), and the southern termination of the Green Mountain massif (north). Across the road from the gift shop is an outcrop of Neoproterozoic to Cambrian Hoosac Schist. It is very similar lithologically to the Greylock Schist on Greylock and the Nassau Formation on the Taconic Crest. They were all deposited as silty mudstones on the continental slope and rise of the Laurentian margin following rifting of Rodinia. Metamorphic grade decreases from our location on Hoosac Summit to the west. Here the Hoosac Schist is a quartz, albite-porphyroblast, muscovite, biotite, garnet schist with lots of quartz veins. The Nassau Formation on the Taconic crest in the distance is a fine-grained phyllite; the Greylock Schist is at an intermediate grade of

metamorphism. Small relict garnet crystals can be found in albite porphyroblasts on the eastern most ridges of Mount Greylock. The southern end of the Green Mountain massif is a south-plunging anticline cored by Mesoproterozoic basement unconformably overlain by Neoproterozoic to Cambrian Dalton Formation and Cambrian Cheshire Quartzite. The east-west valley that connects Williamstown and North Adams between the Green Mountains and Mount Greylock must contain a lateral thrust ramp with many kilometers of structural relief because the Taconic sequence rocks of Mount Greylock must have formerly covered the Green Mountains before erosion stripped them away.

Proceed east on Rt. 2.

3.1 3.1 Turn left on Whitcomb Hill Road.

3.3 0.2 Bear right to stay on Whitcomb Hill Road.

4.1 0.8 Outcrop of Rowe Schist on right.

4.3 0.2 Outcrop of Rowe Schist on right.

4.4 0.1 Pull over to right onto shoulder.

**Stop 2- Rowe Schist.** There is abundant outcrop of Rowe Schist all along Whitcomb Hill Road. This is the best one and it contains a prominent contact between graphitic and non-graphitic schist near the bend in the road. Both contain the same mineral assemblage except for the greater graphite and sulfide content in the rusty-weathering rocks. The Rowe Schist is characterized by alternating graphitic and non-graphitic layers. The graphitic variety tends to be more concentrated in the structurally upper part of the unit close to the contact with the Moretown Formation and near the abundant lens of mafic and ultramafic rocks. The Rowe Schist is a typical pelitic schist with quartz, plagioclase, muscovite, biotite, and garnet. Locally it is more aluminous and contains paragonite (Na-white mica) instead of albit and chloritoid instead of biotite. It also contains a surprisingly large amount of quartz for a sediment that was presumably deposited on the distal Laurentian margin; the quartz-rich layers are best observed on faces perpendicular to the foliation. The two samples of Rowe Schist used for our detrital zircon study came from along this road (Figs. 1C and 3). Both zircon populations are typical of Laurentian-derived sediment with prominent peaks between 1.0 and 1.2 Ga corresponding to the Grenville of North America, and minor Neoproterzoic peaks at approximately 550 Ma, reflecting rift-related magmatism from the breakup of Rodinia.
Note that the boundary between the Rowe Schist and the Moretown Formation is a first-order geophysical feature- the depth to MOHO, as determined by P to S wave conversions, abruptly decreases by 10 to 15 km from west to east approximately below this contact in southern New England (Li et al., 2018).

Continue down Whitcomb Hill Road.

5.4 1.0 Dirt Road on right is Torrey Hill Road. This road leads to the Reed Brook Preserve managed by the Nature Conservancy. A long and winding trail leads uphill to a large ultramafic lens with rare plants. Some large boulders of ultramafic rock are visible in the road a short distance from the paved road.

5.5 0.1 Intersection with River Road. Turn right, south, onto River Road and park in one of the pull outs near the intersection. Walk back toward the intersection and walk across the rickety bridge across the Deerfield River.

After crossing the bridge, continue straight on foot along the dirt road. Go uphill and across the railroad tracks. Turn right and avoid the drive ways to follow Tunnel Road on the far side of the tracks through the woods to get to Stop 3 outcrops. Lots of outcrop of Rowe Schist in woods upslope to left along the road.

**Stop 3- Rowe Schist, Mafic and Ultramafic lenses.** See map in Figure 10 for details of route.
**3A- Rowe Schist**. The large outcrop of Rowe Schist next to the road contains abundant graphite and large garnet porphyroblasts. Note the steeply-dipping well-developed foliation and prominent down-dip lineation.
**3B- Mafic Schist.** The prominent outcrops on the left and right of dirt road are composed of mafic schist and gneiss, likely derived from oceanic crust caught up in the subduction zone between the Moretown terrane and the down-going Laurentian margin rocks.
**3C- Highly altered Ultramafic Rocks of the Hoosac Tunnel Soapstone Quarry**. The large blocks on the right side of the dirt road are waste from a soapstone quarry and talc mine. Soapstone was quarried between 1885 to 1895. In 1909 an adit was drilled in the quarry to mine talc. The operation did not last long. This fine-grained rock contains talc, actinolite, garnet, antigorite, and calcite. Ultramafic lenses are common in the Rowe Schist and Moretown Formation near their contact, and are probably derived from altered mantle peridotite.


**Figure 10. Topographic map showing location of outcrops for Stop 3.**

Return to vehicles and continue south on River Road.

| | | |
|---|---|---|
| 6.9 | 1.4 | Outcrop of Moretown Formation. |
| 9.3 | 2.4 | Bear right to stay on River Road. |
| 10.1 | 0.8 | Pull over to left. |

**Stop 4- Moretown Formation**. This enormous outcrop is a convenient place to see the Moretown Formation in good light. Most of the light-colored rock is quartz, plagioclase, muscovite, biotite granofels with a distinctive pin stripe texture. There are some quartz-rich layers, one of which provided one of our many Moretown Formation detrital zircon samples. Dark layers are mafic dikes and sills with diverse geochemistry (Kim and Jacobi, 1996; Karabinos et al., 2017). The Moretown Formation is Cambrian in age (Macdonald et al., 2014; Karabinos et al., 2017). Based on geochemistry, the undated mafic intrusions most likely include Cambrian to Early Ordovician arc rocks, some of which may have formed during back-arc rifting,

and Silurian or possibly Devonian rift-related rocks coeval with the initiation of the Connecticut Valley basin. Detrital zircons from the Moretown Formation from northern Vermont to southern Massachusetts show prominent 550 to 650 Ma peaks typical of Gondwanan-derived sediment (Figs. 1C and 4) Macdonald et al., 2014; Karabinos et al., 2017). There is a remarkable lack of Grenville peaks in the zircon populations.

Continue south on River Road.

| | | |
|---|---|---|
| 11.1 | 1.0 | Moretown Formation on left |
| 11.3 | 0.2 | Moretown Formation on left |
| 11.6 | 0.3 | Moretown Formation on left |
| 11.8 | 0.2 | Turn left, east, onto Rt. 2. |
| 13.4 | 1.6 | Turn right, south, onto Rt. 8A. |
| 13.5 | 0.1 | Turn right to stay on Rt. 8A south. |
| 16.4 | 2.9 | Turn left onto Pudding Hollow Road. |
| 16.4 | 0.0 | Turn left onto Middle Road. |
| 16.5 | 0.1 | Park on right before bridge. Proceed on foot along Middle Road across bridge and turn left on pleasant dirt road. Make your way down to the Chickley River to the left. Note that this is private property and that permission is needed to access this outcrop. |

**Stop 5- Hawley Formation**. The mafic gneiss exposed here is one of several common rock types in the Hawley Formation. Jon Kim studied these rocks for his doctoral dissertation and Kim and Jacobi (1996) is an excellent account of the geochemistry of this diverse unit. Structures widely interpreted as pillow basalts are present is some parts of this long exposure. The Hawley Formation is part of the Shelburne Falls arc and its Ordovician age is tightly constrained by a TIMS date of 475 Ma on the intrusive Dell Metatrondhjemite and essentially coeval detrital zircons in metasediments (Fig. 6; Macdonald et al., 2014). At least some of the mafic rocks (Kim and Jacobi, 1996) and perhaps most, if not all, of the metasediments formed during an episode of back-arc rifting. An anoxic environment, consistent with the restricted circulation of a rift basin, is required to explain the highly graphitic schist present in the western and eastern exposures of the Hawley Formation. Notable sulfide and manganese deposits in the Hawley Formation are also consistent with intra-arc rifting/splitting.

Our tectonic model described above is strongly driven by the fact that the detrital zircon populations in the Hawley Formation samples indicate both Laurentian and Gondwanan sources. The Gondwanan source is easy to explain because the Shelburne Falls arc formed on the Moretown terrane. The Laurentian detrital zircons component indicates that by about 475 Ma, the Moretown terrane and the Shelburne Falls arc were close enough to Laurentia to receive detritus from the Grenville rocks so prominent along the Laurentian margin.

Return to vehicles and reverse direction back toward Rt. 8A.

| | | |
|---|---|---|
| 16.6 | 0.1 | Turn right onto Pudding Hollow Road. |
| 16.6 | 0.0 | Turn left onto Rt. 8A south. |
| 22.3 | 5.7 | Hallockville Pond. Lunch stop |

Continue south on Rt. 8A

| | | |
|---|---|---|
| 23.3 | 1.0 | Turn right onto Rt. 116 North. |
| 23.4 | 0.1 | Pull over to left in bus turn around circle. Outcrop is on both sides of road but the best exposures are on the north side of Rt. 116. |

**Stop 6- Hallockville Pond Gneiss**. The Hallockville Pond Gneiss is a 475 Ma tonalite (Karabinos and Williamson, 1994; Macdonald et al., 2014) that intruded the Moretown Formation. The intrusive contact is not exposed at this stop, but it is visible nearby on the small hill 0.5 km northwest of the intersection of Hallockville and King Corner Roads in Dubuque State Forest. The arc geochemistry of this pluton (Karabinos et al., 1998) together with the observation that it intruded the Moretown Formation, provides compelling evidence that the Shelburne Falls arc was constructed on the Moretown terrane. The Hallockville Pond Gneiss contains a well-developed foliation that was overprinted by a younger crenulation cleavage. The older fabric, and possibly both, formed during the Taconic orogeny. 20 km to the south the Middlefield Granite at Glendale Falls in Middlefield, MA, is a 447 Ma weakly-foliated granodiorite (Karabinos and Williamson, 1994; Macdonald et al., 2014) that intruded both the Rowe Schist and the Moretown Formation at their contact, but the pluton is not offset at this major terrane boundary. Thus, the suture zone formed before this 447 Ma intrusion. These observations suggest that the strong deformation fabric in the Hallockville Pond Gneiss formed during the Taconic orogeny, and that the Rowe Schist-Moretown Formation fault contact was not greatly modified during the Acadian orogeny.

Reverse direction, and drive easterly on Rt. 116 South.

| | | |
|---|---|---|
| 23.8 | 0.4 | Moretown Formation on left |
| 32.9 | 9.1 | Turn left onto Rt. 112 North and 116 South (?!!?). |
| 34.3 | 1.4 | Straight through intersection to stay on Rt. 112 North. |
| 42.3 | 8.0 | Outcrop of Collinsville Formation on right in arc of road. |
| 42.4 | 0.1 | Turn left onto Rt. 2 East. |
| 42.5 | 0.1 | Outcrop of Collinsville Formation on both sides of road. A sample from this outcrop gave a 475 $\pm$ 1.4 Ma TIMS date (Karabinos et al., 1998). |
| 44.5 | 2.0 | Trailhead for Mahican-Mohawk Trail, alternate way to Stop 7 for those with very low clearance vehicles. |
| 45.0 | 0.5 | Turn right on Wilcox Hollow Road. Dirt road can be rough after severe storms. Use alternate route and hike down Mahican-Mohawk trail if desired. |
| 45.3 | 0.3 | Park without blocking dirt roads. Continue down to power line. Look for small path on right that leads down to the Deerfield River. Long outcrop along the river continues upstream. Pay attention to rising water warnings; this outcrop is just below a hydroelectric dam. |

**Stop 7- Collinsville Formation in the Shelburne Falls dome**. This accessible exposure of the Collinsville Formation includes both tonalite and mafic gneiss. It is great fun to examine and argue about the intrusive relationship between the felsic and mafic rocks. The rocks are strongly foliated, lineated, and folded. The Collinsville Formation makes up the cores of the Shelburne Falls, Goshen, Granville domes. Core rocks from both the Shelburne Falls and Goshen domes are approximately 475 Ma (Karabinos et al., 1998) and surrounded by much younger Devonian metasediments. The contact is not an unconformity, but rather a major extensional shear zone, tops to the south, similar to that described for the Chester dome (Karabinos et al., 2010). Another fascinating feature about this part of the western New England dome belt is the occurrence of potentially ultrahigh-pressure garnet bearing rocks from the Goshen dome just south of the Shelburne Falls dome (Peterman et al., 2016).

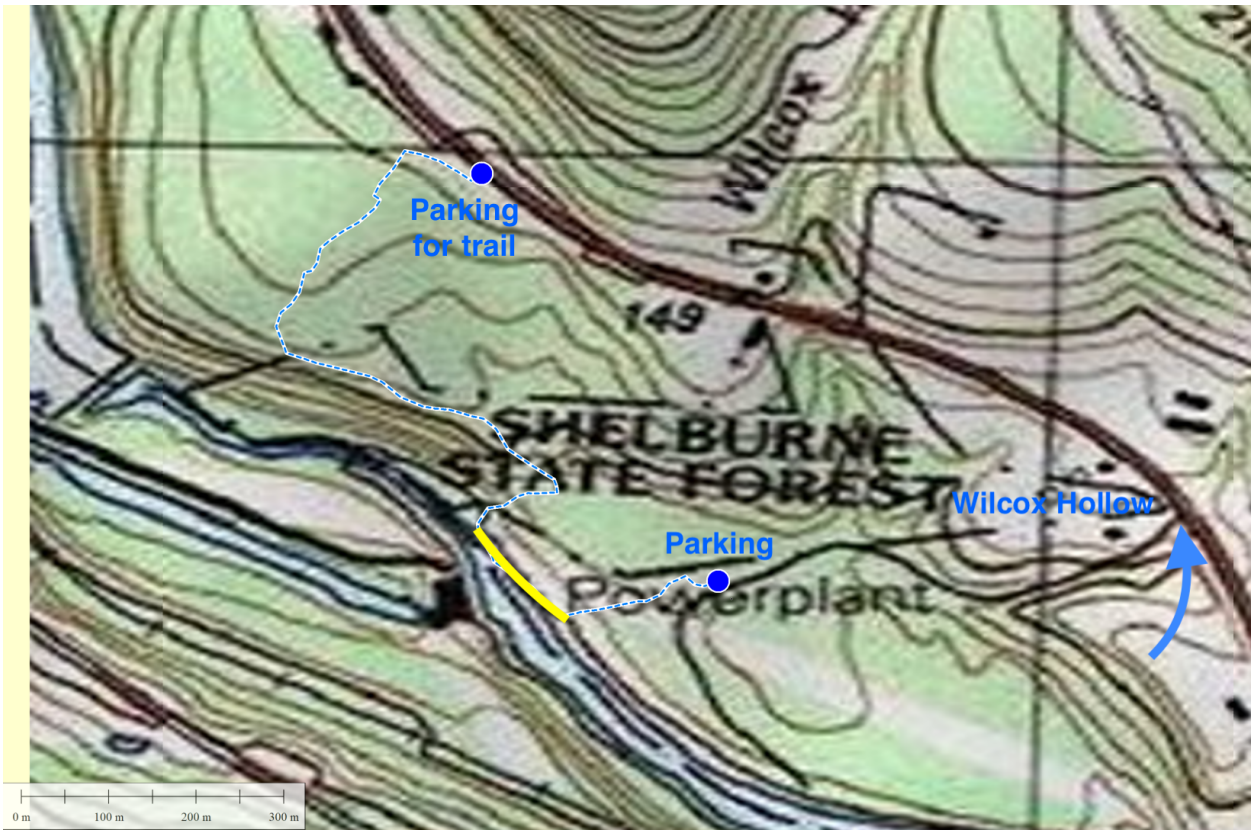


**Figure 11. Topographic map showing dirt road to Wilcox Hollow (arrow) and alternative hiking trail down to Deerfield River and outcrop for Stop 7 (yellow line).**

**END OF TRIP**

## APPENDIX- GEOCHRONOLOGY RESULTS

### *Laurentian Margin*

*Dalton Formation*.-- Two samples of the Dalton Formation come from an unusual facies on Hoosac Mountain (figs. 1C and 2), which is part of an isolated thrust sheet in the northeastern part of the Berkshire massif. Hoosac Mountain is the only part of the Berkshire massif underlain by 960 Ma post-Grenvillian rocks of the Stamford Granite Gneiss (Karabinos and Aleinikoff, 1990, Zen et al., 1983). The overlying basal conglomerate of the Dalton Formation is not dominated by quartz pebbles, but instead contains numerous granitic pebbles and, locally, boulders. The conglomerate grades upward into an albitic schist with pebbly beds, and is stratigraphically overlain by albitic schist of the Hoosac Formation.

*PK45: Dalton Formation*. A granitic boulder extracted from the conglomerate on Hoosac Mountain at 42° 39.838'N, 73° 4.470'W. LA-ICPMS on 35 zircon grains showed a dominant peak at ~960 Ma and four older dates between 1.0 and 1.2 Ga (fig. 3). The thirty-one youngest grains have a weighted mean date of 958 ± 16 Ma (MSWD = 1.4, probability of fit = 0.09).

*F1323: Dalton Formation*. Matrix and granitic pebbles collected on Hoosac Mountain at 42° 39.770'N, 73° 4.159'W. LA-ICPMS on 137 zircon grains showed a dominant peak at 960 Ma and another peak at 1200 Ma (fig. 3).

### *Exotic units*

*Moretown Formation*.-- Macdonald et al. (2014) presented data for three samples of the Moretown Formation from Massachusetts that indicated a Gondwanan provenance for the meta-sediments. Here we present the results from two additional samples (fig. 4). The new samples are from the southern end of the Moretown Formation outcrop belt in Massachusetts near the Connecticut border (fig. 1C).

*F1440: Moretown Formation*. Quartz-rich granofels collected at 42° 10.798'N, 72° 57.031'W. LA-ICPMS on 108 zircon grains showed a dominant peak at ~640 Ma and smaller peaks at ~550, 800, 1200, 1550, and 2000 Ma (fig. 4). The three youngest grains have a weighted mean date of 516 ± 12 Ma (MSWD = 0.05, probability of fit = 0.95).

*F1441: Moretown Formation*. Quartz-rich granofels collected at 42° 13.992'N, 72° 57.805'W. LA-ICPMS on 60 zircon grains showed a dominant peak at ~600 Ma and another large peak at ~770 Ma. There are many small peaks between 0.9 and 2.2 Ga, and another at 2.6 Ga. The three youngest grains have a weighted mean date of 563 ± 12 Ma (MSWD = 0.5, probability of fit = 0.59).

*Cobble Mountain Formation*.-- Figure 4 shows the detrital zircon data from three samples of the Cobble Mountain Formation from southern Massachusetts (fig. 1C).

*F1437: Cobble Mountain Formation*. Quartz-rich biotite schist collected at 42° 7.953'N, 72° 53.824'W. LA-ICPMS on 110 zircon grains showed a dominant peak at 1.55 Ga and another peak at 1.31 Ga. There are five <0.9 Ga grains, three with a weighted mean date of 501 ± 11 Ma (MSWD = 0.2, probability of fit = 0.84) et al. are 606 ± 31 and 623 ± 23 Ma.

*F1438: Cobble Mountain Formation*. Quartz-rich biotite schist collected at 42° 8.076'N, 72° 53.931'W. LA-ICPMS on 107 zircon grains showed a dominant peak at 1.55 Ga and other peaks at 1.35 and 1.75 Ga. One grain yielded a LA-ICPMS date of 766 ± 18 Ma.

*F1439: Cobble Mountain Formation*. Quartz-rich biotite schist collected at 42° 8.076'N, 72° 53.931'W. LA-ICPMS on 111 zircon grains showed a dominant peak at 1.75 Ga and another large peak at 1.50 Ga. There are four <0.9 Ga grains, three with a weighted mean LA-ICPMS date of 547 ± 12 Ma (MSWD = 0.9, probability of fit = 0.42) and one yielded a LA-ICPMS date of 646 ± 20 Ma.

*Albee Formation*.-- We analyzed detrital zircon from seven samples provided by J.N. Aleinikoff, which were originally selected by D.W. Rankin and R.H. Moench to test the stratigraphic assignment of rocks in northern Vermont and New Hampshire. Our LA-ICPMS results (fig. 4) are consistent with unpublished SHRIMP ages obtained by J.N. Aleinikoff, but we were able to analyze a larger number of grains to create more robust age spectra.

*VT-00-257: Albee Formation*. Quartz-rich granofels collected at 44° 22.949'N, 71° 49.680'W. LA-ICPMS on 108 zircon grains showed a dominant peak at 1.5 Ga and another peak at 1.7 Ga. Four <0.9 Ga grains (4%) are 524 ± 22, 536 ± 29, 590 ± 26, and 786 ± 34 Ma.

*VT-00-277: Albee Formation*. Quartz-rich granofels collected at 44° 37.396'N, 71° 33.391'W. LA-ICPMS on 107 zircon grains showed a dominant peak at 620 Ma and other peaks at 1200 Ma and between 1500 and 1600 Ma. Forty-two grains gave LA-ICPMS dates <0.9 Ga (39%). The two youngest yielded LA-ICPMS dates of 492 ± 18 and 503 ± 22 Ma.

*VT-00-276: Albee Formation*. Quartz-rich granofels collected at 44° 32.242'N, 71° 43.559'W. LA-ICPMS on 92 zircon grains showed a dominant peak at 600 Ma and other peaks at 520, 800 and 1200 Ma. Thirty-four grains gave LA-ICPMS dates <0.9 Ga (37%). The five youngest yielded a LA-ICPMS weighted mean date of 519 ± 11 Ma (MSWD = 1.3, probability of fit = 0.29).

*NH-98-141: Albee Formation (Dead River Formation in NH)*. Quartz-rich granofels collected at 44° 19.248'N, 71° 53.574'W. LA-ICPMS on 109 zircon grains showed a dominant peak at 620 Ma and other peaks at 800, 950, 1200 and 1500 Ma. Forty-eight grains gave LA-ICPMS dates <0.9 Ga (44%). The two youngest yielded LA-ICPMS dates of 517 ± 20 and 519 ± 22 Ma.

*NH-98-142: Albee Formation (Dead River Formation in NH)*. Quartz-rich granofels collected at 44° 20.073'N, 71° 54.186'W. LA-ICPMS on 97 zircon grains showed a dominant peak at 620 Ma and other peaks at 550, 1250 and 1520 Ma. Forty-seven grains gave LA-ICPMS dates <0.9 Ga (48%). The three youngest yielded a LA-ICPMS weighted mean date of 511 ± 14 Ma (MSWD = 0.7, probability of fit = 0.47).

*NH-99-158: Albee Formation (Dead River Formation in NH)*. Quartz-rich granofels collected at 43° 57.873'N, 72° 3.127'W. LA-ICPMS on 108 zircon grains showed a dominant peak at 1200 Ma and other peaks at 530 and 630 Ma. Thirty-three grains gave LA-ICPMS dates <0.9 Ga (31%). The six youngest yielded a LA-ICPMS weighted mean date of 526 ± 10 Ma (MSWD = 0.5, probability of fit = 0.75).

*NH-13-397: Albee Formation (Dead River Formation in NH)*. Quartz-rich granofels collected at 44° 12.102'N, 71° 55.991'W. LA-ICPMS on 50 zircon grains showed a dominant peak at 630 Ma and no other peak. Thirty grains gave LA-ICPMS dates <0.9 Ga (60%). The two youngest yielded LA-ICPMS dates of 528 ± 20 and 550 ± 16 Ma.

*Dry Hill Gneiss*.-- *F1314:* Microcline-biotite gneiss containing microcline megacrysts collected at 42° 36.362'N, 72° 25.6748'W. LA-ICPMS on 71 zircon grains from sample yielded scattered dates between 607 ± 23 and 537 ± 19 Ma. The scatter is due to rims with metamorphic zoning seen in CL images that surround grains with igneous zoning. Nine fragments from four grains were analyzed by CA-IDTIMS. All analyses are discordant and

form a line between 607.2 ± 1.9 / 8.6 and 288.8 ± 7.7 / 8.5 Ma (MSWD = 1.2, probability of fit = 0.31). The analyses plot much closer to upper intercept than lower; $^{206}Pb/^{238}U$ dates are 590-498 Ma (fig. 5). The igneous crystallization age is interpreted from the upper intercept and the age of metamorphism from the lower intercept. These results are in excellent agreement with the dates reported by Tucker and Robinson (1990).

***Ordovician Arc-Related Units***

*Hawley and Cram Hill Formations*.-- Macdonald et al. (2014) presented detrital zircon data from two samples of the Hawley Formation, and suggested that the detritus was derived from both Laurentian and Gondwanan sources. Here we present results from three additional samples of the Hawley Formation, and one sample of the correlative Cram Hill Formation along strike in southern Vermont.

*F1442: Hawley Formation*. Graphitic schist collected at 42° 14.321'N, 72° 57.255'W. LA-ICPMS on 8 zircon grains yielded six dates between 1028 ± 61 and 1197 ± 103 Ma, and two others are 460 ± 22 and 469 ± 18 Ma.

*F1444: Hawley Formation*. Hornblende-garnet schist (garbenschieffer) collected at 42° 39.573'N, 72° 51.706'W. LA-ICPMS on 26 zircon grains showed a dominant peak at ~475 Ma and three older grains at 1.55, 1.59, and 1.88 Ga. The twenty youngest grains have a weighted mean date of 474 ± 12 Ma (MSWD = 1.5, probability of fit = 0.08).

*F1446: Cram Hill Formation*. Graphitic schist collected at 42° 46.256'N, 72° 45.972'W. LA-ICPMS on 121 zircon grains showed dominant peaks at ~1.34, 1.55, and 1.74 Ga. There are seven <0.9 Ga grains, the three youngest with a weighted mean date of 611 ± 20 Ma (MSWD = 0.6, probability of fit = 0.58).

*F1507: Hawley Formation*. Graphitic schist collected at 42° 29.629'N, 72° 56.815'W. LA-ICPMS on 109 zircon grains showed a dominant peak between 0.9 and 1.2 Ga. Four <0.9 Ga grains are 530 ± 26, 563 ± 29, 584 ± 27, and 592 ± 27 Ma.

*2836: Barnard Volcanic Member of the Missisquoi Formation (Doll et al., 1961) or Barnard Gneiss (Ratcliffe et al., 2011, Richardson, 1924)*. Felsic granofels collected at 43° 47.691'N, 72° 37.663'W, just below the contact with the Silurian Shaw Mountain Formation (figs. 1D, 5). LA-ICPMS on 84 zircon grains showed a dominant peak at ~460 Ma and one date at 1.1 Ga. Eighty dates yielded a weighted mean date of 458 ± 5 Ma (MSWD = 0.7, probability of fit = 0.96). Six grains analyzed by CA-TIMS have a weighted mean date of 466.00 ± 0.14 / 0.27 / 0.55 Ma (fig. 5; MSWD = 2.1, probability of fit = 0.06). This is the interpreted eruption age.

*F1313: Fourmile Gneiss*. Tonalitic gneiss collected at 42° 36.722'N, 72° 28.721'W. LA-ICPMS on 58 zircon grains yielded scattered dates between 469 ± 19 and 378 ± 20 Ma. The scatter is due to narrow rims with metamorphic zoning seen in CL images that surround grains with igneous zoning. Five whole grains and two fragments from each of three other grains were analyzed by CA-TIMS. The three oldest dates, from one whole grain and two fragments from a grain, have a weighted mean date of 448.16 ± 0.52 / 0.56 / 0.73 Ma (fig. 5; MSWD = 3.7, probability of fit = 0.03). This is the interpreted igneous crystallization age. The eight other dates are younger, between 447.11 ± 0.30 and 444.84 ± 0.31 Ma. These dates are thought to be from grains that are mixtures of igneous and metamorphic zircon. Tucker and Robinson (1990) reported an age of 454 +3/-2 Ma for the Fourmile Gneiss from the same locality.

*F1312: Partridge Formation*. Graphitic schist collected at 42° 40.684'N, 72° 31.009'W. LA-ICPMS on 24 zircon grains from sample (figs. 1C and 6) showed peaks at 1.0, 1.4, and 1.8 Ga. Four <0.9 Ga grains are 452 ± 33, 615 ± 38, 654 ± 40, and 772 ± 36 Ma.

## REFERENCES

Aleinikoff, J., Ratcliffe, N., and Walsh, G., 2011, Provisional zircon and monazite uranium-lead geochronology for selected rocks from Vermont: US Geological Survey Open-File Report, v. 1309, p. 46.

Aleinikoff, J. N., Wintsch, R. P., Tollo, R. P., Unruh, D. M., Fanning, C. M., and Schmitz, M. D., 2007, Ages and origins of rocks of the Killingworth dome, south-central Connecticut: Implications for the tectonic evolution of southern New England: American Journal of Science, v. 307, p. 63-118.

Aleinikoff, J. N., Zartman, R. E., and Lyons, J. B., 1979, U-Th-Pb geochronology of the Massabesic Gneiss and the granite near Milford, south-central New Hampshire: New evidence for Avalonian basement and Taconic and Alleghanian disturbances in eastern New England: Contributions to Mineralogy and Petrology, v. 71, p. 1-11.

Allen, J. S., Thomas, W. A., and Lavoie, D., 2010, The Laurentian margin of northeastern North America, *in* Tollo, R. P., Bartholomew, M. J., Hibbard, J. P., and Karabinos, P. M., editors, From Rodinia to Pangea: The lithotectonic record of the Appalachain region: Denver, CO, Geological Society of America Memoirs, p. 71-90.

Bird, J. M., and Dewey, J. F., 1970, Lithosphere plate-continental margin tectonics and the evolution of the Appalachian orogen: Geological Society of America Bulletin, v. 81, p. 1031-1060.

Bradley, D. C., O'Sullivan, P., Cosca, M. A., Motts, H., Horton, J. D., Taylor, C. D., Beaudoin, G., Lee, G. K., Ramezani, J., and Bradley, D. N., Jone, J., and Bowring, S., 2015, Synthesis of geological, structural, and geochronologic data (phase V, deliverable 53): Chapter A in Second projet de renforcement institutionnel du secteur minier de la République Islamique de Mauritanie (PRISM-II), US Geological Survey. Open-File Report 2013-1280-A.

Castonguay, S., Kim, J., Thompson, P. J., Gale, M. H., Joyce, N., Laird, J., and Doolan, B. L., 2012, Timing of tectonometamorphism across the Green Mountain anticlinorium, northern Vermont Appalachians: 40Ar/39Ar data and correlations with southern Quebec: Geological Society of America Bulletin, v. 124, p. 352-367.

Cawood, P. A., and Nemchin, A. A., 2001, Paleogeographic development of the east Laurentian margin: Constraints from U-Pb dating of detrital zircons in the Newfoundland Appalachians: Geological Society of America Bulletin, v. 113, p. 1234-1246.

Chidester, A. H., Hatch Jr, N. L., Osberg, P. H., Norton, S. A., and Hartshorn, J. H., 1967, Geologic map of the Rowe quadrangle, Franklin and Berkshire Counties, Massachusetts, and Bennignton and Windham Counties, Vermont, GQ-642, scale 1 : 24,000.

Clift, P. D., Schouten, H., and Draut, A. E., 2003, A general model of arc-continent collision and subduction polarity reversal from Taiwan and the Irish Caledonides: Geological Society, London, Special Publications, v. 219, p. 81-98.

Coish, R., Kim, J., Morris, N., Johnson, D., and Murphy, B., 2011, Late stage rifting of the Laurentian continent: evidence from the geochemistry of greenstone and amphibolite in the central Vermont Appalachians 1 1 This article is one of a series of papers published in CJES Special Issue: In honour of Ward Neale on the theme of Appalachian and Grenvillian geology: Canadian Journal of Earth Sciences, v. 49, p. 43-58.

Colman-Sadd, S. P., Dunning, G., and Dec, T., 1992, Dunnage-Gander relationships and Ordovician orogeny in central Newfoundland; a sediment provenance and U/Pb age study: American Journal of Science, v. 292, p. 317-355.

Condon D.J., Schoene B., McLean N.M., Bowring S.A., Parrish R, 2015, Metrology and traceability of U-Pb isotope dilution geochronology (EARTHTIME Tracer Calibration Part I): Geochimica et Cosmochimica Acta 164: 464-480.

Crowley, J., Schoene, B., and Bowring, S., 2007, U-Pb dating of zircon in the Bishop Tuff at the millennial scale: Geology, v. 35, p. 1123-1126.

De Souza, S., and Tremblay, A., 2010, The Rivière-des-Plante ultramafic Complex, southern Québec: Stratigraphy, structure, and implications for the Chain Lakes massif: Geological Society of America Memoirs, v. 206, p. 123-139.

Dean, W., 1985, Relationships of Cambrian-Ordovician faunas in the Caledonide-Appalachian Region, with particular reference to trilobites: The Tectonic Evolution of the Caledonide-Appalachian Orogen, v. 17, p. 47.

Doll, C. G., Cady, W. M., Thompson Jr, J. B., and Billings, M. P., 1961, Centennial geologic map of Vermont: Vermont Geological Survey, scale 1:250,000.

Dorais, M. J., Atkinson, M., Kim, J., West, D. P., Kirby, G. A., and Murphy, B., 2011, Where is the Iapetus suture in northern New England? A study of the Ammonoosuc Volcanics, Bronson Hill terrane, New Hampshire 1 1 This article is one of a series of papers published in this CJES Special Issue: In honour of Ward Neale on the theme of Appalachian and Grenvillian geology: Canadian Journal of Earth Sciences, v. 49, p. 189-205.

Dorais, M.J., Wintsch, R.P., Kunk, M.J., Aleinikoff, J., Burton, W., Underdown, C., and Kerwin, C.M., 2012, P-T-t conditions, Nd and Pb isotopic composiitons and detrital zircon geochronology of the Massabesic Gneiss Comples, New Hampshire: isotopic and metamorphic evidence for the identification of Gander basement, central New England, American Journal of Science, v. 312, p. 1049-1097.

Dubé, B., Dunning, G., Lauziere, K., and Roddick, J., 1996, New insights into the Appalachian Orogen from geology and geochronology along the Cape Ray fault zone, southwest Newfoundland: Geological Society of America Bulletin, v. 108, p. 101-116.

Dunning, G., Wilton, D., and Herd, R., 1989, Geology, geochemistry and geochronology of a Taconic batholith, southwestern Newfoundland: Transactions of the Royal Society of Edinburgh: Earth Sciences, v. 80, p. 159-168.

Fyffe, L. R., Barr, S. M., Johnson, S. C., McLeod, M. J., McNicoll, V. J., Valverde-Vaquero, P., van Staal, C. R., and White, C. E., 2009, Detrital zircon ages from Neoproterozoic and Early Paleozoic conglomerate and sandstone units of New Brunswick and coastal Maine: implications for the tectonic evolution of Ganderia: Atlantic Geology, v. 45, p. Pages 110-144.

Gerbi, C., Johnson, S., and Aleinikoff, J., 2006a, Origin and orogenic role of the Chain Lakes massif, Maine and Quebec: Canadian Journal of Earth Sciences, v. 43, p. 339-366.

Gerbi, C., Johnson, S., Aleinikoff, J., Bédard, J., Dunning, G., and Fanning, C., 2006b, Early Paleozoic development of the Maine-Quebec boundary Mountains region: Canadian Journal of Earth Sciences, v. 43, p. 367-389.

Gerstenberger, H., and Haase, G., 1997, A highly effective emitter substance for mass spectrometric Pb isotope ration determinations: Chemical geology, v. 136, p. 309-312.

Gradstein, F. M., Ogg, J. G., Schmitz, M., and Ogg, G., 2012, The geologic time scale 2012 2-volume set, Elsevier.

Harper, D., Mac Niocaill, C., and Williams, S., 1996, The palaeogeography of early Ordovician Iapetus terranes: an integration of faunal and palaeomagnetic constraints: Palaeogeography, Palaeoclimatology, Palaeoecology, v. 121, p. 297-312.

Harwood, D.S., and Berry, W.B.N., 1967, Fossiliferous Lower Paleozoic rocks in the Cupsuptic quadrangle, west-central Maine, US Geological Survey Professional Paper 575-D, pp. D16–D23.

Hatch, N. L., 1988, Some revisions to the stratigraphy and structure of the Connecticut Valley trough, eastern Vermont: American Journal of Science, v. 288, p. 1041-1059.

Hibbard, J., Van Staal, C., Rankin, D., and Williams, H., 2006, Lithotectonic map of the Appalachian Orogen: Canada–United States of America: Geological Survey of Canada Map A, v. 2096, p. 2.

Hodgkins, C. E., 1985, Major and trace element geochemistry and petrology of the late Precambrian Dry Hill Gneiss, Pelham dome, central Massachusetts: University of Massachusetts, Amherst, 135 p.

Hodych, J. P., and Cox, R. A., 2007, Ediacaran U-Pb zircon dates for the Lac Matapédia and Mt. St.-Anselme basalts of the Quebec Appalachians: support for a long-lived mantle plume during the rifting phase of Iapetus opening: Canadian Journal of Earth Sciences, v. 44, p. 565-581.

Jaffey, A. H., Flynn, K. F., Glendenin, L. E., Bentley, W. C., and Essling, A. M., 1971, Precision measurements of half-lives and specific activities of 235U and 238U: Physical Review C, v. 4, p. 1889-1906.

Johnson, R. J., Pluijm, B. A., and Van der Voo, R., 1991, Paleomagnetism of the Moreton's Harbour Group, northeastern Newfoundland Appalachians: Evidence for an Early Ordovician island arc near the Laurentian margin of Iapetus: Journal of Geophysical Research: Solid Earth (1978–2012), v. 96, p. 11689-11701.

Karabinos, P., 1988, Tectonic significance of basement-cover relationships in the Green Mountain massif, Vermont: The Journal of Geology, p. 445-454.

Karabinos, Paul, 2008, Composite arc terrains in the New England Appalachians, Geological Society of America, Abstracts with Programs: 40, p. 75.

Karabinos, P., Morris, D., Hamilton, M., and Rayner, N., 2008, Age, origin, and tectonic significance of Mesoproterozoic and Silurian felsic sills in the Berkshire massif, Massachusetts: American Journal of Science, v. 308, p. 787-812.

Karabinos, P., Samson, S. D., Hepburn, J. C., and Stoll, H. M., 1998, Taconian orogeny in the New England Appalachians: collision between Laurentia and the Shelburne Falls arc: Geology, v. 26, p. 215-218.

Karabinos, Paul, Samson, S.D., Hepburn, J.C., Stoll, H.M., 1999, Taconian orogeny in the New England Appalachians: Collison between Laurentia and the Shelburne Falls arc, Reply: Geology, v. 27, p. 382.

Karabinos, P., and Williamson, B. F., 1994, Constraints of the timing of Taconian and Acadian deformation in western Massachusetts: Northeastern Geology, v. 16, p. 1-8.

Karabinos, P. A., and Aleinikoff, J. N., 1990, Evidence for a major middle Proterozoic, post-Grenvillian igneous event in western New England: American Journal of Science, v. 290, p. 959-974.

Kim, J., and Jacobi, R. D., 1996, Geochemistry and tectonic implications of Hawley Formation meta-igneous units; northwestern Massachusetts: American Journal of Science, v. 296, p. 1126-1174.

Krough, T. E., 1973, A low contamination method for hydrothermal decompostion of zircon and extraction of U and Pb for isotopic age determination: Geochmica et Cosmochimica Acta, v. 37, p. 485-494.

Kumarapeli, P. S., Dunning, G. R., Pintson, H., and Shaver, J., 1989, Geochemistry and U-Pb zircon age of comenditic metafelsites of the Tibbit Hill Formation, Quebec Appalachians: Canadian Journal of Earth Sciences, v. 26, p. 1374-1383.

Kusky, T., Chow, J., and Bowring, S., 1997, Age and origin of the Boil Mountain ophiolite and Chain Lakes massif, Maine: implications for the Penobscottian orogeny: Canadian Journal of Earth Sciences, v. 34, p. 646-654.

Laird, J., Lanphere, M. A., and Albee, A. L., 1984, Distribution of Ordovician and Devonian metamorphism in mafic and pelitic schists from northern Vermont: American Journal of Science, v. 284, p. 376-413.

Landing, E., 2012, The great American carbonate bank in eastern Laurentia: Its births, deaths, and linkage to paleooceanic oxygenation (Early Cambrian–Late Ordovician).
Li, Cong & Gao, Haiying & Williams, Michael & Levin, Vadim, 2018, Correlation of three-dimensional variations of seismic MOHO with tectonic terranes in the northern Appalachian Mountains, Geophysical Research Letters, v. 45, 10.1130/abs/2018NE-310569.
Liss, M. J., van der Pluijm, B. A., and Van der Voo, R., 1993, Avalonian proximity of the Ordovician Miramichi terrane, northern New Brunswick, northern Appalachians: Paleomagnetic evidence for rifting and back-arc basin formation at the southern margin of Iapetus: Tectonophysics, v. 227, p. 17-30.
Ludwig, K. R., 2003, User's manual for Isoplot 3.00: a geochronological toolkit for Microsoft Excel: Berkeley Geochronology Center Special Publication, v. 4, p. 1-70.
Lyons, J. B., Aleinikoff, J. N., and Zartman, R. E., 1986, Uranium-thorium-lead ages of the Highlandcroft Plutonic Suite, northern New England: American Journal of Science, v. 286, p. 489-509.
Lyons, J.B., Bothner, W.A., Moench, R.H., Thompson Jr., J.B., 1997. Bedrock geologic map of New Hampshire, US Geological Survey; scale 1:250,000.
Mac Niocaill, C., Van der Pluijm, B. A., and Van der Voo, R., 1997, Ordovician paleogeography and the evolution of the Iapetus ocean: Geology, v. 25, p. 159-162.
Macdonald, F. A., Crowley, J. L., Karabinos, P., Hodgin, E. B., and Crockford, P. W., this volume, Bridging the gap between the foreland and the hinterland: Geochronology and tectonic setting of Ordovician magmatism and basin formation on the Laurentian margin of New England and Newfoundland: American Journal of Science.
Macdonald, F. A., Ryan-Davis, J., Coish, R. A., Crowley, J. L., and Karabinos, P., 2014, A newly identified Gondwanan terrane in the northern Appalachian Mountains: Implications for the Taconic orogeny and closure of the Iapetus Ocean: Geology, v. 42, p. 539-542.
Macdonald, F. A., Ryan-Davis, J., Coish, R. A., Crowley, J. L., and Karabinos, P. M., 2015, A newly identified Gondwanan terrane in the northern Appalachian Mountains: Implications for the Taconic orogeny and closure of the Iapetus Ocean Forum Reply: Geology, v. 43, p. e360.
Mattinson, J. M., 2005, Zircon U-Pb chemical abrasion ("CA-TIMS") method: combined annealing and multi-step partial dissolution analysis for improved precision and accuracy of zircon ages: Chemical geology, v. 220, p. 47-66.
McLelland, J. M., Selleck, B. W., Hamilton, M. A., and Bickford, M. E., 2010, Late-to post-tectonic setting of some major Proterozoic anorthosite–mangerite–charnockite–granite (AMCG) suites: The Canadian Mineralogist, v. 48, p. 729-750.
Merschat, A. J., Walsh, G. J., Holm-Denoma, C. S., and McAleer, R. J., 2016, Detrital zircon geochronology of the Bronson Hill anticlinorium and western facies of the Central Maine terrane, southern NH-VT, Geological Society of America Abstracts with Programs.
Moench, R. H., and Aleinikoff, J. N., 2003, Stratigraphy, geochronology, and accretionary terrane settings of two Bronson Hill arc sequences, northern New England: Physics and Chemistry of the Earth, Parts A/B/C, v. 28, p. 113-160.
Moench, R. H., Boone, G. M., Bothner, W. A., Boudette, E. L., Hatch Jr, N. L., Hussey II, A. M., and Marvinney, R. G., 1995, Geologic map of the Sherbrooke–Lewiston area, Maine, New Hampshire, Vermont, United States, and Quebec, Canada, with contributions to geochronology by J.N. Aleinikoff: US Geological Survey pamphlet, 56 p., scale 1:250,000.
Neuman, R. B., 1984, Geology and paleobiology of islands in the Ordovician Iapetus Ocean: Review and implications: Geological Society of America Bulletin, v. 95, p. 1188-1201.
Osberg, P. H., Hussey II, A. M., and Boone, G. M., 1985, Bedrock geologic map of Maine: Maine Geological Survey, scale 1:500,000.
Peterman, E.M., Snoeyenbos, D.R., Jercinovic, M.J., and Kylander-Clark, A., 2016, Dissolution-reprecipitation metasomatism and growth of zircon within phosphatic garnet in metapelites from western Massachusetts. *American Mineralogist,* v. 101, p. 1792-1806.
Potts, S. S., Pluijm, B. A., and Van der Voo, R., 1993, Paleomagnetism of the Ordovician Bluffer Pond Formation: Paleogeographic implications for the Munsungun terrane of northern Maine: Journal of Geophysical Research: Solid Earth, v. 98, p. 7987-7996.
Potts, S. S., Van der Pluijm, B. A., and Van der Voo, R., 1995, Paleomagnetism of the Pennington Mountain terrane: A near-Laurentian back arc basin in the Maine Appalachians: JOURNAL OF GEOPHYSICAL RESEARCH-ALL SERIES-, v. 100, p. 10,003-10,003.

Quinn, A. W., and Moore Jr, G. E., 1968, Sedimentation, tectonism, and plutonism of the Narragansett Basin region: Zen, E-an, White, WS, Jarvis, BH and Thompson, JB (Eds). Studies of Appalachian Geology: Northern and Maritime. Interscience, New YOrk, p. 269-279.

Rankin, D. W., Tucker, R. D., and Amelin, Y., 2013, Reevaluation of the Piermont-Frontenac allochthon in the Upper Connecticut Valley: Restoration of a coherent Boundary Mountains–Bronson Hill stratigraphic sequence: Geological Society of America Bulletin, v. 125, p. 998-1024.

Rast, N., and Skehan, J. W., 1993, Mid-Paleozoic orogenesis in the North Atlantic: the Acadian orogeny: Geological Society of America Special Papers, v. 275, p. 1-26.

Ratcliffe, N. M., Aleinikoff, J. N., Burton, W. C., and Karabinos, P., 1991, Trondhjemitic, 1.35-1.31 Ga gneisses of the Mount Holly Complex of Vermont: evidence for an Elzevirian event in the Grenville Basement of the United States Appalachians: Canadian Journal of Earth Sciences, v. 28, p. 77-93.

Ratcliffe, N.M., Hames, W.E., and Stanley, R.S., 1999, Taconian orogeny in the New England Appalachians: Collision between Laurentia and the Shelburne Falls arc: Comment and Reply: Geology, v. 27, p. 381.

Ratcliffe, N. M., Stanley, R. S., Gale, M. H., Thompson, P. J., Walsh, G. J., Rankin, D. W., Doolan, B. L., Kim, J., Mehrtens, C. J., and Aleinikoff, J. N., 2011, Bedrock geologic map of Vermont, US Geological Survey.

Ratcliffe, N. M., and Zartman, R. E., 1976, Stratigraphy, isotopic ages, and deformational history of basement and cover rocks of the Berkshire Massif, southwestern Massachusetts: Geological Society of America Memoirs, v. 148, p. 373-412.

Reusch, D. N., and van Staal, C. R., 2011, The Dog Bay–Liberty Line and its significance for Silurian tectonics of the northern Appalachian orogen 1 2 1 This article is one of a series of papers published in this CJES Special Issue: In honour of Ward Neale on the theme of Appalachian and Grenvillian geology. 2 Geological Survey of Canada Contribution 20100257: Canadian Journal of Earth Sciences, v. 49, p. 239-258.

Richardson, C. H., 1924, The terranes of Bethel, Vermont, In Perkins, G.H., Report of the State Geologist on the mineral industries and geology of Vermont, 1923-1924: Vermont Geological Survey [Report of the State Geologist], v. 14, p. 77-103.

Riva, J., 1974, A revision of some Ordovician graptolites of eastern North America, Paleontology, v. 17, p. 1-40.

Robinson, P., Tucker, R., Gromet, L., Ashenden, D., Williams, M., Reed, R., and Peterson, V., 1992, The Pelham dome, central Massachusetts: Stratigraphy, geochronology, structure and metamorphism, Guidebook for Field Trips in the Connecticut Valley Region of Massachusetts and Adjacent States, NEIGC 84th Annual Meeting: University of Massachusetts, Department of Geology and Geography Contribution, p. 132-169.

Rodgers, John, compiler, 1985, Bedrock Geological Map of Connecticut: Connecticut Geological and Natural History Survey, Hartford, Connecticut, 2 sheets, scale 1:125,000.

Rowley, D. B., and Kidd, W., 1981, Stratigraphic relationships and detrital composition of the medial Ordovician flysch of western New England: Implications for the tectonic evolution of the Taconic orogeny: The Journal of Geology, p. 199-218.

Schenk, P. E., 1997, Sequence stratigraphy and proveance on Gondwana's margin: the Meguma Zone (Cambrian to Devonian) of Nova Scotia, Canada: Geological Society of America Bulletin, v. 109, p. 395-409.

Schmitz, M. D., and Schoene, B., 2007, Derivation of isotope ratios, errors and error correlations for U-Pb geochronology using 205Pb-235U-(233U)-spiked isotope dilution thermal ionization mass spectrometric data: Geochemistry, Geophysics, Geosystems, v. 8, p. Q08006.

Sevigny, J., and Hanson, G., 1993, Orogenic evolution of the New England Appalachians of southwestern Connecticut: Geological Society of America Bulletin, v. 105, p. 1591-1605.

Sevigny, J., and Hanson, G., 1995, Late-Taconian and pre-Acadian history of the New England Appalachians of southwestern Connecticut: Geological Society of America Bulletin, v. 107, p. 487-498.

Sláma, J., Košler, J., Condon, D. J., Crowley, J. L., Gerdes, A., Hanchar, J. M., Horstwood, M. S., Morris, G. A., Nasdala, L., and Norberg, N., 2008, Plešovice zircon—a new natural reference material for U–Pb and Hf isotopic microanalysis: Chemical geology, v. 249, p. 1-35.

St. Julien, P. S., and Hubert, C., 1975, Evolution of the Taconian orogen in the Quebec Appalachians: American Journal of Science, v. 275, p. 337-362.

Stanley, R. S., and Hatch Jr, N. L., 1988, The pre-Silurian geology of the Rowe-Hawley zone, *in* Hatch Jr, N. L., editor, The bedrock geology of Massachusetts: U.S. Geological Survey Professional Paper 1366, US Geological Survey, p. A1-A39.

Stanley, R. S., and Ratcliffe, N. M., 1985, Tectonic synthesis of the Taconian orogeny in western New England: Geological Society of America Bulletin, v. 96, p. 1227-1250.

Strachan, R., Collins, A., Buchan, C., Nance, R., Murphy, J., and D'Lemos, R., 2007, Terrane analysis along a Neoproterozoic active margin of Gondwana: insights from U–Pb zircon geochronology: Journal of the Geological Society, v. 164, p. 57-60.

Thompson, J.B., Jr., Robinson, Peter, Clifford, T. N., and Trask, N. J. Jr., 1968, Nappes and gneiss domes in west-central New England: *In* Zen E., and W.S. White, Editors, Studies of Appalachian Geology: Northern and Maritime, John Wiley & Sons, New York, p. 203-218, 2 color plates.

Todaro, S., Stamatakos, J., Van der Pluijm, B., and Van der Voo, R., 1996, Near-Laurentian paleogeography of the Lawrence Head volcanics of central Newfoundland, northern Appalachians: Tectonophysics, v. 263, p. 107-121.

Torsvik, T. H., Van der Voo, R., Preeden, U., Mac Niocaill, C., Steinberger, B., Doubrovine, P. V., van Hinsbergen, D. J., Domeier, M., Gaina, C., and Tohver, E., 2012, Phanerozoic polar wander, palaeogeography and dynamics: Earth-Science Reviews, v. 114, p. 325-368.

Tremblay, A., Meshi, A., and Bédard, J. H., 2009, Oceanic core complexes and ancient oceanic lithosphere: insights from Iapetan and Tethyan ophiolites (Canada and Albania): Tectonophysics, v. 473, p. 36-52.

Tremblay, A., and Pinet, N., 2016, Late Neoproterozoic to Permian tectonic evolution of the Quebec Appalachians, Canada, Earth-Science Reviews, v. 160, p. 131-170.

Tucker, R., Bradley, D., Ver Straeten, C., Harris, A., Ebert, J., and McCutcheon, S., 1998, New U–Pb zircon ages and the duration and division of Devonian time: Earth and Planetary Science Letters, v. 158, p. 175-186.

Tucker, R., and McKerrow, W., 1995, Early Paleozoic chronology: a review in light of new U-Pb zircon ages from Newfoundland and Britain: Canadian Journal of Earth Sciences, v. 32, p. 368-379.

Tucker, R. D., and Robinson, P., 1990, Age and setting of the Bronson Hill magmatic arc: A re-evaluation based on U-Pb zircon ages in southern New England: Geological Society of America Bulletin, v. 102, p. 1404-1419.

Valley, P., Walsh, G. J., and McAleer, R. J., 2015, New U-Pb zircon ages from the Bronson Hill arc, west-central New Hampshire, Geological Society of America Abstracts with Programs, p. 41.

van der Pluijm, B. A., Johnson, R. J., and Van der Voo, R., 1990, Early Paleozoic paleogeography and accretionary history of the Newfoundland Appalachians: Geology, v. 18, p. 898-901.

van der Voo, R., Johnson, R. J., van der Pluijm, B. A., and Knutson, L. C., 1991, Paleogeography of some vestiges of Iapetus: paleomagnetism of the Ordovician Robert's Arm, Summerford, and Chanceport groups, central Newfoundland: Geological Society of America Bulletin, v. 103, p. 1564-1575.

Van Staal, C., and Barr, S., 2012, Lithospheric architecture and tectonic evolution of the Canadian Appalachians and associated Atlantic margin: Tectonic styles in Canada: The LITHOPROBE perspective: Geological Association of Canada Special Paper, v. 49, p. 55.

Van Staal, C., Dewey, J., Mac Niocaill, C., and McKerrow, W., 1998, The Cambrian-Silurian tectonic evolution of the northern Appalachians and British Caledonides: history of a complex, west and southwest Pacific-type segment of Iapetus: Geological Society, London, Special Publications, v. 143, p. 197-242.

Van Staal, C., Whalen, J., McNicoll, V., Pehrsson, S., Lissenberg, C. J., Zagorevski, A., van Breemen, O., and Jenner, G., 2007, The Notre Dame arc and the Taconic orogeny in Newfoundland: Geological Society of America Memoirs, v. 200, p. 511-552.

van Staal, C., Wilson, R., Kamo, S., McClelland, W., and McNicoll, V., 2016, Evolution of the Early to Middle Ordovician Popelogan arc in New Brunswick, Canada, and adjacent Maine, USA: Record of arc-trench migration and multiple phases of rifting: Geological Society of America Bulletin, v. 128, p. 122-146.

van Staal, C. R., Chew, D. M., Zagorevski, A., McNicoll, V., Hibbard, J., Skulski, T., Escayola, M. P., Castonguay, S., and Sylvester, P. J., 2013, Evidence of Late Ediacaran hyperextension of the Laurentian Iapetan margin in the Birchy Complex, Baie Verte Peninsula, northwest Newfoundland: implications for the opening of Iapetus, formation of peri-Laurentian microcontinents and Taconic–grampian orogenesis: Geoscience Canada, v. 40, p. 94-117.

van Staal, C. R., Whalen, J. B., Valverde-Vaquero, P., Zagorevski, A., and Rogers, N., 2009, Pre-Carboniferous, episodic accretion-related, orogenesis along the Laurentian margin of the northern Appalachians: Geological Society, London, Special Publications, v. 327, p. 271-316.

Ver Straeten, C. A., 2010, Lessons from the foreland basin: Northern Appalachian basin perspectives on the Acadian orogeny: Geological Society of America Memoirs, v. 206, p. 251-282.

Waldron, J. W., McNicoll, V. J., and van Staal, C. R., 2011, Laurentia-derived detritus in the Badger Group of central Newfoundland: deposition during closing of the Iapetus Ocean 1 2 1 This article is one of a series of papers published in CJES Special Issue: In honour of Ward Neale on the theme of Appalachian and Grenvillian geology. 2 Geological Survey of Canada Contribution 20110273: Canadian Journal of Earth Sciences, v. 49, p. 207-221.

Waldron, J. W., Schofield, D. I., Murphy, J. B., and Thomas, C. W., 2014, How was the Iapetus Ocean infected with subduction?: Geology, p. G36194. 1.

Waldron, J. W., and van Staal, C. R., 2001, Taconian orogeny and the accretion of the Dashwoods block: A peri-Laurentian microcontinent in the Iapetus Ocean: Geology, v. 29, p. 811-814.

Walsh, G. J., and Aleinikoff, J. N., 1999, U-Pb zircon age of metafelsite from the Pinney Hollow Formation; implications for the development of the Vermont Appalachians: American Journal of Science, v. 299, p. 157-170.

Watson, E., Wark, D., and Thomas, J., 2006, Crystallization thermometers for zircon and rutile: Contributions to Mineralogy and Petrology, v. 151, p. 413-433.

Wellensiek, M. R., Pluijm, B. A., Van der Voo, R., and Johnson, R. J., 1990, Tectonic history of the Lunksoos composite terrane in the Maine Appalachians: Tectonics, v. 9, p. 719-734.

Whalen, J., Currie, K., and Van Breemen, O., 1987, Episodic Ordovician-Silurian plutonism in the Topsails igneous terrane, western Newfoundland: Transactions of the Royal Society of Edinburgh: Earth Sciences, v. 78, p. 17-28.

Whalen, J. B., Jenner, G. A., Longstaffe, F. J., Gariepy, C., and Fryer, B. J., 1997a, Implications of granitoid geochemical and isotopic (Nd, O, Pb) data from the Cambrian-Ordovician Notre Dame arc for the evolution of the Central Mobile belt, Newfoundland Appalachians: The nature of magmatism in the Appalachian orogen: Geological Society of America Memoir, v. 191, p. 367-395.

Whalen, J. B., van Staal, C. R., Longstaffe, F. J., Gariépy, C., and Jenner, G. A., 1997b, Insights into tectonostratigraphic zone identification in southwestern Newfoundland based on isotopic (Nd, O, Pb) and geochemical data: Atlantic Geology, v. 33.

White, C. E., and Barr, S. M., 2010, Lithochemistry of the Lower Paleozoic Goldenville and Halifax groups, southwestern Nova Scotia, Canada: Implications for stratigraphy, provenance, and tectonic setting of the Meguma terrane: Geological Society of America Memoirs, v. 206, p. 347-366.

Whitehead, J., Reynolds, P. H., and Spray, J. G., 1996, 40Ar/39Ar age constraints on Taconian and Acadian events in the Quebec Appalachians: Geology, v. 24, p. 359-362.

Williams, H., 1979, Appalachian orogen in Canada: Canadian Journal of Earth Sciences, v. 16, p. 792-807.

Williams, H., Colman-Sadd, S., and Swinden, H., 1988, Tectonic-stratigraphic subdivisions of central Newfoundland: Current Research, Part B. Geological Survey of Canada, Paper, v. 88, p. 91-98.

Williams, H., and Hiscott, R. N., 1987, Definition of the Iapetus rift-drift succession in western Newfoundland: Geology, v. 15, p. 1044-1047.

Willner, A. P., Gerdes, A., Massonne, H.-J., van Staal, C. R., and Zagorevski, A., 2014, Crustal Evolution of the Northeast Laurentian Margin and the Peri-Gondwanan Microcontinent Ganderia Prior to and During Closure of the Iapetus Ocean: Detrital Zircon U–Pb and Hf Isotope Evidence from Newfoundland: Geoscience Canada, v. 41, p. 345-364.

Wintsch, R. P., Webster, J. R., Bernitz, J. A., and Rout, J. S., 1990, Geochemical and geological criteria for the discrimination of high grade gneisses of intrusive and extrusive origin, southern Connecticut, *in* Socci, A. D., Skehan, J. W., and Smith, G. W., editors, Geology of the composite Avalon terrane of southern New England: Geological Society of America Special Paper, p. 187-208.

Wintsch, R. P., Yi, K., and Han, D., 2015, Evidence from U-Pb SHRIMP ages of detrital zircons for evolving provenances for peri-Gondwanan forearc metasediments, western Connecticut, Geological Society of America Abstracts with Programs, p. 42.

Wintsch, R. P., Yi, K., and Lee, T. H., 2016, More about the Moretown terrane in the Bristol dome, western Connecticut, Geological Society of America Abstracts with Programs.

Zagorevski, A., van Staal, C., Rogers, N., McNicoll, V., and Pollock, J., 2010, Middle Cambrian to Ordovician arc-backarc development on the leading edge of Ganderia, Newfoundland Appalachians: Geological Society of America Memoirs, v. 206, p. 367-396.

Zagorevski, A., van Staal, C. R., McNicoll, V., Rogers, N., and Valverde-Vaquero, P., 2008, Tectonic architecture of an arc-arc collision zone, Newfoundland Appalachians: Geological Society of America Special Papers, v. 436, p. 309-333.

Zen, E.A., Goldsmith, R., Ratcliffe, N.M., Robinson, P., Stanley, R.S., Hatch, N.L., Jr., Shride, A.F., Weed, A., and Wones, D.R., 1983, Bedrock geologic map of Massachusetts: United States Geological Survey, scale 1:250,000.

# MOUNT GREYLOCK AS A COSMOGENIC NUCLIDE DIPSTICK TO DETERMINE THE TIMING AND RATE OF SOUTHEASTERN LAURENTIDE ICE SHEET THINNING

By

Christopher T. Halsted[1], Rubenstein School of Environment and Natural Resources, University of Vermont, Burlington, VT 05405
Jeremy D. Shakun[2], Dept. of Earth and Environmental Sciences, Boston College, Chestnut Hill, MA 02467
P. Thompson Davis[3], Dept. of Natural and Applied Sciences, Bentley University, Waltham, MA 02454
Paul R. Bierman[4] and Lee B. Corbett[5], Dept. of Geology, University of Vermont, Burlington, VT 05405
Alexandria J. Koester[6], Dept. of Earth, Atmospheric, and Planetary Sciences, Purdue University, West Lafayette, IN 47907
Email addresses: [1]chalsted@uvm.edu, [2]jeremy.shakun@bc.edu, [3]pdavis@bentley.edu, [4]pbierman@uvm.edu, [5]Ashley.Corbett@uvm.edu,

## INTRODUCTION

This field trip to Mt. Greylock serves several purposes: 1) discuss and review the glacial history of Mt. Greylock and the surrounding region, 2) describe the motivation behind an NSF-funded project to understand the timing and rate of ice thinning in New England and adjacent areas, 3) explain the 'dipstick approach', the primary method being used to reconstruct ice thinning, and demonstrate the field work involved, 4) examine field sampling sites from this project and other glacial features on Mt. Greylock, and 5) discuss implications of initial results for paleoclimate and paleo-sea level change during the last deglaciation. Those interested can participate in a walk along the Appalachian Trail of approximately 2.7 miles (although trip participants are encouraged to lengthen their walk by ~2 miles and return back to the Greylock summit via the AT if desired).

Before beginning this field trip, it is important to reflect on why the fields of glacial geomorphology and ice-sheet reconstructions are areas of interest. Understanding ice sheets and their interactions with other components of the climate is essential to climate change mitigation and adaption discussions, but present projections of future ice sheet stability contain substantial uncertainties (e.g., Stocker et al., 2014; DeConto and Pollard, 2016, Hansen et al., 2016). These large uncertainties are due primarily to a limited understanding and poor model representation of ice sheet decay mechanics, particularly marginal processes such as ice-stream flow, ice-shelf buttressing, and subglacial meltwater drainage (Kleman and Applegate, 2014; Stokes, 2017). Modern observations of ice sheets in Greenland and Antarctica capture only a brief window in their history, and important basal processes are nearly impossible to observe. Reconstructing and studying the behavior of ice sheets during past periods of climate change offers a potential solution to observational and computational limitations.

The largest Northern Hemisphere ice sheet at the Last Glacial Maximum (LGM), the Laurentide Ice Sheet (LIS), is one of the most-investigated paleo-ice sheets, as its size and mixture of terrestrial and marine margins provide a unique opportunity to study the long-term behavior of ice margins analogous to modern-day locations in Greenland and Antarctica (Kleman and Applegate, 2014; Margold et al., 2015; Stokes et al., 2016; Stokes, 2017). Additionally, the near-complete retreat of such a large ice mass in only ~15-kyr illustrates the sensitivity of ice sheets to changing climatic conditions (Abe-Ouchi et al., 2013; Ullman et al., 2015).

The nature of interactions between the LIS and the rest of the climate system during the last deglaciation (~21-11 ka) are the source of much debate in the paleoclimate community. The last deglaciation was marked by a series of abrupt climate change events that are particularly apparent in proxy records from the North Atlantic and Greenland (e.g. Clark et al., 1999; Thornalley et al., 2010). A mechanism for similar abrupt events observed further back in the paleoclimate record (Dansgaard et al., 1993; Johnsen et al., 2001) was originally proposed by Broecker et al. (1985). They argued that changes in the strength of the Atlantic Meridional Overturning Circulation (AMOC) caused the North Atlantic to rapidly shift between two quasi-stable modes of climate. When the AMOC was strong, North Atlantic average annual temperatures were high (interstadial), and when the AMOC was weak, annual North Atlantic temperatures dropped (stadial). Clark et al. (1996) noted that a similar mechanism may have caused the abrupt warming and cooling events observed during the last deglaciation, and eventually hypothesized that the

direction and volume of the LIS meltwater flux may have had a direct influence on the strength of the AMOC (Clark et al., 2001).

## THE PROBLEM AND OUR APPROACH

While proxy evidence has emerged to support the notion of an AMOC with rapid fluctuations in strength during the last deglaciation (e.g., McManus et al., 2004), constraining the volume and source of the LIS meltwater flux through time has proved difficult. While the areal retreat history of the LIS has been refined by decades of research and numerous lines of evidence (e.g., Balco et al., 2002; Dyke, 2004; Ridge et al., 2012), the LIS thinning history is almost wholly unconstrained. Initial attempts to produce data on the thinning history of the LIS relied on $^{14}C$ dating of basal organic material in high- and low-elevation bogs (e.g., Spear, 1989; Spear et al., 1994). While these projects produced robust age/elevation data points, a highly-variable lag-time between deglaciation and deposition of organic matter in the bogs (Davis and Davis, 1980) lent considerable uncertainty to the data. Geophysical models of ice thickness based on inverted isostatic rebound patterns disagree considerably (e.g., Clark and Tarasov, 2014; Peltier et al., 2015), and numerical model simulations of ice thickness based on paleoclimate evolution contain substantial amounts of uncertainty (e.g., Gregoire et al., 2012; Abe-Ouchi et al., 2015).

The lack of suitable data constraints on the LIS thinning history has propagated uncertainty to other areas of paleoclimate. Notably, the volume of the LIS during its decay has remained uncertain, making it difficult to quantify the contribution of the LIS to global sea-level rise (Carlson and Clark, 2012) and discreet meltwater pulse events observed in deglacial sea-level reconstructions (Clark et al., 2002; Clark et al., 2004; Deschamps et al., 2012; Liu et al., 2016). Without constraints on the timing of LIS thinning, the relationships between the variable deglacial AMOC, the volatile North Atlantic climate, and the LIS remain poorly understood. Furthermore, the height of the LIS is an essential boundary condition for deglacial paleoclimate models (e.g., Barron and Pollard, 2002; Ullman et al., 2014). The height of an ice sheet affects atmospheric circulation, with higher ice sheets acting as larger impediments to upper-atmosphere flow (Bromwich et al., 2004; Abe-Ouchi et al., 2007; Langen and Vinther, 2009). Finally, accurate ice-sheet reconstructions are important for ice-sheet models, which are used for future stability projections and depend on data constraints to inform the internal mechanisms within the models (Applegate et al., 2012; Kleman and Applegate, 2014; Stokes et al., 2015).

For this project, we proposed the implementation of a relatively novel method to constrain part of the LIS thinning history: the 'dipstick' approach. In this approach, the 'dipstick' is a series of cosmogenic nuclide exposure ages produced at a range of elevations in an area of significant topography (Fig. 1; see commentary by Bierman, 2007). The theory behind the approach is that as the LIS thinned, it exposed more and more topography, and by taking exposure ages from a range of elevations in one location, the lowering ice surface can essentially be tracked through time. This method has been used to constrain thinning histories of the Scandinavian (Goehring et al., 2008); Antarctic (Stone et al., 2003; Ackert et al., 2007; Mackintosh et al., 2011; Johnson et al., 2014), and Greenland (Corbett et al., 2011) Ice Sheets, but has seen limited use with the LIS. Despite its tremendous size and influence on the deglacial paleoclimate, only three dipsticks have been developed for the LIS (Davis et al., 2015; Koester et al., 2017, Davis et al., 2017). This is primarily a consequence of the fact that the LIS predominately covered flat terrain over the interior regions of the northern United States and Canada, limiting the areas where dipsticks can be produced. While the eastern Canadian Arctic provides sufficient topographic relief for dipstick construction, its polar climate was likely conducive to non-erosive, cold-based ice during the last glacial and deglacial periods (Sugden, 1978; Briner et al., 2003), reducing the effectiveness of the dipstick approach (see Methods section for more detail). Therefore, New England and southern Quebec are the only regions with the necessary topography and paleoclimate for successful LIS dipstick construction.

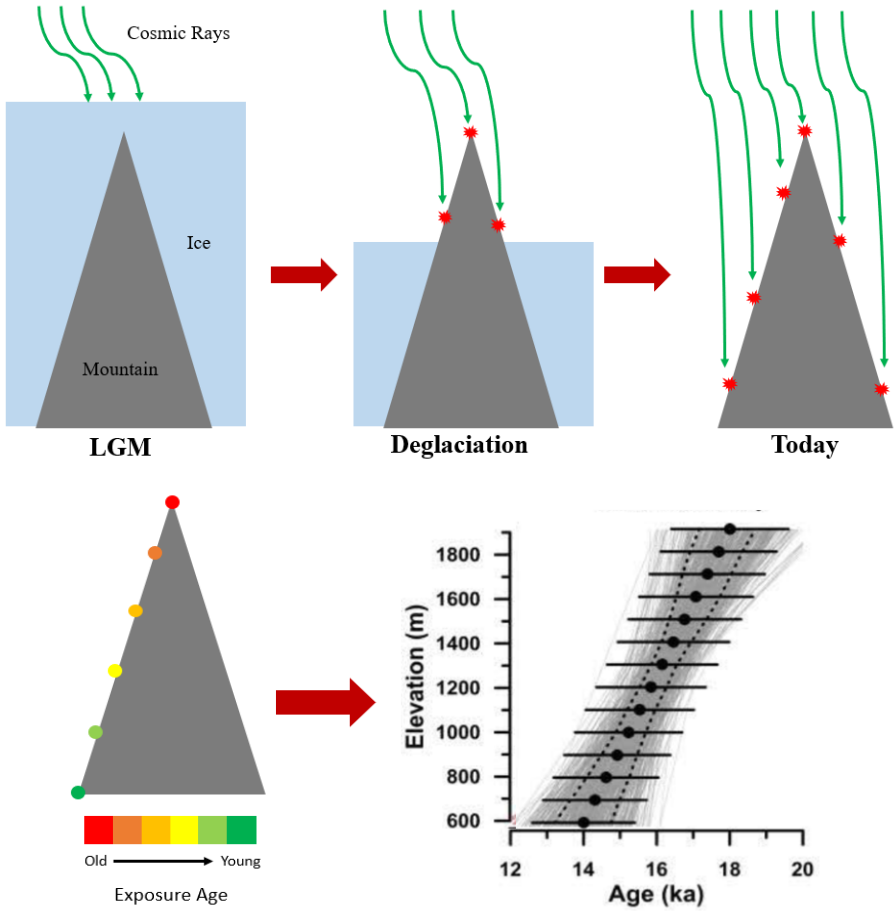


**Figure 1:** A simplified depiction of the dipstick method. Green lines in top panel are cosmic rays, while red starbursts represent the formation of terrestrial *in-situ* cosmogenic nuclides (TCNs). Top-left panel: at the LGM, a mountain is covered by an ice sheet, blocking cosmic rays from interacting with surficial minerals. Top-middle panel: as the ice sheet begins to thin, cosmic rays interact with minerals near the top of the mountain, forming TCNs at higher elevations only. Top-right panel: if the mountain is presently unglaciated, TCNs form at all elevations. Bottom-left panel: typical expected exposure age profile from a mountain in this scenario, due to early exposure of higher elevations. Bottom-right panel: an example of a 'dipstick' plot using synthetic data. The plot shows exposure age on the x-axis vs. elevation on the y-axis. Monte-carlo simulations (grey lines) using the analytical uncertainty on each point (error bars) give a population of possible thinning timing and rates.

## GLOBAL CLIMATE AND SEA LEVEL DURING THE LAST DEGLACIATION

### Last Glacial Maximum to The Oldest Dryas (~21 – 19 ka)

Summer insolation at high northern latitudes (boreal summer insolation) rose following the last eccentricity and precession minimums around 24 ka (Carlson and Winsor, 2012), slowly initiating the retreat of Northern Hemisphere ice sheets. A gradual Northern Hemisphere temperature increase that started around 21 ka has been linked to the shift in insolation forcing, with the temporal lag attributed to inertia within the climate system (He et al., 2013). The gradual Northern Hemisphere warming continued from 21-19 ka, a period characterized by a strong AMOC (McManus et al., 2004; Shakun et al., 2012) and the initial retreat of the southern margins of most Northern Hemisphere ice-sheets (Clark et al., 2009). It is estimated that global average sea level rose about 10 m from 21-19 ka, sourced primarily from Northern Hemisphere ice sheets (Fig. 2; Lambeck et al., 2014). The freshwater flux from this initial retreat may have disturbed the density-driven AMOC, which began reducing in strength around 19 ka (Fig. 2; McManus et al., 2004).

**The Oldest Dryas (19-14.6 ka)**

The AMOC reduction had profound effects on global climate, tipping the bi-polar see-saw and initiating the Oldest Dryas stadial period in the Northern Hemisphere (Liu et al., 2009; Denton et al., 2010; Clark et al., 2012). This stadial period is believed to have been characterized by extreme seasonality, with winter surface air temperatures estimated ~32˚C colder than today, but summer surface air temperatures only ~8˚C colder (Broecker, 2006; Buizert et al., 2014). This pattern is hypothesized to be a consequence of expanded winter sea-ice in the North Atlantic preventing ocean-atmosphere interactions, while continually rising boreal summer insolation maintained mild summer temperatures (Broecker, 2006; Denton et al., 2010). The reduced northward heat transport caused warming in the Southern Hemisphere that ultimately led to a reduction in sea ice and increased upwelling in the Southern Ocean (Denton et al., 2010). The upwelling resulted in a release of sequestered $CO_2$ into the atmosphere starting around 17.5 ka (Shakun et al., 2012; Clark et al., 2012). The subsequent rise of atmospheric $CO_2$ concentration led to greenhouse gas warming, emphasizing interstadial conditions in the Southern Hemisphere and gradually reducing the extreme seasonality dominating the Northern Hemisphere (Denton et al., 2010).

Global average sea level rose slowly in the beginning of the Oldest Dryas (from 19-16.5 ka; Carlson and Clark, 2012), likely due to reduced Northern Hemisphere ice sheet retreat in stadial conditions and a lag in Southern Hemisphere warming. From 16.5 – 14.6 ka, sea-level rise accelerated, increasing ~25 m over this span (Carlson and Clark, 2012; Lambeck et al., 2014). However, the source(s) of this large sea level rise are poorly understood, leading Carlson and Clark (2012) to conclude that, "*the volume contributions of individual ice sheets to sea level change between 19.5 ka and 14.6 ka, which are required to specify freshwater fluxes and their entry points into the ocean, need to be better determined.*"

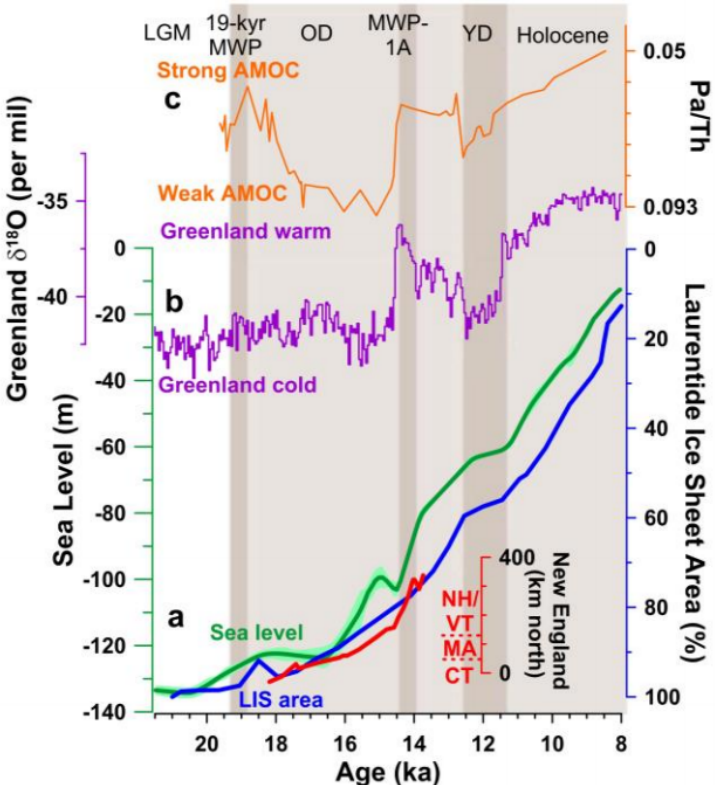


**Figure 1.** Deglacial ice melt, climate, and ocean circulation (figure from Davis et al., 2017). (**a**) Global sea level (green; from Lambeck et al., 2014), LIS extent (blue; from Dyke, 2004), and northward LIS retreat in central New England based on varves (red; Ridge et al., 2012). (**b**) Greenland $\delta^{18}O$, a proxy for temperature (NGRIP members, 2004). (**c**) Protactinium/thorium ratios in a North Atlantic sediment core, a proxy for AMOC strength (McManus et al., 2004).

**Meltwater Pulse 1a and Bølling warming (14.6-14.3 ka)**

Around 14.6 ka, proxy records indicate that the AMOC rapidly strengthened (McManus et al., 2004), closely followed by an abrupt Greenland warming (Fig. 2; NGRIP members, 2004). Around the time of the AMOC recovery, one of the most remarkable and poorly understood events of the last deglaciation occurred. Over a period of approximately 300 years, global average sea level rose between ~9-15 m, suggesting a rate of sea-level rise exceeding 40 mm/yr (Deschamps et al., 2012; Lambeck et al., 2014; Liu et al., 2016). Called Meltwater Pulse 1a (MWP-1A), there is no clear consensus the source(s) and cause(s) of this event. Davis et al. (2017) summarized the ongoing attempts: *"While MWP-1A was first assumed to have originated exclusively from the LIS (Fairbanks, 1989; Peltier, 2005), sea-level fingerprinting and Southern Ocean marine evidence suggest a significant though uncertain Antarctic contribution (Weaver et al., 2003; Deschamps et al., 2012; Weber et al., 2014). Planktonic $\delta^{18}O$ runoff records from the Gulf of Mexico (Wickert et al., 2013), the Arctic (Carlson, 2009), and the Labrador Sea (Obbink et al., 2010) detect only minor contributions from various sectors of the LIS to MWP-1A. Furthermore, LIS areal retreat was no greater during MWP-1A than before or after the event. Therefore, any major LIS sea-level contributions could only have come from rapid ice sheet thinning… An accounting of the sources of sea-level rise during this singular event (MWP-1A) is thus far from complete."*

**The Allerød interstadial, Younger Dryas, and Holocene (14.3-11.7 ka)**

By MWP-1A, the southeastern LIS margin had already retreated north of Mount Greylock. Therefore, subsequent deglacial climate events, although highly interesting and worth further reading for interested trip participants, will only be discussed briefly here. Following MWP-1A, sea-level rise slowed to near the deglacial average rate for the next ~1.5-kyr (Lambeck et al., 2014). The AMOC remained strong during this period (McManus et al., 2004), sustaining interstadial conditions in the Northern Hemisphere that led to high ablation rates and an increased LIS meltwater flux (Ridge et al., 2012). Around 12.9 ka, the AMOC abruptly weakened (Fig. 2; McManus et al., 2004), leading to a brief North Atlantic stadial period known as the Younger Dryas. The cause of this AMOC reduction was initially hypothesized to be a routing of LIS meltwater to the newly exposed St. Lawrence river outlet (Broecker et al., 1989), however, more recent arguments in favor of a northern outlet through the Mackenzie River (Tarasov and Peltier, 2005; Condron and Winsor, 2012) now have robust proxy support (Keigwin et al., 2018). The AMOC recovered around 11.7 ka (Fig. 2; McManus et al., 2004), at the onset of the Holocene.

## SOUTHEASTERN LAURENTIDE DEGLACIATION

The mountains of the northeastern United States and southern Quebec were overridden by the southeastern Laurentide at the LGM (Fig. 3 inset). Numerous data constraints on the retreat history of this ice margin, including minimum-limiting organic $^{14}C$ dates (e.g., Dyke, 2004), $^{14}C$-anchored varve series (e.g., Ridge et al., 2012), and $^{10}Be$ exposure dates on moraines (e.g., Balco et al., 2002; Balco and Schaefer, 2006; Bromley et al., 2015) make it an ideal case study for understanding ice margin-ocean-climate interactions (Fig. 3). However, an almost complete lack of thinning information prevents detailed investigations.

**Ice Extent**

The southeastern margin of the LIS was at its maximum extent by at least 24 ka, as indicated by $^{10}Be$ ages of glacially-deposited boulders on the terminal moraines of Martha's Vineyard (29.2 ± 1.7 ka; Balco et al., 2002) and northern New Jersey (25.2 ± 1.3 ka; Corbett et al., 2017). An initial pullback, likely due to rising boreal summer insolation, placed the ice margin north of Buzzard's Bay by 21.0 ± 1.0 ka (Balco et al., 2002). The North American Varve Chronology indicates that southeastern LIS retreat continued steadily (~50 m/yr) during the Oldest Dryas, despite stadial conditions in the adjacent North Atlantic (Ridge et al., 2012). This pattern might be a consequence of the extreme seasonality that characterized North Atlantic climate during this period. As summer surface air temperatures are the primary control on ice sheet volume, due to their control on ablation (Abe-Ouchi, 2013), the mild summers of the Oldest Dryas may have sustained retreat of the southeastern LIS margin. Several moraine sequences were deposited throughout New England near the transition into the Bølling and MWP-1A (Fig. 3; Balco et al., 2009; Koester et al., 2017). After deposition of these moraines, the southeastern LIS margin retreated at a far higher pace (~300 m/yr), ultimately retreating north of New England by 13 ka (Ridge et al., 2012).

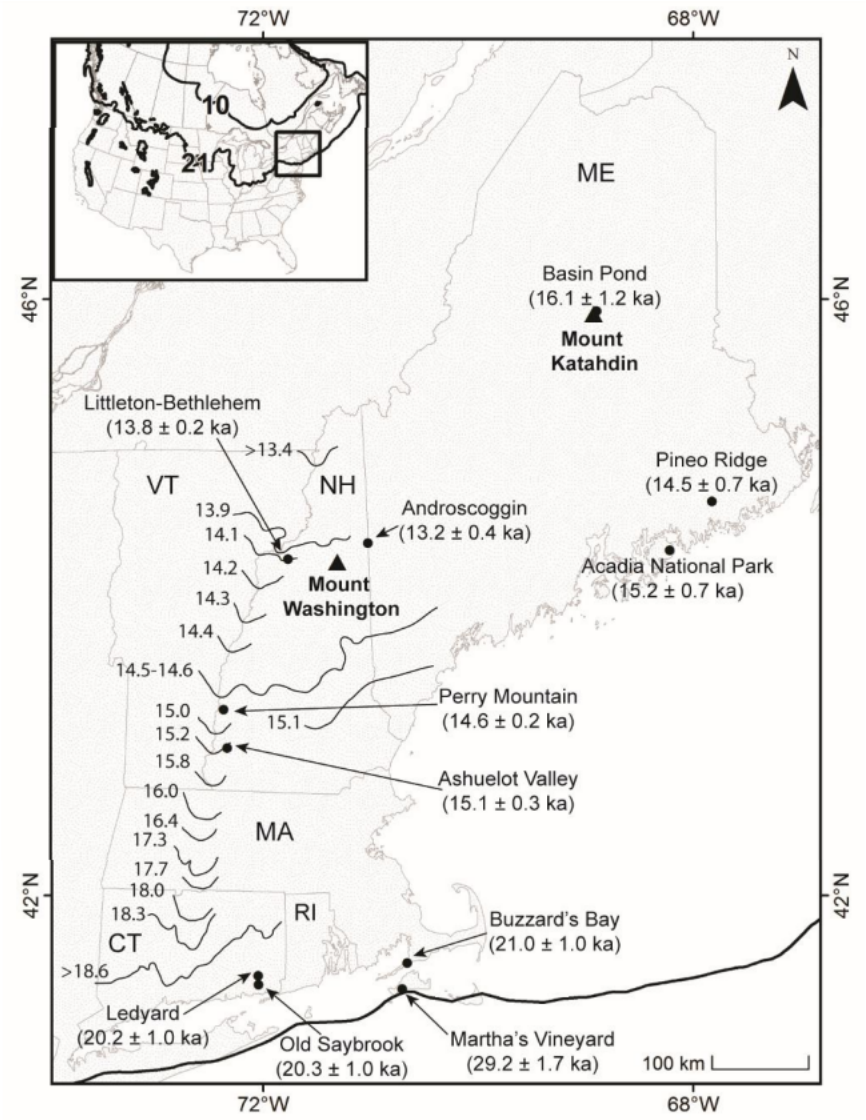


**Figure 3.** Laurentide Ice Sheet lateral extent through time (figure and caption from Davis et al., 2017). Isochrones show the North American Varve Chronology of deglaciation (from Fig. 11 in Ridge et al., 2012). The black dots are moraines dated using $^{10}$Be and calibrated with the northeastern North American production rate (Martha's Vineyard and Buzzard's Bay – Balco et al., 2002; Old Saybrook and Ledyard – Balco and Schaefer, 2006; Ashuelot Valley, Perry Mountain, and Littleton-Bethlehem – Balco et al., 2009; Androscoggin – Bromley et al., 2015; Basin Pond – Davis et al., 2015; Pineo Ridge and Acadia National Park – Koester et al., 2017). Inset figure shows the extent of the LIS at 21 ka and 10 ka (Dyke, 2003).

**Ice Thickness**

While the retreat chronology of the LIS has been clearly defined in most areas using a variety of methods, data on its thinning history is sparse. Initial attempts to reconstruct a southeastern LIS thinning history produced $^{14}$C ages from lake and bog basal sediments in the White Mountains, NH, and Mt. Katahdin, ME, meant to determine minimum-limiting ages for the lowering of the ice surface in the region (Table 1; Davis and Davis, 1980; Spear, 1989; Spear et al., 1994; Rogers, 2003). However, the results contain so much scatter and uncertainty that they are of limited use in determining the timing of ice thinning. It is similarly an open question whether ice sheet drawdown was very rapid (centuries) or much more gradual (millennia).

| Site | Elev (m) | $^{14}$C Age | cal yr BP | Source |
|---|---|---|---|---|
| *Moosilauke* | | | | |
| Deer Lake bog | 1325 | 13,000 ± 400 | 14,195-16,820 | Spear (1989) |
| Mirror Lake | 213 | 13,800 ± 560 | 15,720-17,415 | Davis and Davis (1980) |
| *Franconia Notch* | | | | |
| Lonesome Lake | 831 | 10,535 ± 495 | 11,065-13,355 | Spear et al. (1994) |
| Profile Lake | 593 | 10,660 ± 40 | 12,772-12,885 | Rogers (2003) |
| *Mt. Washington* | | | | |
| Lakes of Clouds | 1538 | 11,530 ± 165 | 10,790-13,355 | Spear (1989) |
| Lost Pond | 625 | 12,870 ± 370 | 14,580-15,760 | Spear et al. (1994) |

**Table 1.** Low versus high-elevation $^{14}$C ages from the White Mountains, NH. Note that the age pairs tend to be fairly similar, suggesting that ice-sheet drawdown may have been rapid. On the other hand, these ages are only minimum0limiting, and the close correspondence in ages may reflect the timing of revegetation and the first occurrence of datable organic material. Indeed, this complication may explain why higher-elevation ages tend to be younger than lower-elevation ages, opposite the pattern expected from top-down deglaciation.

Preliminary cosmogenic exposure ages from our project have yielded more conclusive results, with exposure-age dipsticks providing evidence of rapid ice thinning in central Maine (~16-15 ka; Fig. 5; Davis et al., 2015), the Presidential Range of New Hampshire (starting ~17 ka; Davis et al., 2017), and on the Maine coast (15.2 ± 0.7 ka; Fig. 5; Koester et al., 2017). It should be noted that the dipsticks from central and coastal Maine feature broad 90% confidence intervals, preventing the exclusion of more complex thinning histories with varying thinning rates. Furthermore, nuclide concentrations from the highest summits in this region are higher than expected, likely due to the incomplete removal of cosmogenic nuclides from prior episodes of exposure by non-erosive, cold-based ice (Bierman et al., 2015; Koester et al., 2017). These high-elevation exposure ages, therefore, cannot be meaningfully interpreted because their cosmogenic nuclide concentrations do not reflect a single period of exposure. The dipsticks reported by Davis et al. (2015. 2017) and Koester et al. (2017) are useful, but to extrapolate the timing and pattern of ice thinning observed at these locations to other areas of the LIS would, by necessity, involve significant uncertainty. Accurately reconstructing the thinning behavior of the entire southeastern LIS therefore requires more data covering a large geographic area.

## MOUNT GREYLOCK AND THE SURROUNDING REGION

Mount Greylock is geologically part of the Taconic Mountains but is located near the Berkshire Mountains of northwestern Massachusetts (Fig. 1). It is the tallest mountain in the state, with a summit elevation of 1064 m a.s.l. and a vertical relief of 751 m. Mt. Greylock is composed primarily of metamorphized sedimentary rock, including marble, which is overlain by schist and phyllite of the Taconic allochton (Bierman and Dethier, 1986). Mount Greylock is the product of thrust faulting during the Taconic orogeny, which thrust the Ordovician phyllite and schist over the dolomitic marble (Ratcliffe et al., 1993).

Bedrock is exposed across much of the Mount Greylock uplands, which is otherwise covered by till and colluvial deposits. Glacial striations, chattermarks, and grooves recorded in upland bedrock indicate that the ice-flow was predominately directed southeast, while flow indicators at lower elevations are generally in-line with the valley orientation. This pattern suggests that Laurentide ice became restricted to the valleys at some point in the last deglaciation (Fig. 4a; Bierman and Dethier, 1986). The retreating LIS dammed northward flowing water in the surrounding valleys, forming Glacial Lake Bascom (Fig. 4c), into which extensive deposits of fluvial and subaqueous ice-contact sediment were deposited (Bierman and Dethier, 1986). Lake Bascom reached an elevation of 306-317 m a.s.l. before the Laurentide retreated past a 273 m a.s.l. spillway located at Potter Hill, New York (Fig. 4d).

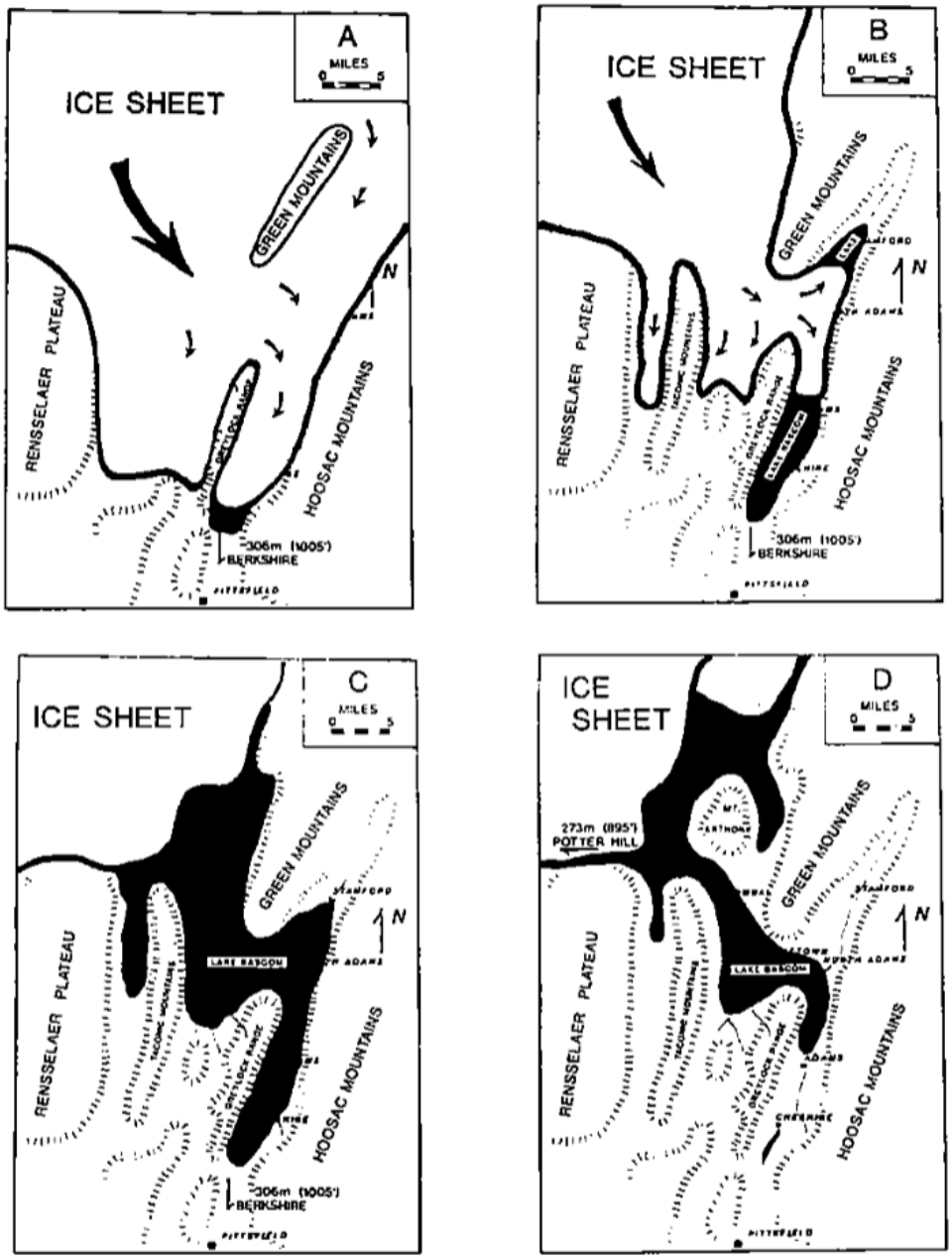


**Figure 4.** Simplified depiction of Laurentide ice retreat around Mount Greylock and formation of Glacial Lake Bascom (figure from Bierman and Dethier, 1986). Note the topographic control of ice in the valleys in (a) and (b).

## RESEARCH MOTIVATIONS.

**1) Did the southeastern LIS thinning rate vary during its deglaciation?**

The last deglaciation encompassed several stadial and interstadial periods, but currently available thinning histories cannot discern if regional climate influenced the thinning rate of the southeastern LIS. Ice extent constraints indicate significant differences in margin retreat rates during stadial vs. interstadial periods (Dyke, 2004; Ridge et al., 2012); are these differences mirrored seen in thinning rates? Of particular interest is the behavior of the southeastern LIS around the time of MWP-1A.

**2) Constrain Individual Ice Sheet Volume Histories**

Uncertainties in volume estimates of the LIS through the last deglaciation are problematic because they prevent further investigations into the mechanisms and influence of freshwater forcing on the AMOC, LIS contribution to sea level rise, and the source(s) of discreet meltwater pulse events. Constraining the timing and rate of LIS thinning, even for just the southeastern sector, could provide valuable insight into these systems.

**3) Improving Confidence and Accuracy in Deglacial Paleoclimate Models**

The height of the LIS is an essential boundary condition for deglacial paleoclimate models (e.g. Barron and Pollard, 2002; Ullman et al., 2014). Ullman et al. (2014) showed that a 20% difference in LIS elevation at the LGM, the difference between published reconstructions by Peltier (2004) and Toscano et al. (2011), resulted in substantial differences in model simulations of the deglacial paleoclimate. Glacial orography has an outsized effect on climate for several reasons. The height of an ice sheet has a direct effect on surface air temperatures through vertical lapse rate, but it also affects atmospheric circulation, with higher ice sheets acting as larger impediments to upper-atmosphere flow (Bromwich et al., 2004; Abe-Ouchi et al., 2007; Langen and Vinther, 2009). The effect of this flow impediment is a re-organization of the atmospheric jet, which has downstream effects on midlatitude storm tracks and wintertime precipitation across much of the NH (Ullman et al., 2014). LIS thickness is also believed to affect the strength of the AMOC, both through its effect on wind stress in the Atlantic (Arzel et al., 2008) and its meltwater flux volume and direction (Clark et al., 2001; Ullman et al., 2014). Present uncertainties about the thickness of the LIS therefore introduce significant uncertainty into paleoclimate models of the last deglacial period.

**4) Improved Understanding of Ice Margin Dynamics**

Finally, an empirically-based three-dimensional reconstruction of the southeastern LIS would prove useful to ice-sheet modelers. Models used to recreate the decay of the LIS and other LGM ice sheets share many similarities with models designed to predict the future stability of the Greenland and Antarctic ice sheets. However, uncertainties in projection models have led to considerable disagreement in predictions of future sea-level rise (e.g. IPCC, 2013; DeConto and Pollard, 2016; Hansen et al., 2016). A three-dimensional southeastern LIS reconstruction would make it possible to gauge the accuracy of ice-sheet models that are used to simulate past, present, and future ice marginal areas.

Recent geomorphic evidence suggests that the southeastern LIS drained into the Atlantic Ocean through several ice streams, some of which occupied present-day New England and southern Quebec (Margold et al., 2015; Stokes, 2017). Additionally, the ice in this region was almost certainly buttressed by ice shelves that extended into the Atlantic (Stokes, 2017). This makes the southeastern LIS retreat through New England a useful case study for the behavior of complex marginal ice systems such as those in southern Greenland.

## RESEARCH STRATEGY

### Sampling

For this project, our nuclide of choice is $^{10}$Be. As one of the most utilized cosmogenic nuclides in earth surface studies, $^{10}$Be has a low analytical uncertainty, offering precise concentration measurements (Gosse and Phillips, 2001). Additionally, a regional calibration data set has been constructed in the northeastern United States by reconciling $^{10}$Be concentration measurements with independent age constraints (Balco et al., 2009), mainly the $^{14}$C-anchored North American Varve Chronology (Ridge et al., 2012). The $^{10}$Be calibration data set has led to more accurate exposure ages in this region (e.g., Bromley et al., 2015; Koester et al., 2017; Davis et al., 2017).

$^{10}$Be forms primarily in quartz (Gosse and Phillips, 2001), so samples for this project are collected from the upper 2-4 cm of quartz-bearing, glacially-transported boulders or glacially-eroded bedrock. Our attempt to constrain southeastern Laurentide thinning takes advantage of the local topography of the northeastern United States and southern Quebec, with samples being collected from 12 mountains with the greatest vertical relief in their regions (Fig. 4). Sample locations include the highest points in the Green Mountains (Jay Peak, 1177 m; Mt. Mansfield,

1330 m; Killington Mt., 1289 m), the White Mountains (Mt. Washington, 1917 m; Mt. Lafayette, 1600 m), central Maine (Mt. Katahdin, 1606 m; Mt. Bigelow, 1247 m), coastal Maine (Cadillac Mt., 466 m), southern New Hampshire (Mt. Monadnock, 965 m), western Massachusetts (Mount Greylock, 1064 m), eastern Massachusetts (Wachusett, 611 m), southern New York (Catskill Mountains, up to 1277 m), and southern Quebec (Mt. Jacques-Cartier, 1268 m).

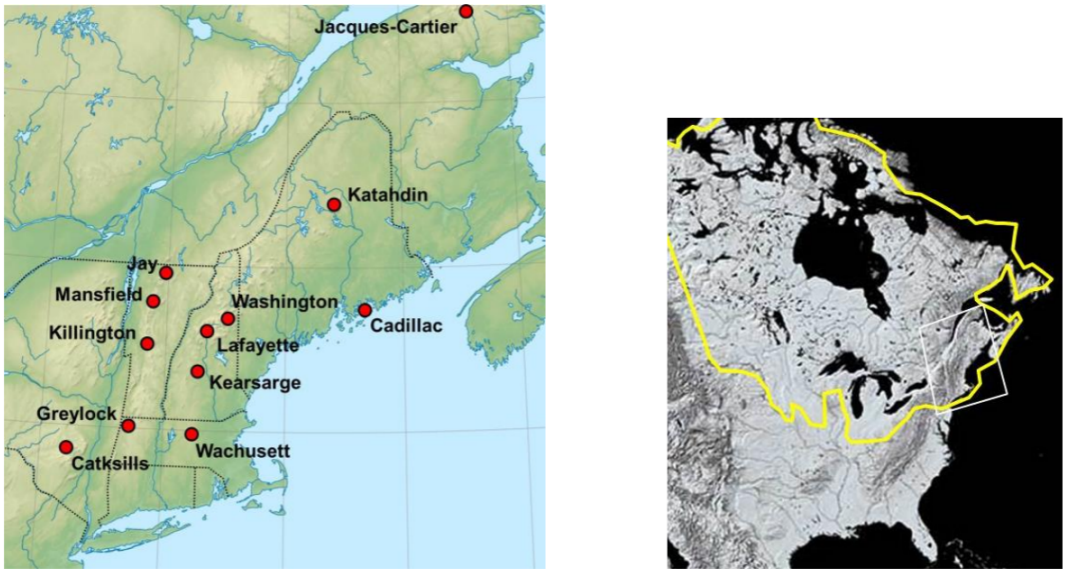


**Figure 5.** Figure from Davis et al. (2017): The locations of 12 ice-sheet mountain dipsticks (red dots) to constrain the thinning history of the southeastern LIS. Note, Mt. Kearsarge has been replaced as a dipstick location by Mt. Monadnock, in southwestern New Hampshire, and Mt. Bigelow, in northwestern Maine, has been added recently. The smaller map shows the LIS outline at the LGM (yellow) and highlights the study region (white box). Note that this region contains the only large mountains underlying interior portions of the LIS, and thus provides a unique opportunity to reconstruct the vertical collapse of the ice sheet.

Nine samples were collected from Mt. Greylock (Fig. 6). MG-01 and -02 were sampled from boulders near the summit composed of the Ordovician phyllite characteristic of the upper reaches of Greylock. MG-03, -04, and -06 were sampled from bedrock quartz veins at 1060, 900, and 780 m a.s.l., respectively. MG-05 and -07 were sampled from boulders at 770 and 900 m a.s.l., respectively, and also seem to be composed of local phyllite. MG-08 and -09 were sampled from large quartzite boulders located on a hillside to the north, across the valley from Mount Greylock, at around 400 m a.s.l.

**Cosmogenic Nuclides**

Terrestrial *in-situ* cosmogenic nuclides are unique isotopes created during nuclear reactions between terrestrial atoms and high energy cosmic rays. They have been used to analyze a variety of surface processes since the development of accelerator mass spectrometry made their detection and measurement possible (Gosse and Phillips, 2001). Davis and Schaeffer (1955) originally noted that rocks continually exposed to cosmic rays become progressively more irradiated at a rate dependent on the cosmic ray flux at that location. They realized that by measuring the present concentration of a (cosmogenic) nuclide in a rock, estimating the nuclide production rate, and accounting for atomic decay if the nuclide is radioactive, the exposure age of that rock could be calculated. Subsequent research revealed that the production rate of *in-situ* cosmogenic nuclides can be affected by a multitude of parameters, including latitude, elevation, and depth below the surface (Lal, 1991). In typical granites and related rocks, the cosmic ray flux attenuates within approximately 2 m of the surface (Gosse and Phillips, 2001), and it is this property that makes cosmogenic nuclides so appealing for glacial chronologies. Warm-based ice, which can move dynamically on a lubricating layer of meltwater at its base, regular erodes more than 2 m of surficial material when advancing, exposing minerals at the surface that were previously shielded from cosmic radiation (Balco,


**Figure 6.** Map of Mount Greylock, surrounding valleys, and sample selection sites. Note: Samples MG-08 and -09 are not pictured, they were sampled on the hill located to the north of Mount Greylock. Stars are locations of field trip stops. Dotted line along Greylock ridge is the optional ~2-mile walk along the Appalachian Trail.

2011). These surficial minerals only begin accumulating cosmogenic nuclides when the overlying ice retreats and exposes them to cosmic rays. Consequently, surface exposure ages from glacially-polished bedrock or glacially-transported boulders generally correspond to the date of ice retreat from that location.

There are, however, cases in which the cosmogenic nuclide concentration in a rock sample does not correspond to a single exposure. If a sample was covered by non-erosive, or cold-based, ice that was frozen to the bed, nuclides from previous exposures may survive glaciation and lead to larger measured concentrations than would be expected due to a single exposure. Conversely, if a sample was covered by till, significant snow accumulation, or relict ice-fields after the retreat of continental ice, there will be a lower nuclide concentration than expected due to partial shielding of the sample. These cases must be considered when analyzing nuclide concentrations.

**Statistical Evaluation of Thinning Time and Rate**

We evaluate the most likely timing and rates of ice thinning at each dipstick location by performing Monte Carlo simulations through the population of exposure age/elevation data points. In each simulation, data points assume a fixed age at random within the bounds of their analytical uncertainty (assuming a Gausian uncertainty distribution), and then a linear regression is run through the resulting absolute age/elevation data points. At least 1000 of these simulations are run, with a filter installed to prevent negative sloping regression lines (indicating thickening ice with time). From these simulations, a population of possible thinning rates and times is generated (Fig. 5; Johnson et al., 2014).

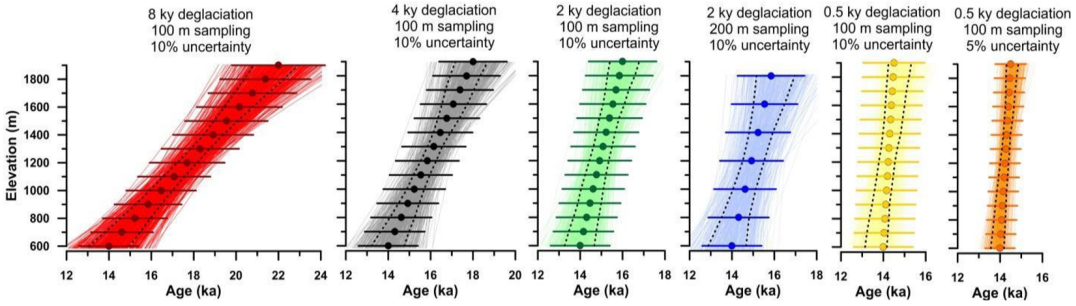


**Figure 7.** Synthetic dipsticks testing sensitivity to deglaciation duration, sampling density, and $^{10}$Be geologic uncertainty typical for cosmogenic datasets. Thin colored lines show 500 Monte Carlo-generated regressions, dotted lines give 68% confidence intervals.

**A New England area grand synthesis**

The ultimate goal of this project is to generate a three-dimensional depiction of statistically-plausible reconstructions for the retreat of the southeastern LIS. One of our project collaborators recently summarized this goal, *"The data we generate will be incorporated into a comprehensive database detailing all extant chronological data from the region – radiocarbon ages (e.g., Dyke, 2004), cosmogenic exposure ages (e.g., Balco et al., 2002; Balco and Schaefer, 2006; Balco et al., 2009; Bromley et al., 2015; Davis et al., 2015; Bierman et al., 2015; Koester et al., 2017; Hall et al., 2017), and varve constraints (Ridge et al., 2012). We envision this reconstruction representing the culmination of decades of glacial geologic work in this data-rich region, with ice volume calculations now possible using the vertical constraints that our cosmogenic exposure age data will provide. This reconstruction will then be compared to offshore marine records, climate records (Fig. 2b), and models to understand the nature of southeastern LIS deglaciation, and infer its possible causes and consequences. Our reconstruction will allow us to estimate New England ice volume losses, which together with a recent reconstruction of the south-central LIS's contribution to deglacial sea-level rise based on ice-sheet models and Gulf of Mexico runoff records (5.5 ± 2.1 m; Wickert et al., 2013), will better constrain the sea-level contribution history of the entire southern part of the LIS."* (Davis et al., 2017).

## INITIAL RESULTS

Of the 84 samples collected for the New England grand synthesis, 42 have been processed and had $^{10}$Be concentrations measured. Of interest to this field trip are exposure ages from samples collected at Mount Greylock (Fig. 6; n = 4) and Peekamoose Mt., in the nearby Catskill mountains of southern NY (Fig. 7; n = 5).

Four exposure ages have been calculated on Mt. Greylock. One of the samples, MG-01, contains more than double the internal uncertainty of any other Greylock sample. This is likely due to the abundance of $K^+$ and $Mg^{2+}$ observed in the sample, which was present even after Be extraction and may have caused slight interferences in AMS ratio measurements. Including 1σ analytical uncertainty, all ages from Mt. Greylock fall between approximately 13-15.5 ka. Monte Carlo dipstick simulations (Fig. 6a) give a 90% confidence interval for simulated thinning rates at Mt. Greylock of 0.06 – 0.41 m yr$^{-1}$ (Fig. 6b), while highest simulated exposure (1060 m asl) occurred at 14.88 ± 1.16 ka (Fig. 6c)

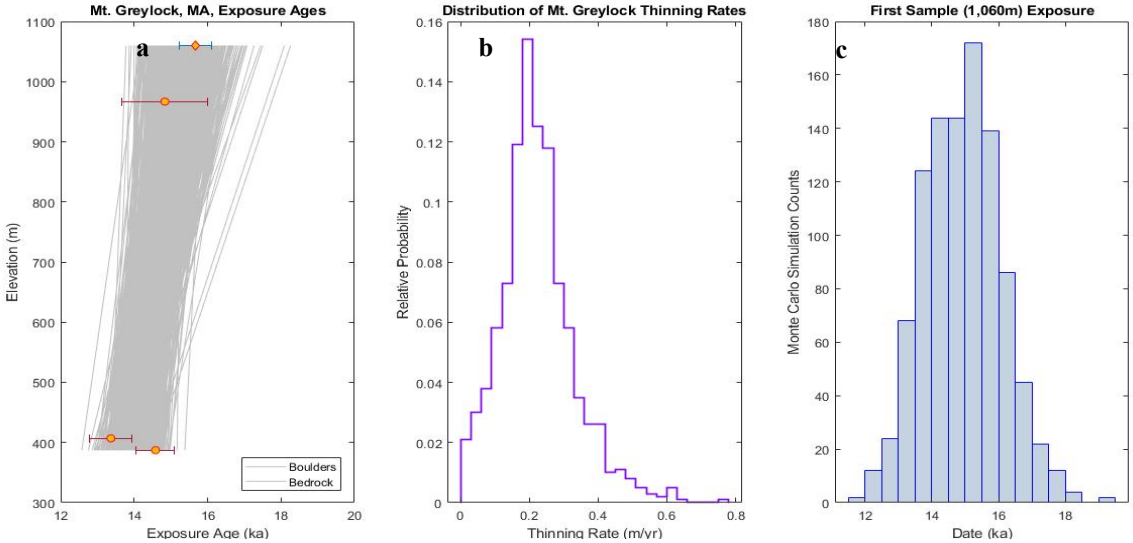


**Figure 8.** Results of Monte Carlo dipstick simulations using exposure ages from Mt. Greylock, MA. (a) Exposure ages with 1σ measurement uncertainties as well as individual Monte Carlo dipstick simulations (gray lines). (b) Probability distribution of simulated thinning rates. (c) Distribution of exposure ages for the highest elevation captured by the Mt. Greylock dipstick

The five processed exposure ages from Peekamoose Mt. are split into two groups that do not overlap within 1σ analytical uncertainty. Higher elevation ages range from 19.8-18.6 ka, while lower elevation samples have ages between 17.2-18.5 ka. Monte Carlo dipstick simulations (Fig. 7a) give a 90% confidence interval ($5^{th}$ – $95^{th}$ percentiles) for the LIS thinning rate in the Catskills of 0.09 – 0.22 m $yr^{-1}$, with a right-skewed distribution that allows for the possibility of much higher thinning rates (Fig. 7b). In addition, the highest elevation simulated, 1170 m asl, was first exposed at 19.46 ± 0.41 ka (Fig. 7c)

The exposure ages from Mount Greylock and Peekamoose Mt. agree within 1σ external uncertainty with the suggested ice retreat in the Connecticut River Valley given by the North American Varve Chronology (Fig. 4; Ridge et al., 2012).

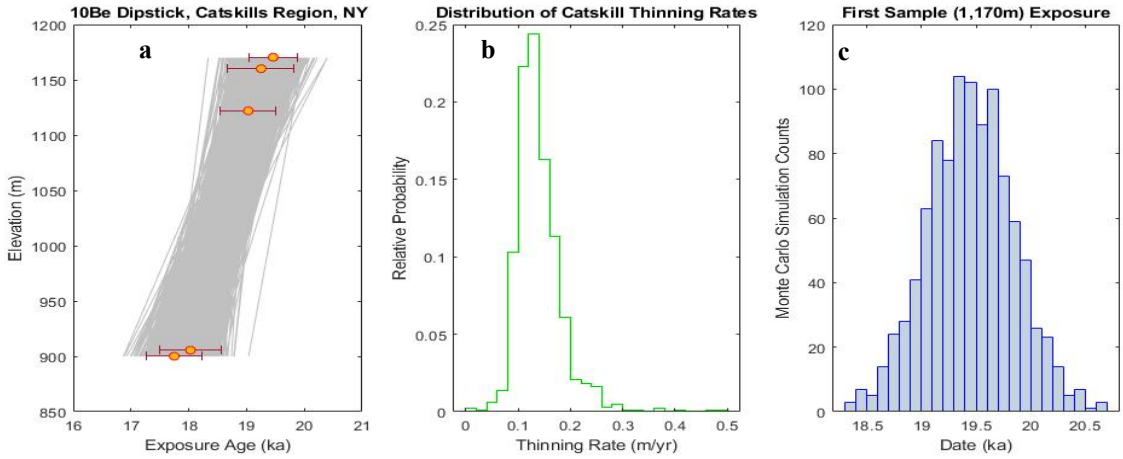


**Figure 9.** Results of Monte Carlo dipstick simulations using exposure ages from the Catskill Mountains, NY. (a) Exposure ages with 1σ measurement uncertainties as well as individual Monte Carlo dipstick simulations (gray lines). (b) Probability distribution of simulated thinning rates. (c) Distribution of exposure ages for the highest elevation captured by the Catskills dipstick.

## DISCUSSION

Together, the exposure ages from Peekamoose Mt. and Mount Greylock provide evidence for southeastern LIS thinning during the Oldest Dryas. This evidence supports the hypothesis of Denton et al. (2005, 2010) that the cold average annual temperatures recorded in Greenland ice cores during the Oldest Dryas were a consequence of extreme seasonality in the North Atlantic, caused primarily by a substantial increase in sea-ice extent during winter. In fact, Buizert et al. (2014) estimated that North Atlantic summer temperatures during the Oldest Dryas may have only been about 8˚C colder than today. Our thinning evidence suggests that summer temperatures in the North Atlantic during the Oldest Dryas were high enough to sustain ablation of the southeastern LIS margin. Additionally, the LIS thinning captured by the Peekamoose Mt. dipstick entirely pre-dates Heinrich Event I (~16 ka; Shaw et al., 2006), indicating that the thinning was not due to drawdown resulting from this ice streaming event. A sustained southeastern LIS thinning during the Oldest Dryas supports the argument of Clark et al. (2001) that the direction and strength of the LIS meltwater flux modulated the strength of the AMOC during the last deglaciation. Southeastern LIS thinning would have had a suppressing effect on the AMOC, and proxy data indicates a suppressed AMOC for over 4-kyr during the Oldest Dryas (McManus et al., 2004).

Despite their locations within 1˚ latitude, samples from Peekamoose Mt. and Mount Greylock appear to capture two different stages of LIS thinning. While Monte Carlo simulations suggest that the lowest sample on Peekamoose Mt. (~900 m a.s.l.) may have been exposed around the same time as the highest Mount Greylock sample (~1050 m a.s.l.), >90% of the simulations have the entirety of the Peekamoose Mt. dipstick exposed at least a thousand years earlier than the highest Mount Greylock sample. This pattern agrees with other New England deglacial chronologies, which suggest that ice retreated slowly during the Oldest Dryas, taking about 2-kyr to retreat northward through Massachusetts (Fig. 4; Ridge et al., 2012). Samples from lower elevations on Peekamoose Mt. might reveal a more extended thinning history, but it is entirely plausible that the mountain was exposed down to 900 m a.s.l. before the summit of Mount Greylock (~1050 m a.s.l.) was exposed from underneath the LIS. The proximity of these two sites combined with the apparent lag of exposure could indicate that the southeastern LIS margin was steeply sloped during its retreat.

With our presently available data, definitive conclusions on the LIS thinning rate at Peekamoose Mt. and Mount Greylock cannot be made, but general statements are offered here. All but two of the samples processed from Mount Greylock have overlapping exposure ages (within 1σ analytical uncertainty), preventing the exclusion of extremely rapid thinning (>1 m/yr). Evidence of rapid LIS thinning has been noted by our project collaborators in coastal Maine (Koester et al., 2017), central Maine (Davis et al., 2015), and the Presidential Range of New Hampshire (Davis et al., 2017). The exposure ages from Peekamoose Mt. suggest a slower thinning rate (<1 m/yr), but again, more data is needed to make conclusive statements.

## ROAD AND TRAIL LOGS

### Time, Place, Logistics

**START TIME AND LOCATION:** Trip begins on Sunday, October 14th, at 9:00 AM outside the Mount Greylock State Reservation Visitor Center located at 30 Rockwell Rd, Lanesborough, MA 01237. The drive to the Visitor Center is about 2 hours from Lake George, NY, and parking and restroom facilities are available.

**DESCRIPTION:** This field trip will begin at the Mount Greylock Visitor Center with a brief introduction to the geologic history of the area, focused primarily on surficial geomorphology and the influence of continental glaciation on Mount Greylock and adjacent valleys. While at the Visitor Center we will try to consolidate vehicles. We will then drive up Rockwell Rd towards the summit, making a detour down Sperry Road to Stony Ledge, a lookout point that offers magnificent views of Mount Greylock. This is one of the few close-up vantage points to view “The Hopper”, the most southerly glacial cirque in New England. More discussion about the influence of glaciation on Mount Greylock will occur here, and field trip participants are encouraged to (carefully) explore Stony Ledge for glacial striations in the exposed bedrock. Following the stop at Stony Ledge, we will return to Rockwell Rd and continue up to the summit. At the summit, trip participants can take advantage of the Bascom Lodge, which has restroom facilities, food and drinks for purchase, a clean water spigot, and information about the surrounding area. At the summit, we will go over a more in-depth review of local and regional geomorphology, with an emphasis on the Laurentide Ice Sheet and its behavior as it overrode and then retreated past Mount Greylock. We will also

briefly discuss the motivations and approach of an NSF-funded research project to constrain the timing and rate of ice thinning in the northeastern United States and point out one of the sample locations on the summit. Weather permitting, interested trip participants are invited to then take a ~2 mile walk north on the historic Appalachian Trail to Mt. Williams, a part of the Greylock ridgeline. Along the way, we will point out other samples for the ice-thinning project and the lead author (a hiking fanatic) will discuss some of the history of the Appalachian Trail and early exploration in the area. For those not participating in the Appalachian Trail walk, the field trip will end by approximately 1 pm. For those participating in the walk, the trip should end by around 3 pm.

**Road Mileage**

0.0 Begin at Mount Greylock State Reservation Visitor Center (30 Rockwell Rd, Lanesborough, MA)

5.5 Take left turn off Rockwell Rd onto Sperry Rd

7.1 **STOP 1.** Park at Stoney Ledge. Sperry Rd makes a loop here, please find parking off the road. Stoney Ledge offers fantastic views of Mount Greylock and The Hopper, a glacial cirque on Greylock's west flank. Exposed bedrock offers the potential to investigate glacial striations!

8.7 After driving back down Sperry Rd, take a left turn back on to Rockwell Rd, heading towards the summit

10.2 Rockwell Rd. joins North Adams Rd, continue right towards summit

11.0 **STOP 2.** Arrive at Mount Greylock summit. Park in designated parking lot and meet outside Bascom Lodge. Bascom Lodge provides restrooms, food for purchase, and free clean drinking water. An in-depth discussion of regional glacial geomorphology, the chronology of the Laurentide Ice Sheet in the area, and the motivations and preliminary results of an NSF-funded ice sheet reconstruction project will take place here. For those not participating in the walk on the Appalachian Trail, the summit marks the end of the trip. Auto roads depart the summit to the north and south (we will drive up the southern road), please drive carefully!

**Trail Mileage for walk along Appalachian Trail**

0.0 Start walk at Mount Greylock summit.

0.25 **STOP 1.** Briefly examine two glacially-transported boulders deposited on the Greylock ridgeline. These boulders were sampled for the NSF dipstick project.

2.2 **STOP 2.** Mt. Williams summit. This is not truly a separate mountain, as it is part of the Greylock ridgeline, but it is a local high-point that offers fantastic views of the surrounding area. Two samples were collected at this location for the NSF dipstick project, one bedrock and one boulder. From here, trip participants can choose to either return via the AT to the Greylock summit or continue down the AT for another half mile, eventually meeting the northern Greylock auto road (Notch Rd). The trip leader will arrange to have a van meet at Notch Rd and transport participants back up to the summit, although participants are welcome to arrange their own transport if desired.

**End of trip; thank you**

**REFERENCES CITED**

Abe-Ouchi, A., Saito, F., Kawamura, K., Raymo, M.E., Okuno, J.i., Takahashi, K., Blatter, H., 2013. Insolationdriven 100,000-year glacial cycles and hysteresis of ice-sheet volume. Nature 500, 190-193.

Abe-Ouchi, A., Saito, F., Kageyama, M., et al., 2015, Ice-sheet configuration in the CMIP5/PMIP3 Last Glacial Maximum experiments: Geoscientific Model Development, v. 8, no. 11, p. 3621-3637.

Abe-Ouchi, A., Segawa, T., and Saito, F., 2007, Climatic Conditions for modelling the Northern Hemisphere ice sheets throughout the ice age cycle: Climate of the Past, v. 3, no. 3, p. 423-438.

Ackert, R.P., Mukhopadhyay, S., Parizek, B.R., Borns, H.W., 2007. Ice elevation near the West Antarctic Ice Sheet divide during the Last Glaciation. Geophysical Research Letters 34, L21506.

Applegate, P.J., Kirchner, N., Stone, E.J., Keller, K., and Greve, R., 2012, An assessment of key model parametric uncertainties in projections of Greenland Ice Sheet behavior: The Cryosphere, v. 6, no. 3, p. 589-606.

Arzel, O., England, M.H., and Sijp, W.P., 2008, Reduced Stability of the Atlantic Meridional Overturning Circulation due to Wind Stress Feedback during Glacial Times: Journal of Climate, v. 21, no. 23, p. 6260-6282.

Balco, G., Briner, J., Finkel, R.C., Rayburn, J.A., Ridge, J.C., Schaefer, J.M., 2009. Regional beryllium-10 production rate calibration for late-glacial northeastern North America. Quaternary Geochronology 4, 93–107. doi:10.1016/j.quageo.2008.09.001

Balco, G., Schaefer, J.M., 2006. Cosmogenic-nuclide and varve chronologies for the deglaciation of southern New England. Quaternary Geochronology 1, 15–28. doi:10.1016/j.quageo.2006.06.014

Balco, G., Stone, J.O., Porter, S.C., Caffee, M.W., 2002. Cosmogenic-nuclide ages for New England coastal moraines, Martha's Vineyard and Cape Cod, Massachusetts, USA. Quaternary Science Reviews 21, 2127–2135. doi:10.1016/S0277-3791(02)00085-9

Barron, E., and Pollard, D., 2002, High-Resolution Climate Simulations of Oxygen Isotope Stage 3 in Europe: Quaternary Research, v. 58, no. 3, p. 296-309.

Bierman, P., 2007. Cosmogenic glacial dating, 20 years and counting. Geology 35, 575-576.

Bierman, P.R., Davis, P.T., Corbett, L.B., Lifton, N.A., Finkel, R.C., 2015. Cold-based Laurentide ice covered New England's highest summits during the Last Glacial Maximum. Geology 43, 1059–1062. doi:10.1130/G37225.1

Bierman, P.R., and Dethier, D., 1986. Lake Bascom and the deglaciation of Northwestern Massachusetts. Northeastern Geology, v. 8, p. 32-43.

Briner, J.P., Miller, G.H., Davis, P.T., Bierman, P.R., Caffee, M., 2003. Last Glacial Maximum ice sheet dynamics in Arctic Canada inferred from young erratics perched on ancient tors. Quaternary Science Reviews 22 (5-7), 437–444.

Broecker, W.S., 2006, Abrupt climate change revisited: Global and Planetary Change, v. 54, no. 3, p. 211-215.

Broecker, W.S., Kennett, J.P., Flower, B.P., Teller, J.T., Trumbore, S., Bonani, G., Wolfli, W., 1989. Routing of meltwater from the Laurentide ice sheet during the Younger Dryas cold episode. Nature 341, 318-321.

Broecker, W.S., Peteet, D.M., and Rind, D., 1985, Does the ocean-atmosphere system have more than one stable mode of operation? Nature, v. 315, no. 6014, p. 21-26.

Bromley, G., Hall, B.L., Thompson, W.B., Kaplan, M.R., Garcia, J.L., Schaefer, J.M., 2015. Late glacial fluctuations of the Laurentide Ice Sheet in the White Mountains of Maine and New Hampshire, U.S.A. Quaternary Research 83(3), 522-530. doi: 10.1016/j.yqres.2015.02.004

Bromwich, D.H., Toracinta, Helin Wei, H., Oglesby, R.J., Fastook, J.L., and Hughes, T.J., 2004, Polar MM5 Simulations of the Winter Climate of the Laurentide Ice Sheet at the LGM: Journal of Climate, v. 17, no. 17, p. 3415-3433.

Buizert, C., Gkinis, V., Severinghaus, J.P., et al., 2014, Greenland temperature response to climate forcing during the last deglaciation: Science, v. 345, no. 6201, p. 1177-1180.

Carlson, A.E., 2009. Geochemical constraints on the Laurentide Ice Sheet contribution to Meltwater Pulse 1A. Quaternary Science Reviews 28, 1625-1630.

Carlson, A.E., Clark, P.U., 2012. Ice sheet sources of sea level rise and freshwater discharge during the last deglaciation. Reviews of Geophysics 50, RG4007. doi: 10.1029/2011RG000371

Carlson, A.E., and Winsor, K., 2012, Northern Hemisphere ice-sheet responses to past climate warming: Nature Geoscience, v. 5, no. 9, p. 607.

Clark, P.U., Alley, R.B., Pollard, D., 1999. Northern hemisphere ice-sheet influences on global climate change. Science 286, 1104-1111.

Clark, P.U., Alley, R.B., Keigwin, L.D., Licciardi, J.M., Johnsen, S.J., Wang, H., 1996. Origin of the first global meltwater pulse following the Last Glacial Maximum. Paleoceanography. doi:10.1029/96PA01419

Clark, P.U., McCabe, A.M., Mix, A.C., and Weaver, A.J., 2004, Rapid Rise of Sea Level 19,000 Years Ago and Its Global Implications: Science, v. 304, no. 5674, p. 1141-1144.

Clark, P.U., Dyke, A.S., Shakun, J.D., Carlson, A.E., Clark, J., Wohlfarth, B., Mitrovica, J.X., Hostetler, S.W., McCabe, A M., 2009. The Last Glacial Maximum. Science 325, 710–714. doi:10.1126/science.1172873

Clark, P.U., Mitrovica, J.X., Milne, G.A., and Tamisiea, M.E., 2002, Sea-Level Fingerprinting as a Direct Test for the Source of Global Meltwater Pulse IA: Science, v. 295, no. 5564, p. 2438-2441.

Clark, P.U., Tarasov, L., 2014. Closing the sea level budget at the Last Glacial Maximum. Proceedings of the National Academy of Sciences 111, 15861-15862.

Clark, P.U., Marshall, S.J., Clarke, G.K.C., Hostetler, S.W., Licciardi, J.M., and Teller, J.T., 2001, Freshwater Forcing of Abrupt Climate Change During the Last Glaciation: Science, v. 293, no. 5528, p. 283-287.

Clark, P.U., Shakun, J.D., Baker, P.A., et al., 2012, Global climate evolution during the last deglaciation: Proceedings of the National Academy of Sciences, v. 109, no. 19, p. E1134.

Corbett, L.B., Bierman, P.R., Stone, B.D., Caffee, M.W., 2017. Cosmogenic nuclide age estimates for Laurentide Ice Sheet recession from the terminal moraine, New Jersey, USA, and constraints on Latest Pleistocene ice sheet behavior: Quaternary Research 87(3), 482-498. https://doi.org/10.1017/qua.2017.11

Corbett, L.B., Young, N.E., Bierman, P.R., Briner, J.P., Neumann, T.A., Rood, D.H., Graly, J.A., 2011. Paired bedrock and boulder 10Be concentrations resulting from early Holocene ice retreat near Jakobshavn Isfjord, western Greenland. Quaternary Science Reviews 30, 1739-1749.

Dansgaard, W., Johnsen, S.J., Clausen, H.B., Dahl-Jensen, D., Gundestrup, N.S., Hammer, C.U., Hvidberg, C.S., Steffensen, J.P., Sveinbjörnsdottir, A.E., Jouzel, J. and Bond, G., 1993. Evidence for general instability of past climate from a 250-kyr ice-core record. *Nature*, *364*(6434), p.218.

Davis, P.T., Bierman, P.R., Corbett, L.B., Finkel, R.C., 2015. Cosmogenic exposure age evidence for rapid Laurentide deglaciation of the Katahdin area, west-central Maine, USA, 16 to 15 ka. Quaternary Science Reviews 116, 95–105. doi:10.1016/j.quascirev.2015.03.021

Davis, P.T., Davis, R.B., 1980. Interpretation of minimum-limiting radiocarbon ages for deglaciation of Mount Katahdin area, Maine. Geology 8, 396-400. doi: 10.1130/0091-7613(1980)8<396:IOMRDF>2.0.CO;2

Davis, P.T., Koester, A.J., Shakun, J.D., Bierman, P.R., and Corbett, L.B., 2017. Applying the Cosmogenic Nuclide Dipstick Model for Deglaciation of Mt. Washington in Johnson, B., and Eusden, J.D., ed., Guidebook for Field Trips in Western Maine and Northern New Hampshire: New England Intercollegiate Geological Conference, Bates College, p. 247-272. https://doi.org/10.26780/2017.001.0014

Davis, R., and Schaeffer, O., 1955, Chlorine-36 in nature: Annals of the New York Academy of Sciences, v. 62, no. 1, p. 107-121.

Denton, G.H., Alley, R.B., Comer, G.C., Broecker, W.S., 2005. The role of seasonality in abrupt climate change. Quaternary Science Reviews 24, 1159-1182.

Denton, G.H., Anderson, R.F., Toggweiler, J.R., Edwards, R.L., Schaefer, J.M., and Putnam, A.E., 2010, The Last Glacial Termination: Science (Washington), v. 328, no. 5986, p. 1650.

DeConto, R.M., and Pollard, D., 2016, Contribution of Antarctica to past and future sea-level rise: Nature, v. 531, no. 7596, p. 591.

Deschamps, P., Durand, N., Bard, E., Hamelin, B., Camoin, G., Thomas, A.L., Henderson, G.M., Okuno, J.I., Yokoyama, Y., 2012. Ice-sheet collapse and sea-level rise at the Bølling warming 14,600 years ago. Nature 483, 559–564. doi:10.1038/nature10902

Dyke, A., 2004. An outline of North American Deglaciation with emphasis on central and northern Canada, in: Ehlers, J., Gibbard, P. (Eds.), Quaternary Glaciations: Extent and Chronology. Elsevier, Amsterdam, pp. 373424.

Dyke, A.S., Moore, A., and Robertson, L., 2003. Deglaciation of North America. Geological Survey of Canada Open File, 1574. Thirty-two digital maps at 1:7,000,000 scale with accompanying digital chronological database and one poster (two sheets) with full map series

Fairbanks, R.G., 1989. A 17,000-year glacio-eustatic sea level record: Influence of glacial melting rates on the Younger Dryas event and deep-ocean circulation. Nature 342, 637–642. doi:10.1038/nrd2468

Goehring, B.M., Brook, E.J., Linge, H., Raisbeck, G.M., Yiou, F., 2008. Beryllium-10 exposure ages of erratic boulders in southern Norway and implications for the history of the Fennoscandian Ice Sheet. Quaternary Science Reviews 27, 320-336.

Gosse, J.C., Phillips, F.M., 2001. Terrestrial in situ cosmogenic nuclides: theory and application. Quaternary Science Reviews 20, 1475–1560. doi:10.1016/S0277-3791(00)00171-2

Gregoire, L.J., Payne, A.J., Valdes, P.J., 2012. Deglacial rapid sea level rises caused by ice-sheet saddle collapses. Nature 487, 219-222.

Hall, B.L., Borns, H.W., Jr., Bromley, G.R.M., Lowell, T.V., 2017. Age of Pineo Ridge system: Implications for behavior of the Laurentide Ice Sheet in eastern Maine, U.S.A., during the last deglaciation. Quaternary Science Reviews 169, 344-356. http://dx.doi.org/10.1016/j.quascirev.2017.06.001

Hansen, J., Sato, M., Hearty, P., et al., 2016, Ice melt, sea level rise and superstorms: evidence from paleoclimate data, climate modeling, and modern observations that 2 °C global warming could be dangerous: Atmospheric Chemistry and Physics, v. 16, no. 6, p. 3761-3812.

He, F., Shakun, J.D., Clark, P.U., Carlson, A.E., Liu, Z., Otto-Bliesner, B.L., Kutzbach, J.E., 2013. Northern Hemisphere forcing of Southern Hemisphere climate during the last deglaciation. Nature 494, 81-85.

Johnsen, S.J., Dahl-Jensen, D., Gundestrup, N., et al., 2001, Oxygen isotope and palaeotemperature records from six Greenland ice-core stations: Camp Century, Dye-3, GRIP, GISP2, Renland and NorthGRIP: Journal of Quaternary Science, v. 16, no. 4, p. 299-307.

Johnson, J.S., Bentley, M.J., Smith, J. A, Finkel, R.C., Rood, D.H., Gohl, K., Balco, G., Larter, R.D., Schaefer, J.M., 2014. Rapid thinning of Pine Island Glacier in the early Holocene. Science 343, 999–1001. doi:10.1126/science.1247385

Keigwin, L.D., Klotsko, S., Zhao, N., Reilly, B., Giosan, L., and Driscoll, N.S., 2018. Deglacial floods in the Beaufort Sea preceded Younger Dryas cooling. Nature Geoscience 11, p. 599-604.

Kleman, J., and Applegate, P.J., 2014, Durations and propagation patterns of ice sheet instability events: Quaternary Science Reviews, v. 92, p. 32-39.

Koester, A.J., Shakun, J.D., Bierman, P.R., Davis, P.T., Corbett, L.B., Braun, D., and Zimmerman, S.R., 2017. Rapid thinning of the Laurentide Ice Sheet in coastal Maine, USA, during late Heinrich Stadial 1. Quaternary Science Reviews 163, 1-13. http://dx.doi.org/10.1016/j.quascirev.2017.03.005

Lal, D., 1991. Cosmic ray labeling of erosional surfaces: in situ nuclide production rates and erosion models. Earth and Planetary Science Letters, v. 104, p. 424-439.

Lambeck, K., Rouby, H., Purcell, A., Sun, Y., Sambridge, M., 2014. Sea level and global ice volumes from the Last Glacial Maximum to the Holocene. Proceedings of the National Academy of Sciences 111 (43), 15296-15303. doi: 10.1073/pnas.1411762111

Langen, P., and Vinther, B., 2009, Response in atmospheric circulation and sources of Greenland precipitation to glacial boundary conditions: Climate Dynamics, v. 32, no. 7, p. 1035-1054.

Liu, J., Milne, G.A., Kopp, R.E., Clark, P.U., Shennan, I., 2016. Sea-level constraints on the amplitude and source distribution of Meltwater Pulse 1A. Nature Geoscience 9(2), 130-134. http://dx.doi.org:10.1038/ngeo2616

Liu, Z., Otto-Bliesner, B.L., He, F., Brady, E.C., Tomas, R., Clark, P.U., Carlson, A.E., Lynch-Stieglitz, J., Curry, W., Brook, E., Erickson, D., Jacob, R., Kutzbach, J., Cheng, J., 2009. Transient simulation of last deglaciation with a new mechanism for Bolling-Allerod warming. Science 325, 310-314.

Mackintosh, A., Golledge, N., Domack, E., Dunbar, R., Leventer, A., White, D., Pollard, D., DeConto, R., Fink, D., Zwartz, D., Gore, D., Lavoie, C., 2011. Retreat of the East Antarctic ice sheet during the last glacial termination. Nature Geoscience 4, 195-202.

Margold, M., Stokes, C.R., Clark, C.D., and Kleman, J., 2015, Ice streams in the Laurentide Ice Sheet: a new mapping inventory: Journal of Maps, v. 11, no. 3, p. 380-395.

McManus, J.F., Francois, R., Gherardi, J.M., Keigwin, L.D., Brown-Leger, S., 2004. Collapse and rapid resumption of Atlantic meridional circulation linked to deglacial climate changes. Nature 428, 834-837.

NGRIP Members, 2004. High-resolution record of Northern Hemisphere climate extending into the last interglacial period. Nature 431, 147-151.

Obbink, E.A., Carlson, A.E., Klinkhammer, G.P., 2010. Eastern North American freshwater discharge during the Bolling-Allerod warm periods. Geology 38, 171-174.

Peltier, W.R., 2005. On the hemispheric origins of meltwater pulse 1a. Quaternary Science Reviews 24, 1655–1671. doi:10.1016/j.quascirev.2004.06.023

Peltier, W.R., Argus, D.F., Drummond, R., 2015. Space geodesy constrains ice age terminal deglaciation: The global ICE-6G_C (VM5a) model. Journal of Geophysical Research: Solid Earth 120, 450-487.

Ratcliffe, N.M., Potter, D.B., and Stanley, R.S., 1993, Bedrock Geologic Map of the Williamstown and North Adams Quadrangles, Massachusetts and Vermont, and Part of the Cheshire Quadrangle, Massachusetts: US Geological survey.

Ridge, J.C., Balco, G., Bayless, R.L., Beck, C.C., Carter, L.B., Dean, J.L., Voytek, E.B., Wei, J.H., 2012. The new North American Varve Chronology: A precise record of southeastern Laurentide Ice Sheet deglaciation and climate, 18.2-12.5 kyr BP, and correlations with Greenland ice core records. American Journal of Science 312, 685-722. doi: 10.2475/07.2012.01

Rogers, J.N., 2003. Major Holocene debris flows of Franconia Notch (White Mountains, New Hampshire) recorded in Profile Lake. University of Massachusetts, Amherst, p. 140.

Shakun, J.D., Clark, P.U., He, F., Marcott, S.A., Mix, A.C., Liu, Z., Otto-Bliesner, B., Schmittner, A., Bard, E., 2012. Global warming preceded by increasing carbon dioxide concentrations during the last deglaciation. Nature 484, 49-54.

Shaw, J., Piper, D.J.W., Fader, G.B.J., King, E.L., Todd, B.J., Bell, T., Batterson, M.J., Liverman, D.G.E., 2006. A conceptual model of the deglaciation of Atlantic Canada. Quaternary Science Reviews 25, 2059-2081.

Spear, R.W., 1989. Late Quaternary history of high-elevation vegetation in the White Mountains of New Hampshire. Ecological Monographs 59 (2), 125-151.

Spear, R.W., Davis, M.B., Shane, L.C.K., 1994. Late Quaternary history of low-and mid-elevation vegetation in the White Mountains of New Hampshire. Ecological Monographs 64 (1), 85-109.

Stocker, T.F., et al. (editors), 2014, Climate change: the physical science basis : Working Group I contribution to the Fifth assessment report of the Intergovernmental Panel on Climate Change: New York, Cambridge University Press.

Stokes, C.R., 2017, Deglaciation of the Laurentide Ice Sheet from the Last Glacial Maximum: Geographical Research Letters, v. 43, no. 2, p. 377-428.

Stokes, C.R., Margold, M., Clark, C.D., and Tarasov, L., 2016, Ice stream activity scaled to ice sheet volume during Laurentide Ice Sheet deglaciation: Nature, v. 530, no. 7590, p. 322.

Stokes, C.R., Tarasov, L., Blomdin, R., Cronin, T.M., Fisher, T.G., Gyllencreutz, R., Hättestrand, C., Heyman, J., Hindmarsh, R.C.A., Hughes, A.L.C., Jakobsson, M., Kirchner, N., Livingstone, S.J., Margold, M., Murton, J.B., Noormets, R., Peltier, W.R., Peteet, D.M., Piper, D.J.W., Preusser, F., Renssen, H., Roberts, D.H., Roche, D.M., Saint-Ange, F., Stroeven, A.P., Teller, J.T., 2015. On the reconstruction of palaeo-ice sheets: Recent advances and future challenges. Quaternary Science Reviews 125, 15-49.

Stone, J.O., Balco, G.A., Sugden, D.E., Caffee, M.W., Sass III, L.C., Cowdery, S.G., Siddoway, C., 2003. Holocene Deglaciation of Marie Byrd Land, West Antarctica. Science 299, 99-102.

Sugden, D.E., 1978, Glacial Erosion by the Laurentide Ice Sheet: Journal of Glaciology, v. 20, no. 83, p. 367-391.

Tarasov, L., and Peltier, W.R., 2005. Arctic freshwater forcing of the Younger Dryas cold reversal. Nature 435(7042), p. 662.

Thornalley, D.J.R., Elderfield, H., and McCave, I.N., 2010, Reconstructing North Atlantic deglacial surface hydrography and its link to the Atlantic overturning circulation: Global and Planetary Change, v. 79, no. 3, p. 163-175.

Ullman, D.J., LeGrande, A.N., Carlson, A.E., Anslow, F.S., Licciardi, J.M., 2014. Assessing the impact of Laurentide Ice Sheet topography on glacial climate. Climate of the Past 10, 487-507.

Ullman, D.J., Carlson, A.E., Anslow, F.S., Legrande, A.N., and Licciardi, J.M., 2015, Laurentide ice-sheet instability during the last deglaciation: Nature Geoscience, v. 8, no. 7, p. 534

Weaver, A.J., Saenko, O., Clark, P.U., Mitrovica, J.X., 2003. Meltwater pulse 1A from Antarctica as a trigger of the Bølling-Allerød warm interval. Science 299, 1709–1713. doi:10.1126/science.1081002

Weber, M.E., Clark, P.U., Kuhn, G., Timmermann, A., Sprenk, D., Gladstone, R., Zhang, X., Lohmann, G., Menviel, L., Chikamoto, M.O., Friedrich, T., Ohlwein, C., 2014. Millennial-scale variability in Antarctic icesheet discharge during the last deglaciation. Nature 510, 134-138.

Wickert, A.D., Mitrovica, J.X., Williams, C., Anderson, R.S., 2013. Gradual demise of a thin southern Laurentide ice sheet recorded by Mississippi drainage. Nature 502, 668-671.

# HEAVY METAL CONTAMINATION FROM ILLEGAL BURN PILES IN AN ECOLOGICALLY SENSITIVE SITE IN WEST HAVEN, VERMONT

By

Helen Mango[1], Department of Natural Sciences, Castleton University, Castleton, VT 05735
Mary Droege[2], Department of Natural Sciences, Castleton University, Castleton, VT 05735
J. Murray McHugh[3], The Nature Conservancy, Southern Vermont Office, 348 Bentley Ave., Poultney, VT 05764
Michele Hluchy[4], Geology and Environmental Studies, Alfred University, Alfred, NY 14802
Email addresses: [1]helen.mango@castleton.edu, [2]mary.droege@castleton.edu, [3]mmchugh@tnc.org, [4]fhluchy@alfred.edu

## INTRODUCTION

The Nature Conservancy owns and manages the Helen W. Buckner Memorial Preserve in West Haven, Vermont. The 3827-acre preserve has one of the highest levels of biodiversity in the state. It is located on the border of New York State, bounded on the south by the Poultney River and on the west by the South Bay of Lake Champlain (Fig. 1). It is an environmentally sensitive and important tract of land, providing habitat for eleven rare/uncommon animal species (including the timber rattlesnake), eighteen rare/uncommon plant species, and ten rare/uncommon natural community types. It encompasses undeveloped lake shoreline, wetlands along the river, floodplain, Clayplain and upland forest, marshes, and cliffs. It includes Austin Hill, composed of Precambrian (Middle Mesoproterozoic) Adirondack biotite tonalite gneiss, and bounded on the west by Cambrian/Ordovician dolostone and quartzite (Fisher, 1984; Ratcliffe et al., 2011).

Illegally dumped and burned garbage piles have existed for years on the access road (Galick Road) along a stretch of the Poultney River. Analysis of ash and soil samples from different burn piles over several years shows elevated levels of many contaminants, including arsenic, copper, lead, zinc, chromium and cobalt, often exceeding background levels by orders of magnitude. The area is seasonally flooded, resulting in both erosion and deposition. As a result of our research, the Vermont Department of Environmental Conservation (DEC) remediated the most contaminated site and installed a parking area and boat launch (allowing for patrol by state law enforcement). However, dumped and burned garbage continues to be a problem at this site.

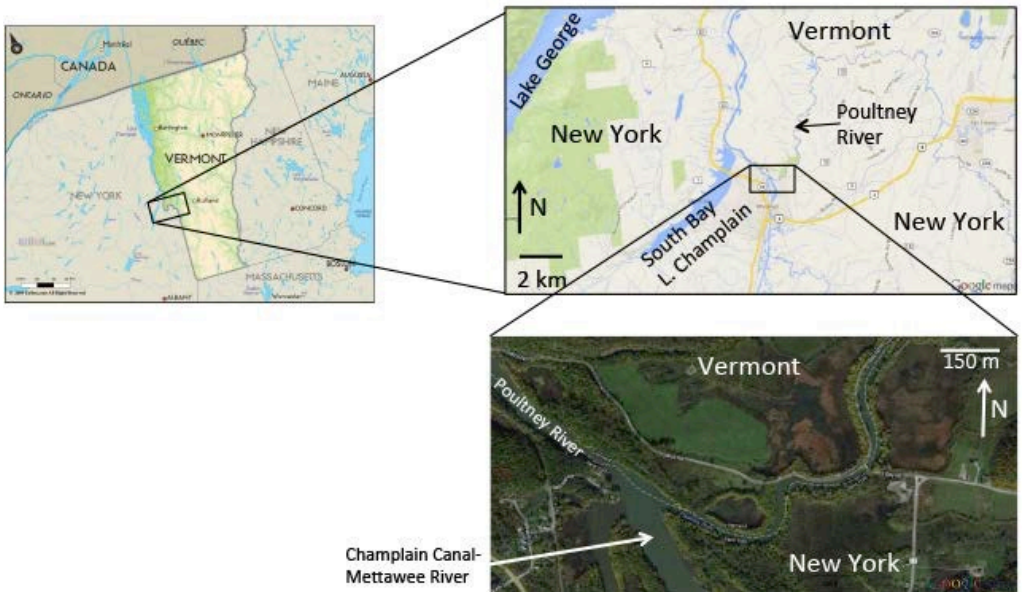


Figure 1. Location maps of the field trip site.

## BURN PILE LOCATION AND CONTENTS

Between 2011 and 2017, burn piles at four different locations along Galick Road were sampled and the samples analyzed for a number of elements. Some burn pile sites were sampled multiple times over the years. The location of the burn piles, and the location where "background" samples were taken, are shown in Figure 2.

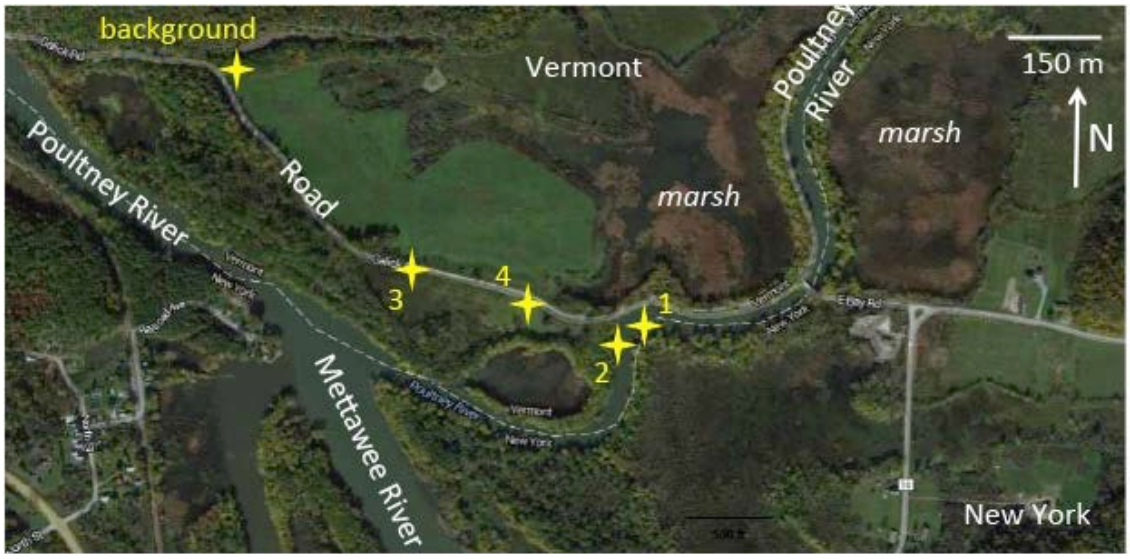


Figure 2. Location of different burn piles and background sampling site.

Sampling and analysis of burn piles began with one grab sample of Burn Pile 1 in 2011. This pile appeared to undergo the most dumping and burning of all the burn piles over the years. Burn Pile 2 was closer to the water's edge, and so was periodically flooded. Burn Piles 3 and 4 were located farther away from where people would congregate, and only appeared to be "active" in 2013. The materials dumped over the years included household trash (from diapers to batteries), junked furniture, construction debris, and commercial waste. There was also refuse related to the bonfires, predominantly beer cans. Table 1 lists the items found over the years of sampling.

Table 1. Burn pile items

| | |
|---|---|
| Particle board, plywood | Window blinds |
| Lumber, wallboard | Cardboard |
| Electronics | Plastic (e.g. tubing, CDs, packaging, PVC) |
| Batteries | Metals (e.g. nails, food storage cans, wire, scrap) |
| Kitchen cabinets | Light bulbs |
| Furniture | General household trash (e.g. diapers, food wrappers) |
| Mattresses | Smoke detectors |

Figure 3 shows Burn Piles 1 and 2, photographed at different times.

(a) (b) (c)

Figure 3. (a) Burn Pile 1 in 2015. (b) Burn Pile 2 in 2014. (c) Burn Pile 1 in 2013.

## GEOCHEMICAL ANALYSIS

Ash from the burn piles was sampled, as was soil in the immediate vicinity of the burn piles, at different depths into and beneath the burn piles, and along transects from burn piles down gradient. Background samples were taken in an undisturbed area at the edge of the forest approximately 0.5 mile (0.8 km) from Burn Pile 1 (see Figure 2). All samples were sent to Activation Laboratories, Inc. (Ancaster, Canada) to be analyzed for 50 major, minor and trace elements by INAA and/or ICP, using 16 standards, and duplicates and blanks.

The results for the elements of most interest are summarized in Table 2. The elements of greatest interest in terms of their potential adverse effect on the ecosystem fauna are copper, lead, zinc, arsenic, manganese, and chromium. Elevated concentrations of all these metals are detrimental to animal health (Jaishankar et al., 2014). Mercury is also in this category, but its concentrations everywhere were below detection level, probably because its relatively low boiling point (357°C) allows it to vaporize in bonfires, thus becoming airborne and settling away from the study area. Gold is also included because while it is not a toxic element, it can be indicative of anthropogenic activity.

Table 2. Geochemistry

(a) Background geochemistry sampled twice (all concentrations in ppm unless otherwise noted). Data from Shacklette and Boerngen (1984) are global averages.

| Element | 2014 | 2015 | Shacklette and Boerngen, 1984 |
|---|---|---|---|
| Cu | 11 | 20 | 30 |
| Pb | 16 | 42 | 10 |
| Zn | 60 | 102 | 50 |
| As | 2.8 | 7.4 | 5 |
| Mn | 601 | 813 | 600 |
| Cr | 67 | 106 | 100 |
| Au (ppb) | b.d. | b.d. | 5 |

b.d. = below detection

(b) Burn Pile 1 geochemistry sampled four times (all concentration in ppm unless otherwise noted)

| Element | Nov. 2011 | Nov. 2013 | June 2014 | May 2015 |
|---|---|---|---|---|
| Cu | >10,000 | 7480 | 424 | 1010 |
| Pb | 4040 | >5,000 | 1270 | 2690 |
| Zn | 2590 | 12500 | 7900 | 16000 |
| As | 59 | 460 | 147 | 261 |
| Br | 19900 | 32 | 14 | 21 |
| Cr | 217 | 1230 | 261 | 556 |
| Mn | 2 | 2170 | 1260 | 1500 |
| Au | 239 ppb | 68 ppb | 19 ppb | 40 ppb |

(c) Nov. 2013 geochemistry (all concentrations in ppm unless otherwise noted)

| Element | Burn Pile 2 | Burn Pile 3 | Burn Pile 4 |
|---|---|---|---|
| Cu | 211 | 204 | 491 |
| Pb | 196 | 122 | 628 |
| Zn | 494 | 467 | 4660 |
| As | 34 | 57 | b.d. |
| Mn | 1590 | 685 | 657 |
| Cr | 66 | 117 | 64 |
| Au (ppb) | b.d. | 152 | 75 |

b.d. = below detection

The background samples were taken within approximately 10 m of each other. In 2014 soil was sampled at the edge of a large meadow, just below the sod. In 2015 soil was sampled just within the woods next to the meadow. The results (Table 2 (a)) show that background concentrations of the elements of interest are quite similar to global averages. Therefore we can assume that elevated concentrations are due to anthropogenic activity.

Burn Pile 1 was sampled four times (Table 2 (b)). The original sampling for this project was done on this pile in November 2011. At that time, there were partially burned electronics scattered all over the pile. The pile was sampled again in November 2013, and this time the unburned material looked to be mostly interior construction waste, such as old kitchen cabinets, window blinds, plywood and wallboard. The pile was sampled again in June 2014. Little new material had been added to the pile, and it appeared to have simply weathered since the last sampling. (Likely not much dumping or burning is done in the winter and early spring.) The final sampling of the pile before site remediation took place was in May 2015. At this time, the burn pile contained ordinary household trash that appeared to be fairly fresh. Note: Br included here because of anomalous 2011 value.

Burn Piles 2, 3 and 4 were sampled in 2014. Unburned material was largely composed of household trash and bonfire detritus such as beer cans and food wrappers. Natural wood appeared to be the main fuel source, and there was no evidence of lumber or manufactured wood products. Concentrations of the selected metals were mostly an order of magnitude greater than background levels, although none as high as concentrations in Burn Pile 1. This is likely due to the greater variety of materials found in Burn Pile 1. These piles were not sampled in 2014 or 2015; the site of Burn Pile 2 was underwater in 2014, and in 2015 no pile remained.

Table 3 lists the possible sources of these selected metals. Almost all items in this table were directly observed at different sampling times.

Table 3. Possible sources of selected metals

**Au**: Electronics, circuitry, appliances, smoke detectors
**Cu**: Electrical/electronic equipment, plumbing, wood preservative (CCA*)
**Pb**: Lead paint (pre-1978), solder, plumbing, window blinds, some PVC
**Zn**: Galvanized metal, furniture/cabinet hardware, cans, batteries, car parts
**As**: Wood preservative (CCA*), semiconductors, batteries, alloys
**Br**: Flame retardants for plastics/electronics/textiles
**Cr**: Wood preservative (CCA* + chromate salts), pigments, steel
**Mn**: Steel alloys, batteries

*CCA = Chromated copper arsenate; used as fungicide/insecticide in pressure-treated lumber and manufactured wood products

Correlations between elements can help identify the source of the metals. Figure 4 shows excellent correlation between chromium and arsenic, suggesting that chromated copper arsenate (CCA), a fungicide/insecticide used in the manufacture of pressure-treated lumber, is the source of these metals. The correlation with copper is less good, but there are also other sources of copper in the burn pile materials, such as electrical and electronic equipment. Figure 5 shows a good correlation between manganese and zinc, suggesting that batteries may be the source of these metals. Figure 6 shows a good correlation between iron and manganese, which may be due to the abundant presence of food storage cans.

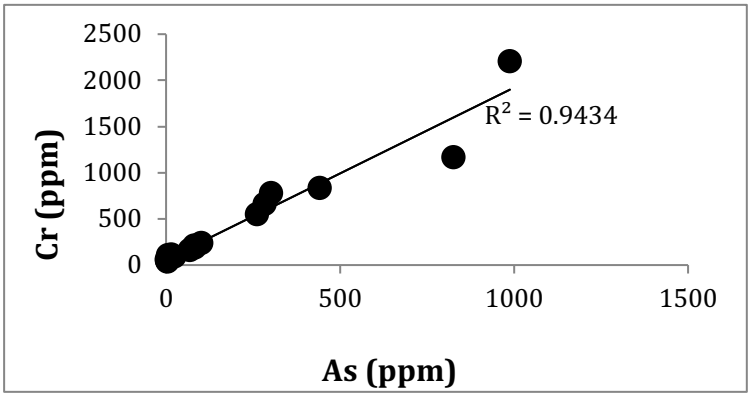


Figure 4a. The good correlation between Cr and As indicates the presence of the wood preservative (CCA), which is used in manufactured wood products.

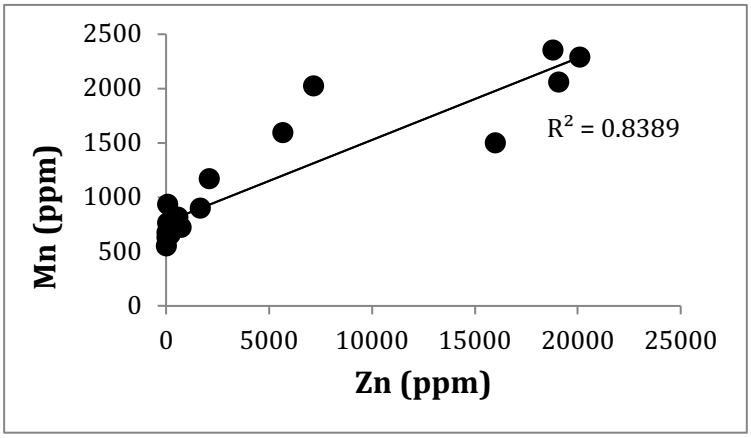


Figure 4b. The correlation between Mn and Zn suggests that batteries are the source of these metals.

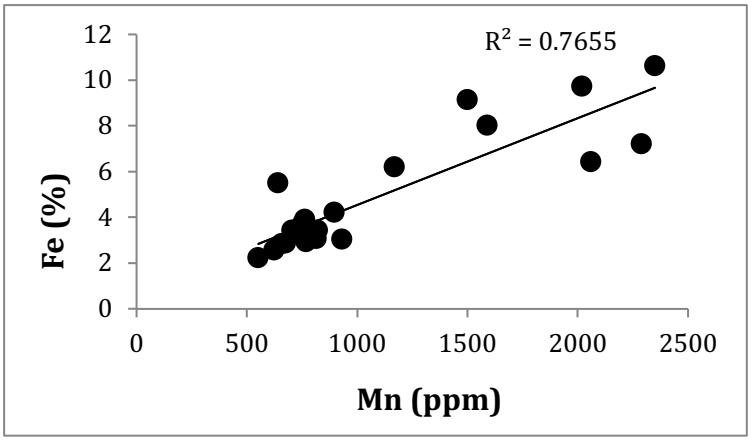


Figure 4c. The correlation between Mn and Fe may be due to the abundance of food storage cans.

Vertical and horizontal sampling along a transect from Burn Pile 1 to the river was accomplished in June, 2015 (Figure 7). Geochemical analysis suggests that contaminants have migrated downward into the underlying soil, as well as laterally towards the river. A 90-cm core from the center of the burn pile shows that metal concentrations are highest from the surface of the pile to a depth of approximately 60 cm down. (Highest values: Pb = 5000 ppm, Zn = 20,000 ppm, As = 1000 ppm, Cu = 4000 ppm, Cr = 2200 ppm and Co = 200 ppm.) This includes ash in the upper 30 cm, and underlying soil beneath the ash. At a distance of 2.1 m from the center of the burn pile in the direction of the river, a core 35 cm long shows metal concentrations highest at the bottom of the core (Pb = 2100 ppm, Zn = 1700 ppm, As = 80 ppm, Cu = 475 ppm, Cr = 215 ppm). A further 2.9 m toward the river, a 40-cm core shows metal contamination spiking at a depth of 15 cm, although at lower concentrations than the previous core. Another 2.5 m toward the river, a 20-cm core shows metal concentrations highest at a depth of 15-20 cm, again at lower amounts than the previous core. This is illustrated in Figure 7. A 30-cm core taken underwater in the riverbed 5 m from the previous core showed no elevated metal concentrations. This suggests that contaminants have migrated away from the burn pile both vertically (presumably by water percolating from the surface) and horizontally (by overland flow, interflow, or both). The different relative concentrations of individual metals from one core to another is the result of differential solubility and transport mechanisms. Contaminants ultimately end up in the river, which flows into Lake Champlain 2 km downstream.

As a result of this study, in 2015 the Vermont Department of Environmental Conservation hired Environmental Compliance Services, Inc., to assess and remediate the site. Four cubic yards of soil was removed and disposed of in a compliant landfill. Clean fill was brought in, and the site of Burn Piles 1 and 2 was re-graded

into a boat launch. Boulders were added along the western edge of the site to prevent people from driving off-road along the banks of the river (which had previously been the site of other burn piles). A parking area was created 50 m along the road. The construction of the boat launch and parking area allows the State of Vermont to patrol the area using law enforcement from the Department of Fish and Wildlife. Since then, it appears as though major dumping has largely ceased. Burn piles still exist, but largely consist of natural firewood and minor trash such as beer cans and food wrappers.

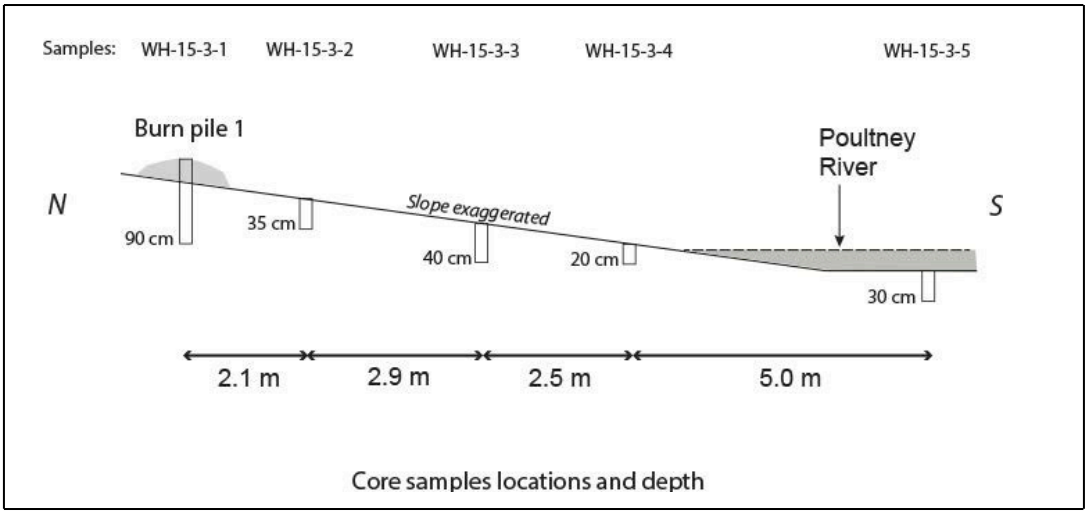


Figure 7. Core depths along a transect from Burn Pile 1 to below the surface of the Poultney River.

## CHAMPLAIN VALLEY CLAYPLAIN FOREST

Prior to European settlement, Clayplain forest dominated the clay and silt soils of the Champlain Valley. Approximately 20,000 years ago, continental ice sheets covered the region. As the ice melted and retreated, a series of lakes filled the Champlain Valley. First, freshwater Lake Vermont flooded most of the valley for 1000-2000 years. When the ice's continued retreated extended far enough to the north, an influx of marine water established the smaller Champlain Sea, which covered the lower elevations of the valley for approximately 2,000 years. The clay that southern Lake Champlain residents know so well settled out in the deep still waters of Lake Vermont and the Champlain Sea. About 11,000 years ago, the connection with the Atlantic Ocean was cut off and present day Lake Champlain began to form. The lake bottom, for thousands of years beneath the water, became exposed lake plain. The word "Clayplain" is shortened from "clay-soil lake plain" – the landform on which the current forest grows (Lapin 2002).

The most common trees of the Clayplain forest type are white oak, red maple, white pine, shagbark hickory and white ash. Associated species are hemlock, sugar maple, beech, swamp white oak and bur oak. Both swamp white oak and bur oak are at the northern extensions of their range in the Champlain Valley.

Because of the relatively warm valley climate, gentle topography, and fertile clay soils, the Champlain Valley was cleared early for agriculture and remains today the predominant agricultural region in Vermont. It is estimate that 90% of the original Clayplain forest (on the Vermont side) has been cut down and converted into use for agriculture or development, making it now a very rare and fragmented forest community (Thompson and Sorenson, 2005).

However, in the very southern end of the Champlain Valley in West Haven and Benson, Lapin et al. (2014) found that 25% of the known and mapped clay soils were forested. This has allowed for some of the best Clayplain forest restoration opportunities in the state. Several of these restoration sites are owned and managed by The Nature Conservancy in the Helen W. Buckner Preserve and the Hubbardton River Clayplain Preserve, both in West Haven (Lapin et al., 2014).

**TIMBER RATTLESNAKE RESEARCH**

Spear et al. (2013) completed a study on timber rattlesnakes in and near the Buckner Preserve in 2011-2012 with the objectives of identifying migration routes and summer foraging habitat, identifying land potentially used by different populations of rattlesnakes to prioritize land protection actions, and determining rattlesnake population status over time. Timber rattlesnakes once ranged widely in eastern North America. In New England today, they are found only in small, isolated populations, and are threatened by human development and illegal hunting. In Vermont, timber rattlesnakes are at the edge of climatic limits, so anthropogenic stressors compound existing natural stressors such as food availability and disease. The timber rattlesnake is currently state-listed as endangered in Vermont. The Buckner Preserve is home to one of only two populations of timber rattlesnakes in Vermont, and there is concern for the survival of the populations considering their relative isolation and the threat of a newly identified fungal disease that has contributed to the severe decline of other New England snake populations. The preserve provides ideal habitat for timber rattlesnakes, which prefer to overwinter in open, rocky areas with southerly aspects; this is limited in Vermont.

For this study, 144 timber rattlesnakes were captured and marked. Radio transmitters were implanted in 17 males, three non-pregnant females and two pregnant females. These snakes were monitored from when they emerged from their hibernacula in the spring until they returned in the fall. They were located an average of 30 times every four days or so.

Distances were measured both as maximum distance from hibernaculum and total distance traveled in the season. The results are given in Table 4.

Table 4. Distances moved by timber rattlesnakes

| | Maximum distance from hibernaculum (km) | Total distance traveled (km) |
|---|---|---|
| Males | 3.56 ± 0.26 | 11.74 ± 0.91 |
| Females | 2.28 ± 0.75 | 5.09 ± 2.16 |

The movement of one radio telemetered male timber rattlesnake during one season is show in Figure 8 as a time-series graph. The "outbound migration" consists of a series of long, rapid movements away from the hibernaculum in the spring. The "core area" consists of a period of slower, shorter movements at a relatively stable distance from the hibernaculum during the summer. The "inbound migration" repeats the long, rapid movements back towards the hibernaculum in the fall.

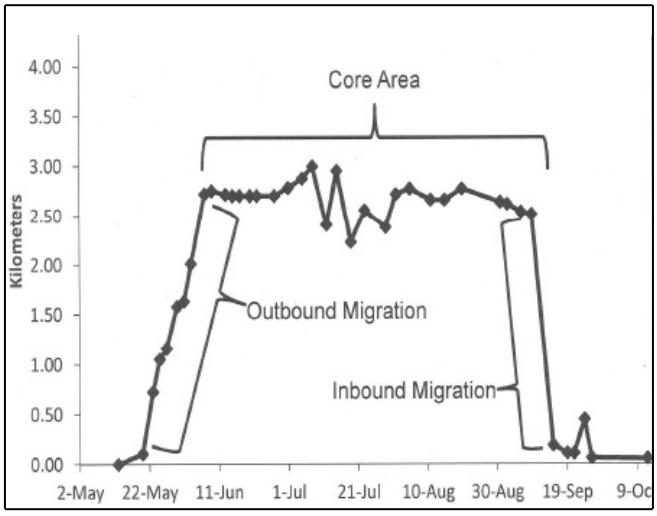


Figure 8. Displacement as a time-series graph for a typical radio-telemetered male rattlesnake.

The snakes used all available habitats in proportion to their availability. (For example, most of the land is forested, so snakes spent most of their summer foraging and mating time on forested land.)

Timber rattlesnake habitat selection:
46% deciduous forest
26% evergreen forest
13% mixed forest
12% wetland
2% agriculture
1% shrub

Most snakes migrated northeast from their hibernacula (Figure 9), spending the summer on private land (which is not protected).

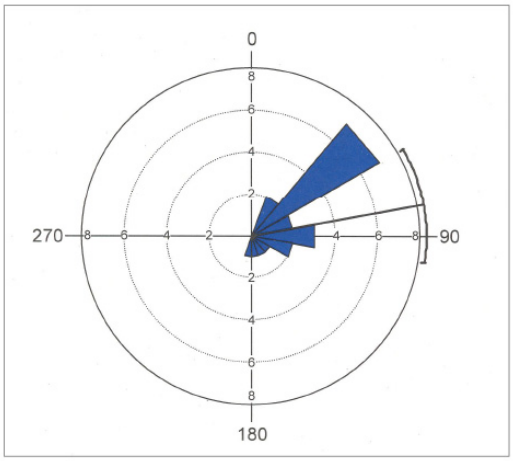


Figure 9. Rose diagram showing the mean bearing of outbound migration for 22 rattlesnakes monitored with radio telemetry in 2011 and 2012.

Additional land protection would therefore provide an enormous benefit for the timber rattlesnake population. It is especially important to prevent the direct mortality of female timber rattlesnakes, because of their slow reproductive output. One approach is the rattlesnake removal program currently underway. On-call trained personnel will go to private property to remove observed rattlesnakes at no cost to the landowner and release them on protected land.

## ARCHAEOLOGY

The Galick Farm to the west of Austin Hill is currently the site of archaeological research led by Professor Matthew Moriarty of Castleton University, who reports:

The Buckner Preserve is home to several important Precontact Native American archaeological sites. The largest of these is spread across an area of roughly five acres in and around the Galick Farm. Archaeological investigations at the Galick Site over the last three years have recovered many artifacts, including projectile points, pottery, animal bone, and thousands of flakes from stone tool production. These artifacts were deposited by Native Americans camping at the site over the course of thousands of years, with the earliest activity dating to nearly 12,000 years ago. Native American foragers likely utilized the Galick Farm area as a seasonal base camp for accessing remarkably diverse local plant and animal resources and as a way station for canoe travel between Lake Champlain and the Hudson River Valley just to the south.

## REFERENCES

Fisher, D.W., 1984, Bedrock geology of the Glens Falls-Whitehall region, New York, New York State Museum Map and Chart Series, no. 35, 60 p., scale 1:48,000.

Jaishankar, M., Tseten, T., Anbalagan, N., Mathew, B.B. and Beeregowda, K.N., 2014, Toxicity, mechanism and health effects of some heavy metals, Interdisip. Toxicol., vol. 7, no.2, p. 60-72.

Lapin, M., 2002, The Champlain Valley Clayplain Forest: A Landowners Guide, Champlain Valley Clayplain Forest Project, 18 p.

Lapin, M., Doyle, K., Graves, J. and Droege, M., 2004, Clayplain and Floodplain Forest Restoration Plan, Hubbardton River and Lower Poultney River Watershed Vermont and New York, The Nature Conservancy, 47 p.

Ratcliffe, N.M., Stanley, R.S., Gale, M.H., Thompson, P.J. and Walsh, G.J., 2011, Bedrock geologic map of Vermont, USGS Scientific Investigations Series Map 3184, 3 sheets, scale 1:100,000.

Shacklette, H.T. and Boerngen, J.G., 1984, Element concentrations in soils and other surficial materials of the conterminous United States, U.S. Geological Survey Professional Paper 1270, 105 p.

Spear, S., Bauder, J., Blodgett, D., Jenkins, C. and Briggs, K., 2013, The ecology of timber rattlesnakes (*Crotalus horridus*) in Vermont, Vermont Dept. of Fish and Wildlife, Rutland, VT.

Thompson, E.H. and Sorenson, E.R. 2005, Wetland, Woodland, Wildland: A Guide to the Natural Communities of Vermont, Vermont Department of Fish and Wildlife/The Nature Conservancy, 468 p.

## ROAD LOG

Assemble at the parking area/boat launch on Galick Road in West Haven, Vermont. From Lake George, NY, take Rt. 9 south approximately 4 miles to Queensbury. Turn left on Rt. 149 east for 11.7 miles to Fort Ann. Turn left on Rt. 4 north for 10.6 miles to Whitehall. Here, Rt. 4 turns right (at the traffic light), going over the Champlain Canal; stay on Broadway (heading north) for almost half a mile, then turn right on Saunders Street. Go over the Canal and then immediately left on N. Williams St. In 0.6 miles turn left on Doig St. In 0.5 miles turn left onto an unmarked dirt road. This will take you over the Poultney River. Just after the bridge, turn left (this is Galick Rd.). The parking area/boat launch is 0.2 miles from the bridge. Vehicles will be left here and the trip will be completed on foot (about 4.5 miles total walking).

We will meet at 9:00 a.m. Bring a lunch and any snacks and beverages you will need for the day. Whitehall is the closest place to purchase anything. We will probably have a late lunch at the last stop, and end the trip early. There are no formal restroom facilities.

Mileage
0.0 Poultney River boat launch

**STOP 1A: SITE OF MAJOR GARBAGE BURN PILES**
(Long. 43.569812 N, Lat. -73.395736 W; UTM 4825346.32N, 629544.54E)

This is the site of Burn Piles 1 and 2. Although geochemistry does not lend itself well to field trips, there are several things worth observing here. As a result of this study, the State of Vermont hired a geologic consulting company to assess the site, remove contaminated soil, place boulders to prevent vehicles from driving further along the river bank, re-grade the burn pile site as an official "boat launch" and create the parking area. Making this an official boat launch allowed Fish and Wildlife law enforcement to patrol the area and issue citations. (Previously, it was up to the town of West Haven to supply law enforcement, which, despite the good efforts of the local sheriff, was completely inadequate to keep up with the illegal/questionable use of the site.)

It is highly likely that there will be a reasonably fresh burn pile, and while we might not see the variety of materials that have been dumped and burned in the past, this will give trip participants a sense of the scale of activity. We can also observe the current river level, and look for evidence of flooding (which periodically erodes burn piles, sending their contents and the contaminated soil around and beneath them, directly into the river and shortly thereafter into Lake Champlain.

**STOP 1B: CLAY PLAIN SOILS AND REFORESTATION**

The Nature Conservancy's Southern Lake Champlain Valley office launched an ambitious 11-year Clayplain forest restoration project in 2004 in multiple sites in West Haven and Benson, Vermont. A decision to use only local seed source lead to the establishment of a small native woody plant nursery called the Champlain Valley Native Plant Nursery. 76,000 native trees and shrubs were planted between 2004 and 2014 on more than 200 acres. Funding was provided by USDA's Wetland Reserve Program, Wildlife Habitat Incentive Program and USFWS Partners For Fish and Wildlife. Survival of the plantings has been mixed, but adjacent to the parking area on Galick Road, which was planted in 2005, survival and growth has been excellent.

0.4 Walk west along Galick Road for 0.4 miles (0.6 km) to the Tim's Trial trailhead.

**STOP 2: SITE OF "BACKGROUND" SAMPLES AND VIEW OF CLIFFS AND TALUS SLOPE**

This is a very brief stop to indicate the location of the "background" samples used in this study. The trailhead is just in the woods next to a large field that is kept open for field-nesting birds, amphibians, and other wildlife. The 2014 background sample was obtained from the very edge of the field, and the 2015 sample was obtained just into the woods, both approximately 100 m from the road.

A little further along the trail (50 m) is an excellent view of the cliffs of Middle Mesoproterozoic gneiss and the talus slope below.

0.6 At the kiosk, go left to take the trail that goes through the woods along the base of the cliff. The trail to the right goes along the edge of the meadow; we will return by this trail.

0.7 The trail is right next to the cliffs here.

**STOP 3: MESOPROTEROZOIC GRANITOID GNEISS/GRANULITE**

This is a brief stop to examine the biotite tonalite gneiss. The rock contains mostly quartz and plagioclase feldspar, with the result that where the foliation is subtle the rock could more appropriately be called a granulite. Minor biotite and pyroxene are visible in hand sample and microscopically. Farther along the trail there is an outcrop that exhibits folded foliation. The rock is very hard, creating the cliffs, and weathers in large blocks, creating the talus slopes that provide critical habitat to a number of species, including the timber rattlesnake.

0.8 Right turn leads to meadow trail back to kiosk. Continue north to start of loop. Take left trail up hill.

0.9 Outcrop of gneiss on right.
1.2 Just off the trail to the left is a view to the south and east.

**STOP 4: WARD MARSH OVERLOOK**

Ward Marsh is visible to the left (east). In addition to the rattlesnake research discussed above, the Buckner Preserve is home to what has recently been recognized as the largest populations of golden-winged warblers, blue-winged warblers and their hybrids in New England. The Nature Conservancy is partnering with Audubon Vermont to monitor the populations and manage areas of the preserve to maintain and improve habitat for these birds.

To the southeast (to the right of Ward Marsh from this vantage point) is Skene Mountain. It consists of Cambrian and Ordovician sedimentary rocks. At the base is Potsdam Sandstone, overlain by Ticonderoga Formation dolostones and above that the Whitehall Formation. The Whitehall Formation consists of interlayered dolostones and limestones; Skene Mountain is capped by the Skene Member, a very hard, massive dolostone.

1.5 Outcrops showing gneissic fabric are plentiful as the trail heads downhill through a hemlock forest.
1.8 Overlook with bench.

**STOP 5: LUNCH AND VIEW**

This overlook provides an excellent view of the Poultney River near its mouth and the South Bay of Lake Champlain. The hill directly south across the Poultney River is made of Hague Gneiss and quartzite of the Lake George Group. Skene Mountain is visible to the east.

To return to the parking area: Either retrace your steps, or continue along the trail for almost 0.2 miles to where Tim's Trail turns east (a connector trail to the west leads down to the Susan Bacher Trail and the Galick Farm). Follow Tim's Trail for 1.1 miles to where it rejoins the trail back to the kiosk and the road.

Thank you

Bruce...

...and Bill